Evaluation and Management of Liver Masses

Lewis R. Roberts
Ju Dong Yang
Sudhakar K. Venkatesh
Editors

Springer

Evaluation and Management of Liver Masses

Lewis R. Roberts • Ju Dong Yang
Sudhakar K. Venkatesh
Editors

Evaluation and Management of Liver Masses

Springer

Editors
Lewis R. Roberts
Division of Gastroenterology and Hepatology
Mayo Clinic
Rochester, MN
USA

Ju Dong Yang
Division of Digestive and Liver Diseases
Cedars-Sinai Medical Center
Los Angeles, CA
USA

Sudhakar K. Venkatesh
Department of Radiology
Mayo Clinic
Rochester, MN
USA

ISBN 978-3-030-46698-5 ISBN 978-3-030-46699-2 (eBook)
https://doi.org/10.1007/978-3-030-46699-2

This Springer imprint is published by the registered company Springer Nature Switzerland AG
The registered company address is: Gewerbestrasse 11, 6330 Cham, Switzerland

Contents

Contributors

Candice A. Bookwalter Department of Radiology, Mayo Clinic, Rochester, MN, USA

Mitesh J. Borad Division of Hematology and Oncology, Mayo Clinic, Rochester, MN, USA

Vishal Chandan Department of Pathology and Laboratory Medicine, University of California-Irvine, Irvine, CA, USA

Sean P. Cleary Department of Surgery, Mayo Clinic, Rochester, MN, USA

Eric C. Ehman Department of Radiology, Mayo Clinic, Rochester, MN, USA

Gaurav Goyal Department of Medical Oncology, Mayo Clinic, Rochester, MN, USA

Rondell P. Graham Department of Laboratory Medicine and Pathology, Mayo Clinic, Rochester, MN, USA

Christopher L. Hallemeier Department of Radiation Oncology, Mayo Clinic, Rochester, MN, USA

Denise M. Harnois Department of Gastroenterology & Hepatology, Mayo Clinic, Jacksonville, FL, USA

Julie K. Heimbach Department of Transplantation Surgery, Mayo Clinic, Rochester, MN, USA

Moira B. Hilscher Department of Gastroenterology and Hepatology, Mayo Clinic, Rochester, MN, USA

Patrick S. Kamath Department of Gastroenterology and Hepatology, Mayo Clinic, Rochester, MN, USA

Benjamin R. Kipp Department of Laboratory Medicine and Pathology, Mayo Clinic, Rochester, MN, USA

Anuhya Kommalapati Department of Internal Medicine, University of South Carolina School of Medicine, Columbia, SC, USA

Amit Mahipal Department of Medical Oncology, Mayo Clinic, Rochester, MN, USA

Lorena Marcano-Bonilla University of Puerto Rico School of Medicine, San Juan, PR, USA

Christine O. Menias Department of Radiology, Mayo Clinic, Scottsdale, AZ, USA

Kabir Mody Division of Hematology/Oncology, Department of Medicine, Mayo Clinic, Jacksonville, FL, USA

Taofic Mounajjed Department of Laboratory Medicine and Pathology, Mayo Clinic, Rochester, MN, USA

Department of Anatomic Pathology, Mayo Clinic, Rochester, MN, USA

Kaitlyn R. Musto Department of Gastroenterology & Hepatology, Mayo Clinic, Jacksonville, FL, USA

Patrick J. Navin Department of Radiology, Mayo Clinic, Rochester, MN, USA

Newton B. Neidert Department of Radiology, Mayo Clinic, Rochester, MN, USA

Tushar C. Patel Department of Transplantation, and Division of Gastroenterology and Hepatology, Mayo Clinic, Jacksonville, FL, USA

Lewis R. Roberts Division of Gastroenterology and Hepatology, Mayo Clinic, Rochester, MN, USA

Douglas A. Simonetto Department of Gastroenterology and Hepatology, Mayo Clinic, Rochester, MN, USA

Rory L. Smoot Department of Surgery, Mayo Clinic, Rochester, MN, USA

Sri Harsha Tella Department of Internal Medicine, University of South Carolina School of Medicine, Columbia, SC, USA

Scott M. Thompson Department of Radiology, Mayo Clinic, Rochester, MN, USA

Michael S. Torbenson Department of Laboratory Medicine and Pathology, Mayo Clinic, Rochester, MN, USA

Wendaline M. VanBuren Department of Radiology, Mayo Clinic, Rochester, MN, USA

Sudhakar K. Venkatesh Department of Radiology, Mayo Clinic, Rochester, MN, USA

Michael L. Wells Department of Radiology, Mayo Clinic, Rochester, MN, USA

Ju Dong Yang Department of Gastroenterology and Hepatology, Mayo Clinic, Rochester, MN, USA

Jason R. Young Department of Radiology, Mayo Clinic, Rochester, MN, USA

Maria Baladron Zanetti Department of Radiology, Mayo Clinic, Rochester, MN, USA

Chapter 1
Hepatocellular Carcinoma

Eric C. Ehman, Michael S. Torbenson, Christopher L. Hallemeier, Julie K. Heimbach, and Lewis R. Roberts

Introduction

Hepatocellular carcinoma (HCC) is the most common primary liver cell cancer. HCC is one of the most common causes of death from cancer worldwide, variably ranking between second and fourth in annual number of deaths and years of life lost from cancer, after lung cancer and essentially tied with gastric cancer and colorectal cancer for the number 2 position [1, 2]. The majority of liver cancers occurring worldwide develop in the context of chronic injury and inflammation of the liver, which results in exhausted liver regeneration and an aberrant healing response with fibrosis leading to cirrhosis. The major etiologies of HCC are chronic hepatitis B

E. C. Ehman (✉)
Department of Radiology, Mayo Clinic, Rochester, MN, USA
e-mail: ehman.eric@mayo.edu

M. S. Torbenson
Department of Laboratory Medicine and Pathology, Mayo Clinic, Rochester, MN, USA
e-mail: torbenson.michael@mayo.edu

C. L. Hallemeier
Department of Radiation Oncology, Mayo Clinic, Rochester, MN, USA
e-mail: hallemeier.christopher@mayo.edu

J. K. Heimbach
Department of Transplantation Surgery, Mayo Clinic, Rochester, MN, USA
e-mail: heimbach.julie@mayo.edu

L. R. Roberts
Division of Gastroenterology and Hepatology, Mayo Clinic, Rochester, MN, USA
e-mail: roberts.lewis@mayo.edu

L. R. Roberts et al. (eds.), *Evaluation and Management of Liver Masses*,
https://doi.org/10.1007/978-3-030-46699-2_1

and C virus infections, alcoholic liver disease, and nonalcoholic fatty liver disease. Other less common causes of liver inflammation and cirrhosis, including hereditary hemochromatosis, primary biliary cirrhosis, and autoimmune hepatitis, are also associated with increased risk of HCC.

The inflammatory microenvironment induced by the different causes of liver injury is characterized by a high concentration of reactive oxygen species that react with hepatocyte genomic DNA to induce DNA mutations and chromosomal aberrations that lead to induction of tumor oncogenes and loss of tumor suppressor function, thus enhancing liver cell growth and inhibiting apoptosis. The inflammatory and fibrotic microenvironment also mediates other tumorigenic processes, including angiogenesis and inhibition of natural antitumor immune responses. In many parts of the world, dietary exposure to mutagenic compounds such as fungal aflatoxins or plant-derived aristolochic acid significantly enhances the risk of HCC, acting synergistically with other etiologic factors such as chronic viral hepatitis [3]. Chronic hepatitis B virus infection and adeno-associated virus 2 infection uniquely cause HCC by viral integration into the host genomic DNA, leading to increased expression of oncogenic proteins.

Imaging techniques have played a central role in improvements in the diagnosis and care of patients with HCC over the past several decades. The use of ultrasound and multiphasic contrast CT to identify new masses developing in patients with liver cirrhosis followed by advancements in angiographic technique and the use of embolization, either bland or with chemotherapy drugs (transarterial chemoembolization, TACE), led to rapid change in the diagnostic and treatment paradigm for HCC. In 2002, two randomized trials showed that chemoembolization was superior to best supportive care in the management of patients with unresectable intermediate stage HCC [4, 5]. TACE is now complemented by transarterial radioembolization (TARE), which uses Yttrium-90 (Y-90) impregnated glass or resin beads to deliver high-activity β-particle radiation to the arterial distribution of HCCs. TARE has been shown to achieve better tumor control and equivalent survival in comparison to TACE for patients with Barcelona Clinic Liver Cancer (BCLC) stages A or B HCC and Child Pugh Class A or B cirrhosis [6].

The next major advances in the use of imaging in HCC were the recognition that multiphasic CT and MRI of the liver could be used for noninvasive diagnosis of newly developing HCC in the cirrhotic liver. At a time when there was concern about the risk of tumor seeding driving recurrence after biopsy, percutaneous ablation, or liver transplantation with posttransplant immunosuppression, the ability to make a noninvasive diagnosis of HCC with high specificity was a substantial advance, as it provided assurance of a lower risk of recurrence for those patients who were eligible for potentially curative ablation or surgical treatment. Further, the arterial vascular enhancement, portal and late venous washout, and other ancillary features characteristic of viable tumor could also be applied to the assessment of treatment response and tumor recurrence, becoming codified as the modified-Response Evaluation Criteria in Solid Tumors (m-RECIST) criteria for HCC [7]. Most recently, expanded evaluation of the diagnostic criteria for

liver masses has resulted in the development of the Liver Imaging Reporting and Data System (LI-RADS), which provides a more systematic classification of liver lesions by imaging [8].

In this chapter, we discuss the current role of liver imaging in the diagnosis and treatment of HCC, including the imaging-intensive treatment modalities of ablation, transarterial chemoembolization (TACE), transarterial radioembolization (TARE), stereotactic body radiation therapy (SBRT), and proton beam therapy. There is a large variability in phenotypic presentation of HCC, ranging from single nodules between 1 and >20 cm in size, to oligonodular tumors with only two or three nodules that may be located in the same segment of the liver, in different segments of the same, right or left, lobe of the liver, or in a bilateral, multilobar distribution, to multinodular tumors presenting with three to ten or more nodules, and then to the extreme end of the spectrum, where there is diffuse involvement of the liver with small, almost miliary nodules or alternatively with a diffusely infiltrative nearly confluent mass of tumor. Consequently, although general principles of care can be produced in guidelines, the optimal treatment of each patient with HCC must be personalized based on the specific presentation.

Knowledge of the spatial geography of tumor nodules within the liver as determined by cross-sectional imaging is critical for making optimal treatment decisions. For example, whether a 2 cm HCC is best treated by liver transplantation, surgical resection, microwave ablation, or transarterial radioembolization depends on its peripheral or central location within the liver and the proximity of large blood vessels or bile ducts, complemented by an assessment of the severity of the underlying liver cirrhosis, loss of liver synthetic function, and associated portal hypertension, and also of the patient's age and comorbidities that may preclude surgical treatment.

Optimal integration of these different factors in treatment selection requires a multidisciplinary team approach including specialists in diagnostic and interventional radiology, pathology, hepatology, medical oncology, radiation oncology, hepatobiliary surgery and liver transplant surgery, and palliative care. Further, since the varying phenotypic presentations almost certainly reflect the underlying biology of the tumors, it is imperative to develop a deeper understanding of the specific biologic determinants of HCC tumor phenotype and outcomes, as these may be directly linked to the response of specific tumors to local, locoregional, targeted, or immune modulatory treatments.

An additional consideration in the care of patients with HCC is the concept of tumor heterogeneity. During the development and progression of liver cancer, once the key molecular alterations needed for the cancer phenotype are established, the malignant clone continues to acquire additional alterations and potentially additional phenotypic characteristics. This may result in HCCs developing a more aggressive, invasive, and metastatic phenotype over time. From an imaging perspective, phenotypic changes acquired by tumors during their growth can often be discerned by differences in their imaging appearances. Perhaps the most well-known imaging proof of tumor progression is the nodule-in-nodule appearance seen when well-differentiated tumors transition into a less well-differentiated

histology, with the more aggressive clone pushing the earlier, less aggressive tumor to the edges of the nodule. Tumor heterogeneity is important in part because the additional changes in tumor biology that occur during tumor progression may be associated with increased resistance to physical, chemical, or systemic anticancer therapies.

Pathologic Features of Hepatocellular Carcinoma

HCC are composed of malignant epithelial cells with hepatocellular differentiation. A tissue proven diagnosis of HCC is based on H&E findings supplemented with immunohistochemical stains. HCC show a number of important architectural changes that help distinguish them from benign liver lesions. They show abnormal arterialization of the hepatic lobules, loss of portal tracts, and abnormal growth patterns (Fig. 1.1), which can include thickened hepatic cords (normally 1–2 cells thick), pseudoglandular structures, and loss of the normal reticulin framework. These architectural changes can be accompanied by cytological abnormalities such as increased nuclear to cytoplasmic ratios, nuclear atypia including hyperchromasia, and prominent nucleoli. Some HCC also develop distinctive cytoplasmic inclusions, including hyaline bodies, Mallory-Denk bodies, or pale bodies.

After a diagnosis is made, HCC are graded from well differentiated to poorly differentiated, based on how closely the tumor cells resemble normal hepatocytes (Fig. 1.2). Tumor grade predicts both patient survival and disease-free survival in all major clinical settings including resections in cirrhotic [9, 10] and non-cirrhotic livers [11], and after liver transplantation [12].

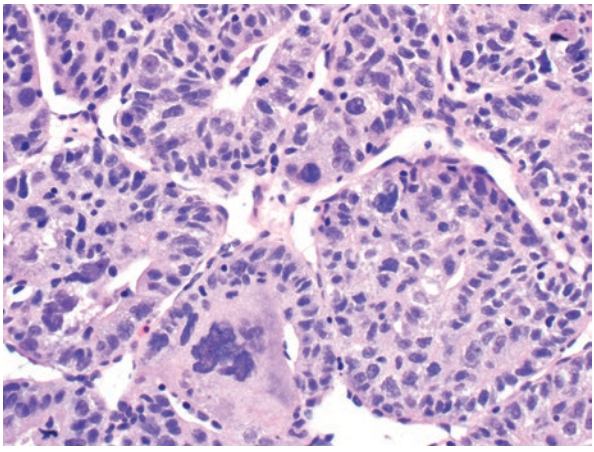

Fig. 1.1 Hepatocellular carcinoma. This hepatocellular carcinoma is growing with thick bulbous plates. The tumor cells show bizarre nuclei

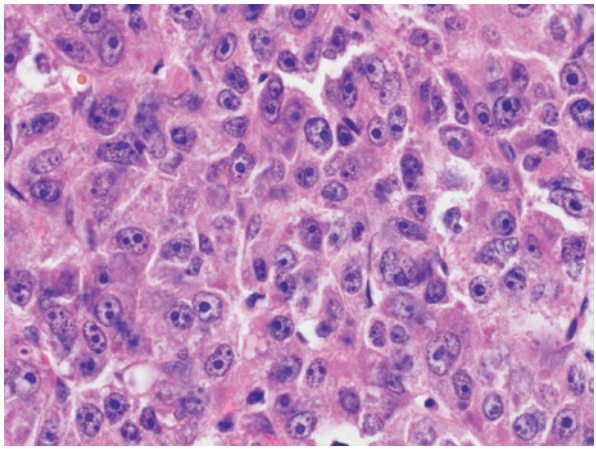

Fig. 1.2 Hepatocellular carcinoma, moderately differentiated. This hepatocellular carcinoma shows enough atypia to indicate that it is malignant, but at the same time shows evidence for hepatic differentiation, with moderately abundant eosinophilic cytoplasm

Histological Subtypes

Up to 35% of HCC can be further classified into histological subtypes or variants, which often have clinical and/or molecular correlates (Table 1.1). The subtypes also have their own potential diagnostic pitfalls, which depend on their morphology (Fig. 1.3). A subtype of HCC is defined by possessing these four key features [13], though all of the features will not be equally well developed when a subtype is first defined and may take many years to fully develop. The key features are the following: (1) unique H&E findings that are reproducibly identifiable and (2) can be confirmed by immunostains or other special studies. These findings in turn have (3) unique clinical correlates and (4) associated molecular findings.

Differential Diagnosis

The histological differential for HCC depends on the degree of differentiation within the tumor and on the presence or absence of cirrhosis in the background liver (Table 1.2). Immunohistochemical stains are used to distinguish between possibilities within the differential and are used in two distinct settings. First, they are used to separate benign hepatic lesions from hepatocellular carcinoma. Stains in this group are predominantly the reticulin stain (Fig. 1.4) and immunostains for glypican 3, glutamine synthetase, and Ki-67. Second, immunostains are used to show hepatocellular differentiation in cases where the differential includes non-hepatic lesions. The most common of these stains in current use are HepPar1 (Fig. 1.5), arginase, and glypican 3.

Table 1.1 Subtypes of hepatocellular carcinoma

Subtype	Frequency (%)	Prognosis[a]	Notes on subtype status
Steatohepatitic	5–20	Similar	Accepted subtype; may be genetically heterogeneous, with morphology reflecting underlying metabolic syndrome or alcohol use
Clear cell	7	Better	Accepted subtype; the percent of clear cell change required has not been well defined
Scirrhous	4	Variable, no strong consensus in literature	Accepted subtype
Chromophobe	3	Similar	Accepted subtype
Cirrhotomimetic	1	Worse	Probable subtype; currently only subtype defined by gross findings
Fibrolamellar carcinoma	1	Similar to HCC in noncirrhotic livers	Accepted subtype
Combined hepatocellular-cholangiocarcinoma	1–3	Worse	Accepted subtype
Combined hepatocellular and neuroendocrine carcinoma	<1	Worse	Accepted subtype
Carcinosarcoma	<1	Worse	Accepted subtype
Granulocyte-colony-stimulating-factor producing	<1	Worse	Accepted subtype
Sarcomatoid	<1	Worse	Accepted subtype
Lymphocyte rich	<1	Better	Accepted subtype
Lipid rich	<1	Unclear	Probable subtype, only a few cases reported

[a]As compared to conventional hepatocellular carcinoma

Pathology Staging and Other Tissue Prognostic Markers

Pathology staging is based on these findings: tumor size (maximum diameter), numbers of tumors, angiolymphatic invasion, and metastatic disease. Angiolymphatic invasion is divided into microscopic type and macrovascular type, where macrovascular invasion involves vessels (portal veins or hepatic veins) that are large enough to be recognized on gross examination or by imaging. The frequency of macrovascular invasion is generally low in resection specimens, because its presence on

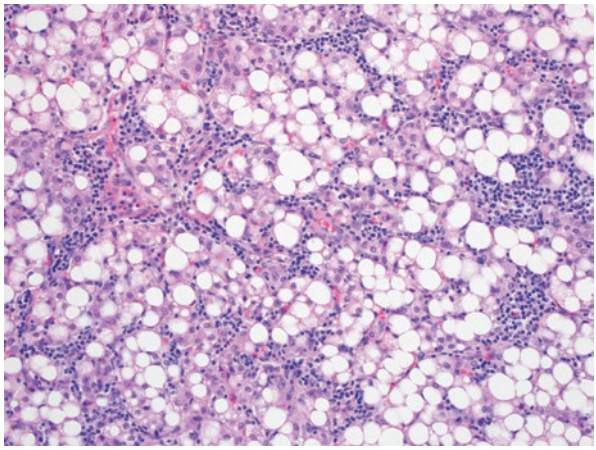

Fig. 1.3 Hepatocellular carcinoma, steatohepatitic subtype. This hepatocellular carcinoma shows fat, inflammation, and fibrosis, which are the key findings in steatohepatitis. This pattern of HCC can sometimes mimic benign liver tissue with steatohepatitis

Table 1.2 Differential for lesions in adult livers

	Well-differentiated hepatocytic lesion	Moderately or poorly differentiated hepatocytic tumor
Cirrhotic background liver	Focal nodular hyperplasia-like lesions[a] Macroregenerative nodule Dysplastic nodule Hepatocellular carcinoma	Hepatocellular carcinoma Cholangiocarcinoma Metastatic carcinoma
Non-cirrhotic background liver	Focal nodular hyperplasia Hepatic adenoma Hepatocellular carcinoma	Hepatocellular carcinoma Fibrolamellar carcinoma Cholangiocarcinoma Metastatic carcinoma

[a]Vascular shunting in cirrhotic livers can sometimes lead to lesions that share many similarities with a focal nodular hyperplasia in the non-cirrhotic liver

imaging is a deterrent to surgical resection. Microvascular invasion is defined as vascular involvement detected only microscopically and is present in about 30% of resected specimens (range from 15% to 60%) [14]. Overall, portal veins are about ten times more likely to be involved than central veins [15], and arterial invasion is even more rare.

A number of other biomarkers of tissue prognosis have been proposed, but to date, expression of CK19 in >5% of tumor cells, which is a negative prognostic indicator, is the most common tissue biomarker in clinical use, largely in Europe and Asia. The lack of underlying liver disease with advanced fibrosis imparts a better prognosis [16]. Targeted molecular-based therapies are also likely to depend on tissue biomarkers.

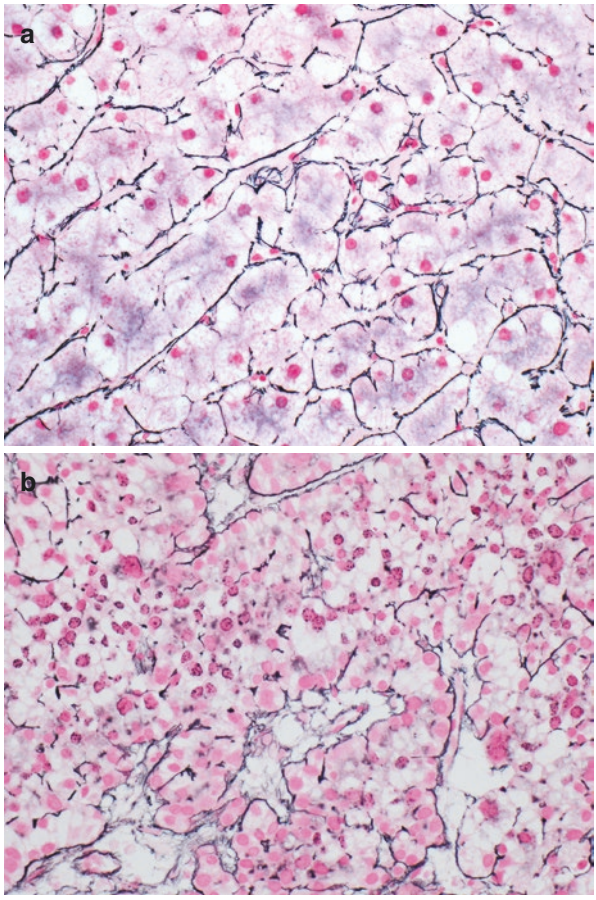

Fig. 1.4 Hepatocellular carcinoma, reticulin loss. The reticulin stain shows thin black lines that represent reticulin. In the normal liver, each hepatocyte is touching reticulin on at least one of its borders (panel **a**), but in hepatocellular carcinoma, many tumor cells are not touching reticulin fibers (panel **b**)

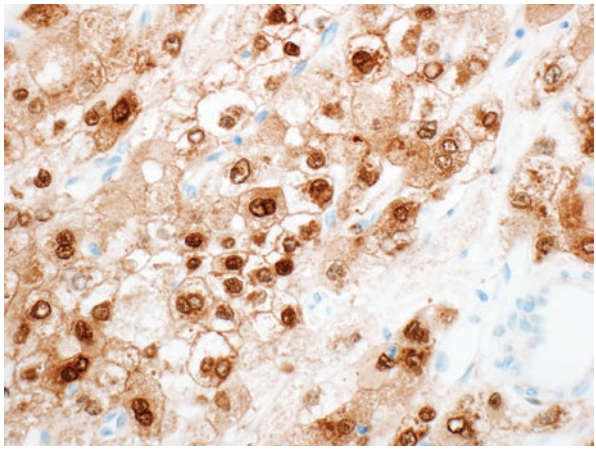

Fig. 1.5 Hepatocellular carcinoma, Arginase 1 stain. The arginase immunostain recognizes a key mitochondrial protein in hepatocytes. Like all immunostains, specificity requires correlation with the H&E findings, as rarely other tumors can also be arginase 1 positive

Imaging Features of Hepatocellular Carcinoma

HCC may be discovered incidentally during imaging for other indications or may be found on surveillance testing in at-risk patients. Historically, ultrasound has been used for surveillance, sometimes performed in an alternating fashion with other cross-sectional imaging including CT and MRI. Various nuclear medicine studies have been investigated, but in general are not being routinely used in the clinical setting. Most current consensus guidelines (American Association for the Study of Liver Diseases (AASLD), European Association for the Study of the Liver (EASL), Japan Society of Hepatology (JSH), Asia Pacific Association for the Study of the Liver (APASL), Korean Liver Cancer Society-National Cancer Center (KLCSG-NCC)) allow a diagnosis of HCC to be made by imaging alone, without the requirement for biopsy confirmation [17–21]. For this reason, it is important that imaging studies intended to diagnose HCC are both sensitive and specific for disease. The Liver Imaging and Reporting Data System (LI-RADS) provides a framework of nomenclature, imaging features, and guidelines to support this goal [8].

Ultrasound (US)

Ultrasound-based surveillance of high-risk patients is recommended by hepatology societies worldwide [17–21], typically every 6 months. Reported sensitivities for HCC in a surveillance population using US range between 47% and 89%, with specificities >90% [22–25]. HCCs have a variable appearance at unenhanced ultrasound, primarily due to the relative background appearance of the liver. In patients with normal liver parenchymal echogenicity, small lesions typically appear hypoechoic to background liver. Larger lesions may appear heterogeneous and have areas of increased or decreased echogenicity secondary to fibrosis, necrosis, internal fat/hemorrhage, or calcification (Fig. 1.6). Because of the variability in echogenicity of HCC, any lesion that is visible by US and cannot be definitely described as benign (cyst, hemangioma, etc.) should be deemed suspicious and follow-up considered. If the lesion is less than 1 cm in maximal diameter, short-term follow-up US is appropriate, but for larger lesions (≥1 cm), further evaluation with contrast-enhanced CT or MRI should be recommended [26].

The ability of US to visualize changes in blood flow using Doppler technique is particularly useful in the evaluation of HCC. Evidence of portal vein thrombus adjacent to a lesion is highly suspicious for HCC and warrants further evaluation with CT or MRI.

Contrast-enhanced ultrasound (CEUS) is an emerging technique in which US imaging is performed following the injection of an IV contrast agent consisting of small bubbles. Because images are obtained in real time as contrast is administered, it is nearly impossible to miss the arterial phase. CEUS is most useful for

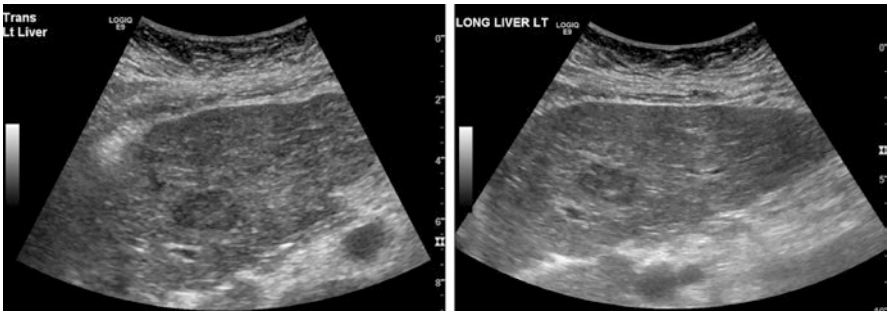

Fig. 1.6 A 72-year-old woman with cirrhosis secondary to primary biliary cirrhosis and autoimmune hepatitis. Gray scale ultrasound images demonstrate a predominantly hypoechoic lesion in the left hepatic lobe, with internal foci of increased echogenicity potentially reflecting internal blood products. No other lesions or venous involvement was seen. Finding is suspicious for hepatocellular carcinoma, and further evaluation with multiphase CT or MRI was recommended

problem-solving or interrogation of lesions seen on prior imaging such as gray scale ultrasound or lesions that are incompletely evaluated at multiphase CT or MRI. A maximum per study dose of IV microbubble contrast agent and a requirement to continuously observe each lesion during the imaging period limit the use of CEUS for whole liver staging. On CEUS, HCC will have non-rim arterial phase hyperenhancement with late (>60 seconds after injection) and mild washout. Care must be taken not to confuse rim-like arterial phase hyperenhancement or early (<60 seconds after injection) and marked washout, as these are features that indicate other types of malignancy such as cholangiocarcinoma or metastases [27]. Reported sensitivity and specificity for HCC using CEUS ranges are 72–94% and 62–69%, respectively [28].

Computed Tomography (CT) and Magnetic Resonance Imaging (MRI)

Noncontrast or single-phase CT or MRI is not sufficient for diagnosis of HCC. If a suspicious observation is made by noncontrast or single-phase imaging, dedicated multiphase imaging of the liver should be recommended.

HCC has a well-recognized temporal pattern of contrast enhancement at CT and MRI using extracellular contrast agents. Because of neovascularization and increased reliance on hepatic arterial supply to feed tumor cells, HCC enhances in an earlier phase of the contrast bolus compared to background liver and contrast washes out more quickly. Imaging diagnosis based on contrast enhancement pattern has been shown to have per lesion sensitivity of 44–78% while maintaining near 100% specificity even for small nodules measuring between 1 and 2 cm [29–32], with even higher sensitivity for larger lesions [33]. Other morphologic and

histologic features provide imaging features that are less frequently seen but may increase specificity for HCC when present.

A multiphase CT examination for HCC must include adequate late arterial phase images (35–40 seconds post injection) for maximum accuracy. Images can quickly be assessed for proper arterial timing by checking for contrast in both the hepatic arteries and the portal vein, without the presence of hepatic vein opacification. Lack of contrast within the portal vein indicates that the timing is too early, and there may be arterial contrast that has not yet reached hepatocytes, while the presence of hepatic veins indicates that the timing is too late, which decreases tumor enhancement to background contrast. A feature strongly associated with HCC is non-rim arterial hyperenhancement. This enhancement should be unequivocally more dense or intense than background liver and, for maximum specificity, should appear mass like or be associated with other imaging features such as visibility on other contrast-enhanced phases, mild T2 hyperintensity, or diffusion restriction [8].

CT and MRI exams should also include portal venous phase (70–80 seconds post injection) and delayed phase (3–5 minutes post injection) images. Adequacy of portal venous phase images can be confirmed by the presence of contrast in portal veins, hepatic veins, and hepatic parenchymal enhancement. Non-rim washout is a feature of HCC that is defined as the visual decrease in density or intensity between an earlier and a later phase of contrast using extracellular agents. This decreased signal may involve the entire observation or part of the observation and can be seen on either portal venous or delayed phase images. Another imaging feature that is strongly associated with HCC but is seen less frequently than are non-rim arterial phase hyperenhancement or non-rim washout is an enhancing "capsule." This feature must be seen on a more delayed phase of contrast (portal venous or true delayed phase) and must be unequivocally more dense/intense or thicker than fibrotic capsules surrounding other nodules. Figure 1.7 shows an example of a lesion demonstrating arterial phase hyperenhancement, washout, and capsule appearance.

Size and specifically an increase in size on consecutive exams is also a characteristic of HCC. Size should be measured as the maximal diameter on the imaging phase in which the observation is most visible, and if possible not on arterial phase images because perilesional enhancement may result in an artifactual increase or decrease in size. A change in size of greater than 50% in less than 6 months is highly suspicious for HCC (Fig. 1.8).

Minor Features and Special Circumstances

In addition to enhancement pattern and lesion growth, there are several additional imaging features that may either suggest HCC, malignancy in general, or a benign alternative. Features favoring HCC include a non-enhancing "capsule," a nodule-in-nodule appearance, mosaic architecture, intralesional hemorrhage, or intralesional fat. Features suggesting malignancy but not specific for HCC include US visibility as a discrete nodule, slow interval growth, restricted diffusion, mild–moderate T2

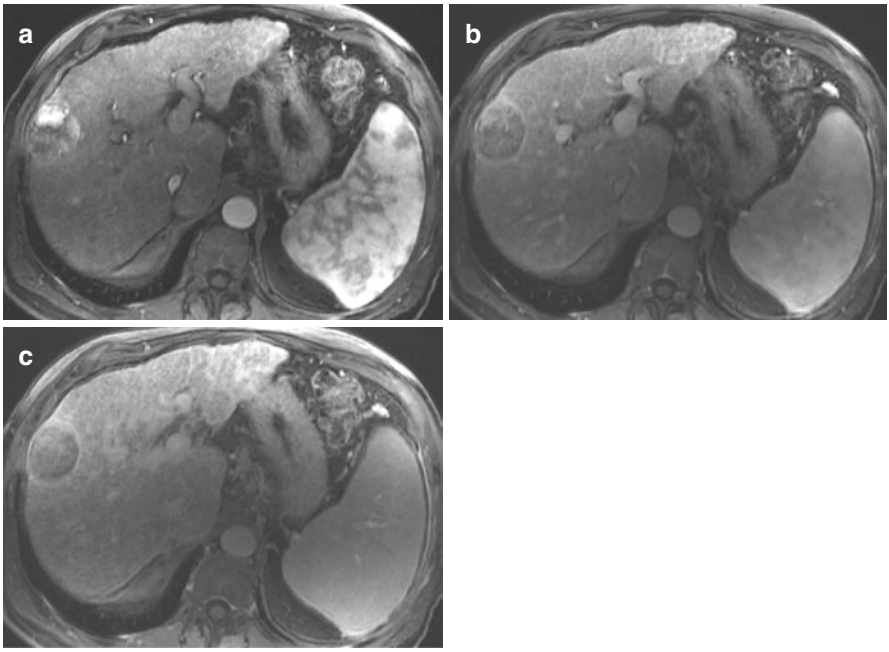

Fig. 1.7 A 69-year-old man with history of cirrhosis secondary to alcohol and steatohepatitis. MR of the liver using an extracellular contrast agent reveals a 5.1 cm lesion in the right hepatic lobe, which has arterial phase hyperenhancement (**a**), washout on both portal venous (**b**), and 5 minute delayed (**c**) phase images, as well as capsule appearance seen on portal venous and delayed phase images. Finding is compatible with a LI-RADS 5/OPTN class 5 lesion and therefore diagnostic of hepatocellular carcinoma

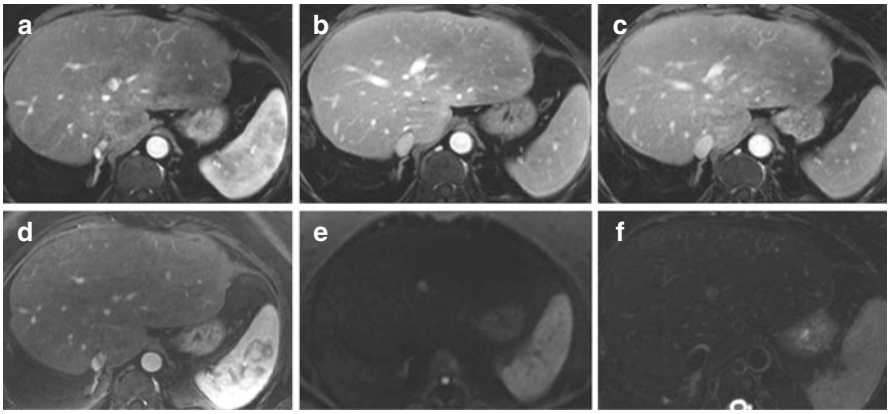

Fig. 1.8 A 53-year-old man with history of HCC status post resection. Multiphase MR images demonstrate an arterially hyperenhancing (**a**) lesion adjacent to the left portal vein, which persists in the portal venous (**b**) and 5 minute delayed phases (**c**). This lesion has restricted diffusion (**e**) and intermediate T2 signal (**f**). MR obtained 4 months prior shows that the lesion has nearly doubled in diameter (from 6 to 11 mm) in the interval (**d**). Given arterial hyperenhancement and threshold growth, this lesion is considered a LI-RADS 5 lesion

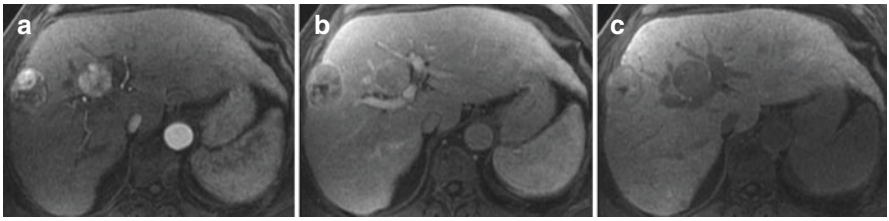

Fig. 1.9 A 68-year-old man with chronic hepatitis C and multiple hepatocellular carcinomas. MRI of the liver performed with a hepatobiliary contrast agent demonstrates two lesions in the right liver. Both lesions show arterial hyperenhancement (**a**), washout, and capsule appearance (**b**). The more lateral lesion shows moderate hepatobiliary contrast agent on 20-minute hepatobiliary phase images (**c**) while the more medial lesion shows no uptake. Both lesions also show a hepatobiliary phase hypointense rim (**c**). Based on imaging appearance, both lesions are LI-RADS 5/OPTN class 5 lesions

hyperintensity at MRI, corona enhancement, focal fatty sparing within a solid mass, focal iron sparing within a solid mass and transitional or hepatobiliary phase hypointensity when using hepatobiliary contrast agents. Features favoring benignity include size stability or reduction, contrast enhancement following blood pool, lack of vessel distortion, iron in mass greater than in liver, marked T2 hyperintensity, and isointensity on the hepatobiliary phase.

There is increased evidence that MRI hepatobiliary contrast agents such as gadoxetate disodium and gadobenate dimeglumine may be useful in the detection and characterization of HCC, providing an increase in per-lesion sensitivity over extracellular contrast-enhanced MRI of 6–15% [34–36]. In general, more poorly differentiated tumors will have decreased expression of the OATP transporter, which normally facilitates hepatobiliary contrast uptake, resulting in hypointensity of these lesions on hepatobiliary phase images. There is the potential for false negatives in lesions which remain well differentiated enough to have adequate OATP expression, and thereby remain hyperintense or isointense to background liver on hepatobiliary phase images (Fig. 1.9). Use of hepatobiliary agents is also limited in patients with severe hepatic dysfunction (total bilirubin >3 mg/dL) due to decreased hepatic uptake of contrast. Further work will be required to identify the most appropriate role for these agents in the evaluation of HCC.

Nuclear Medicine (PET, Scintigraphy)

Currently, the role of positron emission tomography (PET) and single photon emission computed tomography (SPECT) in the evaluation of HCC is limited. 18F-fludeoxyglucose (FDG) is the most commonly used tracer for whole-body PET/CT and is a marker of cellular metabolism. Prior studies have shown that sensitivity using FDG PET/CT is limited with only 50–70% of HCC having FDG uptake beyond background liver [37]. In general, more poorly differentiated HCCs have a greater degree of FDG uptake and are more likely to metastasize; therefore,

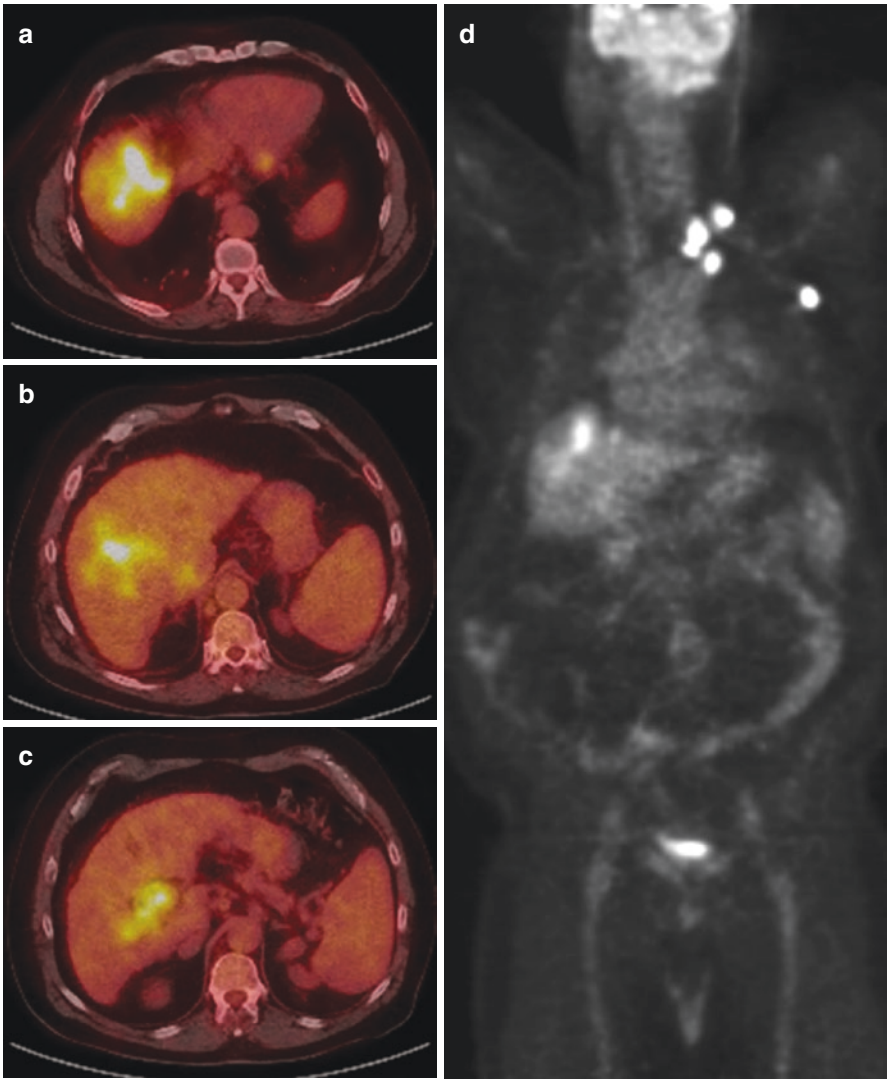

Fig. 1.10 A 66-year-old man with history of hepatitis C found to have a hepatic mass on ultrasound. Biopsy proved hepatocellular carcinoma. Fused FDG PET/CT images (**a**–**c**) show an FDG avid mass in the dome of the liver with extension of abnormal FDG uptake into the portal vein. Coronal PET image (**d**) shows metastatic left supraclavicular and axillary lymphadenopathy, which is also FDG avid

there may be a role for PET/CT in the detection of metastatic disease [38] or in the prognostication of patients at risk for advanced disease [39]. An example of FDG avid metastatic disease is shown in Fig. 1.10.

No reliable SPECT tracer for the detection of HCC exists, but Tc-99 m macroaggregated albumin (MAA) scans are used prior to treatment with Y-90

radioembolization to determine lung shunt fraction and to confirm tumor arterial supply. Bremsstrahlung scanning can be performed immediately after treatment with Y-90 to confirm in-tumor deposition of radioactive particles and absence of nontarget embolization.

Catheter Angiography

Infrequently used for the de novo diagnosis of HCC, catheter angiography typically takes place as a part of catheter-directed therapies including bland embolization, chemoembolization, and radioembolization. Angiographic evaluation of HCC is useful to determine the presence of arterial blood supply to the tumor, the location of the lesion, and whether applied treatment has successfully altered the arterial blood supply to the tumor. Cone-beam CT, which can be performed during catheter-based procedures and allows for 3D reconstruction and display of angiographic images (Fig. 1.11), has been shown to further improve diagnosis and treatment in many HCC lesions [40, 41].

Posttreatment Follow-Up

Imaging following therapy for HCC has an evolving base of knowledge. Given that the range of available treatments includes transarterial embolic, percutaneous chemical and thermal ablation, external beam radiation, and surgical resection, the scope of appearances of treated lesions is broad. In general, treated lesions should no longer demonstrate the suspicious features of HCC, including arterial

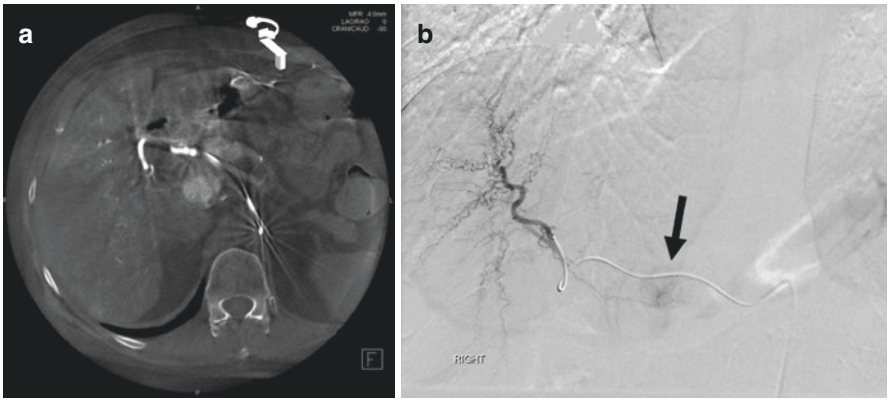

Fig. 1.11 A 63-year-old woman with cirrhosis secondary to nonalcoholic fatty liver disease. Hepatic angiogram (**a**) and cone-beam CT performed during a transarterial chemoembolization procedure (**b**) show an avidly enhancing tumor in the caudate lobe

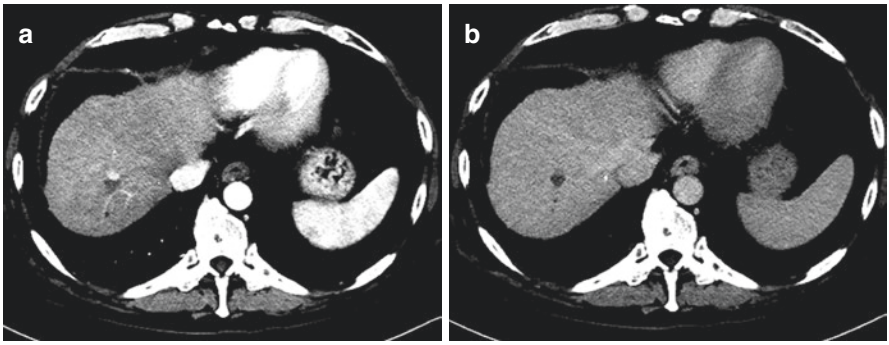

Fig. 1.12 A 61-year-old man with cirrhosis due to nonalcoholic fatty liver disease complicated by multifocal hepatocellular carcinoma. The patient underwent bland embolization to a tumor in the hepatic dome, but follow-up multiphase CT approximately 9 weeks later shows a nodule of residual arterial hyperenhancement (**a**) with washout on delayed phase images (**b**), suggesting residual viable disease

hyperenhancement, washout, or capsule appearance, nor should they enlarge significantly over time. Other features such as low-level progressive enhancement or slow enlargement may represent benign scar tissue or resolving necrosis at the site of treatment. Unfortunately, current imaging techniques are limited in the detection of small areas of viable tumor [42], and therefore any suspicious feature should be examined and followed very carefully (Fig. 1.12).

Imaging Scoring Systems (LI-RADS, OPTN)

The Liver Imaging Reporting and Data System (LI-RADS) is a system created by a multidisciplinary group of diagnostic and interventional radiologists, surgeons, hepatologists, and hepatopathologists and is intended to provide a comprehensive system for standardizing technique, interpretation, and reporting of liver imaging in order to improve communication, research, and ultimately patient care [8].

LI-RADS is a dynamic document that offers guidance for the evaluation of the liver at ultrasound surveillance, contrast-enhanced ultrasound and CT/MRI, as well as for the evaluation of treatment effects. Details of observation categorization and specifics of scoring are beyond the scope of this chapter, but up-to-date instructions may be found at the cited website. LI-RADS major and ancillary imaging features of HCC are listed in Table 1.3. LI-RADS categories range from 1 to 5 with increasing score increasing confidence in HCC and a LI-RADS 5 lesion having very high specificity for HCC.

Another important system for the evaluation of HCC are the Organ Procurement and Transplantation Network (OPTN)/United Network for Organ Sharing (UNOS)

Table 1.3 LI-RADS v2018 major and ancillary imaging features of HCC

Major features	Ancillary features
Determine primary categorization	*Allow adjustment of category after determining major features*
Used with lesion size to diagnose HCC	**Favoring malignancy**
Arterial phase hyperenhancement	US visibility as discrete nodule
Non-peripheral washout	Subthreshold growth
Enhancing capsule	Restricted diffusion
Threshold growth	Mild–moderate T2 hyperintensity
	Corona enhancement
	Fat sparing in solid mass
	Iron sparing in solid mass
	Transitional phase hypointensity
	Hepatobiliary phase hypointensity
	Favoring HCC in particular
	Non-enhancing capsule
	Nodule-in-nodule
	Mosaic architecture
	Blood products in mass
	Fat in mass, greater than adjacent liver

guidelines. The goal of this classification system is to recognize patients who would benefit from liver transplantation as a treatment for HCC in the absence of severe liver dysfunction, and thus grant them priority for allocation of deceased donor liver allografts. Because of the scarcity of donor livers, and lack of histologic confirmation in many cases, a high specificity for HCC is required in order to grant a patient MELD exception points. There is general agreement between the LI-RADS and the OPTN systems for the characteristics which are diagnostic of HCC (LI-RADS 5/OPTN class 5). The precise definitions of the UNOS/OPTN policy are again beyond the scope of this chapter, but are available for review in their most recently revised and published form [43]. In brief, for a nodule that is between 2 and 5 cm to be class 5, it must be hyperenhancing on arterial phase imaging and have washout or a pseudocapsule on delayed phase. Class 5 lesions between 1 and 2 cm are more stringently defined and require hyperenhancement on arterial phase imaging plus washout and a pseudocapsule. Hypervascular lesions which do not have washout or pseudocapsule must then meet specific interval growth criteria to be considered class 5. Biopsy may be considered for lesions that are highly suspicious but do not meet the OPTN class 5 requirements. For patients for whom transplantation may be an option, it is essential to establish the diagnosis of HCC before treating with liver-directed therapy.

Imaging for Liver Fibrosis, Cirrhosis, and Portal Hypertension

An important subclassification that needs to be made early in the evaluation of patients with suspected HCC is the distinction between those with and those without significant liver fibrosis or cirrhosis. Depending on the region of the world and the underlying etiology of liver disease, between 50% and 90% of patients with HCC will have underlying cirrhosis. These patients have two liver diseases, first the underlying etiologic cause of cirrhosis, which is most commonly chronic hepatitis B or C, alcoholic liver disease, or nonalcoholic fatty liver disease, and second, the growing hepatocellular carcinoma, which, if left unchecked, will replace the benign liver tissue and lead to liver failure.

Ultrasound, CT, and MRI Features of Cirrhosis

Liver cirrhosis is associated with the development of a number of characteristic imaging features, including nodularity of the liver, which may be micronodular or macronodular. Liver nodularity may be appreciated on ultrasound or cross-sectional CT or MRI studies as an irregular nodular outline of the liver, coarse echogenicity on ultrasound, or nodular heterogeneity on CT or MRI. Cirrhosis also leads to features of portal hypertension that are visible on imaging, including splenomegaly, patency of the umbilical vein, or the presence of paraumbilical varices, also termed the caput medusa, and upper abdominal or paraesophageal varices. Cirrhosis is also associated with a prothrombotic tendency that may lead to the development of portal vein thrombosis and with decreased liver synthetic function leading to hypoalbuminemia, and in conjunction with increased portal pressure due to increased fibrosis and stiffness of the liver, to the development of ascites.

Noninvasive Assessment of Liver Fibrosis

A number of radiologic techniques have been developed for the assessment of the degree of liver stiffness; these include transient elastography (Fibroscan), ultrasound-based real-time tissue elastography or shear wave elastography, acoustic radiation force impulse imaging, and MR elastography. In those patients found to have underlying liver cirrhosis, the initial step in the treatment plan should be the evaluation and management of any of the sequelae of cirrhosis with portal hypertension, including ascites, esophageal or gastric varices, and hepatic encephalopathy. If not addressed, these sequelae will usually have a detrimental effect on the patient's performance status, often leading to the patient being considered ineligible for therapies that might otherwise be considered optimal.

Radiologic Assessment of Clinically Significant Portal Hypertension

Once the presence or absence of significant fibrosis or cirrhosis has been elucidated and any complications addressed, the next step in the determination of optimal therapy for HCC patients is making the distinction between those who have no cirrhosis and therefore have satisfactory liver synthetic function and the absence of clinically significant portal hypertension—typically defined clinically as patients with normal bilirubin, a platelet count above 120,000, and no varices - versus those with clinically significant portal hypertension, who are at risk for complications after surgical resection or interventions that result in significant decline in already tenuous liver function.

The hepatic venous pressure gradient (HVPG), which is the difference between the wedged (WHVP) and the free hepatic venous pressures, represents the gradient between pressures in the portal vein and the intra-abdominal portion of the inferior vena cava. The HVPG is measured angiographically, usually via a transjugular approach. Where the HVPG is routinely measured, patients with significant portal hypertension have gradients of 10 mmHg or greater. In centers where the Model for End-stage Liver Disease (MELD) score is routinely used, a MELD score of 9 or more has been shown to be associated with a higher risk of hepatic decompensation after surgical resection [44].

Surgical Treatments for Hepatocellular Carcinoma

Patients with a single HCC and a normal serum bilirubin and without clinically significant portal hypertension are usually candidates for consideration of surgical resection with curative intent regardless of the size of the primary tumor. In some patients for whom the remnant liver that would remain after surgical resection is felt to be marginal, portal vein embolization of the affected segment or lobe of the liver can be performed by angiographic techniques. This usually leads to compensatory hypertrophy of the unaffected liver over a 4- to 6-week period and can allow successful resection with a reduced risk of liver failure.

For patients with early stage HCC who have clinically significant portal hypertension and an elevated bilirubin, the most effective treatment currently available is liver transplantation, which has the advantage of removing the malignant tumor and also replacing the cirrhotic liver. The primary barrier to transplantation is the extreme shortage of available liver allografts. In addition, following transplant, patients need to be maintained on lifelong immunosuppression, which is associated with important side effects such as renal insufficiency and an increased risk of infection. While initially patients transplanted with HCC had dismal outcomes because of the high risk of recurrent disease, it was later established that patients with limited HCC disease or with relatively unaggressive, less invasive, and metastatic

features have excellent posttransplant survival and are appropriate candidates for liver transplantation. These were initially codified as the Milan criteria, including patients with a single lesion no more than 5 cm in size or with two or three lesions, each no more than 3 cm in size [45]. Typically, these are patients with a serum alpha fetoprotein (AFP) less than 500 ng/mL. Limited expansion of these criteria is allowed in patients who have favorable biology as demonstrated by response to locoregional or other treatments resulting in downstaging of the tumor to a size and number within the Milan criteria. The most popular extension of the Milan criteria are the University of California San Francisco (UCSF) criteria, which allow transplantation of patients with a solitary tumor smaller than 6.5 cm, or patients having three or fewer nodules, with the largest lesion being smaller than 4.5 cm or having a total tumor diameter less than 8.5 cm without vascular invasion [46].

Nonsurgical Treatment Algorithm for Hepatocellular Carcinoma, Including Radiological Methods

Patients with HCC who are not candidates for surgery and have 1–3 tumors, with the largest being no more than 3 cm in size, have been shown to have excellent results from treatment with local ablation techniques such as radiofrequency ablation or microwave ablation. Local ablation techniques that are less commonly used include irreversible electroporation, laser ablation, and percutaneous ethanol injection. Cryotherapy can be used in specific circumstances when there is a need for high-definition delineation of the extent of therapy such as in the treatment of pelvic metastases where the ability of CT/MRI to visualize the extent of the ice ball facilitates avoidance of injury to the pudendal nerves and other nerve roots.

Patients who are not candidates for treatment with curative intent using surgical resection, ablation, or liver transplantation are currently considered next for locoregional treatment with TACE.

Local Ablation

Local ablation methods typically use heat, cold, or chemical methods to induce necrosis or apoptosis of HCC nodules. The most commonly used methods are radiofrequency ablation and microwave ablation [47, 48]. Both techniques heat the tissue surrounding probes that are placed into the tumor nodule, resulting in coagulative necrosis of the tissue [49]. Microwave ablation is generally more popular than radiofrequency ablation where both are available, due to its similar effectiveness with shorter treatment times [50]. Both techniques rely on US- or CT-guided imaging for placement of the treatment probes, which can be performed percutaneously or surgically. The main contraindication for the use of heat-based ablation methods

is proximity of the tumor nodules to large blood vessels, which act as heat sinks and prevent the achievement of sufficiently high temperatures to effectively destroy the tumor tissue. Microwave ablation may be less susceptible to the heat sink effect than radiofrequency ablation [51]. When necessary, percutaneous ethanol injection can be used close to large vessels to supplement the effects of the heat-based ablative methods. Additional, less commonly used ablation methods include laser ablation, which can be applied with MR imaging, and irreversible electroporation.

Locoregional Transarterial Chemoembolization and Radioembolization

Locoregional treatment of HCC using catheter-based approaches has been in use since the late 1970s and early 1980s. The rationale for the technique is based on the observation that 95% or more of the vascular supply to HCCs is derived from the hepatic arterial branches. Consequently, delivery of absorbable gelatin sponge (Gelfoam) or nonabsorbable polyvinyl alcohol (Ivalon) beads was used to occlude the tumor vasculature, with initial positive results encouraging further development of the technique. The results of transarterial bland embolization (TAE) for HCC were first reported from Japan in 1983, followed by results of transarterial chemoembolization (TACE) using the anticancer agents mitomycin C or adriamycin suspended in Lipiodol in 1985. After a number of equivocal studies, two clinical trials completed in 2002 established the superiority of TACE over best supportive care in patients with intermediate stage HCC, and it subsequently became regarded as the standard of care [4, 5]. The use of TACE has been plagued by a lack of standardization of the techniques and chemotherapy agents used, leading to difficulty in determining the underlying reasons for variable results seen in different studies. More recently, attempts to standardize the administration of TACE have included the use of drug-eluting beads loaded with chemotherapy agents, typically doxorubicin/Adriamycin for HCC or irinotecan for colorectal cancer liver metastases. Increasing evidence suggests that TAE may achieve the same outcomes as TACE in patients with HCC [52, 53].

Transarterial radioembolization (TARE) is a modification of TACE in which glass (TheraSphere) or resin (SIR-Sphere) microspheres bearing Y-90 are infused into the hepatic artery branches supplying HCC nodules in a segment or segments of the liver. Y-90 microspheres are pure beta particle emitters, producing radiation with a mean human tissue penetrance of 2.4 mm and a half-life of 64.2 hours. Because of the limited depth of penetration and short half-life, Y-90 microspheres can be administered on an outpatient basis, and patients do not require special radiation shielding precautions after treatment [54].

TARE has been applied in a number of different circumstances for treatment of HCC. It can be used for “radiation segmentectomy,” in which relatively small regions of the liver are selectively catheterized and treated with very high radiation

doses per unit volume, resulting in complete radiation necrosis of the treated area. This approach can be used in patients with early stage disease, who are not candidates for surgical resection or for whom ablation is contraindicated or not considered an optimal treatment modality. TARE can also be used in place of portal vein embolization. Finally, TARE can be used in place of TACE for patients with intermediate stage disease, or instead of sorafenib or lenvatinib in patients with advanced stage HCC. For these latter indications, TARE has been shown to be capable of downstaging intermediate stage tumors to within criteria for liver transplantation and, in general, appears to be more effective than TACE in inducing tumor regression; however, the higher effectiveness in inducing tissue injury can also put patients at risk for either early or delayed radiation-induced liver injury [55–57]. It is therefore important to carefully assess liver remnant size and function when all but very limited regions of the liver will be treated with TARE.

External Beam Radiotherapy

External beam radiotherapy (EBRT) has been used for several decades for the treatment of HCC. It has long been recognized that the liver is a relatively radiosensitive organ, with whole liver doses of 30 Gy or higher associated with a high risk of radiation-induced liver disease (RILD), a syndrome characterized by anicteric hepatomegaly and ascites, followed by progressive liver failure and death [58]. In the 1970–1980s, the Radiation Therapy Oncology Group (RTOG) conducted several prospective clinical trials (RTOG trials 79-28, 83-01, 83-19, and 88-23) in the United States assessing the safety and efficacy of moderate dose (21–24 Gray) whole liver EBRT with concurrent radiosensitizing systemic chemotherapy for unresectable HCC. Results were not very promising; partial tumor response (>30% reduction) was seen in 22% of patients, and median survival was approximately 6 months [59]. Further attempts to intensify therapy using accelerated hyperfractionated radiotherapy, intra-arterial chemotherapy, and radioimmunotherapy were also unsuccessful. Therefore, EBRT was largely abandoned as a primary treatment for HCC in the United States, with use confined to palliation of local symptoms from metastatic disease.

Significant advances in diagnostic imaging and radiotherapy planning and delivery techniques have sparked renewed interest in the use of EBRT for HCC. Proton beam radiotherapy (PBT) and stereotactic body radiotherapy (SBRT) are advanced EBRT techniques, which allow delivery of high doses of focal radiation with relative sparing of surrounding normal tissues (Fig. 1.13). Furthermore, there is now better recognition of factors associated with increased risk of hepatotoxicity after partial liver radiotherapy, including severity of baseline liver dysfunction and radiotherapy dose-volume parameters for uninvolved liver [58]. Several retrospective and single-arm prospective studies have demonstrated promising safety and efficacy of PBT and SBRT for select patients with nonmetastatic HCC. A recent systematic

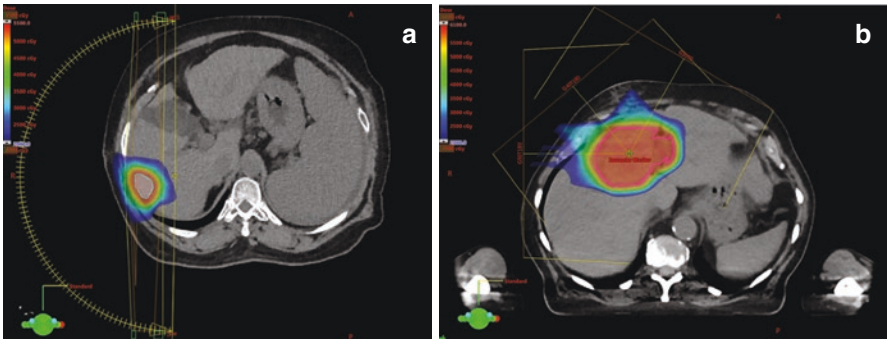

Fig. 1.13 (**a**) A patient with a 3 cm solitary hepatocellular carcinoma (blue outline) treated with stereotactic body radiotherapy (50 Gy in 5 fractions over 1 week) as "bridge to transplantation" therapy, following progression after previous hepatic arterial embolization. The blue indicates the volume receiving 20 Gy or higher, and the red indicates the volume receiving 50 Gy or higher. (**b**) A patient with a 7 cm hepatocellular carcinoma (pink outline) with contiguous left portal vein tumor thrombus treated with proton beam radiotherapy (58.05 Gy in 15 fractions over 3 weeks) as definitive therapy. The blue indicates the volume receiving 20 Gy or higher, and the red indicates the volume receiving 50 Gy or higher

review and meta-analysis found that PBT and SBRT were associated with greater efficacy and reduced toxicity compared to conventional radiotherapy techniques [60]. Ongoing studies will further define the role of EBRT for patients with localized HCC.

Systemic Therapy

For much of the early experience with systemic therapy for cancer, HCC was found not to be effectively treatable with chemotherapy. In particular, patients with cirrhosis often had cytopenias due to portal hypertension and splenomegaly that were exacerbated by treatment with cytotoxic chemotherapy, making them prone to chemotherapy-induced toxicity. In 2007, the first positive clinical trials of targeted therapy using the multikinase inhibitor sorafenib for patients with advanced HCC were reported. Sorafenib was shown to improve the median survival of patients with advanced HCC by 2–3 months [61, 62]. After an approximately 10-year period in which there was no progress in identifying new systemic treatments that significantly improve survival of patients with advanced HCC, several new therapies were approved in 2017 and 2018. Regorafenib was approved for HCC in the second line after progression or intolerance of sorafenib, followed by approval of the anti-PD-1 immune checkpoint inhibitor nivolumab following evidence from Phase I/II studies that nivolumab achieves a 15–20% response rate in advanced HCC. Subsequently, the multikinase inhibitor lenvatinib, an inhibitor

of VEGF receptors 1–3, FGF receptors 1-4, PDGF receptor α, RET, and KIT, was approved for use in the first line after a Phase III study showed non-inferiority to sorafenib in the first line [63–65]. Finally, the anti-PD-1 immune checkpoint inhibitor pembrolizumab was also approved for second-line treatment of HCC in late 2018 [66]. In 2018, two additional Phase III studies of cabozantinib, an inhibitor of MET, vascular endothelial growth factor receptor (VEGFR), and AXL for patients with advanced HCC progressing on sorafenib, and ramucirumab, an anti-VEGF antibody for HCC patients with high AFP levels ≥400 ng/mL, were reported as positive [67, 68]. On the basis of these results, the European Commission approved cabozantinib for treatment of advanced HCC in the second line after sorafenib in late 2018, and it was approved by the US FDA in January 2019. Ramucirumab was also approved for second-line treatment of patients with AFP ≥400 ng/mL, who have been previously treated with sorafenib in May 2019. Early results of combination treatment with immune checkpoint inhibitors and antiangiogenic agents were promising. In late 2018, combination therapy with the PD-L1 inhibitor atezolizumab and the VEGF inhibitor bevacizumab showed promising and durable antitumor activity in a phase Ib study of patients with advanced HCC, with an objective response rate of greater than 30% [69]. The results of the phase III trial comparing combination atezolizumab and bevacizumab to sorafenib in first-line treatment of HCC were reported in November 2019, showing clear superiority of the combination over sorafenib. The combination was approved by the US FDA for treatment of patients with unresectable or metastatic HCC who have not received prior systemic therapy in May 2020 [70]. After years of relative inaction, we are therefore now in a very exciting phase of development of effective systemic therapy for HCC.

Once patients are started on systemic therapy for HCC, close follow-up by cross-sectional imaging is warranted, typically every 3–4 months, in order to assess response to treatment and to identify progressive disease at the earliest possible stage, given the increased number of treatments now available in the first and second line, which can also potentially be administered in subsequent lines of treatment. The availability of additional therapeutic options is also stimulating the need for molecular and genetic analysis of biopsy tissue obtained from patients with intermediate and advanced stage HCC, with the goal of identifying the molecular characteristics that determine response of specific subgroups of HCCs to particular therapies. This trend toward routine biopsy of HCCs is further supported by evidence from large molecular and genetic profiling studies such as the Cancer Genome Atlas Project (TCGA) for HCC that showed that approximately 8% of HCCs that were phenotypically HCC by H&E staining had gene expression patterns typical of cholangiocarcinomas [71]. About 25% of these cholangiocarcinoma-like tumors also carried mutations in the isocitrate dehydrogenase 1 and 2 genes that are characteristic of intrahepatic cholangiocarcinomas.

To complement and potentially extend these predictive strategies, novel efforts are underway in the new field of imaging radiogenomics, using machine learning and artificial intelligence techniques to identify genomic subclasses of HCCs. These efforts represent an exciting new frontier in the use of imaging for determining the optimal systemic treatment for HCC.

References

1. Bray F, Ferlay J, Soerjomataram I, Siegel RL, Torre LA, Jemal A. Global cancer statistics 2018: GLOBOCAN estimates of incidence and mortality worldwide for 36 cancers in 185 countries. CA Cancer J Clin. 2018;68(6):394–424.
2. Fitzmaurice C, Akinyemiju TF, Al Lami FH, Alam T, Alizadeh-Navaei R, Allen C, et al. Global, regional, and national cancer incidence, mortality, years of life lost, years lived with disability, and disability-adjusted life-years for 29 cancer groups, 1990 to 2016: a systematic analysis for the global burden of disease study. JAMA Oncol. 2018;4(11):1553–68.
3. Dhanasekaran R, Nault JC, Roberts LR, Zucman-Rossi J. Genomic medicine and implications for hepatocellular carcinoma prevention and therapy. Gastroenterology. 2019;156(2):492–509.
4. Llovet JM, Real MI, Montana X, Planas R, Coll S, Aponte J, et al. Arterial embolisation or chemoembolisation versus symptomatic treatment in patients with unresectable hepatocellular carcinoma: a randomised controlled trial. Lancet (London, England). 2002;359(9319):1734–9.
5. Lo CM, Ngan H, Tso WK, Liu CL, Lam CM, Poon RT, et al. Randomized controlled trial of transarterial lipiodol chemoembolization for unresectable hepatocellular carcinoma. Hepatology (Baltimore, Md). 2002;35(5):1164–71.
6. Salem R, Gordon AC, Mouli S, Hickey R, Kallini J, Gabr A, et al. Y90 radioembolization significantly prolongs time to progression compared with chemoembolization in patients with hepatocellular carcinoma. Gastroenterology. 2016;151(6):1155–63.e2.
7. Lencioni R, Llovet JM. Modified RECIST (mRECIST) assessment for hepatocellular carcinoma. Semin Liver Dis. 2010;30(1):52–60.
8. American College of Radiology. Liver Imaging Reporting and Data System (LI-RADS). https://www.acr.org/Clinical-Resources/Reporting-and-Data-Systems/LI-RADS.
9. Benckert C, Jonas S, Thelen A, Spinelli A, Schumacher G, Heise M, et al. Liver transplantation for hepatocellular carcinoma in cirrhosis: prognostic parameters. Transplant Proc. 2005;37(4):1693–4.
10. Zhou L, Rui JA, Wang SB, Chen SG, Qu Q, Chi TY, et al. Factors predictive for long-term survival of male patients with hepatocellular carcinoma after curative resection. J Surg Oncol. 2007;95(4):298–303.
11. Lang H, Sotiropoulos GC, Brokalaki EI, Schmitz KJ, Bertona C, Meyer G, et al. Survival and recurrence rates after resection for hepatocellular carcinoma in noncirrhotic livers. J Am Coll Surg. 2007;205(1):27–36.
12. Jonas S, Bechstein WO, Steinmuller T, Herrmann M, Radke C, Berg T, et al. Vascular invasion and histopathologic grading determine outcome after liver transplantation for hepatocellular carcinoma in cirrhosis. Hepatology (Baltimore, Md). 2001;33(5):1080–6.
13. Wood LD, Heaphy CM, Daniel HD, Naini BV, Lassman CR, Arroyo MR, et al. Chromophobe hepatocellular carcinoma with abrupt anaplasia: a proposal for a new subtype of hepatocellular carcinoma with unique morphological and molecular features. Modern Pathol. 2013;26(12):1586–93.
14. Rodriguez-Peralvarez M, Luong TV, Andreana L, Meyer T, Dhillon AP, Burroughs AK. A systematic review of microvascular invasion in hepatocellular carcinoma: diagnostic and prognostic variability. Ann Surg Oncol. 2013;20(1):325–39.
15. Ohashi M, Wakai T, Korita PV, Ajioka Y, Shirai Y, Hatakeyama K. Histological evaluation of intracapsular venous invasion for discrimination between portal and hepatic venous invasion in hepatocellular carcinoma. J Gastroenterol Hepatol. 2010;25(1):143–9.
16. Koike Y, Shiratori Y, Sato S, Obi S, Teratani T, Imamura M, et al. Risk factors for recurring hepatocellular carcinoma differ according to infected hepatitis virus-an analysis of 236 consecutive patients with a single lesion. Hepatology (Baltimore, Md). 2000;32(6):1216–23.

17. Bruix J, Sherman M. Management of hepatocellular carcinoma: an update. Hepatology (Baltimore, Md). 2011;53(3):1020–2.
18. Llovet JM, Ducreux M, Lencioni R, Di Bisceglie A, Galle P, Dufour J. European Association for the Study of the Liver European Organisation for Research and Treatment of Cancer: EASL-EORTC clinical practice guidelines: management of hepatocellular carcinoma. J Hepatol. 2012;56(4):908–43.
19. Kudo M, Izumi N, Kokudo N, Matsui O, Sakamoto M, Nakashima O, et al. Management of hepatocellular carcinoma in Japan: Consensus-Based Clinical Practice Guidelines proposed by the Japan Society of Hepatology (JSH) 2010 updated version. Dig Dis. 2011;29(3):339–64.
20. Omata M, Lesmana LA, Tateishi R, Chen P-J, Lin S-M, Yoshida H, et al. Asian Pacific Association for the Study of the Liver consensus recommendations on hepatocellular carcinoma. Hepatol Int. 2010;4(2):439–74.
21. Jiancheng Z, Xingshun Q, Xiaozhong G. 2014 Korean Liver Cancer Study Group-National Cancer Center Korea practice guideline for the management of hepatocellular carcinoma&58; an excerpt of recommendations. Linchuang Gandanbing Zazhi. 2015;31(7):1031–3.
22. Bolondi L. Screening for hepatocellular carcinoma in cirrhosis. J Hepatol. 2003;39(6): 1076–84.
23. Gambarin-Gelwan M, Wolf DC, Shapiro R, Schwartz ME, Min AD. Sensitivity of commonly available screening tests in detecting hepatocellular carcinoma in cirrhotic patients undergoing liver transplantation. Am J Gastroenterol. 2000;95(6):1535–8.
24. Kim CK, Lim JH, Lee WJ. Detection of hepatocellular carcinomas and dysplastic nodules in cirrhotic liver: accuracy of ultrasonography in transplant patients. J Ultrasound Med. 2001;20(2):99–104.
25. Tzartzeva K, Obi J, Rich NE, Parikh ND, Marrero JA, Yopp A, et al. Surveillance imaging and alpha fetoprotein for early detection of hepatocellular carcinoma in patients with cirrhosis: a meta-analysis. Gastroenterology. 2018;154(6):1706–18.e1.
26. Morgan TA, Maturen KE, Dahiya N, Sun MR, Kamaya A. US LI-RADS: ultrasound liver imaging reporting and data system for screening and surveillance of hepatocellular carcinoma. Abdom Radiol. 2018;43(1):41–55.
27. Piscaglia F, Wilson SR, Lyshchik A, Cosgrove D, Dietrich CF, Jang H-J, et al. American College of Radiology Contrast Enhanced Ultrasound Liver Imaging Reporting and Data System (CEUS LI-RADS) for the diagnosis of Hepatocellular Carcinoma: a pictorial essay. Ultraschall in der Medizin (Stuttgart, Germany: 1980). 2017;38(3):320.
28. Schellhaas B, Görtz RS, Pfeifer L, Kielisch C, Neurath MF, Strobel D. Diagnostic accuracy of contrast-enhanced ultrasound for the differential diagnosis of hepatocellular carcinoma: ESCULAP versus CEUS-LI-RADS. Eur J Gastroenterol Hepatol. 2017;29(9):1036–44.
29. Forner A, Vilana R, Ayuso C, Bianchi L, Sole M, Ayuso JR, et al. Diagnosis of hepatic nodules 20 mm or smaller in cirrhosis: prospective validation of the noninvasive diagnostic criteria for hepatocellular carcinoma. Hepatology (Baltimore, Md). 2008;47(1):97–104.
30. Khalili K, Kim TK, Jang HJ, Haider MA, Khan L, Guindi M, et al. Optimization of imaging diagnosis of 1-2 cm hepatocellular carcinoma: an analysis of diagnostic performance and resource utilization. J Hepatol. 2011;54(4):723–8.
31. Kierans AS, Kang SK, Rosenkrantz AB. The diagnostic performance of dynamic contrast-enhanced MR imaging for detection of small hepatocellular carcinoma measuring up to 2 cm: a meta-analysis. Radiology. 2015;278(1):82–94.
32. Sangiovanni A, Manini MA, Iavarone M, Romeo R, Forzenigo LV, Fraquelli M, et al. The diagnostic and economic impact of contrast imaging techniques in the diagnosis of small hepatocellular carcinoma in cirrhosis. Gut. 2010;59(5):638–44.
33. Lee YJ, Lee JM, Lee JS, Lee HY, Park BH, Kim YH, et al. Hepatocellular carcinoma: diagnostic performance of multidetector CT and MR imaging—a systematic review and meta-analysis. Radiology. 2015;275(1):97–109.
34. Ahn SS, Kim M-J, Lim JS, Hong H-S, Chung YE, Choi J-Y. Added value of gadoxetic acid–enhanced hepatobiliary phase MR imaging in the diagnosis of hepatocellular carcinoma. Radiology. 2010;255(2):459–66.

35. Golfieri R, Renzulli M, Lucidi V, Corcioni B, Trevisani F, Bolondi L. Contribution of the hepatobiliary phase of Gd-EOB-DTPA-enhanced MRI to Dynamic MRI in the detection of hypovascular small (≤2cm) HCC in cirrhosis. Eur Radiol. 2011;21(6):1233–42.
36. Haradome H, Grazioli L, Tinti R, Morone M, Motosugi U, Sano K, et al. Additional value of gadoxetic acid-DTPA-enhanced hepatobiliary phase MR imaging in the diagnosis of early-stage hepatocellular carcinoma: comparison with dynamic triple-phase multidetector CT imaging. J Magn Reson Imaging. 2011;34(1):69–78.
37. Kim MJ, Kim YS, Cho YH, Jang HY, Song JY, Lee SH, et al. Use of (18)F-FDG PET to predict tumor progression and survival in patients with intermediate hepatocellular carcinoma treated by transarterial chemoembolization. Korean J Intern Med. 2015;30(3):308–15.
38. Murakami K. FDG-PET for hepatobiliary and pancreatic cancer: advances and current limitations. World J Clin Oncol. 2011;2(5):229–36.
39. Seo S, Hatano E, Higashi T, Hara T, Tada M, Tamaki N, et al. Fluorine-18 fluorodeoxyglucose positron emission tomography predicts tumor differentiation, P-glycoprotein expression, and outcome after resection in hepatocellular carcinoma. Clin Cancer Res. 2007;13(2 Pt 1):427–33.
40. Iwazawa J, Ohue S, Hashimoto N, Muramoto O, Mitani T. Survival after C-arm CT-assisted chemoembolization of unresectable hepatocellular carcinoma. Eur J Radiol. 2012;81(12): 3985–92.
41. Kakeda S, Korogi Y, Ohnari N, Moriya J, Oda N, Nishino K, et al. Usefulness of cone-beam volume CT with flat panel detectors in conjunction with catheter angiography for transcatheter arterial embolization. J Vasc Interv Radiol. 2007;18(12):1508–16.
42. Ehman EC, Umetsu SE, Ohliger MA, Fidelman N, Ferrell LD, Yeh BM, et al. Imaging prediction of residual hepatocellular carcinoma after locoregional therapy in patients undergoing liver transplantation or partial hepatectomy. Abdom Radiol (New York). 2016;41(11): 2161–8.
43. Wald C, Russo MW, Heimbach JK, Hussain HK, Pomfret EA, Bruix J. New OPTN/UNOS policy for liver transplant allocation: standardization of liver imaging, diagnosis, classification, and reporting of hepatocellular carcinoma. Radiology. 2013;266(2):376–82.
44. Teh SH, Christein J, Donohue J, Que F, Kendrick M, Farnell M, et al. Hepatic resection of hepatocellular carcinoma in patients with cirrhosis: Model of End-Stage Liver Disease (MELD) score predicts perioperative mortality. J Gastroint Surg. 2005;9(9):1207–15; discussion 15
45. Mazzaferro V, Regalia E, Doci R, Andreola S, Pulvirenti A, Bozzetti F, et al. Liver transplantation for the treatment of small hepatocellular carcinomas in patients with cirrhosis. N Engl J Med. 1996;334(11):693–9.
46. Yao FY, Ferrell L, Bass NM, Watson JJ, Bacchetti P, Venook A, et al. Liver transplantation for hepatocellular carcinoma: expansion of the tumor size limits does not adversely impact survival. Hepatology (Baltimore, Md). 2001;33(6):1394–403.
47. Livraghi T, Meloni F, Di Stasi M, Rolle E, Solbiati L, Tinelli C, et al. Sustained complete response and complications rates after radiofrequency ablation of very early hepatocellular carcinoma in cirrhosis: is resection still the treatment of choice? Hepatology (Baltimore, Md). 2008;47(1):82–9.
48. Ahmed M, Brace CL, Lee FT Jr, Goldberg SN. Principles of and advances in percutaneous ablation. Radiology. 2011;258(2):351–69.
49. Lencioni R, Crocetti L. Local-regional treatment of hepatocellular carcinoma. Radiology. 2012;262(1):43–58.
50. Shibata T, Iimuro Y, Yamamoto Y, Maetani Y, Ametani F, Itoh K, et al. Small hepatocellular carcinoma: comparison of radio-frequency ablation and percutaneous microwave coagulation therapy. Radiology. 2002;223(2):331–7.
51. Chinnaratha MA, Chuang MA, Fraser RJ, Woodman RJ, Wigg AJ. Percutaneous thermal ablation for primary hepatocellular carcinoma: a systematic review and meta-analysis. J Gastroenterol Hepatol. 2016;31(2):294–301.

52. Massarweh NN, Davila JA, El-Serag HB, Duan Z, Temple S, May S, et al. Transarterial bland versus chemoembolization for hepatocellular carcinoma: rethinking a gold standard. J Surg Res. 2016;200(2):552–9.
53. Facciorusso A, Bellanti F, Villani R, Salvatore V, Muscatiello N, Piscaglia F, et al. Transarterial chemoembolization vs bland embolization in hepatocellular carcinoma: a meta-analysis of randomized trials. United European Gastroenterol J. 2017;5(4):511–8.
54. Salem R, Thurston KG. Radioembolization with 90Yttrium microspheres: a state-of-the-art brachytherapy treatment for primary and secondary liver malignancies: part 1: technical and methodologic considerations. J Vasc Interv Radiol. 2006;17(8):1251–78.
55. Salem R, Gabr A, Riaz A, Mora R, Ali R, Abecassis M, et al. Institutional decision to adopt Y90 as primary treatment for hepatocellular carcinoma informed by a 1,000-patient 15-year experience. Hepatology (Baltimore, Md). 2018;68(4):1429–40.
56. Vilgrain V, Pereira H, Assenat E, Guiu B, Ilonca AD, Pageaux G-P, et al. Efficacy and safety of selective internal radiotherapy with yttrium-90 resin microspheres compared with sorafenib in locally advanced and inoperable hepatocellular carcinoma (SARAH): an open-label randomised controlled phase 3 trial. Lancet Oncol. 2017;18(12):1624–36.
57. Chow PK, Gandhi M, Tan S-B, Khin MW, Khasbazar A, Ong J, et al. SIRveNIB: selective internal radiation therapy versus sorafenib in Asia-Pacific patients with hepatocellular carcinoma. J Clin Oncol. 2018;36(19):1913–21.
58. Pan CC, Kavanagh BD, Dawson LA, Li XA, Das SK, Miften M, et al. Radiation-associated liver injury. Int J Radiat Oncol Biol Phys. 2010;76(3 Suppl):S94–100.
59. Order SE, Stillwagon GB, Klein JL, Leichner PK, Siegelman SS, Fishman EK, et al. Iodine 131 antiferritin, a new treatment modality in hepatoma: a Radiation Therapy Oncology Group study. J Clin Oncol. 1985;3(12):1573–82.
60. Qi WX, Fu S, Zhang Q, Guo XM. Charged particle therapy versus photon therapy for patients with hepatocellular carcinoma: a systematic review and meta-analysis. Radiother Oncol. 2015;114(3):289–95.
61. Cheng AL, Kang YK, Chen Z, Tsao CJ, Qin S, Kim JS, et al. Efficacy and safety of sorafenib in patients in the Asia-Pacific region with advanced hepatocellular carcinoma: a phase III randomised, double-blind, placebo-controlled trial. Lancet Oncol. 2009;10(1):25–34.
62. Llovet JM, Ricci S, Mazzaferro V, Hilgard P, Gane E, Blanc JF, et al. Sorafenib in advanced hepatocellular carcinoma. N Engl J Med. 2008;359(4):378–90.
63. Bruix J, Qin S, Merle P, Granito A, Huang YH, Bodoky G, et al. Regorafenib for patients with hepatocellular carcinoma who progressed on sorafenib treatment (RESORCE): a randomised, double-blind, placebo-controlled, phase 3 trial. Lancet (London, England). 2017;389(10064):56–66.
64. El-Khoueiry AB, Sangro B, Yau T, Crocenzi TS, Kudo M, Hsu C, et al. Nivolumab in patients with advanced hepatocellular carcinoma (CheckMate 040): an open-label, non-comparative, phase 1/2 dose escalation and expansion trial. Lancet (London, England). 2017;389(10088):2492–502.
65. Kudo M, Finn RS, Qin S, Han KH, Ikeda K, Piscaglia F, et al. Lenvatinib versus sorafenib in first-line treatment of patients with unresectable hepatocellular carcinoma: a randomised phase 3 non-inferiority trial. Lancet (London, England). 2018;391(10126):1163–73.
66. Zhu AX, Finn RS, Edeline J, Cattan S, Ogasawara S, Palmer D, et al. Pembrolizumab in patients with advanced hepatocellular carcinoma previously treated with sorafenib (KEYNOTE-224): a non-randomised, open-label phase 2 trial. Lancet Oncol. 2018;19(7):940–52.
67. Abou-Alfa GK, Meyer T, Cheng AL, El-Khoueiry AB, Rimassa L, Ryoo BY, et al. Cabozantinib in patients with advanced and progressing hepatocellular carcinoma. N Engl J Med. 2018;379(1):54–63.
68. Zhu AX, Kang YK, Yen CJ, Finn RS, Galle PR, Llovet JM, et al. Ramucirumab after sorafenib in patients with advanced hepatocellular carcinoma and increased α-fetoprotein concentrations (REACH-2): a randomised, double-blind, placebo-controlled, phase 3 trial. Lancet Oncol. 2019;20(2):282–96.

69. Stein S, Pishvaian MJ, Lee MS, Lee K-H, Hernandez S, Kwan A, et al. Safety and clinical activity of 1L atezolizumab+ bevacizumab in a phase Ib study in hepatocellular carcinoma (HCC). J Clin Oncol. 2018;36(15_suppl):4074.
70. Finn RS, Qin S, Ikeda M, Galle PR, Ducreux M, Kim TY, et al. Atezolizumab Plus Bevacizumab in Unresectable Hepatocellular Carcinoma. N Engl J Med. 2020;382(20):1894–905.
71. Ally A, Balasundaram M, Carlsen R, Chuah E, Clarke A, Dhalla N, et al. Comprehensive and Integrative Genomic Characterization of Hepatocellular Carcinoma. Cell 2017;169(7): 1327–41.

Chapter 2
Cholangiocarcinoma

Scott M. Thompson, Lorena Marcano-Bonilla, Taofic Mounajjed, Benjamin R. Kipp, Julie K. Heimbach, Christopher L. Hallemeier, Mitesh J. Borad, and Lewis R. Roberts

Epidemiology of BTC

Cholangiocarcinoma (CCA) is a malignancy that arises from the epithelium lining the bile ducts. CCAs are subdivided based on anatomic criteria into intrahepatic (iCCA), perihilar (pCCA), and distal cholangiocarcinoma (dCCA). The most recent estimates from the Global Burden of Disease Study are of 184,000 incident cases of biliary tract cancer (BTC) worldwide in 2016, with 108,000 (59%) occurring in women and 76,000 (41%) in men [1]. Particularly concerning is the evidence for

S. M. Thompson
Department of Radiology, Mayo Clinic, Rochester, MN, USA
e-mail: thompson.scott@mayo.edu

L. Marcano-Bonilla
University of Puerto Rico School of Medicine, San Juan, PR, USA
e-mail: lorena.marcano@upr.edu

T. Mounajjed · B. R. Kipp
Department of Laboratory Medicine and Pathology, Mayo Clinic, Rochester, MN, USA
e-mail: mounajjed.taofic@mayo.edu; kipp.benjamin@mayo.edu

J. K. Heimbach
Department of Transplantation Surgery, Mayo Clinic, Rochester, MN, USA
e-mail: heimbach.julie@mayo.edu

C. L. Hallemeier
Department of Radiation Oncology, Mayo Clinic, Rochester, MN, USA
e-mail: hallemeier.christopher@mayo.edu

M. J. Borad
Division of Hematology and Oncology, Mayo Clinic, Rochester, MN, USA
e-mail: borad.mitesh@mayo.edu

L. R. Roberts (✉)
Division of Gastroenterology and Hepatology, Mayo Clinic, Rochester, MN, USA
e-mail: roberts.lewis@mayo.edu

L. R. Roberts et al. (eds.), *Evaluation and Management of Liver Masses*,
https://doi.org/10.1007/978-3-030-46699-2_2

increasing incidence of CCA in younger birth cohorts. The risk factors most strongly associated with CCA are those characterized by chronic inflammatory states. However, most CCAs are sporadic, with no identifiable risk factors. In Western countries, primary sclerosing cholangitis (PSC) is the most recognized risk factor for CCA. Even though PSC is a well-established risk factor for CCA, the incidence of CCA in patients with PSC is relatively low at 0.5–1.5% per year, reflecting the fact that most of the CCA cases diagnosed in Western countries arise de novo [2–7].

At present, there are no effective screening protocols for early detection of sporadic CCA, nor explicit recommendations for screening of PSC patients for CCA. The most effective strategy for detecting early CCA in PSC involves annual magnetic resonance imaging (MRI) and magnetic resonance cholangiopancreatography (MRCP) or ultrasound and CA 19-9, followed by endoscopic retrograde cholangiopancreatography (ERCP) and brush cytology or forceps biopsy for evaluation of suspicious strictures [8]. This strategy, however, is invasive and costly [9]. The only curative modality for CCA is surgical resection or liver transplantation for early-stage disease [10]. The vast majority of patients with CCA have late-stage disease not amenable to surgical resection with curative intent [11]. The standard of care for intermediate to advanced stage CCA, which is chemotherapy, is typically accompanied by significant toxicity and a high rate of recurrence. In this chapter, we provide a detailed review of the current practices employed to evaluate and manage patients diagnosed with CCA, with a particular emphasis on the imaging features.

Imaging of Cholangiocarcinoma (CCA)

Imaging Classification Overview: Anatomic Location and Morphology

Cholangiocarcinoma (CCA) can be classified at imaging by anatomic location and morphologic growth pattern [12]. CCA classified by location includes (i) intrahepatic CCA (iCCA) occurring proximal to the second-order bile ducts, (ii) perihilar CCA (pCCA) occurring from the second-order bile ducts to the level of the cystic duct origin, and (iii) distal CCA (dCCA) occurring from the cystic duct origin to the ampulla of Vater [13, 14]. CCA classified by morphologic growth pattern includes (i) mass-forming exophytic subtype which appears as a focal hepatic mass, (ii) periductal infiltrating subtype which appears as longitudinal tumor with growth along the bile ducts, (iii) intraductal polypoid type which appears as a focal intraluminal mass, and (iv) mixed pattern [15]. The initial imaging modality for detection of CCA may vary from incidental detection such as in a patient with new onset jaundice versus screening detection in high-risk populations such as those with known cirrhosis or primary sclerosing cholangitis [16] (Figs. 2.1, 2.2, 2.3, 2.4, 2.5, and 2.6).

Imaging Features

Intrahepatic CCA (iCCA)

iCCA or peripheral cholangiocarcinoma occurs proximal to the second-order bile ducts. The mass-forming exophytic type is the most common subtype of iCCA (80%) followed by periductal infiltrating, intraductal growth with or without papillary features, and mixed subtypes [15, 17]. Imaging features of iCCA are dependent on size, morphologic growth pattern, and degree of intratumoral fibrosis, necrosis, or mucin content (Figs. 2.1, 2.2, 2.3, and 2.4).

Ultrasound (US)

On US, mass-forming iCCA may appear as a nonspecific focal mass with variable echogenicity ranging from a hypoechoic (<3 cm) to hyperechoic (>3 cm) mass with heterogeneous echotexture depending on degree of fibrosis, necrosis, mucin content, or calcification and occasional peripheral echogenic rim [18, 19]. The periductal infiltrating subtype may appear as a small mass or with diffuse bile duct thickening with or without a bile duct stricture and peripheral dilated ducts [18, 20]. The intraductal subtype may demonstrate focal or diffuse biliary ductal dilatation with or without an echogenic intraluminal mass with papillary features [18]. A few studies have examined contrast-enhanced US (CEUS) in iCCA and hepatocellular carcinoma (HCC), with

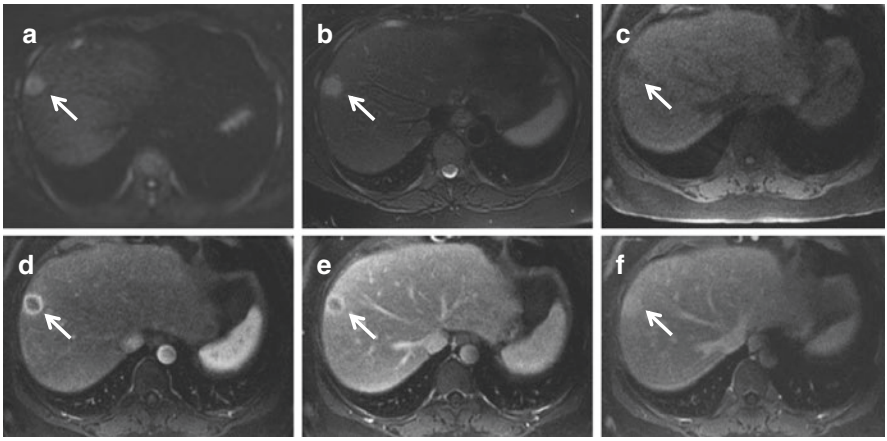

Fig. 2.1 Small mass-forming intrahepatic cholangiocarcinoma (iCCA) evaluated with extravascular contrast on MRI. The mass shows (**a**) peripheral DWI hyperintensity (white arrow), (**b**) T2-weighted hyperintensity, (**c**) T1-weighted hypointensity, (**d**) peripheral arterial phase hyperenhancement (white arrow), and (**e**, **f**) progressive centripetal enhancement on (**e**) portal venous and (**f**) delayed phase MRI (white arrow). DWI diffusion-weighted imaging, MRI magnetic resonance imaging

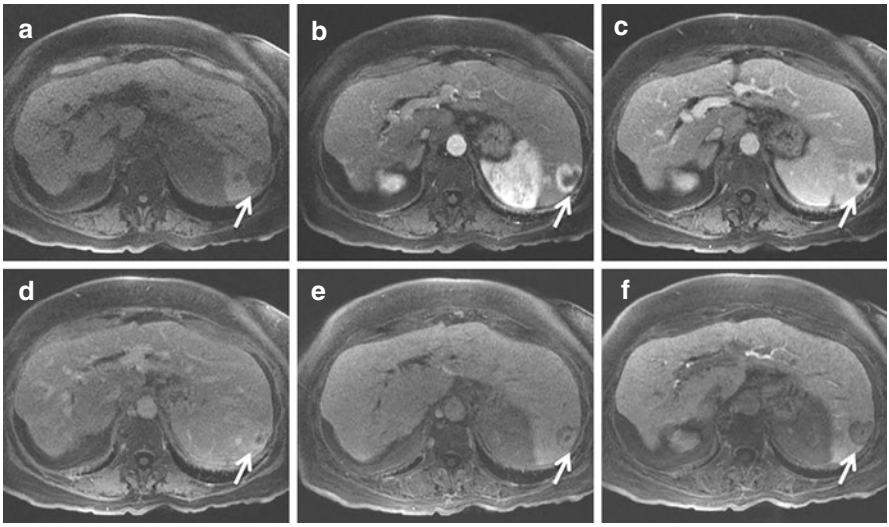

Fig. 2.2 Small mass-forming intrahepatic cholangiocarcinoma (iCCA) evaluated with hepatobiliary contrast on MRI. The mass shows (**a**) T1-weighted hypointensity (white arrow), (**b**) peripheral arterial phase hyperenhancement (white arrow), (**c**, **d**) progressive centripetal enhancement on (**c**) portal venous and (**d**) delayed phases (white arrow), and (**e**, **f**) a rim of peripheral hypointensity with a central hypointense focus on the hepatobiliary phase imaging. DWI diffusion-weighted imaging, MRI magnetic resonance imaging

conflicting results. Although studies have identified similar arterial phase enhancement between iCCA and HCC, both overlapping and nonoverlapping portal venous and delayed phase washout kinetics have been reported with dynamic CEUS [21, 22].

Computed Tomography (CT)

On CT, mass-forming iCCA may appear as a well-defined focal mass or a poorly defined infiltrative mass that is typically homogeneously hypo- to iso-attenuating to the normal hepatic parenchyma on unenhanced CT [19, 21, 23–25]. Typical enhancement characteristics include peripheral or rim arterial phase enhancement followed by gradual centripetal enhancement in the portal venous and delayed phases relative to the normal background liver [18, 26–30]. The viable tumor at the periphery of iCCA may show arterial phase enhancement with subsequent iso- to hypoenhancement during the portal venous phase [28]. This appearance, which is sometimes referred to as the "target pattern," is not specific to iCCA and may also be seen in colon carcinoma metastases. Conversely, the central portion of the iCCA may show central hypoenhancement with centrally necrotic tumors and/or those with higher mucin content [28, 30]. Associated findings include satellite lesions,

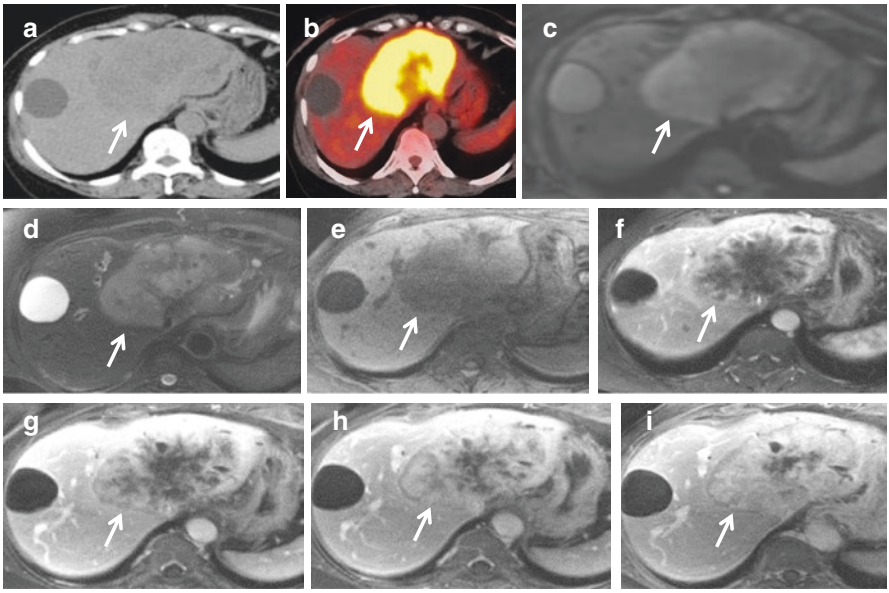

Fig. 2.3 Large mass-forming intrahepatic cholangiocarcinoma (iCCA) CT, 18F-FDG PET, and MRI. The mass is (**a**) isodense with areas of central hypodensity on noncontrast CT (white arrow). (**b**) Axial ^{18}F-FDG-PET/CT show heterogeneous hypermetabolism in the periphery of the hepatic mass (white arrow). The mass shows (**c**) DWI hyperintensity (white arrow), (**d**) heterogenous T2-weighted hyperintensity, (**e**) T1-weighted hypointensity, (**f**) peripheral arterial phase hyperenhancement (white arrow), and (**g–i**) progressive centripetal enhancement on portal venous and delayed phases (white arrow). ^{18}F-FDG 8F-fluorodeoxyglucose, PET positron emission tomography, CT computed tomography, MRI magnetic resonance imaging, DWI diffusion-weighted imaging

hepatic capsular retraction which may be seen in up to 20% of patients, and vascular invasion [20]. Some small mass-forming iCCA may demonstrate arterial phase hyperenhancement (APHE), similar to HCC; as such, portal venous and delayed phase enhancement characteristics become important for differentiating these two. The periductal infiltrating subtype may show diffuse biliary ductal mural thickening and enhancement as well as dilated or narrowed ducts [18]. The CT appearance of the intraductal subtype is the most variable and depends on the presence of an intraluminal mass and the degree of biliary ductal obstruction. Different patterns include (i) an intraluminal mass that is hypo- to isoattenuating to liver on unenhanced CT and enhances with contrast associated with concomitant diffuse severe upstream biliary ductal dilatation, (ii) severe intrahepatic biliary ductal dilatation without an intraductal mass, (iii) an intraductal mass with only localized or mild biliary ductal dilatation, or (iv) a focal biliary stricture with mild proximal biliary ductal dilatation [18]. Primary hepatic tumors with biphenotypic characteristics of both CCA and HCC may demonstrate overlapping imaging features and may ultimately require biopsy for diagnosis and treatment planning [31].

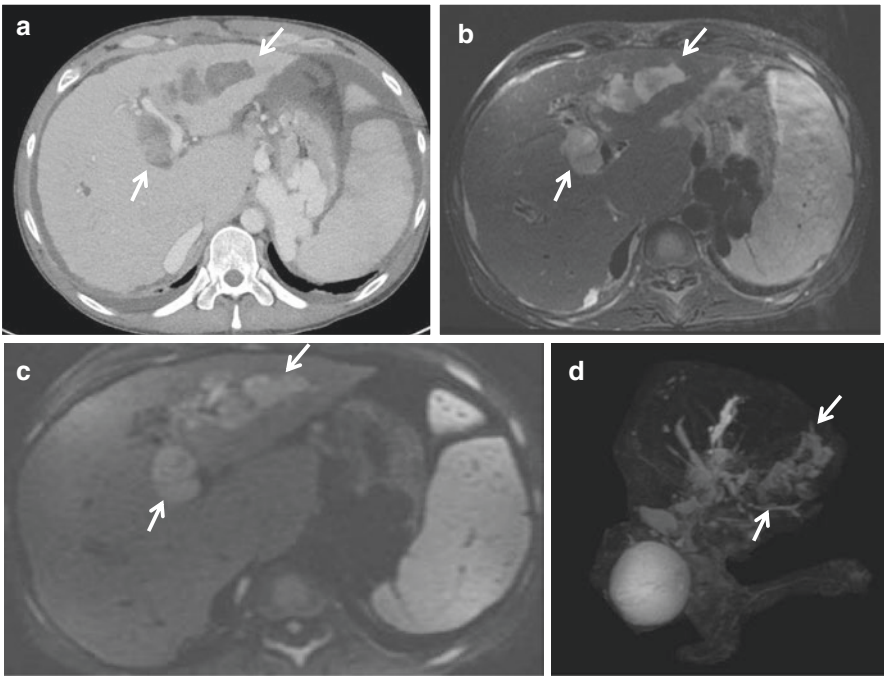

Fig. 2.4 Intraductal intrahepatic cholangiocarcinoma (iCCA) in a patient with ulcerative colitis and primary sclerosing cholangitis evaluated with CT and MRI/MRCP. The ill-defined mass in the left hepatic lobe is (**a**) hypodense with minimal enhancement on portal venous phase CT (white arrows) and shows (**b**) T2-weighted hyperintensity (white arrow) and (**c**) DWI-weighted hyperintensity (white arrow) on MRI. (**d**) Coronal MIP MRCP shows marked intraductal/periductal irregularity of the intrahepatic bile ducts in the left hepatic lobe (white arrows). CT computed tomography, MRI magnetic resonance imaging, MRCP magnetic resonance cholangiopancreatography, DWI diffusion-weighted imaging, MIP maximum intensity projection

Magnetic Resonance Imaging/Magnetic Resonance Cholangiopancreatography (MRI/MRCP)

The morphologic, signal, and enhancement features of iCCA at MRI depend on the morphologic growth pattern and degree of intratumoral fibrosis, necrosis, mucin content, and/or hemorrhage [18, 26]. Mass-forming iCCA is typically iso- to hypointense on T1-weighted (T1W) imaging relative to background liver with possible foci of T1 hyperintensity when intratumoral hemorrhage is present. Additionally, mass-forming iCCA typically shows variable hypo- to hyperintensity on T2-weighted (T2W) imaging depending on the degree of fibrosis (more T2 hypointense) versus necrosis or mucin content (more T2 hyperintense) [18, 25, 27]. On diffusion-weighted imaging (DWI), 50–75% of iCCA may demonstrate target-like central hypointensity with peripheral high signal intensity at high b-values [25, 32, 33].

Additionally, MRCP may show bile duct invasion [20]. Similar to CT, gadolinium-enhanced MRI with extracellular-based agents shows peripheral or rim arterial phase enhancement with patchy central enhancement on portal venous phase and progressive central enhancement on delayed phase imaging [18, 20, 25, 34] with peripheral washout in the portal venous and/or delayed phases. Areas of early enhancement correlate with viable tumor, whereas areas of delayed enhancement correlate with the relatively hypovascular fibrosis. Conversely, gadolinium-enhanced MRI with hepatobiliary-specific contrast agents shows relative hypoenhancement of iCCA relative to the background liver [18, 35]. A target sign has been described in intrahepatic cholangiocarcinoma in the hepatobiliary phase with hepatocyte-specific agents. This is due to circulating contrast agents that tend to remain in the extracellular space associated with fibrosis. This appearance is not specific to iCCA but can also be seen in fibrous tumors such as fibrolamellar hepatocellular carcinoma or treated colorectal metastases. CT and MRI have similar diagnostic performance in the detection of primary and satellite iCCA lesions, but the spatial resolution of CT is superior for the detection of vascular involvement [36]. The morphologic appearance and enhancement characteristics of the periductal infiltrating and intraductal subtypes of iCCA are similar between CT and MRI [18].

Positron Emission Tomography (PET)

18F-florodeoxyglucose (18F-FDG) PET/CT can provide metabolic information related to tumoral glucose uptake and is the most common radiotracer investigated in iCCA. Viable tumor shows FDG uptake, while centrally necrotic or fibrotic portions of the tumor will appear as a photopenic defect. 18F-FDG PET/CT has been shown to be accurate for the evaluation and detection of primary tumors as well as both lymph node and distant metastases in patients with iCCA [37]. Moreover, quantitative tumor standardized uptake value max (SUV-max) has been shown to be an independent prognostic factor for oncological outcomes in patients with resectable iCCA, with tumor SUV-max >8 associated with worse disease-free and overall survival after surgical resection [38, 39]. Moreover, iCCA has been shown to have greater SUV-max compared to extrahepatic CCA [40].

Perihilar CCA (pCCA)

pCCA develops from the second-order bile ducts to the common bile duct at and above the cystic duct origin and may be nodular, sclerosing (periductal infiltrating), or papillary morphologic subtypes [12, 27] (Fig. 2.5). Nodular pCCA tends to grow intraluminally with bile duct invasion resulting in significant fibrotic reaction [41]. Conversely, papillary pCCA grows intraluminally without invasion of the bile duct wall [42]. Sclerosing pCCA produces concentric thickening of the bile duct and

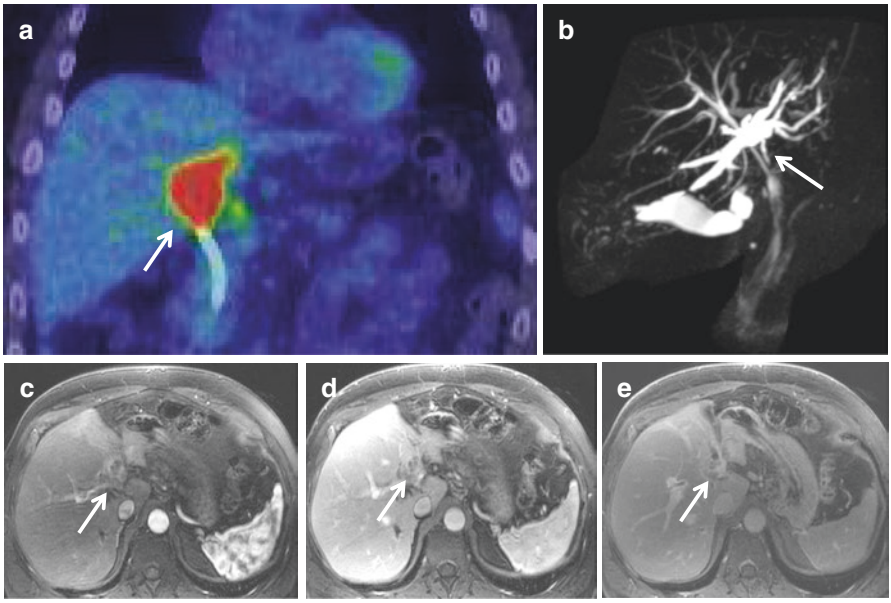

Fig. 2.5 Perihilar cholangiocarcinoma—"Klatskin" tumor—evaluated with 18F-FDG PET/CT and MRI/MRCP. (**a**) Coronal ^{18}F-FDG-PET/CT shows a hypermetabolic mass in the central liver (white arrow). (**b**) Coronal MIP MRCP shows dilatation of intrahepatic bile ducts beginning at the confluence of the left and right hepatic ducts secondary to an hilar obstructing mass and no filling of the extrahepatic bile duct (white arrow). (**c**–**e**) MRI shows an ill-defined mass in the porta hepatis that shows (c) peripheral arterial phase hyperenhancement (white arrow) and (**d**, **e**) slight progressive centripetal enhancement on (**d**) portal venous and (**e**) delayed phases (white arrow). ^{18}F-FDG 18F-fluorodeoxyglucose, PET positron emission tomography, CT computed tomography, MRI magnetic resonance imaging, MRCP magnetic resonance cholangiopancreatography, MIP maximum intensity projection

eventual duct obliteration without a discrete mass [43]. Early pCCA is very difficult to detect due to their small tissue volume that causes only focal thickening of the bile duct wall and relatively less stricturing or complete biliary obstruction.

Ultrasound (US)

Because patients with pCCA often present with obstructive jaundice, US is often the initial imaging modality for evaluation of biliary duct obstruction and is helpful for identifying the level of obstruction [27]. US has a reported sensitivity and specificity of 89% and 80–95% for detection of pCCA [27, 44, 45]. An intraluminal mass with variable echogenicity ranging from hypo- to hyperechoic with upstream ductal dilatation may been seen. Nonetheless, while a mass or stricture may not be directly visualized, US is useful for detecting invasion of the liver parenchyma or portal veins and can help guide next steps for invasive or noninvasive imaging evaluation.

Computed Tomography (CT)

Unenhanced CT may show a variably defined hypodense mass centered near the porta hepatis, which demonstrates variable progressive enhancement of contrast-enhanced imaging. The overall diagnostic accuracy of CT has been reported at 79–92%, and it may be particularly useful for demonstrating the level of biliary obstruction, extent of local invasion into adjacent tissue, and metastatic disease in the abdomen and pelvis [27, 28]. Moreover, CT with angiogram (CTA) and venogram (CTV) protocols are accurate for detection of hepatic arterial and portal vein involvement by pCCA in up to 87–93% of cases [26, 27, 46, 47]. Nevertheless, CT may underestimate the longitudinal extension of tumor along the bile duct for periductal infiltrating subtypes as well as regional lymphadenopathy and peritoneal metastases in up to 50% of cases [36, 46]. Streak artifact from metallic biliary stents may further limit evaluation of locoregional disease extent [46]. As such, CT cholangiography may provide further detail on the biliary anatomy and is an option when MRCP is not available [47]. Nonetheless, CT cholangiography is dependent on a functioning secretory system of the biliary tree, which may be limited in patients with severe biliary obstruction or hyperbilirubinemia.

Magnetic Resonance Imaging/Magnetic Resonance Cholangiopancreatography (MRI/MRCP)

Periductal infiltrating pCCA may be difficult to directly visualize at MRI in the absence of a mass-like lesion. Consequently, tumor extent may be inferred by secondary signs, including proximal biliary ductal dilatation, periductal thickening, and enhancement. Intraductal mass is rare but when present often appears as hyperintense on T2-weighted imaging, hypointense on T1-weighted imaging, and with mild hypoenhancement relative to the liver with the use of extracellular gadolinium-based contrast agents [12, 16, 18, 27]. In addition, hepatobiliary-specific contrast agents may provide the dual benefit of dynamic contrast-enhanced imaging followed by delayed hepatobiliary phase imaging for better delineation of the biliary tree [48]. The utility of hepatobiliary contrast alone for evaluation of pCCA still needs further evaluation as dynamic contrast-enhanced phases are often limited or of inferior quality compared to standard extracellular contrast agents.

MRCP is a particularly accurate method for imaging the biliary tree and is the imaging modality of choice in patients with suspected CCA in conjunction with MRI, particularly for periductal infiltrating tumors [12, 16, 25, 27, 49]. MRCP is ideally performed prior to decompression of the biliary tree by percutaneous or endoscopic techniques. MRCP and ERCP serve complementary roles with MRCP being better able to evaluate the peripheral hepatic ducts. Overall, MRI/MRCP has an overall diagnostic accuracy of 66% for detection of locoregional lymph node metastases, 78% sensitivity and 91% specificity for portal vein invasion, and 58–73% sensitivity and 93% specificity for hepatic arterial invasion, slight

less than CT [50–52]. As such, CT and MRI/MRCP serve complementary roles in the diagnosis and staging of pCCA with CT better at demonstrating vascular involvement while MRI/MRCP better demonstrates extent of biliary neoplastic invasion [51, 53].

Invasive Cholangiography: Endoscopic Retrograde Cholangiopancreatography (ERCP) or Percutaneous Transhepatic Cholangiography (PTC)

Both ERCP and PTC are invasive techniques that can be both diagnostic and therapeutic [54, 55]. Both techniques are useful diagnostically for delineating the biliary tree, location of biliary pathology and/or strictures, and obtaining tissue for histologic, cytologic, or molecular testing. Moreover, ERCP and PTC can be therapeutic with the ability to place internal biliary stents or internal–external biliary drains to decompress an obstructed biliary system [54]. Overall sensitivity and specificity of invasive cholangiography is ~75% with an accuracy of 95% for diagnosis of pCCA [56]. Percutaneous transhepatic biliary drainage (PTBD) has been shown to have a lower complication rate compared to endoscopic biliary drainage (EBD) in the preoperative setting prior to CCA resection [57].

Endoscopic Ultrasound (EUS)

EUS has emerged as an important modality for assessment of pCCA with advantages for evaluating extent of local periductal tumor invasion and regional lymph nodes [58].

Positron Emission Tomography (PET)

Experience with 18F-FDG PET/CT or PET/MRI in pCCA is much more limited than for iCCA, but it may be helpful in detection of distant metastatic disease (Fig. 2.5).

Distal CCA (dCCA)

dCCA develops in the common bile duct between the cystic duct origin and the ampulla of Vater. In general, imaging findings of dCCA and pCCA are similar, with the two subclasses often referred to together as extrahepatic cholangiocarcinoma [12, 18, 27] (Fig. 2.6).

Ultrasound (US)

Similar to pCCA, US may be the first imaging modality in the setting of new obstructive jaundice and is helpful for identifying the level of obstruction, upstream biliary ductal dilatation, and guiding subsequent invasive and noninvasive imaging.

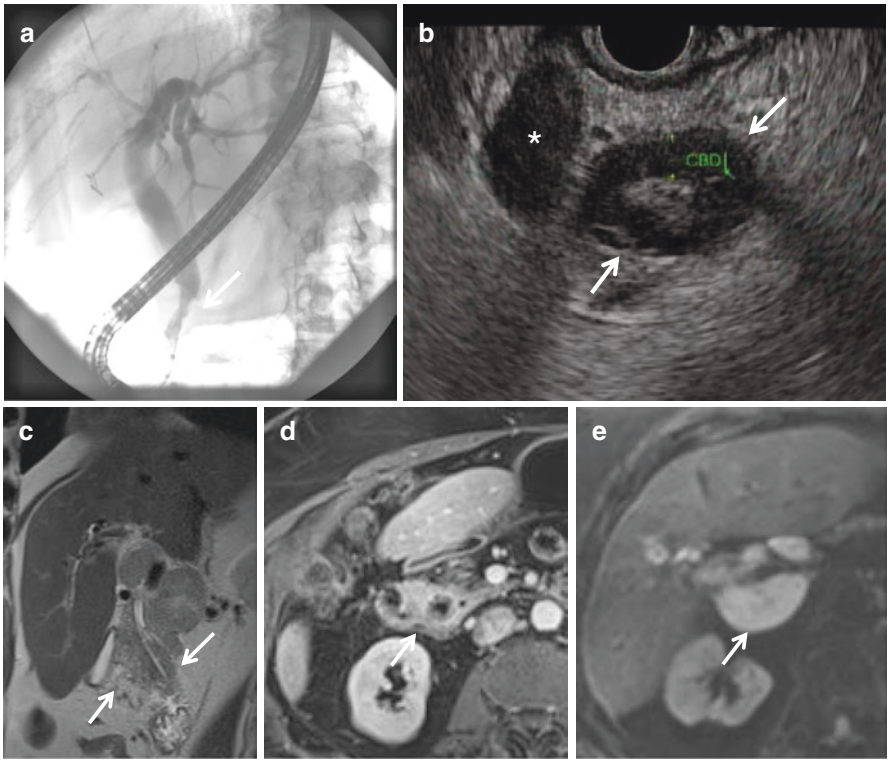

Fig. 2.6 Periductal infiltrating cholangiocarcinoma of the distal common bile duct evaluated with ERC/EUS and MRI. (**a**) Endoscopic retrograde cholangiography (ERC) shows irregular narrowing of the distal common bile duct (CBD) (white arrow). (**b**) Endoscopic ultrasound shows marked mural thickening of the distal common bile duct (white arrow) and a large porta hepatis lymph node (white asterisk). (**c**–**e**) MRI shows (**c**) the periductal infiltrating soft tissue with T2-weighted iso- to hypointensity and (**d**) diffuse enhancement as well as (**e**) multiple enlarged porta hepatis lymph nodes that demonstrate DWI hyperintensity. MRI magnetic resonance imaging, DWI diffusion-weighted imaging

Computed Tomography (CT) and Magnetic Resonance Imaging/Magnetic Resonance Cholangiopancreatography (MRI/MRCP)

CT and MRI/MRCP may demonstrate thickening, enhancement, or stricturing of the common bile duct, with or without an enhancing intraluminal mass. Contrast-enhanced CT or MRI provides important information about tumor involvement of the duodenum and pancreas as well as vascular involvement of the portal vein (PV) or hepatic artery (HA) and locoregional lymph node metastases.

Endoscopic Retrograde Cholangiopancreatography (ERCP) and Endoscopic Ultrasound (EUS)

ERCP has a high diagnostic accuracy for detection of dCCA and evaluating the extent of tumor involvement of the biliary tree. Moreover, EUS is helpful for

evaluating invasion of the biliary wall, hepatic vasculature, and pancreas, as well as detecting porta hepatis lymph node metastases. EUS with fine-needle aspiration (FNA) can be used for sampling the primary tumor as well as locoregional lymph nodes and is often diagnostic. Importantly, individuals who are potential candidates for liver transplantation for their pCCA or dCCA should not have FNA sampling of the primary tumor through the bile duct wall, as that increases the risk of tumor dissemination and is a contraindication to liver transplantation.

Pathology

Grossly, intrahepatic cholangiocarcinoma is typically firm and not encapsulated (Fig. 2.7). It is usually mass forming but can sometimes grow in a diffusely infiltrating periductal distribution or display an intraductal growth pattern [13, 18, 59, 60]. Histologically, cholangiocarcinomas are primarily adenocarcinomas, but other rare histologic variants also exist [61–84]. Extrahepatic cholangiocarcinoma, particularly perihilar cholangiocarcinoma, is typically rich in fibrous stroma, and often has a dense desmoplastic response; this results from extracellular matrix production by activated myofibroblasts present in the stroma [85] (Fig. 2.8). In most

Fig. 2.7 Peripheral intrahepatic cholangiocarcinoma: this cholangiocarcinoma forms a distinct fibrotic mass occupying the peripheral liver parenchyma

Fig. 2.8 Perihilar cholangiocarcinoma: a fibrotic irregular mass is present in the hilum, compressing adjacent ducts

cholangiocarcinomas, the tumor forms glands or tubules which are lined by epithelial cells (Fig. 2.9). Generally, the more centrally located hepatic cholangiocarcinomas are more likely to have well-formed glands lined by columnar epithelial cells with mucin production, whereas cholangiocarcinomas located at the liver periphery are more likely to grow as irregular, anastomosing tubular structures lined by low cuboidal cells that do not produce mucin [65]. Cholangiocarcinoma can also have a variety of growth patterns, often present in the same tumor, including irregular tubules, infiltrating glands, solid nests, trabeculae, and micropapillary structures (Fig. 2.10). Cholangiocarcinoma can grow along sinusoids and spread extensively throughout the liver through the portal venous or lymphatic system (Fig. 2.11). Perineural invasion is usually seen only where the larger nerves of the liver are located, in the large portal areas close to the liver hilum, and is more frequently seen in perihilar cholangiocarcinoma.

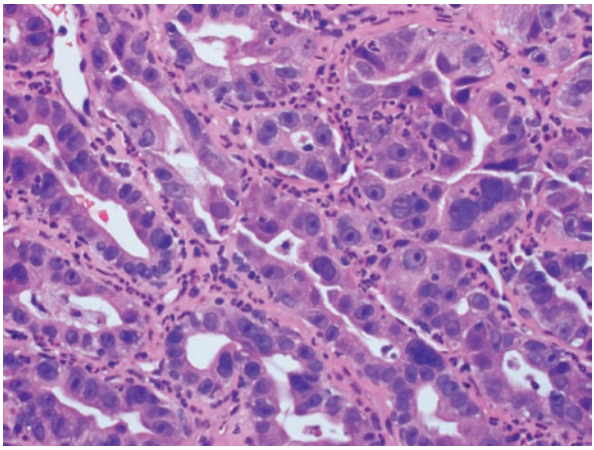

Fig. 2.9 Cholangiocarcinoma with glandular histology. Cholangiocarcinoma is typically an adenocarcinoma, consisting of abnormal glands lined by highly atypical epithelial cells

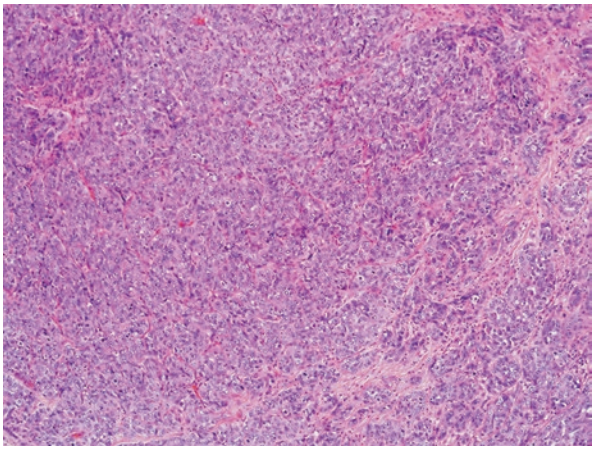

Fig. 2.10 Cholangiocarcinoma with histologic phenotype of solid sheets. Cholangiocarcinoma can also grow in solid sheets and nests of malignant epithelial cells

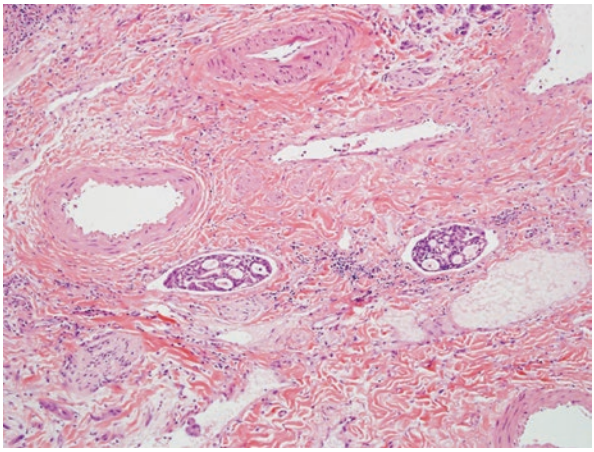

Fig. 2.11 Lymphovascular invasion in a cholangiocarcinoma with dense stroma. Lymphovascular invasion features groups of cholangiocarcinoma cells occupying lymphatic spaces

Although there is not a universally adopted grading system for cholangiocarcinoma, many pathologists in the United States utilize a four-tier grading system adapted by the College of American Pathologists (CAP) and American Joint Committee on Cancer (AJCC), based on the percentage of the glandular component in the tumor [86]. According to this schema, adenocarcinomas are graded as follows: well-differentiated (grade 1), moderately differentiated (grade 2), poorly differentiated (grade 3), and undifferentiated (grade 4). Tumor grade is an independent predictor of patient survival and cancer recurrence [87, 88]. Of note, rare variants of cholangiocarcinoma cannot be graded according to this scheme and are usually not assigned a specific grade.

Immunohistochemical stains are frequently performed on cholangiocarcinoma to exclude metastatic disease to the liver or hepatocellular carcinoma. Cholangiocarcinoma shows positive cytoplasmic staining with polyclonal carcinoembryonic antigen (CEA). CK19 is also positive in 70–80% of cases, and MOC31, a monoclonal antibody that recognizes an epithelial-associated glycoprotein also known as Epithelial Specific Antigen/Ep-CAM, is positive in 90% of cases [89]. Intrahepatic cholangiocarcinoma is virtually always positive for CK7, but varies in CK20 expression. Interestingly, the immunoprofile of cholangiocarcinoma can depend on its location. For example, 50% of peripheral cholangiocarcinomas are CK20 negative, while central and extrahepatic cholangiocarcinomas tend to be CK20 positive [90]. Likewise, peripheral cholangiocarcinomas, especially those with a “bile ductular” pattern, tend to express CD56 [91]. Finally, focal positive staining for HepPar-1, though rare, is more commonly seen in peripherally located tumors.

The histologic differential diagnosis for cholangiocarcinoma includes metastatic adenocarcinoma to the liver, hepatocellular carcinoma, epithelioid hemangioendothelioma, bile duct adenoma, bile duct hamartoma, and biliary adenofibroma. Immunohistochemical stains, when necessary, are used in conjunction with tumor morphology to distinguish cholangiocarcinoma from these tumors.

Cholangiocarcinoma has an immunoprofile that is similar to that of other pancreaticobiliary and upper gastrointestinal adenocarcinomas. In recent times, however, in situ hybridization for albumin has shown high sensitivity and specificity in distinguishing hepatic cholangiocarcinoma from metastatic adenocarcinoma to the liver or carcinoma of unknown origin [92]. Hence, the pathologic diagnosis is based on exclusion of other tumors using morphology, immunostains, in situ hybridization, imaging studies, and clinical findings; once other carcinomas have been excluded, a diagnosis of cholangiocarcinoma can be made.

Diagnosis Using Fluorescence In Situ Hybridization (FISH)

Infiltrating extrahepatic cholangiocarcinoma and pancreatic ductal cancers are often sampled by endoscopic brushing cytology. Although routine cytology has been the primary tool for detecting pancreatobiliary tract malignancy and has near perfect clinical specificity, the diagnostic sensitivity of routine cytology is limited and varies considerably based on stage at diagnosis, cytology collection type, and patient cohort (PSC vs. non-PSC, mass presenting lesions, etc.). More specifically, a review demonstrated a wide range of performance characteristics based on cytology preparation, including pancreatobiliary brushings (sensitivity range, 26–89%; specificity range, 80–100%; accuracy range, 48–96%), bile duct brushings (sensitivity range, 33–54%; specificity range, 100%; accuracy range, 43–67%), pancreatic duct brushings (sensitivity range, 47–66%; specificity range, 100%; accuracy range, 67–79%), and bile cytology (sensitivity range, 6–50%; specificity range, 100%; accuracy range, 31–57%) [93].

The main limitation of cytology is false-negative results in patients with pancreatobiliary tract cancer. As a result, ancillary molecular markers can be utilized to increase diagnostic sensitivity. Cancer genomes contain a wide assortment of genetic alterations that activate oncogenes or that inactivate tumor suppressor genes, including single-nucleotide substitutions, structural rearrangements, small insertions, small deletions, and copy number variation. Fluorescence in situ hybridization (FISH) is a technique that uses fluorescently labeled DNA probes to detect chromosomal copy number variation. For pancreatobiliary testing, FISH probes are specifically designed to assess for neoplastic cells with chromosomal abnormalities (i.e., aneuploidy) in neoplastic cells among a background of diploid nonneoplastic cells. Nonneoplastic cells generally show disomy, with two copies for each of the FISH probes, because each probe targets the two alleles in an individual cell (Fig. 2.12). Specimens are interpreted as abnormal when the number of cells demonstrating losses or gains of probes exceeds the thresholds established in normal value studies for the FISH probes used.

The majority of publications have focused on one of two FISH probe sets. The UroVysion probe set (Abbott Molecular, Inc., Des Plaines, IL) contains a probe directed to the CDKN2A gene located at 9p21 and chromosome enumeration probes directed to chromosomes 3, 7, and 17. In 2009, Fritcher et al. published the most comprehensive report of FISH testing with UroVysion and indicated that the

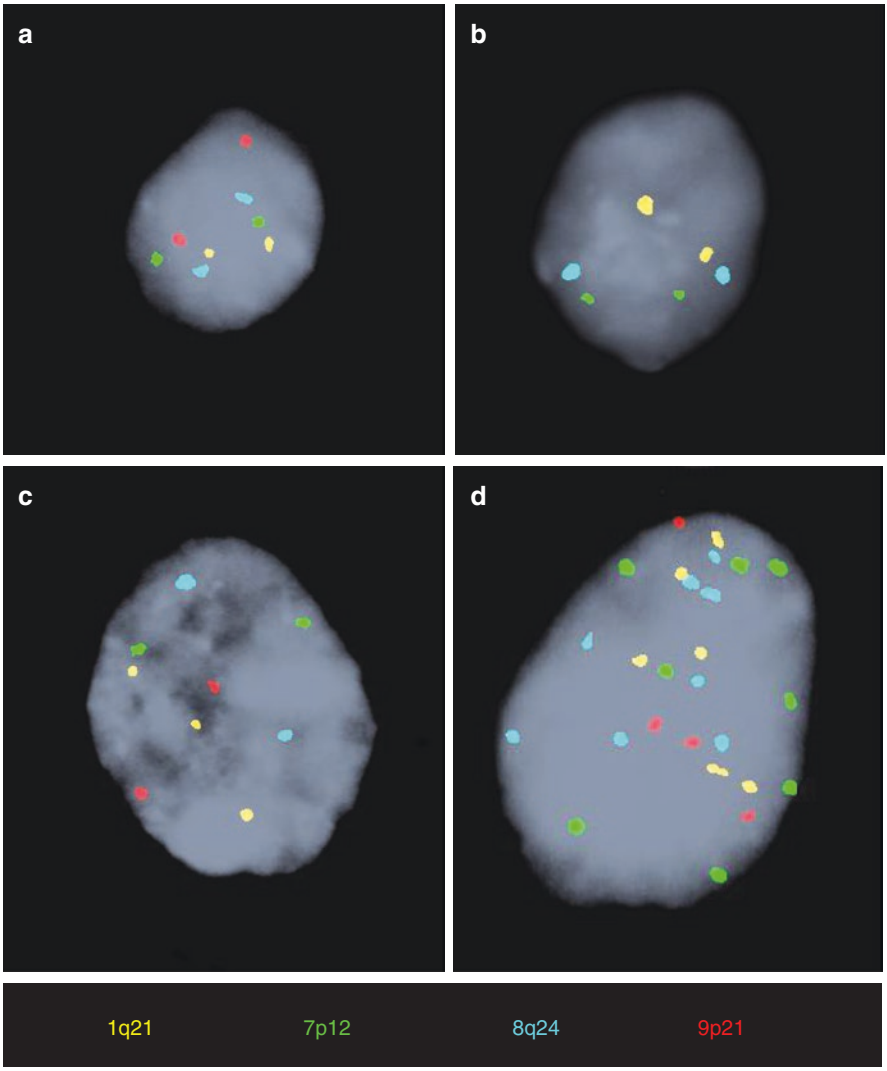

Fig. 2.12 These representative examples of cells demonstrate (**a**) disomic (normal), (**b**) 9p21 loss, (**c**) single locus gain, and (**d**) polysomy FISH signal patterns

sensitivity of FISH was significantly higher than cytology for detecting malignancy (43% vs 20%; $P < 0.001$) [94]. Many other institutions have also reported the improved performance characteristics of FISH using the UroVysion probe set for detecting pancreatobiliary tract malignancy [3]. More recently, a newly tailored pancreatobiliary FISH probe set targeting chromosomal regions 1q21 (*MCL1*), 7p12 (*EGFR*), 8q24 (*MYC*), and 9p21 (*CDKN2A*) has gained acceptance clinically. In a comparison study, the newer tailored pancreatobiliary FISH probe set had a

significantly higher sensitivity (64.7%) than the UroVysion FISH probe set (45.9%) for detecting malignancy and is now the preferred probe set for these specimens [95]. Representative examples of the pancreatobiliary probe set are shown in Fig. 2.12. Future molecular markers and newer technologies for assessing cytology specimens for malignancy will likely continue to improve detection and direct therapeutic decisions.

Treatments with Curative Intent

Surgical resection is the standard treatment for CCA. The goal is complete removal of the tumor with a negative margin and an adequate functional liver remnant (FLR). The use of strategies such as portal vein embolization, preoperative biliary drainage, and complex vascular reconstructive techniques has improved outcomes following surgical resection [96–101]. Staging laparoscopy prior to laparotomy is recommended, especially in patients with high CA 19-9 to assess for evidence of peritoneal metastasis, given that resection is not beneficial in this setting [102].

For iCCA, surgical therapy usually consists of hemi-hepatectomy with excision of regional nodes to ensure adequate staging [103]. Most guidelines recommend resection only for single iCCA tumors, though recent reports have also noted benefit in patients with two or three lesions [104, 105]. Outcomes following resection in patients with iCCA are related to the extent of disease and the ability to obtain a complete resection. In a recent large multicenter series of 1013 patients, those with a single completely resected tumor had a 43% 5-year survival, compared to 28% 5-year survival for those with two tumors [105]. The use of liver transplantation (LT) has been recently described in a multicenter retrospective series of 15 patients with small unresectable (<2 cm) iCCA occurring in the setting of decompensated cirrhosis, achieving a 65% 5-year survival [106, 107]. On the opposite end of the spectrum, favorable outcomes following LT for patients with large, indolent unresectable iCCA occurring in the setting of normal background liver with no evidence of metastasis and a prolonged period of disease stability following chemotherapy have also recently been reported [108]. Prospective data collection from larger series will be needed to confirm these preliminary findings.

Resection is also the standard therapy for patients with pCCA though unfortunately many patients present with unresectable disease either due to metastatic disease, extensive bi-lobar involvement precluding resection, or advanced underlying liver disease such a primary sclerosing cholangitis (PSC). For those who are eligible, resection typically involves an (extended) hemi-hepatectomy including the caudate lobe with en bloc resection of the extrahepatic bile duct as well as regional lymph nodes [109]. Even in those thought to be resectable, a complete resection is only achieved in approximately 70% of cases [109–111]. Outcomes following resection of pCCA depend on the ability to obtain a complete resection as well as the presence of nodal disease, and typically range from 25% to 45% 5-year survival [109–111].

Liver transplantation was initially considered an ideal strategy to improve the likelihood of complete resection for patients with pCCA, but outcomes for LT alone were poor due to a high rate of disease recurrence [112, 113]. Because of this unacceptable rate of disease recurrence for LT alone, a protocol combining neoadjuvant chemoradiotherapy followed by LT for patients with early-stage unresectable pCCA was developed [114, 115]. The use of this combined protocol has achieved 5-year survival rates of 65–70%, leading to the adoption of neoadjuvant chemoradiotherapy followed by liver transplantation as a part of standard organ transplant allocation policy for patients with early-stage pCCA [116–119].

The benefit of combined neoadjuvant therapy and LT for patients with unresectable pCCA has led to the question of whether the same therapy should be offered to patients with resectable pCCA. The severe shortage of available liver allografts and the need for lifelong immunosuppression are key obstacles to this strategy. Recently, a multicenter retrospective analysis found that those with unresectable pCCA undergoing combined neoadjuvant therapy + LT protocol had superior 5-year survival (64% vs 18%; $P < 0.001$), compared to patients undergoing resection who otherwise met LT criteria, and this remained even after accounting for tumor size, nodal status, and PSC ($P = 0.049$) [120].

Surgical resection is often feasible for patients with early-stage distal cholangiocarcinoma with no evidence of local invasion, lymph node, peritoneal, or distant metastases. The most common operation is pancreatoduodenectomy with hepaticojejunostomy (the Whipple procedure). In selected patients in whom the tumor is located above the upper pancreatic border, an extrahepatic bile duct resection may be performed as an alternative [121].

Locoregional Interventional Radiologic Therapies for Treatment of iCCA

Local and locoregional interventional radiologic therapies include image-guided percutaneous thermal and nonthermal ablative therapies using energy-based devices and transarterial chemoembolization (TACE) or radioembolization (TARE).

Percutaneous Ablation

Image-guided percutaneous radiofrequency (RFA) and microwave (MWA) ablation have been shown to be safe and effective for treatment of iCCA in the palliative setting in patients with unresectable tumors or in those patients whose tumors have recurred after surgical resection (Fig. 2.13). Local tumor recurrence has been reported in up to 22% of patients following RFA and MWA with a greater risk of local tumor progression with primary tumors and superficially located tumors [122].

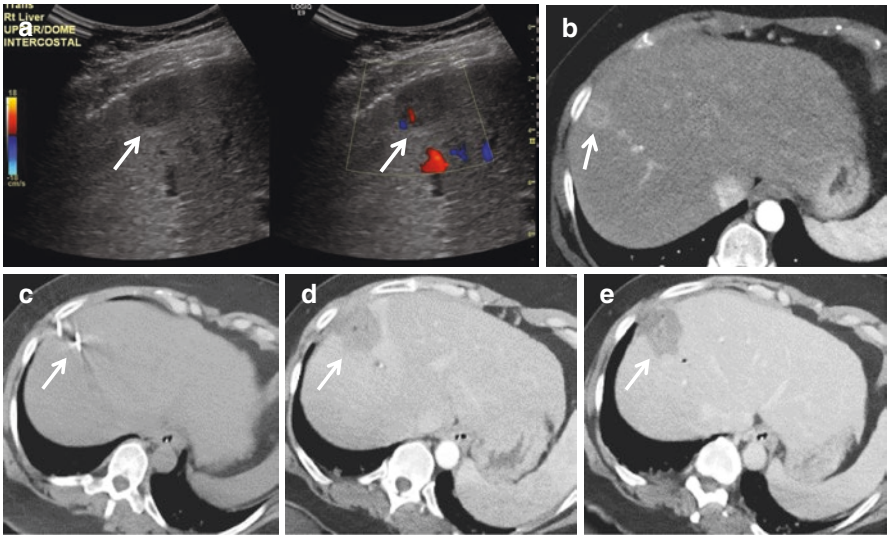

Fig. 2.13 Small mass-forming intrahepatic cholangiocarcinoma (iCCA) evaluated with ultrasound and CT and treated with percutaneous microwave ablation (MWA). (**a**) Grayscale and color Doppler ultrasound shows a small, well-circumscribed hypoechoic mass with mild vascularity (white arrow). (**b**) The mass shows peripheral enhancement on contrast-enhanced CT (white arrow). (**c**) The mass was treated with percutaneous microwave ablation using two microwave antennae (white arrow). (**d**, **e**) Immediate postablation contrast-enhanced CT shows the hypoechoic ablation zone encompassing the tumor without any residual enhancing tumor on (**d**) arterial or (**e**) portal venous phase (white arrow). CT computed tomography

Irreversible Electroporation (IRE)

Percutaneous irreversible electroporation (IRE) is a nonthermal-based ablation treatment option that induces pores in cell membranes, leading to cell death by complex mechanisms. Few reports have demonstrated the safety, feasibility, and early local tumor control of image-guided percutaneous IRE in patients with iCCA and pCCA [123, 124]. Currently, there is an ongoing phase I/II multicenter trial of ablation with IRE in patients with advanced pCCA [125].

Transarterial Chemoembolization (TACE) and Radioembolization (TARE)

Transarterial chemoembolization (TACE) may be performed with drug-eluting beads (DEB-TACE) or with conventional embolic agents mixed with chemotherapeutics (cTACE). Transarterial radioembolization (TARE) is performed with yttrium-90 (Y90) beta-emitting radioactive glass or resin microspheres (Fig. 2.14). DEB-TACE, cTACE, and Y90-TARE have all been shown to be safe and effective

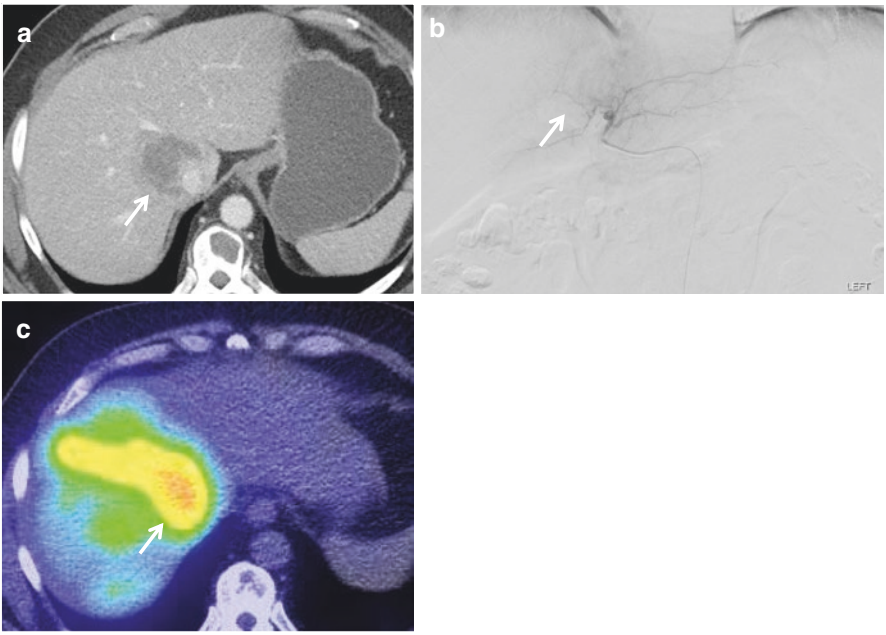

Fig. 2.14 Large mass-forming intrahepatic CCA with hepatic vein invasion evaluated with CT and catheter angiography and treated with transarterial radioembolization (TARE). The mass in the central superior right hepatic lobe shows (**a**) minimal central enhancement on contrast-enhanced CT (white arrow) and (**b**) mild enhancement on selective right hepatic arteriogram (white arrow). The mass was treated with yttrium-90 (Y90) transarterial radioembolization (TARE). (**c**) Post-Y90 SPECT/CT bremsstrahlung scan shows intense uptake within the tumor corresponding with the region of treated tumor. SPECT single-photon emission computed tomography, CT computed tomography

for treatment of unresectable CCA in the palliative setting. Median overall survival for TACE ranges from 12 to 15 months with an improved toxicity profile of DEB-TACE compared to cTACE [126–131]. Similarly, median overall survival for TARE ranges from 11 to 22 months [130, 132–135].

Radiation Therapy

External Beam Radiotherapy

External beam radiotherapy (EBRT) plays a role in the treatment of localized intrahepatic (iCCA) and extrahepatic (eCCA) cholangiocarcinoma. Advances in diagnostic imaging and EBRT planning and delivery allow for potential radiotherapy dose escalation and/or improved protection of normal tissues, which may improve the therapeutic ratio for treatment of CCA.

For patients with resected iCCA or eCCA and features suggestive of a high risk for local/regional recurrence, such as positive surgical margins and/or regional lymph node involvement, postoperative EBRT with concurrent chemotherapy has been utilized, with suggestion of benefit in reducing risk of recurrence and possible improvement in survival [136]. A recent multi-institutional phase II trial evaluated the safety and efficacy of an adjuvant therapy regimen for resected eCCA consisting of initial gemcitabine and capecitabine for 3 months, followed by EBRT (52.5–59.4 Gray in 25–33 fractions) with concurrent capecitabine [137]. The regimen was reasonably well tolerated and associated with promising efficacy, with 2-year overall and disease-free survival of 68% and 54%, respectively. Local/regional recurrence was uncommon, and the most common pattern of recurrence was distant metastasis.

For patients with early stage but unresectable perihilar CCA, a novel treatment approach has been utilized in select patients, consisting of preoperative EBRT (45 Gy in 30 fractions delivered twice per day over 3 weeks) with concurrent 5-flurouracil chemotherapy, followed by intracavitary bile duct brachytherapy, maintenance chemotherapy, and orthotopic liver transplantation. Favorable outcomes have been reported from Mayo Clinic and other institutions [116].

For patients with localized, unresectable iCCA, focal high-dose EBRT, using conformal, hypofractionated photon, or proton techniques, has emerged as a safe and efficacious treatment approach (Fig. 2.15). In a multi-institution phase II trial conducted in the United States, 37 patients with localized, unresectable iCCA were treated with high-dose focal proton beam radiotherapy (median dose 58.05 Gy in 15 fractions). The median overall survival was 22.5 months, and the 2-year local control rate was 94% [138].

For patients with localized eCCA not amenable to resection or liver transplantation, EBRT with concurrent chemotherapy may provide modest benefit in overall survival [139].

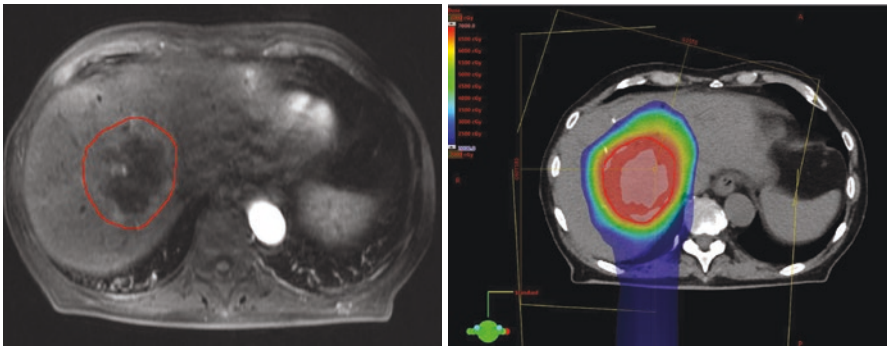

Fig. 2.15 Patient with an unresectable 8-cm central intrahepatic cholangiocarcinoma (red outline) treated with proton beam radiotherapy (67.5 Gy in 15 fractions over 3 weeks). The blue indicates the volume receiving 20 Gy or higher, and the red indicates the volume receiving 67.5 Gy or higher

Chemotherapy and Other Targeted Therapies

Most patients with biliary tract cancers (BTCs) present with advanced stage disease and are only candidates for systemic therapy. Gemcitabine combined with cisplatin has emerged as a standard-of-care regimen for patients with advanced BTCs [140]. Here, we summarize recent advances in systemic and targeted therapies for the treatment of BTCs.

Taxanes have emerged as a class of cytotoxic therapies with promising efficacy in BTCs. In a single-arm Phase 2 clinical study, gemcitabine in combination with nab-paclitaxel yielded a response rate of 30%, progression-free survival (PFS) of 7.7 months, and overall survival (OS) of 12.4 months [141]. A parallel, single-arm Phase 2 trial using a triplet combination of gemcitabine, cisplatin, and nab-paclitaxel (GAP) demonstrated a response rate of 45%, PFS of 11.8 months, and OS of 19.2 months [142]. These promising data have formed the basis for a prospective, multicenter Phase 3 study comparing the GAP triplet to standard-of-care gemcitabine/cisplatin (S1815, NCT03768414) [143]. Similarly, gemcitabine has been tested in combination with fluoropyrimidines using agents such as S-1 (response rate: 15.8%, PFS: 5.8 months, OS: 15.9 months) [144] or capecitabine (PFS: 8 months, OS: 13 months) [145]. Definitive Phase 3 studies comparing these regimens have not been conducted. Nevertheless, these preliminary data are encouraging and provide alternatives for patients who are not suitable for or are found to be intolerant of platinum-based regimens. For patients who progress or have intolerance while on first-line therapies, a Phase 3 trial of modified FOLFOX (5-FU, leucovorin, oxaliplatin) versus best supportive care (ABC-06, NCT01926236) showed a benefit for the combination over best supportive care, and is currently considered the standard of care in the second-line [146].

While therapies that are currently in use in advanced BTCs largely comprise empirical use of cytotoxic therapies, precision medicine has been an area of increasing investigation. Genomic profiling of cancers has become feasible on a large scale, and initial application has been in the context of therapy selection for patients with advanced disease. Tractable targets include receptor tyrosine kinases such as fibroblast growth factor 2 (FGFR2) fusions, HER2/neu amplifications/mutations, epidermal growth factor receptor amplifications/mutations, and MET amplifications. Mutations in the metabolic enzymes isocitrate dehydrogenase 1 and 2 (IDH1/IDH2), RAS/RAF pathway (KRAS/NRAS mutations, BRAF mutations), PI3K-mTOR signaling pathway, and chromatin modifiers have also been observed.

Oncogenic fusions of FGFR2 with other proteins have been found predominantly in patients with iCCA at a frequency of ~10–15%. In this group of patients, promising clinical efficacy has been observed with a number of FGFR small molecule kinase inhibitors. These include infigratinib (BGJ398), derazantinib, and pemigatinib, which have exhibited response rates of 14–48% in single-arm Phase 2 studies [147–149]. Class effects have included hyperphosphatemia, rash, and eye toxicities. Resistance mechanisms are a subject of intense investigation. Emergence of gatekeeper, polyclonal mutations has been observed [150]. In April 2020 pemigatinib was approved by the US FDA for previously treated unresectable locally advanced or metastatic CCA with an FGFR2 fusion or other rearrangement.

Drugs targeting IDH1 (ivosidenib) and IDH2 (enasidenib) are approved for clinical use in patients with acute myeloid leukemia bearing these alterations. IDH1 mutations occur at a frequency of approximately 10–15% in patients with iCCA, predominantly in codon 132 [151]. IDH2 mutations are less common (~5%) and are typically seen in codon 172. In an early-phase clinical trial with ivosidenib (AG-120), a response rate of 6% and 6-month PFS of 40% were observed [152]. This led to a pivotal Phase 3 trial (ClarIDHy, NCT02989857) which demonstrated a significant improvement in progression free survival in patients with advanced IDH1 mutant CCA who had progressed on previous treatment (median 2.7 months [95% CI 1.6–4.2] vs 1.4 months [1.4–1.6]; hazard ratio 0.37; 95% CI 0.25–0.54; one-sided $p < 0.0001$) [153].

While not separately approved for use in advanced BTCs, tumor-agnostic drug approvals have provided a mechanism for rapid availability of promising therapies with genetic alterations amenable to therapeutic intervention. Currently, this includes pembrolizumab in patients with microsatellite instability (MSI-high) or mismatch repair deficiency (MMR). Patients with MSI-high or MMR exhibited deep and durable responses to pembrolizumab, irrespective of the organ of origin of the tumor [154]. Similarly, patients with fusions involving NTRK1, NTRK2, or NTRK3 who received larotrectinib experienced durable tumor-agnostic responses [155]. Both of these trials included patients with advanced BTCs. The prevalence of both sets of markers is only 2–3% in advanced BTC patients, but due the durability of the responses seen, the data are felt to be meaningful in nature.

As highlighted, advances in novel cytotoxic combinations, precision medicine, and immunotherapies are transforming the care of patients with advanced BTCs.

References

1. Fitzmaurice C, Akinyemiju TF, Al Lami FH, Alam T, Alizadeh-Navaei R, Allen C, et al. Global, regional, and national cancer incidence, mortality, years of life lost, years lived with disability, and disability-adjusted life-years for 29 cancer groups, 1990 to 2016. JAMA Oncol. 2018;4(11):1553–68. https://doi.org/10.1001/jamaoncol.2018.2706.
2. Lee YM, Kaplan MM. Primary sclerosing cholangitis. N Engl J Med. 1995;332(14):924–33. https://doi.org/10.1056/NEJM199504063321406.
3. Bergquist A, Ekbom A, Olsson R, Kornfeldt D, Loof L, Danielsson A, et al. Hepatic and extrahepatic malignancies in primary sclerosing cholangitis. J Hepatol. 2002;36(3):321–7. https://doi.org/10.1016/s0168-8278(01)00288-4.
4. Burak K, Angulo P, Pasha TM, Egan K, Petz J, Lindor KD. Incidence and risk factors for cholangiocarcinoma in primary sclerosing cholangitis. Am J Gastroenterol. 2004;99(3):523–6. https://doi.org/10.1111/j.1572-0241.2004.04067.x.
5. Boberg KM, Bergquist A, Mitchell S, Pares A, Rosina F, Broome U, et al. Cholangiocarcinoma in primary sclerosing cholangitis: risk factors and clinical presentation. Scand J Gastroenterol. 2002;37(10):1205–11.
6. Bergquist A, Glaumann H, Persson B, Broome U. Risk factors and clinical presentation of hepatobiliary carcinoma in patients with primary sclerosing cholangitis: a case-control study. Hepatology. 1998;27(2):311–6.

7. Chapman MH, Webster GJM, Bannoo S, Johnson GJ, Wittmann J, Pereira SP. Cholangiocarcinoma and dominant strictures in patients with primary sclerosing cholangitis. Eur J Gastroenterol Hepatol. 2012;24(9):1051–8.
8. Chapman R, Fevery J, Kalloo A, Nagorney DM, Boberg KM, Shneider B, et al. Diagnosis and management of primary sclerosing cholangitis. Hepatology. 2010;51(2):660–78.
9. Razumilava N, Gores GJ. Surveillance for cholangiocarcinoma in patients with primary sclerosing cholangitis: effective and justified? Clin Liver Dis. 2016;8(2):43–7.
10. Vogel A, Wege H, Caca K, Nashan B, Neumann U. The diagnosis and treatment of cholangiocarcinoma. Dtsch Arztebl Int. 2014;111(44):748–54.
11. Jarnagin WR, Fong Y, DeMatteo RP, Gonen M, Burke EC, Bodniewicz BS J, et al. Staging, resectability, and outcome in 225 patients with hilar cholangiocarcinoma. Ann Surg. 2001;234(4):507–17; discussion 517–9.
12. Hennedige TP, Neo WT, Venkatesh SK. Imaging of malignancies of the biliary tract- an update. Cancer Imaging. 2014;14:14.
13. Razumilava N, Gores GJ. Classification, diagnosis, and management of cholangiocarcinoma. Clin Gastroenterol Hepatol. 2013;11(1):13–21.e1; quiz e3–4.
14. Rizvi S, Khan SA, Hallemeier CL, Kelley RK, Gores GJ. Cholangiocarcinoma — evolving concepts and therapeutic strategies. Nat Rev Clin Oncol. 018;15(2):95–111.
15. Yamasaki S. Intrahepatic cholangiocarcinoma: macroscopic type and stage classification. J Hepatobiliary Pancreat Surg. 2003;10(4):288–91.
16. Sandrasegaran K, Menias CO. Imaging and screening of cancer of the gallbladder and bile ducts. Radiol Clin North Am. 2017;55(6):1211–22.
17. Nathan H, Aloia TA, Vauthey J-N, Abdalla EK, Zhu AX, Schulick RD, et al. A proposed staging system for intrahepatic cholangiocarcinoma. Ann Surg Oncol. 2009;16(1):14–22.
18. Chung YE, Kim MJ, Park YN, Choi JY, Pyo JY, Kim YC, et al. Varying appearances of cholangiocarcinoma: radiologic-pathologic correlation. Radiographics. 2009;29(3):683–700.
19. Ros PR, Buck JL, Goodman ZD, Ros AM, Olmsted WW. Intrahepatic cholangiocarcinoma: radiologic-pathologic correlation. Radiology. 1988;167(3):689–93.
20. Lim JH. Cholangiocarcinoma: morphologic classification according to growth pattern and imaging findings. Am J Roentgenol. 2003;181(3):819–27.
21. Vilana R, Forner A, Bianchi L, García-Criado Á, Rimola J, Rodríguez de Lope C, et al. Intrahepatic peripheral cholangiocarcinoma in cirrhosis patients may display a vascular pattern similar to hepatocellular carcinoma on contrast-enhanced ultrasound. Hepatology. 2010;51(6):2020–9.
22. Wildner D, Pfeifer L, Goertz R, Bernatik T, Sturm J, Neurath M, et al. Dynamic contrast-enhanced ultrasound (DCE-US) for the characterization of hepatocellular carcinoma and cholangiocellular carcinoma. Ultraschall der Medizin - Eur J Ultrasound. 2014;35(06):522–7.
23. Bruix J, Sherman M. Management of hepatocellular carcinoma: an update. Hepatology. 2011;53(3):1020–2.
24. Loyer EM, Chin H, DuBrow RA, David CL, Eftekhari F, Charnsangavej C. Hepatocellular carcinoma and intrahepatic peripheral cholangiocarcinoma: enhancement patterns with quadruple phase helical CT—A comparative study. Radiology. 1999;212(3):866–75.
25. Fábrega-Foster K, Ghasabeh MA, Pawlik TM, Kamel IR. Multimodality imaging of intrahepatic cholangiocarcinoma. HepatoBiliary Surg Nutr. 2017;6(2):67–78.
26. Sainani NI, Catalano OA, Holalkere N-S, Zhu AX, Hahn PF, Sahani D V. Cholangiocarcinoma: current and novel imaging techniques. RadioGraphics. 2008;28(5):1263–87.
27. Joo I, Lee JM, Yoon JH. Imaging diagnosis of intrahepatic and perihilar cholangiocarcinoma: recent advances and challenges. Radiology. 2018;288(1):7–13.
28. Kim TK, Choi BI, Han JK, Jang HJ, Cho SG, Han MC. Peripheral cholangiocarcinoma of the liver: two-phase spiral CT findings. Radiology. 1997;204(2):539–43.
29. Iavarone M, Piscaglia F, Vavassori S, Galassi M, Sangiovanni A, Venerandi L, et al. Contrast enhanced CT-scan to diagnose intrahepatic cholangiocarcinoma in patients with cirrhosis. J Hepatol. 2013;58(6):1188–93.

30. Lacomis JM, Baron RL, Oliver JH, Nalesnik MA, Federle MP. Cholangiocarcinoma: delayed CT contrast enhancement patterns. Radiology. 1997;203(1):98–104.
31. Wells ML, Venkatesh SK, Chandan VS, Fidler JL, Fletcher JG, Johnson GB, et al. Biphenotypic hepatic tumors: imaging findings and review of literature. Abdom Imaging. 2015;40(7):2293–305.
32. Kim R, Lee JM, Shin C-I, Lee ES, Yoon JH, Joo I, et al. Differentiation of intrahepatic mass-forming cholangiocarcinoma from hepatocellular carcinoma on gadoxetic acid-enhanced liver MR imaging. Eur Radiol. 2016;26(6):1808–17.
33. Park HJ, Kim YK, Park MJ, Lee WJ. Small intrahepatic mass-forming cholangiocarcinoma: target sign on diffusion-weighted imaging for differentiation from hepatocellular carcinoma. Abdom Imaging. 2013;38(4):793–801.
34. Kim SH, Lee CH, Kim BH, Kim WB, Yeom SK, Kim KA, et al. Typical and atypical imaging findings of intrahepatic cholangiocarcinoma using gadolinium ethoxybenzyl diethylenetriamine pentaacetic acid–enhanced magnetic resonance imaging. J Comput Assist Tomogr. 2012;36(6):704–9.
35. Ringe KI, Husarik DB, Sirlin CB, Merkle EM. Gadoxetate disodium–enhanced MRI of the liver: part 1, protocol optimization and lesion appearance in the noncirrhotic liver. Am J Roentgenol. 2010;195(1):13–28.
36. Vilgrain V. Staging cholangiocarcinoma by imaging studies. HPB. 2008;10(2):106–9.
37. Hu J-H, Tang J, Lin C-H, Chu Y-Y, Liu N-J. Preoperative staging of cholangiocarcinoma and biliary carcinoma using 18F-fluorodeoxyglucose positron emission tomography: a meta-analysis. J Investig Med. 2018;66(1):52–61.
38. Ma KW, Cheung TT, She WH, Chok KSH, Chan ACY, Dai WC, et al. Diagnostic and prognostic role of 18-FDG PET/CT in the management of resectable biliary tract cancer. World J Surg. 2018;42(3):823–34.
39. Yoh T, Seo S, Morino K, Fuji H, Ikeno Y, Ishii T, et al. Reappraisal of prognostic impact of tumor SUVmax by 18F-FDG-PET/CT in intrahepatic cholangiocarcinoma. World J Surg. 2019;43(5):1323–31.
40. Sabaté-Llobera A, Gràcia-Sánchez L, Reynés-Llompart G, Ramos E, Lladó L, Robles J, et al. Differences on metabolic behavior between intra and extrahepatic cholangiocarcinomas at 18F-FDG–PET/CT: prognostic implication of metabolic parameters and tumor markers. Clin Transl Oncol. 2019;21(3):324–33.
41. Cleary SP, Dawson LA, Knox JJ, Gallinger S. Cancer of the gallbladder and extrahepatic bile ducts. Curr Probl Surg. 2007;44(7):396–482.
42. Lim JH, Yoon K-H, Kim SH, Kim HY, Lim HK, Song SY, et al. Intraductal papillary mucinous tumor of the bile ducts. RadioGraphics. 2004;24(1):53–66.
43. Choi BI, Lee JM, Han JK. Imaging of intrahepatic and hilar cholangiocarcinoma. Abdom Imaging. 2004;29(5):548–57.
44. Slattery JM. What is the current state-of-the-art imaging for detection and staging of cholangiocarcinoma? Oncologist. 2006;11(8):913–22.
45. Sharma MP, Ahuja V. Aetiological spectrum of obstructive jaundice and diagnostic ability of ultrasonography: a clinician's perspective. Trop Gastroenterol. 1999;20(4):167–9.
46. Choi J-Y, Kim M-J, Lee JM, Kim KW, Lee JY, Han JK, et al. Hilar cholangiocarcinoma: role of preoperative imaging with sonography, MDCT, MRI, and direct cholangiography. Am J Roentgenol. 2008;191(5):1448–57.
47. Lee HY, Kim SH, Lee JM, Kim S-W, Jang J-Y, Han JK, et al. Preoperative assessment of resectability of hepatic hilar cholangiocarcinoma: combined CT and cholangiography with revised criteria. Radiology. 2006;239(1):113–21.
48. Seale MK, Catalano OA, Saini S, Hahn PF, Sahani D V. Hepatobiliary-specific MR contrast agents: role in imaging the liver and biliary tree. RadioGraphics. 2009;29(6):1725–48.
49. Manfredi R, Masselli G, Maresca G, Brizi MG, Vecchioli A, Marano P. MR imaging and MRCP of hilar cholangiocarcinoma. Abdom Imaging. 2003;28(3):319–25.

50. Hänninen EL, Pech M, Jonas S, Ricke J, Thelen A, Langrehr J, et al. Magnetic resonance imaging including magnetic resonance cholangiopancreatography for tumor localization and therapy planning in malignant hilar obstructions. Acta Radiol. 2005;46(5):462–70.
51. Masselli G, Manfredi R, Vecchioli A, Gualdi G. MR imaging and MR cholangiopancreatography in the preoperative evaluation of hilar cholangiocarcinoma: correlation with surgical and pathologic findings. Eur Radiol. 2008;18(10):2213–21.
52. Lee M-G, Park KB, Shin YM, Yoon HK, Sung KB, Kim MH, et al. Preoperative evaluation of hilar cholangiocarcinoma with contrast-enhanced three-dimensional fast imaging with steady-state precession magnetic resonance angiography: comparison with intraarterial digital subtraction angiography. World J Surg. 2003;27(3):278–83.
53. Ruys AT, van Beem BE, Engelbrecht MRW, Bipat S, Stoker J, Van Gulik TM. Radiological staging in patients with hilar cholangiocarcinoma: a systematic review and meta-analysis. Br J Radiol. 2012;85(1017):1255–62.
54. Anderson MA, Appalaneni V, Ben-Menachem T, Decker GA, Early DS, Evans JA, et al. The role of endoscopy in the evaluation and treatment of patients with biliary neoplasia. Gastrointest Endosc. 2013;77(2):167–74.
55. Saad WEA, Wallace MJ, Wojak JC, Kundu S, Cardella JF. Quality improvement guidelines for percutaneous transhepatic cholangiography, biliary drainage, and percutaneous cholecystostomy. J Vasc Interv Radiol. 2010;21(6):789–95.
56. Park M-S, Kim TK, Kim KW, Park SW, Lee JK, Kim J-S, et al. Differentiation of extrahepatic bile duct cholangiocarcinoma from benign stricture: findings at MRCP versus ERCP. Radiology. 2004;233(1):234–40.
57. Al Mahjoub A, Menahem B, Fohlen A, Dupont B, Alves A, Launoy G, et al. Preoperative biliary drainage in patients with resectable perihilar cholangiocarcinoma: is percutaneous transhepatic biliary drainage safer and more effective than endoscopic biliary drainage? A meta-analysis. J Vasc Interv Radiol. 2017;28(4):576–82.
58. Nguyen K, James T Sing Jr. Review of endoscopic techniques in the diagnosis and management of cholangiocarcinoma. World J Gastroenterol. 2008;14(19):2995-9.
59. Sasaki A, Aramaki M, Kawano K, Morii Y, Nakashima K, Yoshida T, et al. Intrahepatic peripheral cholangiocarcinoma: mode of spread and choice of surgical treatment. Br J Surg. 1998;85(9):1206–9.
60. Shimada K, Sano T, Sakamoto Y, Esaki M, Kosuge T, Ojima H. Surgical outcomes of the mass-forming plus periductal infiltrating types of intrahepatic cholangiocarcinoma: a comparative study with the typical mass-forming type of intrahepatic cholangiocarcinoma. World J Surg. 2007;31(10):2016–22.
61. Kajiyama K, Maeda T, Takenaka K, Sugimachi K, Tsuneyoshi M. The significance of stromal desmoplasia in intrahepatic cholangiocarcinoma: a special reference of “scirrhous-type” and “nonscirrhous-type” growth. Am J Surg Pathol. 1999;23(8):892–902.
62. Shiota K, Taguchi J, Nakashima O, Nakashima M, Kojiro M. Clinicopathologic study on cholangiolocellular carcinoma. Oncol Rep. 2001;8(2):263-8.
63. Nakajima T, Kondo Y, Miyazaki M, Okui K. A histopathologic study of 102 cases of intrahepatic cholangiocarcinoma: histologic classification and modes of spreading. Hum Pathol. 1988;19(10):1228–34.
64. Chow LT, Ahuja AT, Kwong KH, Fung KS, Lai CK, Lau JW. Mucinous cholangiocarcinoma: an unusual complication of hepatolithiasis and recurrent pyogenic cholangitis. Histopathology. 1997;30(5):491–4.
65. Shimonishi T, Miyazaki K, Nakanuma Y. Cytokeratin profile relates to histological subtypes and intrahepatic location of intrahepatic cholangiocarcinoma and primary sites of metastatic adenocarcinoma of liver. Histopathology. 2000;37(1):55–63.
66. Tsou Y-K, Wu R-C, Hung C-F, Lee C-S. Intrahepatic sarcomatoid cholangiocarcinoma: clinical analysis of seven cases during a 15-year period. Chang Gung Med J. 2008;31(6):599–605.
67. Craig JR, Peters RL, Edmondson HA AFI of P, (U.S.) O. Tumors of the liver and intrahepatic bile ducts. Armed Forces Inst Pathol Supt Docs, US GPO.

68. Haas S, Gütgemann I, Wolff M, Fischer H-P. Intrahepatic clear cell cholangiocarcinoma: immunohistochemical aspects in a very rare type of cholangiocarcinoma. Am J Surg Pathol. 2007;31(6):902–6.
69. Isa T, Kusano T, Muto Y, Furukawa M, Kiyuna M, Toda T. Clinicopathologic features of resected primary adenosquamous carcinomas of the liver. J Clin Gastroenterol. 1997;25(4):623–7.
70. Maeda T, Takenaka K, Taguchi K, Kajiyama K, Shirabe K, Shimada M, et al. Adenosquamous carcinoma of the liver: clinicopathologic characteristics and cytokeratin profile. Cancer. 1997;80(3):364–71.
71. Takahashi H, Hayakawa H, Tanaka M, Okamura K, Kosaka A, Mizumoto R, et al. Primary adenosquamous carcinoma of liver resected by right trisegmentectomy: report of a case and review of the literature. J Gastroenterol. 1997;32(6):843–7.
72. Sasaki M, Nakanuma Y, Nagai Y, Nonomura A. Intrahepatic cholangiocarcinoma with sarcomatous transformation: an autopsy case. J Clin Gastroenterol. 1991;13(2):220–5.
73. Komuta M, Spee B, Vander Borght S, De Vos R, Verslype C, Aerts R, et al. Clinicopathological study on cholangiolocellular carcinoma suggesting hepatic progenitor cell origin. Hepatology. 2008;47(5):1544–56.
74. 74. Bloustein PA, Silverberg SG. Squamous cell carcinoma originating in an hepatic cyst. Case report with a review of the hepatic cyst-carcinoma association. Cancer. 1976;38(5):2002–5.
75. Gresham GA, Rue LW. Squamous cell carcinoma of the liver. Hum Pathol. 1985;16(4):413–6.
76. Lynch MJ, McLeod MK, Weatherbee L, Gilsdorf JR, Guice KS, Eckhauser FE. Squamous cell cancer of the liver arising from a solitary benign nonparasitic hepatic cyst. Am J Gastroenterol. 1988;83(4):426–31.
77. Pliskin A, Cualing H, Stenger RJ. Primary squamous cell carcinoma originating in congenital cysts of the liver. Report of a case and review of the literature. Arch Pathol Lab Med. 1992;116(1):105–7.
78. Kanamoto M, Yoshizumi T, Ikegami T, Imura S, Morine Y, Ikemoto T, et al. Cholangiolocellular carcinoma containing hepatocellular carcinoma and cholangiocellular carcinoma, extremely rare tumor of the liver: a case report. J Med Invest. 2008;55(1–2):161–5.
79. Theise ND, Saxena R, Portmann BC, Thung SN, Yee H, Chiriboga L, et al. The canals of Hering and hepatic stem cells in humans. Hepatology. 1999;30(6):1425–33.
80. Nakanuma Y, Sasaki M, Ikeda H, Sato Y, Zen Y, Kosaka K, et al. Pathology of peripheral intrahepatic cholangiocarcinoma with reference to tumorigenesis. Hepatol Res. 2008;38(4):325–34.
81. Nakanuma Y, Sato Y, Harada K, Sasaki M, Xu J, Ikeda H. Pathological classification of intrahepatic cholangiocarcinoma based on a new concept. World J Hepatol. 2010;2(12):419–27.
82. Nakanuma Y, Sato Y, Ikeda H, Harada K, Kobayashi M, Sano K, et al. Intrahepatic cholangiocarcinoma with predominant “ductal plate malformation” pattern: a new subtype. Am J Surg Pathol. 2012;36(11):1629–35.
83. Jeng YM, Chen CL, Hsu HC. Lymphoepithelioma-like cholangiocarcinoma: an Epstein-Barr virus-associated tumor. Am J Surg Pathol. 2001;25(4):516–20.
84. Chen TC, Ng KF, Kuo TT. Intrahepatic cholangiocarcinoma with lymphoepithelioma-like component. Mod Pathol. 2001;14(5):527–32.
85. Terada T, Makimoto K, Terayama N, Suzuki Y, Nakanuma Y. Alpha-smooth muscle actin-positive stromal cells in cholangiocarcinomas, hepatocellular carcinomas and metastatic liver carcinomas. J Hepatol. 1996;24(6):706–12.
86. Edge SB, Compton CC. The American Joint Committee on Cancer: the 7th edition of the AJCC cancer staging manual and the future of TNM. Ann Surg Oncol. 2010;17:1471–4.
87. Khan SA, Davidson BR, Goldin RD, Heaton N, Karani J, Pereira SP, et al. Guidelines for the diagnosis and treatment of cholangiocarcinoma: an update. Gut. 2012;61(12):1657–69.
88. Nuzzo G, Giuliante F, Ardito F, De Rose AM, Vellone M, Clemente G, et al. Intrahepatic cholangiocarcinoma: prognostic factors after liver resection. Updates Surg. 2010;62(1):11–9.
89. Chan ES, Yeh MM. The use of immunohistochemistry in liver tumors. Clin Liver Dis. 2010;14(4):687–703.

90. Rullier A, Le Bail B, Fawaz R, Blanc JF, Saric J, Bioulac-Sage P. Cytokeratin 7 and 20 expression in cholangiocarcinomas varies along the biliary tract but still differs from that in colorectal carcinoma metastasis. Am J Surg Pathol. 2000;24(6):870–6.
91. Kozaka K, Sasaki M, Fujii T, Harada K, Zen Y, Sato Y, et al. A subgroup of intrahepatic cholangiocarcinoma with an infiltrating replacement growth pattern and a resemblance to reactive proliferating bile ductules: "bile ductular carcinoma". Histopathology. 2007;51(3):390–400.
92. Ferrone CR, Ting DT, Shahid M, Konstantinidis IT, Sabbatino F, Goyal L, et al. The ability to diagnose intrahepatic cholangiocarcinoma definitively using novel branched DNA-enhanced albumin RNA in situ hybridization technology. Ann Surg Oncol. 2016;23(1):290–6.
93. Volmar KE, Vollmer RT, Routbort MJ, Creager AJ. Pancreatic and bile duct brushing cytology in 1000 cases: review of findings and comparison of preparation methods. Cancer. 2006;108(4):231–8.
94. Fritcher EG, Kipp BR, Halling KC, Oberg TN, Bryant SC, Tarrell RF, et al. A multivariable model using advanced cytologic methods for the evaluation of indeterminate pancreatobiliary strictures. Gastroenterology. 2009;136(7):2180-6.
95. Barr Fritcher EG, Voss JS, Brankley SM, Campion MB, Jenkins SM, Keeney ME, et al. An optimized set of fluorescence in situ hybridization probes for detection of pancreatobiliary tract cancer in cytology brush samples. Gastroenterology. 2015;149(7):1813–1824.
96. Abbas S, Sandroussi C. Systematic review and meta-analysis of the role of vascular resection in the treatment of hilar cholangiocarcinoma. HPB (Oxford). 2013;15(7):492–503.
97. van Vugt JLA, Gaspersz MP, Coelen RJS, Vugts J, Labeur TA, de Jonge J, et al. The prognostic value of portal vein and hepatic artery involvement in patients with perihilar cholangiocarcinoma. HPB (Oxford). 2018;20(1):83–92.
98. Farges O, Regimbeau JM, Fuks D, Le Treut YP, Cherqui D, Bachellier P, et al. Multicentre European study of preoperative biliary drainage for hilar cholangiocarcinoma. Br J Surg. 2013;100(2):274–83.
99. Coelen RJS, Roos E, Wiggers JK, Besselink MG, Buis CI, Busch ORC, et al. Endoscopic versus percutaneous biliary drainage in patients with resectable perihilar cholangiocarcinoma: a multicentre, randomised controlled trial. Lancet Gastroenterol Hepatol. 2018;3(10):681–90.
100. Esposito F, Lim C, Lahat E, Shwaartz C, Eshkenazy R, Salloum C, et al. Combined hepatic and portal vein embolization as preparation for major hepatectomy: a systematic review. HPB (Oxford) 2019;21(9):1099-1106.
101. Nuzzo G, Giuliante F, Ardito F, Giovannini I, Aldrighetti L, Belli G, et al. Improvement in perioperative and long-term outcome after surgical treatment of hilar cholangiocarcinoma: results of an Italian multicenter analysis of 440 patients. Arch Surg. 2012;147(1):26–34.
102. Bird N, Elmasry M, Jones R, Elniel M, Kelly M, Palmer D, et al. Role of staging laparoscopy in the stratification of patients with perihilar cholangiocarcinoma. Br J Surg. 2017;104(4):418–25.
103. Weber SM, Ribero D, O'Reilly EM, Kokudo N, Miyazaki M, Pawlik TM. Intrahepatic cholangiocarcinoma: expert consensus statement. HPB (Oxford). 2015;17(8):669–80.
104. Buettner S, Ten Cate DWG, Bagante F, Alexandrescu S, Marques HP, Lamelas J, et al. Survival after resection of multiple tumor foci of intrahepatic cholangiocarcinoma. J Gastrointest Surg. 2019;23(11):2239-2246.
105. Conci S, Ruzzenente A, Viganò L, Ercolani G, Fontana A, Bagante F, et al. Patterns of distribution of hepatic nodules (single, satellites or multifocal) in intrahepatic cholangiocarcinoma: prognostic impact after surgery. Ann Surg Oncol. 2018;25(12):3719–27.
106. Sapisochin G, de Lope CR, Gastaca M, de Urbina JO, López-Andujar R, Palacios F, et al. Intrahepatic cholangiocarcinoma or mixed hepatocellular-cholangiocarcinoma in patients undergoing liver transplantation: a Spanish matched cohort multicenter study. Ann Surg. 2014;259(5):944–52.
107. Sapisochin G, Facciuto M, Rubbia-Brandt L, Marti J, Mehta N, Yao FY, et al. Liver transplantation for "very early" intrahepatic cholangiocarcinoma: international retrospective study supporting a prospective assessment. Hepatology 2016;64(4):1178–88. Sapisochin G,

Facciuto M, Rubbia-Brandt L, Marti J, Mehta N, Yao FY, et al. Liver transplantation for "very early" intrahepatic cholangiocarcinoma: international retrospective study supporting a prospective assessment. Hepatology. 2016;64(4):1178–88.
108. Lunsford KE, Javle M, Heyne K, Shroff RT, Abdel-Wahab R, Gupta N, et al. Liver transplantation for locally advanced intrahepatic cholangiocarcinoma treated with neoadjuvant therapy: a prospective case-series. Lancet Gastroenterol Hepatol. 2018;3(5):337–48.
109. Hartog H, Ijzermans JNM, van Gulik TM, Groot Koerkamp B. Resection of perihilar cholangiocarcinoma. Surg Clin North Am. 2016;96(2):247–67.
110. Nagino M, Ebata T, Yokoyama Y, Igami T, Sugawara G, Takahashi Y, et al. Evolution of surgical treatment for perihilar cholangiocarcinoma: a single-center 34-year review of 574 consecutive resections. Ann Surg. 2013;258(1):129–40.
111. Ebata T, Mizuno T, Yokoyama Y, Igami T, Sugawara G, Nagino M. Surgical resection for Bismuth type IV perihilar cholangiocarcinoma. Br J Surg. 2018;105(7):829–38.
112. Meyer CG, Penn I, James L. Liver transplantation for cholangiocarcinoma: results in 207 patients. Transplantation. 2000;69(8):1633–7.
113. Robles R, Figueras J, Turrión VS, Margarit C, Moya A, Varo E, et al. Spanish experience in liver transplantation for hilar and peripheral cholangiocarcinoma. Ann Surg. 2004;239:265–71.
114. Rea DJ, Heimbach JK, Rosen CB, Haddock MG, Alberts SR, Kremers WK, et al. Liver transplantation with neoadjuvant chemoradiation is more effective than resection for hilar cholangiocarcinoma. Ann Surg. 2005;242(3):451–8; discussion 458–61.
115. Sudan D, DeRoover A, Chinnakotla S, Fox I, Shaw B, McCashland T, et al. Radiochemotherapy and transplantation allow long-term survival for nonresectable hilar cholangiocarcinoma. Am J Transplant. 2002;2(8):774–9.
116. Darwish Murad S, Kim WR, Harnois DM, Douglas DD, Burton J, Kulik LM, et al. Efficacy of neoadjuvant chemoradiation, followed by liver transplantation, for perihilar cholangiocarcinoma at 12 US centers. Gastroenterology. 2012;143(1):88–98.e3.
117. Darwish Murad S, Kim WR, Therneau T, Gores GJ, Rosen CB, Martenson JA, et al. Predictors of pretransplant dropout and posttransplant recurrence in patients with perihilar cholangiocarcinoma. Hepatology. 2012;56(3):972–81.
118. Duignan S, Maguire D, Ravichand CS, Geoghegan J, Hoti E, Fennelly D, et al. Neoadjuvant chemoradiotherapy followed by liver transplantation for unresectable cholangiocarcinoma: a single-centre national experience. HPB. 2014;16(1):91–8.
119. Policies – OPTN [Internet]. [cited 2019 Aug 30]. Available from: https://optn.transplant.hrsa.gov/governance/policies
120. Ethun CG, Lopez-Aguiar AG, Anderson DJ, Adams AB, Fields RC, Doyle MB, et al. Transplantation versus resection for hilar cholangiocarcinoma: an argument for shifting treatment paradigms for resectable disease. Ann Surg. 2018;267(5):797–805.
121. Schreuder AM, Engelsman AF, van Roessel S, Verheij J, Besselink MG, van Gulik TM, et al. Treatment of mid-bile duct carcinoma: local resection or pancreatoduodenectomy? Eur J Surg Oncol. 2019;45(11):2180–7.
122. Takahashi EA, Kinsman KA, Schmit GD, Atwell TD, Schmitz JJ, Welch BT, et al. Thermal ablation of intrahepatic cholangiocarcinoma: safety, efficacy, and factors affecting local tumor progression. Abdom Radiol. 2018;43(12):3487–92.
123. Melenhorst MCAM, Scheffer HJ, Vroomen LGPH, Kazemier G, van den Tol MP, Meijerink MR. Percutaneous irreversible electroporation of unresectable hilar cholangiocarcinoma (Klatskin tumor): a case report. Cardiovasc Intervent Radiol. 2016;39(1):117–21.
124. Mafeld S, Wong JJ, Kibriya N, Stenberg B, Manas D, Bassett P, et al. Percutaneous irreversible electroporation (IRE) of hepatic malignancy: a bi-institutional analysis of safety and outcomes. Cardiovasc Intervent Radiol. 2019;42(4):577–83.
125. Coelen RJS, Vogel JA, Vroomen LGPH, Roos E, Busch ORC, van Delden OM, et al. Ablation with irreversible electroporation in patients with advanced perihilar cholangiocarcinoma (ALPACA): a multicentre phase I/II feasibility study protocol. BMJ Open. 2017;7(9):e015810.

126. Kiefer M V., Albert M, McNally M, Robertson M, Sun W, Fraker D, et al. Chemoembolization of intrahepatic cholangiocarcinoma with cisplatinum, doxorubicin, mitomycin C, ethiodol, and polyvinyl alcohol. Cancer. 2011;117(7):1498–505.
127. Park S-Y, Kim JH, Yoon H-J, Lee I-S, Yoon H-K, Kim K-P. Transarterial chemoembolization versus supportive therapy in the palliative treatment of unresectable intrahepatic cholangiocarcinoma. Clin Radiol. 2011;66(4):322–8.
128. Vogl TJ, Naguib NNN, Nour-Eldin N-EA, Bechstein WO, Zeuzem S, Trojan J, et al. Transarterial chemoembolization in the treatment of patients with unresectable cholangiocarcinoma: results and prognostic factors governing treatment success. Int J Cancer 2012;131(3):733–40.
129. Kuhlmann JB, Euringer W, Spangenberg HC, Breidert M, Blum HE, Harder J, et al. Treatment of unresectable cholangiocarcinoma. Eur J Gastroenterol Hepatol. 2012;24(4):437-43.
130. Boehm LM, Jayakrishnan TT, Miura JT, Zacharias AJ, Johnston FM, Turaga KK, et al. Comparative effectiveness of hepatic artery based therapies for unresectable intrahepatic cholangiocarcinoma. J Surg Oncol. 2015;111(2):213–20.
131. Aliberti C, Carandina R, Sarti D, Pizzirani E, Ramondo G, Mulazzani L, et al. Chemoembolization with drug-eluting microspheres loaded with doxorubicin for the treatment of cholangiocarcinoma. Anticancer Res. 2017;37(4):1859–63.
132. Hoffmann R-T, Paprottka PM, Schön A, Bamberg F, Haug A, Dürr E-M, et al. Transarterial hepatic yttrium-90 radioembolization in patients with unresectable intrahepatic cholangiocarcinoma: factors associated with prolonged survival. Cardiovasc Intervent Radiol. 2012;35(1):105–16.
133. Rafi S, Piduru SM, El-Rayes B, Kauh JS, Kooby DA, Sarmiento JM, et al. Yttrium-90 radioembolization for unresectable standard-chemorefractory intrahepatic cholangiocarcinoma: survival, efficacy, and safety study. Cardiovasc Intervent Radiol. 2013;36(2):440–8.
134. Mosconi C, Gramenzi A, Ascanio S, Cappelli A, Renzulli M, Pettinato C, et al. Yttrium-90 radioembolization for unresectable/recurrent intrahepatic cholangiocarcinoma: a survival, efficacy and safety study. Br J Cancer. 2016;115(3):297–302.
135. Reimer P, Virarkar MK, Binnenhei M, Justinger M, Schön MR, Tatsch K. Prognostic factors in overall survival of patients with unresectable intrahepatic cholangiocarcinoma treated by means of yttrium-90 radioembolization: results in therapy-naïve patients. Cardiovasc Intervent Radiol. 2018;41(5):744–52.
136. Horgan AM, Amir E, Walter T, Knox JJ. Adjuvant therapy in the treatment of biliary tract cancer: a systematic review and meta-analysis. J Clin Oncol. 2012;30(16):1934–40.
137. El-Khoueiry AB, Rankin CJ, Ben-Josef E, Lenz HJ, Gold PJ, Hamilton RD, et al. SWOG 0514: a phase II study of sorafenib in patients with unresectable or metastatic gallbladder carcinoma and cholangiocarcinoma. Investig New Drugs. 2012;30(4):1646–51.
138. Hong TS, Wo JY, Yeap BY, Ben-Josef E, McDonnell EI, Blaszkowsky LS, et al. Multi-institutional phase II study of high-dose hypofractionated proton beam therapy in patients with localized, unresectable hepatocellular carcinoma and intrahepatic cholangiocarcinoma. J Clin Oncol. 2016;34(5):460–8.
139. Torgeson A, Lloyd S, Boothe D, Cannon G, Garrido-Laguna I, Whisenant J, et al. Chemoradiation therapy for unresected extrahepatic cholangiocarcinoma: a propensity score-matched analysis. Ann Surg Oncol. 2017;24(13):4001–8.
140. Valle J, Wasan H, Palmer DH, Cunningham D, Anthoney A, Maraveyas A, et al. Cisplatin plus gemcitabine versus gemcitabine for biliary tract Cancer. N Engl J Med. 2010;362(14):1273–81.
141. Sahai V, Catalano PJ, Zalupski MM, Lubner SJ, Menge MR, Nimeiri HS, et al. Nab-paclitaxel and gemcitabine as first-line treatment of advanced or metastatic cholangiocarcinoma. JAMA Oncol. 2018;4(12):1707.
142. Shroff RT, Javle MM, Xiao L, Kaseb AO, Varadhachary GR, Wolff RA, et al. Gemcitabine, cisplatin, and nab-paclitaxel for the treatment of advanced biliary tract cancers: a phase 2 clinical trial. JAMA Oncol. 2019;5(6):824-830.

143. Gemcitabine hydrochloride and cisplatin with or without nab-paclitaxel in treating patients with newly diagnosed advanced biliary tract cancers - ClinicalTrials.gov. [cited 2019 May 13]. Available from: https://clinicaltrials.gov/ct2/show/NCT03768414
144. Arima S, Shimizu K, Okamoto T, Toki M, Suzuki Y, Okano N, et al. A multicenter phase II study of gemcitabine plus S-1 chemotherapy for advanced biliary tract Cancer. Anticancer Res. 2017;37(2):909–14.
145. Gabriel E, Gandhi S, Attwood K, Kuvshinoff B, Hochwald S, Iyer R. Gemcitabine and capecitabine for advanced biliary cancer. J Gastrointest Oncol. 2017;8(4):728–36.
146. Lamarca A, Palmer DH, Wasan HS, Ross PJ, Ma YT, Arora A, et al. ABC-06 | A randomised phase III, multi-centre, open-label study of active symptom control (ASC) alone or ASC with oxaliplatin/5-FU chemotherapy (ASC+mFOLFOX) for patients (pts) with locally advanced/metastatic biliary tract cancers (ABC) previouslytreated with cisplatin/gemcitabine (CisGem) chemotherapy. Journal of Clinical Oncology. 2019;37(15_suppl):4003–4003.
147. Mazzaferro V, El-Rayes BF, Droz Dit Busset M, Cotsoglou C, Harris WP, Damjanov N, et al. Derazantinib (ARQ 087) in advanced or inoperable FGFR2 gene fusion-positive intrahepatic cholangiocarcinoma. Br J Cancer. 2019;120(2):165–71.
148. Javle M, Lowery M, Shroff RT, Weiss KH, Springfeld C, Borad MJ, et al. Phase II study of BGJ398 in patients with FGFR-altered advanced cholangiocarcinoma. J Clin Oncol. 2018;36(3):276–82.
149. Abou-Alfa GK, Sahai V, Hollebecque A, Vaccaro G, Melisi D, Al-Rajabi R, et al. Pemigatinib for previously treated, locally advanced or metastatic cholangiocarcinoma: a multicentre, open-label, phase 2 study. Lancet Oncol. 2020;21(5):671–84.
150. Goyal L, Saha SK, Liu LY, Siravegna G, Leshchiner I, Ahronian LG, et al. Polyclonal secondary FGFR2 mutations drive acquired resistance to FGFR inhibition in patients with FGFR2 fusion-positive cholangiocarcinoma. Cancer Discov. 2017;7(3):252–63.
151. Kipp BR, Voss JS, Kerr SE, Barr Fritcher EG, Graham RP, Zhang L, et al. Isocitrate dehydrogenase 1 and 2 mutations in cholangiocarcinoma. Hum Pathol. 2012;43(10):1552–8.
152. Lowery MA, Abou-Alfa GK, Burris HA, Janku F, Shroff RT, Cleary JM, et al. Phase I study of AG-120, an IDH1 mutant enzyme inhibitor: results from the cholangiocarcinoma dose escalation and expansion cohorts. J Clin Oncol. 2017;35(15_suppl):4015–4015.
153. Abou-Alfa GK, Macarulla T, Javle MM, Kelley RK, Lubner SJ, Adeva J, et al. Ivosidenib in IDH1-mutant, chemotherapy-refractory cholangiocarcinoma (ClarIDHy): a multicentre, randomised, double-blind, placebo-controlled, phase 3 study. Lancet Oncol. 2020;21(6):796-807.
154. Le DT, Durham JN, Smith KN, Wang H, Bartlett BR, Aulakh LK, et al. Mismatch repair deficiency predicts response of solid tumors to PD-1 blockade. Science. 2017;357(6349):409–13.
155. Drilon A, Laetsch TW, Kummar S, DuBois SG, Lassen UN, Demetri GD, et al. Efficacy of larotrectinib in TRK fusion-positive cancers in adults and children. N Engl J Med. 2018;378(8):731–9.

Chapter 3
Biphenotypic Tumors

Vishal Chandan, Michael L. Wells, and Kabir Mody

Epidemiology of Combined HCC-CCA

Primary liver cancer is broadly recognized as a spectrum marked by hepatocellular carcinoma (HCC) at one end, intrahepatic cholangiocarcinoma (iCCA) at the other end, and biphenotypic or combined hepatocellular-cholangiocarcinoma (cHCC-CCA) in the middle [1]. Classical HCC demonstrates hepatocytic differentiation while the CCA shows cholangiocytic differentiation. Primary liver cancers with features of both hepatocytic and cholangiocytic differentiation that do not completely fit cytologically or architecturally into either the HCC or CCA category have been broadly categorized as "mixed" or "combined" HCC-CCA. They have also been called "biphenotypic" primary liver cancers, combined liver and bile duct carcinoma, or hepato-cholangiocarcinoma [2, 3]. The term "collision tumor" is discouraged.

The most recent edition of the World Health Organization (WHO) classification of tumors of the digestive system defines cHCC-CCA as a tumor composed of an unequivocal mixture of both HCC and CCA [4]. They should have two distinct morphologies evident on the Hematoxylin and Eosin (H&E) stain, one of HCC and

V. Chandan (✉)
Department of Pathology and Laboratory Medicine, University of California-Irvine, Irvine, CA, USA
e-mail: vchandan@hs.uci.edu

M. L. Wells
Department of Radiology, Mayo Clinic, Rochester, MN, USA
e-mail: wells.michael@mayo.edu

K. Mody
Division of Hematology/Oncology, Department of Medicine, Mayo Clinic, Jacksonville, FL, USA
e-mail: mody.kabir@mayo.edu

L. R. Roberts et al. (eds.), *Evaluation and Management of Liver Masses*,
https://doi.org/10.1007/978-3-030-46699-2_3

one of CCA. The two components can be found as adjacent nodules or areas within the same tumor, sometimes even with a transition zone.

The first case of a biphenotypic hepatic tumor was reported in 1903 [5]. The frequency of cHCC-CCA is about 1–6% of all primary liver cancers [6–10]. Patients with cHCC-CCA have a similar median age (of 62 years) compared with HCC (median age of 61 years) but are younger than those with CCA (median age 67 years) [11]. cHCC-CCA is seen more frequently in males than females [11]. The overall risk factors for cHCC-CCA are similar to those of conventional HCC such as viral hepatitis B and C as well as cirrhosis of any cause.

Pathology of Combined HCC-CCA

cHCC-CCA tumors can develop in both cirrhotic and non-cirrhotic livers [7, 10, 12]. Approximately 80% are unifocal while 20% are multifocal [8, 13–15]. Most cHCC-CCA tumors measure between 5 and 10 cm in greatest dimension at the time of diagnosis [11]. A diagnosis of cHCC-CCA requires that both the HCC and CCA components are present in one nodule or in immediately adjacent nodules. Cases in which the liver shows HCC and CCA but in clearly separate nodules with intervening normal liver should be classified as double primaries and not as cHCC-CCA.

cHCC-CCA tumors must show the two distinct HCC and CCA morphologies on the H&E stained sections. Morphological features of HCC include the presence of trabecular or pseudo-acinar architecture with neoplastic cells showing similarity to normal liver cells up to a variable extent (hepatocytic differentiation) (Fig. 3.1a). Bile production may also be seen within this component. Features of CCA include acinar or glandular architecture similar to an adenocarcinoma, often with a desmoplastic stromal reaction (Fig. 3.1b). The two components may be intermixed or may be seen in separate regions of the same tumor. There are no published consensus guidelines for the minimum proportions of HCC or CCA to make the diagnosis of cHCC-CCA on either biopsy or resection specimens [16]. A recent study has shown that recurrent and/or metastatic cHCC-CCA can show a wide range of histomorphological patterns, replicating the heterogeneity of the primary tumor [17]. The originally minute foci of divergent differentiation in the primary tumor can become predominant later on. Hence, histological comparison between the primary liver tumor and their metastatic deposits can be informative and should be included in the management of patients with metastatic cHCC-CCA.

Special stains should be used only to confirm the H&E impression. The HCC component is positive for typical markers of hepatocellular differentiation such as HepPar1, arginase-1, and glypican 3 (Fig. 3.1c, d). The CCA is positive for biliary type keratins such as CK7 and CK19 and negative for markers of hepatocellular differentiation (Fig. 3.1e, f). Mucin production may also be seen in the CCA but is not a requirement. A diagnosis of cHCC-CCA should not be based on immunohistochemical findings only, without morphological correlation. The diagnosis of cHCC-CCA can be challenging on a needle core biopsy as it depends on the area of

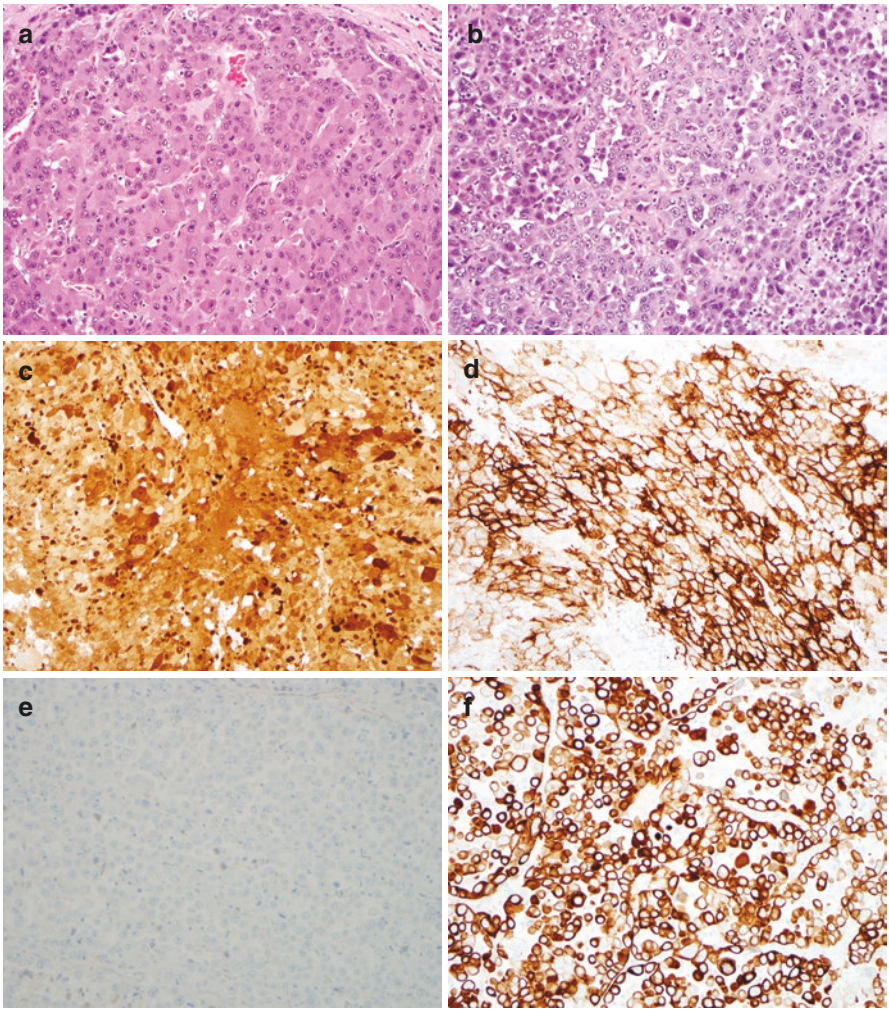

Fig. 3.1 Histology of biphenotypic tumor. Hepatocellular carcinoma component showing trabecular arrangement of the tumor cells with typical hepatocellular carcinoma morphology (**a**). Cholangiocarcinoma component within the same tumor showing a glandular architecture (**b**). Arginase-1 immunostain showing positivity within the hepatocellular carcinoma component of the tumor (**c**). Glypican-3 immunostain is also positive within the hepatocellular carcinoma component of the tumor (**d**). Arginase-1 immunostain is negative within the cholangiocarcinoma component (**e**). Cytokeratin 7 immunostain is positive within the cholangiocarcinoma component (**f**)

the tumor sampled [18]. The true histopathology may only be confirmed after the evaluation of a resected surgical specimen. This clearly may create difficulties in the evaluation of unresectable cHCC-CCAs.

The current WHO classification divides cHCC-CCA into two subcategories: classic cHCC-CCA and cHCC-CCA with stem cell features when morphological

and/or immunophenotypical features of stem/progenitor cells predominate within the tumor [4]. The stem cell type is further subdivided into three subtypes, namely, typical subtype, intermediate–cell subtype, and cholangiolocellular subtype. The first two subtypes are associated with areas of hepatic differentiation, whereas the cholangiolocellular subtype shows CCA differentiation. Dense intratumoral fibrosis is a common finding in all subtypes. However, recent work has shown that stem cell phenotypes can be seen in other forms of primary liver cancers and hence these different WHO categories are not clearly separable [19, 20]. It is also now recommended that there should no longer be formal diagnostic subtypes of cHCC-CCA based on the identification of stem/progenitor cells [16].

Molecular studies, although limited in number, have highlighted significant heterogeneity within these tumors [21–23]. A stem cell that differentiates into both hepatocytes and bile duct epithelial cells is suspected to be the cell of origin for these tumors [24–28]. Molecular studies have shown that cHCC-CCA shares some traits with HCC and others with CCA, supporting its status as a distinct entity [21, 29–31].

The reported 3-year and 5-year overall survival rates range between 11–47% and 10–40% for cHCC-CCA [3]. Its prognosis falls in between that of CCA and HCC and is reportedly worse than that of conventional HCC [9]. A recent retrospective review of the National Cancer Data Base (NCDB) showed the unadjusted median overall survival for cHCC-CCA to be 7.9 months [11]. Some studies have shown the overall prognosis of cHCC-CCA to be similar to that of CCA, but this is debatable as other studies have shown variable outcomes [9, 13, 32]. cHCC-CCA has a higher rate of recurrence after resection and liver transplantation [33, 34]. In the recent 8th edition AJCC staging system, cHCC-CCA is staged using the CCA protocol [35]. This is not unreasonable as the CCA component appears to drive the worse prognosis of these tumors.

Imaging of Combined HCC-CCA

Combined HCC-CCA liver tumors contain cellular and architectural elements of both HCC and CCA. These lesions consequently have a spectrum of imaging appearances including lesions with typical imaging findings of HCC, some with an appearance typical of CCA, and others with a mixture of features. The dominant histologic component tends to determine the appearance of the mass at imaging [36–40].

Combined HCC-CCA tumors most commonly resemble intrahepatic mass-forming CCA or a metastasis at imaging [41]. These masses characteristically have the greatest cellularity at the periphery of the lesion and a fibrous component centrally, which may result in a targetoid appearance at cross-sectional imaging. The masses are hypoattenuating to background liver at computed tomography (CT) and T2 hyperintense and T1 hypointense at magnetic resonance imaging (MRI) [41]. At

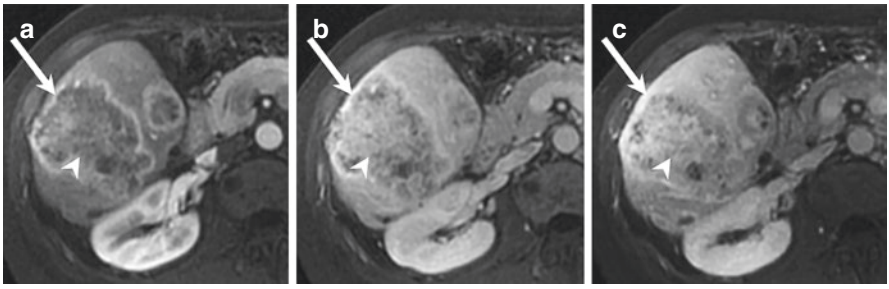

Fig. 3.2 cHCC-CCA with imaging appearance resembling cholangiocarcinoma. (**a**) T1-weighted fat saturated MRI image demonstrates a mass with continuous peripheral late arterial hyperenhancement (arrow) and heterogenous hypointensity centrally (arrowhead). (**b**) Portal venous and (**c**) delayed phase images show the fade of the peripheral enhancement to near iso-intensity with the adjacent liver (**b**, **c**, arrows) and progressively increasing central enhancement (**b**, **c**, arrowheads)

dynamic contrast-enhanced CT or MRI, the peripheral portion of the tumor enhances in the late arterial or portal venous phase of imaging (Fig. 3.2). On subsequent phases the peripheral enhancement may fade to a degree similar to the surrounding parenchyma or may demonstrate a washout appearance and become hypoattenuating (CT) or hypointense (MRI). The central component initially enhances poorly in the late arterial phase, but as injected contrast material equilibrates to the extravascular, extracellular space, there is progressively greater enhancement in the delayed phases. Combined HCC-CCA cannot be reliably differentiated from CCA by imaging alone; however, imaging features reported to be suggestive of cHCC-CCA tumor in a mass which otherwise resembles CCA include: strong arterial phase enhancement, washout, lipid content, hemorrhage, and venous tumor thrombus [41, 42].

The cHCC-CCA tumors most likely to demonstrate an imaging pattern similar to HCC have a predominance of the HCC histologic subtype [36, 37, 39, 40, 43]. The tumors may demonstrate characteristic imaging findings of HCC, including late arterial phase hyperenhancement, portal venous and/or delayed phase washout, and capsule appearance (Fig. 3.3) [41]. These tumors may also have additional findings associated with HCC including mosaic architecture, lipid content, or venous invasion [44]. It has been reported that up to 30–40% of biphenotypic tumors may have an imaging appearance mimicking HCC, and prior studies have confirmed the difficulty in differentiating the two based on imaging [42, 45, 46]. This is particularly problematic for patients at risk for HCC in whom imaging criteria may be used to make a definitive diagnosis before instituting therapy. Tumors demonstrating enhancement features potentially representative of HCC by traditional OPTN criteria can be referred for inappropriate therapy, including transplant [41, 45]. Fortunately, many cHCC-CCA with enhancement characteristics similar to HCC will also demonstrate American College of Radiology, Liver Imaging and Reporting Data System (LIRADS) ancillary findings favoring non-HCC malignancy. These

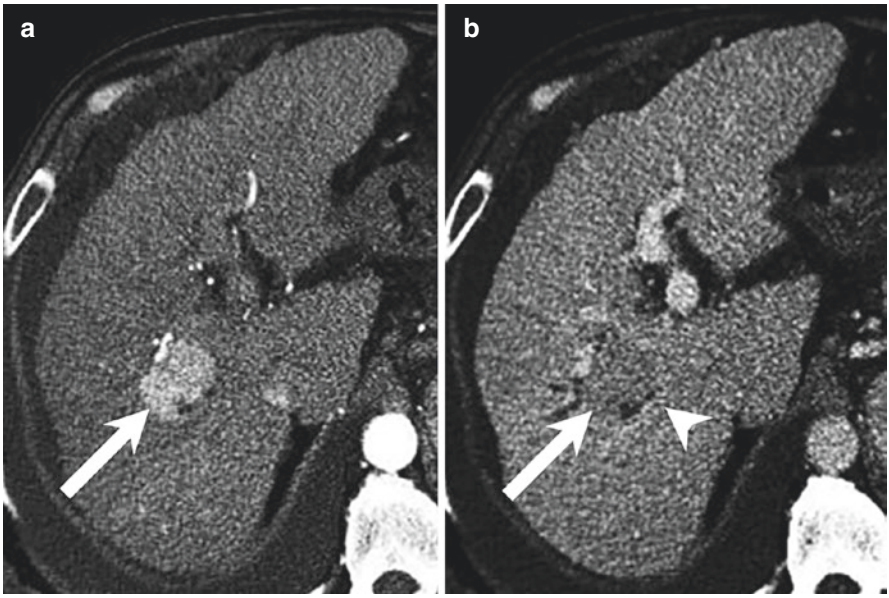

Fig. 3.3 cHCC-CCA with imaging appearance resembling HCC. (**a**) Late arterial phase CT image demonstrates a homogenously hyperenhancing mass (arrow). (**b**) Portal venous phase image shows the lesion becoming hypoattenuating when compared with the adjacent liver (arrow) consistent with a washout appearance. A subtle hyperattenuating capsule appearance is also seen at the periphery of the lesion (arrowhead)

ancillary findings are important for maintaining specificity for the diagnosis of HCC, and they include: peripheral pattern of enhancement/washout, biliary obstruction out of proportion to size of the mass, progressive central enhancement, liver capsular retraction, or marked restricted diffusion [41, 45, 46].

Combined HCC-CCA may demonstrate imaging findings typical of CCA and HCC in separate regions within a single mass (Fig. 3.4). This imaging pattern is uncommon but is highly suggestive of a cHCC-CCA tumor. The imaging pattern must also be carefully scrutinized for evidence of a collision tumor, as HCC and CCA which originate separately within the same liver but grow into one another are not considered a cHCC-CCA by WHO criteria [47].

Ultrasound and positron emission tomography (PET) may also be used to evaluate cHCC-CCA tumors. A tumor may be initially discovered at ultrasound. Unfortunately, routine grayscale and Doppler ultrasound findings are not specific and are unable to diagnose a cHCC-CCA tumor [41]. Ultrasound may be helpful for identifying important secondary findings such as biliary ductal obstruction or vascular tumor thrombus. Limited information is available regarding the PET-CT features of cHCC-CCA [41, 48, 49]. PET-CT has a limited role in diagnosis of HCC and CCA due to variable lesion tracer activity and relatively high background liver activity [50, 51]. When imaged with F-18 labeled fluorodeoxyglucose, cHCC-CCA

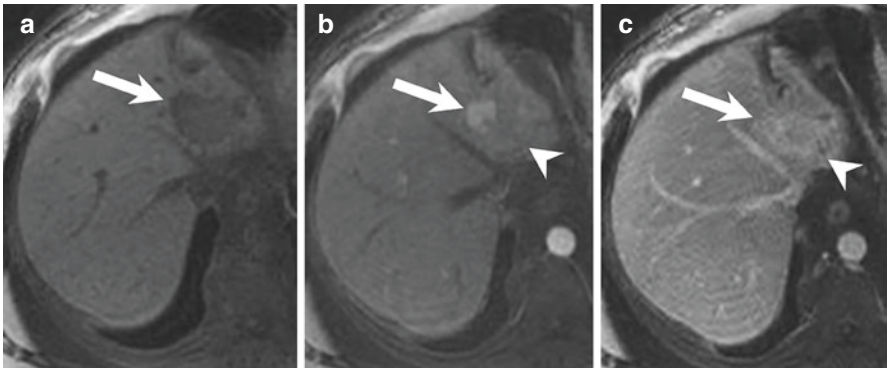

Fig. 3.4 cHCC-CCA with mixed imaging features of both HCC and CCA. (**a**) Precontrast T1-weighted fat saturated MRI image shows a hypoattenuating hepatic lesion (arrow). (**b**) Late arterial phase image demonstrates a nodular region of hyperenhancement (arrow), while the larger portion of the tumor has become iso-attenuating when compared with the adjacent liver (arrowhead). (**c**) Delayed phase image shows subtle washout of the previously hyperenhancing component of the tumor (arrow). The remainder of the tumor has become progressively more intense (arrowhead)

tumors have been reported to demonstrate marked hypermetabolism with high standard uptake values. This suggests a possible role for PET-CT for initial diagnosis, staging, or follow-up after treatment.

A comparison of cross-sectional imaging findings with laboratory values may be helpful for diagnosis. Serum markers including C19-9, which is associated with cholangiocarcinoma and alpha fetoprotein (AFP), which is associated with HCC, can be a helpful adjunct to image interpretation when they are elevated. Combined HCC-CCA tumor should be included in the differential diagnosis when the cross-sectional imaging findings are consistent with hepatocellular carcinoma, but there is elevation of the serum CA 19-9. Conversely, imaging findings consistent with CCA or metastasis in the setting of an elevated AFP are also suggestive of a cHCC-CCA tumor.

Management of Combined HCC-CCA

There are no clear guidelines with regard to the management of cHCC-CCA. As is the case with other malignancies of the liver, surgical resection is the only treatment offering the possibility of a cure. However, many patients present with disease too advanced for surgical management, and their disease is, given the paucity of any trials dedicated to the management specifically of cHCC-CCA, managed via therapeutic strategies utilized in the management of either HCC or ICC alone.

Surgery

Surgical management strategies remain the sole modality associated with a possibility of cure for patients with cHCC-CCA. Eligibility for surgery in this unique population of patients hinges on a number of factors including underlying cirrhosis, the patient's general medical condition, tumor extent, and local anatomic conditions. Complete surgical excision with negative margins and limited impingement upon liver function is the ultimate goal of therapy. Severe liver dysfunction, of course, predicts a poor prognosis, regardless of the success of the actual procedure, and usually precludes resection.

In one series from a Western academic medical center, 78% of patients seen with cHCC-CCA were eligible for surgical resection [10]. This high proportion may have been due in part to referral bias, but nevertheless, it showed that many cHCC-CCAs may be eligible for resection with curative intent. cHCC-CCA tends to behave like HCC with respect to portal and hepatic venous infiltration and like CCA with regard to lymph node metastasis [52]. In autopsy studies, lymph node metastases have been observed in 76% of patients with cHCC-CCA [53]. Comparatively, lymph node metastases were present in only 30% of HCC patients and 69% of CCA patients [53]. Hence, hilar lymph node dissection is recommended as part of the surgical management of cHCC-CCA. However, the prognostic benefit of lymphadenectomy for cHCC-CCA remains controversial [54–57]. Also of significance and an open question for investigation is whether the addition of neoadjuvant or adjuvant systemic chemotherapy overall and, also more specifically, in patients undergoing lymph node dissection improves prognosis.

A unique consideration in the management of patients with liver cancers in general is that of the underlying liver disease. For cirrhotic patients, given their reduced functional reserve, hepatic resection has the potential for debilitating complications, so the adoption of strict selection criteria is imperative to avoid significant perioperative and overall morbidity and mortality due to post-operative liver decompensation [58].

Data regarding survival outcomes with non-transplant surgical management of cHCC-CCA has come mostly in the form of retrospective case series. Generally, 5-year overall survival has ranged between 24% and 31% while disease-free survival at 3 years ranges between 26% and 41% [59–62]. One study also carefully evaluated whether a difference in survival outcomes existed based on the predominance of the CCA component and found no such difference [59]. Differences in outcomes have also been evaluated among the three liver malignancies (HCC, cHCC-CCA, and CCA), and it has been noted that post-resection tumor recurrence rates do not differ significantly, whereas differences in survival rates have been significant, with a median survival after tumor recurrence of 51, 8, and 6 months, respectively, reflecting the general propensity of cHCC-CCA to behave in a similar manner to CCA [60].

Liver Transplantation

The role of liver transplantation in the treatment of HCC is well established as an effective option for patients with HCC, generally guided by the Milan criteria [63]. Contrary to this, the role of transplantation for cHCC-CCA is undefined and controversial at this time, primarily because of the high rate of tumor recurrence and variable survival outcomes [64, 65].

Data regarding survival outcomes of cHCC-CCA patients treated with liver transplantation is limited and has come mostly in the form of retrospective studies. Overall, 3- and 5-year overall survival rates reported in the existing literature have ranged between 39–78% and 16–78%, respectively [8, 61, 66–70]. Disease free survival at 3 and 5 years in the existing literature has ranged between 30–47% and 28–45%, respectively [61, 69–71]. Recurrence rates within 5 years of transplant have ranged between 32% and 60% [71–73].

To come to a consensus on the role of transplant for cHCC-CCA, comparing outcomes to those of transplant for HCC has been done in a number of studies, though most have been small single institution studies. Lunsford et al. sought to compare post-transplant oncologic outcomes for cHCC-CCA to a matched cohort of HCC liver transplant recipients in a retrospective, single-center analysis of 12 patients with cHCC-CCA diagnosed on explant pathology. When matched to an HCC cohort with similar explant pathology, cHCC-CCA had similar 5-year disease-free survival (42% vs 44%, $P = 0.45$) but trended toward higher post-transplant recurrence (50% vs 27%, $P = 0.13$) [71]. Another study evaluated 42 patients undergoing a transplant for HCC but with a diagnosis of cHCC-CCA or iCCA on pathologic evaluation. Compared to a control group of 84 patients with HCC, no differences in 1-, 3-, and 5-year actuarial survival rates were observed between the cHCC-CCA subgroup and the HCC controls [67]. Another group reported their experience with living donor liver transplantation for cHCC-CCA from a cohort of 710 patients at a single institution. Of this group, 377 of them received transplantation for HCC and 11 patients were diagnosed with cHCC-CCA pathologically in the explant livers. Outcomes for patients with cHCC-CCA undergoing transplant were worse than outcomes for those with HCC [69]. The Mayo Clinic group also retrospectively reviewed their experience in 12 patients with a finding of cHCC-CCA post-transplant. They noted that 5-year survival was comparable to or better than liver transplantation for iCCA, but poorer than for HCC patients who met the Milan criteria [66]. In a departure from other studies, Vilchez and colleagues utilized data from a much bigger sample size, 4049 patients in the United Network for Organ Sharing (UNOS) database, to compare outcomes in patients undergoing liver transplantation for cHCC-CCA versus patients with HCC or iCCA in a retrospective analysis. Of this group 94 had cHCC-CCA, 3515 HCC, and 440 iCCA. Overall survival rates at 1, 3 and 5 years for cHCC-CCA were similar to the rates for iCCA, but significantly worse than for HCC [74].

Comparisons of outcomes with resection versus liver transplantation for cHCC-CCA have also been carried out, but again, the data is sparse and

conflicting. Jung et al. evaluated the long-term outcomes following liver transplantation and hepatic resection for cHCC-CCA in 32 patients. Tumor recurrence and survival rates did not differ significantly between the transplant and resection groups [73]. Groeschl et al. questioned the benefit of transplantation, compared with resection, for patients with cHCC-CCA and evaluated a much larger sample size, 3378 patients, with localized HCC or cHCC-CCA treated with surgical resection or transplant identified using the Surveillance, Epidemiology, and End Results (SEER) database. Of this group, 43% received liver transplants and 57% resection, including 54 patients with cHCC-CCA, of whom 35% were transplanted and 65% resected. Transplantation for localized cHCC-CCA conferred a survival benefit similar to liver resection for cHCC-CCA. Patients undergoing resection of HCC and cHCC-CCA had similar 3-year overall survival; however 3-year overall survival for patients undergoing transplant was significantly greater for HCC (78%) than for cHCC-CCA (48%) [8]. These results suggest that cHCC-CCA generally have more aggressive biology and worse outcomes than HCC, with outcomes that are more similar to the outcomes for iCCA. However, the generation of additional robust data evaluating liver transplantation in the management of cHCC-CCA is an area of unmet clinical need.

Locoregional Therapies

Locoregional treatments, such as transarterial chemoembolization and radioembolization, are some of the most widely used treatments for HCC [75, 76]. Data for the outcomes of these embolic therapies in the management of cHCC-CCA is lacking, however. cHCC-CCA tumors with a substantial CCA component may be less vascular and more fibrotic than HCC and thus may be less responsive to embolic therapies. Chan et al. demonstrated radioembolization to be a safe and promising treatment option, albeit in a small cohort of patients. Patients with histopathologically confirmed cHCC-CCA treated with radioembolization were retrospectively evaluated. Ten patients with unresectable cHCC-CCA underwent 14 radioembolization treatments with resin ($n = 6$) or glass ($n = 4$ patients) microspheres. Clinical toxicities were limited to grade 1–2 fatigue, anorexia, nausea, or abdominal pain. Median overall survival from the first radioembolization treatment and from initial diagnosis was 10.2 and 17.7 months, respectively. Best radiological response was 60% partial response and 40% stable disease by mRECIST criteria [77].

Ablation-based treatments are also a possible option for the treatment of disease recurrence in select patients [78]. Patients who are unresectable due to locally advanced disease or those with local recurrence may also be candidates for palliative stereotactic body radiation therapy with or without concomitant chemotherapy. Symptomatic and local tumor control has been reported with such treatment [52, 79].

Systemic Therapy

For those patients with advanced disease, systemic chemotherapy may be an option. However, there is no clear standard therapeutic strategy or regimen for the management of this cohort of patients with cHCC-CCA. Additionally, response rates reported thus far have been low [80–82]. Recently, data reporting experiences with systemic therapy have provided more updated outcomes data with newer therapeutics. One group reported on 39 cases of recurrent unresectable or metastatic cHCC-CCA. In 28 patients, first-line systemic therapy included: gemcitabine or 5-fluorouracil monotherapy (18%), chemotherapy (43%), sorafenib (29%), or clinical trials (11%). Six patients who received chemotherapy also received sorafenib. The median progression free survival (PFS) and overall survival (OS) from the time of first systemic treatment were 2.4 and 10 months, respectively. The median PFS for monotherapy, sorafenib, chemotherapy, and chemotherapy + sorafenib were 1.8, 3.1, 4.5, and 8.2 months, respectively. Overall survival favored chemotherapy + sorafenib with median OS of 1.8, 7.6, 8.4, and 14.7 months (Log rank $p = 0.01$), respectively [81]. Rogers et al. reported on 7 patients who received first-line sorafenib (3 patients), gemcitabine plus bevacizumab (2 patients), gemcitabine alone (1 patient), and gemcitabine plus cisplatin (1 patient). Progressive disease at first reimaging was seen in 71% of patients. Front-line treatment showed a median PFS of just 3.4 months. Of the 3 patients who received second-line therapy, a median PFS of 6.5 months was noted with regimens such as gemcitabine plus oxaliplatin (1 patient), gemcitabine plus oxaliplatin plus bevacizumab (1 patient), and fluorouracil plus leucovorin plus irinotecan (FOLFIRI) (1 patient). The group concluded, albeit in this small cohort, that all patients who received a platinum (cisplatin or oxaliplatin) in combination with gemcitabine during their disease course showed disease control and an impressive median OS of 11.7 months, compared with a median OS for the entire cohort of 8.3 months, regardless of the timing of the therapy [83].

In the era of genomics and precision medicine, with novel therapies being approved for HCC and with significant strides made in therapeutically important genomic subtyping of cholangiocarcinoma in recent years, an understanding of the unique molecular profile underpinning the pathogenesis of cHCC-CCA is critical. Such information is generally lacking thus far. One study sought to identify genetic and gene expression alterations in cHCC-CCA versus iCCA in a Chinese population. Analyses were performed on 10 iCCA and 10 cHCC-CCA samples, each controlled by matched adjacent non-tumor liver tissue, and the results compared with datasets from The Cancer Genome Atlas (TCGA) project. Differences in mutational and transcriptional landscapes of cHCC-CCA and iCCA were clearly delineated [23]. Sasaki et al. specifically examined the mutational statuses of KRAS, IDH1 or IDH2 (IDH1/2), ARID1A, the TERT promoter, and TP53 and their relationships with clinicopathological features in 53 patients with cHCC-CCA. Mutations in TP53, the TERT promoter, ARID1A, IDH1/2, and KRAS were detected in 45.3%, 31.3%, 13.2%, 11.8%, and 7.5% of patients, respectively. TP53 mutations correlated with α-fetoprotein (AFP) positivity. TERT promoter mutations correlated with

hepatitis B etiology, female-predominance, an intermediate subtype-predominant histology, higher clinical stage, the presence of lymph node metastases, and previous therapy. ARID1A mutations correlated with alcoholic liver disease, smaller tumor size, a lower grade of coexistent HCC, and AFP positivity and were also associated with cholangiolocellular carcinoma subtype predominance. KRAS mutations correlated with high histological diversity scores and the presence of distant metastasis [84]. These initial observations suggest that there may be an opportunity to molecularly subclassify cHCC-CCA in a manner that allows better prediction of response to specific therapies and clinical outcomes.

Overall, with significant advances being made in the management of both HCC and iCCA and with advances in our ability to investigate the genomic changes underlying these diseases, our understanding of cHCC-CCA as a distinct entity is sure to grow and this should expand the repertoire of therapeutic options for patients with cHCC-CCA.

References

1. Brunt EM, Paradis V, Sempoux C, Theise ND. Biphenotypic (hepatobiliary) primary liver carcinomas: the work in progress. Hepat Oncol. 2015;2(3):255–73.
2. Allen RA, Lisa JR. Combined liver cell and bile duct carcinoma. Am J Pathol. 1949;25(4):647–55.
3. Gera S, Ettel M, Acosta-Gonzalez G, Xu R. Clinical features, histology, and histogenesis of combined hepatocellular-cholangiocarcinoma. World J Hepatol. 2017;9(6):300–9.
4. Theise ND, Nakashima O, Park YN, Nakanuma Y. Combined hepatocellular-cholangiocarcinoma. WHO classification of tumours of the digestive system. 2010:225-7.
5. Wells HG. Primary carcinoma of the liver. Am J Sci. 1903;126:403–17.
6. Garancini M, Goffredo P, Pagni F, Romano F, Roman S, Sosa JA, et al. Combined hepatocellular-cholangiocarcinoma: a population-level analysis of an uncommon primary liver tumor. Liver Transpl. 2014;20(8):952–9.
7. Chu KJ, Lu CD, Dong H, Fu XH, Zhang HW, Yao XP. Hepatitis B virus-related combined hepatocellular-cholangiocarcinoma: Clinicopathological and prognostic analysis of 390 cases. Eur J Gastroenterol Hepatol. 2014;26(2):192–9.
8. Groeschl RT, Turaga KK, Gamblin TC. Transplantation versus resection for patients with combined hepatocellular carcinoma-cholangiocarcinoma. J Surg Oncol. 2013;107(6):608–12.
9. Lee JH, Chung GE, Yu SJ, Hwang SY, Kim JS, Kim HY, et al. Long-term prognosis of combined hepatocellular and cholangiocarcinoma after curative resection comparison with hepatocellular carcinoma and cholangiocarcinoma. J Clin Gastroenterol. 2011;45(1):69–75.
10. Jarnagin WR, Weber S, Tickoo SK, Koea JB, Obiekwe S, Fong Y, et al. Combined hepatocellular and cholangiocarcinoma: demographic, clinical, and prognostic factors. Cancer. 2002;94(7):2040–6.
11. Bergquist JR, Groeschl RT, Ivanics T, Shubert CR, Habermann EB, Kendrick ML, et al. Mixed hepatocellular and cholangiocarcinoma: a rare tumor with a mix of parent phenotypic characteristics. HPB (Oxford). 2016;18(11):886–92.
12. Fowler KJ, Sheybani A, Parke Iii RA, Doherty S, Brunt EM, Chapman WC, et al. Combined hepatocellular and cholangiocarcinoma (biphenotypic) tumors: imaging features and diagnostic accuracy of contrast-enhanced CT and MRI. Am J Roentgenol. 2013;201(2):332–9.

13. Yin X, Zhang BH, Qiu SJ, Ren ZG, Zhou J, Chen XH, et al. Combined hepatocellular carcinoma and cholangiocarcinoma: clinical features, treatment modalities, and prognosis. Ann Surg Oncol. 2012;19(9):2869–76.
14. Kim SH, Park YN, Lim JH, Choi GH, Choi JS, Kim KS. Characteristics of combined hepatocelluar-cholangiocarcinoma and comparison with intrahepatic cholangiocarcinoma. Eur J Surg Oncol. 2014;40(8):976–81.
15. Song S, Moon HH, Lee S, Kim TS, Shin M, Kim JM, et al. Comparison between resection and transplantation in combined hepatocellular and cholangiocarcinoma. Transplant Proc. 2013;45(8):3041–6.
16. Brunt E, Aishima S, Clavien PA, Fowler K, Goodman Z, Gores G, et al. cHCC-CCA: consensus terminology for primary liver carcinomas with both hepatocytic and cholangiocytic differentation. Hepatology. 2018;68:113.
17. De Vito C, Sarker D, Ross P, Heaton N, Quaglia A. Histological heterogeneity in primary and metastatic classic combined hepatocellular-cholangiocarcinoma: a case series. Virchows Arch. 2017;471(5):619–29.
18. O'Connor K, Walsh JC, Schaeffer DF. Combined hepatocellular-cholangiocarcinoma (cHCC-CC): a distinct entity. Ann Hepatol. 2014;13(3):317–22.
19. Akiba J, Nakashima O, Hattori S, Tanikawa K, Takenaka M, Nakayama M, et al. Clinicopathologic analysis of combined hepatocellular-cholangiocarcinoma according to the latest who classification. Am J Surg Pathol. 2013;37(4):496–505.
20. Sasaki M, Sato H, Kakuda Y, Sato Y, Choi JH, Nakanuma Y. Clinicopathological significance of 'subtypes with stem-cell feature' in combined hepatocellular-cholangiocarcinoma. Liver Int. 2015;35(3):1024–35.
21. Coulouarn C, Cavard C, Rubbia-Brandt L, Audebourg A, Dumont F, Jacques S, et al. Combined hepatocellular-cholangiocarcinomas exhibit progenitor features and activation of Wnt and TGFβ signaling pathways. Carcinogenesis. 2012;33(9):1791–6.
22. Moeini A, Sia D, Zhang Z, Camprecios G, Stueck A, Dong H, et al. Mixed hepatocellular cholangiocarcinoma tumors: Cholangiolocellular carcinoma is a distinct molecular entity. J Hepatol. 2017;66(5):952–61.
23. Liu ZH, Lian BF, Dong QZ, Sun H, Wei JW, Sheng YY, et al. Whole-exome mutational and transcriptional landscapes of combined hepatocellular cholangiocarcinoma and intrahepatic cholangiocarcinoma reveal molecular diversity. Biochim Biophys Acta. 2018;1864(6 Pt B):2360–8.
24. Yeh MM. Pathology of combined hepatocellular-cholangiocarcinoma. J Gastroenterol Hepatol. 2010;25(9):1485–92.
25. Theise ND, Yao JL, Harada K, Hytiroglou P, Portmann B, Thung SN, et al. Hepatic 'stem cell' malignancies in adults: four cases. Histopathology. 2003;43(3):263–71.
26. Kim H, Park C, Han KH, Choi J, Kim YB, Kim JK, et al. Primary liver carcinoma of intermediate (hepatocyte-cholangiocyte) phenotype. J Hepatol. 2004;40(2):298–304.
27. Itoyama M, Hata M, Yamanegi K, Yamada N, Ohyama H, Hirano H, et al. Expression of both hepatocellular carcinoma and cholangiocarcinoma phenotypes in hepatocellular carcinoma and cholangiocarcinoma components in combined hepatocellular and cholangiocarcinoma. Med Mol Morphol. 2012;45(1):7–13.
28. Ogasawara S, Akiba J, Nakayama M, Nakashima O, Torimura T, Yano H. Epithelial cell adhesion molecule-positive human hepatic neoplastic cells: development of combined hepatocellular-cholangiocarcinoma in mice. J Gastroenterol Hepatol. 2015;30(2):413–20.
29. Xue TC, Zhang BH, Ye SL, Ren ZG. Differentially expressed gene profiles of intrahepatic cholangiocarcinoma, hepatocellular carcinoma, and combined hepatocellular-cholangiocarcinoma by integrated microarray analysis. Tumor Biol. 2015;36(8):5891–9.
30. Woo HG, Lee JH, Yoon JH, Kim CY, Lee HS, Jang JJ, et al. Identification of a cholangiocarcinoma-like gene expression trait in hepatocellular carcinoma. Cancer Res. 2010;70(8):3034–41.

31. Fujimoto A, Furuta M, Shiraishi Y, Gotoh K, Kawakami Y, Arihiro K, et al. Whole-genome mutational landscape of liver cancers displaying biliary phenotype reveals hepatitis impact and molecular diversity. Nat Commun. 2015;6:1–8.
32. Zuo HQ, Yan LN, Zeng Y, Yang JY, Luo HZ, Liu JW, et al. Clinicopathological characteristics of 15 patients with combined hepatocellular carcinoma and cholangiocarcinoma. Hepatobiliary Pancreat Dis Int. 2007;6(2):161–5.
33. Yap AQ, Chen CL, Yong CC, Kuo FY, Wang SH, Lin CC, et al. Clinicopathological factors impact the survival outcome following the resection of combined hepatocellular carcinoma and cholangiocarcinoma. Surg Oncol. 2013;22(1):55–60.
34. Park YH, Hwang S, Ahn CS, Kim KH, Moon DB, Ha TY, et al. Long-term outcome of liver transplantation for combined hepatocellular carcinoma and cholangiocarcinoma. Transplant Proc. 2013;45(8):3038–40.
35. Aloia T, Pawlik TM, Taouli B, Rubbia-Brandt L, Vauthey J. Intrahepatic bile ducts. AJCC cancer staging manual. 8th ed. NewYork: Springer; 2017.
36. Aoki K, Takayasu K, Kawano T, Muramatsu Y, Moriyama N, Wakao F, et al. Combined hepatocellular carcinoma and cholangiocarcinoma: clinical features and computed tomographic findings. Hepatology. 1993;18(5):1090–5.
37. Fukukura Y, Taguchi J, Nakashima O, Wada Y, Kojiro M. Combined hepatocellular and cholangiocarcinoma: correlation between CT findings and clinicopathological features. J Comput Assist Tomogr. 1997;21(1):52–8.
38. Hashimoto T, Nakamura H, Hori S, Tomoda K, Mitani T, Murakami T, et al. MR imaging of mixed hepatocellular and cholangiocellular carcinoma. Abdom Imaging. 1994;19(5): 430–2.
39. Sanada Y, Shiozaki S, Aoki H, Takakura N, Yoshida K, Yamaguchi Y. A clinical study of 11 cases of combined hepatocellular–cholangiocarcinoma Assessment of enhancement patterns on dynamics computed tomography before resection. Hepatol Res. 2005;32(3):185–95.
40. Shin CI, Lee JM, Kim SH, Choi JY, Lee JY, Han JK, et al. Recurrence patterns of combined hepatocellular-cholangiocarcinoma on enhanced computed tomography. J Comput Assist Tomogr. 2007;31(1):109–15.
41. Wells ML, Venkatesh SK, Chandan VS, Fidler JL, Fletcher JG, Johnson GB, et al. Biphenotypic hepatic tumors: imaging findings and review of literature. Abdom Imaging. 2015;40(7):2293–305.
42. Sammon J, Fischer S, Menezes R, Hosseini-Nik H, Lewis S, Taouli B, et al. MRI features of combined hepatocellular- cholangiocarcinoma versus mass forming intrahepatic cholangiocarcinoma. Cancer Imaging. 2018;18(1):8.
43. Lin G, Toh CH, Wu RC, Ko SF, Ng SH, Chou WC, et al. Combined hepatocellular cholangiocarcinoma: prognostic factors investigated by computed tomography/magnetic resonance imaging. Int J Clin Pract. 2007;62(8):1199–205.
44. Sheng RF, Xie YH, Ji Y, Chen CZ, Yang L, Jin KP, et al. MR comparative study of combined hepatocellular-cholangiocarcinoma in normal, fibrotic, and cirrhotic livers. Abdom Radiol (NY). 2016;41(11):2102–14.
45. Potretzke TA, Tan BR, Doyle MB, Brunt EM, Heiken JP, Fowler KJ. Imaging features of Biphenotypic primary liver carcinoma (Hepatocholangiocarcinoma) and the potential to mimic hepatocellular carcinoma: LI-RADS analysis of CT and MRI features in 81 cases. AJR Am J Roentgenol. 2016;207(1):25–31.
46. Fowler KJ, Sheybani A, Parker RA, Doherty S, et al. Combined hepatocellular and cholangiocarcinoma (biphenotypic) tumors: imaging features and diagnostic accuracy of contrast-enhanced CT and MRI. Am J Roentgenol. 2013;201(2):332–9.
47. Theise ND, Nakashima O, Park YN, Nakanuma Y. WHO classification of tumours of the digestive system. Lyon, France: IARC Press; 4th ed. 2010, p. 225–7.
48. Shiomi S, Sasaki N, Kawashima D, Jomura H, Fukuda T, Kuroki T, et al. Combined hepatocellular carcinoma and cholangiocarcinoma with high F-18 fluorodeoxyglucose positron emission tomographic uptake. Clin Nucl Med. 1999;24(5):370–1.

49. Ijichi H, Shirabe K, Taketomi A, Yoshizumi T, Ikegami T, Mano Y, et al. Clinical usefulness of (18) F-fluorodeoxyglucose positron emission tomography/computed tomography for patients with primary liver cancer with special reference to rare histological types, hepatocellular carcinoma with sarcomatous change and combined hepatocellular and cholangiocarcinoma. Hepatol Res. 2013;43(5):481–7.
50. Sacks A, Peller PJ, Surasi DS, Chatburn L, Mercier G, Subramaniam RM. Value of PET/CT in the management of primary hepatobiliary tumors, part 2. Am J Roentgenol. 2011;197(2):W260–W5.
51. Cheung TT, Ho CL, Lo CM, Chen S, Chan SC, Chok KSH, et al. 11C-acetate and 18F-FDG PET/CT for clinical staging and selection of patients with hepatocellular carcinoma for liver transplantation on the basis of Milan criteria: surgeon's perspective. J Nucl Med. 2013;54(2):192–200.
52. Goodman ZD, Ishak KG, Langloss JM, Sesterhenn IA, Rabin L. Combined hepatocellular-cholangiocarcinoma. A histologic and immunohistochemical study. Cancer. 1985;55(1):124–35.
53. The general rule for the clinical and pathological study of primary liver cancer. Liver cancer study group of Japan. Jpn J Surg. 1989;19(1):98–129.
54. Nakamura S, Suzuki S, Sakaguchi T, Serizawa A, Konno H, Baba S, et al. Surgical treatment of patients with mixed hepatocellular carcinoma and cholangiocarcinoma. Cancer. 1996;78(8):1671–6.
55. Sasaki A, Kawano K, Aramaki M, Ohno T, Tahara K, Takeuchi Y, et al. Clinicopathologic study of mixed hepatocellular and cholangiocellular carcinoma: modes of spreading and choice of surgical treatment by reference to macroscopic type. J Surg Oncol. 2001;76(1):37–46.
56. Ercolani G, Grazi GL, Ravaioli M, Grigioni WF, Cescon M, Gardini A, et al. The role of lymphadenectomy for liver tumors: further considerations on the appropriateness of treatment strategy. Ann Surg. 2004;239(2):202–9.
57. Vauthey JN, Pawlik TM, Abdalla EK, Arens JF, Nemr RA, Wei SH, et al. Is extended hepatectomy for hepatobiliary malignancy justified? Ann Surg. 2004;239(5):722–30; discussion 30–2.
58. Llovet JM, Burroughs A, Bruix J. Hepatocellular carcinoma. Lancet. 2003;362(9399):1907–17.
59. Ariizumi S, Kotera Y, Katagiri S, Nakano M, Yamamoto M. Combined hepatocellular-cholangiocarcinoma had poor outcomes after hepatectomy regardless of Allen and Lisa class or the predominance of intrahepatic cholangiocarcinoma cells within the tumor. Ann Surg Oncol. 2012;19(5):1628–36.
60. Yoon YI, Hwang S, Lee YJ, Kim KH, Ahn CS, Moon DB, et al. Postresection outcomes of combined hepatocellular carcinoma-cholangiocarcinoma, hepatocellular carcinoma and intrahepatic cholangiocarcinoma. J Gastrointest Surg. 2016;20(2):411–20.
61. Wu CH, Yong CC, Liew EH, Tsang LL, Lazo M, Hsu HW, et al. Combined hepatocellular carcinoma and cholangiocarcinoma: diagnosis and prognosis after resection or transplantation. Transplant Proc. 2016;48(4):1100–4.
62. Kim KH, Lee SG, Park EH, Hwang S, Ahn CS, Moon DB, et al. Surgical treatments and prognoses of patients with combined hepatocellular carcinoma and cholangiocarcinoma. Ann Surg Oncol. 2009;16(3):623–9.
63. Mazzaferro V, Regalia E, Doci R, Andreola S, Pulvirenti A, Bozzetti F, et al. Liver transplantation for the treatment of small hepatocellular carcinomas in patients with cirrhosis. N Engl J Med. 1996;334(11):693–9.
64. Meyer CG, Penn I, James L. Liver transplantation for cholangiocarcinoma: results in 207 patients. Transplantation. 2000;69(8):1633–7.
65. Shimoda M, Farmer DG, Colquhoun SD, Rosove M, Ghobrial RM, Yersiz H, et al. Liver transplantation for cholangiocellular carcinoma: analysis of a single-center experience and review of the literature. Liver Transpl. 2001;7(12):1023–33.
66. Panjala C, Senecal DL, Bridges MD, Kim GP, Nakhleh RE, Nguyen JHH, et al. The diagnostic conundrum and liver transplantation outcome for combined hepatocellular-cholangiocarcinoma. Am J Transplant. 2010;10(5):1263–7.

67. Sapisochin G, De Lope CR, Gastaca M, De Urbina JO, López-Andujar R, Palacios F, et al. Intrahepatic cholangiocarcinoma or mixed hepatocellular-cholangiocarcinoma in patients undergoing liver transplantation: a spanish matched cohort multicenter study. Ann Surg. 2014;259(5):944–52.
68. Vilchez V, Shah MB, Daily MF, Pena L, Tzeng CW, Davenport D, et al. Long-term outcome of patients undergoing liver transplantation for mixed hepatocellular carcinoma and cholangiocarcinoma: an analysis of the UNOS database. HPB (Oxford). 2016;18:29–34.
69. Chang CC, Chen YJ, Huang TH, Chen CH, Kuo FY, Eng HL, et al. Living donor liver transplantation for combined hepatocellular carcinoma and cholangiocarcinoma: experience of a single center. Ann Transplant. 2017;22:115–20.
70. Magistri P, Tarantino G, Serra V, Guidetti C, Ballarin R, Di Benedetto F. Liver transplantation and combined hepatocellular-cholangiocarcinoma: feasibility and outcomes. Dig Liver Dis. 2017;49(5):467–70.
71. Lunsford KE, Court C, Lee YS, Lu DS, Naini BV, Harlander-Locke MP, et al. Propensity matched analysis of patients with mixed hepatocellular-cholangiocarcinoma and hepatocellular carcinoma undergoing liver transplantation. Liver Transpl. 2018;24(10):1384–97.
72. Sapisochin G, Fidelman N, Roberts JP, Yao FY. Mixed hepatocellular cholangiocarcinoma and intrahepatic cholangiocarcinoma in patients undergoing transplantation for hepatocellular carcinoma. Liver Transpl. 2011;17(8):934–42.
73. Jung DH, Hwang S, Song GW, Ahn CS, Moon DB, Kim KH, et al. Longterm prognosis of combined hepatocellular carcinoma-cholangiocarcinoma following liver transplantation and resection. Liver Transpl. 2017;23(3):330–41.
74. Vilchez V, Shah MB, Daily MF, Pena L, Tzeng CWD, Davenport D, et al. Long-term outcome of patients undergoing liver transplantation for mixed hepatocellular carcinoma and cholangiocarcinoma: an analysis of the UNOS database. HPB. 2016;18(1):29–34.
75. Llovet JM, Real MI, Montana X, Planas R, Coll S, Aponte J, et al. Arterial embolisation or chemoembolisation versus symptomatic treatment in patients with unresectable hepatocellular carcinoma: a randomised controlled trial. Lancet. 2002;359(9319):1734–9.
76. Okada S. Local ablation therapy for hepatocellular carcinoma. Semin Liver Dis. 1999;19(3):323–8.
77. Chan LS, Sze DY, Poultsides GA, Louie JD, Abdelrazek Mohammed MA, Wang DS. Yttrium-90 radioembolization for unresectable combined hepatocellular-cholangiocarcinoma. Cardiovasc Intervent Radiol. 2017;40(9):1383–91.
78. Dick EA, Taylor-Robinson SD, Thomas HC, Gedroyc WM. Ablative therapy for liver tumours. Gut. 2002;50(5):733–9.
79. Olnes MJ, Erlich R. A review and update on cholangiocarcinoma. Oncology. 2004;66(3):167–79.
80. Kajanti M, Pyrhonen S. Epirubicin-sequential methotrexate-5-fluorouracil-leucovorin treatment in advanced cancer of the extrahepatic biliary system. A phase II study. Am J Clin Oncol. 1994;17(3):223–6.
81. Connell LC, Harding JJ, Lowery M, Kemeny N, Cercek A, Abdelgawad M, et al. Platinum-based combination therapy (PCT) and outcomes for patients (pts) with mixed hepatocellular carcinoma and intrahepatic cholangiocarcinoma (mHCC/ICC). J Clin Oncol. 2015;33(15_Suppl):e15146.
82. Takada T, Kato H, Matsushiro T, Nimura Y, Nagakawa T, Nakayama T. Comparison of 5-fluorouracil, doxorubicin and mitomycin C with 5-fluorouracil alone in the treatment of pancreatic-biliary carcinomas. Oncology. 1994;51(5):396–400.
83. Rogers JE, Bolonesi RM, Rashid A, Elsayes KM, Elbanan MG, Law L, et al. Systemic therapy for unresectable, mixed hepatocellular-cholangiocarcinoma: treatment of a rare malignancy. J Gastrointest Oncol. 2017;8(2):347–51.
84. Sasaki M, Sato Y, Nakanuma Y. Mutational landscape of combined hepatocellular carcinoma and cholangiocarcinoma, and its clinicopathological significance. Histopathology. 2017;70(3):423–34.

Chapter 4
Hepatocellular Adenoma

Jason R. Young, Taofic Mounajjed, Rory L. Smoot, Denise M. Harnois, Kaitlyn R. Musto, and Sudhakar K. Venkatesh

Introduction

Hepatocelluar adenoma (HCA) is the third most common benign hepatic mass following cavernous hemangiomas and focal nodular hyperplasia (FNH). Most cases of HCA occur in women who have increased levels of estrogen, particularly those taking estrogen-based oral contraception. The overall annual incidence of HCA for women between 16 and 44 years of age is slightly over 1 per million while the incidence is 3.4 per 100,000 in those on long-term estrogen-based oral estrogen contraception [1]. Increased risk of HCA development has been associated with longer duration of oral contraceptives use, higher estrogen content, and age over 30 years [1, 2]. More recently, obesity and metabolic syndrome have also been associated with the development of HCA and hepatic adenomatosis [3]. HCAs are rare in males; however, those taking anabolic steroids and men with metabolic syndrome are at increased risk [4]. Other conditions associated with the increased risk of developing HCA include aplastic anemia and inherited disorders

J. R. Young (✉) · S. K. Venkatesh
Department of Radiology, Mayo Clinic, Rochester, MN, USA
e-mail: Young.Jason@mayo.edu; Venkatesh.Sudhakar@mayo.edu

T. Mounajjed
Department of Laboratory Medicine and Pathology, Mayo Clinic, Rochester, MN, USA

Department of Anatomic Pathology, Mayo Clinic, Rochester, MN, USA
e-mail: Mounajjed.Taofic@mayo.edu

R. L. Smoot
Department of Surgery, Mayo Clinic, Rochester, MN, USA
e-mail: Smoot.Rory@mayo.edu

D. M. Harnois · K. R. Musto
Department of Gastroenterology & Hepatology, Mayo Clinic, Jacksonville, FL, USA
e-mail: Harnois.Denise@mayo.edu; Musto.Kaitlyn@mayo.edu

L. R. Roberts et al. (eds.), *Evaluation and Management of Liver Masses*,
https://doi.org/10.1007/978-3-030-46699-2_4

such as glycogen storage disease and maturity onset diabetes of the young, type 3 (MODY3) [5, 6].

HCAs are often discovered incidentally when patients undergo imaging for unrelated clinical symptoms or staging of a synchronous carcinoma. Most patients are asymptomatic at the time of HCA diagnosis [7]. Right upper quadrant discomfort is the most common presenting symptom (up to 43%) and is usually associated with hemorrhage in or around the lesion [7, 8]. Patients can present with abnormal liver function tests including elevated levels of serum transaminases, alkaline phosphatase, and gamma-glutamyl-transferase levels [2].

Multiple synchronous HCA lesions are common, occurring in nearly half of patients. Hepatic adenomatosis (defined as >10 HCA lesions) can occur in up to 10% of patients and, while previously thought to be a distinct entity, is now known to occur in all subtypes of HCAs including men, women, and those with glycogen storage disorders [1]. The risk of hemorrhage (27–29%) combined with a risk of malignant transformation (4–5%) results in HCAs being treated differently than most benign hepatic tumors [9–11]. A common challenge is distinguishing HCAs from focal nodular hyperplasia (FNH), hepatocellular carcinoma (HCC), and metastases. While major complications from percutaneous biopsy of HCA are relatively low (2%), there is a 10% discordance between histological diagnosis obtained by biopsy and final pathological diagnosis of surgical resection specimens [12].

Pathologic Features

Histologically, HCAs consist of benign hepatocytes; they differ from the background liver by their lack of portal tracts. Instead of portal tracts, aberrant naked arteries are typically scattered throughout the lesion. The hepatocytes within the tumor are indistinguishable from normal hepatocytes at high power magnification. They typically have no cytological atypia and essentially no mitotic activity. One exception is androgen-related HCAs, which can demonstrate mild cytological atypia. Fatty change can occur in HCAs, but this tends to be characterized by steatosis only, without Mallory hyaline, ballooning, or perisinusoidal fibrosis. A true steatohepatitic pattern is atypical for HCA and should raise consideration for a steatohepatitic variant of hepatocellular carcinoma. HCAs can also demonstrate focal areas of prominent congestion, hemorrhage, and necrosis.

HCAs are usually non-encapsulated; they can be either sharply delimited from adjacent non-tumor liver or can blend into the background liver. The background liver usually shows no significant pathology or fibrosis. Exceptions include individuals with glycogen storage disease, in whom some fibrosis can be seen. In

addition, inflammatory-type HCAs commonly arise in individuals with obesity and background fatty liver changes.

By special stains, HCAs show an intact reticulin meshwork, similar to that of normal liver. They are strongly and diffusely positive for HepPar1 and Arginase-1 and are negative for Glypican 3. CD34 typically shows patchy sinusoidal staining, in contrast to the diffuse sinusoidal staining typical of hepatocellular carcinoma. In isolation, however, this marker does not reliably distinguish HCAs from hepatocellular carcinoma [13]. Ki-67 of HCA typically shows a very low proliferative index (<1–2%).

The main histologic differential diagnoses for HCA are focal nodular hyperplasia (FNH) and hepatocellular carcinoma (HCC). In contrast to HCA, FNH has a nodular configuration with fibrous septa and some cases have a central scar. Bile ductular proliferation tends to be a more prominent feature in FNH. Further, FNH often has a "map-like" staining pattern with glutamine synthetase (GS) staining. In contrast, HCAs do not demonstrate this "map-like" pattern on GS staining, rather being frankly negative or positive for GS stain, depending on the beta-catenin activation status of the HCA [14].

Well-differentiated HCC can be difficult to differentiate from HCA; features that favor malignancy include cytologic atypia, mitotic activity, and steatohepatitic features. Special stains can also help in differentiating HCC from HCA; reticulin stain usually shows loss or reduction of the reticulin meshwork in HCC compared to reticulin preservation in HCA. Glypican-3 immunostain can be positive in HCC but is usually negative in HCA [15, 16]. Ki-67 can show an increased proliferative index in HCC but is usually low in HCA.

Four common subtypes of HCA have been described based on histologic appearance, immunohistochemical staining, genetic mutations, and associated clinical features [17] (Table 4.2): β-catenin-activating mutated HCA (β-HCA) accounting for 10–15% of HCAs have a male predilection and higher risk of transformation into HCC (Fig. 4.1). Inflammatory (I-HCA) accounting for 40–50% of HCAs have an association with alcohol abuse, obesity, background hepatic steatosis and increased risk of hemorrhage when large. 10% of I-HCA have a β-catenin-activating mutation (Fig. 4.2). HNF1α inactivated (H-HCA) are the second most common type accounting for 35–40% of HCAs, have higher rates of tumor steatosis, hepatic adenomatosis, and maturity-onset diabetes of the young (Fig. 4.3). The fourth unclassified type (U-HCA), accounting for 5–10% of HCAs, characteristically are lacking mutations or the inflammatory phenotype (Fig. 4.4). More recently, Nault et al. described an additional subtype of hepatic adenoma characterized by the fusion of the promoter of INHBE1 with GLI1, leading to activation of the hedgehog pathway. This hedgehog-activated HCA subtype has an increased risk of hemorrhage [18]. Other uncommon types include myxoid HCA [19, 20] and pigmented HCA [21].

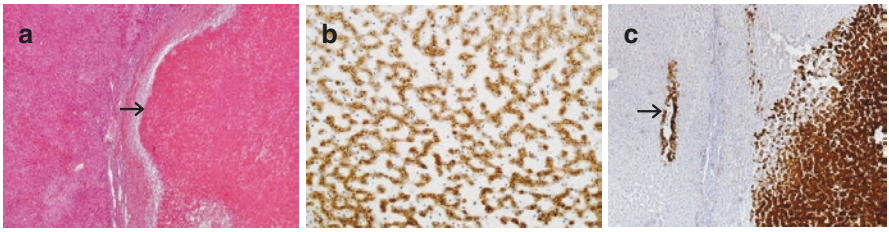

Fig. 4.1 β-Catenin-activating mutated HCA. (**a**) This hepatic adenoma shows an area of hemorrhagic necrosis (arrow) in its center. (**b**) The adenoma shows strong diffuse immunohistochemical expression of Serum Amyloid A, supporting an inflammatory phenotype. (**c**) An immunostain for glutamine synthetase also shows diffuse positive staining in the tumor (right) and only perivenular staining in the background liver (left, arrow). This immunoprofile supports beta-catenin activation (inflammatory adenoma with beta catenin activation)

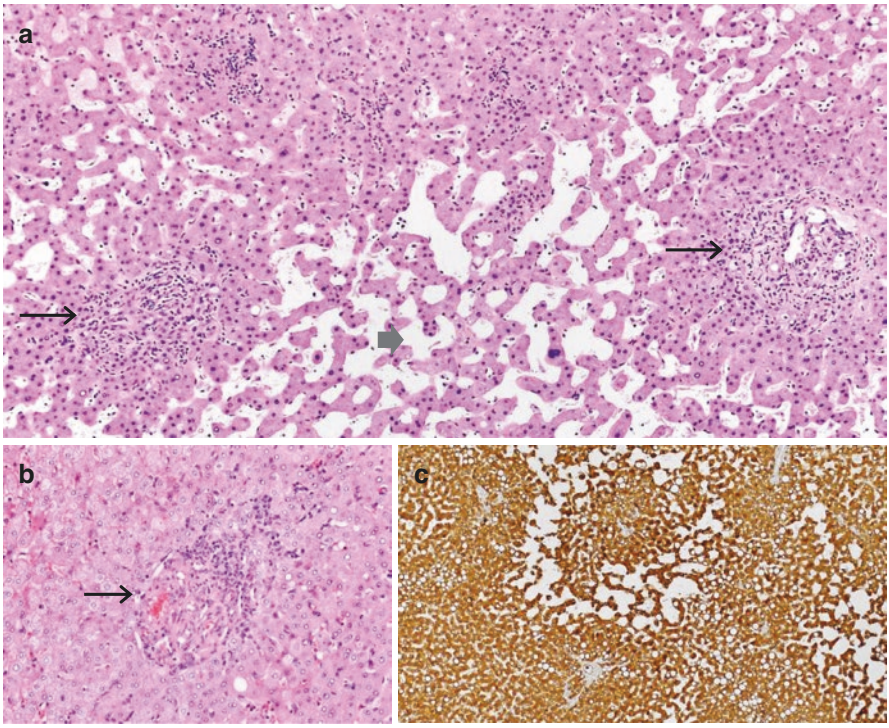

Fig. 4.2 Inflammatory HCA. (**a**) This hepatic adenoma shows typical histologic features of inflammatory phenotype, including sinusoidal dilatation (short arrow) and multiple faux portal tracts (long arrows). (**b**) A higher power view of a faux portal tract (arrow); these structures resemble portal tracts but lack the structures found in normal portal tracts (normal bile ducts, portal vein branches). (**c**) The adenoma shows strong diffuse immunohistochemical expression of C-reactive protein, supporting the inflammatory phenotype

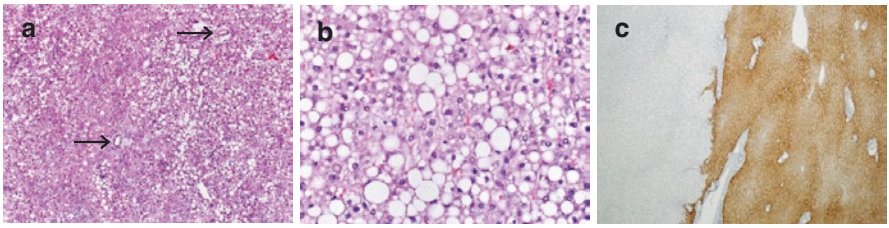

Fig. 4.3 HNF-1A inactivated HCA. (**a**) This hepatic adenoma consists of benign-appearing hepatocytes with fatty change. Scattered aberrant or naked arteries are observed (arrows). (**b**) The tumor consists of bland uniform sheets of hepatocytes with steatosis. (**c**) The tumor shows aberrant loss of liver fatty acid–binding protein (L-FABP) (left) by immunostain, but L-FABP is preserved in the background liver (right). This phenotype is typical of HNF-1 alpha inactivation

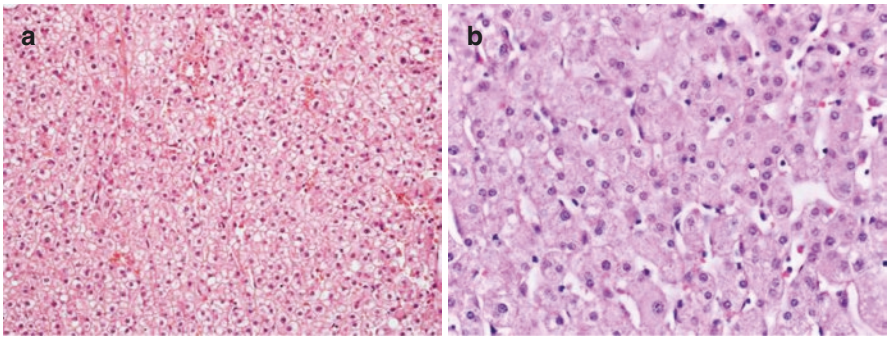

Fig. 4.4 Unclassified HCA. (**a**) This hepatic adenoma consists of normal-appearing hepatocytes and lacks specific features to suggest a certain phenotype. (**b**) A high power view shows nondescript uniform and bland hepatocytes without specific features. By immunohistochemistry (not shown), the tumor showed normal retained expression of liver fatty acid–binding protein (L-FABP) and was negative for C-reactive protein, serum Amyloid A, β-catenin, and glutamine synthetase (not shown). This immunoprofile supports an "unclassified" type

Radiologic Features

Understanding the histopathologic changes of hepatocellular adenomas (HCA) is fundamental to their imaging appearance. HCAs have radial growth of essentially normal, albeit crowded hepatocytes. Lacking the portal vein and bile duct of the portal triad, HCAs have a predominantly arterial blood supply. Hence, HCAs are often best visualized during the arterial phase of contrast-enhanced imaging. Uncomplicated HCA may otherwise be difficult to detect, only evident by subtle architectural distortion. Hepatocytes in HCAs can also show fatty change which can be seen on imaging, a feature useful to differentiate from other lesions. The altered blood supply and lack of a true capsule predispose HCA to necrosis and

uncontained hemorrhage [11]. The risk of hemorrhage (27–29%) and malignant transformation (4–5%) result in HCAs being treated with greater scrutiny and caution, often imaged with greater frequency and with various modalities [9–11].

When imaging with computed tomography (CT) and magnetic resonance imaging (MRI), HCAs are often undetectable on non-contrast-enhanced CT or T1-weighted MR images. HCAs tend to have similar signal characteristics to surrounding liver parenchyma on T2-weighted images but may be hyperintense on diffusion-weighted imaging (DWI). The presence of fat within HCAs renders them hypodense to the normal liver on CT and hypointense on fat-suppressed MRI sequences. However, HCA with fat occurring in a diffuse fatty liver may be obscured on both non-contrast-enhanced CT and MRI [22]. On contrast-enhanced CT and MRI, uncomplicated HCAs typically show homogeneous arterial phase hyperenhancement, becoming isodense/isointense on portal venous and delayed phases. Therefore, arterial phase imaging is the key to detecting HCA. Intra-tumoral fat will be evident by hypoattenuation on CT and fat signal on MRI, a finding that can be obscured by hepatic steatosis [22]. Necrosis of HCA will often result in a heterogeneous appearance and cystic changes. Hemorrhage within a HCA will produce a variety of appearances with blood products of various ages, cystic changes, and rarely calcifications.

Compared to CT, HCAs are often better detected with MRI given the inherent strengths of various sequences and greater contrast resolution. On DWI, HCAs are seen well with high signal at low b-values. Several lesions including FNH and HCCs appear hyperintense on DWI. Hepatobiliary MRI contrast agents such as gadoxetic acid have been reported to help distinguish HCA from FNH, HCA tending to lack enhancement in the delayed hepatobiliary phase compared to FNH [23]. However, there is significant overlap in the imaging appearance of HCA and FNH in the hepatobiliary phase, particularly the inflammatory type of FNH [24–26]. Useful differentiating features are the presence of fat, hemorrhage, and necrosis in HCAs along with the multiplicity of HCAs versus FNHs, which are usually solitary or few.

The imaging features of HCA and HCC overlap, with both typically being arterially enhancing with diffusion restriction. While loss of signal on opposed phase imaging may point toward HCA, the same imaging feature can occur in 20% of HCC with an even higher rate (36%) for lesions between 1.0 and 1.5 cm in size [27]. Washout in the portal venous and/or delayed phases is a typical feature for HCC but may also be rarely seen in HCAs. An enhancing capsule is a useful distinguishing feature for HCC from other lesions but is only present in less than 50% of HCCs. Invasive features such as tumor in the portal or hepatic vein or biliary obstruction favor HCC. Historically, the clinical setting has played a strong role in distinguishing HCA from HCC. The prototypical presentation is of a young healthy female on estrogen-based contraceptives for HCA versus a person with chronic liver disease such as alcoholic cirrhosis or chronic viral hepatitis B or C for HCC. However, times have changed in middle-to-high-income countries worldwide with an epidemic of obesity and metabolic syndrome. Non-alcoholic fatty liver disease (NAFLD), particularly non-alcoholic steatohepatitis (NASH), increases the risk of HCC [28–31]. In tandem, higher body fat results in a state of elevated systemic estrogen which not only predisposes to HCA but has been proposed as a major risk

factor for malignant transformation of HCA, warranting close monitoring and tissue biopsy diagnosis when appropriate [32].

Both HCA and metastases may present with multiple hepatic lesions. Hypovascular metastases are differentiated from HCA by decreased enhancement throughout all phases and their irregular outline. However, the imaging features of HCA and metastases overlap. In the setting of a primary malignancy with potential for hepatic metastases, the diagnosis of HCA by imaging features on a single exam should be made with caution. Ideally, even patients with typical imaging features of HCA on first evaluation should have follow-up imaging in 4–6 months to confirm lack of substantial nodule growth. This provides a failsafe against misdiagnosis of malignancy and also allows assessment of growth, hemorrhage, and/or malignant transformation of HCA.

The ultrasound features of HCA are generally non-specific. Ultrasound is useful for the detection of HCA, often being the means by which asymptomatic HCAs are initially found, as well as for monitoring the size of HCAs and development of necrosis or hemorrhage within the lesions. The sonographic appearance of HCA is varied, depending on the echogenicity of surrounding hepatic parenchyma and the tumor itself. Most HCAs present as hypoechoic lesions which are more pronounced in a background fatty liver [33]. However, intracellular lipid within HCA can produce an isoechoic to hyperechoic appearance, typically more isoechoic in a background fatty liver. Necrosis, hemorrhage, and subsequent calcification of HCA will result in a mixed sonographic appearance with cystic changes, regional heterogeneity, and acoustic shadowing of calcified portions of the lesion [34]. Large HCAs tend to have prominent disorganized peripheral vascularity.

The most common Doppler finding within HCA is a low-resistance venous waveform (either within or at the tumor periphery) and lack of intra-tumoral arterial waveform, in contrast to FNH [35, 36]. Ultrasound microbubble contrast agents can help characterize HCA. Most commonly, HCAs have homogenous early arterial enhancement. However, large HCA will tend to have more peripheral and heterogeneous arterial enhancement [37]. The most common dynamic fill-in pattern of HCA is centripetal (peripheral to central). Some HCAs may have a mixed fill-in pattern. However, HCAs almost never display centrifugal (central to peripheral) enhancement, distinguishing them from FNH [38]. The sonographic portal venous and delayed enhancement features of HCA are overall inconsistent.

While there is a limited role for scintigraphic evaluation of suspected HCA, it can be helpful with atypical conventional imaging findings, inability to obtain an MRI or history of serious CT/MRI contrast allergy. There is no role for scintigraphic evaluation of small hepatic lesions due to limitations of scintigraphic resolution. However, a handful of radionuclides can be used to answer specific questions. When trying to distinguish HCA from FNH, Tc-99m sulfur colloid is helpful. HCAs more commonly have diminished Tc-99m sulfur colloid uptake compared to focal nodular hyperplasia which usually have normal–to-increased uptake [39, 40]. However, malignant hepatic tumors will also lack sulfur colloid uptake. When trying to distinguish HCA and FNH from malignant lesions, hepatobiliary agents such as Tc-99m mebrofenin can be helpful. Although not specific, scintigraphic hepatobiliary agents will tend to have uptake

in both FNH and HCA (often more intense in HCA due to absent bile ducts). This is in contrast to HCC and hepatic metastases which generally lack hepatobiliary agent uptake (less so for well-differentiated HCC). The best hepatobiliary technique is a three-phase approach with multiple planar images at 5, 10, and 60–90 minutes, with adjustments in acquisition timing for poor hepatic function [41].

There is little data regarding FDG PET-CT imaging of HCA. However, almost every case in the literature has reported HCA to be FDG avid (4–10 SUVmax) and often mimic metastatic disease [42–52]. The mechanism of increased FDG uptake within HCAs is somewhat speculative, possibly from increased blood supply, inflammation, fatty change, activated Kupffer cells, and altered protein expression.

Efforts to distinguish HCA subtypes have been focused on MRI characteristics. There does not seem to be a difference in DWI signal between the different HCA subtypes [53]. Both H-HCA and U-HCA tend to have relatively lower signal intensity on intracellular hepatobiliary MRI contrast enhancement compared to I-HCA and β-HCA [54, 55].

β-Catenin-Activating Mutated HCA (β-HCA)

This HCA subtype has the highest risk for malignant transformation but unfortunately also has the least distinguishing imaging features (Fig. 4.5). A smudgy irregular T2 hyperintense central scar that may enhance in the portal venous phase has been reported as a characteristic feature [56]. Aggressive features over time include an increase in size, invasion of normal surrounding structures, and a shift to hypoenhancement (washout) on portal venous and delayed phases of MRI enhancement [57]. A definite diagnosis of *β-HCA* cannot be made based on imaging features alone.

Inflammatory HCA (I-HCA)

The MRI feature most characteristic of I-HCA is slightly elevated T2-weighted signal intensity. This is the only subtype to have a more intense peripheral rim of T2 signal as an “atoll” sign, occurring in about half the cases [56]. These lesions may show persistent delayed enhancement on CT and MRI (Fig. 4.6). The combination of increased T2 signal and persistent delayed enhancement has a sensitivity of 85% and specificity of 88% for diagnosing I-HCA [58]. This subtype may uptake hepatobiliary contrast agents similar to FNH. The uptake is usually heterogeneous or peripheral rim-like as compared to homogeneous and diffuse uptake (except for the central scar) in cases of FNH.

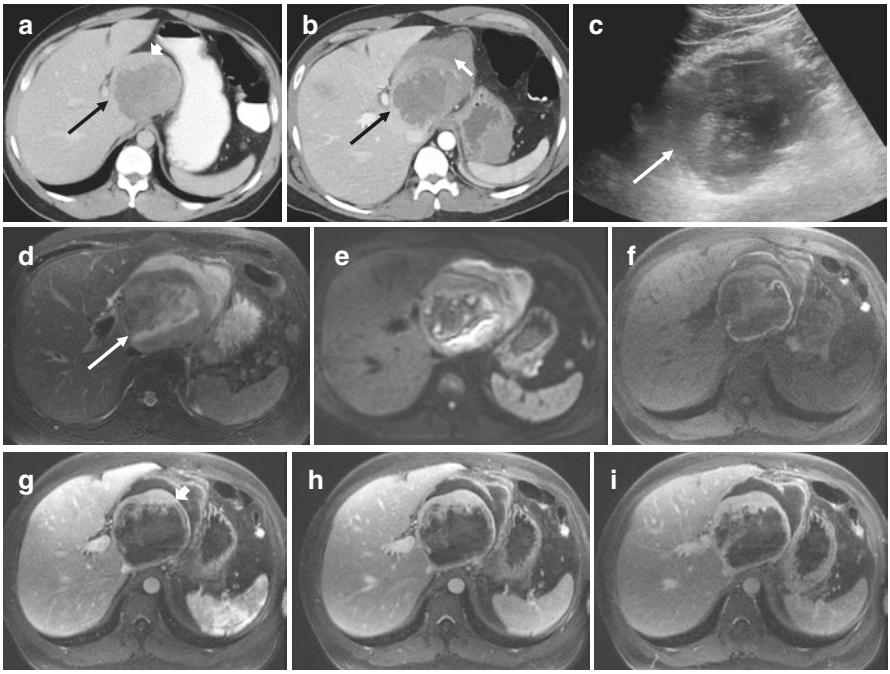

Fig. 4.5 β-Catenin-activating mutated HCA in a 42-year-old male presenting with abdominal pain. Non-contrast-enhanced CT showed a mixed density mass. Post-contrast-enhanced axial CT (**a**) showing a hypodense mass (black arrow) in caudate lobe of liver with enhancing rind (arrowhead). A day after admission the patient complained of worsening pain and a contrast-enhanced CT (**b**) showed an increased size of the lesion with perilesional fluid (white arrow) and mass effect consistent with rupture and hemorrhage. Ultrasound (**c**) shows a heterogeneous but predominantly echogenic mass, a finding most consistent with hemorrhage within the mass. A follow-up MRI shows a heterogeneous mass on axial T2W (**d**), DWI (**e**) and T1 (**f**)-weighted images, again consistent with internal hemorrhage and organizing hematoma around the tumor. Post contrast, there is nodular enhancement of the periphery of the mass on arterial (**g**), portal venous (**h**), and delayed phases (**i**) consistent with viable tumor. The mass was surgically resected and histologically found to be a β-catenin-activating mutated HCA

HNF1α Inactivated HCA (H-HCA)

The finding most characteristic of H-HCA is intracellular fat, which will drop signal on opposed-phase MRI imaging and on fat-suppressed MRI sequences (Fig. 4.7). The presence of homogeneous intracellular fat is 87% sensitive and 100% specific for the H-HCA subtype [58, 59]. This type of HCA tend to show washout of contrast in the portal venous and delayed phases which overlaps with HCC. However, the clinical presentation and history of chronic liver disease in case of HCC may be helpful to distinguish the two lesions.

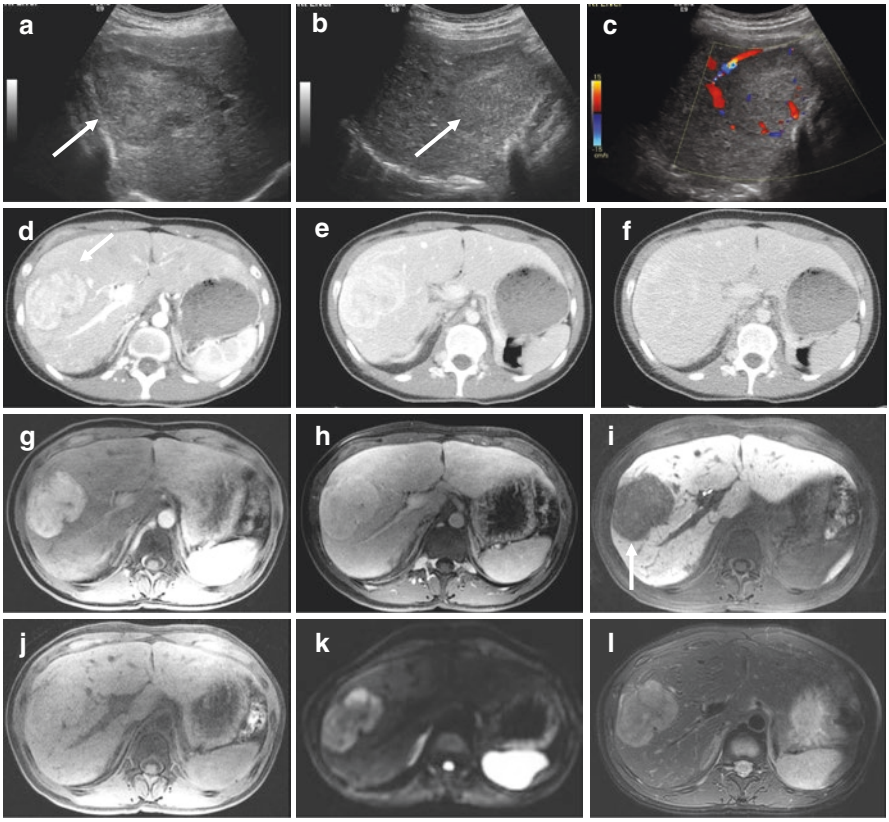

Fig. 4.6 Inflammatory HCA in a 35-year-old female. Ultrasound images in transverse (**a**) and longitudinal (**b**) views show heterogeneous, slightly echogenic mass in the right lobe subcapsular location (arrows). Color Doppler (**c**) shows internal and peripheral vascularity. Contrast-enhanced CT in arterial (**d**), portal venous (**e**), and delayed (**f**) phases shows a heterogeneous hyperenhancing lesion (arrow) with persistent enhancement in portal venous phase, becoming nearly isodense in the delayed phase. MRI study shows similar arterial phase enhancing (**g**) and persistent enhancement in portal venous phase (**h**). This particular lesion does not uptake hepatobiliary contrast, shown in the 20-minute hepatobiliary phase with Gd-EOB-DTPA (**i**). The lesion is nearly isointense on T1W (**j**) but hyperintense on DWI (**k**) and T2W (**l**) images

Unclassified HCA (U-HCA)

Distinct MRI features of U-HCA have been difficult to identify (Fig. 4.8). While U-HCAs have the morphologic features of HCA, they lack immunohistochemical and genetic abnormalities, resulting in an essentially bland subtype with expected generic HCA imaging findings.

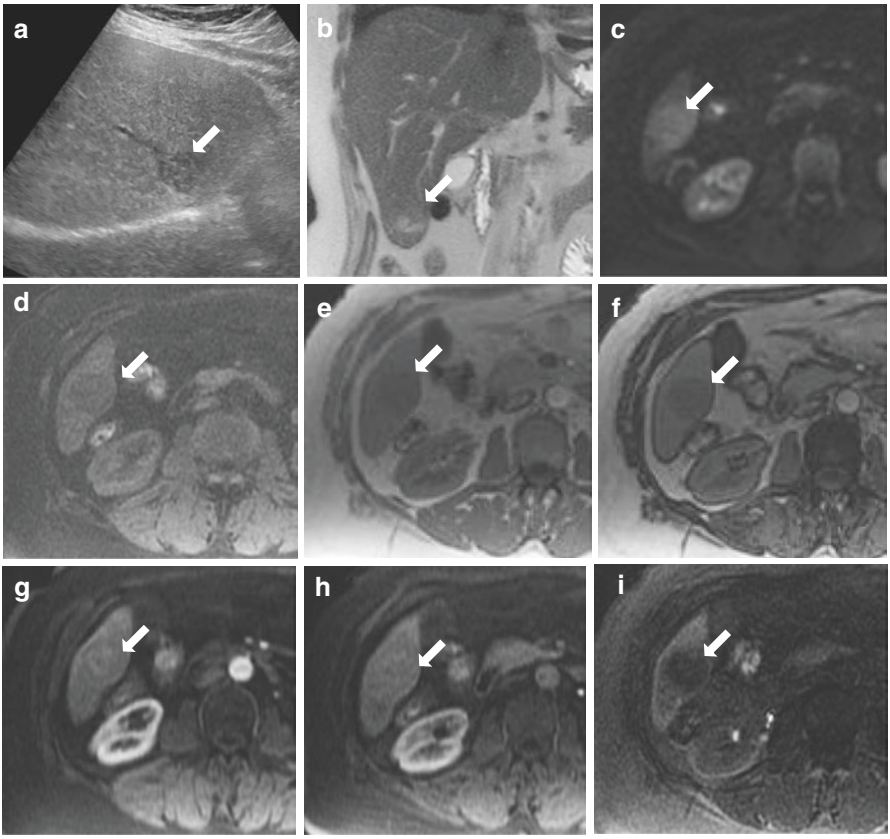

Fig. 4.7 HNF-1A inactivated HCA in a 49-year-old female. Ultrasound image (**a**) showing mixed echogenicity lesion in inferior right lobe (arrow). The lesion appears hyperintense on coronal T2W (**b**) and axial DWI (**c**) images and hypointense on T1W images (**d**). In-phase (**e**) and opposed phase (**f**) images showing signal loss in the lesion consistent with intralesional fat. Post–contrast-enhanced arterial phase (**g**) and portal venous phase (**h**) images showing enhancing lesion without any washout. Delayed 20-minute hepatobiliary phase image (**i**) shows no significant uptake of contrast by the lesion

Myxoid Hepatocellular Neoplasm HCA (MHN-HCA)

More recently a unique myxoid hepatocellular neoplasm (MHN) has been described. When these features occur in HCA, there is an elevated risk for HCC [20]. Given their high mucin content, these MHNs have a marked hyperintense signal on T2-weighted imaging with thin T2 hypointense septations. The enhancement pattern of MHN is somewhat unique with moderate peripheral arterial enhancement and progressive centripetal fill-in on portal venous and delayed phases, similar to

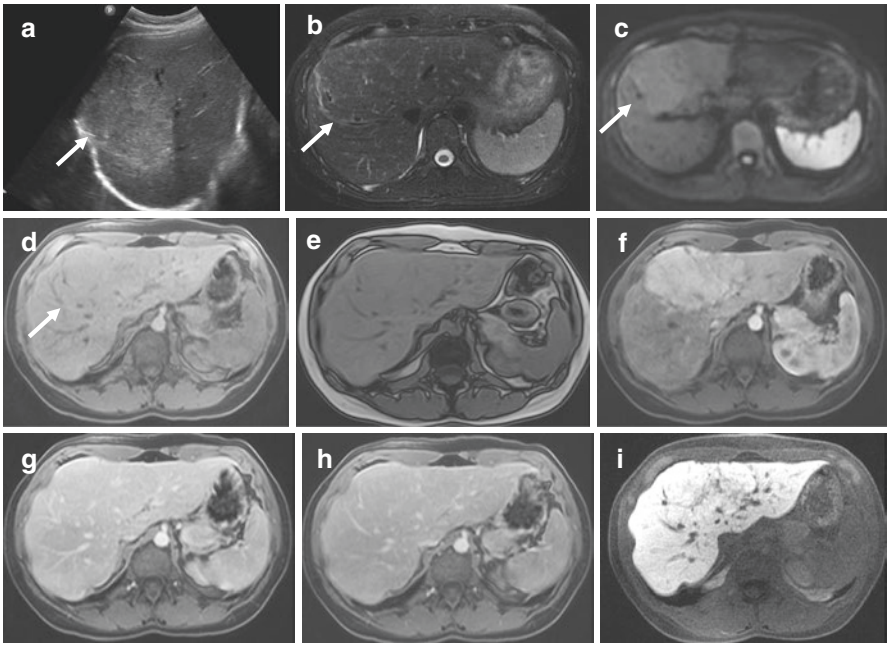

Fig. 4.8 Unclassified HCA in a 34-year-old female. Ultrasound (**a**) shows an echogenic mass in the right hepatic lobe. MRI shows a corresponding nearly isointense mass (arrow) in the right lobe on T2W image (**b**) with mild hyperintense signal on the DWI (**c**), and isointense signal on T1W (**d**) sequences. No evidence of intralesional fat on the opposed-phase sequence (**e**). Post contrast, there is arterial phase hyperenhancement (**f**), isointensity on portal venous (**g**), and delayed (**h**) phases. Gd-EOB-DTPA shows uptake of the contrast similar to liver parenchyma in the hepatobiliary phase (**i**). Overall the imaging features mimic focal nodular hyperplasia. However, percutaneous biopsy and surgical excision were both consistent with HCA unclassified type

hepatic hemangiomas yet more heterogeneous, lacking the well-defined interrupted nodular appearance of a hemangioma [19].

Atypical HCA

Adenomas that show some concerning features for malignancy but are not characteristic of an HCC are classified as atypical HCAs. These are different from the unclassified HCA subtype. The features that should raise the possibility of this uncommon variant include adenoma occurring in an older male, cytoarchitectural atypia and histological features mimicking HCC, and adenomas occurring in the background of chronic liver disease. Close follow-up or resection is the preferred management of these lesions [60].

Diagnosis of the subtype of HCA is important in the management as B-HCA and MXN-HCA subtypes carry higher risk of malignancy. Table 4.2 highlights the key features of the four most common HCA subtypes. With percutaneous biopsy, a well-differentiated HCC can be difficult to differentiate from HCA, prompting complete excision of the lesion for definitive diagnosis. Larger lesions and atypical imaging features would also validate surgical removal.

Medical Management

Medical management of HCA is often determined by tumor size, the number of lesions, symptoms, gender, and history of OC use [61]. Table 4.1 highlights the primary HCA risk factors. The HCA subtype must now also be considered [7]. Obesity and metabolic syndrome are risk factors for HCA development. With rising obesity in the United States, management guidelines may need to be updated to include these risk factors [3].

The risk of hemorrhage has been associated with tumor size >5 cm, I-HCA subtype, increasing size over time, OC use within 6 months, and pregnancy [7]. Tumor rupture may present with acute abdominal pain and free intraperitoneal or intratumoral hemorrhage on imaging; hemodynamic instability is uncommon and conservative management is indicated in most cases [8]. Transarterial embolization (TAE) is recommended in the setting of hemodynamic instability and/or to reduce tumor size [7]. Emergent surgical resection is generally not recommended in the acute phase and has been associated with greater mortality (5–10%), increased morbidity, and longer length of hospital admissions [7, 62].

Malignant transformation has been seen in up to 46% of *β-HCA*, and approximately 10% of I-HCAs have β-catenin gene mutations [7]. Risk of malignant transformation is highest in male patients, *β-HCA*, large tumor size (>8 cm), and those with glycogen storage disease (particularly type 1 and type 3) [8, 57, 63]. Germline mutations of HNF1α also result in maturity onset diabetes of the young-type 3 (MODY3), and this is also the only subtype associated with familial adenomatosis

Table 4.1 Risk factors for HCA complications

Hemorrhage	Malignant transformation
Size >5 cm	Size >8 cm
Increasing size of lesion	Male
I-HCA subtype	B-HCA
OC use within 6 months	Glycogen storage disease
Pregnancy	Androgen use

OC oral contraceptive

Table 4.2 Features of four common HCA subtypes

Subtype	Frequency	Clinical	Risk factors	Pathologic features	MRI features
B-HCA	10–15%	Highest HCC risk	OC Male > female Androgen use Glycogen Storage Disease	Cytologic atypia, positive for gluthamine synthetase (immunohistochemistry) Aberrant nuclear expression of beta-catenin by immunohistochemical stain	Smudgy T2 hyperintense central scar that enhances in the portal venous phase may be seen
I-HCA	40–50%	Higher risk of hemorrhage	OC Female > male Obesity ETOH abuse Metabolic syndrome	"Faux-portal tracts" ± ductular proliferation Sinusoidal dilatation Congestion Inflammation Positive for CRP and SAA by immunohistochemistry	Slightly elevated T2 signal with atoll sign and persistent delayed enhancement. Rim-like uptake with gadoxetate
H-HCA	35–40%	Higher hepatic adenomatosis	OC Women Maturity-onset diabetes of the young type 3 (MODY3)	Fatty change in HCA Aberrant loss of L-FABP by immunohistochemistry	Homogeneous intracellular fat content; and washout on portal venous and delayed phases
U-HCA	5–10%	None	OC	None	Bland with no distinctive features

OC oral contraceptives, *CRP* C-reactive protein, *SAA* serum amyloid-A, *L-FABP* liver fatty acid–binding protein

[8, 63]. Genetic counseling is recommended for diabetes and HCA screening in those found to have HNF1α HCA subtypes (Table 4.2) [63].

In all cases, discontinuation of OC or androgens is recommended as regression of HCA has been observed after hormone withdrawal [61, 63]. Follow-up imaging to monitor for regression should be performed in 3–6 months [57]. If there is lesion growth after discontinuation of hormones or anabolic steroids, diagnostic doubt, or atypical appearance of suspected HCA, biopsy and/or surgical resection may be indicated [8, 57]. The use of percutaneous liver biopsy is somewhat controversial due to sampling error and lack of expertise in histopathologic and cytologic experience in some hospitals [8]. However, as recommended by S. Agrawal et al., selective liver biopsy is indicated for tumors approaching 5 cm that are not being considered for resection [7].

Conservative management is recommended with radiologic follow-up for single or multiple lesions <5 cm in women or larger steatotic lesions that are not β-catenin activated on liver biopsy [7]. Due to the lower risk of malignant transformation, smaller H-HCAs with typical features on MRI do not need biopsy and can be followed with imaging [63]. In these circumstances, the optimal duration and

frequency of imaging surveillance is unclear [8]. Some recommend annual imaging with CT or MRI until menopause [8].

Surgical resection is recommended for HCA that does not regress with OC or androgen cessation, lesions >5 cm, the β-catenin-activated HCA subtype, or HCAs in male patients regardless of tumor size [7, 63]. There is no consensus on the resumption of OC after the resection of HCA, but radiologic surveillance is recommended if OCs are restarted [7].

There is limited data about pregnancy and HCA. A study by Dokmak et al. indicated that pregnancy should not be contraindicated in patients with HCA [1]. However, in patients with small HCA (<5 cm), close observation and serial liver imaging are recommended with liver ultrasound every 6 weeks during pregnancy [64, 65]. Treatment of large HCA (>5 cm) should be completed prior to planned pregnancy, but in cases when intervention is required during pregnancy, it seems to be safest in the 2nd trimester [63, 65].

Liver-Directed Therapy

The recommendations regarding treatment for HCAs are based on the risk of complications. As noted previously, the most common complication is hemorrhage, which will occur in approximately 25% of known adenomas [1, 66]. The true incidence is lower as the denominator is unknown. The more feared complication is malignant transformation with a historical risk of approximately 4%, although the true incidence is likely much lower [67]. The improved understanding of molecular mechanisms that drive adenoma growth, and delineation of the specific subtypes, have allowed more accurate prognostication regarding risk, leading to more informed recommendations regarding treatment [17, 68, 69]. Ongoing studies seek to further identify HCAs with a higher risk of complications such as hemorrhage, and additional molecular-based subtypes have been proposed [18, 70].

Historically, recommendations for adenoma removal included: (i) size over 5 cm, (ii) any adenoma in a male, (iii) any symptomatic adenoma, and (iv) diagnostic uncertainty with concern for hepatocellular carcinoma [1, 68, 71]. The recommendation regarding size was based on longitudinal data suggesting that essentially no adenoma under 5 cm in a woman had been described to harbor malignancy. These recommendations can now be further refined based on malignancy risk essentially being limited to the *β-HCA* and I-HCA subtypes of adenoma with the inflammatory subtype requiring a concomitant beta-catenin mutation to elevate malignant risk [18]. The more likely complication in an adenoma over 5 cm is hemorrhage, and this may be more associated with beta-catenin mutated and sonic hedgehog-associated adenomas, yet not all hemorrhage is symptomatic and a portion go undetected [18]. In the largest current pathologic-molecular-clinical correlation study, symptomatic hemorrhage was more common in the sonic hedgehog adenomas [18].

Adenomas in men bear special mention, and the recommendation is still removal regardless of size. The underlying pathology of adenoma suggests a role for

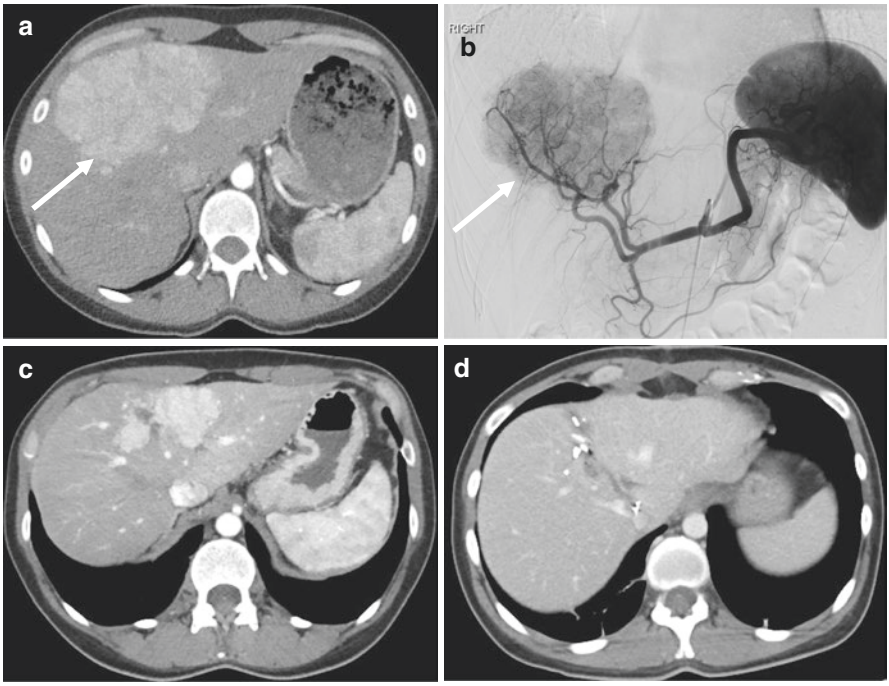

Fig. 4.9 A 34-year-old female with an unclassified type HCA. She initially presented with right upper quadrant pain and a CT (**a**) showed an 11 cm enhancing mass (arrow) in the anterior liver involving both right and left lobes. The patient underwent two embolization procedures to reduce the size for surgical excision via central hepatectomy. An angiogram through the celiac artery (**b**) shows a vascular mass (arrow). After two bland embolizations, there was significant reduction in the size of the lesion as shown on follow-up CT (**c**). The patient underwent a central hepatectomy without complication. Post-surgery CT (**d**) shows central hepatectomy changes without residual tumor

estrogen, and the risk of malignant transformation in men is higher in retrospective series, especially in those suffering from metabolic syndrome [71].

Standard operative approaches are utilized for resection with a negative margin. Whether this is approached in an open or laparoscopic fashion is dependent on the surgical expertise of the institution. Expected mortality rates for liver resection, even major resections, should be less than 2% with low morbidity typically ranging from 10% to 30% depending on the extent of resection required. Other approaches are possible and have been described such as transarterial embolization (TAE), (Fig. 4.9). TAE is the *only* appropriate approach for an acutely bleeding adenoma at an institution where this modality is available. The role of TAE in the elective setting is more controversial. A recent systematic review of the outcomes demonstrated low complication rates, with the ability to "avoid surgery" in up to 45% of patients. The indications across the 20 studies in this review varied widely; however, what is clear is that TAE can be done safely in the majority of patients [72]. Ablation, both

radiofrequency and microwave, has also been described in small case series [73, 74]. Treated adenomas typically are in the standard size range for HCC ablations ~3 cm or less, with at least one 8 cm adenoma being treated in a staged approach via ablation [74]. However, there are currently no standardized recommendations regarding percutaneous treatment (either ablation or TAE) of adenomas.

Special Circumstances

Adenomatosis

The role of liver-directed therapy becomes less clear in patients with adenomatosis [75–78]. Generally, the approach is to target symptomatic (hemorrhagic) adenomas or those that are growing rapidly with concern for possible malignant transformation [75]. Liver transplant is very rarely considered for patients with adenomatosis and typically only in the setting of confirmed or suspected malignant transformation or rapidly progressive adenomatosis that is unresectable [79].

Timing of Intervention After Acute Hemorrhage

There is no data to guide recommendations regarding the timing of definitive intervention following TAE for acute hemorrhage of adenomas. We generally wait 3–6 months with serial imaging at 3-month intervals to monitor the continued involution of the hemorrhagic mass. The underlying adenoma typically is much smaller than the acute hemorrhagic mass, and a less radical resection is often possible with continued observation. Repeat bleeding episodes or ongoing symptoms may argue for earlier intervention.

References

1. Rooks JB, Ory HW, Ishak KG, Strauss LT, Greenspan JR, Hill AP, Tyler CW. Epidemiology of hepatocellular adenoma: the role of contraceptive use. JAMA. 1979;242(7):644–8.
2. Dokmak S, Paradis V, Vilgrain V, Sauvanet A, Farges O, Valla D, et al. A single-center surgical experience of 122 patients with single and multiple hepatocellular adenomas. Gastroenterology. 2009;137(5):1698–705. https://doi.org/10.1053/j.gastro.2009.07.061.
3. Chang CY, Hernandez-Prera JC, Roayaie S, Schwartz M, Thung SN. Changing epidemiology of hepatocellular adenoma in the United States: review of the literature. Int J Hepatol. 2013;2013:604860. https://doi.org/10.1155/2013/604860.
4. Socas L, Zumbado M, Perez-Luzardo O, Ramos A, Perez C, Hernandez JR, et al. Hepatocellular adenomas associated with anabolic androgenic steroid abuse in bodybuilders: a report of two cases and a review of the literature. Br J Sports Med. 2005;39(5):e27. https://doi.org/10.1136/bjsm.2004.013599.

5. Nakao A, Sakagami K, Nakata Y, Komazawa K, Amimoto T, Nakashima K, et al. Multiple hepatic adenomas caused by long-term administration of androgenic steroids for aplastic anemia in association with familial adenomatous polyposis. J Gastroenterol. 2000;35(7):557–62.
6. Labrune P, Trioche P, Duvaltier I, Chevalier P, Odievre M. Hepatocellular adenomas in glycogen storage disease type I and III: a series of 43 patients and review of the literature. J Pediatr Gastroenterol Nutr. 1997;24(3):276–9.
7. Agrawal S, Agarwal S, Arnason T, Saini S, Belghiti J. Management of hepatocellular adenoma: recent advances. Clin Gastroenterol Hepatol. 2014;13:1221. https://doi.org/10.1016/j.cgh.2014.05.023.
8. Shanbhogue A, Shah SN, Zaheer A, Prasad SR, Takahashi N, Vikram R. Hepatocellular adenomas: current update on genetics,taxonomy, and management. J Comput Assist Tomogr. 2011;35(2):159–66.
9. Cho SW, Marsh JW, Steel J, Holloway SE, Heckman JT, Ochoa ER, et al. Surgical management of hepatocellular adenoma: take it or leave it? Ann Surg Oncol. 2008;15(10):2795–803. https://doi.org/10.1245/s10434-008-0090-0.
10. Stoot JH, Coelen RJ, De Jong MC, Dejong CH. Malignant transformation of hepatocellular adenomas into hepatocellular carcinomas: a systematic review including more than 1600 adenoma cases. HPB (Oxford). 2010;12(8):509–22. https://doi.org/10.1111/j.1477-2574.2010.00222.x.
11. van Aalten SM, de Man RA, Ijzermans JN, Terkivatan T. Systematic review of haemorrhage and rupture of hepatocellular adenomas. Br J Surg. 2012;99(7):911–6. https://doi.org/10.1002/bjs.8762.
12. Doolittle DA, Atwell TD, Sanchez W, Mounajjed T, Hough DM, Schmit GD, et al. Safety and outcomes of percutaneous biopsy of 61 hepatic adenomas. AJR Am J Roentgenol. 2016;206(4):871–6. https://doi.org/10.2214/AJR.15.15301.
13. Bellamy CO, Maxwell RS, Prost S, Azodo IA, Powell JJ, Manning JR. The value of immunophenotyping hepatocellular adenomas: consecutive resections at one UK centre. Histopathology. 2013;62(3):431–45. https://doi.org/10.1111/his.12011.
14. Bioulac-Sage P, Cubel G, Taouji S, Scoazec JY, Leteurtre E, Paradis V, et al. Immunohistochemical markers on needle biopsies are helpful for the diagnosis of focal nodular hyperplasia and hepatocellular adenoma subtypes. Am J Surg Pathol. 2012;36(11):1691–9. https://doi.org/10.1097/PAS.0b013e3182653ece.
15. Libbrecht L, Severi T, Cassiman D, Vander Borght S, Pirenne J, Nevens F, et al. Glypican-3 expression distinguishes small hepatocellular carcinomas from cirrhosis, dysplastic nodules, and focal nodular hyperplasia-like nodules. Am J Surg Pathol. 2006;30(11):1405–11. https://doi.org/10.1097/01.pas.0000213323.97294.9a.
16. Coston WM, Loera S, Lau SK, Ishizawa S, Jiang Z, Wu CL, et al. Distinction of hepatocellular carcinoma from benign hepatic mimickers using Glypican-3 and CD34 immunohistochemistry. Am J Surg Pathol. 2008;32(3):433–44. https://doi.org/10.1097/PAS.0b013e318158142f.
17. Bioulac-Sage P, Balabaud C, Zucman-Rossi J. Subtype classification of hepatocellular adenoma. Dig Surg. 2010;27(1):39–45. https://doi.org/10.1159/000268406.
18. Nault JC, Couchy G, Balabaud C, Morcrette G, Caruso S, Blanc JF, et al. Molecular classification of hepatocellular adenoma associates with risk factors, bleeding, and malignant transformation. Gastroenterology. 2017;152(4):880–94. e6. https://doi.org/10.1053/j.gastro.2016.11.042.
19. Young JT, Kurup AN, Graham RP, Torbenson MS, Venkatesh SK. Myxoid hepatocellular neoplasms: imaging appearance of a unique mucinous tumor variant. Abdom Radiol (NY). 2016;41(11):2115–22. https://doi.org/10.1007/s00261-016-0812-x.
20. Salaria SN, Graham RP, Aishima S, Mounajjed T, Yeh MM, Torbenson MS. Primary hepatic tumors with myxoid change: morphologically unique hepatic adenomas and hepatocellular carcinomas. Am J Surg Pathol. 2015;39(3):318–24. https://doi.org/10.1097/PAS.0000000000000382.
21. Mounajjed T, Yasir S, Aleff PA, Torbenson MS. Pigmented hepatocellular adenomas have a high risk of atypia and malignancy. Modern Pathol. 2015;28(9):1265–74. https://doi.org/10.1038/modpathol.2015.83.

22. Venkatesh SK, Hennedige T, Johnson GB, Hough DM, Fletcher JG. Imaging patterns and focal lesions in fatty liver: a pictorial review. Abdom Radiol. 2017;42(5):1374–92. https://doi.org/10.1007/s00261-016-1002-6.
23. Grazioli L, Bondioni MP, Haradome H, Motosugi U, Tinti R, Frittoli B, et al. Hepatocellular adenoma and focal nodular hyperplasia: Value of gadoxetic acid-enhanced MR imaging in differential diagnosis. Radiology. 2012;262(2):520–9. https://doi.org/10.1148/radiol.11101742.
24. McInnes MDF, Hibbert RM, Inacio JR, Schieda N. Focal nodular hyperplasia and hepatocellular adenoma: accuracy of gadoxetic acid-enhanced MR imaging – a systematic review. Radiology. 2015;277(2):413–23. https://doi.org/10.1148/radiol.2015142986.
25. Agarwal S, Fuentes-Orrego JM, Arnason T, Misdraji J, Jhaveri KS, Harisinghani M, et al. Inflammatory hepatocellular adenomas can mimic focal nodular hyperplasia on gadoxetic acid-enhanced MRI. Am J Roentgenol. 2014;203(4):W408–W14. https://doi.org/10.2214/AJR.13.12251.
26. Glockner JF, Lee CU, Mounajjed T. Inflammatory hepatic adenomas: characterization with hepatobiliary MRI contrast agents. Magn Reson Imaging. 2017;47:103–10. https://doi.org/10.1016/j.mri.2017.12.006.
27. Kutami R, Nakashima Y, Nakashima O, Shiota K, Kojiro M. Pathomorphologic study on the mechanism of fatty change in small hepatocellular carcinoma of humans. J Hepatol. 2000;33(2):282–9.
28. Baffy G, Brunt EM, Caldwell SH. Hepatocellular carcinoma in non-alcoholic fatty liver disease: an emerging menace. J Hepatol. 2012;56(6):1384–91. https://doi.org/10.1016/j.jhep.2011.10.027.
29. Hashimoto E, Tokushige K. Hepatocellular carcinoma in non-alcoholic steatohepatitis: growing evidence of an epidemic? Hepatol Res. 2012;42(1):1–14. https://doi.org/10.1111/j.1872-034X.2011.00872.x.
30. Sanyal AJ, Banas C, Sargeant C, Luketic VA, Sterling RK, Stravitz RT, et al. Similarities and differences in outcomes of cirrhosis due to nonalcoholic steatohepatitis and hepatitis C. Hepatology. 2006;43(4):682–9. https://doi.org/10.1002/hep.21103.
31. Ascha MS, Hanouneh IA, Lopez R, Tamimi TA, Feldstein AF, Zein NN. The incidence and risk factors of hepatocellular carcinoma in patients with nonalcoholic steatohepatitis. Hepatology. 2010;51(6):1972–8. https://doi.org/10.1002/hep.23527.
32. Bioulac-Sage P, Taouji S, Possenti L, Balabaud C. Hepatocellular adenoma subtypes: the impact of overweight and obesity. Liver Int. 2012;32(8):1217–21. https://doi.org/10.1111/j.1478-3231.2012.02786.x.
33. Dong Y, Zhu Z, Wang W-P, Mao F, Ji Z-B. Ultrasound features of hepatocellular adenoma and the additional value of contrast-enhanced ultrasound. Hepatobiliary Pancreat Dis Int. 2016;15(1):48–54.
34. Grazioli L, Federle MP, Brancatelli G, Ichikawa T, Olivetti L, Blachar A. Hepatic adenomas: imaging and pathologic findings. Radiographics. 2001;21(4):877–92. https://doi.org/10.1148/radiographics.21.4.g01jl04877; discussion 92–4.
35. Bartolozzi C, Lencioni R, Paolicchi A, Moretti M, Armillotta N, Pinto F. Differentiation of hepatocellular adenoma and focal nodular hyperplasia of the liver: comparison of power Doppler imaging and conventional color Doppler sonography. Eur Radiol. 1997;7(9):1410–5. https://doi.org/10.1007/s003300050308.
36. Golli M, Van Nhieu JT, Mathieu D, Zafrani ES, Cherqui D, Dhumeaux D, et al. Hepatocellular adenoma: color Doppler US and pathologic correlations. Radiology. 1994;190(3):741–4. https://doi.org/10.1148/radiology.190.3.8115621.
37. Bartolotta TV, Vernuccio F, Taibbi A, Lagalla R. Contrast-enhanced ultrasound in focal liver lesions: where do we stand? Semin Ultrasound CT MR. 2016;37(6):573–86. https://doi.org/10.1053/j.sult.2016.10.003.
38. Roche V, Pigneur F, Tselikas L, Roux M, Baranes L, Djabbari M, et al. Differentiation of focal nodular hyperplasia from hepatocellular adenomas with low-mechanical-index contrast-enhanced sonography (CEUS): effect of size on diagnostic confidence. Eur Radiol. 2015;25(1):186–95. https://doi.org/10.1007/s00330-014-3363-y.

39. Rubin RA, Lichtenstein GR. Hepatic scintigraphy in the evaluation of solitary solid liver masses. J Nucl Med. 1993;34(4):697–705.
40. Lubbers PR, Ros PR, Goodman ZD, Ishak KG. Accumulation of technetium-99m sulfur colloid by hepatocellular adenoma: scintigraphic-pathologic correlation. AJR Am J Roentgenol. 1987;148(6):1105–8. https://doi.org/10.2214/ajr.148.6.1105.
41. Kotzerke J, Schwarzrock R, Krischek O, Wiese H, Hundeshagen H. Technetium-99m DISIDA hepatobiliary agent in diagnosis of hepatocellular carcinoma, adenoma, and focal nodular hyperplasia. J Nucl Med. 1989;30(7):1278–80.
42. Liu W, Delwaide J, Bletard N, Delvenne P, Meunier P, Hustinx R, et al. 18-Fluoro-deoxyglucose uptake in inflammatory hepatic adenoma: a case report. World J Hepatol. 2017;9(11):562–6. https://doi.org/10.4254/wjh.v9.i11.562.
43. Fosse P, Girault S, Hoareau J, Testard A, Couturier O, Morel O. Unusual uptake of 18FDG by a hepatic adenoma. Clin Nucl Med. 2013;38(2):135–6. https://doi.org/10.1097/RLU.0b013e318279b95a.
44. Lim D, Lee SY, Lim KH, Chan CY. Hepatic adenoma mimicking a metastatic lesion on computed tomography-positron emission tomography scan. World J Gastroenterol. 2013;19(27):4432–6. https://doi.org/10.3748/wjg.v19.i27.4432.
45. Patel PM, Alibazoglu H, Ali A, Fordham E, LaMonica G. 'False-positive' uptake of FDG in a hepatic adenoma. Clin Nucl Med. 1997;22(7):490–1.
46. Sumiyoshi T, Moriguchi M, Kanemoto H, Asakura K, Sasaki K, Sugiura T, et al. Liver-specific contrast agent-enhanced magnetic resonance and (1)(8)F-fluorodeoxyglucose positron emission tomography findings of hepatocellular adenoma: report of a case. Surg Today. 2012;42(2):200–4. https://doi.org/10.1007/s00595-011-0067-7.
47. Sanli Y, Bakir B, Kuyumcu S, Ozkan ZG, Gulluoglu M, Bilge O, et al. Hepatic adenomatosis may mimic metastatic lesions of liver with 18F-FDG PET/CT. Clin Nucl Med. 2012;37(7):697–8. https://doi.org/10.1097/RLU.0b013e3182443ced.
48. Magini G, Farsad M, Frigerio M, Serra C, Colecchia A, Jovine E, et al. C-11 acetate does not enhance usefulness of F-18 FDG PET/CT in differentiating between focal nodular hyperplasia and hepatic adenoma. Clin Nucl Med. 2009;34(10):659–65. https://doi.org/10.1097/RLU.0b013e3181b53488.
49. Nakashima T, Takayama Y, Nishie A, Asayama Y, Baba S, Yamashita Y, et al. Hepatocellular adenoma showing high uptake of (18)F-fluorodeoxyglucose (FDG) via an increased expression of glucose transporter 2 (GLUT-2). Clin Imaging. 2014;38(6):888–91. https://doi.org/10.1016/j.clinimag.2014.06.005.
50. Delbeke D, Martin WH, Sandler MP, Chapman WC, Wright JK Jr, Pinson CW. Evaluation of benign vs malignant hepatic lesions with positron emission tomography. Arch Surg. 1998;133(5):510–5. discussion 5-6
51. Ozaki K, Harada K, Terayama N, Matsui O, Saitoh S, Tomimaru Y, et al. Hepatocyte nuclear factor 1alpha-inactivated hepatocellular adenomas exhibit high ^{18}F-fludeoxyglucose uptake associated with glucose-6-phosphate transporter inactivation. Br J Radiol. 2016;89(1063):20160265. https://doi.org/10.1259/bjr.20160265.
52. Buc E, Dupre A, Golffier C, Chabrot P, Flamein R, Dubois A, et al. Positive PET-CT scan in hepatocellular adenoma with concomitant benign liver tumors. Gastroenterol Clin Biol. 2010;34(4–5):338–41. https://doi.org/10.1016/j.gcb.2010.01.018.
53. Agnello F, Ronot M, Valla DC, Sinkus R, Van Beers BE, Vilgrain V. High-b-value diffusion-weighted MR imaging of benign hepatocellular lesions: quantitative and qualitative analysis. Radiology. 2012;262(2):511–9. https://doi.org/10.1148/radiol.11110922.
54. Ba-Ssalamah A, Antunes C, Feier D, Bastati N, Hodge JC, Stift J, et al. Morphologic and molecular features of hepatocellular adenoma with gadoxetic acid-enhanced MR imaging. Radiology. 2015;277(1):104–13. https://doi.org/10.1148/radiol.2015142366.
55. Guo Y, Li W, Cai W, Zhang Y, Fang Y, Hong G. Diagnostic value of gadoxetic acid-enhanced MR imaging to distinguish HCA and its subtype from FNH: a systematic review. Int J Med Sci. 2017;14(7):668–74. https://doi.org/10.7150/ijms.17865.

56. Van Aalten SM, Thomeer MGJ, Terkivatan T, Dwarkasing RS, Verheij J, De Man RA, et al. Hepatocellular adenomas: correlation of MR imaging findings with pathologic subtype classification. Radiology. 2011;261(1):172–81. https://doi.org/10.1148/radiol.11110023.
57. Dharmana H, Saravana-Bawan S, Girgis S, Low G. Hepatocellular adenoma: imaging review of the various molecular subtypes. Clin Radiol. 2017;72(4):276–85. https://doi.org/10.1016/j.crad.2016.12.020.
58. Laumonier H, Bioulac-Sage P, Laurent C, Zucman-Rossi J, Balabaud C, Trillaud H. Hepatocellular adenomas: magnetic resonance imaging features as a function of molecular pathological classification. Hepatology. 2008;48(3):808–18. https://doi.org/10.1002/hep.22417.
59. Tse JR, Naini BV, Lu DSK, Raman SS. Qualitative and quantitative gadoxetic acid-enhanced MR imaging helps subtype hepatocellular adenomas. Radiology. 2016;279(1):118–27. https://doi.org/10.1148/radiol.2015142449.
60. Bedossa P, Burt AD, Brunt EM, Callea F, Clouston AD, Dienes HP, et al. Well-differentiated hepatocellular neoplasm of uncertain malignant potential: proposal for a new diagnostic category. Hum Pathol. 2014;45(3):658–60. https://doi.org/10.1016/j.humpath.2013.09.020.
61. Karkar AM, Tang LH, Kashikar ND, Gonen M, Solomon SB, Dematteo RP, et al. Management of hepatocellular adenoma: comparison of resection, embolization and observation. HPB (Oxford). 2013;15(3):235–43. https://doi.org/10.1111/j.1477-2574.2012.00584.x.
62. Bieze M, Phoa SS, Verheij J, van Lienden KP, van Gulik TM. Risk factors for bleeding in hepatocellular adenoma. Br J Surg. 2014;101(7):847–55. https://doi.org/10.1002/bjs.9493.
63. Nault JC, Bioulac-Sage P, Zucman-Rossi J. Hepatocellular benign tumors-from molecular classification to personalized clinical care. Gastroenterology. 2013;144(5):888–902. https://doi.org/10.1053/j.gastro.2013.02.032.
64. Broker ME, Ijzermans JN, van Aalten SM, de Man RA, Terkivatan T. The management of pregnancy in women with hepatocellular adenoma: a plea for an individualized approach. Int J Hepatol. 2012;2012:725735. https://doi.org/10.1155/2012/725735.
65. Noels JE, van Aalten SM, van der Windt DJ, Kok NF, de Man RA, Terkivatan T, et al. Management of hepatocellular adenoma during pregnancy. J Hepatol. 2011;54(3):553–8. https://doi.org/10.1016/j.jhep.2010.07.022.
66. Deneve JL, Pawlik TM, Cunningham S, Clary B, Reddy S, Scoggins CR, et al. Liver cell adenoma: a multicenter analysis of risk factors for rupture and malignancy. Ann Surg Oncol. 2009;16(3):640–8. https://doi.org/10.1245/s10434-008-0275-6.
67. Stoot JH, Coelen RJ, De Jong MC, Dejong CH. Malignant transformation of hepatocellular adenomas into hepatocellular carcinomas: a systematic review including more than 1600 adenoma cases. HPB. 2010;12(8):509–22. https://doi.org/10.1111/j.1477-2574.2010.00222.x.
68. Bioulac-Sage P, Laumonier H, Couchy G, Le Bail B, Sa Cunha A, Rullier A, et al. Hepatocellular adenoma management and phenotypic classification: the Bordeaux experience. Hepatology. 2009;50(2):481–9. https://doi.org/10.1002/hep.22995.
69. Bioulac-Sage P, Rebouissou S, Thomas C, Blanc JF, Saric J, Sa Cunha A, et al. Hepatocellular adenoma subtype classification using molecular markers and immunohistochemistry. Hepatology. 2007;46(3):740–8. https://doi.org/10.1002/hep.21743.
70. Henriet E, Abou Hammoud A, Dupuy JW, Dartigues B, Ezzoukry Z, Dugot-Senant N, et al. Argininosuccinate synthase 1 (ASS1): a marker of unclassified hepatocellular adenoma and high bleeding risk. Hepatology. 2017;66(6):2016–28. https://doi.org/10.1002/hep.29336.
71. Farges O, Ferreira N, Dokmak S, Belghiti J, Bedossa P, Paradis V. Changing trends in malignant transformation of hepatocellular adenoma. Gut. 2011;60(1):85–9. https://doi.org/10.1136/gut.2010.222109.
72. van Rosmalen BV, Coelen RJS, Bieze M, van Delden OM, Verheij J, Dejong CHC, et al. Systematic review of transarterial embolization for hepatocellular adenomas. Br J Surg. 2017;104(7):823–35. https://doi.org/10.1002/bjs.10547.

73. Atwell TD, Brandhagen DJ, Charboneau JW, Nagorney DM, Callstrom MR, Farrell MA. Successful treatment of hepatocellular adenoma with percutaneous radiofrequency ablation. AJR Am J Roentgenol. 2005;184(3):828–31. https://doi.org/10.2214/ajr.184.3.01840828.
74. Smolock AR, Cristescu MM, Potretzke TA, Ziemlewicz TJ, Lubner MG, Hinshaw JL, et al. Microwave ablation for the treatment of hepatic adenomas. J Vasc Interv Radiol. 2016;27(2):244–9. https://doi.org/10.1016/j.jvir.2015.09.021.
75. Ribeiro A, Burgart LJ, Nagorney DM, Gores GJ. Management of liver adenomatosis: results with a conservative surgical approach. Liver Transpl Surg. 1998;4(5):388–98.
76. Vetelainen R, Erdogan D, de Graaf W, ten Kate F, Jansen PL, Gouma DJ, et al. Liver adenomatosis: re-evaluation of aetiology and management. Liver Int. 2008;28(4):499–508. https://doi.org/10.1111/j.1478-3231.2008.01669.x.
77. Yoshidome H, McMasters KM, Edwards MJ. Management issues regarding hepatic adenomatosis. Am Surg. 1999;65(11):1070–6.
78. Chiche L, Dao T, Salame E, Galais MP, Bouvard N, Schmutz G, et al. Liver adenomatosis: reappraisal, diagnosis, and surgical management: eight new cases and review of the literature. Ann Surg. 2000;231(1):74–81.
79. Chiche L, David A, Adam R, Oliverius MM, Klempnauer J, Vibert E, et al. Liver transplantation for adenomatosis: European experience. Liver Transpl. 2016;22(4):516–26. https://doi.org/10.1002/lt.24417.

Chapter 5
Infectious and Inflammatory Lesions of the Liver

Patrick J. Navin, Christine O. Menias, Rondell P. Graham, Maria Baladron Zanetti, Sudhakar K. Venkatesh, and Wendaline M. VanBuren

Introduction

Imaging plays an important role in the diagnosis and treatment of infectious and inflammatory diseases of the liver. Infectious pathogens may be bacterial, viral, parasitic, or fungal whereas other inflammatory lesions have an unknown etiology. Early diagnosis and management is crucial as many infections can be fatal if not treated early. Ultrasonography (US), computed tomography (CT), and magnetic resonance (MR) imaging allow for accurate detection of most hepatic infections and may provide features which may help identify the underlying pathogen.

However, imaging often lacks specificity in the diagnosis of the causative pathogen. As a result, more invasive methods such as serology, fluid analysis, and tissue sampling are typically required to allow for a definitive diagnosis and to guide possible curative management.

P. J. Navin · M. B. Zanetti · W. M. VanBuren (✉) · S. K. Venkatesh
Department of Radiology, Mayo Clinic, Rochester, MN, USA
e-mail: Navin.patrick@mayo.edu; VanBuren.Wendaline@mayo.edu; Venkatesh.Sudhakar@mayo.edu

C. O. Menias
Department of Radiology, Mayo Clinic, Scottsdale, AZ, USA
e-mail: Menias.Christine@mayo.edu

R. P. Graham
Department of Laboratory Medicine and Pathology, Mayo Clinic, Rochester, MN, USA
e-mail: Graham.Rondell@mayo.edu

L. R. Roberts et al. (eds.), *Evaluation and Management of Liver Masses*,
https://doi.org/10.1007/978-3-030-46699-2_5

This chapter will provide a background of the more common infectious and inflammatory hepatic diseases with a focus on their associated imaging characteristics.

Bacterial

Pyogenic Abscess

Pyogenic (bacterial) abscesses of the liver were first described at the time of Hippocrates in 400 BC. They account for approximately 48% of all visceral abscesses [1]. The incidence of liver abscesses varies per country with a rate of 1.1 per 100,000 population per year in Canada, 2.3 per 100,000 in Denmark, and up to 17.6 per 100,000 in Taiwan. The rate in the US is reported as 3.6–4.1 cases per 100,000 population [2, 3]. The incidence of liver abscesses has increased two-fold over the past 35 years [3]. This increase is multifactorial, with increasing hepatobiliary disease and interventional procedures as possible causes [2].

The portal vein is an important source of spread from a gastrointestinal source with portal pyemia implicated in 20% of cases [4]. Biliary obstruction and resultant ascending cholangitis is also a significant source of hepatic abscesses [4]. Direct inoculation and hematogenous seeding from the systemic circulation are less common causes [5–7].

The bacterium implicated depends on the mode of spread and the population affected. Traditionally, *Escherichia coli* has been reported as the most common bacterium; however, Asian studies report that *Klebsiella pneumoniae* is the most common pathogen in pyogenic liver abscesses [2, 8, 9]. E. coli is implicated in abscesses from a biliary source whereas *Klebsiella pneumoniae* is associated with cryptogenic abscesses [10]. E. coli, Enterobacter cloacae, and Enterococcus faecalis have been implicated in abscesses developing post-transarterial embolization of hepatic malignancy [10, 11].

Treatment is centered on antibiotic coverage with percutaneous drainage depending on locularity and size. Access into the abscess is always beneficial in order to allow microbiological analysis of the contents and guide antibiotic coverage. In unilocular abscesses, percutaneous needle aspiration or catheter placement may be possible, with catheter placement preferred in abscesses greater than 5 cm [12]. In multiloculated abscesses, the decision to aspirate is on a case-by-case basis, depending on patient status, radiologist's skill or comfort with the procedure, and position/locularity of the abscess. Surgical management is often warranted in more severe cases.

The clinical presentation and initial laboratory studies may raise the initial suspicion of a pyogenic abscess; however, imaging studies are required to establish the diagnosis.

When assessed in the emergency department, US demonstrates a sensitivity of 86% for pyogenic abscess [13]. Microabscesses (<2 cm) are typically seen as small hypoechoic structures or ill-defined areas of architectural distortion [14]. Larger abscesses are classically identified as an ill-defined hypoechoic structure with posterior acoustic enhancement and absence of internal vascularity on color Doppler imaging. Fluid-debris levels may be present [14–16]. The presence of internal echogenicity is variable and the lesion may mimic a solid mass (Fig. 5.1). These characteristics are most commonly observed early in the disease process when gas bubbles are also often present. Klebsiella or Clostridium species are the most common causative agents of gas-containing abscesses [15, 17–19]. US is operator dependent and often limited by patient factors such as subcutaneous adiposity and hepatic steatosis which may decrease visualization.

The imaging of pyogenic abscesses on CT is variable with a sensitivity of 97% [20]. The typical CT appearance is of a low attenuation lesion with peripheral rim enhancement (Figs. 5.1 and 5.2) [16]. The presence of air is best appreciated on CT [21]. Certain specific features are also appreciated on contrast-enhanced CT, such as the "double target sign," defined as a central area of fluid attenuation surrounded by an inner ring of high attenuation and outer ring of low attenuation (Figs. 5.1 andd 5.2), which is seen in 30% of hepatic abscesses. The inner ring demonstrates early and persistent contrast enhancement whereas the outer ring demonstrates enhancement on delayed phase only [22]. The "cluster sign" describes a coalescence of small low attenuation lesions that forms a larger abscess, seen in early infection [15, 23]. In a retrospective study of 92 patients with a monomicrobial Klebsiella hepatic abscess, 58% were described as solid on CT and 95% multilocular (Fig. 5.3). This compares to a 36% solid and 72% multilocular appearance in a comparison group caused by other bacteria [24]. Multiple internal enhancing septations have also been described in a "turquoise pattern" (Fig. 5.4).

Pyogenic abscesses typically demonstrate internal low T1 signal and high T2 signal (Fig. 5.3), which can be seen in 91% of abscesses [25]. The presence of proteinaceous material or gas may alter the internal signal intensity [25, 26]. Perilesional edema is identified as surrounding high T2 signal and is present in 35% of cases [26]. Appearances post administration of extracellular contrast agent are similar to appearances on contrast-enhanced CT imaging with capsular enhancement seen in up to 100% of cases and a recognized "double target sign" [25, 27]. The absence of capsular enhancement has however been noted in immunocompromised patients [28]. Pyogenic abscesses universally demonstrate abnormal diffusion restriction [27].

Pyogenic abscesses may mimic a necrotic tumor on all imaging modalities, and definitive diagnosis often requires tissue sampling. Certain features such as a layered wall appearance with early inner rim enhancement and delayed enhancement of the outer layer are characteristic of an abscess [22]. Other features such as transient segmental enhancement and abnormal restricted diffusion may allow for greater differentiation [27, 29].

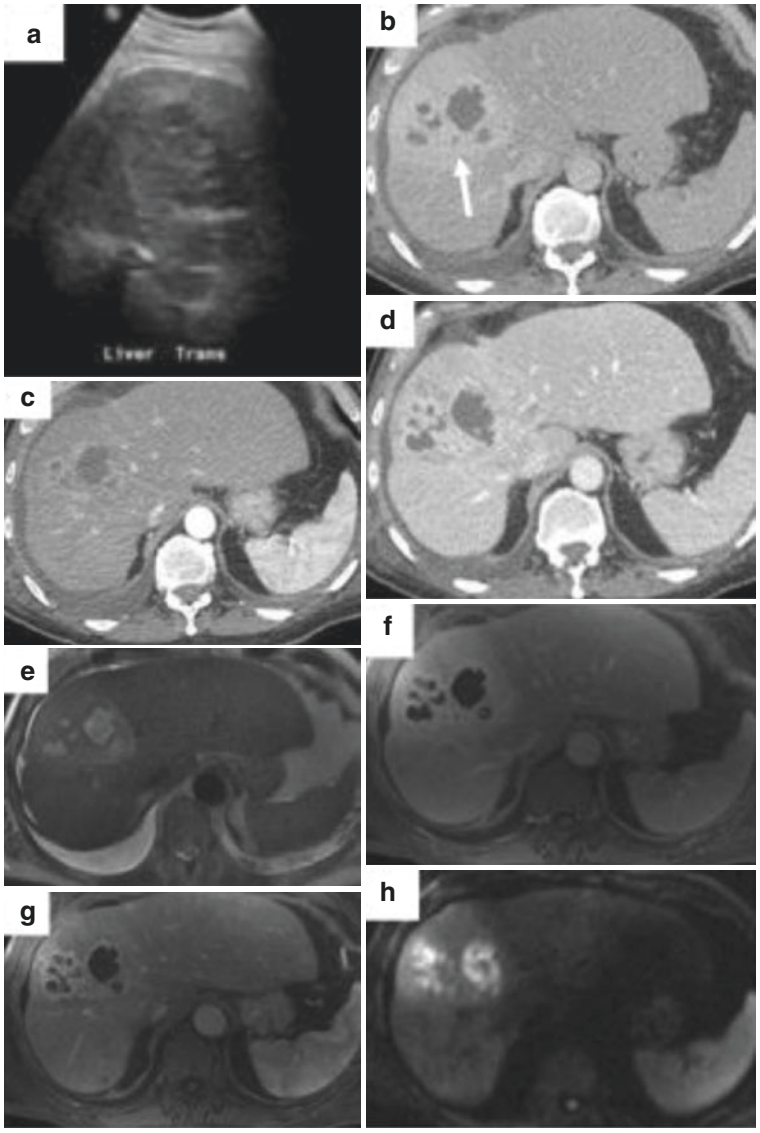

Fig. 5.1 Ultrasound of a 74-year-old patient with abnormal liver function tests, abdominal pain, and fever. Subsequent biopsy and aspiration grew streptococcal species, consistent with a pyogenic abscess. There is a well-defined mass in the right liver, slightly hypoechoic compared to the surrounding liver with minimal posterior acoustic enhancement (**a**). CT of the same patient demonstrates a multiloculated mass, hypoattenuating centrally on noncontrast CT (**b**). Arterial phase contrast-enhanced CT demonstrates peripheral rim enhancement and an outer ring of low attenuation (double target sign) (**c**). There is persistent peripheral enhancement on portal venous phase without fill-in (**d**). MRI of the same patient. Multiloculated fluid collection again noted. There is central high signal on T2-weighted sequences with ill-defined zone of high signal intensity correlating to perilesional edema (**e**). The lesion is of low signal intensity on T1-weighted sequences (**f**) with rim enhancement post-administration of gadolinium (**g**). There are areas of abnormal restricted diffusion on apparent diffusion coefficient map and diffusion-weighted images (**h**, **i**). Subsequent biopsy and aspiration grew streptococcal species

Fig. 5.1 (continued)

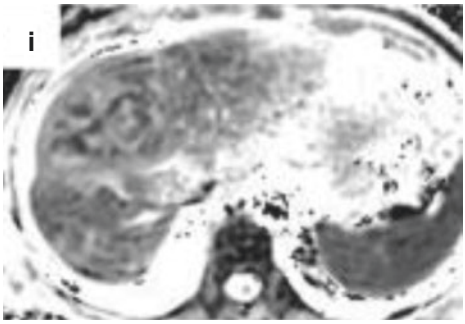

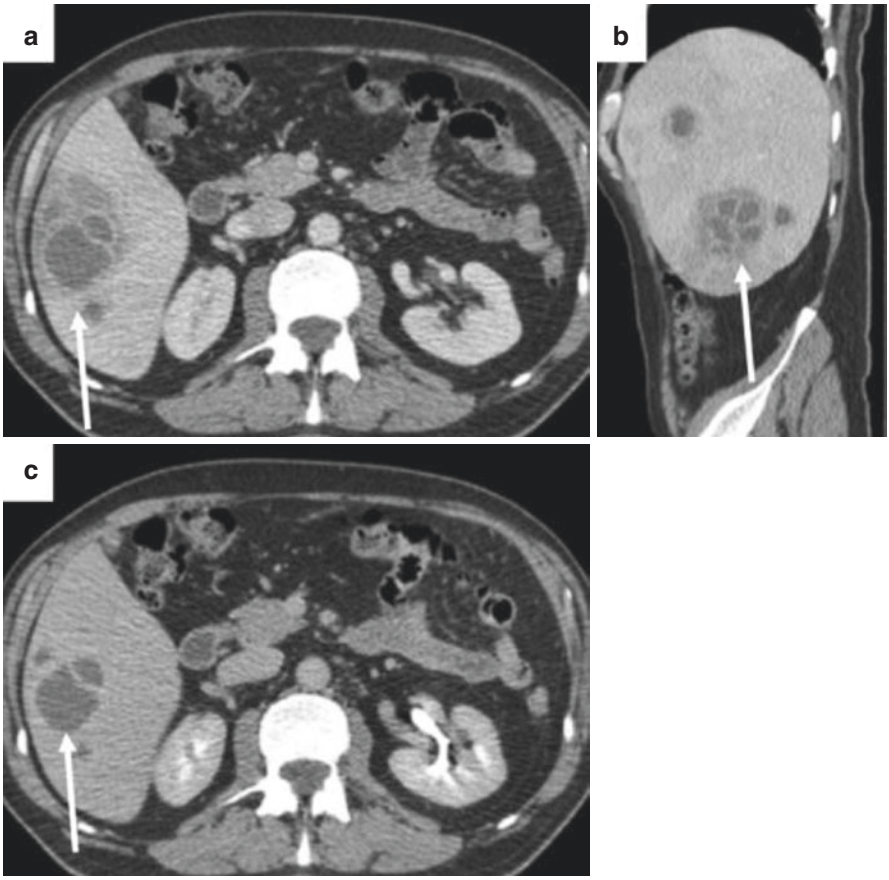

Fig. 5.2 Contrast-enhanced CT in a 50–year-old female patient with pyogenic abscess. Portal venous phase (**a**, **b**) and delayed phase images (**c**) demonstrate a loculated collection separated by septae. Note the double target sign on portal venous phase imaging consisting of a hypodense, avascular central area, surrounded by an enhancing rim, and a hypoenhancing, ill-defined area. This external area demonstrates late phase contrast enhancement (**c**)

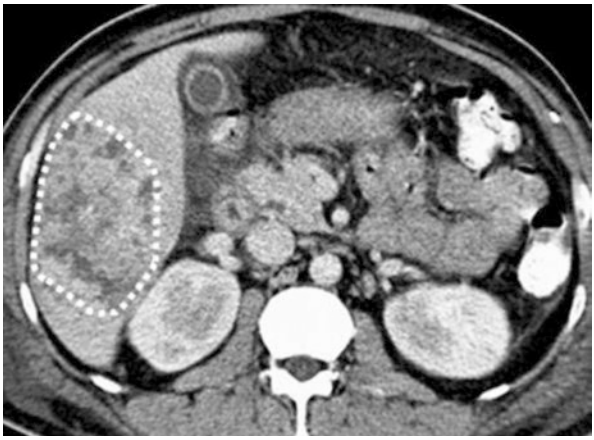

Fig. 5.3 Contrast-enhanced CT of a 63-year-old man who presented with fever and abdominal pain. There is a solid appearing mass in the right liver with hypodense areas consistent with liquefaction. Pus and blood cultures were positive for *Klebsiella pneumoniae*. (Images courtesy of: Alsaif et al. [24])

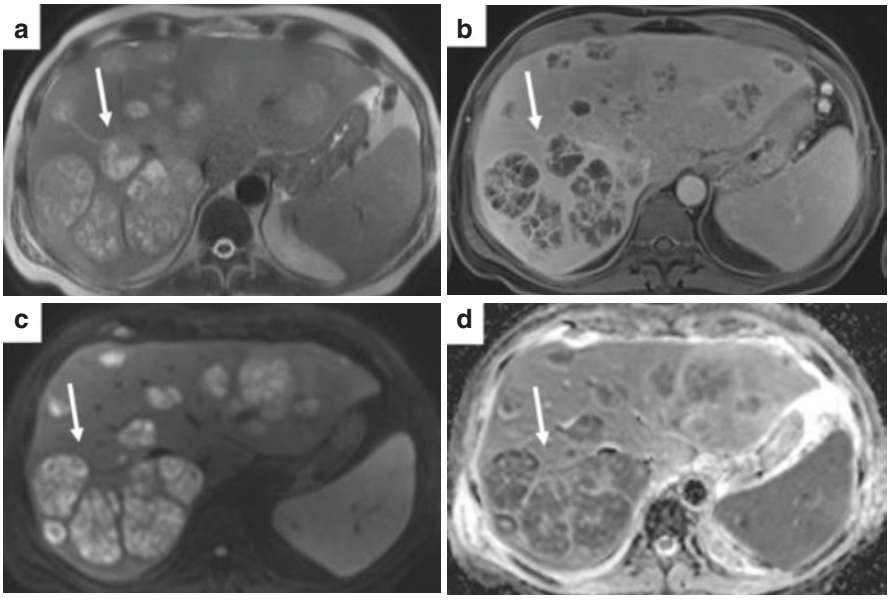

Fig. 5.4 MR abdomen of a 45-year-old male presenting with fever, abdominal pain, and bacteremia. Aspiration and culture demonstrated streptococcal species. Abdominal MR axial T2 WI (**a**), T1 FS post-contrast (**b**), and Diffusion with ADC map (**c**, **d**). Note the numerous septal bands resembling a turquoise pattern

Hepatobiliary Tuberculosis

Tuberculosis (TB) caused by the bacillus *Mycobacterium tuberculosis* is predominantly a disease of the developing world with 95% of deaths due to TB occurring in developing countries [30]. In the United States, incidence rates are on the decline

with a nationwide incidence rate of 2.9 cases per 100,000 per year [31]. Hepatobiliary TB accounts for approximately 1.2% of all cases of TB. Primary hepatic TB is exceedingly rare [32, 33].

The transmission of hepatobiliary TB may be via the hepatic artery, portal vein, or lymphatic vessels. The hepatic artery is the most common route with the dissemination of miliary TB from a pulmonary source [32, 34]. Portal or lymphatic spread is via the GI tract or lymphatics [35]. Irrespective of the mode of transmission, a granulomatous reaction occurs within the liver [36].

The classification of hepatobiliary TB is confusing with multiple systems offered. Based on imaging and histopathological patterns, involvement may be divided into the parenchymal type, serohepatic type, and tuberculous cholangitis.

Two types of parenchymal hepatobiliary TB are generally recognized in the radiology literature: a micronodular and macronodular form [16, 37]; however imaging is nonspecific. Tuberculous abscesses can also develop but are very rare [38]. The diagnosis is usually via a combination of clinical findings, imaging, biopsy, and mycobacterial culture. Biopsy is deemed the most specific diagnostic tool [33, 39].

The micronodular form is more common, accounting for 79% of cases, and is due to miliary dissemination with the formation of tuberculomas ranging from 0.6 to 2 mm [39]. Tuberculomas generally seed close to the portal tracts [38]. Autopsy studies demonstrate hepatobiliary TB in 50–80% of patients with pulmonary TB [40, 41]. The micronodular form, however, is often not visualized. Hepatomegaly and a diffusely echogenic liver are the most common imaging features on ultrasound [42]. On CT, diffuse low-density foci are occasionally seen (Figs. 5.5 and 5.6) [42, 43]. Healing micronodular tuberculomas can calcify, which make them more readily identifiable on CT imaging [44, 45]. MRI may demonstrate superior performance in identifying micronodular foci, yet the sensitivity remains low [46]. The micronodular lesions are seen as foci with low signal intensity on T1-weighted sequences and high signal on T2-weighted sequences [43]. The use of

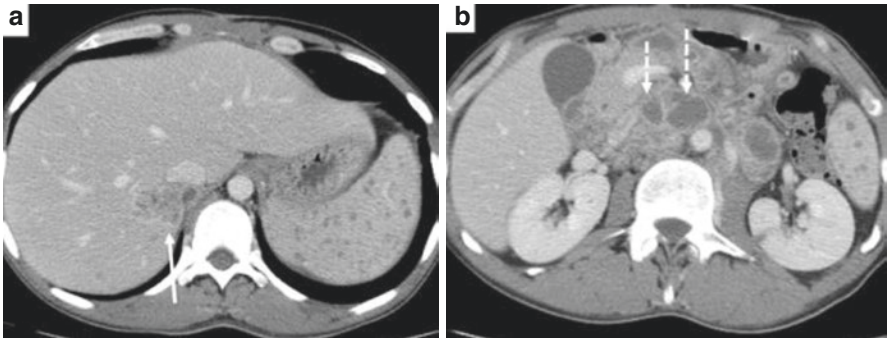

Fig. 5.5 Contrast-enhanced CT of a 28-year-old male patient with HIV and disseminated, micronodular TB. Multiple hypodense lesions are visualized in the liver and spleen consistent with micronodular disease. Note the confluent mass in right hepatic lobe consistent with a tuberculoma (**a** arrow). Extensive mesenteric and retroperitoneal cavitary lymphadenopathy is also seen (**b** broken arrows)

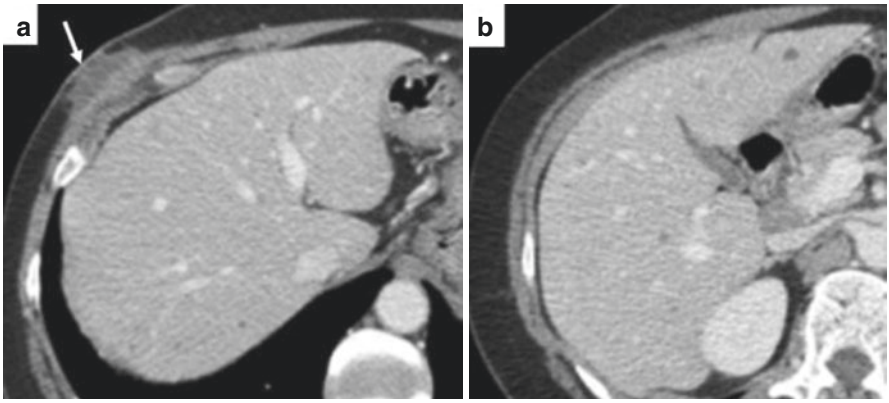

Fig. 5.6 Contrast-enhanced CT at different liver levels (**a** & **b**) demonstrates small round hypodense hepatic lesions consistent with disseminated micronodular TB. A subcutaneous abscess with underlying rib involvement is present (arrow)

18F-fluorodeoxyglucose Positron Emission Tomography adds minimal diagnostic information. The micronodular form may at times present as significantly increased radiotracer uptake in the liver or a "hepatic superscan" [47, 48].

The macronodular form predominantly arises via the gastrointestinal tract and forms a tubercle greater than 2 mm [32]. This presentation, also described as local or pseudotumoral TB, is rarer, being seen in 21% of hepatobiliary TB cases [39]. The process is often focal and tends to occur at the portal triads [32, 49]. Lesions are predominantly hypoechoic on ultrasound but may be hyperechoic early in the disease process before the onset of necrosis [35, 37]. Macronodular tubercles on contrast-enhanced CT are of low attenuation centrally with a variable hyperenhancing rim representing granulation tissue (Fig. 5.7) [38, 50]. On T1-weighted MR images, tuberculomas appear as an area of hypointensity with a hypointense rim. On T2-weighted sequences, they predominantly appear as hyperintense or isointense, again depending on the presence of necrosis, with peripheral rim or internal septal enhancement after the administration of extracellular contrast [43, 51]. Serohepatic tuberculosis is the rarest form of hepatobiliary TB. It describes the involvement of the subserosal plane of the liver. Imaging findings typically demonstrate focal areas of capsule thickening with a classical "frosted" appearance [43].

Tuberculous involvement of the biliary system is rare, and transmission is via portal spread from the GI tract or by direct extension from hepatic parenchyma or lymphatics [51]. The intrahepatic ducts are more commonly affected [52, 53]. Obstruction of the extrahepatic ducts in the presence of TB is generally secondary to mass effect from periportal lymph nodes [53–55]. Extrahepatic biliary TB is very rare [56–58]. Imaging features are nonspecific. US, CT, endoscopic retrograde cholangiopancreatography (ERCP), and MR cholangiopancreatography (MRCP) may be utilized. Imaging generally demonstrates ductal wall thickening with stricturing and resultant proximal dilatation [59, 60]. Focal calcifications along the biliary system have also been described in the presence of military TB and are best appreciated

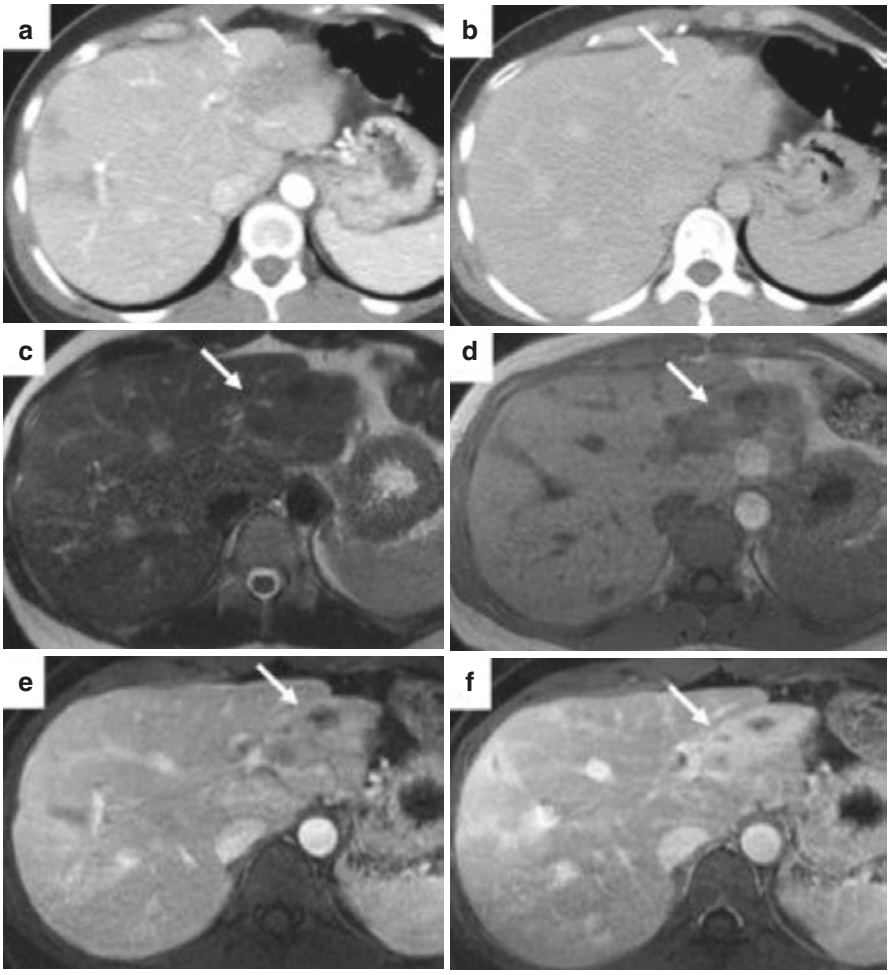

Fig. 5.7 A 45-year-old woman who presented with fever of unknown origin and was ultimately diagnosed with disseminated macronodular TB. Contrast-enhanced CT demonstrates a hypoenhancing area in the left liver on late arterial phase imaging (**a**) which demonstrates subtle enhancement on delayed images (**b**). MRI abdomen demonstrates a correlating mass isointense on T2- (**c**) and hypointense on T1-weighted sequences (**d**). This lesion demonstrates patchy enhancement on late arterial phase contrast-enhanced images (**e**) and more homogenous enhancement on portal venous phase images (**f**)

on US and CT imaging [60]. The presence of TB features elsewhere such as nodal or pulmonary involvement may suggest the diagnosis; however, tissue sampling through ERCP is typically required for a definitive diagnosis. Differentials to consider include benign inflammatory strictures secondary to sclerosing cholangitis, Mirizzi's syndrome, pancreatitis, or malignant strictures secondary to cholangiocarcinoma, particularly the diffuse sclerosing type [61].

Bartonellosis

Bartonellosis describes an infectious disease caused by bacteria from the *Bartonella* genus. These are gram-negative facultative intracellular parasites that can cause an array of infectious syndromes. *Bartonella henselae* is a particular strain which may affect immunocompetent and immunosuppressed hosts.

Cat-scratch disease is an infection in immunocompetent individuals caused by B henselae. Rare cases have been described caused by *B clarridgeiae* and *Afipia felis* [62, 63]. It affects children or young adults; however 6% of cases occur in adults over 60 years [64]. A large retrospective study identified 12,000 cases of CSD per year in the United States from 2005 to 2013. Those most affected were children aged 5–9 and individuals in the south-eastern states [65]. Cats act as a natural reservoir for *B. henselae*, and transmission is typically via a scratch or bite from an infected cat, especially those with fleas [66].

The initial presentation is typically with a local papular or pustular lesion at the site of inoculation with fever and painful lymphadenopathy. These findings generally appear approximately 1–3 weeks post exposure [67]. Disseminated infection can involve the liver, spleen, eye, or nervous system and occurs in 5–10% [68].

The involvement of the liver and spleen is rare but important to recognize [69, 70]. Disseminated cat-scratch disease to the liver is identified on imaging as multiple granulomatous lesions measuring 3–30 mm. Hepatomegaly may or may not be present. On ultrasound these lesions appear hypoechoic with either ill-defined or well-defined borders (Fig. 5.8) [14, 67]. CT demonstrates hypoattenuating lesions on noncontrast images (Figs. 5.8 and 5.9) [14, 71]. Variable enhancement characteristics have been described. The lesions may demonstrate hypoenhancement in relation to background liver, may be isoenhancing to background liver, or may demonstrate peripheral hyperenhancement [71, 72]. Findings on MRI are nonspecific with the granulomatous lesions having low T1 and high T2 signal with rim enhancement [16, 73].

The differential diagnosis based on imaging alone is wide, with sarcoidosis, infective causes such as disseminated fungal infections and malignancies such as lymphoma and metastasis as possibilities. The presentation becomes more specific when the presence of these nodules is in an immunocompetent young patient with splenic nodules. Tissue sampling or blood serological analysis is required for definitive diagnosis [16].

The infection of an immunocompromised host with Bartonella henselae, almost exclusively secondary to HIV, may be associated with peliosis hepatis. The mode of transmission is unclear, but animal or insect vectors are likely involved [74, 75]. Peliosis is the formation of blood-filled, dilated sinusoids, typically measuring 2–10 mm. The pathophysiology is not completely understood, but the proliferation of hepatic endothelial cells secondary to vascular endothelial growth factor is believed to play a central role [76].

The sonographic appearance reveals hypoechoic lesions with CT imaging typically demonstrating multiple small hypoattenuating areas [77, 78]. On MRI the

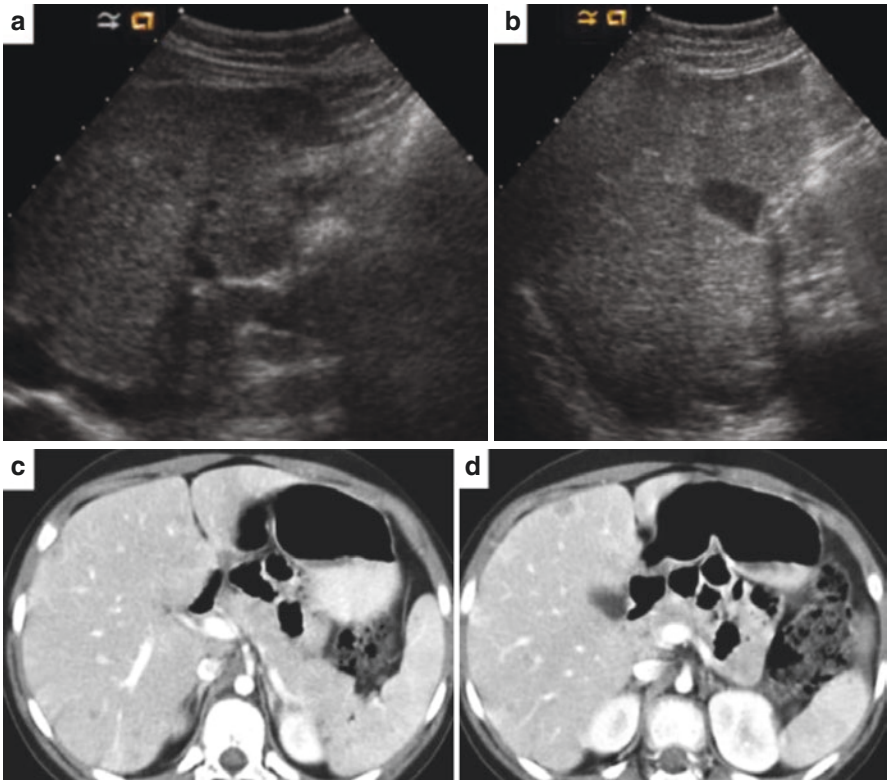

Fig. 5.8 A 9-year-old female with a 9-day history of fever, headache, and stiff neck. LP was negative on the 1st day of symptoms with normal CT and MRI brain on repeat visit. History of exposure to kittens. Serology demonstrated high *Bartonella henselae* IgG titers, consistent with cat-scratch disease. Ultrasound abdomen demonstrates multiple tiny hypoechoic lesions within the liver and spleen, suspicious for abscesses (**a**, **b**). There is mild hepatomegaly. Contrast-enhanced CT demonstrates multiple small hypoattenuating areas in the liver and spleen. These demonstrate mild peripheral enhancement most consistent with hepatic and splenic microabscesses (**c**, **d**)

lesions are of low signal intensity on T1-weighted imaging and high signal intensity on T2-weighted sequences with internal foci of high T1 signal related to hemorrhagic material [79]. There is typically no significant mass effect on the surrounding vasculature [80]. The enhancement pattern is similar on CT and MRI. Peliosis hepatis can demonstrate multiple enhancement patterns which vary depending on the presence of hemorrhage, presence of thrombus, or the size of the lesion. Smaller lesions may demonstrate arterial phase hyperenhancement which persists on portal venous phase imaging [79]. For larger lesions, a globular enhancement pattern predominates on early phases. Fill-in is predominantly centrifugal but may be centripetal [79, 81]. In delayed phases, a persistent peripheral ring like enhancement has been described; however, blood pooling is typical with a persistent homogenous enhancement [79, 82].

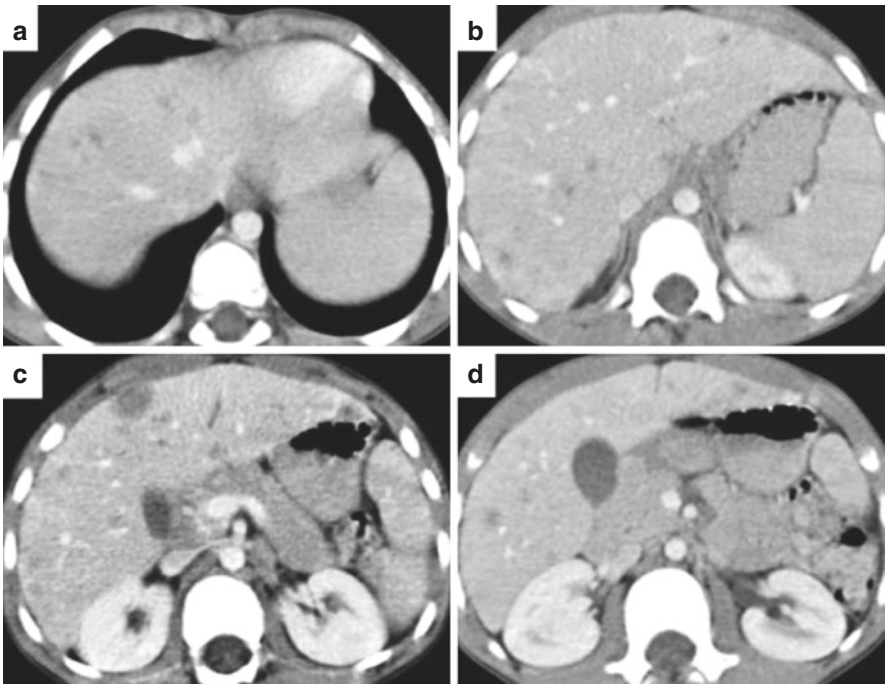

Fig. 5.9 A 6-year-old boy with cat-scratch disease. After multiple presentations to emergency room with fever of unknown origin, serology demonstrated high *Bartonella henselae* henselae IgG titers. Contrast-enhanced CT demonstrated multiple ill-defined, hypoattenuating lesions throughout the liver (**a**, **b**, **c**) with portal adenopathy (**d**). Given the clinical presentation the primary differential was multiple abscesses secondary to bacterial or fungal infection. Metastatic disease or lymphoma was considered less likely

Viral

Viral Hepatitis

Viral hepatitis can arise secondary to infection from various pathogens. In the United States, most causes are secondary to hepatitis A, hepatitis B, and hepatitis C which account for more than 90% of cases [83]. Other possible causes include hepatitis D, hepatitis E, HIV, Coxsackie virus, rubella virus, varicella, and herpes simplex virus.

The clinical presentation varies and is dependent on the individual and the causative agent. Classically, there are four phases described: the asymptomatic viral replication phase; the prodromal phase with nonspecific symptoms such as nausea, vomiting, and malaise; the icteric phase with jaundice, dark urine, and pale stools; and finally the convalescent phase during which symptoms resolve. Progression to chronic liver disease and cirrhosis is more commonly seen in hepatitis B and

hepatitis C infections. Hepatitis D can be transmitted as a co-infection at the same time as hepatitis B virus infection or as a superinfection of patients with existing chronic hepatitis B [84].

The clinical presentation, hematological, histopathological, and imaging tests are often utilized to form the diagnosis of viral hepatitis. Imaging is nonspecific but may allow other hepatitis mimics to be excluded [14]. The imaging presentation is usually one of a diffuse hepatitis; however, occasionally focal lesions are identified, particularly in varicella and herpes simplex involvement [85–87].

In acute hepatitis, ultrasound appearances vary and may range from normal to hepatomegaly with a diffusely hypoechoic parenchymal appearance. The portal venous walls may appear hyperechoic in comparison, giving the classical "starry sky" pattern [14, 88]. Geographical heterogeneity is appreciated on CT with well-defined areas of low attenuation [89]. Nonspecific findings such as hepatomegaly and periportal edema are visualized on CT and MR imaging [14].

Fulminant hepatic failure is a severe acute liver injury characterized by coagulopathy and encephalopathy in patients without chronic liver disease. It is characterized on CT by focal or diffuse areas of necrosis (hypoattenuation) and portal vein dilatation. It can be distinguished from acute hepatitis without encephalopathy by the absence of hepatomegaly and progressive decrease in size on serial CT.

When focal nodules are visualized, they are multiple, small, ill-defined nodules, hypoechoic on ultrasound and hypodense on CT imaging (Fig. 5.10) [85–87]. This appearance is nonspecific with pathologies such as pyogenic abscess, fungal abscess, metastatic disease, and lymphoma in the differential diagnosis [85].

The imaging appearances of chronic hepatitis may range from normal to cirrhosis. Ultrasound may demonstrate coarsened hepatic echotexture with diffusely increased echogenicity [14]. On CT and MRI periportal lymphadenopathy may be the only abnormality [88].

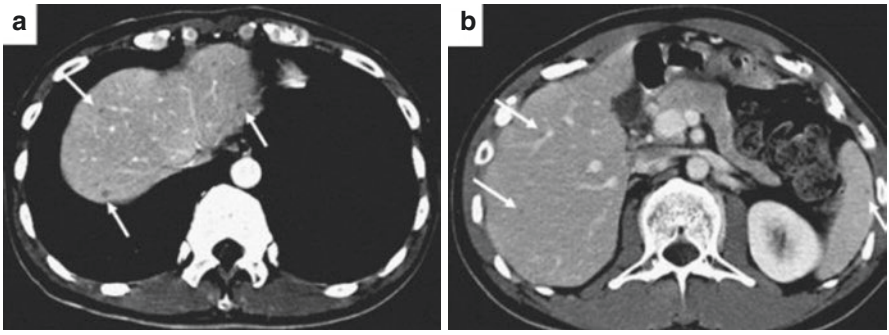

Fig. 5.10 Contrast-enhanced CT of the liver in a 42-year-old male with hepatosplenic varicella. The patient presented with a 5-day history of a vesicular rash, fever, abdominal pain, cough, and excessive tearing. Multiple, well-defined, small hypodense nodules (white arrows) are seen in both lobes of the liver and also in the spleen (**a** & **b**). Symptoms and imaging appearance resolved following acyclovir therapy. (Courtesy of: Venkatesh and Lo [85])

Fungal Infections

Candidiasis

Hepatosplenic candidiasis almost exclusively presents in immunocompromised patients. Its prevalence has decreased since the 1980s with the introduction of prophylaxis in at-risk individuals [90]. It typically develops in individuals undergoing chemotherapy for a hematological infection with absolute neutrophil counts below 500/μL for more than 10 days [91].

The presentation is of a recently neutropenic patient whose neutrophils have normalized with a fever that does not respond to standard antibiotic therapy. Blood cultures are unreliable with a definitive diagnosis only possible by biopsy [92]. The mainstay of treatment is an antifungal regimen. Despite treatment, mortality rates remain high [93].

US typically demonstrates multiple hypoechoic lesions measuring up to 2 cm; this appearance is most common yet least specific. Various other appearances have been described depending on the stage of the disease and the degree of immunosuppression. A "bulls-eye" appearance is seen with a central hyperechoic area encircled by a hypoechoic area. These lesions correspond to histopathological appearances of central inflammatory cells surrounded by an area of fibrosis. Lesions with a similar layered appearance, except with a central hypoechoic nidus, are also described. These are typically termed the "wheel within a wheel" appearance. The central hypoechoic nidus corresponds to an area of necrosis. A homogenous, hyperechoic pattern is also seen and typically represents resolution with variable degrees of posterior acoustic shadowing indicating resolution and calcification [14, 16, 94]. Contrast-enhanced ultrasound may be beneficial. Lesions may be hypoechoic in all phases; however, there may also be evidence of rim hyper- or iso-enhancement [95].

CT and MR imaging are valuable imaging tools as these modalities can identify hepatosplenic candidiasis in these immunocompromised patients before the recovery of absolute neutrophil count. Lesions in the acute phase are best appreciated in early arterial phase imaging with a "bulls-eye" appearance, similar to US, or a nonspecific hypoattenuating microabscess on CT (Fig. 5.11) [96]. As the lesion progresses into the subacute or chronic stages of the disease, the lesions may become hyperattenuating secondary to hemorrhagic products or calcification [97].

Fungal lesions on MRI are often hypointense on T1-weighted sequences and hyperintense on T2-weighted sequences, demonstrate intense peripheral ring enhancement on arterial phase contrast enhanced imaging, and restrict diffusion [44, 98]. MRI in the clinical setting of known or suspected hepatosplenic candidiasis has a sensitivity of 100% and a specitivity of 97% [98].

Histopathological analysis typically describes microabscesses with central fungus and a surrounding necrotic area. Granulomas may also form with branching hyphae visualized depending on the particular stain (Fig. 5.11) [14].

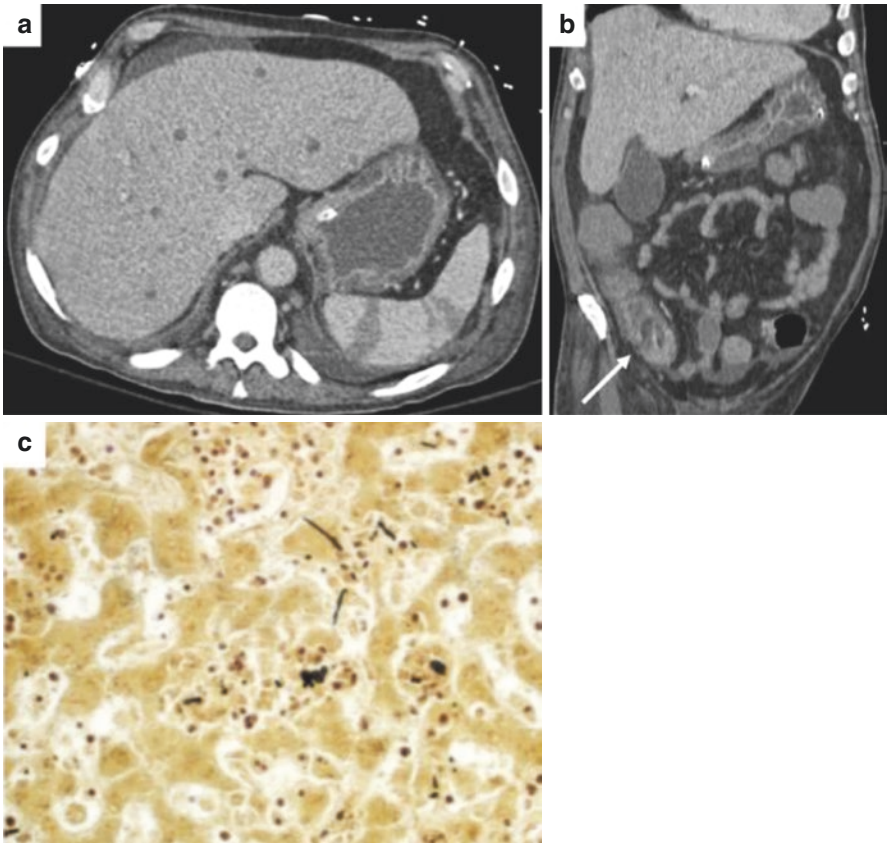

Fig. 5.11 A 35-year-old male patient on chemotherapy with hepatic candidiasis. Axial (**a**) and coronal (**b**) images of a portal venous phase contrast-enhanced CT. Multiple hypoattenuating areas in the left and right liver. Evidence of typhlitis on coronal image (arrow). A hepatic lesion was biopsied with findings consistent with candidiasis (**c**). This silver stain shows branching hyphae of *Candida* species

Histoplasmosis

Histoplasmosis is caused by *Histoplasma capsulatum* and is endemic in North and South America, particularly in the Mississippi river valleys [99]. The mode of transmission is typically through the lungs via inhalation of spores in individuals exposed to bird and bat droppings [100]. Only 1% of individuals exposed develop symptoms [14]. During the 1980s, histoplasmosis was diagnosed in 5–27% of patients with AIDS living in endemic areas for histoplasmosis [101]. This figure has decreased with improved antiretroviral therapy.

Disseminated histoplasmosis occurs in 1 in 2000 patients with acute infection [102]. It predominantly arises in the immunosuppressed and is an AIDS-defining

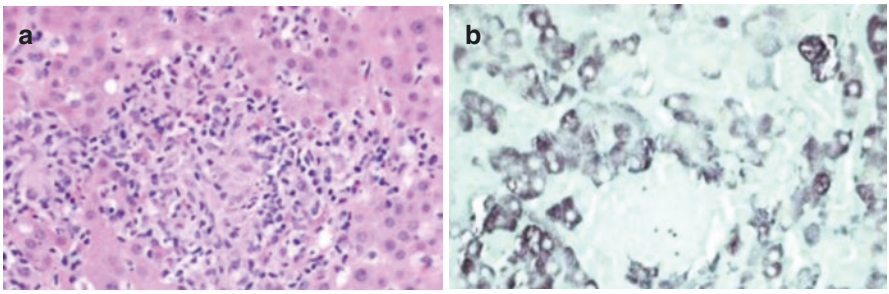

Fig. 5.12 A 56-year-old male with disseminated histoplasmosis to the liver. Photomicrograph of a non-necrotizing granuloma within the liver parenchyma (**a**). A Grocott methanamine silver stain highlights the *Histoplasma* organisms within the granuloma characterized by small black oval-shaped structures (**b**)

illness. Patients with hepatic involvement may present with pyrexia of unknown origin, abnormal liver function tests, nausea and vomiting, and fatigue [103].

The value of imaging in the diagnosis of hepatic histoplasmosis is limited. In a study of 16 patients, the only liver abnormality on CT imaging was hepatomegaly [104]. The presence of small diffuse granulomas has also been described. Appearances are nonspecific and similar to other granulomatous conditions with the formation of small punctate calcifications on healing [14].

Pathological analysis demonstrates portal lymphohistiocytic inflammation with small granulomas [14]. Grocott methanamine silver stain may identify the Histoplasma organisms within the granuloma to help differentiate histoplasmosis from other granulomatous diseases (Fig. 5.12).

Parasitic Infections

Amebic Abscess

Hepatic amebic abscess is caused by the protozoan parasite, Entamoeba histolytica. It is transmitted to the human host through contamination of water or food by human feces [105]. Entamoeba infects approximately 500 million people worldwide with rates highest in India, Africa, and Central and South America. Many Entamoeba infections are due to Entamoeba disbar, which is largely asymptomatic [106, 107]. The presentation of a hepatic amebic abscess is usually of right upper quadrant pain and fever with one third of patients complaining of diarrhea and approximately 10% presenting with jaundice [108].

The diagnosis of a hepatic amebic abscess typically requires multiple diagnostic modalities. The imaging appearance of an amebic abscess is not easily differentiated from other forms of abscess, and when aspirated, the contents are usually acellular brown fluid with a typical “anchovy paste” appearance. Trophozoites are

present in approximately 20% of samples and typically observed when the cyst wall is biopsied [106]. Amebic serology is often required and is present in 92–97% of patients with amebic liver abscesses [109].

On imaging, amebic liver abscess is classically unilocular, although septa may be present, and often solitary and located in the right hepatic lobe, typically near the liver capsule. It may thus be indistinguishable from unilocular pyogenic abscess from another source. US typically demonstrates a unilocular cystic lesion in the right liver with low-level internal echoes and minimal wall echoes (Fig. 5.13) [110]. Improvements in imaging techniques, however, have demonstrated an increased frequency of multiple abscesses [106]. CT demonstrates a well-defined cystic fluid collection with an enhancing wall measuring 3–15 mm and a peripheral edematous area (Fig. 5.13) [14, 104, 110]. Extrahepatic extension through the diaphragm into the gastrointestinal tract or into the retroperitoneum has been described [104]. T1-weighted sequences on MRI demonstrate a well-circumscribed, heterogeneous mass. This area is hyperintense on T2-weighted sequences with a surrounding less marked hyperintensity corresponding to edema on CT [111].

Histological analysis demonstrates mild marginal inflammatory reaction with a fibrin lining [14]. Amebic organisms may be visualized on high magnification (Fig. 5.13).

Echinococcal Disease

Echinococcal disease describes infection by the Echinococcus tapeworm. Two species of Echinococcus have been identified to cause infection in humans. Echinococcus granulosus causes cystic echinococcus (CE) and Echinococcus multilocularis causes alveolar echinococcus.

Echinococcus Granulosus

Humans serve only as an incidental host for echinococcus granulosus with the typical life cycle requiring an intermediate host in the form of sheep, cattle, and goats and a definitive host, typically a dog. Transmission to humans is through contact with feces from an infected dog. Highly resistant eggs produced by the adult tapeworm in the definitive host are ingested. Ultimately, oncospheres invade into the blood stream and migrate to the liver or other organ [112]. The prevalence is highest in South America, the eastern Mediterranean region, sub-Saharan Africa, Russia, and China [113].

Cystic echinococcus may not present for several years due to the slow development of the cyst. Symptoms, when they arise, are typically due to mass effect, and patients may present with upper abdominal pain and obstructive jaundice [114, 115]. Occasionally a cyst may rupture, leading to a potentially life-threatening anaphylactic reaction. If biopsy of a potential echinococcal cyst is warranted, consideration for anesthesiology support should be considered for the management of severe reactions.

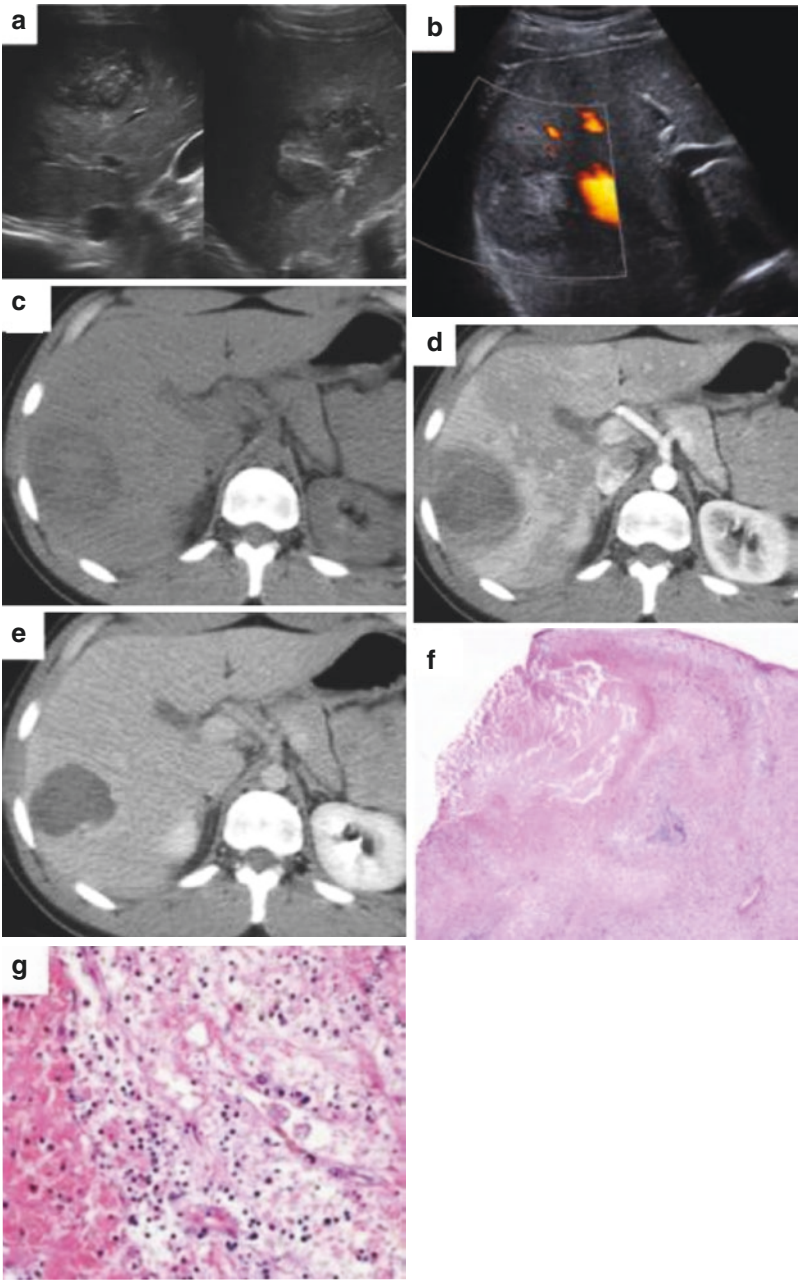

Fig. 5.13 A 25-year old male with an amebic abscess. The patient presented with abdominal pain and fever. There is a unilocular right hepatic liver lesion near the liver capsule with significant internal echoes (**a**). There is no internal flow on color Doppler imaging (**b**). Axial, non-contrast (**c**), arterial phase (**d**) and portal venous phase (**e**) images of the same individual demonstrate complex fluid attenuation (**c**) with well-defined, rim-enhancement (**d**), and surrounding edema (**e**). Hepatic amebiasis forming a focal hepatic abscess (panel **f**). On high magnification, rare round Amoeba organisms can be noted just right of center in the necrotic debris (**g**)

Table 5.1 WHO-Informal Working Group for Classification of Echinococcus classification system for cystic echinococcus

WHO classification	Features	Stage
CL	Unilocular cystic lesion with anechoic contents	Active
CE1	Unilocular cystic lesion with fine echoes (Hydatid sand/"snow flake sign")	Active
CE2	Multivesicular, multiseptated cyst. Daughter cysts may partly or completely fill cyst structure. Structure described as "wheel-like," "rosette-like," or "honeycomb-like"	Active
CE3	Anechoic cyst with detachment of laminated inner membrane or endocyst ("water-lily sign")	Transitional
CE4	Cysts with heterogeneous matrix, no daughter cysts	Inactive
CE5	Thick calcified wall	Inactive

Diagnosis is achieved from clinical history of potential exposure, imaging, and serological tests. Appearances on imaging are dependent on the stage of the cyst. A classification system by the WHO-Informal Working Group Classification on Echinococcus is the most commonly referred-to system (Table 5.1) [116].

Cystic echinococcus on plain radiograph may be identified by the presence of a calcified rim which is present in up to 30% of cases (Fig. 5.14) [117]. Ultrasound is useful as a screening tool for diagnosis and for follow-up imaging. Sensitivities of 93–98% and a specificity of 93% have been quoted for the diagnosis of CE [118]. Sonographic features depend on the stage and are outlined in Table 5.1 (Figs. 5.15 and 5.16). CT and MRI findings again vary through the cycle of the cyst and are similar to the sonographic appearance as outlined in the WHO classification system (Figs. 5.15, 5.16, and 5.17). Early in the process, the cyst may be simple with the possible development of daughter cysts in 75% [88]. The cyst wall is typically hyperattenuating on noncontrast studies with coarse calcification present in 50% (Fig. 5.16) [88, 119].

The outer layer or pericyst of the lesion is identified as a hypointense structure on T1- and T2-weighted sequences. Depending on the contents the matrix may demonstrate intermediate to high signal on T2-weighted sequences and intermediate to low signal on T1-weighted sequences. Daughter cysts have higher signal intensity than the mother cyst (Fig. 5.14) and resemble CSF intensity (Fig. 5.17). The "water lily sign" can be appreciated if present (Fig. 5.15). There is occasional delayed enhancement of the pericyst (Fig. 5.17); however the cyst contents and septations are usually nonenhancing [16, 119].

Three outer layers are identified on pathological analysis: the endocyst, ectocyst, and pericyst (Fig. 5.19). The endocyst can invaginate and create daughter cysts. Silver stain may highlight the microorganism (Fig. 5.19d).

Echinococcus Multilocularis

The definitive host of the *Echinococcus multilocularis,* where the adult form exists, is the red fox, with rodents as the intermediate host. Humans, like in the E. granulosus life cycle, are accidental hosts of the parasite. Alveolar echinococcus is most

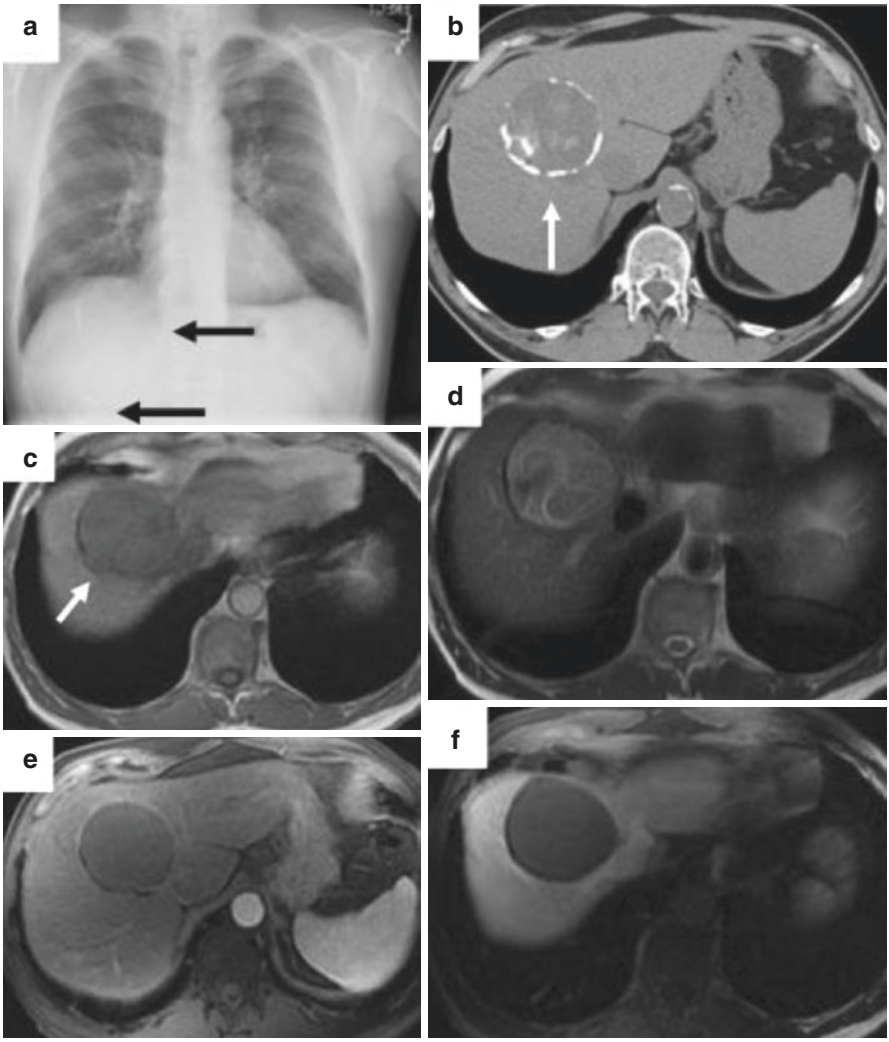

Fig. 5.14 Chest x-ray in a 64-year-old female with echinococcus granulosus infection who presented with cough. Curvilinear calcifications were noted incidentally in the liver (**a**). Noncontrast CT on the same patient demonstrates two separate peripherally calcified masses in the liver (**b**). MRI abdomen of the same patient shows a mildly T1 hypointense mass in the right liver (**c**) which is predominantly hyperintense on T2-weighted sequences (**d**) and with no appreciable enhancement (**e**, **f**). Note the water lily sign on T2-weighted sequence (**d**), consistent with a type CE3 lesion in the WHO classification system

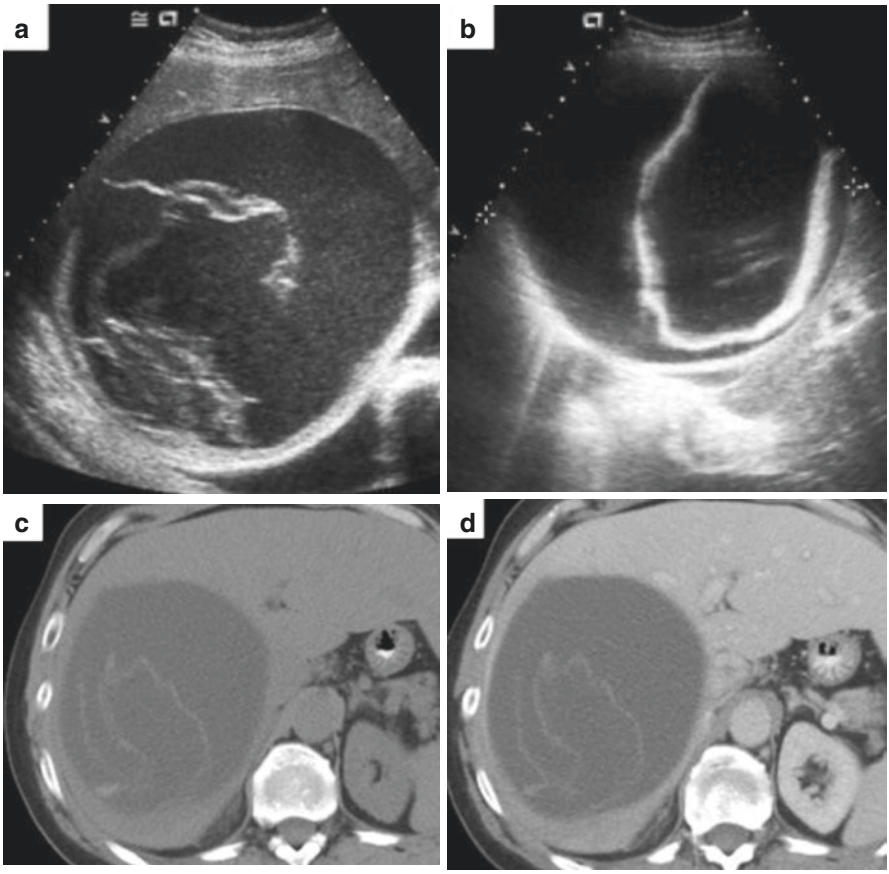

Fig. 5.15 A 60-year-old male with echinococcus granulosus infection. Abdominal ultrasound demonstrates a large cystic mass occupying much of the right lobe of the liver with a maximum diameter of 17 cm. There are membranes or linear densities within this cystic mass along with some dependent calcifications and mildly echogenic debris on sonographic imaging (**a**, **b**). Findings consistent with a type CE3 lesion. CT of the abdomen without (**c**) and with IV contrast (**d**) in the portal venous phase on the same patient. Findings correlate with the US appearance of the mass, with several irregular, partially calcified septations within the cystic liver lesion, representing a delaminated endocyst (water lily sign). There is no septal contrast enhancement

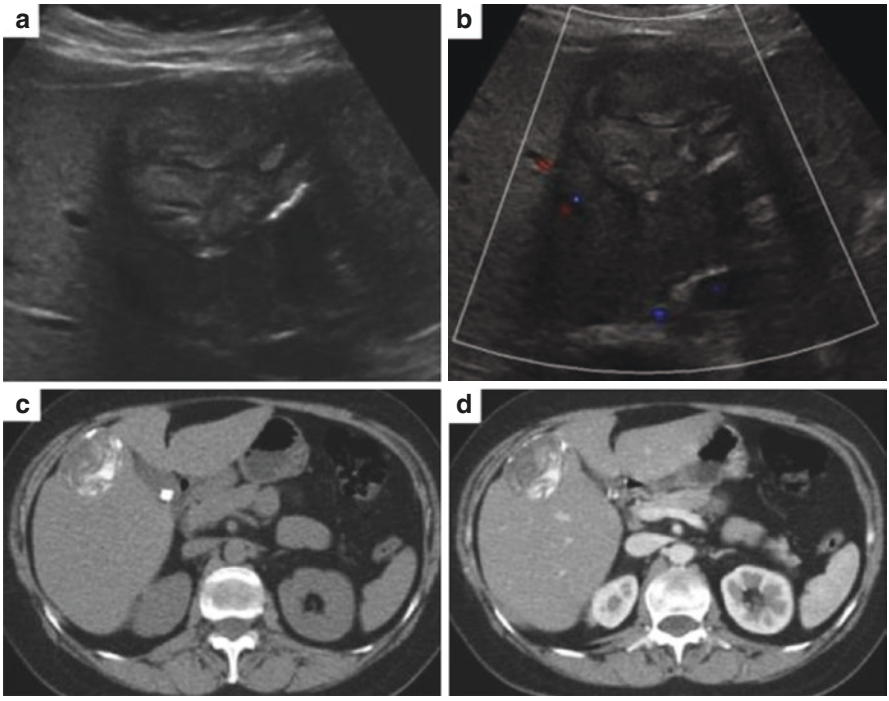

Fig. 5.16 A 54-year-old female with echinococcus granulosus infection. Abdominal US demonstrates peripheral calcifications in a complex predominantly isoechoic lesion (**a**). No flow was demonstrated inside the lesion on color Doppler imaging (**b**). Abdominal CT without contrast (**c**) and with contrast (**d**) in arterial phase demonstrates cystic lesion with thick coarsened calcifications in the right hepatic lobe. Findings consistent with a type CE 5 lesion

prevalent in the northern hemisphere, most common in countries such as Turkey, Russia, Iran, Iraq, China, and Japan [120]. The liver is the most common site of infection, involved in 90% of cases [14].

Diagnosis is achieved using multiple modalities including clinical history and examination, imaging, histopathology, and serological analysis [121].

The US appearances can vary. In 70% of cases, a large, ill-defined mass in the right liver is observed containing adjacent areas of hyper- and hypoechogenicity. Foci of calcification may be present with a central cystic area correlating to necrosis. Multiple hyperechoic nodules are often visualized giving a "hailstorm appearance" [122].

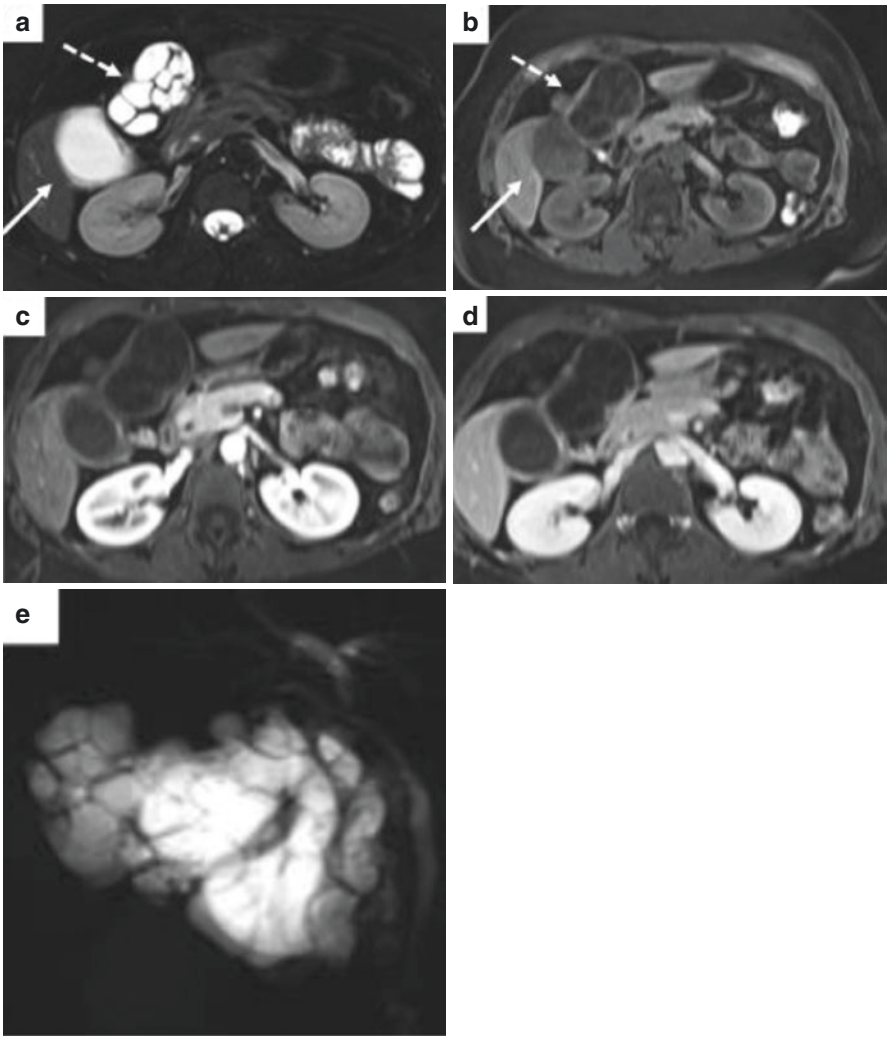

Fig. 5.17 A 42-year-old female with echinococcus granulosus infection. Abdominal MRI with axial T2 fat saturation (**a**), T1 pre-Gadolinium (**b**), arterial phase (**c**), portal venous phase, (**d**) and MRCP (**e**). There are multiple daughter cysts within a large cystic mass. The daughter cysts are markedly hyperintense on T2-weighted imaging (a broken arrow) and hypointense on T1-weighted imaging relative to the matrix (solid arrow). Daughter cysts are pathognomonic of a viable cyst Type CE2

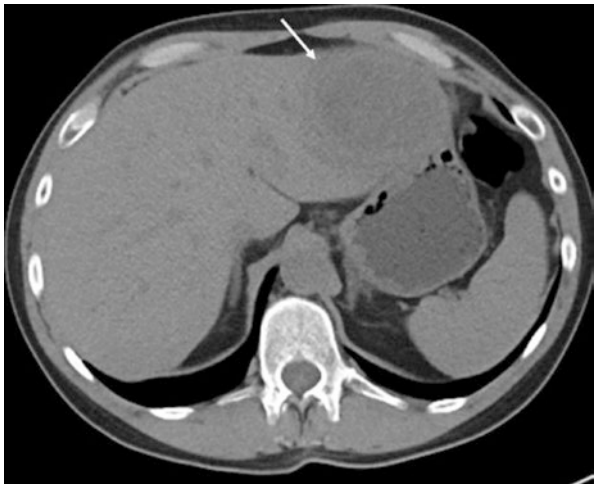

Fig. 5.18 A 54-year-old male patient with mantle cell lymphoma and synchronous echinococcus multilocularis infection. Non-contrast CT demonstrates an ill-defined, heterogeneous mass noted in the left liver. Subsequent biopsy and resection demonstrated a necrotizing granulomatous process consistent with echinococcus multilocularis

CT demonstrates a large, ill-defined, infiltrating mass in the liver (Fig. 5.18). The mass is usually heterogeneous with areas of calcification and necrosis. There is typically no internal enhancement following the administration of contrast with mild, delayed enhancement of the peripheral fibroinflammatory component [123].

MRI is often used preoperatively to assess vascular, biliary, or extrahepatic involvement [122]. Similar to CT, MRI demonstrates an ill-defined, heterogeneous, infiltrating mass with a necrotic center. The lesion is heterogeneous in signal intensity on both T1- and T2-weighted sequences with cystic or necrotic areas demonstrating typical high T2 and low T1 signal intensity. There is no associated restricted diffusion with minimal to no enhancement post contrast administration, which may help differentiate the lesion from malignancy [123].

Histopathological analysis demonstrates infiltrative masses with areas of central necrosis and peripheral palisades of histiocytes. The organism membranes are seen as discrete well-formed multilocular structures in the areas of necrosis (Fig. 5.19).

Fascioliasis

Fasciola hepatica is a trematode which resides in two hosts during its life cycle. The definitive host includes herbivorous mammals with the intermediate host a freshwater snail. The metacercaria are ingested by the definitive host through aquatic plants, which the parasite attaches itself onto after leaving the dead snail [124]. There are two separate phases once the metacercaria are inside the definitive (human) host. The parenchymal phase describes the passage of the larvae through the intestinal wall and into the liver parenchyma. Here, they form tracts with inflammatory change, abscess formation, granulation, and fibrosis. The biliary or ductal phase begins when the immature fluke enters the hepatic bile duct, matures into an adult fluke, and begins laying eggs. Endemic regions of fascioliasis include Bolivia, Peru, Chile, Cuba, Egypt, Iran, and parts of Southern Europe and East Asia [125].

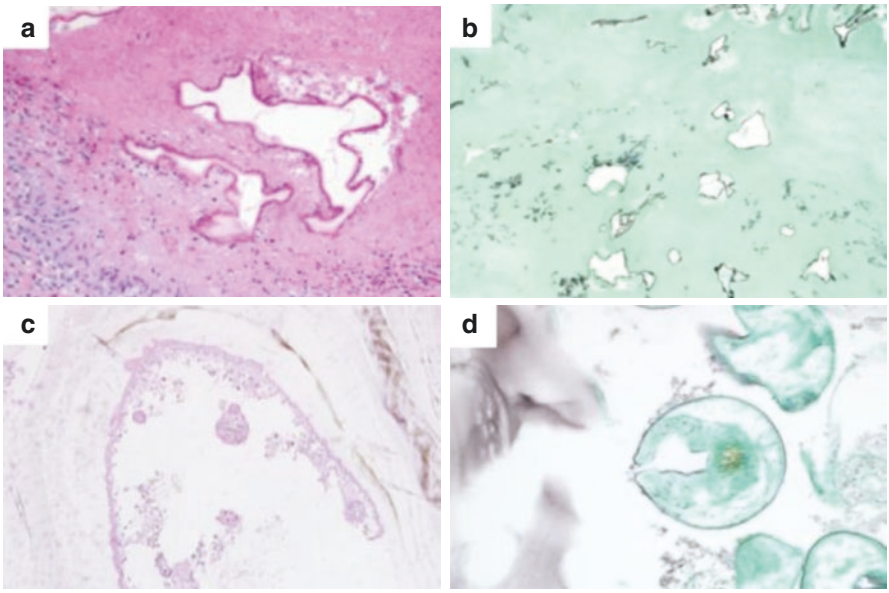

Fig. 5.19 Echinococcus multilocularis forms infiltrative masses (alveolar echinococcosis) with extensive areas of central necrosis and a peripheral palisade of histiocytes (**a**). The organism membranes are seen as discrete well-formed multilocular structures in the areas of necrosis. This Grocott methanamine silver stain highlights the infiltrative quality of echinococcus multilocularis infection (**b**). Echinococcus granulosus causes hydatid cyst disease or cystic echinococcosis (**c**). This cystic structure shows a discrete multilayered membrane with a micro-organism just above center. High magnification photomicrograph of a silver stain highlighting the microorganism and its retractile hooklets (**d**)

Patients typically present with right upper quadrant pain and hepatomegaly with possible fever and weight loss. Diagnosis is based on direct visualization of eggs in stool, duodenal fluid, and bile samples or by visualization of the adult fluke in endoscopic or surgical specimens. Imaging may provide an indirect, noninvasive adjunct to diagnosis.

US in the parenchymal phase is nonspecific with multiple hypoechoic lesions in 90% of patients. Rarely these lesions may be hyperechoic [126]. Diffuse, increased hepatic echogenicity has also been described [127]. In the biliary or ductal phase, the fluke is frequently seen in the gallbladder lumen or common bile duct. Other nonspecific findings such as gallbladder wall thickening, common bile duct dilatation, and gallbladder dilatation are less frequently seen [126].

Similar to US, CT in the parenchymal phase demonstrates multiple, clustered, hypoattenuating lesions (Fig. 5.20). These lesions may be ill-defined with peripheral contrast enhancement and arise in the subcapsular liver early in the disease. Focal thickening of the hepatic capsule may be present with subcapsular fluid and periportal lymph nodes [126, 127]. Changes in the biliary phase are best appreciated on ultrasound; however, biliary dilatation and wall enhancement are infrequent findings [126].

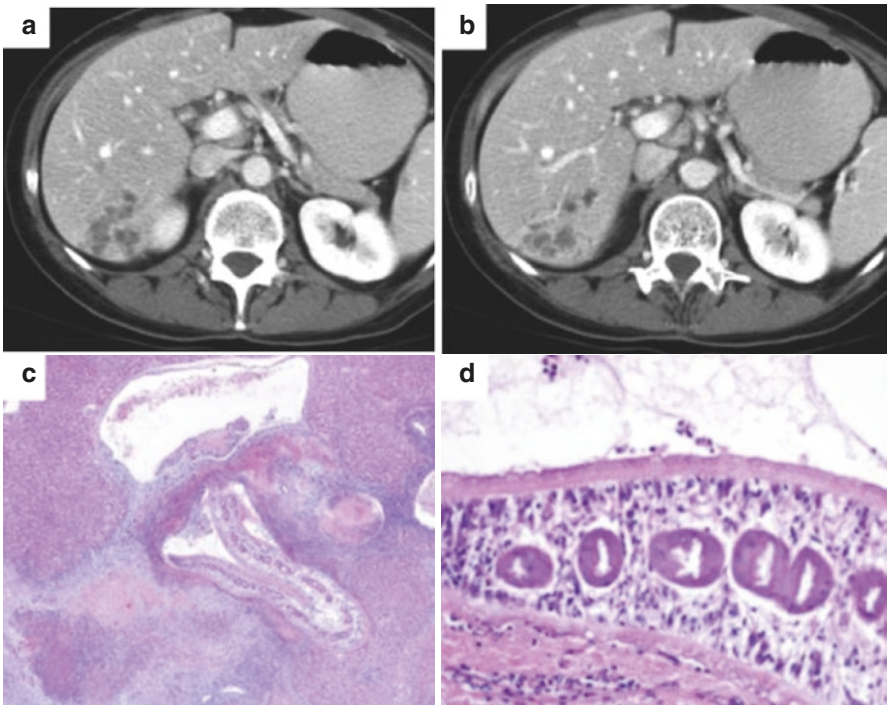

Fig. 5.20 A 58-year-old female patient with fascioliasis. The patient presented with nonspecific symptoms of abdominal pain and intermittent fever. Contrast-enhanced CT demonstrates multiple clustered hypoattenuating lesions in the right liver (**a**, **b**). Serology was positive for fascioliasis. Pathology specimen demonstrates *Fasciola hepatica* invading the liver parenchyma from the bile duct leading to marked parenchymal inflammation (**c**). The adult organism has a single highly branched digestive tube (ceca) in a coarse integument (**d**)

MRI in the parenchymal phase demonstrates the subcapsular lesions as hypointense on T1-weighted, and hyperintense on T2-weighted which peripherally enhance after the administration of an extracellular contrast agent. Focal areas of capsular T2 hyperintensity and thickening can also be best appreciated on MRI and correlate with the invasive tract of the immature fluke [127]. Based on imaging findings in 29 patients, five separate presentations on MRI are described. These include type-1 lesion described as hyperintensity of the liver capsule on T2-weighted sequences with post-contrast enhancement; type-2 lesion, described as ill-defined T2 hyperintense linear areas correlating to the immature fluke tract; type-3 and 4 lesions, described as T1 signal hypointense and T2 signal hyperintense lesions without (type-3) and with (type-4) peripheral contrast enhancement, and finally type-5 lesions described as a hypointense focus on T1- and T2-weighted sequences with homogenous enhancement [128].

Marked parenchymal inflammation is noted on pathological analysis. Adult flukes may be visualized in the hepatic parenchyma or dilated biliary ducts (Fig. 5.20). Eosinophilic granulomas may also be seen.

Schistosomiasis

There are five schistosome species known to cause infections in humans: *Schistosoma mansoni, S. japonicum, S. haematobium, S. mekongi*, *and S. intercalatum.* Of these*, S. mansoni, S. japonicum*, and rarely *S mekongi* can cause hepatic schistosomiasis.

These trematodes require two hosts to complete their life cycle. Fresh water snails act as intermediate hosts and are specific to the schistosome. When infective schistosome cercaria are released from the snail, they reside in fresh water until they come in contact with human skin. After penetrating the skin, they migrate through the blood stream to the liver where they mature into adult worms [129].

The diagnosis of schistosomiasis is based on clinical history, presence of eosinophilia, and imaging. Serological analysis for circulating antibodies and antigens specific to schistosomiasis can be performed with antibody-based assays and labelled monoclonal antibodies. Examination of stool and urine for eggs, however, remains the gold standard. Hepatic schistosomiasis describes two separate syndromes: an inflammatory, acute response to ova and a chronic, fibrotic condition seen many years following the initial infection [130].

Most imaging changes do not arise for some years following infection. In the inflammatory stage, hepatomegaly may be the only abnormality on ultrasound [131]. Multiple hypoenhancing nodules in the liver have been described in one case report on contrast-enhanced CT [132].

In the fibrotic stage, imaging varies depending on the schistosome species. It centers on deposition of collagen in the periportal space with progressive occlusion and resultant portal hypertension [133]. With S japonicum, the US features consist of hyperechoic polygonal septa, which demarcate essentially normal hepatic parenchyma in the periphery of the liver consistent with a "fish scale" appearance [134]. Due to the larger size of the S mansoni eggs, changes in imaging are often noted centrally, in and adjacent to larger vessels. The "bulls-eye" appearance is often described, consisting of an anechoic portal vein surrounded by echogenic fibrous tissue [14].

CT and MR imaging in the fibrotic stage demonstrate calcified septae, perpendicular to the capsule in infection with S japonicum. This has been described as a "tortoiseshell" or "turtle back" appearance [14]. In S mansoni, CT features include low attenuation areas in the periportal regions consistent with fibrotic tissue.

On MR imaging in the fibrotic stage, infection by S japonicum manifests as low T1 signal and high T2 signal septae that demonstrate enhancement post

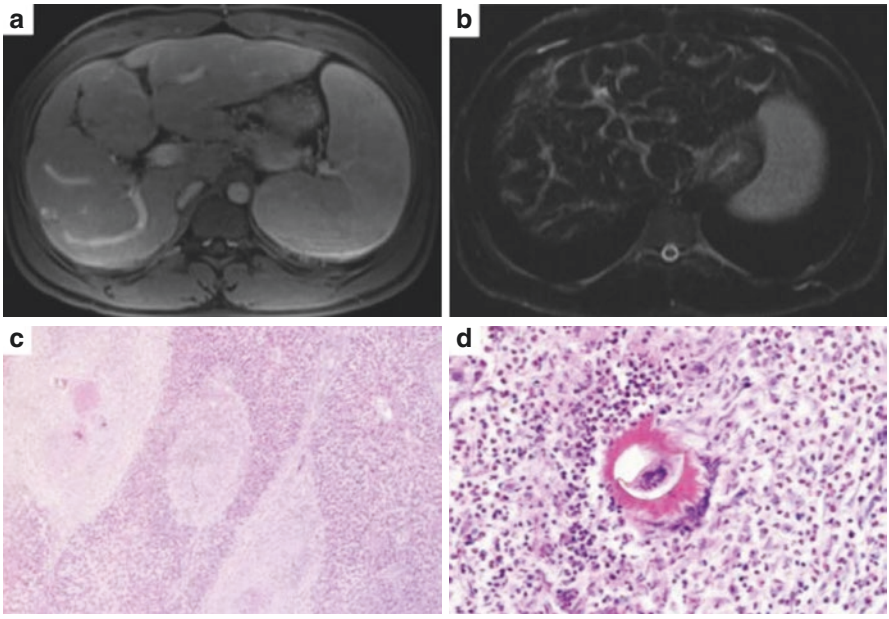

Fig. 5.21 MR abdomen of a patient with serology positive for schistosomiasis. Enhancing periportal fibrosis in the liver on portal venous phase scanning (**a**) which was high signal on T2-weighted sequences (**b**). Schistosoma organisms involve the liver and give rise to granuloma formation and fibrosis after years of infection. This is the histologic correlate of Symmers' "pipestem" fibrosis shown here (**c**). On high magnification, the Schistosoma eggs with central dark pigment and surrounding starburst like Splendore-Hoeppli phenomenon can be seen within the inflammatory background. Tissue and peripheral eosinophilia are common (**d**)

administration of extracellular contrast [134]. Periportal fibrosis with S mansoni infection demonstrates low T1 signal and high T2 signal intensity with enhancement post administration of contrast (Fig. 5.21) [135, 136].

Multiple small granulomas are noted on pathological analysis composed of macrophages, lymphocytes, neutrophils, and eosinophils [14]. A schistosome egg can be seen within the inflammatory background (Fig. 5.21).

Clonorchiasis

Clonorchiasis is caused by the trematode *Clonorchiasis sinensis.* The life cycle is complex and involves two intermediate hosts (snails and fresh water fish) and a definitive host (fish eating mammals). Humans serve as an incidental host. *C sinensis* is endemic in far-east Asia [137]. There are approximately 35 million people infected worldwide [138].

Transmission to humans is via ingestion of raw or undercooked fish. Once in the duodenum the immature fluke ascends the biliary tree where it matures. The

development of symptoms depends on worm burden [139]. Patients may be asymptomatic in low burden disease to presenting with nonspecific symptoms such as nausea, diarrhea, abdominal pain, and headache. Tender hepatomegaly and jaundice may be present on physical examination [140]. As the disease progresses, cholelithiasis, cholangitis, and cholecystitis may develop [141, 142]. There is also a link between clonorchiasis and cholangiocarcinoma with an odds ratio ranging from 4.5 to 6.1 [143–145].

The gold standard for diagnosis is the visualization of eggs in stool via the Kato-Katz method. Eggs may also be visualized in bile, allowing diagnosis in cases of biliary obstruction. The use of PCR is increasing, which allows easier differentiation of *C sinensis* from other trematode species. ELISA is also utilized but lacks specificity [140].

Imaging features are nonspecific. On US, clonorchiasis can present with diffuse dilatation of the intrahepatic bile ducts with intraductal stones with minimal dilatation of larger bile ducts without an obstructing lesion. The flukes or aggregates of eggs may be seen as nonshadowing echogenic foci or casts within the bile ducts. Echogenic bile duct walls, consistent with cholangitis and periductal fibrosis, may be visualized. Echogenic, non-shadowing, mobile structures may also be seen in the gallbladder which reflects adult flukes [146]. Similar appearances are appreciated on CT. Mild, diffuse intrahepatic duct dilatation without evidence of extrahepatic biliary dilatation is most commonly appreciated. Gallstones and pyogenic liver abscesses may also be present [147]. On MR imaging, in addition to diffuse intrahepatic duct dilatation, other findings such as periductal enhancement and direct visualization of flukes on MRCP allow greater specificity and assessment of disease activity [148].

Clonorchiasis flukes are visualized in the biliary tree. Adenomatous proliferation and goblet cell metaplasia are appreciated with fibrotic replacement of adenomatous tissue in chronic infection [149]. Two digestive tubes are commonly visualized in contrast to the single tract in fasciola (Fig. 5.22).

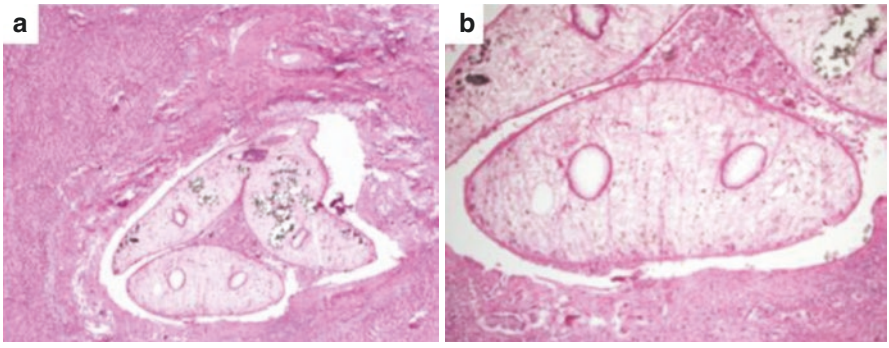

Fig. 5.22 Clonorchis sinensis remains within the intrahepatic bile duct in contrasts to Fasciola hepatica (**a**). Clonorchis sinensis has two digestive tubes and the surrounding integument is smooth rather than coarse (**b**). The eggs of Clonorchis stain black and are located within the highly branched uterus of the organism

Other Inflammatory Conditions

Sarcoidosis

Sarcoidosis is an idiopathic condition characterized by diffuse non-caseating granulomas in multiple organs. Incidence rates vary depending on geographical location, ranging from 1/100,000 in Japan to 39/100,000 in African-American females in the United States [150–152].

The liver is commonly involved with granulomas found in 50–65% of patients with sarcoidosis [153]. Symptomatic disease is less prevalent, however, quoted at 5–15%. Symptoms include abdominal pain, fever, weight loss, and jaundice. Hepatomegaly may be present on physical examination. Histopathological assessment is required for definitive diagnosis [154–157].

Hepatomegaly is the most common finding on imaging [158]. On ultrasound, the hepatic parenchyma is often of increased echogenicity with a coarsened echotexture. Diffuse nodularity may also be present, representing multiple small granulomas. These nodules are predominantly hypoechoic and measure 1–2 mm (Fig. 5.23). They may coalesce to form larger conglomerates [159].

Multiple nodules are also appreciated on contrast-enhanced CT imaging (Figs. 5.23 and 5.24). These are predominantly hypodense and hypoenhancing to surrounding hepatic parenchyma without peripheral enhancement [160]. Multiple low-density septae have also been described [161].

MRI again demonstrates multiple nodules measuring 5–20 mm [162]. The nodules are of low signal on all standard sequences and hypoenhance compared to

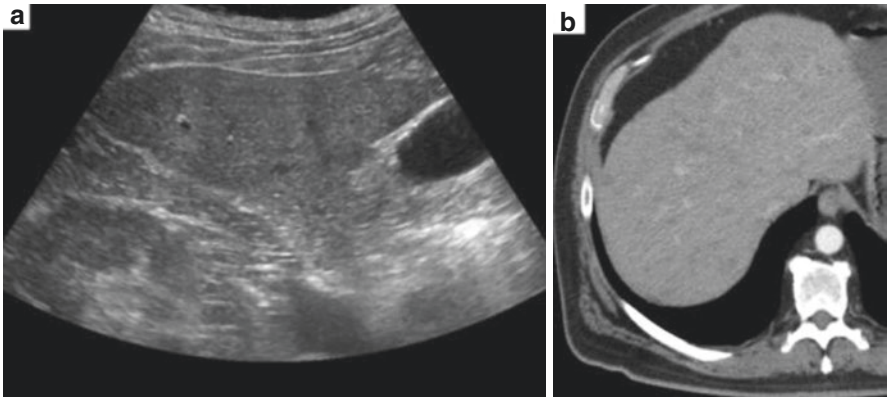

Fig. 5.23 A 60-year-old patient with sarcoidosis. The patient presented with cough and an abnormal chest x-ray. Ultrasound demonstrates coarsened hepatic parenchyma with multiple small hypoechoic nodules. On initial imaging, due to the nodularity and coarsened echotexture, this was reported as cirrhotic change (**a**). Contrast-enhanced CT on the same patient however demonstrated innumerable nonenhancing lesions throughout the liver (**b**). Biopsy confirmed sarcoidosis

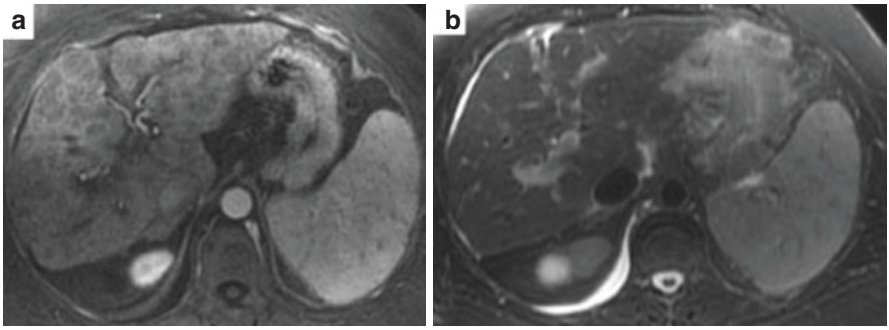

Fig. 5.24 A 57-year-old female with hepatic sarcoidosis. MRI of the abdomen confirmed the diffuse nodularity which was hypointense and nonenhancing on gadolinium enhanced T1-weighted sequences (**a**) and isointense on T2-weighted sequences (**b**). Subsequent biopsy confirmed sarcoidosis

background hepatic parenchyma (Fig. 5.24) [159, 162]. Increased periportal signal on T2-weighted sequences, contour irregularity, and focal calcifications can also be appreciated [159].

Inflammatory Myofibroblastic Tumor (IMT) of the Liver

Inflammatory myofibroblastic tumor (Inflammatory pseudotumor, plasma cell granuloma, xanthomatous pseudotumor) is a rare and much-debated process which can develop in multiple locations throughout the body. The exact cause is not definitively known. Associations include previous surgery or trauma, autoimmune conditions, and IgG4-related conditions [163–166]. Originally described in the lung, IMT was previously considered a benign post-inflammatory condition [167, 168]. More recent case series, however, have demonstrated evidence of local recurrence and metastasis [169, 170]. IMTs are now considered along the same spectrum and indistinguishable from inflammatory fibrosarcoma [171].

IMTs of the liver are rare, accounting for approximately 8% of IMT outside of the lung [172, 173]. They are predominantly seen in men and young adults [172]. Patients most commonly present with abdominal pain, fever, or symptoms associated with biliary obstruction [172]. Clinical assessment, laboratory studies, and imaging findings are not specific. As a result, biopsy or surgical excision is often required for definitive diagnosis.

Sonographic appearances demonstrate predominantly hypoechoic lesions although hyperechoic lesions have been described, possibly due to alterations in the degree of fibrosis. Posterior acoustic enhancement and septations may be present (Fig. 5.25) [174–176].

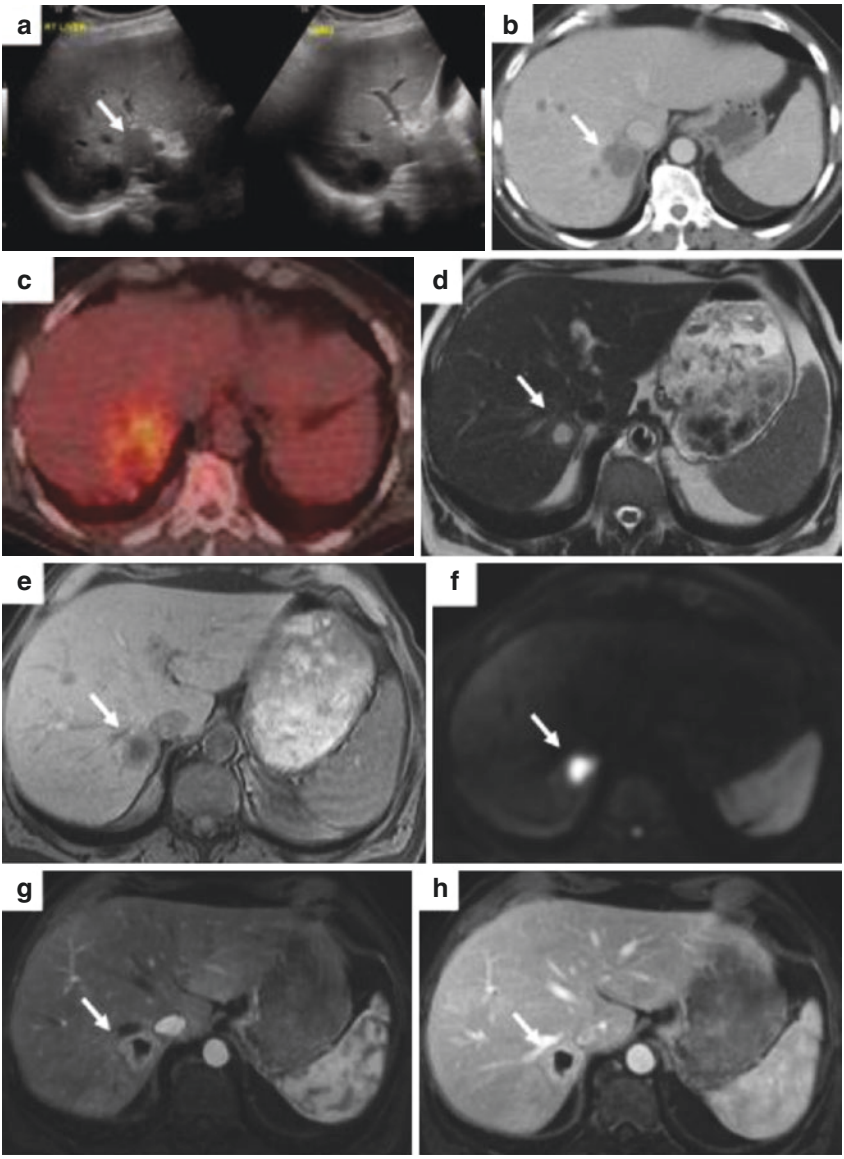

Fig. 5.25 A 59-year-old male with inflammatory myofibroblastic tumor of the liver. The patient presented with abnormal liver function tests and biopsy proven carcinoma in cervical lymph nodes. Ultrasound of the liver demonstrates a hypoechoic mass in the right liver centrally with posterior acoustic enhancement (**a**). Contrast-enhanced CT demonstrated a hypoattenuating lesion adjacent to the inferior vena cava with subtle peripheral and internal septal enhancement. Multiple smaller nonenhancing lesions were also noted throughout the liver (**b**). The mass demonstrated F18 Fluorodeoxyglucose avidity on PET imaging (**c**). MRI of the abdomen demonstrated a central area of high T2 (**d**) and low T1 (**e**) signal intensity with an ill-defined high *T2* low T1 ring. This peripheral area demonstrated enhancement on arterial phase imaging (**f**) which persisted on portal venous phase (**g**). Abnormal restricted diffusion was noted (**h**). This was thought to be consistent with metastatic disease. Subsequent biopsy demonstrated dense fibrosis with mixed lymphocytes and plasma cells, consistent with an inflammatory myofibroblastic tumor

CT demonstrates a low attenuation lesion on unenhanced images. The enhancement pattern is variable with peripheral enhancement only, peripheral enhancement with fill-in, complete homogenous enhancement, and complete heterogeneous enhancement all described (Fig. 5.25) [163, 177, 178]. FDG avidity is often appreciated on PET CT.

IMTs of the liver on MRI are typically of low signal intensity on T1-weighted sequences, high signal on T2-weighted sequences with, similar to CT, various enhancement patterns on portal venous phase such as peripheral enhancement, central nodular enhancement, septal enhancement, or a mixture of all (Fig. 5.25) [179].

References

1. Altemeier WA, Culbertson WR, Fullen WD, Shook CD. Intra-abdominal abscesses. Am J Surg. 1973;125(1):70–9.
2. Meddings L, Myers RP, Hubbard J, Shaheen AA, Laupland KB, Dixon E, et al. A population-based study of pyogenic liver abscesses in the United States: incidence, mortality, and temporal trends. Am J Gastroenterol. 2010;105(1):117–24.
3. Sharma A, Sharma A, Mukewar S, Mara KC, Dierkhising RA, Kamath PS, Cummins N. Epidemiologic actors, clinical presentation, causes, and outcomes of liver abscess: a 35-year olmsted county study. Mayo Clin Proc Innov Qual Outcomes. 2018;2(1):16–25.
4. Branum GD, Tyson GS, Branum MA, Meyers WC. Hepatic abscess. Changes in etiology, diagnosis, and management. Ann Surg. 1990;212(6):655–62.
5. Huang CJ, Pitt HA, Lipsett PA, Osterman FA Jr, Lillemoe KD, Cameron JL, et al. Pyogenic hepatic abscess. Changing trends over 42 years. Ann Surg. 1996;223(5):600–7; discussion 7–9.
6. Rahimian J, Wilson T, Oram V, Holzman RS. Pyogenic liver abscess: recent trends in etiology and mortality. Clin Infect Dis. 2004;39(11):1654–9.
7. Lam YH, Wong SK, Lee DW, Lau JY, Chan AC, Yiu RY, et al. ERCP and pyogenic liver abscess. Gastrointest Endosc. 1999;50(3):340–4.
8. Ruiz-Hernandez JJ, Leon-Mazorra M, Conde-Martel A, Marchena-Gomez J, Hemmersbach-Miller M, Betancor-Leon P. Pyogenic liver abscesses: mortality-related factors. Eur J Gastroenterol Hepatol. 2007;19(10):853–8.
9. Chemaly RF, Hall GS, Keys TF, Procop GW. Microbiology of liver abscesses and the predictive value of abscess gram stain and associated blood cultures. Diagn Microbiol Infect Dis. 2003;46(4):245–8.
10. Chou FF, Sheen-Chen SM, Chen YS, Chen MC. Single and multiple pyogenic liver abscesses: clinical course, etiology, and results of treatment. World J Surg. 1997;21(4):384–8; discussion 8–9.
11. Lv WF, Lu D, He YS, Xiao JK, Zhou CZ, Cheng DL. Liver abscess formation following transarterial chemoembolization: clinical features, risk factors, bacteria spectrum, and percutaneous catheter drainage. Medicine. 2016;95(17):e3503.
12. Cai YL, Xiong XZ, Lu J, Cheng Y, Yang C, Lin YX, Zhang J, Cheng NS. Percutaneous needle aspiration versus catheter drainage in the management of liver abscess: a systematic review and meta-analysis. HPB (Oxford). 2015;17(3):195–201. https://doi.org/10.1111/hpb.12332.
13. Lin AC, Yeh DY, Hsu YH, Wu CC, Chang H, Jang TN, et al. Diagnosis of pyogenic liver abscess by abdominal ultrasonography in the emergency department. Emerg Med J. 2009;26(4):273–5.
14. Mortele KJ, Segatto E, Ros PR. The infected liver: radiologic-pathologic correlation. Radiographics. 2004;24(4):937–55.
15. Benedetti NJ, Desser TS, Jeffrey RB. Imaging of hepatic infections. Ultrasound Q. 2008;24(4):267–78.

16. Bachler P, Baladron MJ, Menias C, Beddings I, Loch R, Zalaquett E, et al. Multimodality imaging of liver infections: differential diagnosis and potential pitfalls. Radiographics. 2016;36(4):1001–23.
17. Subramanyam BR, Balthazar EJ, Raghavendra BN, Horii SC, Hilton S, Naidich DP. Ultrasound analysis of solid-appearing abscesses. Radiology. 1983;146(2):487–91.
18. Hui JY, Yang MK, Cho DH, Li A, Loke TK, Chan JC, et al. Pyogenic liver abscesses caused by Klebsiella pneumoniae: US appearance and aspiration findings. Radiology. 2007;242(3):769–76.
19. Kuligowska E, Connors SK, Shapiro JH. Liver abscess: sonography in diagnosis and treatment. AJR Am J Roentgenol. 1982;138(2):253–7.
20. Halvorsen RA Jr, Foster WL Jr, Wilkinson RH Jr, Silverman PM, Thompson WM. Hepatic abscess: sensitivity of imaging tests and clinical findings. Gastrointest Radiol. 1988;13(2):135–41.
21. Halvorsen RA, Korobkin M, Foster WL, Silverman PM, Thompson WM. The variable CT appearance of hepatic abscesses. AJR Am J Roentgenol. 1984;142(5):941–6.
22. Mathieu D, Vasile N, Fagniez PL, Segui S, Grably D, Larde D. Dynamic CT features of hepatic abscesses. Radiology. 1985;154(3):749–52.
23. Jeffrey RB Jr, Tolentino CS, Chang FC, Federle MP. CT of small pyogenic hepatic abscesses: the cluster sign. AJR Am J Roentgenol. 1988;151(3):487–9.
24. Alsaif HS, Venkatesh SK, Chan DS, Archuleta S. CT appearance of pyogenic liver abscesses caused by Klebsiella pneumoniae. Radiology. 2011;260(1):129–38.
25. Balci NC, Semelka RC, Noone TC, Siegelman ES, de Beeck BO, Brown JJ, et al. Pyogenic hepatic abscesses: MRI findings on T1- and T2-weighted and serial gadolinium-enhanced gradient-echo images. J Magn Reson Imaging. 1999;9(2):285–90.
26. Mendez RJ, Schiebler ML, Outwater EK, Kressel HY. Hepatic abscesses: MR imaging findings. Radiology. 1994;190(2):431–6.
27. Chan JH, Tsui EY, Luk SH, Fung AS, Yuen MK, Szeto ML, et al. Diffusion-weighted MR imaging of the liver: distinguishing hepatic abscess from cystic or necrotic tumor. Abdom Imaging. 2001;26(2):161–5.
28. Leyendecker JR, Brown JJ, Merkle EM. Practical guide to abdominal and pelvic MRI. 2nd ed. Philadelphia: Lippincott, Williams and Wilkins; 2010.
29. Gabata T, Kadoya M, Matsui O, Kobayashi T, Kawamori Y, Sanada J, et al. Dynamic CT of hepatic abscesses: significance of transient segmental enhancement. AJR Am J Roentgenol. 2001;176(3):675–9.
30. WHO|Global tuberculosis report 2017. WHO. 2017.
31. Prevention CfDCa. Tuberculosis 2018. Available from: https://www.cdc.gov/tb/default.htm.
32. Hersch C. Tuberculosis of the liver. A study of 200 cases. S Afr Med J. 1964;38:857–63.
33. Essop AR, Posen JA, Hodkinson JH, Segal I. Tuberculosis hepatitis: a clinical review of 96 cases. Q J Med. 1984;53(212):465–77.
34. Terry RB, Gunnar RM. Primary miliary tuberculosis of the liver. J Am Med Assoc. 1957;164(2):150–7.
35. Leder RA, Low VH. Tuberculosis of the abdomen. Radiol Clin N Am. 1995;33(4):691–705.
36. Turhan N, Kurt M, Ozderin YO, Kurt OK. Hepatic granulomas: a clinicopathologic analysis of 86 cases. Pathol Res Pract. 2011;207(6):359–65.
37. Vanhoenacker FM, De Backer AI, de Beeck BO, Maes M, Van Altena R, Van Beckevoort D, et al. Imaging of gastrointestinal and abdominal tuberculosis. Eur Radiol. 2004;14(Suppl 3):E103–15.
38. Karaosmanoglu AD, Onur MR, Sahani DV, Tabari A, Karcaaltincaba M. Hepatobiliary tuberculosis: imaging findings. AJR Am J Roentgenol. 2016;207(4):1–11.
39. Hickey AJ, Gounder L, Moosa MY, Drain PK. A systematic review of hepatic tuberculosis with considerations in human immunodeficiency virus co-infection. BMC Infect Dis. 2015; 15:209.
40. Saphir O. Changes in the liver and pancreas in chronic pulmonary tuberculosis. Arch Path. 1929;7:1026549–56.

41. Torrey RG. Occurrence of miliary tuberculosis of the liver in course of pulmonary tuberculosis. Am J Med Sci. 1916;151:549.
42. Pereira JM, Madureira AJ, Vieira A, Ramos I. Abdominal tuberculosis: imaging features. Eur J Radiol. 2005;55(2):173–80.
43. Yu RS, Zhang SZ, Wu JJ, Li RF. Imaging diagnosis of 12 patients with hepatic tuberculosis. World J Gastroenterol. 2004;10(11):1639–42.
44. Doyle DJ, Hanbidge AE, O'Malley ME. Imaging of hepatic infections. Clin Radiol. 2006;61(9):737–48.
45. Jadvar H, Mindelzun RE, Olcott EW, Levitt DB. Still the great mimicker: abdominal tuberculosis. AJR Am J Roentgenol. 1997;168(6):1455–60.
46. Bomanji JB, Gupta N, Gulati P, Das CJ. Imaging in tuberculosis. Cold Spring Harb Perspect Med. 2015;5(6):a017814.
47. Ito K, Morooka M, Minamimoto R, Miyata Y, Okasaki M, Kubota K. Imaging spectrum and pitfalls of (1)(8)F-fluorodeoxyglucose positron emission tomography/computed tomography in patients with tuberculosis. Jpn J Radiol. 2013;31(8):511–20.
48. Wong SS, Yuen HY, Ahuja AT. Hepatic tuberculosis: a rare cause of fluorodeoxyglucose hepatic superscan with background suppression on positron emission tomography. Singap Med J. 2014;55(7):e101–3.
49. Chien RN, Lin PY, Liaw YF. Hepatic tuberculosis: comparison of miliary and local form. Infection. 1995;23(1):5–8.
50. Wu Z, Wang WL, Zhu Y, Cheng JW, Dong J, Li MX, et al. Diagnosis and treatment of hepatic tuberculosis: report of five cases and review of literature. Int J Clin Exp Med. 2013;6(9):845–50.
51. Kawamori Y, Matsui O, Kitagawa K, Kadoya M, Takashima T, Yamahana T. Macronodular tuberculoma of the liver: CT and MR findings. AJR Am J Roentgenol. 1992;158(2):311–3.
52. Abascal J, Martin F, Abreu L, Pereira F, Herrera J, Ratia T, et al. Atypical hepatic tuberculosis presenting as obstructive jaundice. Am J Gastroenterol. 1988;83(10):1183–6.
53. Ratanarapee S, Pausawasdi A. Tuberculosis of the common bile duct. HPB Surg. 1991;3(3):205–8.
54. Pombo F, Soler R, Arrojo L, Juega J. US and CT findings in biliary obstruction due to tuberculous adenitis in the periportal area. 2 cases. Eur J Radiol. 1989;9(1):71–3.
55. Kohen MD, Altman KA. Jaundice due to a rare cause: tuberculous lymphadenitis. Am J Gastroenterol. 1973;59(1):48–53.
56. Morris E. Tuberculosis of the liver. Am Rev Tuberc. 1930;22:585–92.
57. Bearer EA, Savides TJ, McCutchan JA. Endoscopic diagnosis and management of hepatobiliary tuberculosis. Am J Gastroenterol. 1996;91(12):2602–4.
58. Fan ST, Ng IO, Choi TK, Lai EC. Tuberculosis of the bile duct: a rare cause of biliary stricture. Am J Gastroenterol. 1989;84(4):413–4.
59. Chong VH, Lim KS. Hepatobiliary tuberculosis. Singap Med J. 2010;51(9):744–51.
60. Kakkar C, Polnaya AM, Koteshwara P, Smiti S, Rajagopal KV, Arora A. Hepatic tuberculosis: a multimodality imaging review. Insights Imaging. 2015;6(6):647–58.
61. Inal M, Aksungur E, Akgul E, Demirbas O, Oguz M, Erkocak E. Biliary tuberculosis mimicking cholangiocarcinoma: treatment with metallic biliary endoprothesis. Am J Gastroenterol. 2000;95(4):1069–71.
62. Giladi M, Avidor B, Kletter Y, Abulafia S, Slater LN, Welch DF, et al. Cat scratch disease: the rare role of Afipia felis. J Clin Microbiol. 1998;36(9):2499–502.
63. Kordick DL, Hilyard EJ, Hadfield TL, Wilson KH, Steigerwalt AG, Brenner DJ, et al. Bartonella clarridgeiae, a newly recognized zoonotic pathogen causing inoculation papules, fever, and lymphadenopathy (cat scratch disease). J Clin Microbiol. 1997;35(7):1813–8.
64. Ben-Ami R, Ephros M, Avidor B, Katchman E, Varon M, Leibowitz C, et al. Cat-scratch disease in elderly patients. Clin Infect Dis. 2005;41(7):969–74.
65. Nelson CA, Saha S, Mead PS. Cat-scratch disease in the United States, 2005–2013. Emerg Infect Dis. 2016;22(10):1741–6.

66. Zangwill KM, Hamilton DH, Perkins BA, Regnery RL, Plikaytis BD, Hadler JL, et al. Cat scratch disease in Connecticut. Epidemiology, risk factors, and evaluation of a new diagnostic test. N Engl J Med. 1993;329(1):8–13.
67. Florin TA, Zaoutis TE, Zaoutis LB. Beyond cat scratch disease: widening spectrum of Bartonella henselae infection. Pediatrics. 2008;121(5):e1413–25.
68. Carithers HA. Cat-scratch disease. An overview based on a study of 1,200 patients. Am J Dis Child. 1985;139(11):1124–33.
69. Lenoir AA, Storch GA, DeSchryver-Kecskemeti K, Shackelford GD, Rothbaum RJ, Wear DJ, et al. Granulomatous hepatitis associated with cat scratch disease. Lancet. 1988;1(8595):1132–6.
70. Fretzayas A, Papadopoulos NG, Moustaki M, Bossios A, Koukoutsakis P, Karpathios T. Unsuspected extralymphocutaneous dissemination in febrile cat scratch disease. Scand J Infect Dis. 2001;33(8):599–603.
71. Hopkins KL, Simoneaux SF, Patrick LE, Wyly JB, Dalton MJ, Snitzer JA. Imaging manifestations of cat-scratch disease. AJR Am J Roentgenol. 1996;166(2):435–8.
72. Rappaport DC, Cumming WA, Ros PR. Disseminated hepatic and splenic lesions in cat-scratch disease: imaging features. AJR Am J Roentgenol. 1991;156(6):1227–8.
73. Danon O, Duval-Arnould M, Osman Z, Boukobza B, Kazerouni F, Cadranel JF, et al. Hepatic and splenic involvement in cat-scratch disease: imaging features. Abdom Imaging. 2000;25(2):182–3.
74. Relman DA, Loutit JS, Schmidt TM, Falkow S, Tompkins LS. The agent of bacillary angiomatosis. An approach to the identification of uncultured pathogens. N Engl J Med. 1990;323(23):1573–80.
75. Berger TG, Koehler JE. Bacillary angiomatosis. AIDS Clin Rev. 1993:43–60.
76. Kempf VA, Volkmann B, Schaller M, Sander CA, Alitalo K, Riess T, et al. Evidence of a leading role for VEGF in Bartonella henselae-induced endothelial cell proliferations. Cell Microbiol. 2001;3(9):623–32.
77. Moore EH, Russell LA, Klein JS, White CS, McGuinness G, Davis LG, et al. Bacillary angiomatosis in patients with AIDS: multiorgan imaging findings. Radiology. 1995;197(1):67–72.
78. Wyatt SH, Fishman EK. Hepatic bacillary angiomatosis in a patient with AIDS. Abdom Imaging. 1993;18(4):336–8.
79. Iannaccone R, Federle MP, Brancatelli G, Matsui O, Fishman EK, Narra VR, et al. Peliosis hepatis: spectrum of imaging findings. AJR Am J Roentgenol. 2006;187(1):W43–52.
80. Gouya H, Vignaux O, Legmann P, de Pigneux G, Bonnin A. Peliosis hepatis: triphasic helical CT and dynamic MRI findings. Abdom Imaging. 2001;26(5):507–9.
81. Torabi M, Hosseinzadeh K, Federle MP. CT of nonneoplastic hepatic vascular and perfusion disorders. Radiographics. 2008;28(7):1967–82.
82. Sandrasegaran K, Hawes DR, Matthew G. Hepatic peliosis (bacillary angiomatosis) in AIDS: CT findings. Abdom Imaging. 2005;30(6):738–40.
83. Prevention CfDCa. Viral hepatitis 2016 [cited 2018 May 31st]. Available from: https://www.cdc.gov/hepatitis/statistics/index.htm.
84. Mills P, Saverymuttu S, Fallowfield M, Nussey S, Joseph AE. Ultrasound in the diagnosis of granulomatous liver disease. Clin Radiol. 1990;41(2):113–5.
85. Venkatesh SK, Lo LL. CT appearance of varicella zoster lesions in liver and spleen in an immunocompetent patient. J Clin Virol. 2006;36(4):303–5.
86. Ak O, Uygur Bayramicli O, Ozer S, Yilmaz B. A case of herpes simplex hepatitis with hepatic nodules in an immunocompetent patient. Turk J Gastroenterol. 2007;18(2):115–8.
87. Ruehm SG, Trojan A, Vogt P, Krause M, Krestin GP. CT appearances of hepatic involvement in systemic varicella-zoster. Br J Radiol. 1998;71(852):1317–9.
88. Mortele KJ, Ros PR. Imaging of diffuse liver disease. Semin Liver Dis. 2001;21(2):195–212.
89. Rofsky NM, Fleishaker H. CT and MRI of diffuse liver disease. Semin Ultrasound CT MR. 1995;16(1):16–33.
90. van Burik JH, Leisenring W, Myerson D, Hackman RC, Shulman HM, Sale GE, et al. The effect of prophylactic fluconazole on the clinical spectrum of fungal diseases in bone marrow

transplant recipients with special attention to hepatic candidiasis. An autopsy study of 355 patients. Medicine. 1998;77(4):246–54.
91. Pagano L, Mele L, Fianchi L, Melillo L, Martino B, D'Antonio D, et al. Chronic disseminated candidiasis in patients with hematologic malignancies. Clinical features and outcome of 29 episodes. Haematologica. 2002;87(5):535–41.
92. Thaler M, Pastakia B, Shawker TH, O'Leary T, Pizzo PA. Hepatic candidiasis in cancer patients: the evolving picture of the syndrome. Ann Intern Med. 1988;108(1):88–100.
93. Andes DR, Safdar N, Baddley JW, Playford G, Reboli AC, Rex JH, et al. Impact of treatment strategy on outcomes in patients with candidemia and other forms of invasive candidiasis: a patient-level quantitative review of randomized trials. Clin Infect Dis. 2012;54(8):1110–22.
94. Pastakia B, Shawker TH, Thaler M, O'Leary T, Pizzo PA. Hepatosplenic candidiasis: wheels within wheels. Radiology. 1988;166(2):417–21.
95. Gorg C, Bert T, Klassen E, Neesse A, Barth P, Neubauer A. Contrast enhanced sonographic patterns of hepatic candidiasis. Z Gastroenterol. 2010;48(6):678–82.
96. Metser U, Haider MA, Dill-Macky M, Atri M, Lockwood G, Minden M. Fungal liver infection in immunocompromised patients: depiction with multiphasic contrast-enhanced helical CT. Radiology. 2005;235(1):97–105.
97. Hepatosplenic candidiasis – Cornely – 2015 – Clinical liver disease – Wiley Online Library. 2018.
98. Semelka RC, Kelekis NL, Sallah S, Worawattanakul S, Ascher SM. Hepatosplenic fungal disease: diagnostic accuracy and spectrum of appearances on MR imaging. AJR Am J Roentgenol. 1997;169(5):1311–6.
99. Lamps LW, Molina CP, West AB, Haggitt RC, Scott MA. The pathologic spectrum of gastrointestinal and hepatic histoplasmosis. Am J Clin Pathol. 2000;113(1):64–72.
100. Benedict K, Mody RK. Epidemiology of histoplasmosis outbreaks, United States, 1938–2013. Emerg Infect Dis. 2016;22(3):370–8.
101. Wheat LJ, Connolly-Stringfield PA, Baker RL, Curfman MF, Eads ME, Israel KS, et al. Disseminated histoplasmosis in the acquired immune deficiency syndrome: clinical findings, diagnosis and treatment, and review of the literature. Medicine (Baltimore). 1990;69(6):361–74.
102. Goodwin RA Jr, Shapiro JL, Thurman GH, Thurman SS, Des Prez RM. Disseminated histoplasmosis: clinical and pathologic correlations. Medicine (Baltimore). 1980;59(1):1–33.
103. Kibria R, Bari K, Ali SA, Barde CJ. "Ohio River valley fever" presenting as isolated granulomatous hepatitis: a case report. South Med J. 2009;102(6):656–8.
104. Radin DR. Disseminated histoplasmosis: abdominal CT findings in 16 patients. AJR Am J Roentgenol. 1991;157(5):955–8.
105. Salit IE, Khairnar K, Gough K, Pillai DR. A possible cluster of sexually transmitted Entamoeba histolytica: genetic analysis of a highly virulent strain. Clin Infect Dis. 2009;49(3):346–53.
106. Stanley SL Jr. Amoebiasis. Lancet. 2003;361(9362):1025–34.
107. Salles JM, Moraes LA, Salles MC. Hepatic amebiasis. Braz J Infect Dis. 2003;7(2):96–110.
108. Maltz G, Knauer CM. Amebic liver abscess: a 15-year experience. Am J Gastroenterol. 1991;86(6):704–10.
109. Anesi JA, Gluckman S. Amebic liver abscess. Clin Liver Dis. 2015;6(2):41–3.
110. Landay MJ, Setiawan H, Hirsch G, Christensen EE, Conrad MR. Hepatic and thoracic amaebiasis. AJR Am J Roentgenol. 1980;135(3):449–54.
111. Elizondo G, Weissleder R, Stark DD, Todd LE, Compton C, Wittenberg J, et al. Amebic liver abscess: diagnosis and treatment evaluation with MR imaging. Radiology. 1987;165(3):795–800.
112. Pakala T, Molina M, Wu GY. Hepatic echinococcal cysts: a review. J Clin Transl Hepatol. 2016;4(1):39–46.
113. Jenkins DJ, Romig T, Thompson RC. Emergence/re-emergence of Echinococcus spp.–a global update. Int J Parasitol. 2005;35(11–12):1205–19.

114. Siracusano A, Delunardo F, Teggi A, Ortona E. Host-parasite relationship in cystic echinococcosis: an evolving story. Clin Dev Immunol. 2012;2012:639362.
115. Langer JC, Rose DB, Keystone JS, Taylor BR, Langer B. Diagnosis and management of hydatid disease of the liver. A 15-year North American experience. Ann Surg. 1984;199(4):412–7.
116. WHO Informal Working Group. International classification of ultrasound images in cystic echinococcosis for application in clinical and field epidemiological settings. Acta Trop. 2003;85(2):253–61.
117. Beggs I. The radiology of hydatid disease. AJR Am J Roentgenol. 1985;145(3):639–48.
118. Caremani M, Benci A, Maestrini R, Accorsi A, Caremani D, Lapini L. Ultrasound imaging in cystic echinococcosis. Proposal of a new sonographic classification. Acta Trop. 1997;67(1–2):91–105.
119. Pedrosa I, Saiz A, Arrazola J, Ferreiros J, Pedrosa CS. Hydatid disease: radiologic and pathologic features and complications. Radiographics. 2000;20(3):795–817.
120. Vuitton DA, Zhou H, Bresson-Hadni S, Wang Q, Piarroux M, Raoul F, et al. Epidemiology of alveolar echinococcosis with particular reference to China and Europe. Parasitology. 2003;127(Suppl):S87–107.
121. Kern P. Clinical features and treatment of alveolar echinococcosis. Curr Opin Infect Dis. 2010;23(5):505–12.
122. Bresson-Hadni S, Delabrousse E, Blagosklonov O, Bartholomot B, Koch S, Miguet JP, et al. Imaging aspects and non-surgical interventional treatment in human alveolar echinococcosis. Parasitol Int. 2006;55(Suppl):S267–72.
123. Kantarci M, Bayraktutan U, Karabulut N, Aydinli B, Ogul H, Yuce I, et al. Alveolar echinococcosis: spectrum of findings at cross-sectional imaging. Radiographics. 2012;32(7):2053–70.
124. Dusak A, Onur MR, Cicek M, Firat U, Ren T, Dogra VS. Radiological imaging features of Fasciola hepatica infection – a pictorial review. J Clin Imaging Sci. 2012;2:2.
125. Mas-Coma S, Bargues MD, Valero MA. Fascioliasis and other plant-borne trematode zoonoses. Int J Parasitol. 2005;35(11–12):1255–78.
126. Kabaalioglu A, Ceken K, Alimoglu E, Saba R, Cubuk M, Arslan G, et al. Hepatobiliary fascioliasis: sonographic and CT findings in 87 patients during the initial phase and long-term follow-up. AJR Am J Roentgenol. 2007;189(4):824–8.
127. Gonzalo-Orden M, Millan L, Alvarez M, Sanchez-Campos S, Jimenez R, Gonzalez-Gallego J, et al. Diagnostic imaging in sheep hepatic fascioliasis: ultrasound, computer tomography and magnetic resonance findings. Parasitol Res. 2003;90(5):359–64.
128. Cevikol C, Karaali K, Senol U, Kabaalioglu A, Apaydin A, Saba R, et al. Human fascioliasis: MR imaging findings of hepatic lesions. Eur Radiol. 2003;13(1):141–8.
129. Gryseels B, Polman K, Clerinx J, Kestens L. Human schistosomiasis. Lancet. 2006;368(9541):1106–18.
130. Gryseels B, Polderman AM. Morbidity, due to schistosomiasis mansoni, and its control in Subsaharan Africa. Parasitol Today. 1991;7(9):244–8.
131. Gryseels B, Polderman AM. The morbidity of schistosomiasis mansoni in Maniema (Zaire). Trans R Soc Trop Med Hyg. 1987;81(2):202–9.
132. Passos MC, Silva LC, Ferrari TC, Faria LC. Ultrasound and CT findings in hepatic and pancreatic parenchyma in acute schistosomiasis. Br J Radiol. 2009;82(979):e145–7.
133. Cheever AW. A quantitative post-mortem study of Schistosomiasis mansoni in man. Am J Trop Med Hyg. 1968;17(1):38–64.
134. Manzella A, Ohtomo K, Monzawa S, Lim JH. Schistosomiasis of the liver. Abdom Imaging. 2008;33(2):144–50.
135. Patel SA, Castillo DF, Hibbeln JF, Watkins JL. Magnetic resonance imaging appearance of hepatic schistosomiasis, with ultrasound and computed tomography correlation. Am J Gastroenterol. 1993;88(1):113–6.
136. Nompleggi DJ, Farraye FA, Singer A, Edelman RR, Chopra S. Hepatic schistosomiasis: report of two cases and literature review. Am J Gastroenterol. 1991;86(11):1658–64.

137. Lai DH, Hong XK, Su BX, Liang C, Hide G, Zhang X, et al. Current status of Clonorchis sinensis and clonorchiasis in China. Trans R Soc Trop Med Hyg. 2016;110(1):21–7.
138. Keiser J, Utzinger J. Emerging foodborne trematodiasis. Emerg Infect Dis. 2005;11(10): 1507–14.
139. Kim TI, Yoo WG, Kwak BK, Seok JW, Hong SJ. Tracing of the Bile-chemotactic migration of juvenile Clonorchis sinensis in rabbits by PET-CT. PLoS Negl Trop Dis. 2011;5(12):e1414.
140. Qian MB, Utzinger J, Keiser J, Zhou XN. Clonorchiasis. Lancet. 2016;387(10020):800–10.
141. Qiao T, Ma RH, Luo XB, Luo ZL, Zheng PM. Cholecystolithiasis is associated with Clonorchis sinensis infection. PLoS One. 2012;7(8):e42471.
142. Qiao T, Ma RH, Luo ZL, Yang LQ, Luo XB, Zheng PM. Clonorcis sinensis eggs are associated with calcium carbonate gallbladder stones. Acta Trop. 2014;138:28–37.
143. Shin HR, Oh JK, Lim MK, Shin A, Kong HJ, Jung KW, et al. Descriptive epidemiology of cholangiocarcinoma and clonorchiasis in Korea. J Korean Med Sci. 2010;25(7):1011–6.
144. Furst T, Keiser J, Utzinger J. Global burden of human food-borne trematodiasis: a systematic review and meta-analysis. Lancet Infect Dis. 2012;12(3):210–21.
145. Qian MB, Chen YD, Liang S, Yang GJ, Zhou XN. The global epidemiology of clonorchiasis and its relation with cholangiocarcinoma. Infect Dis Poverty. 2012;1(1):4.
146. Lim JH, Ko YT, Lee DH, Kim SY. Clonorchiasis: sonographic findings in 59 proved cases. AJR Am J Roentgenol. 1989;152(4):761–4.
147. Choi BI, Kim HJ, Han MC, Do YS, Han MH, Lee SH. CT findings of clonorchiasis. AJR Am J Roentgenol. 1989;152(2):281–4.
148. Choi D, Hong ST. Imaging diagnosis of clonorchiasis. Korean J Parasitol. 2007;45(2):77–85.
149. Sun T. Pathology and immunology of Clonorchis sinensis infection of the liver. Ann Clin Lab Sci. 1984;14(3):208–15.
150. Rybicki BA, Major M, Popovich J Jr, Maliarik MJ, Iannuzzi MC. Racial differences in sarcoidosis incidence: a 5-year study in a health maintenance organization. Am J Epidemiol. 1997;145(3):234–41.
151. Morimoto T, Azuma A, Abe S, Usuki J, Kudoh S, Sugisaki K, et al. Epidemiology of sarcoidosis in Japan. Eur Respir J. 2008;31(2):372–9.
152. Hillerdal G, Nou E, Osterman K, Schmekel B. Sarcoidosis: epidemiology and prognosis. A 15-year European study. Am Rev Respir Dis. 1984;130(1):29–32.
153. Irani SK, Dobbins WO 3rd. Hepatic granulomas: review of 73 patients from one hospital and survey of the literature. J Clin Gastroenterol. 1979;1(2):131–43.
154. Lehmuskallio E, Hannuksela M, Halme H. The liver in sarcoidosis. Acta Med Scand. 1977;202(4):289–93.
155. Chamuleau RA, Sprangers RL, Alberts C, Schipper ME. Sarcoidosis and chronic intrahepatic cholestasis. Neth J Med. 1985;28(10):470–6.
156. Klatskin G. Hepatic granulomata: problems in interpretation. Ann N Y Acad Sci. 1976;278:427–32.
157. Devaney K, Goodman ZD, Epstein MS, Zimmerman HJ, Ishak KG. Hepatic sarcoidosis. Clinicopathologic features in 100 patients. Am J Surg Pathol. 1993;17(12):1272–80.
158. Warshauer DM, Dumbleton SA, Molina PL, Yankaskas BC, Parker LA, Woosley JT. Abdominal CT findings in sarcoidosis: radiologic and clinical correlation. Radiology. 1994;192(1):93–8.
159. Kessler A, Mitchell DG, Israel HL, Goldberg BB. Hepatic and splenic sarcoidosis: ultrasound and MR imaging. Abdom Imaging. 1993;18(2):159–63.
160. Warshauer DM, Molina PL, Hamman SM, Koehler RE, Paulson EK, Bechtold RE, et al. Nodular sarcoidosis of the liver and spleen: analysis of 32 cases. Radiology. 1995;195(3):757–62.
161. Tsukada T, Katayama N, Taniguchi M, Miwa H, Kobayashi T, Deguchi K, et al. Liver sarcoidosis showing low-density intrahepatic septa on postcontrast computed tomography. Gastroenterol Jpn. 1993;28(5):730–3.

162. Warshauer DM, Semelka RC, Ascher SM. Nodular sarcoidosis of the liver and spleen: appearance on MR images. J Magn Reson Imaging. 1994;4(4):553–7.
163. Narla LD, Newman B, Spottswood SS, Narla S, Kolli R. Inflammatory pseudotumor. Radiographics. 2003;23(3):719–29.
164. Maves CK, Johnson JF, Bove K, Malott RL. Gastric inflammatory pseudotumor in children. Radiology. 1989;173(2):381–3.
165. Sanders BM, West KW, Gingalewski C, Engum S, Davis M, Grosfeld JL. Inflammatory pseudotumor of the alimentary tract: clinical and surgical experience. J Pediatr Surg. 2001;36(1):169–73.
166. Kamisawa T, Takuma K, Egawa N, Tsuruta K, Sasaki T. Autoimmune pancreatitis and IgG4-related sclerosing disease. Nat Rev Gastroenterol Hepatol. 2010;7(7):401–9.
167. Brunn H. Two interesting benign tumors of contradictory histopathology. Remarks on the necessity for maintaining the Chest Tumor Registry. J Thorac Surg. 1939;9:119–31.
168. Umiker WO, Iverson L. Postinflammatory tumors of the lung; report of four cases simulating xanthoma, fibroma, or plasma cell tumor. J Thorac Surg. 1954;28(1):55–63.
169. Meis JM, Enzinger FM. Inflammatory fibrosarcoma of the mesentery and retroperitoneum. A tumor closely simulating inflammatory pseudotumor. Am J Surg Pathol. 1991;15(12):1146–56.
170. Coffin CM, Watterson J, Priest JR, Dehner LP. Extrapulmonary inflammatory myofibroblastic tumor (inflammatory pseudotumor). A clinicopathologic and immunohistochemical study of 84 cases. Am J Surg Pathol. 1995;19(8):859–72.
171. Gleason BC, Hornick JL. Inflammatory myofibroblastic tumours: where are we now? J Clin Pathol. 2008;61(4):428–37.
172. Tang L, Lai EC, Cong WM, Li AJ, Fu SY, Pan ZY, et al. Inflammatory myofibroblastic tumor of the liver: a cohort study. World J Surg. 2010;34(2):309–13.
173. Park JY, Choi MS, Lim YS, Park JW, Kim SU, Min YW, et al. Clinical features, image findings, and prognosis of inflammatory pseudotumor of the liver: a multicenter experience of 45 cases. Gut Liver. 2014;8(1):58–63.
174. Nam KJ, Kang HK, Lim JH. Inflammatory pseudotumor of the liver: CT and sonographic findings. AJR Am J Roentgenol. 1996;167(2):485–7.
175. Caramella T, Novellas S, Fournol M, Saint-Paul MC, Bruneton JN, Chevallier P. Imaging of inflammatory pseudotumors of the liver. J Radiol. 2007;88(6):882–8.
176. Celik H, Ozdemir H, Yucel C, Gultekin S, Oktar SO, Arac M. Characterization of hyperechoic focal liver lesions: quantitative evaluation with pulse inversion harmonic imaging in the late phase of levovist. J Ultrasound Med. 2005;24(1):39–47.
177. Brunello F, Caremani M, Marcarino C, Benci A, Menchetti D, Emanuelli G. Inflammatory pseudotumour of the liver: diagnosis by fine needle biopsy in two cases and a review of the literature. Ital J Gastroenterol. 1994;26(3):151–3.
178. Levy S, Sauvanet A, Diebold MD, Marcus C, Da Costa N, Thiefin G. Spontaneous regression of an inflammatory pseudotumor of the liver presenting as an obstructing malignant biliary tumor. Gastrointest Endosc. 2001;53(3):371–4.
179. Yan FH, Zhou KR, Jiang YP, Shi WB. Inflammatory pseudotumor of the liver: 13 cases of MRI findings. World J Gastroenterol. 2001;7(3):422–4.

Chapter 6
Focal Nodular Hyperplasia

Michael L. Wells, Rondell P. Graham, and Douglas A. Simonetto

Introduction, Epidemiology, and Manifestations

Focal nodular hyperplasia (FNH) is a reactive nodular proliferation of hepatocytes, often associated with central fibrosis and believed to be etiologically related to arteriovenous shunts [1–4]. It is useful to note that these blood flow abnormalities may be developmental or acquired, for example, after cancer therapy [5, 6]. While vascular changes are accepted as the underlying cause of FNH, the diagnosis of hepatocellular nodules in the context of vascular abnormalities of the liver can be a clinical and pathologic challenge leading to multiple clinical tests [7].

There is a scarcity of epidemiologic data on FNH, and population-based frequency data are lacking. The available data indicate that FNH is the second most common hepatic lesion with a frequency 3- to 10-fold that of hepatocellular adenoma and a prevalence of approximately 0.2–3% [4, 8–11]. FNH is often solitary,

M. L. Wells (✉)
Department of Radiology, Mayo Clinic, Rochester, MN, USA
e-mail: Wells.Michael@mayo.edu

R. P. Graham
Department of Laboratory Medicine and Pathology, Mayo Clinic, Rochester, MN, USA
e-mail: Graham.Rondell@mayo.edu

D. A. Simonetto
Department of Gastroenterology and Hepatology, Mayo Clinic, Rochester, MN, USA
e-mail: Simonetto.Douglas@mayo.edu

L. R. Roberts et al. (eds.), *Evaluation and Management of Liver Masses*,
https://doi.org/10.1007/978-3-030-46699-2_6

but in approximately 20–30% of patients, multiple nodules of FNH are identified [10, 12]. There is a female predominance noted in multiple studies from the Western hemisphere [12–14].

FNH arises in noncirrhotic livers and should be distinguished from FNH-like lesions, which occur in patients with abnormal parenchyma including fibrosis and cirrhosis. The underlying biology of the two lesions appears to differ [15]. The vast majority of FNH cases are asymptomatic and incidentally discovered during abdominal imaging or autopsy. Right upper quadrant abdominal pain and a palpable mass have been reported in symptomatic cases. Tumor rupture, bleeding, or necrosis is exceedingly rare in FNH.

Radiologic Evaluation

FNH is most commonly detected on imaging as an incidental solitary mass within an otherwise normal appearing liver [12, 16]. In this setting, FNH is often incompletely characterized and raises concern for a potential malignancy. Fortunately, with properly protocoled exams, a combination of characteristic imaging findings can be identified in most cases, allowing a confident diagnosis of this benign entity.

FNH may be identified initially on an ultrasound exam. As with other hepatic masses, routine grayscale and Doppler ultrasound imaging often does not provide sufficient characterization for confident diagnosis of FNH; further imaging is required with computed tomography (CT) or magnetic resonance imaging (MRI). At grayscale ultrasound, FNH appears as a solid well-circumscribed, lobulated mass with echogenicity similar or slightly less than that of the adjacent liver [17]. Color Doppler imaging may demonstrate a feeding artery coursing toward the center of the mass with radial branching outward to the periphery of the lesion, in a characteristic spoke-wheel pattern (Fig. 6.1). Recent developments in the use of microbubble-based intravenous contrast agents for ultrasound may improve characterization of FNH. Specifically, if prior imaging has not been able to clearly differentiate FNH from adenoma, contrast-enhanced ultrasound has been shown to be helpful for evaluating small lesions (<3 cm) by demonstrating a centrifugal pattern of enhancement which is specific to FNH [18]. In a study of patients with FNH and adenoma, contrast-enhanced ultrasound showed a sensitivity and specificity of 95% and 86% for correctly diagnosing FNH [19].

With CT and MRI exams performed without IV contrast, FNH characteristically appears homogenous and very similar to the background normal hepatic parenchyma. On CT, a typical FNH is nearly isoattenuating to the background liver, and at MRI the signal is isointense or demonstrates only a slight variation on T1-weighted, T2-weighted and diffusion-weighted imaging (Fig. 6.2). The tendency of FNH to resemble background normal liver has led to the nickname term “stealth lesion.” If the background liver contains abnormally high lipid or iron content, it may change the appearance of FNH on routine sequences (Fig. 6.3). Abnormally high liver lipid content may make FNH appear hyperintense on fat-suppressed T1- and T2-weighted

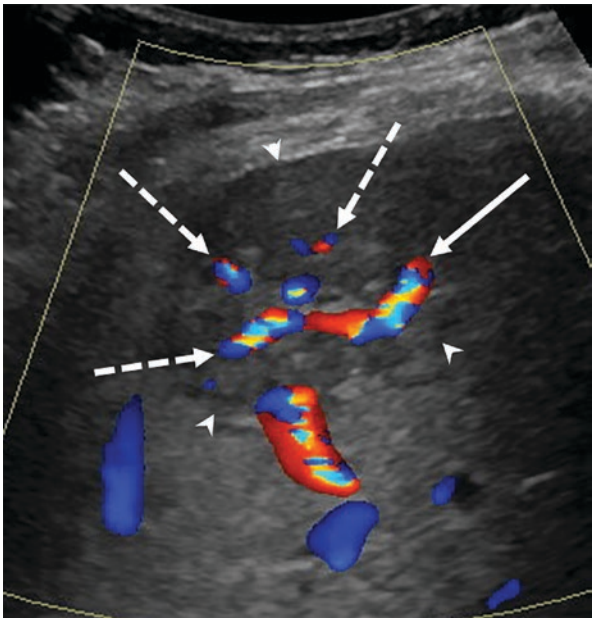

Fig. 6.1 Spoke-wheel ultrasound appearance of focal nodular hyperplasia. (**a**) Grayscale ultrasound image with Doppler flow overlay demonstrates a hypoechoic mass (arrowheads). A feeding artery (arrow) is seen coursing into the center of the mass, and smaller arteries are seen radiating from the center to the periphery of the mass (dashed arrows)

images [20]. Abnormally high liver iron content may result in FNH appearing hyperintense on all imaging sequences [21]. CT and MRI imaging may identify a central scar within an FNH, which is a characteristic finding [22]. The presence of a central scar increases in frequency as the lesion enlarges, being present in 35% of lesions less than 3 cm, and 65% of lesions larger in size [23]. The scar is usually small and demonstrates high T2 signal intensity [24, 25]. Fibrolamellar hepatocellular carcinoma (FL-HCC) is another hepatic lesion which may have a central scar. In contrast to FNH, the scar of fibrolamellar HCC is low in signal on T2-weighted sequences and is often large and calcified [24].

The enhancement pattern of FNH is an important feature allowing confident diagnosis [23, 26, 27]. With both CT and MRI, the lesions enhance avidly and homogeneously in the late arterial phase (25–40 seconds from the start of intravenous contrast injection) (Fig. 6.4). With increasing time delay, the mass fades to isoattenuation (CT) or isointensity (MRI) on the portal venous or delayed phase images. A washout appearance, with the lesion becoming hypoattenuating or hypointense to the background parenchyma on portal venous or delayed phase imaging, should not occur in the setting of a normal liver. A central scar will show poor arterial phase enhancement. As intravascular contrast redistributes to the extravascular, extracellular space, it progressively accumulates within the central scar, leading to a hyperattenuating or hyperintense appearance in the delayed phase. The delayed phase enhancement of the scar is not specific and may also be seen in fibrolamellar HCC [24]

Imaging with hepatobiliary contrast agents (HBCA) increases both the detection and specificity of diagnosis of FNH made by MRI imaging. The sinusoidal

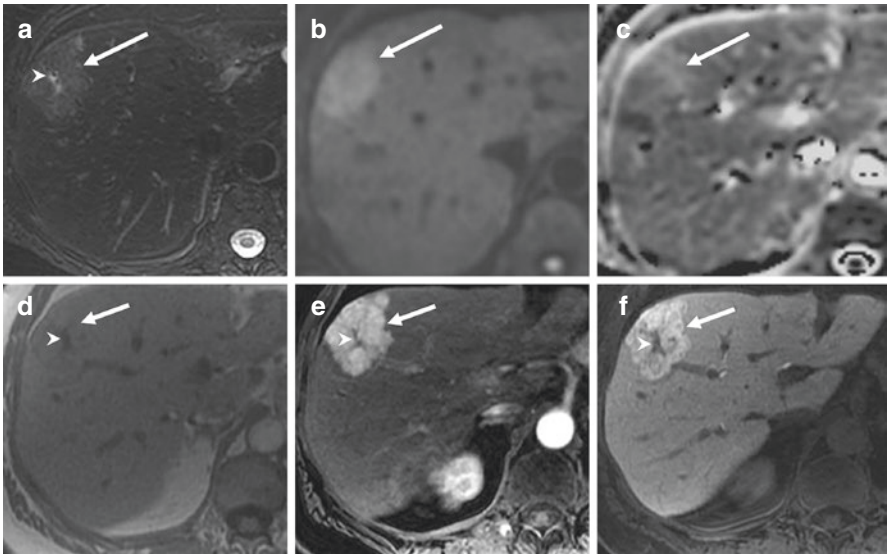

Fig. 6.2 Typical MRI findings of focal nodular hyperplasia. (**a**) Axial fat-suppressed T2-weighted MRI image shows a slightly T2 hyperintense mass with a markedly T2 hyperintense central scar (arrowhead). (**b**) Axial diffusion-weighted image shows slight hyperintensity of the mass (arrow). (**c**) Axial apparent diffusion coefficient map shows the lesion to be isointense to slightly hyperintense (arrow), with the T2 "shine through effect" and absence of restricted diffusion. (**d**) Axial T1-sweighted image shows the mass to be isointense (arrow) with a hypointense central scar (arrowhead). (**e**, **f**) Axial fat-suppressed T1-weighted images enhanced with hepatobiliary agent in the late arterial (**e**) and 20-minute delayed phases (**f**). The late arterial phase image shows diffuse avid contrast enhancement (**e**, arrow) with a T1 hypointense central scar (**e**, arrowhead). The 20-minute delayed phase shows retention of contrast agent (**f**, arrow) to a degree greater than that of the surrounding liver, which is typical of an FNH. The central scar does not retain the hepatobiliary contrast agent (**f**, arrowhead)

transporter OATP1B3 which delivers HBCA into the hepatocytes is upregulated in FNH. This transporter and the enzyme glutamine synthetase are downstream targets of the Wnt/beta-catenin signaling pathway, and both are expressed in a characteristic, map-like pattern when FNH is examined immunohistochemically [28] (Fig. 6.5). Thus, there is a correlation between uptake of HBCA detected at MRI and the pathologic diagnosis of FNH based on glutamine synthetase expression. FNH retains HBCA to a degree similar or greater than background liver in 90% of lesions [29, 30] (Figs. 6.2, 6.3, and 6.6). This enhancement pattern is uncommonly seen in other entities within the differential of a hyperenhancing hepatic mass such as hepatic adenoma, hepatocellular carcinoma, or hypervascular metastases. The elevated HBCA retention in FNH is most commonly found in a diffuse pattern but may be seen in a peripheral ring-like distribution in up to 41% [31].

FNH characteristically does not demonstrate imaging evidence of lipid, iron, or hemorrhagic contents. Rarely, FNH may contain detectable lipid content which may raise suspicion of hepatocellular adenoma or well-differentiated HCC [32]. Steatotic

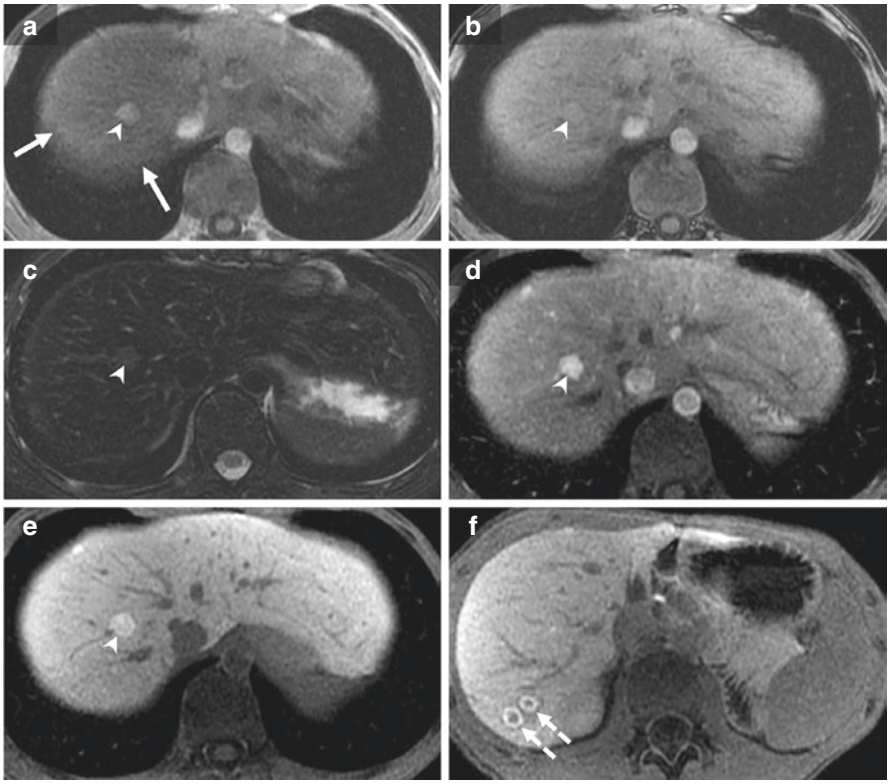

Fig. 6.3 FNH in a patient previously treated with chemotherapy for Wilms tumor. In-phase (**a**) and opposed-phase (**b**) images show low signal of the liver on the in-phase (**a**, arrows) due to the presence of iron. The low signal of the background liver results in the FNH (**a**, **b** arrowheads) appearing hyperintense. (**c**) T2-weighted image shows abnormally low signal of the liver due to iron and a mildly T2 hyperintense FNH (arrowhead). (**d**) Late arterial phase image shows hyperenhancement of the FNH (arrowhead). (**e**) 20-minute delayed phase image with HBCA shows marked retention of the contrast agent in the FNH (arrowhead). (**f**) The patient had numerous FNH, several of which demonstrated a peripheral pattern of HBCA retention (dashed arrows) on 20-minute delayed phase imaging

FNH (fat-containing FNH) most commonly occurs in the background of hepatic steatosis. Despite the presence of steatosis, it is still possible to make a reliable imaging diagnosis of FNH, so long as the lesion demonstrates classic findings on the remaining sequences. If the remaining imaging findings are not typical, then biopsy may be needed for diagnosis of steatotic FNH.

Radionucleotide imaging of FNH with technetium sulfur colloid (Tc-SC) or technetium iminodiacetic acid (Tc-IDA) analogs has been performed in the past but is rarely used today. FNH contain Kupffer cells which accumulate Tc-SC particles sized 0.3–1.0 μm. FNH imaged with Tc-SC demonstrates activity greater than the background liver in 40%, similar in 30% and less than in 30% [33]. In contrast, most adenomas and HCC appear as a photopenic defect when imaged with Tc-SC due to

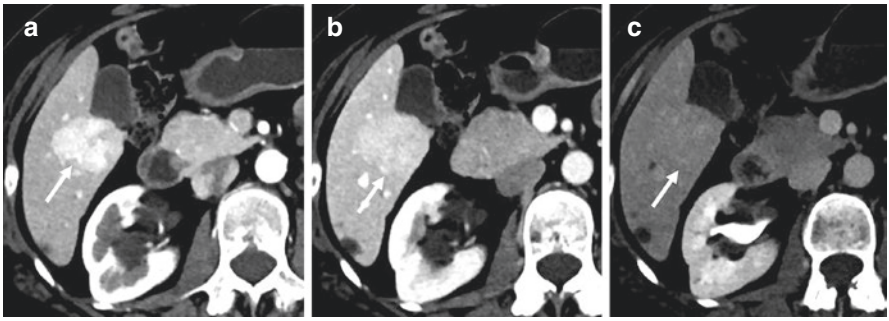

Fig. 6.4 Typical enhancement pattern of FNH. Late arterial phase CT image (**a**) shows homogenous hyperenhancement of a lobulated mass within segment 6 of the liver. Portal venous phase image (**b**) shows the lesion to slightly fade but remain slightly hyperintense. (**c**) On the delayed phase image, the mass is isoattenuating to the background liver

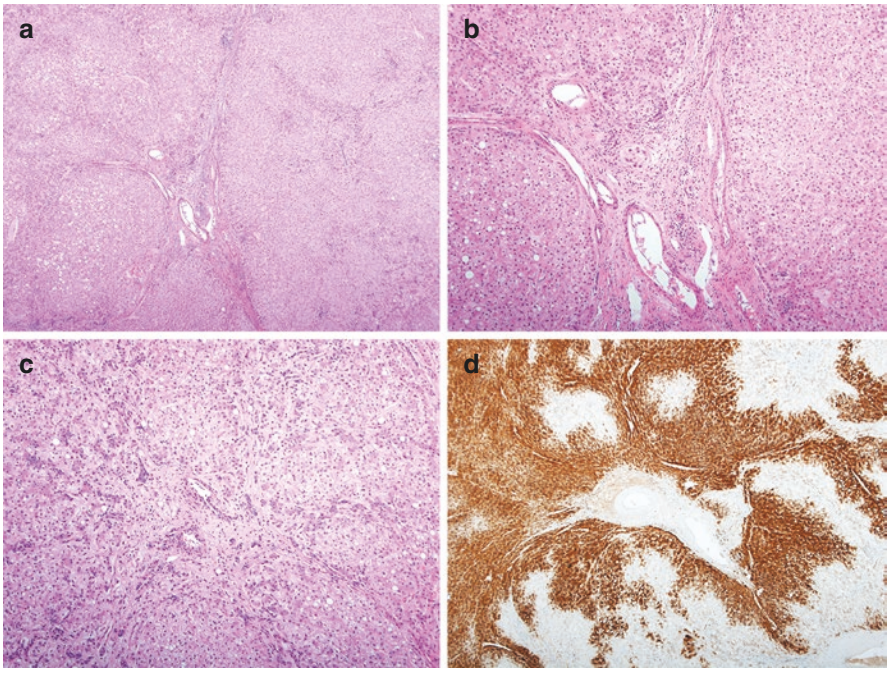

Fig. 6.5 (**a**) A representative photomicrograph of focal nodular hyperplasia (FNH) characterized by a multinodular proliferation of hepatocytes with a central scar. (**b**) The central scar displays dystrophic thick-walled arterioles, which are often identified at diagnosis. (**c**) An accompanying bile ductular reaction is often noted. (**d**) Glutamine synthetase immunohistochemistry reveals a map-like pattern of expression indicative of the Wnt signaling pathway activation that underlies FNH

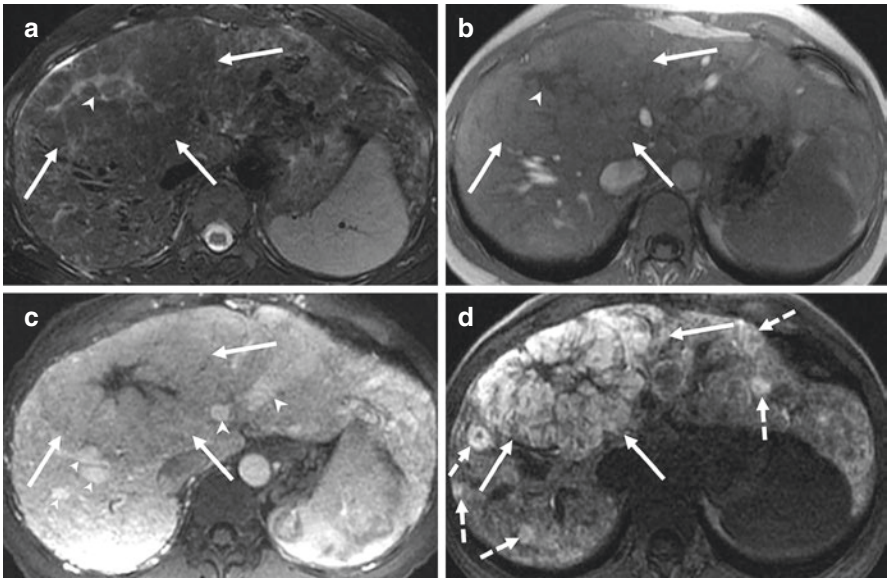

Fig. 6.6 FNH in a patient with hereditary hemorrhagic telangiectasia. (**a**) T2-weighted image shows a large FNH (arrows) in the liver which is abnormally T2 hypointense to the adjacent liver and contains a markedly T2 hyperintense central scar (arrowhead). Note the reticular high T2 signal intensity of the background liver which is likely responsible for the abnormally hypointense appearance of the FNH. (**b**) T1-weighted image shows the mass to be isointense to the surrounding liver with a hypointense central scar. (**c**) Imaging obtained at typical arterial phase timing shows extensive shunting through the liver with very early opacification of the hepatic veins (arrowheads). The FNH (arrows) is abnormally hypointense at this time due to the extensive shunting and early enhancement of the background liver. (**d**) 20-minute delayed phase image obtained with HBCA shows avid retention of contrast agent in the large FNH (arrows) and also within several smaller lesions (dashed arrows) scattered throughout the liver

a paucity of Kupffer cells. Tc-IDA analogs are taken up into normal hepatocytes and excreted into the bile ducts. Ninety percent of FNH demonstrate rapid uptake and delayed clearance of these agents [34]. Adenomas do not demonstrate uptake, and HCC may show only delayed retention.

Several conditions predispose to development of FNH, such as biliary atresia, hepatic vascular abnormalities, passive congestion, and prior chemotherapy. In the setting of one of these predisposing conditions, FNH are frequently multiple, and their appearance may be altered by imaging abnormalities of the background liver (Fig. 6.6). For example, increased delayed phase contrast retention within a congested or fibrotic liver may create the appearance of washout in an FNH nodule, raising concern for HCC [28, 35]. When FNH demonstrates a washout appearance in a background of hepatic congestion, the additional findings of a homogenous appearance, retention of HBCA, and stability over time help to support the benign nature of the nodule. Several years after exposure to chemotherapy, FNH nodules may develop and raise concern for potential metastases [5, 21] (Fig. 6.2). Benign

regenerative nodules may also develop after chemotherapy and can have an appearance identical to FNH, with the exception that they tend not to develop central scars [21]. MRI evaluation of these hepatic lesions developing after chemotherapy exposure is helpful, as the typical findings of FNH, including HBCA retention, remain specific to a benign lesion.

Pathologic Evaluation

For pathologists, most cases of FNH can be confidently diagnosed due to the recognition of the hallmark features, a multinodular mass of bland-appearing hepatocytes inclusive of a central scar with radiating fibrous septa, a bile ductular reaction, and thick-walled arterioles [36]. Cholestasis, which can be confirmed by a copper stain, is a common finding but in an individual case is not of much use in distinguishing FNH from their morphologic mimic inflammatory-type hepatocellular adenoma [37]. Morphologically, classic cases of FNH often show the typical expected immunohistochemical pattern with glutamine synthetase. Challenging cases do occur however. For example, a well-developed central scar is not seen in all cases of FNH. In small biopsies, the limited sample may not include all of the classic findings and may even sample only the periphery of the lesion. Further, the expression of glutamine synthetase can be challenging on small biopsies and, in some cases, it may simply not show the expected pattern of expression [38]. Also a potential histologic pitfall, steatohepatitis-like change has also been reported in FNH [39]. A detailed discussion of the pathologic approach to challenging cases is beyond the scope of this chapter. Nevertheless, the salient point for clinicians is that, while a definite diagnosis of FNH is often provided by the pathologist after a review of the morphology with the occasional aid of immunohistochemistry, there are infrequent cases where a descriptive diagnosis is rendered, and additional investigation or sampling may be needed.

Natural History and Management

FNH carries a low rate of complications and does not typically change in size or character over time. Additionally, FNH is not at risk of malignant transformation. Therefore, patients with confirmed asymptomatic FNH do not require treatment or follow-up imaging. In those with severe symptoms suspected to be related to FNH, surgical resection may be an option after extensive evaluation has ruled out other possible causes [40]. Moreover, resection may also be performed whenever there is diagnostic uncertainty in the setting of significant tumor growth. Percutaneous radiofrequency ablation has also been used in the management of symptomatic FNH, and offers a safe and effective alternative to surgery [41].

References

1. Brenard R, Chapaux X, Deltenre P, Henrion J, De Maeght S, Horsmans Y, et al. Large spectrum of liver vascular lesions including high prevalence of focal nodular hyperplasia in patients with hereditary haemorrhagic telangiectasia: the Belgian Registry based on 30 patients. Eur J Gastroenterol Hepatol. 2010;22(10):1253–9.
2. Buscarini E, Danesino C, Plauchu H, de Fazio C, Olivieri C, Brambilla G, et al. High prevalence of hepatic focal nodular hyperplasia in subjects with hereditary hemorrhagic telangiectasia. Ultrasound Med Biol. 2004;30(9):1089–97.
3. Wanless IR, Albrecht S, Bilbao J, Frei JV, Heathcote EJ, Roberts EA, et al. Multiple focal nodular hyperplasia of the liver associated with vascular malformations of various organs and neoplasia of the brain: a new syndrome. Mod Pathol. 1989;2(5):456–62.
4. Wanless IR, Mawdsley C, Adams R. On the pathogenesis of focal nodular hyperplasia of the liver. Hepatology. 1985;5(6):1194–200.
5. Furlan A, Brancatelli G, Dioguardi Burgio M, Grazioli L, Lee JM, Murmura E, et al. Focal nodular hyperplasia after treatment with oxaliplatin: a multiinstitutional series of cases diagnosed at MRI. AJR Am J Roentgenol. 2018;210(4):775–9.
6. Joyner BL Jr, Levin TL, Goyal RK, Newman B. Focal nodular hyperplasia of the liver: a sequela of tumor therapy. Pediatr Radiol. 2005;35(12):1234–9.
7. Sempoux C, Balabaud C, Paradis V, Bioulac-Sage P. Hepatocellular nodules in vascular liver diseases. Virchows Arch. 2018;473(1):33–44.
8. Kaltenbach TE, Engler P, Kratzer W, Oeztuerk S, Seufferlein T, Haenle MM, et al. Prevalence of benign focal liver lesions: ultrasound investigation of 45,319 hospital patients. Abdom Radiol (NY). 2016;41(1):25–32.
9. Karhunen PJ. Benign hepatic tumours and tumour like conditions in men. J Clin Pathol. 1986;39(2):183–8.
10. Vilgrain V, Uzan F, Brancatelli G, Federle MP, Zappa M, Menu Y. Prevalence of hepatic hemangioma in patients with focal nodular hyperplasia: MR imaging analysis. Radiology. 2003;229(1):75–9.
11. Horta G, Lopez M, Dotte A, Cordero J, Chesta C, Castro A, et al. Benign focal liver lesions detected by computed tomography: review of 1,184 examinations. Rev Med Chil. 2015;143(2):197–202.
12. Nguyen BN, Flejou JF, Terris B, Belghiti J, Degott C. Focal nodular hyperplasia of the liver: a comprehensive pathologic study of 305 lesions and recognition of new histologic forms. Am J Surg Pathol. 1999;23(12):1441–54.
13. Busireddy KK, Ramalho M, AlObaidy M, Matos AP, Burke LM, Dale BM, et al. Multiple focal nodular hyperplasia: MRI features. Clin Imaging. 2018;49:89–96.
14. Luciani A, Kobeiter H, Maison P, Cherqui D, Zafrani ES, Dhumeaux D, et al. Focal nodular hyperplasia of the liver in men: is presentation the same in men and women? Gut. 2002;50(6):877–80.
15. Rebouissou S, Couchy G, Libbrecht L, Balabaud C, Imbeaud S, Auffray C, et al. The beta-catenin pathway is activated in focal nodular hyperplasia but not in cirrhotic FNH-like nodules. J Hepatol. 2008;49(1):61–71.
16. Cha DI, Yoo SY, Kim JH, Jeon TY, Eo H. Clinical and imaging features of focal nodular hyperplasia in children. AJR Am J Roentgenol. 2014;202(5):960–5.
17. Venturi A, Piscaglia F, Vidili G, Flori S, Righini R, Golfieri R, et al. Diagnosis and management of hepatic focal nodular hyperplasia. J Ultrasound. 2007;10(3):116–27.
18. Bertin C, Egels S, Wagner M, Huynh-Charlier I, Vilgrain V, Lucidarme O. Contrast-enhanced ultrasound of focal nodular hyperplasia: a matter of size. Eur Radiol. 2014;24(10):2561–71.
19. Kim TK, Jang HJ, Burns PN, Murphy-Lavallee J, Wilson SR. Focal nodular hyperplasia and hepatic adenoma: differentiation with low-mechanical-index contrast-enhanced sonography. AJR Am J Roentgenol. 2008;190(1):58–66.

20. Venkatesh SK, Hennedige T, Johnson GB, Hough DM, Fletcher JG. Imaging patterns and focal lesions in fatty liver: a pictorial review. Abdom Radiol (NY). 2017;42(5):1374–92.
21. Yoo SY, Kim JH, Eo H, Jeon TY, Sung KW, Kim HS. Dynamic MRI findings and clinical features of benign hypervascular hepatic nodules in childhood-cancer survivors. AJR Am J Roentgenol. 2013;201(1):178–84.
22. Mortele KJ, Praet M, Van Vlierberghe H, Kunnen M, Ros PR. CT and MR imaging findings in focal nodular hyperplasia of the liver: radiologic-pathologic correlation. AJR Am J Roentgenol. 2000;175(3):687–92.
23. Brancatelli G, Federle MP, Grazioli L, Blachar A, Peterson MS, Thaete L. Focal nodular hyperplasia: CT findings with emphasis on multiphasic helical CT in 78 patients. Radiology. 2001;219(1):61–8.
24. Ganeshan D, Szklaruk J, Kundra V, Kaseb A, Rashid A, Elsayes KM. Imaging features of fibrolamellar hepatocellular carcinoma. AJR Am J Roentgenol. 2014;202(3):544–52.
25. Mattison GR, Glazer GM, Quint LE, Francis IR, Bree RL, Ensminger WD. MR imaging of hepatic focal nodular hyperplasia: characterization and distinction from primary malignant hepatic tumors. AJR Am J Roentgenol. 1987;148(4):711–5.
26. Choi BY, Nguyen MH. The diagnosis and management of benign hepatic tumors. J Clin Gastroenterol. 2005;39(5):401–12.
27. Choi CS, Freeny PC. Triphasic helical CT of hepatic focal nodular hyperplasia: incidence of atypical findings. AJR Am J Roentgenol. 1998;170(2):391–5.
28. Yoneda N, Matsui O, Kitao A, Kozaka K, Kobayashi S, Sasaki M, et al. Benign hepatocellular nodules: hepatobiliary phase of gadoxetic acid-enhanced MR imaging based on molecular background. Radiographics. 2016;36(7):2010–27.
29. Zech CJ, Grazioli L, Breuer J, Reiser MF, Schoenberg SO. Diagnostic performance and description of morphological features of focal nodular hyperplasia in Gd-EOB-DTPA-enhanced liver magnetic resonance imaging: results of a multicenter trial. Investig Radiol. 2008;43(7):504–11.
30. Grazioli L, Bondioni MP, Haradome H, Motosugi U, Tinti R, Frittoli B, et al. Hepatocellular adenoma and focal nodular hyperplasia: value of gadoxetic acid-enhanced MR imaging in differential diagnosis. Radiology. 2012;262(2):520–9.
31. Mohajer K, Frydrychowicz A, Robbins JB, Loeffler AG, Reed TD, Reeder SB. Characterization of hepatic adenoma and focal nodular hyperplasia with gadoxetic acid. J Magn Reson Imaging. 2012;36(3):686–96.
32. Ronot M, Paradis V, Duran R, Kerbaol A, Vullierme MP, Belghiti J, et al. MR findings of steatotic focal nodular hyperplasia and comparison with other fatty tumours. Eur Radiol. 2013;23(4):914–23.
33. Mettler FA, Guiberteau MJ. Essentials of nuclear medicine imaging. 5th ed. Philadelphia: Saunders/Elsevier; 2006. xi, 577 p. p.
34. Ziessman HA, O'Malley JP, Thrall JH. Nuclear medicine : the requisites in radiology. 3rd ed. Philadelphia: Mosby Elsevier; 2006. xii, 580 p., 16 p. of plates p.
35. Wells ML, Hough DM, Fidler JL, Kamath PS, Poterucha JT, Venkatesh SK. Benign nodules in post-Fontan livers can show imaging features considered diagnostic for hepatocellular carcinoma. Abdom Radiol (NY). 2017;42:2623.
36. Makhlouf HR, Abdul-Al HM, Goodman ZD. Diagnosis of focal nodular hyperplasia of the liver by needle biopsy. Hum Pathol. 2005;36(11):1210–6.
37. Chandan VS, Shah SS, Mounajjed T, Torbenson MS, Wu TT. Copper deposition in focal nodular hyperplasia and inflammatory hepatocellular adenoma. J Clin Pathol. 2018;71(6):504–7.
38. Joseph NM, Ferrell LD, Jain D, Torbenson MS, Wu TT, Yeh MM, et al. Diagnostic utility and limitations of glutamine synthetase and serum amyloid-associated protein immunohistochemistry in the distinction of focal nodular hyperplasia and inflammatory hepatocellular adenoma. Mod Pathol. 2014;27(1):62–72.

39. Deniz K, Moreira RK, Yeh MM, Ferrell LD. Steatohepatitis-like changes in focal nodular hyperplasia, a finding to distinguish from steatohepatitic variant of hepatocellular carcinoma. Am J Surg Pathol. 2017;41(2):277–81.
40. Perrakis A, Demir R, Muller V, Mulsow J, Aydin U, Alibek S, et al. Management of the focal nodular hyperplasia of the liver: evaluation of the surgical treatment comparing with observation only. Am J Surg. 2012;204(5):689–96.
41. Hedayati P, VanSonnenberg E, Shamos R, Gillespie T, McMullen W. Treatment of symptomatic focal nodular hyperplasia with percutaneous radiofrequency ablation. J Vasc Interv Radiol. 2010;21(4):582–5.

Chapter 7
Hemangiomas and Other Vascular Tumors

Eric C. Ehman, Douglas A. Simonetto, and Michael S. Torbenson

Introduction

The liver consists primarily of hepatocytes and cholangiocytes, while endothelial cells, Kupffer cells, stellate cells, and immune cells all serve ancillary roles. There are several types of hepatic masses or mass-like lesions which may arise from the endothelial cells that line the hepatic arteries, sinusoids, portal veins, and hepatic venous system. These entities span the spectrum from rare and aggressive lesions such as angiosarcoma to common benign masses such as hemangiomas. Knowledge of the various vascular tumors of the liver may allow accurate differentiation based on a combination of clinical and imaging features. Tables 7.1 and 7.2 summarize the clinical, histologic, and imaging features of these entities.

E. C. Ehman (✉)
Department of Radiology, Mayo Clinic, Rochester, MN, USA
e-mail: ehman.eric@mayo.edu

D. A. Simonetto
Department of Gastroenterology and Hepatology, Mayo Clinic, Rochester, MN, USA
e-mail: simonetto.douglas@mayo.edu

M. S. Torbenson
Department of Laboratory Medicine and Pathology, Mayo Clinic, Rochester, MN, USA
e-mail: torbenson.michael@mayo.edu

L. R. Roberts et al. (eds.), *Evaluation and Management of Liver Masses*,
https://doi.org/10.1007/978-3-030-46699-2_7

Table 7.1 Overview of vascular tumors of the liver

Lesion	Cell of origin	Incidence and demographics	Clinical features	Gross appearance	Microscopic appearance	Differential diagnosis
Angiosarcoma	Endothelial cells	Rare. Age 50–60. M:F ratio of 3:1	Pain, systemic symptoms such as weight loss and fatigue. Rarely cases may present secondary to tumor hemorrhage	Numerous ill-defined nodules. Hemorrhage and central thrombosis are often seen	Hypercellular tumor exhibiting pleomorphic and spindle to epithelioid cells with minimal stroma	Epithelioid hemangioendothelioma Kaposi sarcoma Carcinoma
Hepatic epithelioid hemangioendothelioma (HEHE)	Endothelial cells	Very rare. Age 10–80. F:M ratio of 2:1	Pain, palpable abdominal mass, constitutional symptoms	Firm gray-white, red or tan tumor with irregular borders	Cords and nests of tumor cells in an abundant myxoid stromal background	Angiosarcoma Intrahepatic cholangiocarcinoma Atypical hemangioma
Cavernous hemangioma	Venous malformation (not technically a neoplasm)	Affect 2–7% of the population. F:M ratio of 4–6:1	Typically encountered incidentally. Symptoms such as pain, bleeding, or consumptive coagulopathy are rare and seen only in the largest lesions	Measure from 3 mm up to greater than 20 cm and are seen throughout the liver. Spongy cystic tissue, with areas of involution depending on age. Calcifications may be seen	Dilated vascular channels lined by bland endothelial cells. May contain areas of thrombus and scarring	Metastases Hereditary hemorrhagic telangiectasia Infantile hemangioma Peliosis hepatis Angiosarcoma Epithelioid hemangioendothelioma

Modified, with permission: Ehman et al. [53]

Table 7.2 Summary of imaging features of vascular tumors of the liver

Lesion morphology	US	NCCT	T1	T2	DWI	Extracellular contrast	Hepatobiliary contrast	FDG PET
Angiosarcoma Single or multiple masses.	Heterogeneous echogenicity	Hypoattenuating masses. Some may be dense due to hemorrhage	Heterogeneous. Increased signal	Heterogeneous increased signal	Heterogeneous increased signal	Arterial phase enhancement in various patterns. Hemangioma or reverse hemangioma patterns	No uptake	Intensely FDG avid
Hepatic epithelioid hemangioendothelioma (HEHE) Single or multiple nodules, or confluent disease	Heterogeneously hypoechoic to liver parenchyma. May be hyperechoic	Hypoattenuating. May contain calcifications	Hypointense core. Hyperintense rim and hypointense halo "dark-bright-dark ring sign" is classic	Hyperintense centrally. May have alternating layers of targetoid high/low T2 signal peripherally	Variable. Can be influenced by T2 shine through	Mild central enhancement of stroma. Possible progressive peripheral enhancement. Washout is not seen	"Trapping" phenomenon of retained central contrast on delayed images has been described, but is not uniformly seen	Variable uptake
Cavernous hemangioma	Hyperechoic to background liver	Hypo to isodense to liver	Hypointense	Hyperintense	Mild diffusion restriction, may be complicated by T2 shine through	Classical pattern of nodular discontinuous arterial enhancement followed by progressive fill-in on delayed phase images. Atypical variants may show either diffuse early enhancement (flash filling) or incomplete fill-in on delayed imaging (sclerosed type)	No uptake	Not FGD avid

Modified, with permission: Ehman et al. [53]
NCCT Noncontrast CT

Hemangioma

Epidemiology and Manifestations

Hemangiomas are the most common benign hepatic tumors with a reported prevalence of 1.4–3% based on surgical or ultrasonographic series [1, 2]. Hemangiomas are more common in women between 30 and 50 years of age with a 2:1 female-to-male ratio although a hormonal effect has not been proven. The majority of cases are asymptomatic and the tumors are often incidentally found on abdominal imaging obtained for other indications. A small proportion of patients with giant hemangiomas greater than 8 cm in size may present with vague symptoms, including abdominal distention, right upper quadrant abdominal pain, and early satiety due to extrinsic gastric compression. Subcapsular hemangiomas may also present with acute severe abdominal pain resulting from thrombosis or bleeding within the tumor and consequent irritation of the hepatic capsule; however, given the high prevalence of hepatic hemangiomas and the rarity of reports of bleeding from pathologically confirmed hemangiomas, this complication appears to be exceedingly rare [3]. Chronic, recurrent fevers have also been reported in the setting of large hemangiomas, likely related to intratumoral necrosis [4].

Giant hemangiomas, particularly in children, have been associated with high-output heart failure [5], hypothyroidism, and Kasabach–Merritt syndrome, a consumptive coagulopathy presenting with thrombocytopenia and hemolytic anemia [6, 7].

Pathology

Hemangiomas are benign vascular tumors. They have no malignant potential and are not precursor lesions for angiosarcoma. Based on the size and morphology of the blood vessels, hemangiomas are subdivided into cavernous hemangiomas, capillary hemangiomas, and anastomosing hemangiomas.

The most common type of hemangioma is the cavernous hemangioma (>95% of all cases), which consists of a generally well-circumscribed and unencapsulated cluster of large caliber and thin-walled vessels (Fig. 7.1). The vessels are closely approximated, with little intervening stroma. The vessels are lined by bland endothelial cells. Over time, hemangiomas can become sclerosed and sometimes partially calcified.

Cavernous hemangiomas in rare cases grow large enough to be called giant cavernous hemangiomas—there is no universally applied size criterion for using this term, but a common criterion is greater than 8 cm. Giant cavernous hemangiomas overall look similar to smaller hemangiomas histologically, but often have somewhat infiltrative borders at the interface with the background liver, a finding called

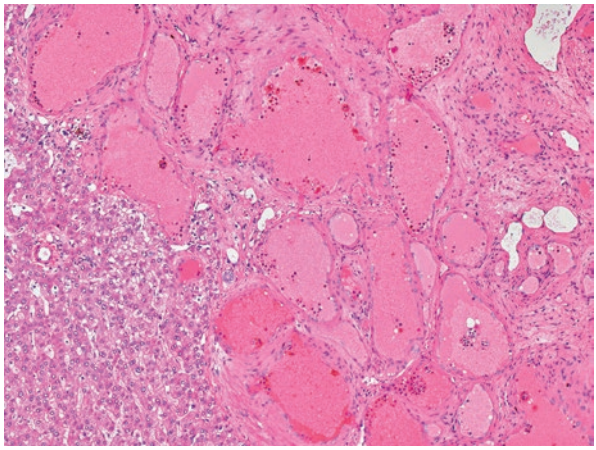

Fig. 7.1 Hemangioma, cavernous. The tumor is composed of large dilated blood vessels. Normal liver is seen in the lower left of the image

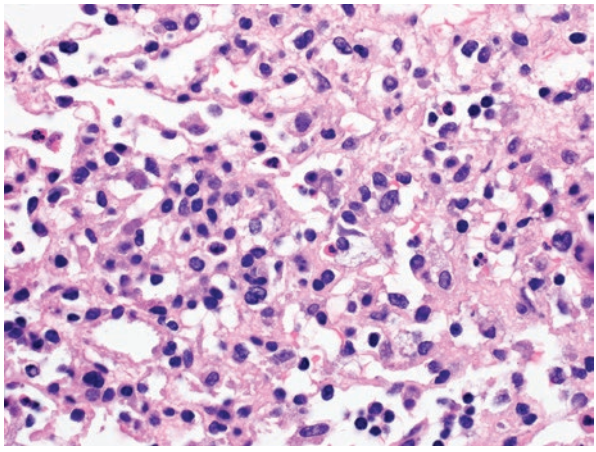

Fig. 7.2 Hemangioma, anastomosing. Small-sized and interconnecting vessels are seen, lined by plump endothelial cells

"hemangiomatosis" or "hemangioma-like vessels" [8]. They are also more likely to have areas of fibrosis.

The rare capillary hemangioma is composed of small thin-walled vessels with a lobular arrangement. The lumens are lined by plump but cytologically bland endothelial cells. In some cases, the vascular lumens can be compressed and inconspicuous, obscuring the vascular nature of the lesion. Rare cases with capsules have been reported [9].

The anastomosing hemangioma is composed of interconnecting small- to medium-sized vascular spaces (Fig. 7.2). The lining endothelial cells can be plump or "hobnailed," often with mild cytological atypia, sometimes causing confusion with angiosarcoma [10]. About 70% of anastomosing hemangiomas have GNAQ mutations [11]. Similar histological and molecular findings have been reported under the term "hepatic small vessel neoplasm" [12].

Imaging Features

Hemangiomas most often occur with a set of classic imaging features which typically results in an unequivocal diagnosis; however, atypical variants may lack classic features and therefore present a more difficult diagnosis.

Classically, hepatic hemangiomas appear hyperechoic at ultrasound, isodense or hypodense to liver parenchyma at noncontrast CT, hypointense to liver at T1 precontrast MRI and moderately T2 hyperintense, with variable diffusion restriction. With the administration of contrast at either US, CT, or MRI, there should be initial nodular, discontinuous, peripheral contrast enhancement with progressive central fill-in over time [13, 14, 15].

Atypical hemangioma variants based on imaging appearance have been described as giant, flash filling, calcified, hyalinized, cystic, and pedunculated. Giant hemangiomas are described as those measuring greater than 8 cm and usually show peripheral nodular enhancement, but delayed phase fill-in may be incomplete, possibly owing to their very large size [16, 17]. The so-called flash-filling hemangiomas are often small and follow the aorta on each vascular phase of imaging [18, 19]. Based on their enhancement pattern, these lesions may serve as mimics for other small hypervascular lesions such as metastases. Because they are slow-flow vascular lesions, hemangiomas sometimes contain calcifications or phleboliths. Hyalinized or sclerotic hemangiomas may mimic hypoenhancing metastases due to their low density/signal intensity and mild peripheral enhancement. At MRI, these sclerotic hemangiomas may have mild T2 signal and will not take up hepatobiliary contrast agents. Stability in size or biopsy may be the only ways to tell these from more sinister lesions. Cystic hemangiomas can contain cystic spaces with fluid–fluid levels visible at CT and MRI but not at US [20, 21, 22]. Examples of classic cavernous hemangiomas (Fig. 7.3) as well as several atypical variants are shown (Fig. 7.4).

Natural History and Management

Hemangiomas are associated with a low risk of complications or significant progression and do not carry malignant potential. Therefore, treatment or follow-up of small asymptomatic hemangiomas is not recommended. Tumor growth may be observed in giant hemangiomas, which in turn may lead to symptoms and possible complications, such as rupture and bleeding [23]. Fortunately, spontaneous tumor rupture resulting in intraperitoneal hemorrhage is exceedingly rare and mostly observed in large, peripheral, and exophytic tumors [24]. Percutaneous ultrasound-guided radiofrequency ablation [25], transcatheter arterial embolization [26], or surgical enucleation [27] has been performed for severely symptomatic or complicated giant hemangiomas. Symptomatic improvement postablative therapy or surgery has been reported in 75–96% of patients; however, extensive evaluation to rule out other possible causes of symptoms is imperative [28, 29].

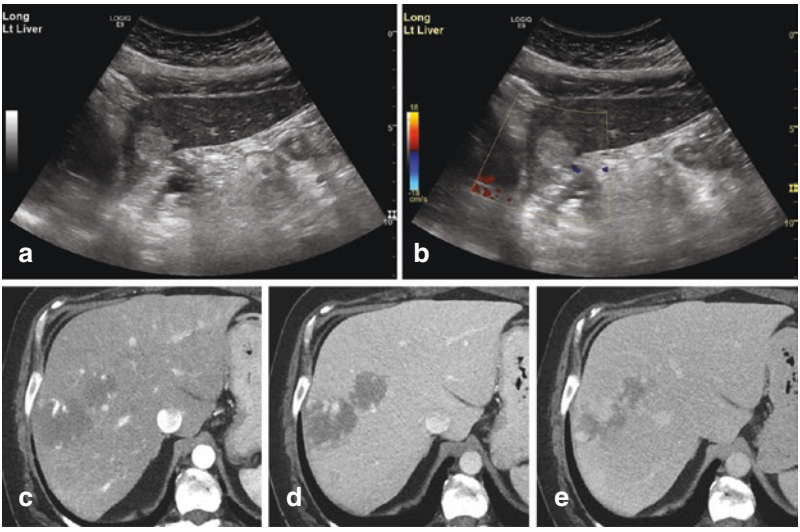

Fig. 7.3 Hemangiomas, classic appearance. Grayscale sonographic images of the left lobe (**a**) show a homogeneously hyperechoic mass with no increased blood on color Doppler (**b**). While the sonographic appearance alone is nonspecific, this mass was later imaged with multiphase CT confirming the diagnosis of a cavernous hemangioma. Axial CT images in the arterial (**c**), portal venous (**d**), and 3-minute delayed (**e**) phases show two adjacent hypodense foci with discontinuous nodular enhancement and progressive fill-in over time, classic features of a cavernous hemangioma

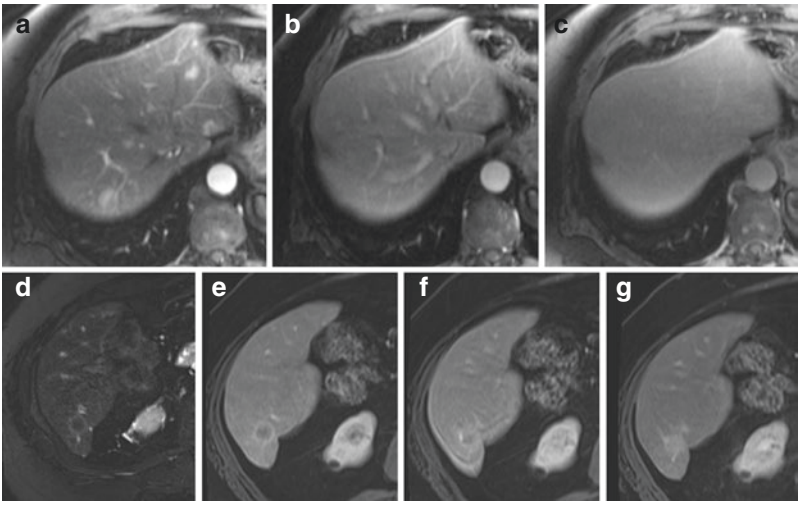

Fig. 7.4 Hemangiomas, atypical appearance. MRI of the liver in a patient with multiple vertebral body and splenic hemangiomas shows an avidly arterially enhancing focus (**a**) which is isointense to liver parenchyma on other phases (**b**, **c**). Several other lesions with similar enhancement pattern were seen throughout the liver, compatible with flash filling hemangiomas. MR images from a patient being followed up after renal mass ablation demonstrate a lesion in the posterior right hepatic lobe with a rim of T2 hyperintensity and a hypointense core (**d**) as well as rim-like arterial enhancement (**e**) with progressive central fill-in on delayed (**f**, **g**) phase images. This finding was stable for greater than 4 years and therefore compatible with a partially sclerosed hemangioma

Hepatic Epithelioid Hemangioendothelioma

Epidemiology and Manifestations

Hepatic epithelioid hemangioendothelioma (HEHE) is a locally aggressive vascular tumor with metastatic potential and shared features between hemangioma and angiosarcoma. The estimated prevalence of HEHE is less than one in 1 million, affecting predominantly females (1:3–4 male-to-female ratio) with a usual age at diagnosis between 20 and 60 years [30]. Patients are often asymptomatic at early stages but are at risk of liver failure with disease progression and extensive organ involvement. Initial symptoms are nonspecific and include upper abdominal pain or fullness, weight loss, fever, jaundice, and fatigue [31].

Pathology

HEHE are vascular malignancies that are clinically lower grade than angiosarcomas. The tumor cells can be epithelioid and dendritic, without well-formed blood vessels, potentially leading to diagnostic challenges. The tumor cells often have intracytoplasmic lumens, leading to a signet ring cell-type morphology. The tumor cells are embedded in a distinctive myxoid or hyalinized matrix (Fig. 7.5). HEHE form mass lesions, but tumor cells can also extend outside the main mass along the sinusoids, portal veins, and central veins, leading to fibro-obliteration of the veins and subsequent parenchymal atrophy with hepatocyte dropout.

Because the tumor has signet ring-type cells and abundant extracellular matrix, the histological findings can mimic cholangiocarcinoma or other adenocarcinomas [32]. In challenging cases, immunostains are used to prove vascular differentiation. At the molecular level, many HEHE have a t(1;3)(p36.3;q25) translocation that leads to a CAMTA1–WWTR1 fusion product.

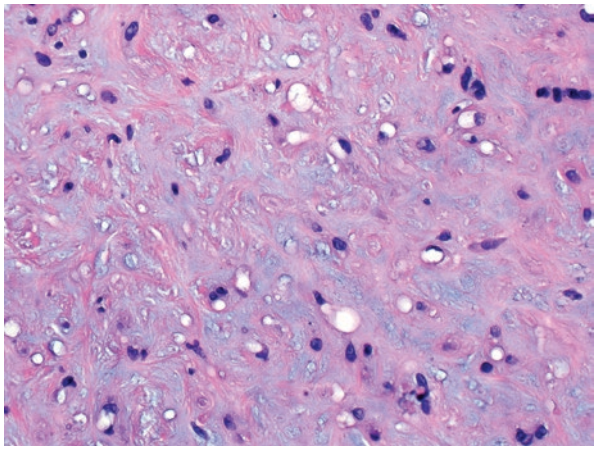

Fig. 7.5 Epithelioid hemangioendothelioma. The tumor cells have small lumens, resembling signet ring cells, and are embedded in a dense myxoid matrix

Imaging Features

The imaging appearance of HEHE is described to follow three subtypes: solitary nodular type, multiple nodular type, and diffuse confluent nodular type. It is theorized that a solitary lesion progresses to multiple nodules which then coalesce over time to form confluent disease. Solitary lesions are classically found in the subcapsular right hepatic lobe, measuring between 1 and 5 cm [33]. Less frequently, solitary lesions can be found in the central liver [34]. Multiple masses tend to be larger, measuring between 1 and 12 cm and may be found either peripherally or in the central liver [35]. Multinodular lesions will most frequently exhibit the classic finding of capsular retraction [34]. This finding should be differentiated from the capsular bulge seen in cholangiocarcinoma. Solitary nodular type (Fig. 7.6) and multinodular type (Fig. 7.7) are shown.

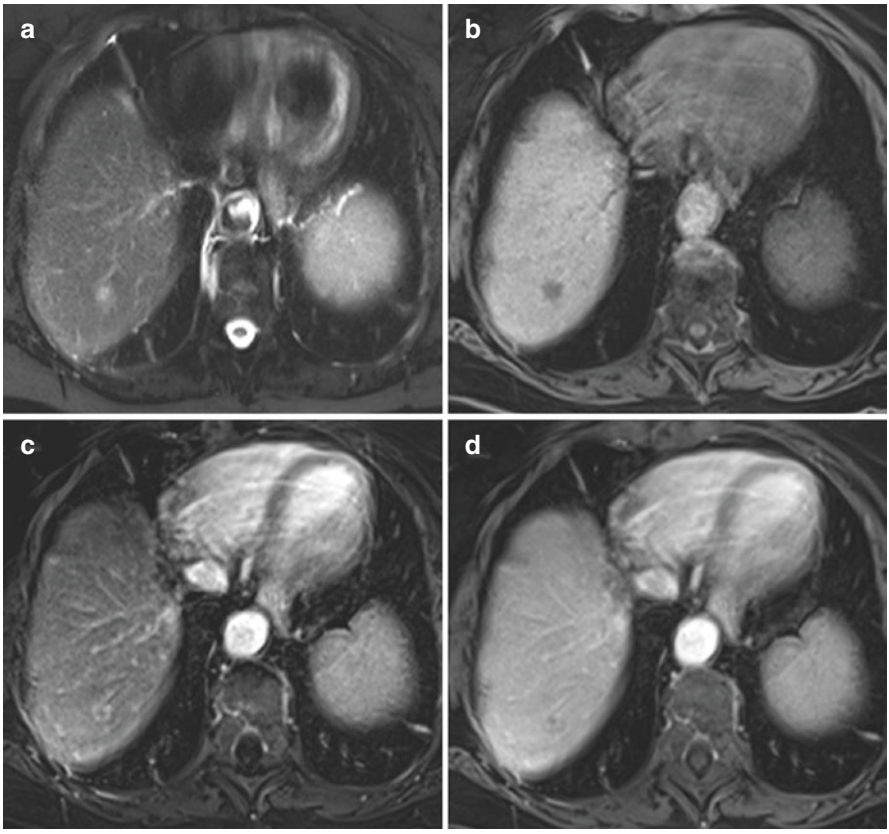

Fig. 7.6 Epithelioid hemangioendothelioma. MRI images from a 76-year-old woman show a solitary lesion in the hepatic dome which was thought to represent cholangiocarcinoma and went on to be resected. Histology confirmed a hepatic epithelioid hemangioendothelioma (HEHE). Note the T2 hyperintense center with intermediate T2 signal rim (**a**), T1 hypointensity (**b**), early peripheral enhancement (**c**), and laminated delayed central fill-in (**d**)

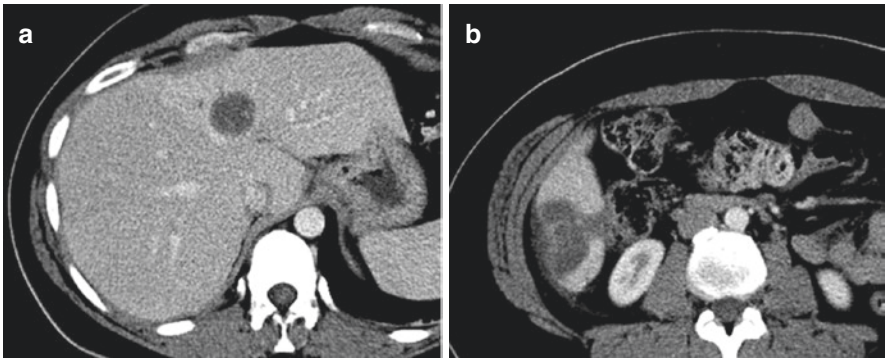

Fig. 7.7 Epithelioid hemangioendothelioma. Single-phase CT images from a 31-year-old woman with biopsy-proven hepatic epithelioid hemangioendothelioma. Multiple hypoenhancing hepatic lesions are seen in the anterior left lobe (**a**) and the inferior right lobe (**b**). Note the presence of capsular retraction adjacent to both lesions. Alternative etiologies with similar single-phase imaging features would be expected to result in capsular bulge

Sonographically, HEHE should show hypoechoic nodules, though a minority of nodules may appear hyperechoic to surrounding liver. As with other modalities, capsular retraction can be seen. At CT, lesions should be hypointense to hepatic parenchyma and at MRI, lesions should be T1 hypointense. T2 appearance is variable, but many lesions are T2 hyperintense centrally due to a core of fibrous stroma. Others may demonstrate alternating rings of T2 signal in the so-called "dark-bright-dark ring" sign [36]. When performed, diffusion-weighted imaging will also show a multicentric pattern of high and low signals. After contrast administration, some lesions show a rim of enhancement followed by fill-in on delayed phase, in a pattern similar to that of cholangiocarcinoma or metastases. In contrast to hemangiomas, globular peripheral enhancement is not seen. There have been reports of HEHE lesions "trapping" hepatobiliary contrast agents and resulting in a hypointense rim with a hyperintense core, though this is not frequently observed [34]. Extrahepatic HEHE has been described in the lung, lymphatic system, peritoneum, bone marrow, and spleen.

Natural History and Management

HEHE is associated with a high risk of metastasis, particularly to the lungs, bone, peritoneum, and lymph nodes. Untreated patients carry a 5-year mortality risk greater than 50% and, therefore, expectant management is not recommended. Surgical resection and liver transplantation are the treatments of choice, while the role of chemotherapy and radiation has not been well established. Unfortunately, surgical resection is an option in only about 10% of cases, as the majority of patients present with multifocal bilobar disease and about a third have extrahepatic involvement at diagnosis. In those with limited disease, surgical resection carries a good prognosis with 75% survival at 5 years [37]. Liver transplantation is the preferred treatment modality

for unresectable HEHE and is associated with 1-year and 5-year survival rates of 96% and 80%, respectively [37, 38, 39]. Extrahepatic metastases do not significantly affect long-term outcomes posttransplant and, therefore, are not a contraindication to transplant. Currently, patients with HEHE do not qualify for automatic MELD exception points, as do patients with hepatocellular carcinoma listed for liver transplantation. However, given the acceptable outcomes with transplant, selected patients with HEHE may be granted exception MELD points upon request to the Regional Review Board of the United Network for Organ Sharing (UNOS).

Angiosarcoma

Epidemiology and Manifestations

Hepatic angiosarcoma (HAS) is a rare and aggressive vascular tumor, which accounts for <1% of all primary liver tumors [40, 41]. HAS is associated with exposure to known carcinogens in 25% of cases, including vinyl chloride monomer, radiocontrast material thorotrast, androgenic steroid use, chronic arsenic ingestion, and exposure to radium [42]. The other 75% of tumors have no known etiology. HAS is more common in men (3:1 male-to-female ratio) in their sixth to seventh decade of life [43]. Patients often present with vague, nonspecific symptoms including fatigue, weight loss, and upper abdominal pain [40]. About half of the patients present with symptoms of liver failure or portal hypertension, such as jaundice, hepatosplenomegaly, ascites, and possibly hepatic encephalopathy [42]. Angiosarcoma has also been associated with Kasabach–Merritt syndrome [44] and spontaneous tumor rupture resulting in hemoperitoneum [45]. In contrast to hemangiomas, the diagnosis of HAS often relies on histopathologic assessment, which in turn depends on adequate tumor sampling. Due to the increased risk of bleeding, percutaneous needle biopsy is not recommended, and rather fine-needle aspiration cytology is preferred [46].

Pathology

Angiosarcomas are high-grade malignant vascular tumors that can be primary to the liver or metastatic. They are composed of malignant cells that have evidence for vascular differentiation by morphology or by immunostains such as CD34, FLi-1, or ERG. In most cases, angiosarcomas form distinct mass lesions, but rarely they grow as a subtle diffuse sinusoidal infiltrate, leading to hepatomegaly without a mass lesion (Fig. 7.8). When forming mass lesions, the tumor cells can be epithelioid (Fig. 7.9), spindle cell, or show irregular poorly formed vascular structures (Fig. 7.10), often with slit-like spaces that contain red blood cells. The tumor cells show cytological atypia and numerous mitotic figures.

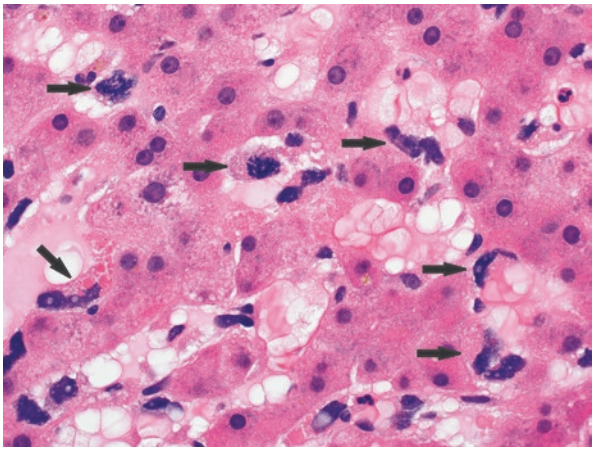

Fig. 7.8 Angiosarcoma, sinusoidal pattern. There was no mass lesion, but a biopsy showed diffuse infiltration of the sinusoids by malignant endothelial cells (arrows). Most of the remaining cells in the image are benign hepatocytes

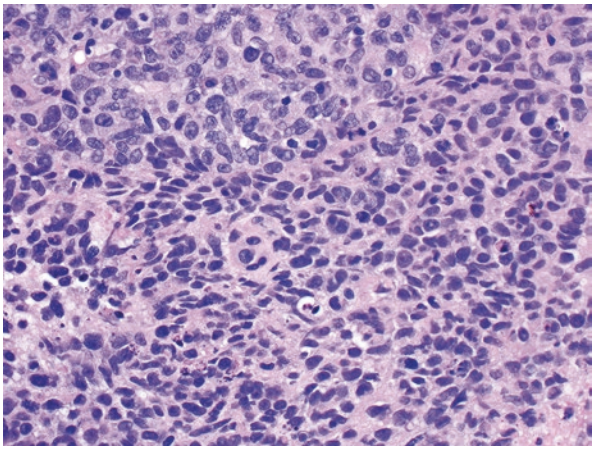

Fig. 7.9 Angiosarcoma, solid pattern. This mass-forming angiosarcoma shows no evident blood vessels, and the diagnosis required immunostains

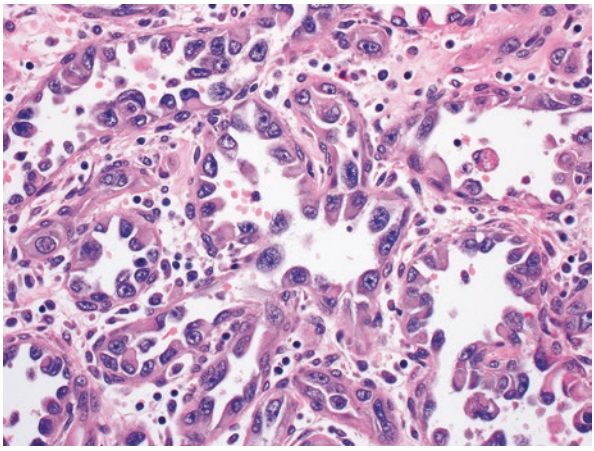

Fig. 7.10 Angiosarcoma, vessel-forming pattern. This mass-forming angiosarcoma had vascular-like spaces lined by highly atypical cells

Imaging Features

Due to their rarity, knowledge of the appearance of angiosarcomas is largely limited to observations published in case series ranging from 7 to 35 patients [47, 48, 49]. At imaging, tumors are found to be multifocal in nearly all patients, and the dominant tumor may range in size from 3 to 20 cm. While most lesions are found to involve both hepatic lobes, a subgroup has been described to involve only the left hepatic lobe. Metastases, most commonly to spleen, peritoneum, lungs, or bone marrow, are seen in 45–60% of patients at presentation.

At multiphase CT, hepatic angiosarcomas should follow the blood pool attenuation. Prior to the administration of contrast, lesions will be hypodense to liver parenchyma, though areas of hemorrhage or blood products may be denser. Several patterns of contrast enhancement have been described, including nodular, rim, branching, and diffuse enhancement. At least one type of arterial phase enhancement is seen in over 90% of tumors [49]. On portal venous and delayed phase images, lesions will enhance progressively in one of two patterns, either hemangioma-like peripheral to central or a reverse hemangioma pattern with central early enhancement with delayed peripheral fill-in [48, 49].

At MRI, angiosarcoma has an overall low T1 signal except for areas of hemorrhage which may have a high intrinsic T1 signal. Angiosarcomas usually have central heterogeneous T2 hyperintensity, and larger lesions may demonstrate serpiginous DWI hyperintensity. Enhancement patterns using extracellular contrast agents mirror those seen at CT. An example of a well-differentiated angiosarcoma is shown in Fig. 7.11.

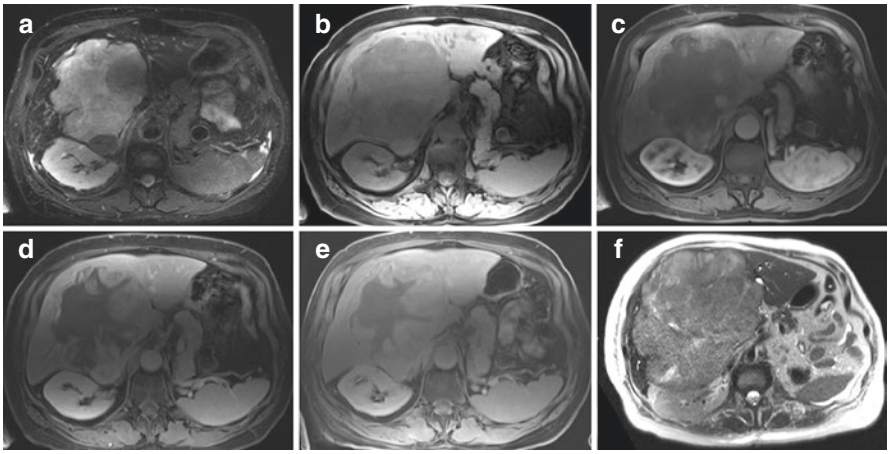

Fig. 7.11 Angiosarcoma. Biopsy-proven angiosarcoma spanning both hepatic lobes (**a**) in a 74-year-old man. The T1 signal is somewhat heterogeneous suggesting internal hemorrhage (**b**). Following administration of contrast there is peripheral arterial enhancement (**c**) followed by progressive fill-in on delayed phase images (**d**, **e**). Although based on enhancement pattern alone, this lesion could be mistaken for a giant hemangioma; rapid growth in 5 weeks seen on a follow-up scan (**f**) is more indicative of an aggressive process such as angiosarcoma

Imaging differentiation of angiosarcoma from other etiologies is difficult, as hemangiomas, epithelioid hemangioendotheliomas, and hypervascular metastases as well as primary hepatic neoplasms such as HCC and intrahepatic cholangiocarcinoma may all have overlapping features. Rapid progression over serial exams is the most reliable differentiator; however, prospective diagnosis is challenging and ultimately may require histologic sampling.

Natural History and Management

Hepatic angiosarcoma carries an extremely poor prognosis with a median survival of only 1 month [50]. Surgical resection of localized tumors may prolong survival, and is the therapy of choice for early solitary tumors. Systemic therapy or transarterial chemoembolization with palliative intent has shown potential benefits in patients with dominant HAS [51]. Additionally, transarterial embolization can be used to achieve hemostasis in ruptured HAS with hemoperitoneum. Liver transplantation is contraindicated in HAS due to aggressive early recurrence posttransplant, observed in up to 80% of patients [52].

Summary

Vascular tumors of the liver span the spectrum from exceedingly rare to very common and from malignant with a dismal prognosis to benign and incidental. While the clinical and imaging features may possess a large amount of overlap, classic findings may allow for noninvasive diagnosis in some cases. Histologic sampling may be required for others.

References

1. Gandolfi L, Leo P, Solmi L, Vitelli E, Verros G, Colecchia A. Natural history of hepatic haemangiomas: clinical and ultrasound study. Gut. 1991;32:677–80.
2. Kaltenbach TE, Engler P, Kratzer W, Oeztuerk S, Seufferlein T, Haenle MM, Graeter T. Prevalence of benign focal liver lesions: ultrasound investigation of 45,319 hospital patients. Abdom Radiol (NY). 2016;41:25–32. https://doi.org/10.1007/s00261-015-0605-7.
3. Tait N, Richardson AJ, Muguti G, Little JM. Hepatic cavernous haemangioma: a 10 year review. Aust N Z J Surg. 1992;62:521–4.
4. Liu X, Yang Z, Tan H, Zhou W, Su Y. Fever of unknown origin caused by giant hepatic hemangioma. J Gastrointest Surg. 2018;22:366–7. https://doi.org/10.1007/s11605-017-3522-y.

5. Smith AA, Nelson M. High-output heart failure from a hepatic hemangioma with exertion-induced hypoxia. Am J Cardiol. 2016;117:157–8. https://doi.org/10.1016/j.amjcard.2015.10.019.
6. Concejero AM, Chen CL, Chen TY, Eng HL, Kuo FY. Giant cavernous hemangioma of the liver with coagulopathy: adult Kasabach-Merritt syndrome. Surgery. 2009;145:245–7. https://doi.org/10.1016/j.surg.2007.07.039.
7. Shimizu M, Miura J, Itoh H, Saitoh Y. Hepatic giant cavernous hemangioma with microangiopathic hemolytic anemia and consumption coagulopathy. Am J Gastroenterol. 1990;85:1411–3.
8. Jhaveri KS, Vlachou PA, Guindi M, Fischer S, Khalili K, Cleary SP, Ayyappan AP. Association of hepatic hemangiomatosis with giant cavernous hemangioma in the adult population: prevalence, imaging appearance, and relevance. AJR Am J Roentgenol. 2011;196:809–15. https://doi.org/10.2214/ajr.09.4143.
9. Jhuang JY, Lin LW, Hsieh MS. Adult capillary hemangioma of the liver: case report and literature review. Kaohsiung J Med Sci. 2011;27:344–7. https://doi.org/10.1016/j.kjms.2011.03.003.
10. Lin J, Bigge J, Ulbright TM, Montgomery E. Anastomosing hemangioma of the liver and gastrointestinal tract: an unusual variant histologically mimicking angiosarcoma. Am J Surg Pathol. 2013;37:1761–5. https://doi.org/10.1097/PAS.0b013e3182967e6c.
11. Bean GR, Joseph NM, Gill RM, Folpe AL, Horvai AE, Umetsu SE. Recurrent GNAQ mutations in anastomosing hemangiomas. Mod Pathol. 2017;30:722–7. https://doi.org/10.1038/modpathol.2016.234.
12. Gill RM, et al. Hepatic small vessel neoplasm, a rare infiltrative vascular neoplasm of uncertain malignant potential. Hum Pathol. 2016;54:143–51. https://doi.org/10.1016/j.humpath.2016.03.018.
13. Johnson CM, Sheedy P 2nd, Stanson AW, Stephens DH, Hattery R, Adson M. Computed tomography and angiography of cavernous hemangiomas of the liver. Radiology. 1981;138:115–21.
14. Tung G, Vaccaro J, Cronan J, Rogg J. Cavernous hemangioma of the liver: pathologic correlation with high-field MR imaging. AJR Am J Roentgenol. 1994;162:1113–7.
15. Yamashita Y, Ogata I, Urata J, Takahashi M. Cavernous hemangioma of the liver: pathologic correlation with dynamic CT findings. Radiology. 1997;203:121–5.
16. Choi B, Han M, Park J, Kim SH, Han M, Kim C. Giant cavernous hemangioma of the liver: CT and MR imaging in 10 cases. Am J Roentgenol. 1989;152:1221–6.
17. Soyer P, Dufresne A, Somveille E, Scherrer A. Hepatic cavernous hemangioma: appearance on T2-weighted fast spin-echo MR imaging with and without fat suppression. AJR Am J Roentgenol. 1997;168:461–5.
18. Hanafusa K, Ohashi I, Himeno Y, Suzuki S, Shibuya H. Hepatic hemangioma: findings with two-phase CT. Radiology. 1995;196:465–9.
19. Quinn SF, Benjamin G. Hepatic cavernous hemangiomas: simple diagnostic sign with dynamic bolus CT. Radiology. 1992;182:545–8.
20. Hihara T, Araki T, Katou K, Odashima H, Ounishi H, Kachi K, Uchiyama G. Cystic cavernous hemangioma of the liver. Gastrointest Radiol. 1990;15:112–4.
21. Itai Y, Ohtomo K, Kokubo T, Yamauchi T, Okada Y, Makita K. CT demonstration of fluid-fluid levels in nonenhancing hemangiomas of the liver. J Comput Assist Tomogr. 1987;11:763–5.
22. Soyer P, Bluemke D, Fishman E, Rymer R. Fluid–fluid levels within focal hepatic lesions: imaging appearance and etiology. Abdom Imaging. 1998;23:161–5.
23. Jing L, Liang H, Caifeng L, Jianjun Y, Feng X, Mengchao W, Yiqun Y. New recognition of the natural history and growth pattern of hepatic hemangioma in adults. Hepatol Res. 2016;46:727–33. https://doi.org/10.1111/hepr.12610.
24. Mocchegiani F, et al. Prevalence and clinical outcome of hepatic haemangioma with specific reference to the risk of rupture: a large retrospective cross-sectional study. Dig Liver Dis. 2016;48:309–14. https://doi.org/10.1016/j.dld.2015.09.016.

25. Park SY, Tak WY, Jung MK, Jeon SW, Cho CM, Kweon YO, Kim KC. Symptomatic-enlarging hepatic hemangiomas are effectively treated by percutaneous ultrasonography-guided radiofrequency ablation. J Hepatol. 2011;54:559–65. https://doi.org/10.1016/j.jhep.2010.07.024.
26. Sun JH, et al. Transcatheter arterial embolization alone for giant hepatic hemangioma. PLoS One. 2015;10:e0135158. https://doi.org/10.1371/journal.pone.0135158.
27. Abdel Wahab M, et al. Surgical management of giant hepatic hemangioma: single center's experience with 144 patients. J Gastrointest Surg. 2018;22:849–58. https://doi.org/10.1007/s11605-018-3696-y.
28. Farges O, Daradkeh S, Bismuth H. Cavernous hemangiomas of the liver: are there any indications for resection? World J Surg. 1995;19:19–24.
29. Yoon SS, Charny CK, Fong Y, Jarnagin WR, Schwartz LH, Blumgart LH, DeMatteo RP. Diagnosis, management, and outcomes of 115 patients with hepatic hemangioma. J Am Coll Surg. 2003;197:392–402. https://doi.org/10.1016/S1072-7515(03)00420-4.
30. Sardaro A, Bardoscia L, Petruzzelli MF, Portaluri M. Epithelioid hemangioendothelioma: an overview and update on a rare vascular tumor. Oncol Rev. 2014;8:259. https://doi.org/10.4081/oncol.2014.259.
31. Lauffer JM, Zimmermann A, Krahenbuhl L, Triller J, Baer HU. Epithelioid hemangioendothelioma of the liver. A rare hepatic tumor. Cancer. 1996;78:2318–27.
32. Makhlouf HR, Ishak KG, Goodman ZD. Epithelioid hemangioendothelioma of the liver: a clinicopathologic study of 137 cases. Cancer. 1999;85:562–82.
33. Miller W, Dodd G 3rd, Federle M, Baron R. Epithelioid hemangioendothelioma of the liver: imaging findings with pathologic correlation. AJR Am J Roentgenol. 1992;159:53–7.
34. Kim EH, Rha SE, Lee YJ, Yoo IR, Jung ES, Byun JY. CT and MR imaging findings of hepatic epithelioid hemangioendotheliomas: emphasis on single nodular type. Abdom Imaging. 2015;40:500–9.
35. Paolantonio P, Laghi A, Vanzulli A, Grazioli L, Morana G, Ragozzino A, Colagrande S. MRI of hepatic epithelioid hemangioendothelioma (HEH). J Magn Reson Imaging. 2014;40:552–8.
36. Economopoulos N, Kelekis NL, Argentos S, Tsompanlioti C, Patapis P, Nikolaou I, Gouliamos A. Bright-dark ring sign in MR imaging of hepatic epithelioid hemangioendothelioma. J Magn Reson Imaging. 2008;27:908–12.
37. Mehrabi A, et al. Primary malignant hepatic epithelioid hemangioendothelioma: a comprehensive review of the literature with emphasis on the surgical therapy. Cancer. 2006;107:2108–21. https://doi.org/10.1002/cncr.22225.
38. Nudo CG, et al. Liver transplantation for hepatic epithelioid hemangioendothelioma: the Canadian multicentre experience. Can J Gastroenterol. 2008;22:821–4.
39. Rodriguez JA, Becker NS, O'Mahony CA, Goss JA, Aloia TA. Long-term outcomes following liver transplantation for hepatic hemangioendothelioma: the UNOS experience from 1987 to 2005. J Gastrointest Surg. 2008;12:110–6. https://doi.org/10.1007/s11605-007-0247-3.
40. Molina E, Hernandez A. Clinical manifestations of primary hepatic angiosarcoma. Dig Dis Sci. 2003;48:677–82.
41. Zocchetti C. Liver angiosarcoma in humans: epidemiologic considerations. Med Lav. 2001;92:39–53.
42. Chaudhary P, Bhadana U, Singh RA, Ahuja A. Primary hepatic angiosarcoma. Eur J Surg Oncol. 2015;41:1137–43. https://doi.org/10.1016/j.ejso.2015.04.022.
43. Bioulac-Sage P, Laumonier H, Laurent C, Blanc JF, Balabaud C. Benign and malignant vascular tumors of the liver in adults. Semin Liver Dis. 2008;28:302–14. https://doi.org/10.1055/s-0028-1085098.
44. Fujii F, et al. Hepatic angiosarcoma with Kasabach-Merritt phenomenon: a case report and review of the literature. Ann Hepatol. 2018;17:655–60. https://doi.org/10.5604/01.3001.0012.0949.
45. Leowardi C, et al. Ruptured angiosarcoma of the liver treated by emergency catheter-directed embolization. World J Gastroenterol. 2006;12:804–8.
46. Wong JW, Bedard YC. Fine-needle aspiration biopsy of hepatic angiosarcoma: report of a case with immunocytochemical findings. Diagn Cytopathol. 1992;8:380–3.

47. Bruegel M, Muenzel D, Waldt S, Specht K, Rummeny EJ. Hepatic angiosarcoma: cross-sectional imaging findings in seven patients with emphasis on dynamic contrast-enhanced and diffusion-weighted MRI. Abdom Imaging. 2013;38:745–54.
48. Koyama T, Fletcher JG, Johnson CD, Kuo MS, Notohara K, Burgart LJ. Primary hepatic angiosarcoma: findings at CT and MR imaging. Radiology. 2002;222:667–73.
49. Pickhardt PJ, Kitchin D, Lubner MG, Ganeshan DM, Bhalla S, Covey AM. Primary hepatic angiosarcoma: multi-institutional comprehensive cancer centre review of multiphasic CT and MR imaging in 35 patients. Eur Radiol. 2015;25:315–22.
50. Groeschl RT, Miura JT, Oshima K, Gamblin TC, Turaga KK. Does histology predict outcome for malignant vascular tumors of the liver? J Surg Oncol. 2014;109:483–6. https://doi.org/10.1002/jso.23517.
51. Park YS, Kim JH, Kim KW, Lee IS, Yoon HK, Ko GY, Sung KB. Primary hepatic angiosarcoma: imaging findings and palliative treatment with transcatheter arterial chemoembolization or embolization. Clin Radiol. 2009;64:779–85. https://doi.org/10.1016/j.crad.2009.02.019.
52. Bonaccorsi-Riani E, Lerut JP. Liver transplantation and vascular tumours. Transpl Int. 2010;23:686–91. https://doi.org/10.1111/j.1432-2277.2010.01107.x.
53. Ehman EC, et al. Hepatic tumors of vascular origin: imaging appearances. Abdom Radiol. 2018;43(8):1978–90.

Chapter 8
Rare Liver Tumors

Patrick J. Navin, Ju Dong Yang, Michael S. Torbenson, and Sudhakar K. Venkatesh

Introduction

Various neoplastic entities can arise in the liver originating from a hepatocytic, biliary, or mesenchymal cell type. While differentiating benign from malignant tumors is crucial, imaging features are often nonspecific and thus differentiation of these lesions is difficult. Hepatic tumors occur less commonly in the pediatric population than in adults. Up to 70% of pediatric liver tumors are malignant and associated with a poor prognosis [1]. The aim of this chapter is to provide a brief overview of some of the more uncommon hepatic tumors affecting the adult and pediatric populations.

Hepatic Angiomyolipoma

Angiomyolipomas (AMLs) are mesenchymal tumors characterized by the presence of variable mixtures of adipose tissue, smooth muscle cells, and thick-walled blood vessels. AMLs are thought to belong to a group of type of tumor known as a

P. J. Navin · S. K. Venkatesh (✉)
Department of Radiology, Mayo Clinic, Rochester, MN, USA
e-mail: Navin.patrick@mayo.edu; Venkatesh.Sudhakar@mayo.edu

J. D. Yang
Department of Gastroenterology and Hepatology, Mayo Clinic, Rochester, MN, USA
e-mail: Yang.JuDong@mayo.edu

M. S. Torbenson
Department of Laboratory Medicine and Pathology, Mayo Clinic, Rochester, MN, USA
e-mail: Torbenson.Michael@mayo.edu

L. R. Roberts et al. (eds.), *Evaluation and Management of Liver Masses*,
https://doi.org/10.1007/978-3-030-46699-2_8

"PEComa." This entity is defined by the World Health Organization as a "mesenchymal tumor composed of histologically and immunohistochemically distinctive perivascular epithelioid cells" [2]. The PEComa group includes tumors such as pulmonary lymphangioleiomyomatosis, clear cell "sugar" tumor (CCST), clear-cell myomelanocytic tumor of the falciform ligament, and AMLs [3].

Hepatic AMLs are a very rare entity. They were first described in 1976. Only approximately 200 cases were reported up until 2005 [4, 5]. The incidence of hepatic AMLs is higher in females, with a large age range from 26 to 86 years [6–12]. There are limited data to suggest any viral or genetic association; however, hepatic AMLs have been associated with certain genetic variants of tuberous sclerosis [13, 14]. Hepatic AMLs are only seen in 6% of patients with tuberous sclerosis, whereas renal AMLs are more commonly present in 20% of tuberous sclerosis patients [15].

The clinical presentation is predominantly of an asymptomatic hepatic lesion found incidentally on imaging. When symptoms arise, they are generally secondary to mass effect and take the form of abdominal pain [6, 11]. Liver tests, viral serology, and tumor markers are generally normal [10, 11].

Imaging

The appearance of hepatic AMLs on imaging is inconsistent given the variation in the proportions of tumor components [16]. Although imaging is an essential component of the diagnostic evaluation, a definitive conclusion is only achieved in approximately 5% of cases, with lesions often misdiagnosed as hepatocellular carcinoma (HCC) or focal nodular hyperplasia (FNH) [16]. Intralesional fat is seen in only 50% of hepatic AMLs in comparison to renal AMLs where it is more commonly seen [6].

The sonographic appearance is generally of a solitary, echogenic lesion, ranging from 5 to 6 cm in size (Fig. 8.1d) [14, 17]. Unless features such as speed propagation artifact and refraction artifact are present, hepatic AMLs are virtually identical to hemangiomas [12, 18]. On CT, lesions demonstrate varying amounts of intralesional fat from obvious fat attenuation (Fig. 8.1) to a more heterogenous mixed attenuation appearance. When fat is present, the lesion can be described as two specific components: a peripheral angiomyomatous component and a central fatty component with CT number less than – 20 Hounsfield units (HU) [19]. On MRI, hepatic AML demonstrate high signal on T1 and T2 weighted images with signal decrease on opposed phase imaging when fat is present. Features on CT or MRI such as intense arterial enhancement later than that of HCC (Fig. 8.2), a peripheral rim of contrast washout on equilibrium and delayed phases, and the presence of an early draining vein are more specific to hepatic AML [16]. The fatty areas are also generally hypervascular in AMLs and relatively hypovascular in HCCs [20]. AML

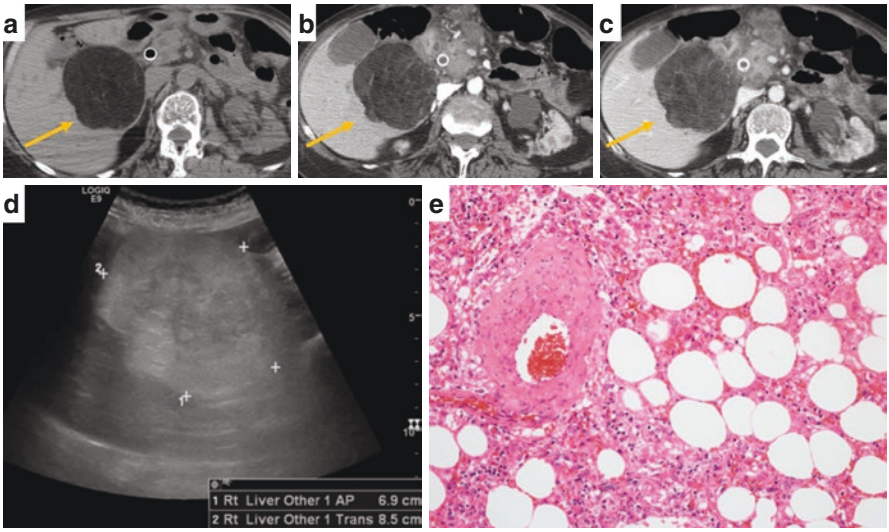

Fig. 8.1 Angiomyolipoma of the liver in a 64-year-old lady with tuberous sclerosis. Noncontrast CT (**a**) demonstrates a mass of predominantly fat attenuation in segment 5 of the liver with minimal progressive internal enhancement on arterial (**b**) and portal venous phases (**c**). Ultrasound (**d**) demonstrates a large echogenic mass in the right liver with poor penetration of the ultrasound beam. Biopsy (**e**) of the tumor demonstrates fat, myoid cells, and large vessels confirming the diagnosis of angiomyolipoma

occurring in a patient with chronic liver disease may be diagnosed and treated as HCC, as biopsy confirmation is often not required for making the diagnosis of HCC.

Pathology

AMLs are composed of neoplastic cells that show a mixture of steatosis, smooth muscle (myoid) differentiation, and large thick-walled vessels (Figs. 8.1e and 8.2f). The myoid cells can be either spindled or epithelioid. The proportion of each component varies considerably between tumors, leading to difficulties in diagnosis. For example, a subset of angiomyolipomas are composed mostly of spindled myoid cells and can mimic smooth muscle tumors [21], while others are composed mostly of epithelioid cells that can closely mimic hepatic tumors (Fig. 8.2f), such as hepatic adenomas or HCC [6].

Extramedullary hematopoiesis is commonly found in tumors that have significant fatty differentiation. A small number of AMLs can have marked lymphoplasmacytic rich inflammation, mimicking inflammatory pseudotumors [6]. Other rare

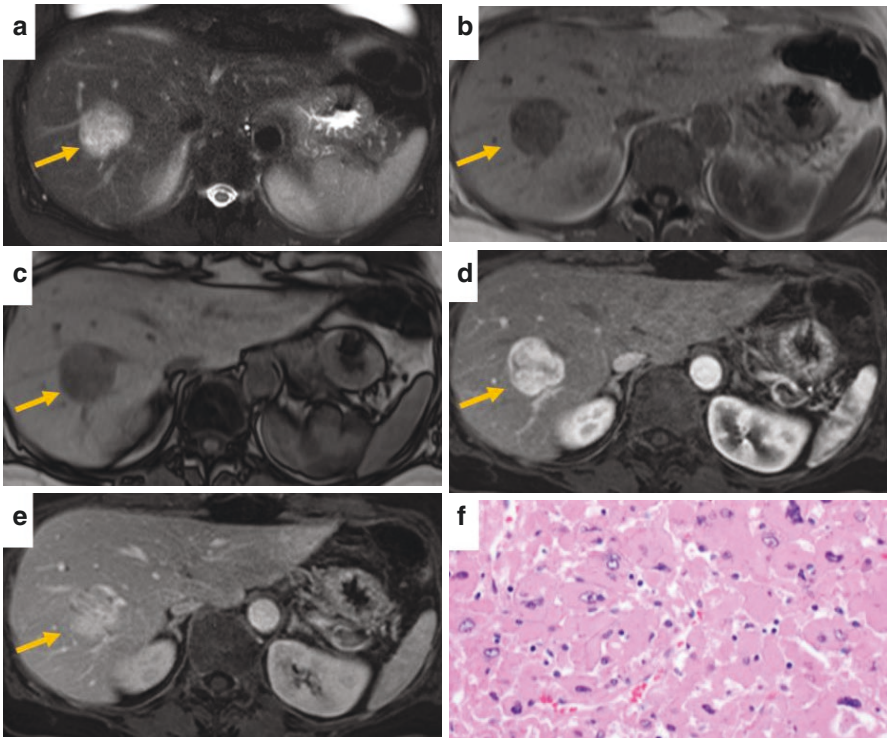

Fig. 8.2 Angiomyolipoma of liver. A 63-year-old lady with rectal cancer and a liver mass. MRI of the abdomen demonstrates a heterogeneously hyperintense mass on T2 weighted sequences (**a**), hypointense on T1 weighted sequences (**b**) with no loss of signal on out-of-phase images (**c**) indicating no intralesional fat. The lesion demonstrates avid enhancement on arterial phase imaging (**d**) with residual less marked enhancement in the portal venous phase (**e**). Histopathology demonstrates sheets and trabeculae of epithelioid and spindle cells separated by vascular spaces, consistent with AML. The myoid cells in this case resemble epithelial cells, which can mimic the tumor cells of hepatic adenomas or hepatocellular carcinoma (**f**)

histological findings include striking peliotic changes, hemorrhage, and necrosis. Finally, in a small percent of cases, the myoid cells can be large, pleomorphic, and multinucleated with hyperchromatic nuclei, a finding that is not necessarily associated with a more malignant phenotype.

Very rarely, AMLs can be clinically aggressive. Findings that raise concern for a more malignant phenotype include vascular invasion [22], coagulative necrosis [23], and marked cytological atypia associated with increased mitotic activity [24].

Because of the diagnostic challenges in recognizing AML on H&E, in most cases, the diagnosis is confirmed by immunohistochemistry. AMLs are negative for both cytokeratins and markers of hepatic differentiation, but are positive for β-Hydroxy β-Methylbutyrate (HMB) 45 and Melan A, with the strongest staining in the myoid components. It is important to distinguish AML from gastrointestinal stromal tumors, as most AMLs are c-Kit positive by immunostain [25].

Surgical resection is warranted if there is diagnostic uncertainty, if the lesion is symptomatic, or if the size is greater than 5 cm or enlarging over a short period of observation [8, 26].

Primary Hepatic Lymphoma

Primary hepatic lymphoma is a rare entity, first described in 1965 [27]. It is defined as lymphoma confined to the liver with perihepatic nodal sites, without disease involvement elsewhere [28, 29]. Typically, distal disease should not be present for approximately 6 months after the onset of hepatic lesions [30]. The distinction between primary and secondary hepatic lymphoma is important as the treatment and prognosis vary considerably.

The factors leading to primary lymphoma in the liver are not completely understood. Various etiological factors such as chronic hepatitis, cirrhosis, treatment with immunosuppressive therapy, systemic lupus erythematosus, continuous B-cell proliferation posttransplant, and acquired immune deficiency syndrome have been suggested [31–44]. However, most associations are based on case reports and no unifying etiological factors have been identified.

Patients typically present with abdominal pain, jaundice, and other nonspecific symptoms such as weight loss, nausea and vomiting, and night sweats [29, 45]. On clinical exam, hepatomegaly is the most common finding, seen in approximately 50% [29, 45–47]. Liver tests are inconsistently elevated, predominantly alkaline phosphatase and lactate dehydrogenase [48]. Serum calcium and tumor markers such as alpha-fetoprotein and carcinoembryonic antigen may also be raised [48, 49].

Imaging

Imaging presentation may be with a solitary mass, multiple well-defined masses, or as an infiltrating lesion [50, 51]. A single solitary mass is reported as most common, occurring in 55–60% of presentations [29]. The mass may grow into the hepatic veins, inferior vena cava, and the right atrium, mimicking an HCC. Approximately 35–40% of patients have multiple lesions [52]. Diffuse infiltration is rare [53].

On ultrasound, lesions are typically solid and hypoechoic or anechoic, often resembling cysts (Fig. 8.3a) [30, 53]. A target lesion has also been described [28]. In the infiltrating form of the disease, the only imaging feature is often hepatomegaly [54].

Focal hepatic lymphoma lesions are hypoattenuating on noncontrast CT with rim enhancement often seen with contrast administration (Fig. 8.3b). A target type lesion can also occur on CT with lesions consisting of central necrosis, rim enhancement, and a peripheral ill-defined hypoattenuating area [28].

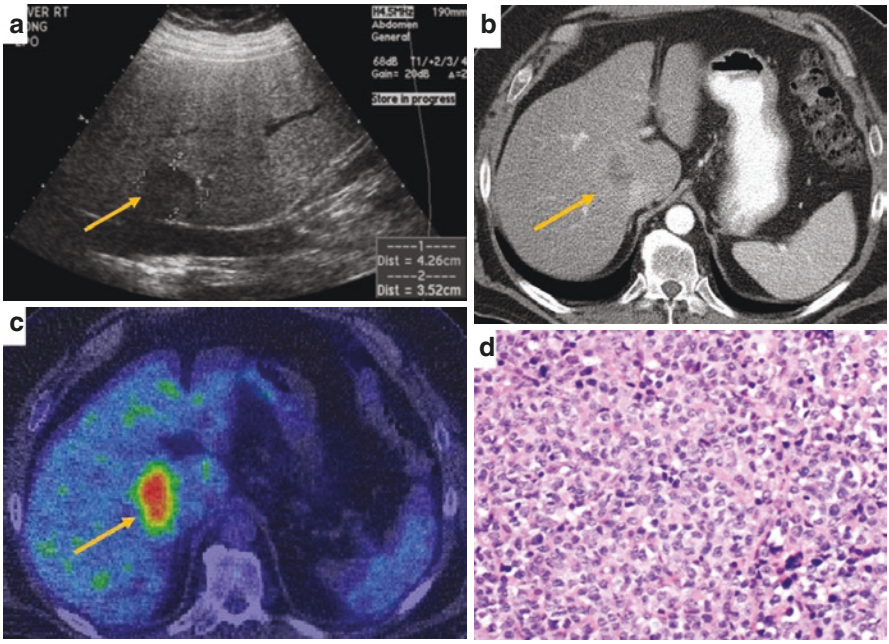

Fig. 8.3 Large B-cell lymphoma of liver. A 62-year-old male with rectal cancer detected on colonoscopy. Work up demonstrated a mass in the liver. Ultrasound (**a**) demonstrates a predominantly hypoechoic mass in the central liver adjacent to the IVC. Contrast-enhanced CT (**b**) demonstrates a hypoattenuating mass with minimal peripheral enhancement. The lesion was FDG avid on PET CT (**c**) with no evidence of disease elsewhere. Biopsy demonstrated diffuse large B-cell lymphoma (**d**). The tumor formed a large destructive mass and is composed of sheets of atypical B cells

On MRI, focal lesions are hypointense on T1 weighted images and hyperintense on T2 weighted images. Diffusion weighted imaging (DWI) and apparent diffusion coefficient (ADC) are measures of Brownian motion of water molecules in a particular tissue voxel. Increased signal on DWI and decreased signal on ADC would indicate decreased diffusion of water or "restricted diffusion" within that volume of tissue. Primary hepatic lymphoma typically demonstrates marked diffusion restriction with signal on ADC mapping typically lower than most other benign and malignant hepatic lesions. In the arterial and portal venous phases, the lesions typically demonstrate heterogenous, but predominantly decreased enhancement compared to the surrounding hepatic parenchyma. In the hepatobiliary phase, however, hepatic lymphoma is markedly and homogenously hypointense [55].

Positron emission tomography with flourine-18-fluoro-2-deoxyglucose is often used to assess distant disease. Increased disease activity often correlates with increased radiotracer uptake (Fig. 8.3c) [56].

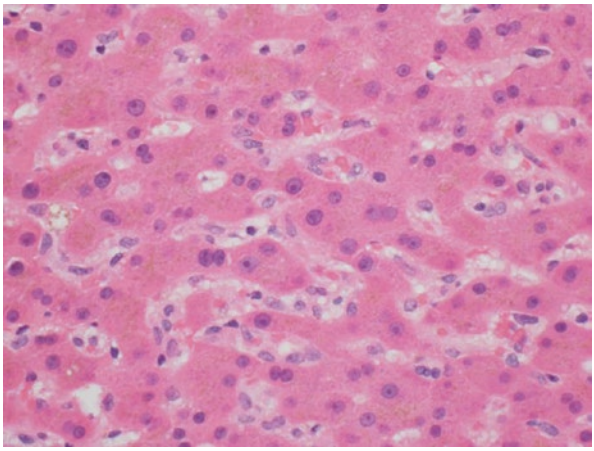

Fig. 8.4 Hepatosplenic T-cell lymphoma. Biopsy specimen showing sinusoids with a subtle infiltrate of atypical T cells

Pathology

Lymphomas that originate from any site in the body can eventually spread to the liver, and most lymphomas involving the liver are not primary to the liver. The majority of primary hepatic lymphomas are non-Hodgkin lymphoma, with about two-thirds being first diagnosed at liver biopsy [57]. The most common primary lymphomas of the liver are diffuse large B-cell lymphoma, which comprise approximately 75% of cases, and marginal zone lymphoma, which accounts for approximately 20% of cases [36, 58].

The major known risk factors for diffuse large B cell lymphoma of the liver are chronic hepatitis C and immunosuppression [59]. Diffuse large B-cell lymphomas are composed of sheets of atypical B cells that are more than twice the size of normal lymphocytes. Most diffuse large B cell lymphomas are mass-forming lesions associated with destruction of the normal liver architecture (Fig. 8.3d). They are diagnosed and further subtyped using immunostains and fluorescence in situ hybridization (FISH). The major known risk factors for primary marginal zone lymphomas of the liver are primary biliary cirrhosis, autoimmune hepatitis, and chronic hepatitis B and C [36]. Lymphoepithelial lesions involving the bile ducts are common but are neither sensitive nor specific for the diagnosis of lymphoma.

Most patients with hepatosplenic T-cell lymphoma are men, with a median age at diagnosis of about 35 years. This lymphoma predominately involves the hepatic sinusoids (Fig. 8.4), without forming a mass lesion. The tumor cells show subtle enlargement and atypia in comparison to normal lymphocytes.

Treatment modalities include chemotherapy, radiation therapy, and perhaps surgery. Surgical resection may be attempted if disease is localized or for debulking prior to chemotherapy [47, 60]. Chemotherapy or chemotherapy with radiotherapy is often utilized with varying degrees of success [29, 47, 61, 62]. The overall prognosis is poor with reported median survival rates of 3–124 months [47].

Primary Hepatic Neuroendocrine Neoplasm

Neuroendocrine neoplasms arise from neuroendocrine cells in the endocrine tissues, which demonstrate various characteristics depending on the hormonal profile of the cell [63–66]. The classification is based on tumor grade using a system developed by the World Health Organization, which was most recently updated in 2010. The system differentiates neuroendocrine neoplasms into well-differentiated, consisting of low grade and intermediate grade neoplasms, and poorly differentiated, consisting of high-grade neoplasms. Grading is based on mitotic count and Ki-67 Index [67].

Most neuroendocrine tumors develop in the gastroenteropancreatic system followed by the bronchopulmonary system. These areas account for 84% of neuroendocrine tumors. Primary hepatic neuroendocrine neoplasms (PHNEN) are rare; however, their incidence is increasing [68–72]. PHNEN are more common in male patients and in the fifth or sixth decade [73]. There is no documented relationship to underlying liver disease [74].

Presenting symptoms include right upper quadrant pain, fatigue, and weight loss. Carcinoid syndrome can occur but is rare [69]. Laboratory tests such as a 24-hour urine collection demonstrate high 5-hydroxyindoleacetic acid [75]. Serum chromogranin A levels may be elevated with good sensitivity and specificity levels [76]. Tumor markers such as carcinoembryonic antigen, CA19-9, and alpha-fetoprotein may also be elevated; however, their specificity is poor.

Imaging

Imaging demonstrates a focal mass or masses typically in the right liver which vary in appearance depending on histologic grade [74]. Lesions on ultrasound can be variable ranging from solid hypoechoic masses to heterogeneous (Fig. 8.5a) or hyperechoic masses [74]. Low-grade PHNENs typically demonstrate a single mass on CT and MR imaging. On CT, the lesions are homogenously hypoattenuating with enhancement in the arterial phase post administration of contrast. Necrosis, hemorrhage, or calcification are infrequently present [74, 77]. Low-grade PHNENs on MRI are low signal intensity on T1 weighted sequences and high signal on T2 weighted sequences, with homogeneous arterial phase hyperenhancement on postcontrast images. On delayed postcontrast sequences, an enhancing capsule is commonly seen [77].

Intermediate grade PHNENs on CT are more heterogeneous with necrotic change and peripheral nodular enhancement on postcontrast images (Fig. 8.5b, c). MRI also demonstrates heterogeneity on T1 and T2 weighted sequences with peripheral nodular enhancement (Fig. 8.5d–i).

High-grade PHNEN lesions demonstrate further progression in heterogeneity on CT and MR imaging with peripheral nodular enhancement [74, 77]. MRI

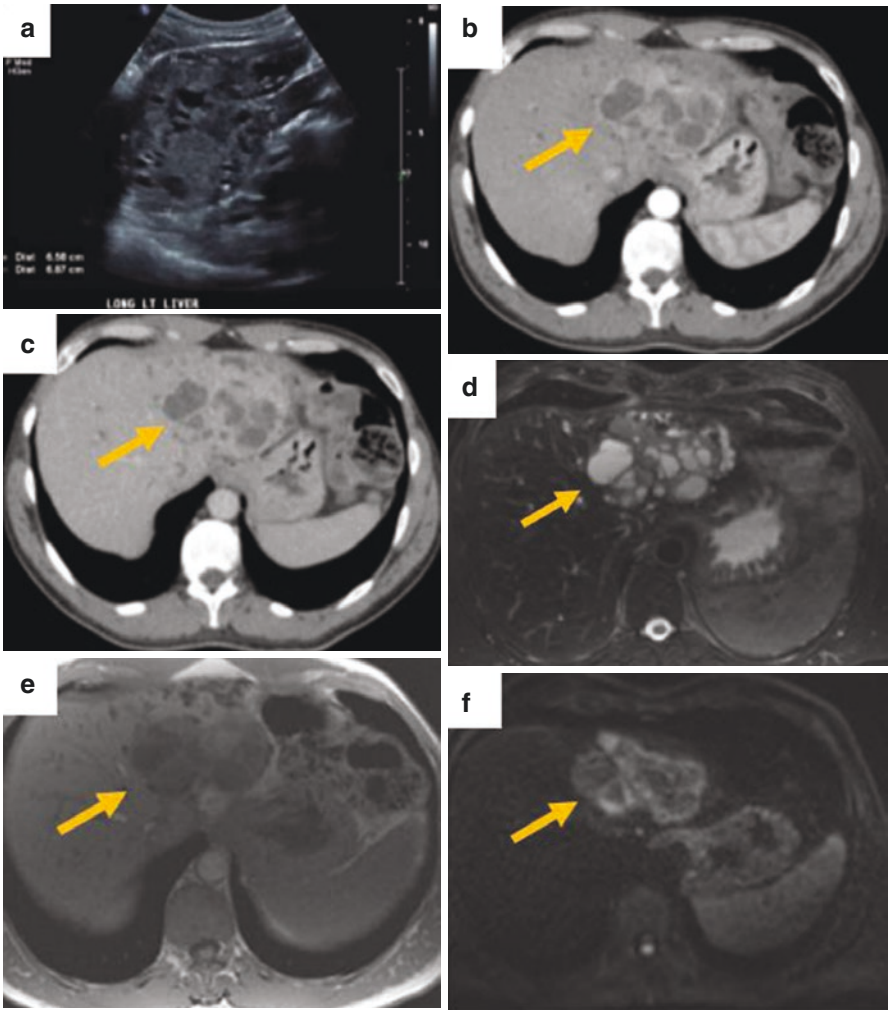

Fig. 8.5 Primary hepatic neuroendocrine neoplasm in a 44-year-old male presenting with abdominal pain and jaundice. Ultrasound (**a**) demonstrates a well-defined mass, predominantly isoechoic to surrounding hepatic parenchyma with multiple internal cystic areas. Contrast-enhanced CT demonstrates arterial phase hyperenhancement of the solid regions (**b**) which become isoattenuating on portal venous phase imaging (**c**). MRI demonstrates a heterogeneous mass in the left liver on T2 weighted sequences with a multiloculated cystic component (**d**). This was predominantly of low signal on T1 weighted sequences (**e**) with evidence of restricted diffusion (**f**). Postcontrast images with a hepatocyte specific contrast agent demonstrates early contrast enhancement of the solid areas on arterial phase (**g**), which persists on portal venous phase (**h**). There is no residual uptake on hepatobiliary phase images (**i**). 111 In-pentetreotide SPECT CT (**j**) demonstrates radiotracer uptake correlating to the mass on other imaging. There was no evidence of disseminated disease. Surgical resection (**k**) demonstrated a single 10.5 × 9.4 × 4.4 cm tan-red mass growing within the intrahepatic ducts. Pathology demonstrated a well-differentiated neuroendocrine tumor, WHO grade 2, involving the liver and bile ducts

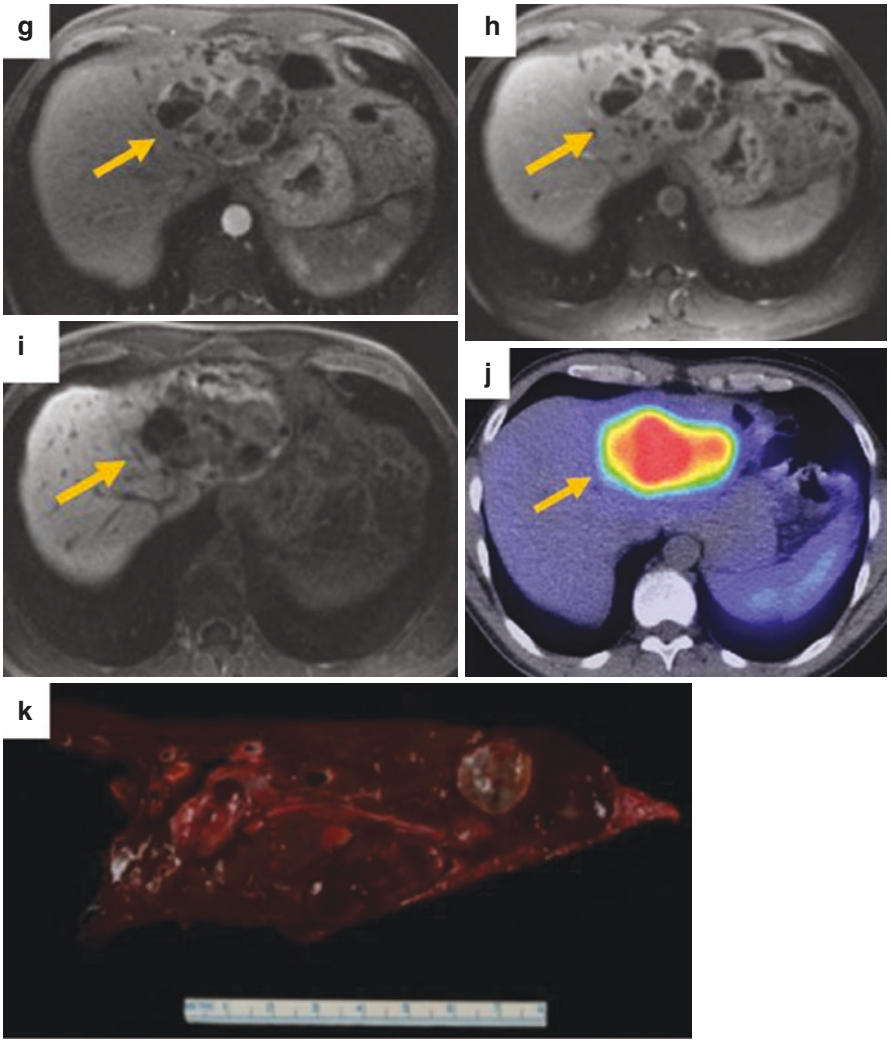

Fig. 8.5 (continued)

demonstrates increased necrosis and hemorrhagic change with progressive restricted diffusion and decreasing mean ADC values (Fig. 8.5f) [77].

Multiple radiopharmaceuticals have been employed in the detection of neuroendocrine neoplasms. Scintigraphy using ^{111}In-pentetreotide or octreotide scanning has demonstrated a sensitivity of 90% and specificity of 83% (Fig. 8.5j) [78, 79]. Positron emission tomography (PET)/CT with gallium-68 labeled somatostatin analogs has improved diagnostic performance with 68 Ga-DOTATATE and 68Ga-DOTATOC demonstrating sensitivities of 96% and 93%, respectively, and

specificities of 100% and 85%, respectively [80]. PET/CT is now the preferred functional imaging study for neuroendocrine neoplasms.

Pathology

It is very difficult to use pathological techniques to prove that a neuroendocrine tumor is primary to the liver, as there are no morphological, immunostain, or molecular findings that indicate a neuroendocrine tumor is likely to be primary to the liver. Thus, the final diagnosis requires (1) establishing that the tumor in the liver is a neuroendocrine tumor by morphology and immunostain findings and (2) ruling out another primary site by imaging findings, which tends to be challenging.

Treatment depends on presentation. The role of chemotherapy is limited [71]. Curative resection is possible for a single mass. Liver transplant is also possible for liver-confined disease [71, 81, 82]. Transcatheter arterial embolization can provide excellent outcomes for unresectable tumors, given the sensitivity of neuroendocrine neoplasms to alteration in blood flow [83]. Percutaneous ablation and somatostatin analogs may also be utilized [84–86]. The theranostic application of Lutetium-177 has recently been employed with promising results in advanced disease [87–89].

Desmoplastic Small Round Cell Tumor

Desmoplastic small round cell tumors (DSRCT) are rare tumors of young adults first described in 1989 [90]. They belong to a family of small round blue cell tumors with other malignancies such as non-Hodgkin's lymphoma, rhabdomyosarcoma, Ewing sarcoma, Wilms' tumor, poorly differentiated synovial cell sarcoma, small cell osteosarcoma, and neuroectodermal tumor. They are most commonly present in males with a ratio to females of approximately 5 to 1. The mean age at presentation is 22 years with a mean survival time of less than 3 years [91–93].

DSRCT most commonly originates in the mesothelium of the abdomen, involving the omentum and peritoneum. Organ involvement including the liver and lungs is infrequent and likely represents metastatic disease [94]. Patients present with abdominal mass, abdominal pain, and weight loss most commonly, with symptoms such as diaphoresis, back pain, and lethargy [95].

Imaging

Imaging commonly demonstrates a large intra-abdominal mass involving the peritoneum. Hepatic involvement is often associated with a retrovesical or rectouterine space mass in approximately 85% of patients [96]. Hepatic masses are

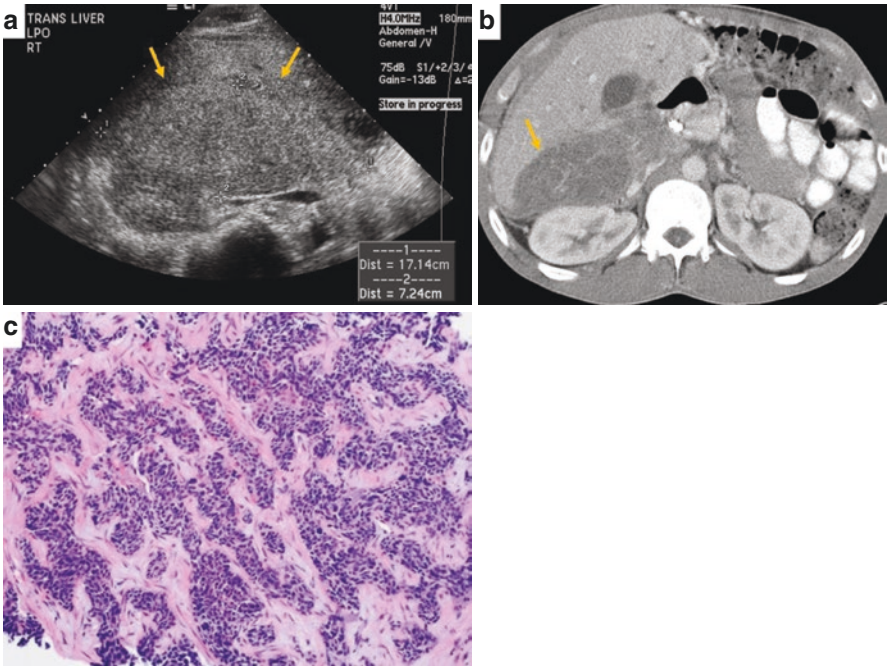

Fig. 8.6 Desmoplastic round cell tumor in a 24-year-old male presenting with abdominal pain, clay colored stools, dark urine, abdominal distension, and weight loss. Ultrasound demonstrates a subtle, slightly hyperechoic mass in the right liver (**a**). On contrast-enhanced CT (**b**), this mass was hypoattenuating compared to the surrounding liver and was compressing the common bile duct, with the requirement of stent placement. Biopsy demonstrated small, round, and blue tumor cells growing in trabeculae, with a background desmoplastic response (**c**)

heterogeneously hypoattenuating on contrast-enhanced CT (Figs. 8.6 and 8.7) [95, 97]. MRI demonstrates lesions of high signal intensity on T2 weighted sequences and low signal intensity on T1 weighted images. Heterogenous enhancement is seen post administration of gadolinium. Areas of internal hemorrhage or necrosis may be present [95, 98].

Pathology

DSRCT are histologically primitive tumors composed of small round blue cells that elicit a desmoplastic response (Fig. 8.6c). The tumor cells are uniform in appearance and grow in cords and nests surrounded by fibrotic stroma. Other cytological changes can include spindled areas, signet ring-like cells, pseudorosette formation, and cystic degeneration [99]. The tumors are positive for keratin, a marker of epithelial differentiation, and desmin, a marker of rhabdoid differentiation [91]. Greater

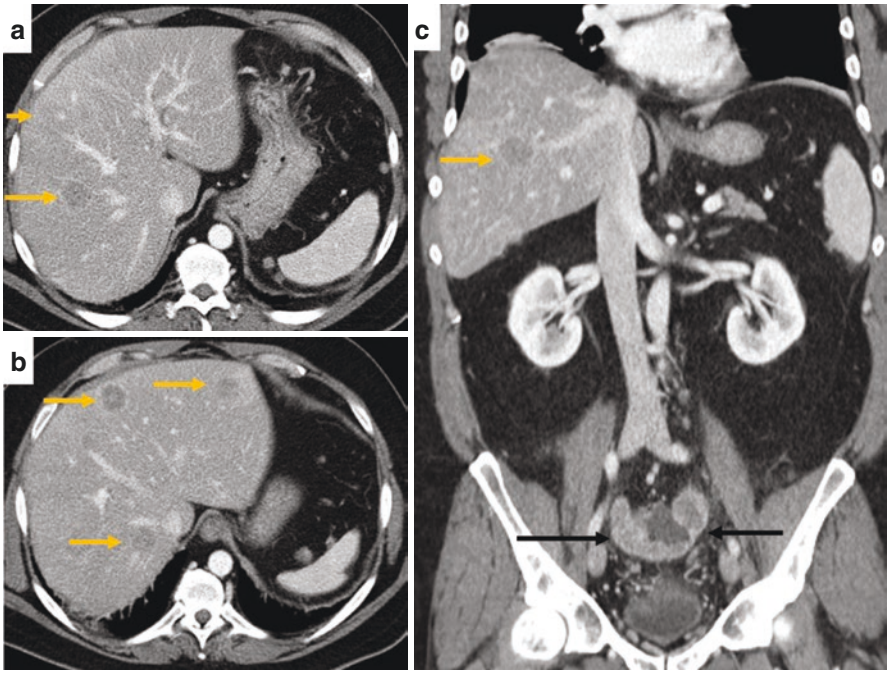

Fig. 8.7 A 39-year-old patient with biopsy-proven intra-abdominal desmoplastic small round cell tumor. Contrast-enhanced CT demonstrates heterogeneous but largely hypoattenuating masses in the left and right liver (**a**–**c**). Note peritoneal disease in the recto vesical space (black arrow). The disease continued to progress despite six cycles of chemotherapy and surgical debulking

than 95% of tumors have a translocation (t(11;22) (p13;q12)) resulting in a EWS-WT1 gene fusion [100], which can be detected by molecular methods.

Treatment involves surgical debulking, combination cytotoxic chemotherapy, and radiation therapy in varying proportions. Improved survival is demonstrated with radiotherapy and surgical resection for localized disease [96, 101].

Hepatoblastoma

Hepatoblastoma is the most common primary hepatic malignancy in children. It is still rare, however, with a prevalence of 10.5 cases per million in children less than 1 year old in the United States [102]. The rate is increasing in the US with a 4% increase reported between 1992 and 2004 [103]. There is a slight male preponderance and hepatoblastoma is associated with a number of genetic syndromes such as familial adenomatous polyposis, Beckwith–Wiedemann syndrome, and Trisomy 18 [104–107]. The prognosis is generally poor compared to other pediatric cancers, with an overall 5-year survival in the US of 74% [102].

Patients generally present with an enlarging abdominal mass with weight loss and decreased appetite. Rarely, excess β-human chorionic gonadotropin may lead to precocious puberty [108]. The serum alpha-fetoprotein (AFP) is generally elevated and is an important clinical marker. Hepatoblastoma without a raised AFP carries a worse prognosis and is often associated with small cell undifferentiated morphology [109].

Imaging

Imaging typically demonstrates a large well-defined mass most commonly in the right lobe of the liver [110]. Ultrasound demonstrates an echogenic mass which increases in heterogeneity as tumor size increases. Increased vascularity may be appreciated on color Doppler imaging [111, 112]. On contrast-enhanced CT, the mass is heterogeneous and largely hypoattenuating with areas of necrosis visualized. Calcifications are visualized in up to 50% (Fig. 8.8a) [110, 113]. Hepatoblastomas are predominantly of low signal on T1 weighted images and high signal on T2 weighted sequences with heterogeneity depending on the extent of hemorrhage and necrosis. Heterogenous enhancement post administration of gadolinium is also most commonly seen (Fig. 8.8d, e) and a variable degree of washout may be seen in the delayed phases. MRI may also allow for better appreciation of hepatic segmental involvement leading to improved staging [110]. A large heterogeneous liver mass with heterogeneous enhancement occurring in a child along with a raised serum AFP is characteristic of hepatoblastoma.

Pathology

Hepatoblastomas are epithelial malignancies of infants and children. An epithelial component is required, but the tumors can be composed entirely of epithelial cells or can have both epithelial and mesenchymal components. Hepatoblastomas are further classified into seven subtypes based on the extent of hepatic differentiation and, for cases with fetal growth patterns, the amount of cytological atypia and mitotic count: small cell undifferentiated, embryonal, pure fetal with low mitotic activity, fetal with mitotic activity, pleomorphic fetal, macrotrabecular, and cholangioblastic [114]. Currently, the most clinically important patterns are the small cell undifferentiated pattern, because it requires more aggressive chemotherapy and the pure fetal pattern with low mitotic activity (Fig. 8.8f), because it is cured with complete excision and does not require chemotherapy.

There can be diagnostic challenges at both ends of the tumor differentiation spectrum. Small cell undifferentiated hepatoblastoma can mimic other small round blue cell tumors on small biopsies and additional stains are usually needed to confirm the diagnosis and exclude other entities in the differential. On the other hand,

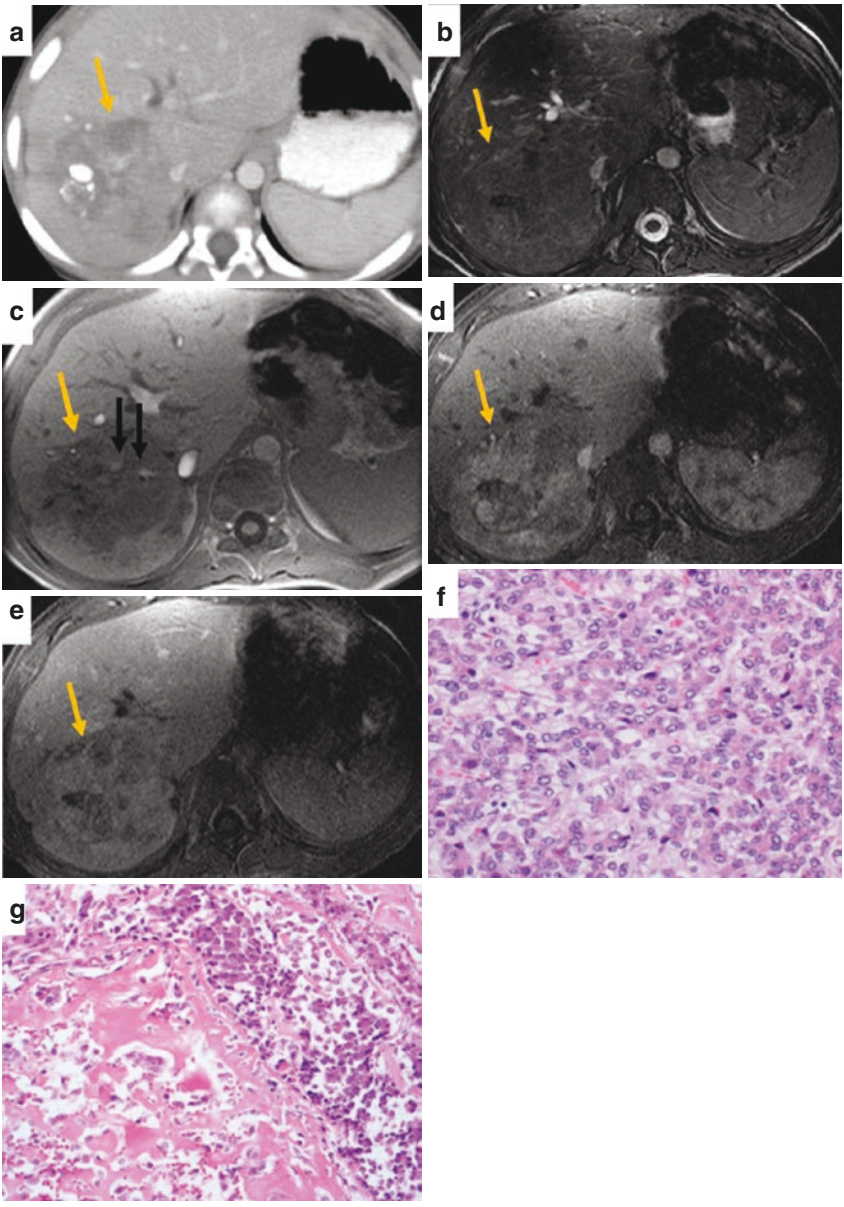

Fig. 8.8 Hepatoblastoma in a 28-month-old child presenting with precocious puberty. Abdominal distension with enlarged liver noted on clinical examination. Contrast-enhanced CT demonstrates an ill-defined, heterogeneous mass in the right liver with coarse calcification (**a**). MRI demonstrates an ill-defined mass in the right liver, isointense to surrounding liver on T2 weighted images (**b**), and hypointense on T1 weighted sequences (**c**). Note areas of high T1 signal consistent with hemorrhagic change (black arrows). Heterogeneous enhancement noted on arterial and portal venous phase postcontrast-enhanced images (**d**, **e**). The mass was biopsied with mixed epithelial and mesenchymal hepatoblastoma diagnosed. In the fetal morphology, the tumor cells resemble hepatocytes found in the fetal liver (**f**). In the mesenchymal component osteoid material is present (**g**)

tumors with a pure fetal growth pattern can closely resemble conventional hepatocellular carcinoma. There are no molecular or immunostain findings that have high value for distinguishing these two possibilities, so the diagnosis is made on morphological and clinical findings. Underlying liver disease and/or advanced fibrosis strongly favor conventional hepatocellular carcinoma. Embryonal or mesenchymal components strongly favor hepatoblastoma. Mesenchymal components are found in up to 40% of cases. The mesenchymal component usually consists of nondescript spindled cells, but osteoid material (Fig. 8.8g), skeletal muscle, or cartilage can also be found.

Staging by imaging is based on the PRETEXT system and is described with reference to involvement of the mass with hepatic segments. There is close correlation to prognosis [115]. Surgical resection is the cornerstone of treatment. Approximately 30% of tumors are resectable on presentation which increases significantly with neoadjuvant chemotherapy [116, 117].

Mesenchymal Hamartoma

Mesenchymal hamartoma is an uncommon tumor of the liver and is composed of loosely organized mesenchymal tissue, bile ducts, and hepatic parenchyma. Unencapsulated fluid accumulates giving the characteristic cystic appearance [118].

The lesion is most commonly seen in patients less than 2 years old, with a male preponderance [118]. Patients commonly present with an asymptomatic enlarging mass. Other symptoms such as vomiting, fever, diarrhea, respiratory distress, and weight loss are less common [118]. The prognosis is generally good with rare fatal complications reported secondary to fetal hydrops, respiratory distress, compression of vital vessels, and congestive cardiac failure secondary to arteriovenous shunting within the mass.

Laboratory tests may demonstrate an elevated serum AFP; however, liver function tests are usually normal.

Imaging

Imaging typically demonstrates a cystic lesion in the right liver with both solid and solid/cystic lesions rarely identified [119]. Sonography demonstrates a cystic mass with thick septations [120]. Rarely, a solid mass has been described (Fig. 8.9a) [121]. The mass is well defined and heterogeneous on noncontrast CT with heterogeneous enhancement of the solid components post administration of iodinated contrast (Fig. 8.9b, c) [120–122]. MRI demonstrates a multiloculated cystic mass with internal low signal on T1 weighted sequences and high signal on T2 weighted sequences (Fig. 8.9d–f). The signal may vary depending on the protein content of the fluid [123, 124].

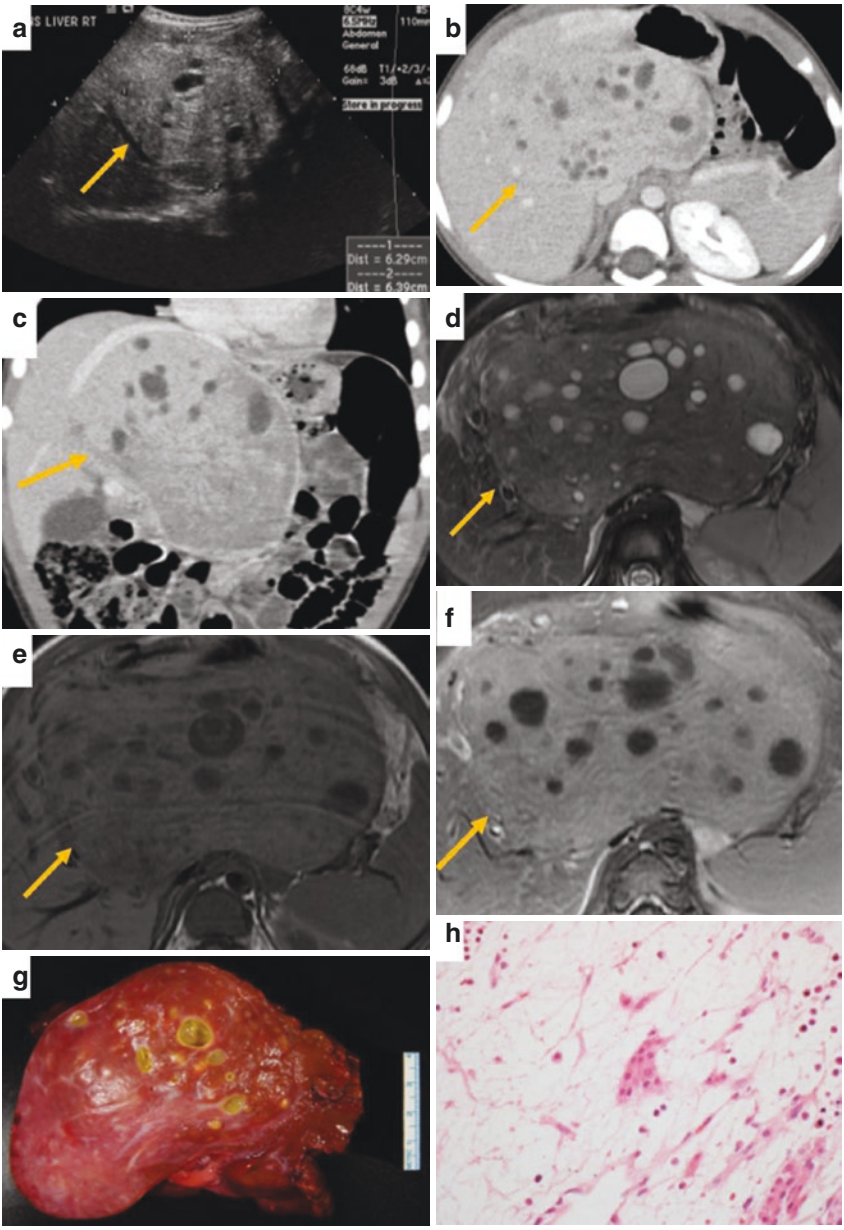

Fig. 8.9 Mesenchymal hamartoma of the liver in a 3-year-old child presenting with abdominal distension. Echogenic mass with cystic areas noted on US (**a**). Axial (**b**) and coronal (**c**) contrast-enhanced CT demonstrates heterogeneously enhancing mass, centered in the left liver with cystic areas. MRI demonstrates a slightly hyperintense, well-defined mass on T2 weighted sequences interspersed with cystic areas (**d**). Mass was slightly hypointense on T1 weighted sequences (**e**) with homogenous enhancement of the solid components (**f**). Extended left hepatectomy demonstrated mesenchymal hamartoma (**g**). The tumor is composed of loose, edematous spindle cells with rare small clusters of hepatocytes (**h**)

Pathology

Mesenchymal hamartomas are composed of loose, edematous mesenchymal tissue, often with cystic degeneration (Fig. 8.9g, h). The mesenchymal tissue contains cytologically bland spindled cells as well as occasional clusters of benign hepatocytes. Hyalinized portal tract-like areas can also be found, more commonly at the periphery of the tumor. In some cases, the bile ducts in the portal tract-like areas can show a ductal plate malformation pattern. Rarely, the bile ducts in these portal tract-like areas become dilated, forming a small biliary cyst.

Surgical resection is the predominant mode of therapy with improved survival in those where surgical resection is possible [119]. Marsupialization or even aspiration has been reported in unresectable cases [125].

Undifferentiated Embryonal Sarcoma of the Liver

Undifferentiated embryonal sarcoma of the liver describes a rare, highly malignant, undifferentiated mesenchymal neoplasm. It is the third most common hepatic malignancy in children with peak incidence between 6 and 10 years [126, 127]. The tumor is rare in adults with a female preponderance [128, 129].

Patients present with an enlarging abdominal mass. Abdominal pain may or may not be present. Features such as fever, decreased appetite, weight loss, vomiting, and diarrhea are less frequent [126, 130, 131]. Laboratory tests are not useful with liver function tests, tumor markers, and inflammatory markers typically within normal ranges. Cases have been reported of elevated aminotransferases, leukocytosis, increased erythrocyte sedimentation rate, and increased alpha-fetoprotein or CA-125 [126, 132, 133].

Imaging

Imaging typically presents a large, well-circumscribed mass in the liver. The sonographic appearance is variable. A complex cystic mass with multiple septations and mural nodularity is most commonly described with a solid echogenic lesion also possible [134]. CT and MRI demonstrate a well-defined mass with necrotic and hemorrhagic change to varying degrees. The lesion is hypoattenuating on noncontrast CT (Fig. 8.10a, b) with MRI demonstrating low signal on T1 weighted sequences and high signal on T2 weighted sequences. At times, the mass may resemble a cystic lesion due to the high water content of the myxoid stroma [134, 135]. Minimal enhancement is noted on early postcontrast phase imaging with subtle enhancement on delayed phases (Fig. 8.10c–f) [136].

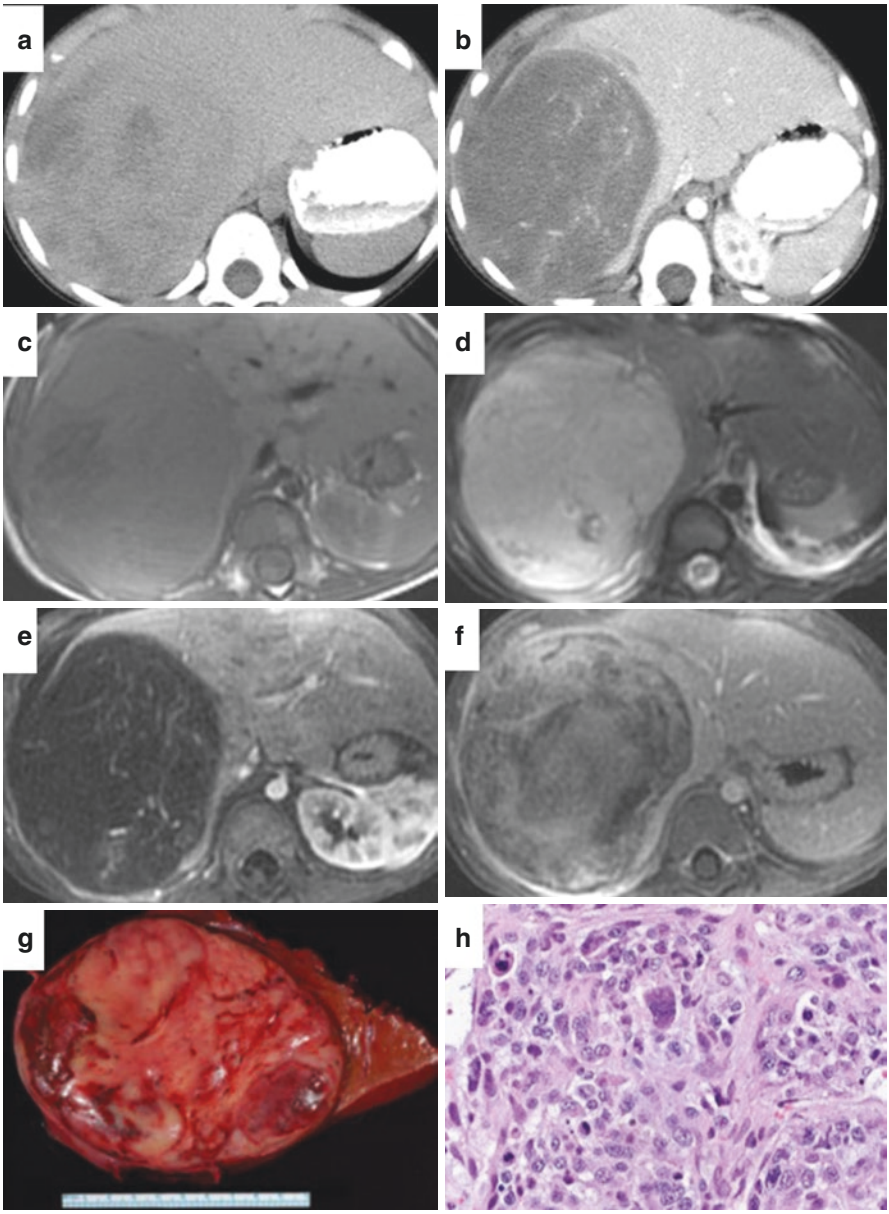

Fig. 8.10 Embryonal cell sarcoma of the liver. A 4-year-old boy with nonspecific abdominal pain progressing to fevers over 1 year. Non-contrast CT demonstrates a heterogeneous area in the right liver with ill-defined hypoattenuating areas (**a**). Contrast-enhanced CT demonstrates the mass to be well-defined and largely hypoattenuating (**b**), resembling a complex cyst. MRI demonstrates a well-defined mass, hypointense on T1 weighted sequences (**c**), and mildly hyperintense on T2 weighted sequences (**d**). The mass demonstrates minimal linear enhancement on arterial phase postcontrast sequences (**e**) which fills in on delayed sequences consistent with a solid mass (**f**). Resection demonstrates embryonal sarcoma (**g**). The tumor is composed of anaplastic spindled and epithelioid cells (**h**)

Pathology

Embryonal sarcomas are high-grade sarcomas with high cellularity and numerous anaplastic cells, frequently with giant cell transformation (Fig. 8.10h). Tumor cells often contain cytoplasmic hyaline globules, but this finding is neither highly sensitive nor specific. The stroma can vary from loose and myxoid to dense and collagenized. Embryonal sarcomas can arise from mesenchymal hamartomas, so some cases will have residual mesenchymal hamartomas at their edges.

Surgical resection is the treatment of choice in undifferentiated embryonal sarcoma. Survival is poor with a reported 37% 3-year survival in 1990 [137]. With improved multimodal treatment in the form of neoadjuvant chemotherapy and radiation therapy, more recent survival rates have improved to 70–100% over a follow-up period of 21–68 months [130, 138–140].

Hepatic Lymphangioma

Hepatic lymphangioma is a rare tumor characterized by cystic dilatation of lymphatic vessels in the hepatic parenchyma [141]. The mass is believed to develop secondary to congenital obstruction of the lymphatic system in the liver with resultant dilatation [141, 142]. Intra-abdominal lesions account for only 5% of all lymphangiomas [143]. Solitary hepatic lymphangiomas are rare with lesions usually occurring with other masses in multiple organs and occur predominantly in children or adolescents [144–146].

Patients are typically asymptomatic, with symptoms when present, usually nonspecific, such as abdominal pain, fever, nausea, and vomiting [147–149]. Laboratory tests such as liver function tests and tumor markers are typically negative [149–151].

Imaging

On ultrasound, masses are multiloculated cystic masses with echogenic debris. Hyperechoic lesions have also been described [152]. MRI demonstrates a heterogeneous mass, low signal intensity on T1 weighted images, and high signal on T2 weighted images. Septal enhancement can occur and may mimic a solid lesion in the microcystic variant [151, 153].

Pathology

Hepatic lymphangiomas consist of variably sized cyst-like spaces lined by benign endothelial cells. The cysts-like spaces often contain a thin proteinaceous fluid. In most cases, lymphangiomas are not isolated to the liver and there is systemic involvement, with similar lesions in the spleen, skeleton, and other organs.

Surgical resection is the treatment of choice with a complete cure possible [147]. Recurrence has been described post resection of lymphangiomas elsewhere at a rate of 0–27% for complete resection and 10–100% for incomplete resection [154]. Where complete resection is not possible, percutaneous ablation using alcohol and OK-432 has been described in lesions outside of the liver [155–157].

Lipoma

Lipomas are focal areas of mature fat cells surrounded by a thin fibrous capsule. They can occur anywhere throughout the body, most frequently in the subcutaneous tissues. Lipomas of the liver are very uncommon with only a small number of cases reported. The first description was an incidental finding on an autopsy study in 1970 [158].

Patients are typically asymptomatic at presentation [159–161]. Rarely, vague abdominal pain has been reported and is likely secondary to mass effect and stretching of the hepatic capsule [162].

Imaging

Ultrasound demonstrates a homogeneous, hyperechoic mass. It is typically solitary with a well-demarcated border and posterior acoustic enhancement. A phenomenon of apparent discontinuity of the diaphragm, secondary to refractive effects at the interface between the lipoma and normal hepatic tissue has been described [162]. Hepatic lipomas on CT are well-demarcated, homogenous, hypoattenuating masses with attenuation values less than −20 HU. The lesions do not enhance. If enhancement is present, it indicates the presence of an adenomatous or angiomatous component [123, 159, 163]. MRI demonstrates a hyperintense mass on T1 weighted sequences with signal reduction on out-of-phase imaging [159]. Imaging should follow retroperitoneal fat on all sequences [164].

Pathology

Lipomas are composed of mature adipose tissue. The adipocytes are uniform in size and without nuclear atypia. Rarely, they can be admixed with other benign soft tissue elements, such as fibrous tissue in fibroliopomas.

Lipomas are S100 positive and are negative for MDM2 amplification (MDM2 amplification is found in many well-differentiated liposarcomas). Before a diagnosis of lipoma is made, other tumors such as AML should also be excluded.

Malignant degeneration of lipoma to liposarcoma is exceedingly rare in lesions found elsewhere in the body and is never described in hepatic lipomas [165]. Imaging appearances should allow a diagnosis with no biopsy or surgery typically warranted [123].

References

1. Newman KD. Malignant liver tumors of children. Semin Pediatr Surg. 1992;1(2):145–51.
2. Folpe A. Neoplasms with perivascular epithelioid cell differentiation (PEComas). Lyon: IARC Press; 2002.
3. Petrolla AA, Xin W. Hepatic angiomyolipoma. Arch Pathol Lab Med. 2008;132(10):1679–82.
4. Ishak K. Mesenchymal tumors of the liver. New York: Wiley; 1976.
5. Jiang TA, Zhao QY, Chen MY, Wang LJ, Ao JY. Diagnostic analysis of hepatic angiomyolipoma. Hepatobiliary Pancreat Dis Int. 2005;4(1):152–5.
6. Tsui WM, Colombari R, Portmann BC, Bonetti F, Thung SN, Ferrell LD, et al. Hepatic angiomyolipoma: a clinicopathologic study of 30 cases and delineation of unusual morphologic variants. Am J Surg Pathol. 1999;23(1):34–48.
7. Terris B, Flejou JF, Picot R, Belghiti J, Henin D. Hepatic angiomyolipoma. A report of four cases with immunohistochemical and DNA-flow cytometric studies. Arch Pathol Lab Med. 1996;120(1):68–72.
8. Ren N, Qin LX, Tang ZY, Wu ZQ, Fan J. Diagnosis and treatment of hepatic angiomyolipoma in 26 cases. World J Gastroenterol. 2003;9(8):1856–8.
9. Nonomura A, Enomoto Y, Takeda M, Tamura T, Kasai T, Yosikawa T, et al. Invasive growth of hepatic angiomyolipoma; a hitherto unreported ominous histological feature. Histopathology. 2006;48(7):831–5.
10. Wang SN, Tsai KB, Lee KT. Hepatic angiomyolipoma with trace amounts of fat: a case report and literature review. J Clin Pathol. 2006;59(11):1196–9.
11. Xu AM, Zhang SH, Zheng JM, Zheng WQ, Wu MC. Pathological and molecular analysis of sporadic hepatic angiomyolipoma. Hum Pathol. 2006;37(6):735–41.
12. Prasad SR, Wang H, Rosas H, Menias CO, Narra VR, Middleton WD, et al. Fat-containing lesions of the liver: radiologic-pathologic correlation. Radiographics. 2005;25(2):321–31.
13. Dabora SL, Jozwiak S, Franz DN, Roberts PS, Nieto A, Chung J, et al. Mutational analysis in a cohort of 224 tuberous sclerosis patients indicates increased severity of TSC2, compared with TSC1, disease in multiple organs. Am J Hum Genet. 2001;68(1):64–80.
14. Black ME, Hedgire SS, Camposano S, Paul E, Harisinghani M, Thiele EA. Hepatic manifestations of tuberous sclerosis complex: a genotypic and phenotypic analysis. Clin Genet. 2012;82(6):552–7.
15. Cha I, Cartwright D, Guis M, Miller TR, Ferrell LD. Angiomyolipoma of the liver in fine-needle aspiration biopsies: its distinction from hepatocellular carcinoma. Cancer. 1999;87(1):25–30.

16. Cai PQ, Wu YP, Xie CM, Zhang WD, Han R, Wu PH. Hepatic angiomyolipoma: CT and MR imaging findings with clinical-pathologic comparison. Abdom Imaging. 2013;38(3):482–9.
17. Wang Z, Xu HX, Xie XY, Xie XH, Kuang M, Xu ZF, et al. Imaging features of hepatic angiomyolipomas on real-time contrast-enhanced ultrasound. Br J Radiol. 2010;83(989):411–8.
18. Musante F, Derchi LE, Zappasodi F, Bazzocchi M, Riviezzo GC, Banderali A, et al. Myelolipoma of the adrenal gland: sonographic and CT features. AJR Am J Roentgenol. 1988;151(5):961–4.
19. Ahmadi T, Itai Y, Takahashi M, Onaya H, Kobayashi T, Tanaka YO, et al. Angiomyolipoma of the liver: significance of CT and MR dynamic study. Abdom Imaging. 1998;23(5):520–6.
20. Yan F, Zeng M, Zhou K, Shi W, Zheng W, Da R, et al. Hepatic angiomyolipoma: various appearances on two-phase contrast scanning of spiral CT. Eur J Radiol. 2002;41(1):12–8.
21. Nonomura A, Minato H, Kurumaya H. Angiomyolipoma predominantly composed of smooth muscle cells: problems in histological diagnosis. Histopathology. 1998;33(1):20–7.
22. Dalle I, Sciot R, de Vos R, Aerts R, van Damme B, Desmet V, et al. Malignant angiomyolipoma of the liver: a hitherto unreported variant. Histopathology. 2000;36(5):443–50.
23. Nguyen TT, Gorman B, Shields D, Goodman Z. Malignant hepatic angiomyolipoma: report of a case and review of literature. Am J Surg Pathol. 2008;32(5):793–8.
24. Deng YF, Lin Q, Zhang SH, Ling YM, He JK, Chen XF. Malignant angiomyolipoma in the liver: a case report with pathological and molecular analysis. Pathol Res Pract. 2008;204(12):911–8.
25. Makhlouf HR, Remotti HE, Ishak KG. Expression of KIT (CD117) in angiomyolipoma. Am J Surg Pathol. 2002;26(4):493–7.
26. Yang CY, Ho MC, Jeng YM, Hu RH, Wu YM, Lee PH. Management of Hepatic Angiomyolipoma. J Gastrointest Surg. 2007;11(4):452–7.
27. Ata AA, Kamel IA. Primary reticulum cell sarcoma of the liver. A case report. J Egypt Med Assoc. 1965;48(7):514–21.
28. Elsayes KM, Menias CO, Willatt JM, Pandya A, Wiggins M, Platt J. Primary hepatic lymphoma: imaging findings. J Med Imaging Radiat Oncol. 2009;53(4):373–9.
29. Noronha V, Shafi NQ, Obando JA, Kummar S. Primary non-Hodgkin's lymphoma of the liver. Crit Rev Oncol Hematol. 2005;53(3):199–207.
30. Tomasian A, Sandrasegaran K, Elsayes KM, Shanbhogue A, Shaaban A, Menias CO. Hematologic malignancies of the liver: spectrum of disease. Radiographics. 2015;35(1):71–86.
31. Lisker-Melman M, Pittaluga S, Pluda JM, Kleiner DE, Thompson P, Martin P, et al. Primary lymphoma of the liver in a patient with acquired immune deficiency syndrome and chronic hepatitis B. Am J Gastroenterol. 1989;84(11):1445–8.
32. Mohan C, Alurkar SS, Sharma OP, Advani SH. Primary liver lymphoma: a diagnostic dilemma. AJR Am J Roentgenol. 1991;157(2):413.
33. Mohamed M, Fernando R. Diagnostic and therapeutic quandaries in a patient with primary hepatic lymphoma and concurrent hepatitis C infection. Indian J Hematol Blood Transfus. 2014;30(Suppl 1):394–7.
34. Sekiguchi Y, Yoshikawa H, Shimada A, Imai H, Wakabayashi M, Sugimoto K, et al. Primary hepatic circumscribed Burkitt's lymphoma that developed after acute hepatitis B: report of a case with a review of the literature. J Clin Exp Hematop. 2013;53(2):167–73.
35. Somaglino C, Pramaggiore P, Polastri R. Primary hepatic lymphoma in a patient with chronic hepatitis B and C infection: diagnostic pitfalls and therapeutic challenge. Updat Surg. 2014;66(1):89–90.
36. Kikuma K, Watanabe J, Oshiro Y, Shimogama T, Honda Y, Okamura S, et al. Etiological factors in primary hepatic B-cell lymphoma. Virchows Arch. 2012;460(4):379–87.
37. Nakayama S, Yokote T, Kobayashi K, Hirata Y, Akioka T, Miyoshi T, et al. Primary hepatic MALT lymphoma associated with primary biliary cirrhosis. Leuk Res. 2010;34:e17–20.
38. Sato S, Masuda T, Oikawa H, Satoh T, Suzuki Y, Takikawa Y, et al. Primary hepatic lymphoma associated with primary biliary cirrhosis. Am J Gastroenterol. 1999;94(6):1669–73.

39. Chowdhary VR, Crowson CS, Poterucha JJ, Moder KG. Liver involvement in systemic lupus erythematosus: case review of 40 patients. J Rheumatol. 2008;35(11):2159–64.
40. Sutton E, Malatjalian D, Hayne OA, Hanly JG. Liver lymphoma in systemic lupus erythematosus. J Rheumatol. 1989;16(12):1584–8.
41. Honda H, Franken EA Jr, Barloon TJ, Smith JL. Hepatic lymphoma in cyclosporine-treated transplant recipients: sonographic and CT findings. AJR Am J Roentgenol. 1989;152(3):501–3.
42. Palazzo JP, Lundquist K, Mitchell D, Mittal KR, Hann HW, Munoz S, et al. Rapid development of lymphoma following liver transplantation in a recipient with hepatitis B and primary hemochromatosis. Am J Gastroenterol. 1993;88(1):102–4.
43. Rostaing L, Suc B, Fourtanier G, Baron E, Lloveras JJ, Durand D. Liver B cell lymphoma after liver transplantation. Transplant Proc. 1995;27(2):1781–2.
44. Caccamo D, Pervez NK, Marchevsky A. Primary lymphoma of the liver in the acquired immunodeficiency syndrome. Arch Pathol Lab Med. 1986;110(6):553–5.
45. Ugurluer G, Miller RC, Li Y, Thariat J, Ghadjar P, Schick U, et al. Primary hepatic lymphoma: a retrospective, multicenter rare cancer network study. Rare Tumors. 2016;8(3):6502.
46. Lei KI. Primary non-Hodgkin's lymphoma of the liver. Leuk Lymphoma. 1998;29(3–4):293–9.
47. Avlonitis VS, Linos D. Primary hepatic lymphoma: a review. Eur J Surg. 1999;165(8):725–9.
48. Page RD, Romaguera JE, Osborne B, Medeiros LJ, Rodriguez J, North L, et al. Primary hepatic lymphoma: favorable outcome after combination chemotherapy. Cancer. 2001;92(8):2023–9.
49. Seymour JF, Gagel RF, Hagemeister FB, Dimopoulos MA, Cabanillas F. Calcitriol production in hypercalcemic and normocalcemic patients with non-Hodgkin lymphoma. Ann Intern Med. 1994;121(9):633–40.
50. Maher MM, McDermott SR, Fenlon HM, Conroy D, O'Keane JC, Carney DN, et al. Imaging of primary non-Hodgkin's lymphoma of the liver. Clin Radiol. 2001;56(4):295–301.
51. Kelekis NL, Semelka RC, Siegelman ES, Ascher SM, Outwater EK, Woosley JT, et al. Focal hepatic lymphoma: magnetic resonance demonstration using current techniques including gadolinium enhancement. Magn Reson Imaging. 1997;15(6):625–36.
52. Emile JF, Azoulay D, Gornet JM, Lopes G, Delvart V, Samuel D, et al. Primary non-Hodgkin's lymphomas of the liver with nodular and diffuse infiltration patterns have different prognoses. Ann Oncol. 2001;12(7):1005–10.
53. Gazelle GS, Lee MJ, Hahn PF, Goldberg MA, Rafaat N, Mueller PR. US, CT, and MRI of primary and secondary liver lymphoma. J Comput Assist Tomogr. 1994;18(3):412–5.
54. Rajesh S, Bansal K, Sureka B, Patidar Y, Bihari C, Arora A. The imaging conundrum of hepatic lymphoma revisited. Insights Imaging. 2015;6(6):679–92.
55. Colagrande S, Calistri L, Grazzini G, Nardi C, Busoni S, Morana G, et al. MRI features of primary hepatic lymphoma. Abdom Radiol (NY). 2018;49:2277.
56. Goldberg MA, Lee MJ, Fischman AJ, Mueller PR, Alpert NM, Thrall JH. Fluorodeoxyglucose PET of abdominal and pelvic neoplasms: potential role in oncologic imaging. Radiographics. 1993;13(5):1047–62.
57. Loddenkemper C, Longerich T, Hummel M, Ernestus K, Anagnostopoulos I, Dienes HP, et al. Frequency and diagnostic patterns of lymphomas in liver biopsies with respect to the WHO classification. Virchows Arch. 2007;450(5):493–502.
58. Swadley MJ, Deliu M, Mosunjac MB, Gunthel CJ, Nguyen ML, Hanley KZ. Primary and secondary hepatic lymphomas diagnosed by image-guided fine-needle aspiration: a retrospective study of clinical and cytomorphologic findings. Am J Clin Pathol. 2014;141(1):119–27.
59. Bronowicki JP, Bineau C, Feugier P, Hermine O, Brousse N, Oberti F, et al. Primary lymphoma of the liver: clinical-pathological features and relationship with HCV infection in French patients. Hepatology. 2003;37(4):781–7.
60. Scoazec JY, Degott C, Brousse N, Barge J, Molas G, Potet F, et al. Non-Hodgkin's lymphoma presenting as a primary tumor of the liver: presentation, diagnosis and outcome in eight patients. Hepatology. 1991;13(5):870–5.
61. Chowla A, Malhi-Chowla N, Chidambaram A, Surick B. Primary hepatic lymphoma in hepatitis C: case report and review of the literature. Am Surg. 1999;65(9):881–3.

62. Coiffier B, Lepage E, Briere J, Herbrecht R, Tilly H, Bouabdallah R, et al. CHOP chemotherapy plus rituximab compared with CHOP alone in elderly patients with diffuse large-B-cell lymphoma. N Engl J Med. 2002;346(4):235–42.
63. Cho MY, Kim JM, Sohn JH, Kim MJ, Kim KM, Kim WH, et al. Current trends of the incidence and pathological diagnosis of Gastroenteropancreatic Neuroendocrine Tumors (GEP-NETs) in Korea 2000-2009: multicenter study. Cancer Res Treat. 2012;44(3):157–65.
64. Klimstra DS, Modlin IR, Coppola D, Lloyd RV, Suster S. The pathologic classification of neuroendocrine tumors: a review of nomenclature, grading, and staging systems. Pancreas. 2010;39(6):707–12.
65. Kloppel G, Perren A, Heitz PU. The gastroenteropancreatic neuroendocrine cell system and its tumors: the WHO classification. Ann N Y Acad Sci. 2004;1014:13–27.
66. Kloppel G, Couvelard A, Perren A, Komminoth P, McNicol AM, Nilsson O, et al. ENETS consensus guidelines for the standards of care in neuroendocrine tumors: towards a standardized approach to the diagnosis of gastroenteropancreatic neuroendocrine tumors and their prognostic stratification. Neuroendocrinology. 2009;90(2):162–6.
67. Rindi G, Arnold R, Bosman F. Nomenclature and classification of neuroendocrine neoplasms of the digestive system. In: Bosman F, Carneiro F, Hruban R, Theise N, editors. WHO classification of tumors of the digestive system. Lyon: IARC; 2010.
68. Iwao M, Nakamuta M, Enjoji M, Kubo H, Fukutomi T, Tanabe Y, et al. Primary hepatic carcinoid tumor: case report and review of 53 cases. Med Sci Monit. 2001;7(4):746–50.
69. Donadon M, Torzilli G, Palmisano A, Del Fabbro D, Panizzo V, Maggioni M, et al. Liver resection for primary hepatic neuroendocrine tumours: report of three cases and review of the literature. Eur J Surg Oncol. 2006;32(3):325–8.
70. Huang YQ, Xu F, Yang JM, Huang B. Primary hepatic neuroendocrine carcinoma: clinical analysis of 11 cases. Hepatobiliary Pancreat Dis Int. 2010;9(1):44–8.
71. Park CH, Chung JW, Jang SJ, Chung MJ, Bang S, Park SW, et al. Clinical features and outcomes of primary hepatic neuroendocrine carcinomas. J Gastroenterol Hepatol. 2012;27(8):1306–11.
72. Yao JC, Hassan M, Phan A, Dagohoy C, Leary C, Mares JE, et al. One hundred years after "carcinoid": epidemiology of and prognostic factors for neuroendocrine tumors in 35,825 cases in the United States. J Clin Oncol. 2008;26(18):3063–72.
73. Oberg K, Astrup L, Eriksson B, Falkmer SE, Falkmer UG, Gustafsen J, et al. Guidelines for the management of gastroenteropancreatic neuroendocrine tumours (including bronchopulmonary and thymic neoplasms). Part I-general overview. Acta Oncol. 2004;43(7):617–25.
74. Yang K, Cheng YS, Yang JJ, Jiang X, Guo JX. Primary hepatic neuroendocrine tumors: multimodal imaging features with pathological correlations. Cancer Imaging. 2017;17(1):20.
75. Sippel RS, Chen H. Carcinoid tumors. Surg Oncol Clin N Am. 2006;15(3):463–78.
76. Campana D, Nori F, Piscitelli L, Morselli-Labate AM, Pezzilli R, Corinaldesi R, et al. Chromogranin A: is it a useful marker of neuroendocrine tumors? J Clin Oncol. 2007;25(15):1967–73.
77. Wang LX, Liu K, Lin GW, Jiang T. Primary hepatic neuroendocrine tumors: comparing CT and MRI features with pathology. Cancer Imaging. 2015;15:13.
78. Critchley M. Octreotide scanning for carcinoid tumours. Postgrad Med J. 1997;73(861):399–402.
79. Knox CD, Anderson CD, Lamps LW, Adkins RB, Pinson CW. Long-term survival after resection for primary hepatic carcinoid tumor. Ann Surg Oncol. 2003;10(10):1171–5.
80. Yang J, Kan Y, Ge BH, Yuan L, Li C, Zhao W. Diagnostic role of Gallium-68 DOTATOC and Gallium-68 DOTATATE PET in patients with neuroendocrine tumors: a meta-analysis. Acta Radiol. 2014;55(4):389–98.
81. Fenwick SW, Wyatt JI, Toogood GJ, Lodge JP. Hepatic resection and transplantation for primary carcinoid tumors of the liver. Ann Surg. 2004;239(2):210–9.
82. de Liguori CN, Manzia TM, Tariciotti L, Berlanda M, Orlando G, Tisone G. Liver transplantation in primary hepatic carcinoid tumor: case report and literature review. Transplant Proc. 2009;41(4):1386–9.

83. Kress O, Wagner HJ, Wied M, Klose KJ, Arnold R, Alfke H. Transarterial chemoembolization of advanced liver metastases of neuroendocrine tumors--a retrospective single-center analysis. Digestion. 2003;68(2–3):94–101.
84. Yao KA, Talamonti MS, Nemcek A, Angelos P, Chrisman H, Skarda J, et al. Indications and results of liver resection and hepatic chemoembolization for metastatic gastrointestinal neuroendocrine tumors. Surgery. 2001;130(4):677–82; discussion 82-5.
85. Gamblin TC, Christians K, Pappas SG. Radiofrequency ablation of neuroendocrine hepatic metastasis. Surg Oncol Clin N Am. 2011;20(2):273–9, vii-viii.
86. Kvols LK, Moertel CG, O'Connell MJ, Schutt AJ, Rubin J, Hahn RG. Treatment of the malignant carcinoid syndrome. Evaluation of a long-acting somatostatin analogue. N Engl J Med. 1986;315(11):663–6.
87. Das T, Banerjee S. Theranostic applications of Lutetium-177 in radionuclide therapy. Curr Radiopharm. 2016;9(1):94–101.
88. Kam BL, Teunissen JJ, Krenning EP, de Herder WW, Khan S, van Vliet EI, et al. Lutetium-labelled peptides for therapy of neuroendocrine tumours. Eur J Nucl Med Mol Imaging. 2012;39(Suppl 1):S103–12.
89. Claringbold PG, Turner JH. NeuroEndocrine tumor therapy with Lutetium-177-octreotate and Everolimus (NETTLE): a phase I study. Cancer Biother Radiopharm. 2015;30(6):261–9.
90. Gerald WL, Rosai J. Case 2. Desmoplastic small cell tumor with divergent differentiation. Pediatr Pathol. 1989;9(2):177–83.
91. Gerald WL, Ladanyi M, de Alava E, Cuatrecasas M, Kushner BH, LaQuaglia MP, et al. Clinical, pathologic, and molecular spectrum of tumors associated with t(11;22)(p13;q12): desmoplastic small round-cell tumor and its variants. J Clin Oncol. 1998;16(9):3028–36.
92. Kushner BH, LaQuaglia MP, Wollner N, Meyers PA, Lindsley KL, Ghavimi F, et al. Desmoplastic small round-cell tumor: prolonged progression-free survival with aggressive multimodality therapy. J Clin Oncol. 1996;14(5):1526–31.
93. Quaglia MP, Brennan MF. The clinical approach to desmoplastic small round cell tumor. Surg Oncol. 2000;9(2):77–81.
94. Dufresne A, Cassier P, Couraud L, Marec-Berard P, Meeus P, Alberti L, et al. Desmoplastic small round cell tumor: current management and recent findings. Sarcoma. 2012;2012:714986.
95. Thomas R, Rajeswaran G, Thway K, Benson C, Shahabuddin K, Moskovic E. Desmoplastic small round cell tumour: the radiological, pathological and clinical features. Insights Imaging. 2013;4(1):111–8.
96. Bellah R, Suzuki-Bordalo L, Brecher E, Ginsberg JP, Maris J, Pawel BR. Desmoplastic small round cell tumor in the abdomen and pelvis: report of CT findings in 11 affected children and young adults. AJR Am J Roentgenol. 2005;184(6):1910–4.
97. Kis B, O'Regan KN, Agoston A, Javery O, Jagannathan J, Ramaiya NH. Imaging of desmoplastic small round cell tumour in adults. Br J Radiol. 2012;85(1010):187–92.
98. Pickhardt PJ, Fisher AJ, Balfe DM, Dehner LP, Huettner PC. Desmoplastic small round cell tumor of the abdomen: radiologic-histopathologic correlation. Radiology. 1999;210(3):633–8.
99. Ordonez NG. Desmoplastic small round cell tumor: I: a histopathologic study of 39 cases with emphasis on unusual histological patterns. Am J Surg Pathol. 1998;22(11):1303–13.
100. Gerald WL, Rosai J, Ladanyi M. Characterization of the genomic breakpoint and chimeric transcripts in the EWS-WT1 gene fusion of desmoplastic small round cell tumor. Proc Natl Acad Sci U S A. 1995;92(4):1028–32.
101. Wong HH, Hatcher HM, Benson C, Al-Muderis O, Horan G, Fisher C, et al. Desmoplastic small round cell tumour: characteristics and prognostic factors of 41 patients and review of the literature. Clin Sarcoma Res. 2013;3(1):14.
102. Howlader N. Surveillance epidemiology and end results (SEER) cancer statistics review, 1975–2008. Bethesda: National Cancer Institute; 2011.
103. Linabery AM, Ross JA. Trends in childhood cancer incidence in the U.S. (1992-2004). Cancer. 2008;112(2):416–32.

104. Ries LAG, Smith MA, Gurney JG, Linet M, Tamra T, Young JL, et al. Cancer incidence and survival among children and adolescents: United States SEER Program 1975–1995. 1999.
105. Giardiello FM, Offerhaus GJ, Krush AJ, Booker SV, Tersmette AC, Mulder JW, et al. Risk of hepatoblastoma in familial adenomatous polyposis. J Pediatr. 1991;119(5):766–8.
106. DeBaun MR, Tucker MA. Risk of cancer during the first four years of life in children from the Beckwith-Wiedemann syndrome registry. J Pediatr. 1998;132(3 Pt 1):398–400.
107. Kitanovski L, Ovcak Z, Jazbec J. Multifocal hepatoblastoma in a 6-month-old girl with trisomy 18: a case report. J Med Case Rep. 2009;3:8319.
108. Hiyama E. Pediatric hepatoblastoma: diagnosis and treatment. Transl Pediatr. 2014;3(4):293–9.
109. De Ioris M, Brugieres L, Zimmermann A, Keeling J, Brock P, Maibach R, et al. Hepatoblastoma with a low serum alpha-fetoprotein level at diagnosis: the SIOPEL group experience. Eur J Cancer. 2008;44(4):545–50.
110. Adeyiga AO, Lee EY, Eisenberg RL. Focal hepatic masses in pediatric patients. AJR Am J Roentgenol. 2012;199(4):W422–40.
111. Dachman AH, Pakter RL, Ros PR, Fishman EK, Goodman ZD, Lichtenstein JE. Hepatoblastoma: radiologic-pathologic correlation in 50 cases. Radiology. 1987;164(1):15–9.
112. Gubernick JA, Rosenberg HK, Ilaslan H, Kessler A. US approach to jaundice in infants and children. Radiographics. 2000;20(1):173–95.
113. King SJ, Babyn PS, Greenberg ML, Phillips MJ, Filler RM. Value of CT in determining the resectability of hepatoblastoma before and after chemotherapy. AJR Am J Roentgenol. 1993;160(4):793–8.
114. Lopez-Terrada D, Alaggio R, de Davila MT, Czauderna P, Hiyama E, Katzenstein H, et al. Towards an international pediatric liver tumor consensus classification: proceedings of the Los Angeles COG liver tumors symposium. Mod Pathol. 2014;27(3):472–91.
115. Roebuck DJ, Aronson D, Clapuyt P, Czauderna P, de Ville de Goyet J, Gauthier F, et al. 2005 PRETEXT: a revised staging system for primary malignant liver tumours of childhood developed by the SIOPEL group. Pediatr Radiol. 2007;37(2):123–32; quiz 249-50.
116. Venkatramani R, Stein JE, Sapra A, Genyk Y, Jhaveri V, Malogolowkin M, et al. Effect of neoadjuvant chemotherapy on resectability of stage III and IV hepatoblastoma. Br J Surg. 2015;102(1):108–13.
117. Ortega JA, Douglass EC, Feusner JH, Reynolds M, Quinn JJ, Finegold MJ, et al. Randomized comparison of cisplatin/vincristine/fluorouracil and cisplatin/continuous infusion doxorubicin for treatment of pediatric hepatoblastoma: a report from the Children's Cancer Group and the Pediatric Oncology Group. J Clin Oncol. 2000;18(14):2665–75.
118. Stocker JT, Ishak KG. Mesenchymal hamartoma of the liver: report of 30 cases and review of the literature. Pediatr Pathol. 1983;1(3):245–67.
119. Isaacs H Jr. Fetal and neonatal hepatic tumors. J Pediatr Surg. 2007;42(11):1797–803.
120. Stanley P, Hall TR, Woolley MM, Diament MJ, Gilsanz V, Miller JH. Mesenchymal hamartomas of the liver in childhood: sonographic and CT findings. AJR Am J Roentgenol. 1986;147(5):1035–9.
121. Kim SH, Kim WS, Cheon JE, Yoon HK, Kang GH, Kim IO, et al. Radiological spectrum of hepatic mesenchymal hamartoma in children. Korean J Radiol. 2007;8(6):498–505.
122. Thampy R, Elsayes KM, Menias CO, Pickhardt PJ, Kang HC, Deshmukh SP, et al. Imaging features of rare mesenychmal liver tumours: beyond haemangiomas. Br J Radiol. 2017;90(1079):20170373.
123. Horton KM, Bluemke DA, Hruban RH, Soyer P, Fishman EK. CT and MR imaging of benign hepatic and biliary tumors. Radiographics. 1999;19(2):431–51.
124. Roberts EA, Liu P, Stringer D, Superina RA, Mancer K. Mesenchymal hamartoma in a 10-month-old infant: appearance by magnetic resonance imaging. Can Assoc Radiol J. 1989;40(4):219–21.
125. Ito H, Kishikawa T, Toda T, Arai M, Muro H. Hepatic mensenchymal hamartoma of an infant. J Pediatr Surg. 1984;19(3):315–7.

126. Stocker JT, Ishak KG. Undifferentiated (embryonal) sarcoma of the liver: report of 31 cases. Cancer. 1978;42(1):336–48.
127. Weinberg AG, Finegold MJ. Primary hepatic tumors of childhood. Hum Pathol. 1983;14(6):512–37.
128. Lenze F, Birkfellner T, Lenz P, Hussein K, Langer F, Kreipe H, et al. Undifferentiated embryonal sarcoma of the liver in adults. Cancer. 2008;112(10):2274–82.
129. Nishio J, Iwasaki H, Sakashita N, Haraoka S, Isayama T, Naito M, et al. Undifferentiated (embryonal) sarcoma of the liver in middle-aged adults: smooth muscle differentiation determined by immunohistochemistry and electron microscopy. Hum Pathol. 2003;34(3):246–52.
130. Bisogno G, Pilz T, Perilongo G, Ferrari A, Harms D, Ninfo V, et al. Undifferentiated sarcoma of the liver in childhood: a curable disease. Cancer. 2002;94(1):252–7.
131. Pachera S, Nishio H, Takahashi Y, Yokoyama Y, Oda K, Ebata T, et al. Undifferentiated embryonal sarcoma of the liver: case report and literature survey. J Hepato-Biliary-Pancreat Surg. 2008;15(5):536–44.
132. Wei ZG, Tang LF, Chen ZM, Tang HF, Li MJ. Childhood undifferentiated embryonal liver sarcoma: clinical features and immunohistochemistry analysis. J Pediatr Surg. 2008;43(10):1912–9.
133. Almogy G, Lieberman S, Gips M, Pappo O, Edden Y, Jurim O, et al. Clinical outcomes of surgical resections for primary liver sarcoma in adults: results from a single centre. Eur J Surg Oncol. 2004;30(4):421–7.
134. Ros PR, Olmsted WW, Dachman AH, Goodman ZD, Ishak KG, Hartman DS. Undifferentiated (embryonal) sarcoma of the liver: radiologic-pathologic correlation. Radiology. 1986;161(1):141–5.
135. Buetow PC, Buck JL, Pantongrag-Brown L, Marshall WH, Ros PR, Levine MS, et al. Undifferentiated (embryonal) sarcoma of the liver: pathologic basis of imaging findings in 28 cases. Radiology. 1997;203(3):779–83.
136. Psatha EA, Semelka RC, Fordham L, Firat Z, Woosley JT. Undifferentiated (embryonal) sarcoma of the liver (USL): MRI findings including dynamic gadolinium enhancement. Magn Reson Imaging. 2004;22(6):897–900.
137. Leuschner I, Schmidt D, Harms D. Undifferentiated sarcoma of the liver in childhood: morphology, flow cytometry, and literature review. Hum Pathol. 1990;21(1):68–76.
138. May LT, Wang M, Albano E, Garrington T, Dishop M, Macy ME. Undifferentiated sarcoma of the liver: a single institution experience using a uniform treatment approach. J Pediatr Hematol Oncol. 2012;34(3):e114–6.
139. Plant AS, Busuttil RW, Rana A, Nelson SD, Auerbach M, Federman NC. A single-institution retrospective cases series of childhood undifferentiated embryonal liver sarcoma (UELS): success of combined therapy and the use of orthotopic liver transplant. J Pediatr Hematol Oncol. 2013;35(6):451–5.
140. Weitz J, Klimstra DS, Cymes K, Jarnagin WR, D'Angelica M, La Quaglia MP, et al. Management of primary liver sarcomas. Cancer. 2007;109(7):1391–6.
141. Asch MJ, Cohen AH, Moore TC. Hepatic and splenic lymphangiomatosis with skeletal involvement: report of a case and review of the literature. Surgery. 1974;76(2):334–9.
142. Enzinger F, Weiss S. Soft tissue tumour. 3rd ed. St Louis: Mosby; 1998.
143. Losanoff JE, Richman BW, El-Sherif A, Rider KD, Jones JW. Mesenteric cystic lymphangioma. J Am Coll Surg. 2003;196(4):598–603.
144. Stavropoulos M, Vagianos C, Scopa CD, Dragotis C, Androulakis J. Solitary hepatic lymphangioma. A rare benign tumour: a case report. HPB Surg. 1994;8(1):33–6.
145. Koh CC, Sheu JC. Hepatic lymphangioma--a case report. Pediatr Surg Int. 2000;16(7):515–6.
146. O'Sullivan DA, Torres VE, de Groen PC, Batts KP, King BF, Vockley J. Hepatic lymphangiomatosis mimicking polycystic liver disease. Mayo Clin Proc. 1998;73(12):1188–92.
147. Allen JG, Riall TS, Cameron JL, Askin FB, Hruban RH, Campbell KA. Abdominal lymphangiomas in adults. J Gastrointest Surg. 2006;10(5):746–51.

148. Matsumoto T, Ojima H, Akishima-Fukasawa Y, Hiraoka N, Onaya H, Shimada K, et al. Solitary hepatic lymphangioma: report of a case. Surg Today. 2010;40(9):883–9.
149. Liu Q, Sui CJ, Li BS, Gao A, Lu JY, Yang JM. Solitary hepatic lymphangioma: a one-case report. Springerplus. 2014;3:314.
150. Biondi A, Malaguarnera G, Vacante M, Berretta M, D'Agata V, Malaguarnera M, et al. Elevated serum levels of Chromogranin A in hepatocellular carcinoma. BMC Surg. 2012;12(Suppl 1):S7.
151. Choi WJ, Jeong WK, Kim Y, Kim J, Pyo JY, Oh YH. MR imaging of hepatic lymphangioma. Korean J Hepatol. 2012;18(1):101–4.
152. Levy AD, Cantisani V, Miettinen M. Abdominal lymphangiomas: imaging features with pathologic correlation. AJR Am J Roentgenol. 2004;182(6):1485–91.
153. Siegel MJ, Glazer HS, St Amour TE, Rosenthal DD. Lymphangiomas in children: MR imaging. Radiology. 1989;170(2):467–70.
154. Roisman I, Manny J, Fields S, Shiloni E. Intra-abdominal lymphangioma. Br J Surg. 1989;76(5):485–9.
155. Stein M, Hsu RK, Schneider PD, Ruebner BH, Mina Y. Alcohol ablation of a mesenteric lymphangioma. J Vasc Interv Radiol. 2000;11(2 Pt 1):247–50.
156. De Santis M, Calo GF, Trombini P, Romagnoli R. Percutaneous sclerosing treatment with ethanol of a large cystic lymphangioma of the neck in an adult. Radiol Med. 2003;105(1–2):127–30.
157. Banieghbal B, Davies MR. Guidelines for the successful treatment of lymphangioma with OK-432. Eur J Pediatr Surg. 2003;13(2):103–7.
158. Ramchand S, Ahmed Y, Baskerville L. Lipoma of the liver. Arch Pathol. 1970;90(4):331–3.
159. Marti-Bonmati L, Menor F, Vizcaino I, Vilar J. Lipoma of the liver: US, CT, and MRI appearance. Gastrointest Radiol. 1989;14(2):155–7.
160. Roberts JL, Fishman EK, Hartman DS, Sanders R, Goodman Z, Siegelman SS. Lipomatous tumors of the liver: evaluation with CT and US. Radiology. 1986;158(3):613–7.
161. Reading CC, Charboneau JW. Case of the day. Ultrasound. Hepatic lipoma. Radiographics. 1990;10(3):511–2.
162. Puljiz Z, Petricevic M, Bratanic A, Barisic I, Puljiz M, Karin Z. An unusually large liver lipoma. Med Glas (Zenica). 2012;9(2):411–4.
163. Bruneton JN, Kerboul P, Drouillard J, Menu Y, Normand F, Santini N. Hepatic lipomas: ultrasound and computed tomographic findings. Gastrointest Radiol. 1987;12(4):299–303.
164. Valls C, Iannacconne R, Alba E, Murakami T, Hori M, Passariello R, et al. Fat in the liver: diagnosis and characterization. Eur Radiol. 2006;16(10):2292–308.
165. Dalal KM, Antonescu CR, Singer S. Diagnosis and management of lipomatous tumors. J Surg Oncol. 2008;97(4):298–313.

Chapter 9
Liver Lesions in Congestive Hepatopathy

Moira B. Hilscher, Michael L. Wells, and Patrick S. Kamath

Introduction

The liver is a highly vascular organ, which receives approximately 30% of cardiac output, and is prone to a spectrum of circulatory disturbances and vascular insults [1]. Congestive hepatopathy (CH) describes the manifestations of chronic, passive congestion of the liver in the setting of impaired hepatic venous outflow [2]. CH most commonly occurs secondary to cardiac disease although obstruction of the hepatic venous outflow at the level of the supra-hepatic inferior vena cava (IVC) or hepatic veins can also induce hepatic congestion. Any etiology of right ventricular heart failure may precipitate hepatic congestion, including constrictive pericarditis, tricuspid regurgitation, cardiomyopathy, and cor pulmonale. The prevalence of CH is increasing in the setting of an aging population with expanding therapeutic options which prolong survival [3]. In addition, patients who have undergone surgical palliation for congenital heart disease with the Fontan procedure are at risk for chronic congestion. The Fontan procedure, which is considered the definitive palliation for patients with single-ventricle physiology, returns systemic venous blood to the pulmonary circulation via an anastomosis between the vena cava or right atrium and the pulmonary arteries. As survival of patients who have undergone the Fontan procedure and other corrective procedures improves [4, 5], hepatic manifestations of congestion are increasingly evident [6]. Chronic congestion may culminate in hepatic fibrosis, cirrhosis, and portal hypertension with associated complications. Indeed, recent studies reveal an increasing incidence of hepatocellular carcinoma

M. B. Hilscher · P. S. Kamath
Department of Gastroenterology and Hepatology, Mayo Clinic, Rochester, MN, USA
e-mail: Hilscher.moira@mayo.edu; Kamath.patrick@mayo.edu

M. L. Wells (✉)
Department of Radiology, Mayo Clinic, Rochester, MN, USA
e-mail: Wells.Michael@mayo.edu

L. R. Roberts et al. (eds.), *Evaluation and Management of Liver Masses*,
https://doi.org/10.1007/978-3-030-46699-2_9

(HCC) in patients with CH and Fontan physiology [7]. However, benign liver masses such as focal nodular hyperplasia (FNH) also occur in this setting. This emphasizes the need for precise diagnostic studies, which are able to accurately differentiate benign lesions from HCC in this patient population.

Hepatic Circulation: Normal Physiology

The liver receives dual blood supply from the portal vein and the hepatic artery. Well-oxygenated arterial blood from the celiac trunk of the aorta comprises only approximately 25% of total hepatic blood flow. The remaining 75% of hepatic blood flow consists of blood supplied by the portal vein at venous pressure (approximately 6 mm Hg) [8]. Blood from the portal vein converges with hepatic arterial blood within hepatic sinusoids. The hepatic artery autoregulates blood flow via the hepatic arterial buffer response (HABR), whereby decreased portal flow instigates compensatory upregulation of hepatic arterial flow and vice versa [9]. This regulatory response maintains hepatic oxygenation and preserves a constant level of total hepatic blood flow [10, 11]. It is estimated that the HABR can compensate for a 25–60% decrease in portal blood flow [9, 12]. On the other hand, portal venous flow is not autoregulated and is therefore dependent on mesenteric circulation and the gradient between portal and hepatic venous pressures to maintain venous circulation to the liver.

Pathophysiology of Congestive Hepatopathy

Among the key factors in the pathophysiology of CH is the presence of elevated central venous pressure which transmits to the hepatic veins and sinusoids and thereby decreases portal venous inflow [13, 14]. Increased hepatic venous pressure also causes sinusoidal congestion, dilation of sinusoidal fenestrae, and exudation of protein and fluid into the Space of Disse. Accumulation of exudate into the Space of Disse impairs diffusion of oxygen and nutrients to hepatocytes [13, 15]. Decreased hepatic blood flow further increases susceptibility to injury in settings which compromise arterial flow, such as hypotension, arrhythmias, or left-sided heart failure, which can precipitate ischemic hepatopathy [14] . Patients with CH and the Fontan physiology may have lower baseline arterial oxygen saturations which further predispose to hepatocyte ischemia [16]. Sinusoidal congestion, impaired portal venous inflow, depressed cardiac output, and compromised arterial oxygenation culminate in hepatocyte ischemia in a process described as “parenchymal extinction” [17]. Chronic vascular shear stress and injury also instigate fibrogenic pathways that can culminate in cirrhosis. A murine model of CH was recently developed which entails partial ligation of the suprahepatic inferior vena cava. This model revealed that

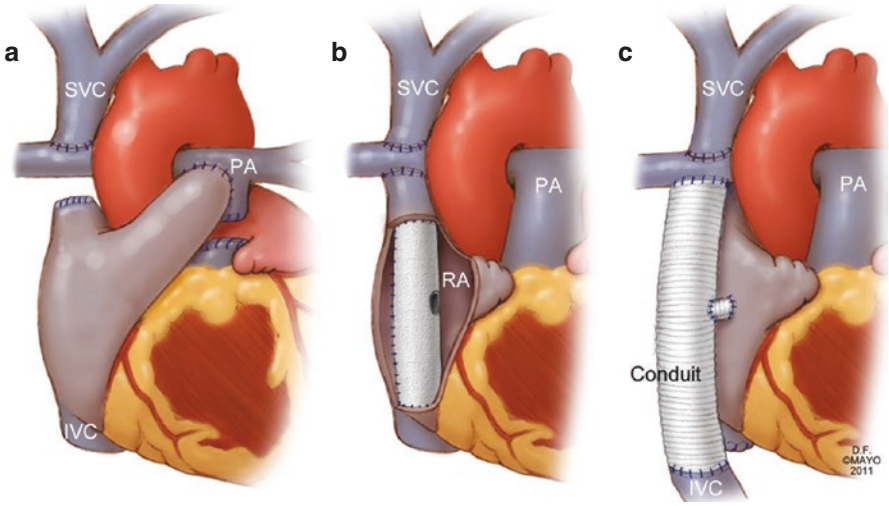

Fig. 9.1 (**a**) This depicts a bidirectional cavopulmonary shunt, which entails ligation of the superior vena cava to the right pulmonary artery. The inferior vena cava is anastomosed to the pulmonary artery to supply blood to the lungs. (**b**) Fontan with an intra-atrial conduit which channels blood from the inferior vena cava to the pulmonary artery through the right atrium. Blood from the superior vena cava is channeled to the pulmonary artery. (**c**) An extracardiac Fontan utilizes a conduit from the inferior vena cava to the right pulmonary artery with anastomosis of the superior vena cava to the pulmonary artery. IVC inferior vena cava, PA pulmonary artery, RA right atrium, SVC superior vena cava

mechanical forces imposed by congestion and microvascular thrombosis are key mediators of fibrosis in CH [18].

In the Fontan circulation, systemic venous blood returns to the lungs without utilizing a pumping chamber [19, 20] (Fig. 9.1). The Fontan operation maintains near-normal systemic oxygenation while inducing systemic venous hypertension and relatively decreased cardiac output [20]. Hepatic dysfunction after the Fontan procedure is multifactorial and is due to hypoxemia in the setting of chronic low cardiac output state, chronic elevation of central venous pressure, and increased mesenteric vascular resistance. Continuous systemic venous back-pressure on the liver results in hepatic changes secondary to passive venous congestion. This passive venous congestion is continuous, in contrast to the more intermittent or pulsatile back-pressure experienced with other cardiac defects, such as tricuspid regurgitation.

Histologically, passive congestion of the liver is reflected by sinusoidal dilation, congestion, and hepatocyte atrophy most prominent in zone 3 which comprises the centrilobular parenchyma surrounding the central hepatic veins [21, 22] (Fig. 9.2). In CH due to heart disease, the extent of sinusoidal dilation correlates with the degree of right atrial and hepatic venous pressure elevation [16]. Elevated hepatic venous pressures may precipitate extravasation of red blood cells into the space of Disse. The extent of necrosis, inflammation, and dilation has been correlated with

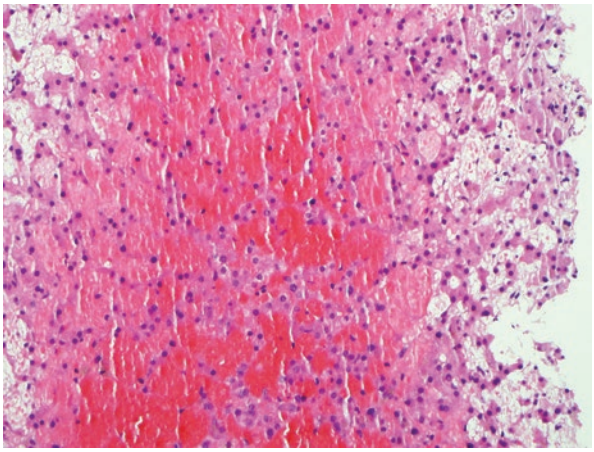

Fig. 9.2 Characteristic histologic changes of congestive hepatopathy, including sinusoidal dilatation, congestion, hepatic cord atrophy, and extravasation of red blood cells into the hepatocytes

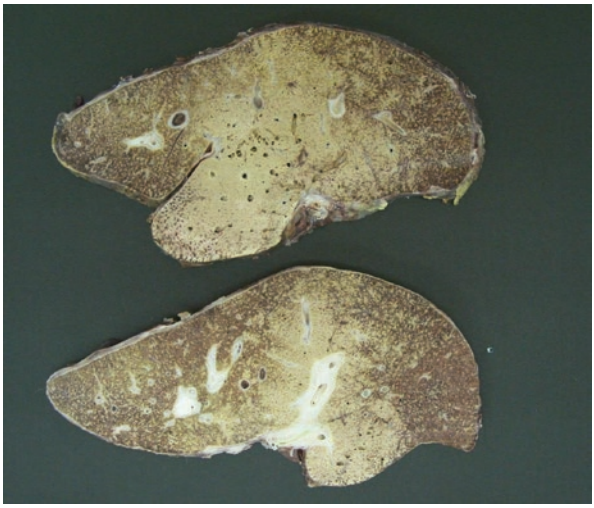

Fig. 9.3 "Nutmeg liver" characteristic of congestive hepatopathy. Dark centrilobular zones reflecting sinusoidal congestion alternate with pale periportal zones

right atrial and hepatic pressures [16]. Chronic congestion leads to perivenular and perisinusoidal fibrosis [21]. Fibrosis initially forms in zone 3 of the hepatic acinus, but over time may progress to bridging fibrosis between hepatic veins [21]. This is in contrast to noncardiac fibrosis which is characterized instead by fibrosis which extends between portal triads. Grossly, the congested liver has been characterized as a "nutmeg liver," [23] (Fig. 9.3) with dark centrilobular zones reflecting sinusoidal congestion alternating with pale periportal zones with normal or fatty liver tissue [23, 24]. Regenerative nodules or focal nodular hyperplasia (FNH) are commonly described in livers with chronic congestion [25–27]. Such regenerative nodules typically contain arteries and have been attributed to compromise in venous flow, which increases reliance on hepatic arterial flow to maintain parenchymal perfusion [25]. However, chronic congestion can culminate in fibrosis and cirrhosis, and

therefore also predisposes to HCC, which is important to distinguish from benign nodules.

Clinical Manifestations of Congestive Hepatopathy

Patients with congestive hepatopathy may remain asymptomatic from their liver disease. When symptomatic, patients may note jaundice or dull right upper quadrant discomfort secondary to pressure imposed on the liver capsule. Clinical stigmata of portal hypertension including ascites, hepatic encephalopathy, and varices, may be apparent with progression to cirrhosis.

Congestive hepatopathy is frequently identified through abnormalities noted on routine laboratory assessment. Characteristic laboratory findings include elevations in serum aminotransferases to 2–3 times the upper limit of normal and unconjugated hyperbilirubinemia which rarely exceeds 3 mg/dL. Acute cardiac ischemia resulting from hypotension in patients with passive venous congestion of the liver may precipitate a more abrupt onset of jaundice with marked elevation of aminotransferases to greater than 50 times the upper limit of normal.

Morbidity and mortality in congestive hepatopathy are frequently predicated by the gravity of cardiac disease. Management of congestive hepatopathy relies on treatment of the underlying cardiac condition and optimization of cardiac output. Patients with cirrhosis require screening for esophageal varices and hepatocellular carcinoma.

Liver Masses in Congestive Hepatopathy

Chronic congestive hepatopathy predisposes the liver to development of both benign and malignant focal hepatic lesions which may be detected either incidentally or as part of surveillance imaging. Lesions within the congested liver detected incidentally are often incompletely evaluated and raise concern for malignancy. In most cases, assessment with properly designed imaging protocols is able to differentiate benign lesions from those that require biopsy or additional evaluation and treatment. The congested liver itself also demonstrates several characteristic imaging abnormalities which are important to review, as they can both alter the normal appearance of hepatic lesions and may simulate focal lesions.

Several characteristic parenchymal abnormalities are seen within the congested liver at computed tomography (CT) and magnetic resonance imaging (MRI) (Figs. 9.4 and 9.5) [28]. Congestion causing parenchymal edema results in unusually low attenuation at CT and unusually high T2 signal and low T1 signal at MRI. These imaging abnormalities are greatest at the periphery of the liver. If congestion leads to liver injury and steatosis, the liver parenchyma will also be lower

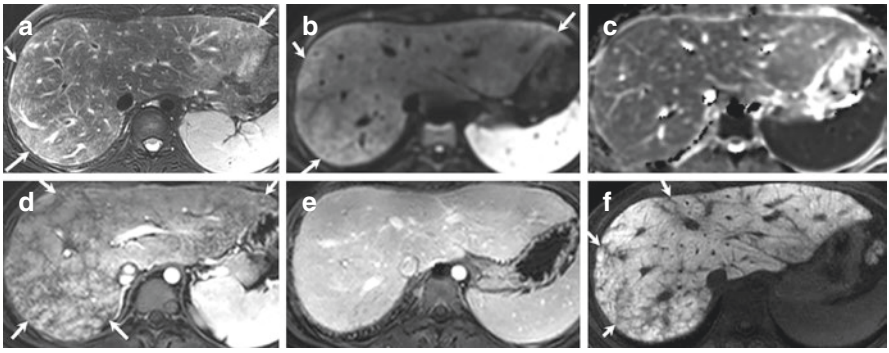

Fig. 9.4 MRI findings of hepatic congestion in a 20-year-old female who had undergone the Fontan procedure for palliation of complex congenital heart disease. (**a**) T2-weighted fast spin echo (FSE) MRI demonstrates high signal in the periphery of the liver (arrows), representative of edema or fibrosis. (**b**, **c**) Corresponding DWI (**b**) and ADC (**c**) images show high signal on DWI without low signal on the ADC map. The findings represent T2 shine through and correspond to high signal found on the T2 FSE image. (**d**, **e**) Portal venous and delayed phase images enhanced with extracellular contrast show reticular regions of poor enhancement in the portal venous phase (**d**, arrows) which correspond with high T2 signal images on the T2 FSE image. The abnormal regions of enhancement become indistinct on the delayed phase (**e**). (**f**) Hepatobiliary phase image from MRI examination performed with hepatocyte-specific contrast agent clearly shows reticular regions of poor contrast uptake in the periphery of the liver (arrows). These findings correspond to abnormalities demonstrated on the remaining sequences and may represent bands of fibrosis

than normal in attenuation at CT and will demonstrate low signal at MRI on both T1-weighted opposed phase images and fat-saturated sequences.

Reticular bands of low attenuation related to edema and fibrosis are seen on CT [28]. These irregular bands are found most commonly at the periphery of the liver, and progress centrally as the congestion worsens. At MRI, they appear as high signal on T2-weighted images and low on T1-weighted images. On both CT and MRI, the reticular regions demonstrate poor early phase enhancement, and are most conspicuous at the portal venous phase, when the adjacent parenchyma is maximally enhanced. On delayed phase imaging, conventional contrast media redistributes to the extravascular, extracellular space, and the reticular regions become less conspicuous. If liver injury leads to parenchymal fibrosis, a nodular cirrhotic liver with bands of fibrosis may be seen at imaging. Differentiating fibrosis from congestion may be difficult at imaging, as both bands of fibrosis and edema appear low-attenuation at CT and high in T2 signal, low in T1 signal at MRI. The presence of portosystemic shunts may help identify cirrhosis, as these are characteristically absent in passive congestion with elevated central venous pressures.

Periportal edema related to the engorgement of perivascular lymphatics is also seen at CT and MRI. In the delayed phase, contrast media may diffuse into the perivascular space, creating a ring appearance which may be mistaken as an enhancing vessel wall surrounding a luminal thrombus [29].

Hepatobiliary-specific agents used for MRI imaging are actively transported into the hepatocytes [30]. There may be a heterogenous pattern of uptake in the liver

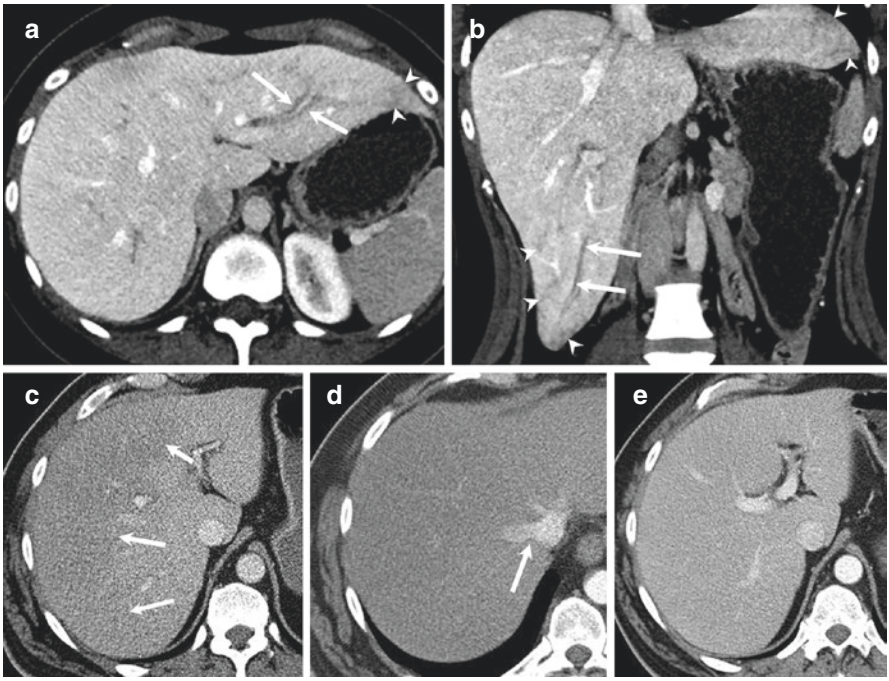

Fig. 9.5 Acute hepatic congestion. (**a**, **b**) A 30-year-old female being evaluated for routine follow-up of Crohn's disease. New periportal edema (arrows) and peripheral hepatic perfusion irregularity (arrowheads) was new from prior examination. The patient had received an IV infusion of 2 liters normal saline shortly prior to the CT examination for clinically suspected dehydration. (**c**–**e**) A 47-year-old male presenting to the emergency room after his motor vehicle collided with a tree. Trauma CT scan shows poor perfusion in the periphery of the liver (**c**, arrows) and reflux of injected contrast bolus into the hepatic veins (**d**, arrow). Patient was found to have an inferior ST elevated myocardial infarction and subsequently underwent right coronary artery thrombectomy with stent placement. Follow-up CT scan (**e**) shows resolution of the hepatic perfusion abnormalities

parenchyma as a result of hepatocyte dysfunction [28]. Focal regions of parenchyma which poorly accumulate hepatobiliary contrast agent can be mistaken for focal malignant masses [31, 32]. The reticular regions of poor enhancement seen with conventional contrast media also do not retain hepatobiliary contrast and are prominently seen in the hepatobiliary phase (Fig. 9.4).

The congested liver is predisposed to development of benign regenerative nodules or focal nodular hyperplasia (FNH) and malignant hepatocellular carcinoma (HCC). Despite atypical imaging findings of the background congested liver parenchyma, most benign regnerative nodules and FNH demonstrate typical imaging, allowing a confident diagnosis of the benign lesion [27]. These nodules should have a well-circumscribed, round, or slightly lobulated margin. The nodules enhance avidly in the late arterial phase and fade into isoattenuation or isointensity on subsequent imaging phases when using an extracellular contrast agent [33–35]. When using a hepatobiliary-specific contrast agent, 90–91% of FNH nodules retain

contrast to a degree similar to or greater than the background liver [36, 37]. The pattern of hepatobiliary contrast agent retention is most commonly diffuse but may be found in a peripheral ring-like distribution in up to 41% [38]. A central scar may be present in FNH, the frequency of which increases as the mass enlarges [33]. The central scar of FNH is low attenuation at CT, high in signal on T2-weighted images, and low on T1-weighted images on the MRI. A central scar enhances poorly in the early phase and progressively accumulates extracellular contrast in the delayed phase.

Abnormalities of the background liver may result in an atypical appearance of benign regenerative nodules or FNH. Hepatic steatosis may result in FNH appearing hyperattenuating at CT or hyperintense on the MRI T1-weighted opposed phase, or fat-saturated sequences. Excess iron accumulation within the background liver results in MRI signal loss and a relative increase in signal intensity of nodules which do not accumulate iron. It is important to recognize that edematous or fibrous hepatic parenchyma in the setting of hepatic congestion causes relative hypoattenuating or hypointense appearance of the benign nodules in delayed phase simulating washout [27, 39].

A nodule with the combination of arterial hyperenhancment followed by washout in the portal venous or delayed phase may result in an imaging diagnosis of HCC when using traditional organ procurement and transplant network criteria. The Liver Imaging Reporting and Data System (LIRADS) criteria no longer consider traditional enhancement characteristics applicable in patients with cardiac congestion and hepatic vascular disease, including hereditary hemorrhagic telangiectasia, Budd–Chiari syndrome, and chronic portal vein occlusion [40]. A washout appearance of a benign nodule may be related to abnormally increased redistribution of extracellular contrast into the expanded extracellular space of the edematous or fibrotic background liver (Fig. 9.6) [27]. Benign nodules which show an abnormal washout appearance also tend to have relatively low T2 signal; this is likely due to abnormally high T2 signal of the edematous and fibrotic background parenchyma (Fig. 9.7). A nodule which resembles FNH at imaging but has delayed phase washout and low T2 signal intensity should be assessed with hepatobiliary contrast agent-enhanced MRI. Hepatobiliary agent contrast-enhanced MRI may be helpful as a homogeneous pattern of retention greatly increases the likelihood of a benign lesion [41–43]. If the nodule does not retain hepatobiliary contrast agent in a pattern consistent with FNH, then either follow-up imaging in 3 months or a biopsy is recommended.

Patients with passive hepatic congestion are also at increased risk for development of HCC [7, 27]. Previous reports of HCC developing within a congested liver have uniformly reported concerning imaging findings in addition to washout [7, 27, 44–51]. Imaging findings concerning for HCC include a heterogeneous or mosaic appearance of a mass, necrosis, internal lipid content, rapid growth, and venous tumor thrombus (Fig. 9.8). The serum alpha-fetoprotein level is helpful for image interpretation as it raises suspicion for HCC when elevated. When a hyperenhancing nodule in a congested liver shows delayed phase washout, the presence of a cirrhotic background liver also significantly increases the likelihood of HCC being present [27].

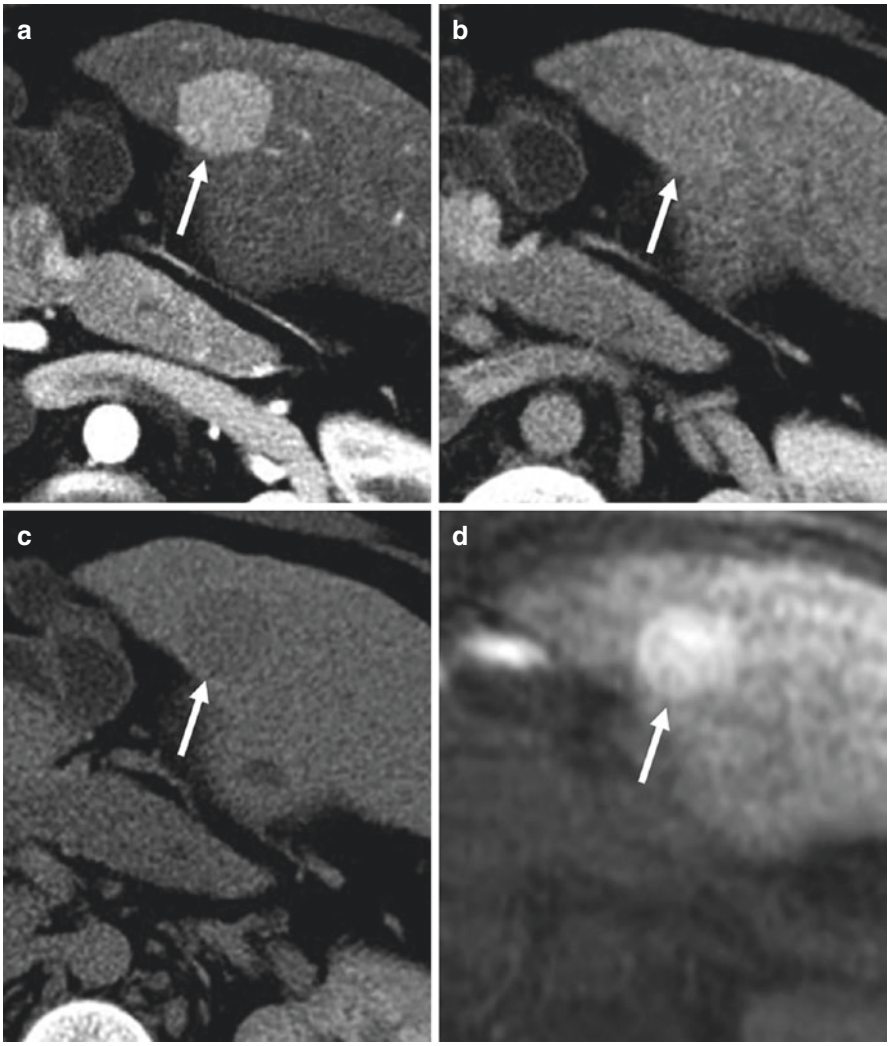

Fig. 9.6 Hypervascular lesion (arrow, **a**) fades into isointensity on portal venous phase (arrow, **b**) and shows washout (arrow, **c**) on delayed images. Imaging with Eovist in the hepatobiliary phase however shows retention of contrast (arrow, **d**). This patient had numerous hyper-enhancing lesions with washout which were all stable on 25 months of imaging follow-up

Post-Fontan patients with cirrhosis should have regular surveillance for HCC with twice annual ultrasonography and measurement of AFP (Fig. 9.9) [51]. If a hepatic nodule is detected on ultrasound imaging, either a contrast enhanced CT or MRI scan should be carried out. The presence of a cardiac pacemaker or implantable defibrillator may make MR imaging more challenging. MRI is still possible if the patient is not pacemaker dependent and the test is performed under MRI physicist supervision. Patients who have hepatic nodules with

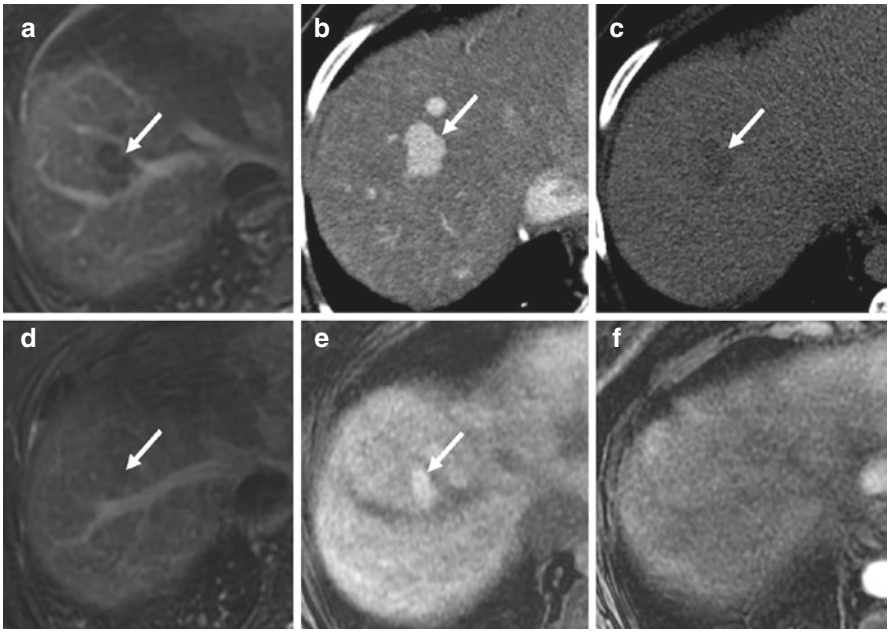

Fig. 9.7 Patient with multiple T2 hypointense masses, one of which is shown (arrow, **a**). Nodules in this patient showed arterial phase hyperintensity (arrow, **b**) and delayed phase washout (arrow, **c**) on CT scan obtained near the time of the initial MRI (MRI was enhanced with gadoxetate disodium making assessment of delayed phase washout unreliable). This patient had numerous follow-up examinations over 25 months of imaging follow-up which demonstrated resolution of both the T2 hypointensity (arrow, **d**) and delayed phase washout (not shown), possibly reflecting a change in the composition of the background liver parenchyma. The nodule remained present when imaged in the arterial phase and with extracellular contrast agent or in the hepatobiliary phase with intracellular contrast agent (arrow, **e**). A precontrast image (**f**) from the study performed in image (**e**) is provided for reference

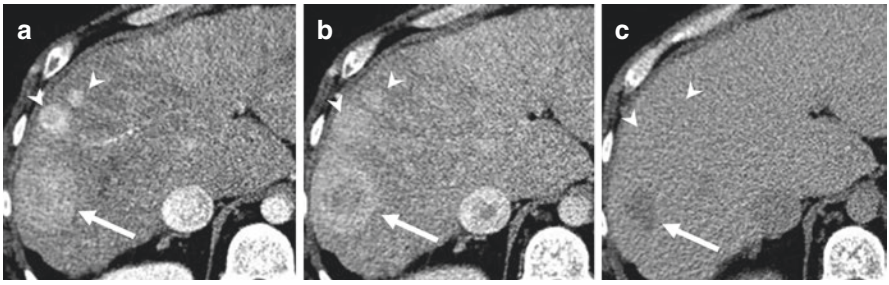

Fig. 9.8 Biopsy-proven hepatocellular carcinoma (arrow, **a**) in a patient with numerous hypervascular nodules, two of which are shown (arrowheads, **a**, **b**). The HCC was unique due to its size and heterogenous washout on portal venous and delayed phase images (arrows, **b**, **c**) while the remaining hepatic nodules fade to iso-attenuation on delayed phase images (arrowheads, **c**)

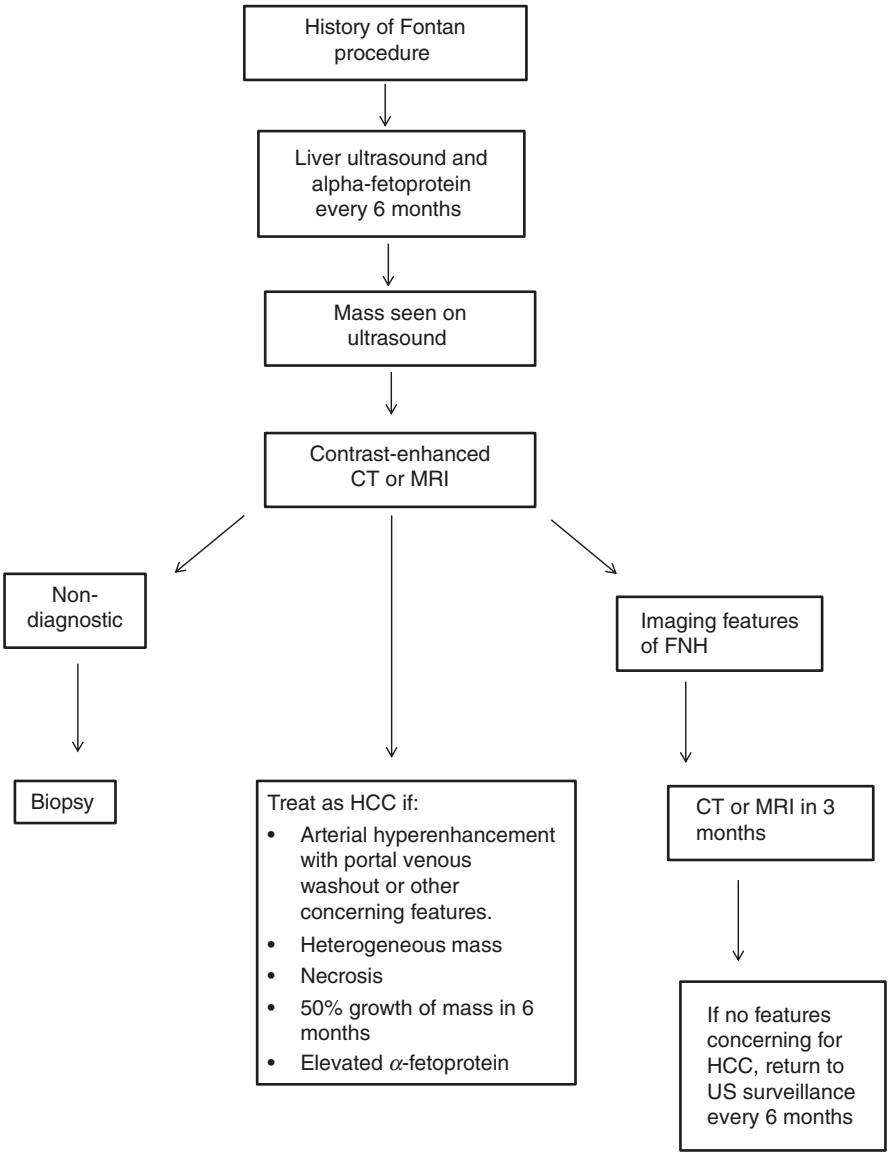

Fig. 9.9 Algorithm for evaluation and management of liver lesions detected in patients with congestive hepatopathy

characteristic features on either CT or MR imaging (arterial hyperenhancement and portal venous washout, heterogeneous appearance, necrosis), or hepatic masses with concomitant AFP levels >200 ng/mL should be considered to have HCC and treated appropriately. A mass which shows more than 50% growth over a 6-month period is also concerning for HCC. A mass with characteristics of

FNH requires reimaging with CT or MRI after 3 months. If imaging characteristics remain convincing for FNH, then routine surveillance every 6 months can be resumed.

References

1. Ford RM, Book W, Spivey JR. Liver disease related to the heart. Transplant Rev (Orlando). 2015;29(1):33–7.
2. Weisberg IS, Jacobson IM. Cardiovascular diseases and the liver. Clin Liver Dis. 2011;15(1):1–20.
3. Ahmed A. American College of Cardiology/American Heart Association Chronic Heart Failure Evaluation and Management guidelines: relevance to the geriatric practice. J Am Geriatr Soc. 2003;51(1):123–6.
4. Atz AM, et al. Survival data and predictors of functional outcome an average of 15 years after the Fontan procedure: the pediatric heart network Fontan cohort. Congenit Heart Dis. 2015;10(1):E30–42.
5. Gersony WM. Fontan operation after 3 decades: what we have learned. Circulation. 2008;117(1):13–5.
6. Pundi K, et al. Liver disease in patients after the Fontan operation. Am J Cardiol. 2016;117(3):456–60.
7. Asrani SK, Warnes CA, Kamath PS. Hepatocellular carcinoma after the Fontan procedure. N Engl J Med. 2013;368(18):1756–7.
8. Lautt WW. Hepatic circulation: physiology and pathophysiology. California, USA: San Rafael; 2009.
9. Lautt WW. Mechanism and role of intrinsic regulation of hepatic arterial blood flow: hepatic arterial buffer response. Am J Phys. 1985;249(5 Pt 1):G549–56.
10. Lautt WW. The hepatic artery: subservient to hepatic metabolism or guardian of normal hepatic clearance rates of humoral substances. Gen Pharmacol. 1977;8(2):73–8.
11. Eipel C, Abshagen K, Vollmar B. Regulation of hepatic blood flow: the hepatic arterial buffer response revisited. World J Gastroenterol. 2010;16(48):6046–57.
12. Lautt WW. Relationship between hepatic blood flow and overall metabolism: the hepatic arterial buffer response. Fed Proc. 1983;42(6):1662–6.
13. Giallourakis CC, Rosenberg PM, Friedman LS. The liver in heart failure. Clin Liver Dis. 2002;6(4):947–67, viii-ix.
14. Asrani SK, et al. Congenital heart disease and the liver. Hepatology. 2012;56(3):1160–9.
15. Safran AP, Schaffner F. Chronic passive congestion of the liver in man. Electron microscopic study of cell atrophy and intralobular fibrosis. Am J Pathol. 1967;50(3):447–63.
16. Myers RP, et al. Cardiac hepatopathy: clinical, hemodynamic, and histologic characteristics and correlations. Hepatology. 2003;37(2):393–400.
17. Wanless IR, Liu JJ, Butany J. Role of thrombosis in the pathogenesis of congestive hepatic fibrosis (cardiac cirrhosis). Hepatology. 1995;21(5):1232–7.
18. Simonetto DA, et al. Chronic passive venous congestion drives hepatic fibrogenesis via sinusoidal thrombosis and mechanical forces. Hepatology. 2015;61(2):648–59.
19. Driscoll DJ. Long-term results of the Fontan operation. Pediatr Cardiol. 2007;28(6):438–42.
20. Gewillig M, Goldberg DJ. Failure of the fontan circulation. Heart Fail Clin. 2014;10(1):105–16.
21. Dai DF, et al. Congestive hepatic fibrosis score: a novel histologic assessment of clinical severity. Mod Pathol. 2014;27(12):1552–8.
22. Arcidi JM Jr, Moore GW, Hutchins GM. Hepatic morphology in cardiac dysfunction: a clinicopathologic study of 1000 subjects at autopsy. Am J Pathol. 1981;104(2):159–66.

23. Sherlock S. The liver in heart failure; relation of anatomical, functional, and circulatory changes. Br Heart J. 1951;13(3):273–93.
24. Lefkowitch JH, Mendez L. Morphologic features of hepatic injury in cardiac disease and shock. J Hepatol. 1986;2(3):313–27.
25. Tanaka M, Wanless IR. Pathology of the liver in Budd-Chiari syndrome: portal vein thrombosis and the histogenesis of veno-centric cirrhosis, veno-portal cirrhosis, and large regenerative nodules. Hepatology. 1998;27(2):488–96.
26. Koehne de Gonzalez AK, Lefkowitch JH. Heart disease and the liver: pathologic evaluation. Gastroenterol Clin N Am. 2017;46(2):421–35.
27. Wells ML, et al. Benign nodules in post-Fontan livers can show imaging features considered diagnostic for hepatocellular carcinoma. Abdom Radiol (NY). 2017;42(11):2623–31.
28. Wells ML, et al. Imaging findings of congestive hepatopathy. Radiographics : a review publication of the Radiological Society of North America, Inc. 2016;36(4):1024–37.
29. Gore RM, et al. Passive hepatic congestion: cross-sectional imaging features. AJR Am J Roentgenol. 1994;162(1):71–5.
30. Yoneda N, et al. Benign hepatocellular nodules: hepatobiliary phase of gadoxetic acid-enhanced MR imaging based on molecular background. Radiographics. 2016;36(7):2010–27.
31. Uchino K, et al. Oxaliplatin-induced liver injury mimicking metastatic tumor on images: a case report. Jpn J Clin Oncol. 2013;43(10):1034–8.
32. Choi JH, et al. Oxaliplatin-induced sinusoidal obstruction syndrome mimicking metastatic colon cancer in the liver. Oncol Lett. 2016;11(4):2861–4.
33. Brancatelli G, et al. Focal nodular hyperplasia: CT findings with emphasis on multiphasic helical CT in 78 patients. Radiology. 2001;219(1):61–8.
34. Choi BY, Nguyen MH. The diagnosis and management of benign hepatic tumors. J Clin Gastroenterol. 2005;39(5):401–12.
35. Choi CS, Freeny PC. Triphasic helical CT of hepatic focal nodular hyperplasia: incidence of atypical findings. AJR Am J Roentgenol. 1998;170(2):391–5.
36. Zech CJ, et al. Diagnostic performance and description of morphological features of focal nodular hyperplasia in Gd-EOB-DTPA-enhanced liver magnetic resonance imaging: results of a multicenter trial. Investig Radiol. 2008;43(7):504–11.
37. Grazioli L, et al. Hepatocellular adenoma and focal nodular hyperplasia: value of gadoxetic acid-enhanced MR imaging in differential diagnosis. Radiology. 2012;262(2):520–9.
38. Mohajer K, et al. Characterization of hepatic adenoma and focal nodular hyperplasia with gadoxetic acid. J Magn Reson Imaging. 2012;36(3):686–96.
39. Choi JY, et al. Focal nodular hyperplasia or focal nodular hyperplasia-like lesions of the liver: a special emphasis on diagnosis. J Gastroenterol Hepatol. 2011;26(6):1004–9.
40. Radiology, A.C.o., American College of Radiology. Liver imaging reporting and data system in Version 2017.
41. Choi JY, Lee JM, Sirlin CB. CT and MR imaging diagnosis and staging of hepatocellular carcinoma: part II. Extracellular agents, hepatobiliary agents, and ancillary imaging features. Radiology. 2014;273(1):30–50.
42. Hope TA, et al. Hepatobiliary agents and their role in LI-RADS. Abdom Imaging. 2015;40(3):613–25.
43. Suh YJ, et al. Differentiation of hepatic hyperintense lesions seen on gadoxetic acid-enhanced hepatobiliary phase MRI. AJR Am J Roentgenol. 2011;197(1):W44–52.
44. Elder RW, Parekh S, Book WM. More on hepatocellular carcinoma after the Fontan procedure. N Engl J Med. 2013;369(5):490.
45. Ewe SHT, Ju L. Hepatotocellular carcinoma—a rare complication post Fontan operation. Congenit Heart Dis. 2009;4(2):103–6.
46. Ghaferi AA, Hutchins GM. Progression of liver pathology in patients undergoing the Fontan procedure: chronic passive congestion, cardiac cirrhosis, hepatic adenoma, and hepatocellular carcinoma. J Thorac Cardiovasc Surg. 2005;129(6):1348–52.

47. Josephus Jitta D, et al. Three cases of hepatocellular carcinoma in Fontan patients: review of the literature and suggestions for hepatic screening. Int J Cardiol. 2016;206:21–6.
48. Rajoriya N, et al. A liver mass post-Fontan operation. QJM. 2014;107(7):571–2.
49. Rosenbaum J, et al. Cardiac cirrhosis and hepatocellular carcinoma in a 13-year-old treated with doxorubicin microbead transarterial chemoembolization. J Paediatr Child Health. 2012;48(3):E140–3.
50. Saliba T, et al. Hepatocellular carcinoma in two patients with cardiac cirrhosis. Eur J Gastroenterol Hepatol. 2010;22(7):889–91.
51. Yamada K, et al. Transarterial embolization for pediatric hepatocellular carcinoma with cardiac cirrhosis. Pediatr Int. 2015;57(4):766–70.

Chapter 10
Fibrolamellar Carcinoma

Scott M. Thompson, Michael S. Torbenson, Lewis R. Roberts, and Sudhakar K. Venkatesh

Introduction

Fibrolamellar carcinoma (FLC) is a rare primary liver cancer that characteristically presents in teenagers or young adults without any prior history of chronic liver disease. In part because of the absence of known liver disease and the young age of the patients, the tumor is typically not diagnosed until patients become symptomatic, usually with vague or increasing abdominal pain or a palpable mass. The symptoms are frequently initially attributed to causes other than a malignant tumor. Consequently, the tumors are commonly large and sometimes metastatic to other sites by the time of diagnosis. Epidemiologically, FLC is rare, representing about 1–5% of all primary liver malignancies, with an age-adjusted incidence of 0.02 per 100,000 persons per year in the United States [1]. US population-based studies using cancer registries of the Surveillance, Epidemiology, and End Results

S. M. Thompson (✉)
Department of Radiology, Mayo Clinic, Rochester, MN, USA
e-mail: thompson.scott@mayo.edu

M. S. Torbenson
Department of Laboratory Medicine and Pathology, Mayo Clinic, Rochester, MN, USA
e-mail: torbenson.michael@mayo.edu

L. R. Roberts
Division of Gastroenterology and Hepatology, Mayo Clinic, Rochester, MN, USA
e-mail: roberts.lewis@mayo.edu

S. K. Venkatesh
Department of Radiology, Mayo Clinic, Rochester, MN, USA
e-mail: venkatesh.sudhakar@mayo.edu

L. R. Roberts et al. (eds.), *Evaluation and Management of Liver Masses*,
https://doi.org/10.1007/978-3-030-46699-2_10

(SEER) Program have described two age-specific incidence peaks from 10–30 years and 70–79 years of age. FLC occurs with equal frequency in males and females [2]. The incidence rates of FLC remained relatively stable between 2000 and 2010. In terms of prognosis, recent studies suggest that the outcomes of patients with FLC up to 39 years in age were better than those of patients with primary hepatocellular carcinoma (HCC), but this difference in outcome was not seen in older patients [2].

Genetically, almost all FLCs are characterized by a single 400 kb deletion in chromosome 19 that results in a distinctive fusion between the heat-shock protein DNAJB1 and protein kinase A (PRKACA) genes, which leads to formation of J-PKAcα, a kinase fusion chimera of the J domain of DnaJB1 with PKAcα, which exhibits constitutive activation of protein kinase A [3].

Comparison of the crystal structure of the chimeric fusion $RI\alpha_2$:J-$PKAc\alpha_2$ holoenzyme formed by J-PKAcα and the PKA regulatory (R) subunit RIα to the structure of the wild-type (WT) $RI\alpha_2$:$PKAc\alpha_2$ holoenzyme suggests substantial differences that may potentially be exploited in the development of novel therapeutics against the fusion enzyme [4]. A small percentage of FLCs occur in patients with the Carney complex. In these patients, the tumors show mutations of the PRKAR1A gene instead of the classic DNAJB1–PRKACA fusion.

Pathologic Features of Fibrolamellar Carcinoma

FLCs occur in noncirrhotic livers and are not associated with underlying liver disease. The tumors have a median age of presentation of about 25 years, with 85% of all cases presenting before the age of 35 [5]. There is no strong gender predilection.

Histologically, FLCs are composed of eosinophilic tumor cells with abundant cytoplasm and prominent nucleoli (Fig. 10.1). The abundant cytoplasm is filled

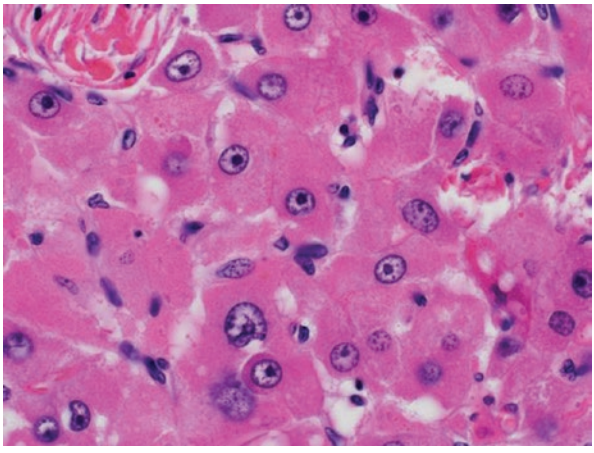

Fig. 10.1 Fibrolamellar carcinoma, morphology. The tumor cells have abundant eosinophilic cytoplasm and prominent nucleoli

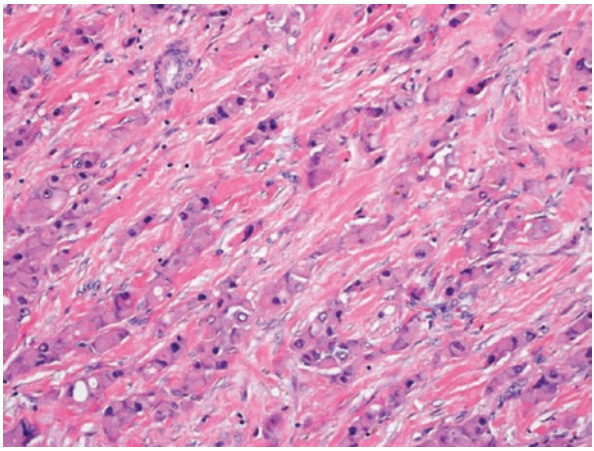

Fig. 10.2 Fibrolamellar carcinoma, intratumoral fibrosis. The fibrosis in this image is dense and runs in parallel bands

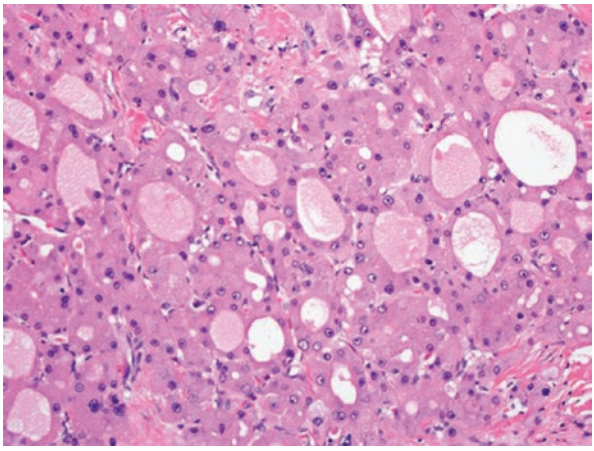

Fig. 10.3 Fibrolamellar carcinoma, intratumoral fibrosis. Pseudoglands are prominent in this image

with mitochondria and lysosomes. FLCs commonly have striking intratumoral fibrosis (Fig. 10.2). The fibrosis can be organized into somewhat parallel, or lamellar, bands, or can be more haphazard in organization. In some areas of the tumor, the fibrosis can be sparse or absent. The three findings of large eosinophilic cells, prominent nucleoli, and intratumoral fibrosis are considered key diagnostic findings.

There are a number of other common histological features of FLC. The tumor can form pseudoglandular structures composed of tumor cells surrounding a central area containing tumor secretions (Fig. 10.3). Individual tumor cells often have pale bodies or hyaline bodies, can show bile production, and occasionally have macrovesicular steatosis. Small calcifications can be found either as single calcified tumor cells or as small calcified foci in the fibrous bands.

The clinical and histological findings can strongly suggest the diagnosis of FLC, but they are not perfectly specific, nor are immunostains that are used to

demonstrate hepatic differentiation, as FLCs are positive for hepatocyte markers such as HepPar1 and arginase. In the context of comparable morphology, coexpression of CD68 (a marker of lysosomes) and CK7 can help confirm the diagnosis of FLC [6]. Essentially all sporadic FLCs have a somatic microdeletion that leads to a DNAJB1–PRKACA fusion [3], which is a major driver of tumorigenesis. FISH-based molecular tests can detect this molecular event and have been validated for clinical care on cytology, biopsy, and resection specimens [7]. Generation of the Dnajb1–Prkaca fusion gene in the liver of wild-type mice using Crispr-Cas technology and hydrodynamic tail vein injection has been shown to be sufficient to initiate development of tumors bearing many features of human FLC [8]. In keeping with the unique molecular etiology of FLC, comprehensive analysis of FLC specimens included in the Cancer Genome Atlas project revealed a distinctive gene and non-coding RNA signature of FLC [9].

A small subset of FLC occurs in individuals with the Carney complex, a rare multiple endocrine and nonendocrine neoplastic syndrome first described in 1985 by J Aidan Carney as a "complex of myxomas, spotty pigmentation and endocrine overactivity" [10, 11]. The Carney complex can be familial or occur sporadically. Individuals with the Carney complex may have spotty skin pigmentation, cardiac and other myxomas, endocrine tumors, and psammomatous melanotic schwannomas. Carney complex is characterized by germline or somatic mutations in the PRKAR1A gene, which encodes the regulatory unit of protein kinase A (RIα). The mutations lead to loss of function of the regulatory unit, resulting in decreased basal PKA activity, but an increase in cAMP-stimulated activity which appears to induce tumor formation [12, 13].

FLCs developing in the setting of the DNAJB1–PRKACA fusion as well as the Carney complex PRKAR1A gene mutations are histologically identical [11].

FLC can be associated with the clinical syndrome of noncirrhotic hyperammonemic encephalopathy [14]. The diagnosis requires a high index of suspicion, as the clinical features can be subtle [15]. A number of potential mechanisms can contribute to this syndrome, which can be exacerbated by the use of catabolic steroids. It has been proposed that pathophysiologic overexpression of the chimeric J-PKAcα fusion kinase results in downstream overexpression of Aurora Kinase A, driving expression of the c-Myc oncogene. This results in ornithine decarboxylase dysfunction and leads to depletion of amino acids crucial to urea cycle function [16]. Dysfunction of the urea cycle leads to accumulation of ammonia in the bloodstream and encephalopathy. The appreciation that urea cycle dysfunction due to metabolite consumption is responsible for the hyperammonemia has led to the development of a rational treatment paradigm based on the use of the ammonia scavenging drugs sodium benzoate and phenylbutyrate in combination with supplementation of the relevant amino acids citrulline, ornithine and arginine. This approach has achieved complete recovery from hyperammonemic encephalopathy in affected patients, resulting in substantial reductions in the mortality of FLC-related hyperammonemic encephalopathy [17]. However, not all FLC patients with hyperammonemic encephalopathy show evidence of urea cycle abnormalities [18].

Imaging Features of Fibrolamellar Carcinoma

FLC usually presents with a large mass associated with lymphadenopathy at the time of diagnosis. Due to their higher prevalence in children and young adults, ultrasound is often the first imaging modality performed. Further evaluation is then performed with computed tomography (CT) or magnetic resonance imaging (MRI) (Table 10.1).

Table 10.1 Imaging features of fibrolamellar hepatocellular carcinoma (FL-HCC)

Modality	Description	Comments
Grayscale US		
Size	Large, solitary	
Margins	Well-defined, lobulated	
Echogenicity	Variable	
Central scar	Hypoechoic	
Calcifications	Common	Calcifications are better seen on CT
Color Doppler US	Increased vascularity	
Contrast-enhanced US (CEUS)	AP: Heterogeneous enhancement PV/DP: Variable washout	Enhancement features are similar to other primary liver tumors
CT		Rare intratumoral cystic change/ necrosis or hemorrhage. No macroscopic fat
Size	Large, solitary	
Margins	Well-circumscribed, lobulated	
Non-contrast attenuation	Hypodense	
Enhancement	Art: Heterogeneously hyperenhancing PV: Variable DP: Variable	Features may simulate a hepatocellular carcinoma (HCC).
Central scar	Hypodense. May show delayed enhancement	
Calcifications	Common (best seen)	
Vascular/biliary invasion	Uncommon	
Biliary ductal dilatation	Uncommon	
Lymphadenopathy	Common (>50%)	A differentiating feature from HCC
MRI		
Size	Large, solitary	
Margins	Well-circumscribed, lobulated	
Signal	T1W: Hypointense > isointense T2W: Mildly hyperintense DWI: Hyperintense	Rare intratumoral cystic change/ necrosis or hemorrhage. No macroscopic fat. Presence of fat should raise suspicion of HCC

(continued)

Table 10.1 (continued)

Modality	Description	Comments
Enhancement (ECM)	Art: Heterogeneously hyperenhancing PV: Variable, iso to hypoenhancing DP: Variable, iso to hypoenhancing	
Enhancement (HBCA)	Homogenously hypoenhancing	
Central scar	T1W: Hypointense T2W: Hypointense May show delayed enhancement	Rarely T2W hyperintense scar may simulate scar in focal nodular hyperplasia
Calcifications	Not well seen	
Vascular/biliary invasion	Uncommon	
Biliary ductal dilatation	More common than at CT	
FDG-PET/CT	FDG avid (few cases)	May be useful for initial staging, re-staging and/or detection of occult lymph node metastasis
Nuclear scintigraphy		No longer used
Tc-99 m sulfur colloid	Photopenic defect	Previously useful for differentiating FNH from FLC
Tc-99 m RBCs	Arterial: Increased activity Delayed: Decreased activity	
Catheter angiography	Hypervascular mass with a hypovascular central scar (if present) Arteriovenous, arterioportal shunting and portal vein tumor thrombus rare	No longer used for diagnosis; may be used during locoregional therapy (TAE, TACE, TARE).

US ultrasound, *CT* computed tomography, *MRI* magnetic resonance imaging, *FDG* fluorodeoxyglucose, *PET* positron emission tomography, *Tc-99 m* technetium 99 m, *RBCs* red blood cells, *Art* arterial phase, *PV* portal venous phase, *DP* delayed phase, *T1W* T1-weighted, *T2W* T2-weighted, *DWI* diffusion weighted imaging, *HCC* hepatocellular carcinoma; *ECM* extracellular contrast medium, *HBCA* hepatobiliary contrast agent, *TAE* transarterial embolization, *TACE* transarterial chemoembolization, *TARE* transarterial radioembolization

Ultrasound (US) (Fig. 10.4)

Ultrasound features of FLC are nonspecific. Grayscale ultrasound typically shows a large, well-defined, lobulated mass of variable echogenicity ranging from hyperechoic to hypoechoic to mixed [19–23]. A hypoechoic central scar and small, focal calcifications may be seen. Color-Doppler and spectral US may show increased tumor vascularity with a low-resistance arterial waveform in the setting of arteriovenous shunting [24]. Contrast-enhanced ultrasound (CEUS) may be useful to show similar enhancement characteristics to dynamic contrast-enhanced CT (CE-CT) or MRI (CE-MRI) [25].

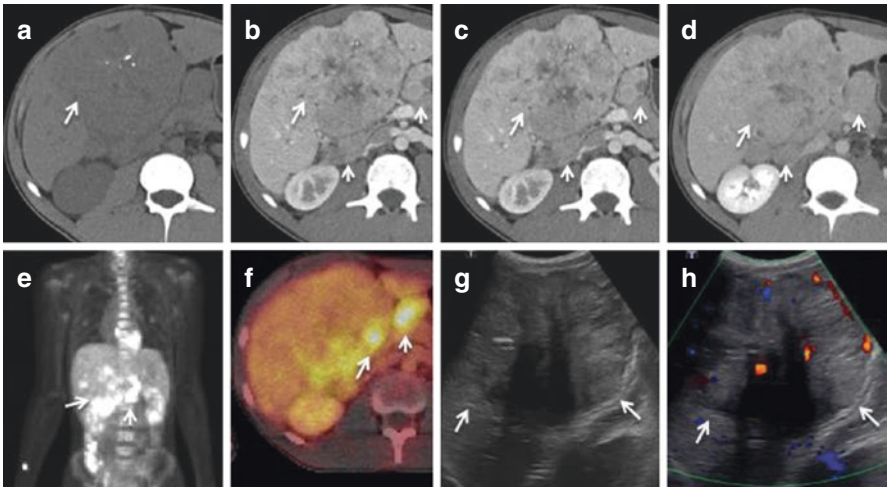

Fig. 10.4 A 16-year-old male with a 12.5 cm fibrolamellar carcinoma in hepatic segment IVb. The mass is (**a**) mildly hypodense with several central calcifications on noncontrast CT (white arrow) and shows (**b**) heterogeneous arterial phase enhancement with a hypoenhancing central scar (white arrow) that shows (**c**–**d**) progressive enhancement on (**c**) portal venous and (**d**) delayed phase imaging (white arrow). (**b**–**d**) Numerous enlarged gastrohepatic and perihepatic lymph nodes (short white arrow). (**e**–**f**) Coronal MIP 18F-FDG-PET and (**f**) PET/CT show heterogeneous hypermetabolism in the periphery of the hepatic mass (white arrow) as well as FDG avid right cardiophrenic angle, gastrohepatic ligament, and perihepatic lymph node metastases (short white arrow). (**g**) Grayscale and (**h**) color Doppler ultrasound show a large, lobulated mass with mixed echogenicity, central posterior acoustic shadowing, and mild vascularity. (*18F-FDG* 18F-fluorodeoxyglucose, *PET* positron emission tomography, *CT* computed tomography)

Computed Tomography (CT) (Fig. 10.4)

Computed tomography often shows a large (>10 cm), solitary, well-circumscribed, lobulated mass that is heterogeneously hypoattenuating (75%–100%) on noncontrast-enhanced imaging [19–23, 26–28]. Less commonly, satellite nodules within the liver may be seen [20]. Intratumoral areas of cystic change, necrosis, and hemorrhage are often present but no gross macroscopic fat [27, 28]. Most FLCs are heterogeneously hyperenhancing at arterial phase contrast-enhanced imaging (80%–100%) [19, 22, 26–28]. However, FLCs show more heterogeneous enhancement during portal venous imaging (hypoenhancing 36%; isoenhancing 48%; hyperenhancing 16%) and delayed phase imaging (hypoenhancing 56%; isoenhancing 22%; hyperenhancing 22%) [26, 28]. A central, stellate, hypodense scar with or without radiating septa/fibrosis is present in 33%–71% of FLCs [19, 22, 23, 26–28]. The central scar is frequently hypoenhancing during arterial and portal venous phase imaging but may rarely show mild delayed phase enhancement [26–28]. Small, predominantly central focal calcifications have been reported in 40% to 95% of FLCs [19, 20, 22, 23, 26–28]. Macroscopic vascular invasion (10%–22%),

intrahepatic biliary ductal dilatation (40%), and ascites (35%) are less commonly seen (40%) [22, 27]. Lymphadenopathy (>1 cm short-axis), particularly hilar as well as upper abdominal and retroperitoneal, may be seen in up to two-thirds of patients at the time of diagnosis [22, 26, 28]. The combination of young age at presentation, absence of chronic liver disease, large heterogeneous mass, hypoenhancing scar, presence of calcification and lymphadenopathy is highly suggestive of FLC.

Magnetic Resonance Imaging (MRI) (Fig. 10.5)

Magnetic resonance imaging often shows a large (>10 cm), solitary, well-circumscribed and lobulated mass that is homogenously hypointense on T1-weighted imaging (T1W; 62%–100%) and heterogeneously hyperintense on T2-weighted imaging (T2W; 54%–100%) [21, 23, 27–30]. A T1W and T2W hypointense capsule (36%) and intratumoral areas of cystic change/necrosis (36%) and hemorrhage (22%) have been reported less commonly. There is no macroscopic intratumoral fat on T1-weighted or in-phase and opposed-phase imaging [27–29]. At contrast-enhanced MRI using extracellular gadolinium agents, most FLCs are heterogeneously hyperenhancing at arterial phase imaging (81%–100%) [27–30]. Similar to CT, FLCs show more heterogeneous enhancement during portal venous phase imaging (hypoenhancing 67%, isoenhancing 33%) and more homogenous enhancement during delayed phase imaging [29, 30]. Palm et al. noted arterial phase hyperenhancement (APHE) and portal venous phase washout (PVWO) in 3 of 6 patients, findings more commonly seen in classical HCC [30]. In three small series, 100% of FLCs showed homogenous hypoenhancement at delayed phase imaging with hepatobiliary contrast agents [27,

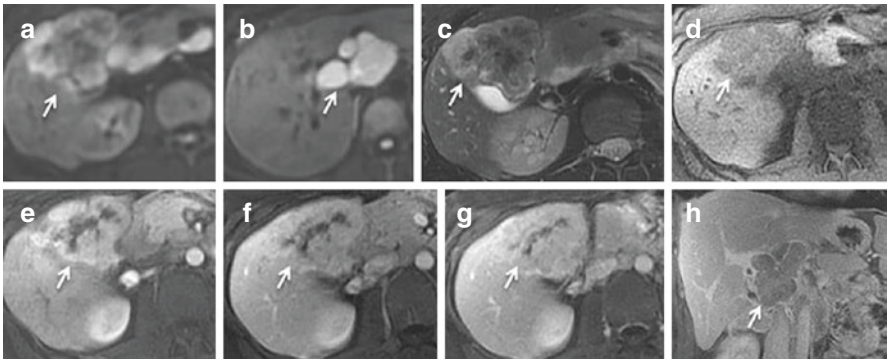

Fig. 10.5 A 33-year-old female with a 6.5 cm fibrolamellar carcinoma within hepatic segment IVb/V. (**a**) On MRI, the mass shows mild heterogeneous DWI hyperintensity (white arrow). (**b**) There are numerous DWI hyperintense periportal lymph nodes (white arrow) which show (**h**) washout on portal venous phase imaging. The mass shows (**c**) mild T2-weighted hyperintensity, (**d**) T1-weighted hypointensity, (**e**) arterial phase hyperenhancement (white arrow) and (**f–g**) portal venous, and delayed phase isointensity (white arrow). There is a (**a**) DWI hypointense and (**c**) T2 hypointense irregularly shaped central scar with (**e–g**) heterogeneous delayed enhancement

28, 30]. Diffusion-weighted imaging (DWI) has infrequently been reported in FLCs, but in a few studies, the majority of FLCs are hyperintense at DWI (83%–100%) [27, 30]. A central, stellate, T1W and T2W hypointense scar with or without radiating septa/fibrosis is present in 46%–86%% of FLCs [27–29]. Rarely the central scar may be T2W hyperintense (8%), which may mimic focal nodular hyperplasia (FNH) [29]. The central scar is typically homogenously hypoenhancing during arterial phase imaging but mildly hyperenhancing during portal venous and delayed phase imaging [29, 31]. Small calcifications are not well seen at MRI. Macroscopic vascular invasion (17%–18%) and bile duct invasion (17%) are less commonly seen while intrahepatic biliary ductal dilatation (50%–72%) and ascites (64%) are reported in a higher proportion of cases [27, 30]. MR elastography (MRE) has been studied in HCC, but not FLC [32].

Positron Emission Tomography (PET) (Fig. 10.4)

The role of 18-fluorodeoxyglucose (18F-FDG)-positron emission tomography/computed tomography (PET/CT) in FLC has not been systemically evaluated. However, case reports and small series suggest that FLCs may be FDG avid and FDG PET/CT may be useful for initial staging and restaging of intrahepatic and extrahepatic FLC in conjunction with dedicated CT or MRI, particularly for detection of occult lymph node metastases [21, 33–35].

Nuclear Medicine Scintigraphy

Nuclear medicine scintigraphy techniques have been replaced by CE-CT and CE-MRI. Historically, technetium-99 m (Tc-99 m)-sulfur colloid scintigraphy was useful for differentiating FLC from FNH. Sulfur colloid is taken up by the reticuloendothelial system, particularly the Kupffer cells within the liver. Given the presence of Kupffer cells within FNH, FNH shows focal sulfur colloid uptake while FLC appears as a photopenic defect [20, 23, 29]. In the AFIP series, 100% of FLCs were photopenic at Tc-99 m-sulfur colloid scintigraphy [29]. Tc99m-red blood cell (RBC) scintigraphy would show increased activity during arterial phase imaging and washout resulting in photopenia during delayed phase imaging [29].

Catheter Angiography

Catheter angiography is no longer routinely used in the diagnosis of FLC but rather in the setting of hepatic locoregional therapies, including transarterial embolization (TAE) or radioembolization (TARE). At angiography, FLC typically appears as a

hypervascular mass with enlarged feeding arteries, a hypovascular central scar and mildly enhancing fibrous septa. Arteriovenous and arterioportal shunting and portal vein tumor thrombus are rare, unlike with classic HCC [19, 20, 22, 23, 29].

Posttreatment Follow-Up

Intrahepatic FLC recurrence following resection has similar US, CT, and MRI imaging characteristics to the primary tumor, but calcifications are not usually present [31, 36].

Surgical Treatment of Fibrolamellar Carcinoma

Patients with a single large FLC and normal liver function are candidates for surgical resection with curative intent usually performed with concomitant lymph node dissection. Unfortunately, up to 40% of patients have positive surgical margins after resection and a similar proportion have evidence of vascular invasion. This results in high rates of recurrent disease, most typically in the liver, regional or adjacent lymph nodes, or the lungs. Even in the presence of lymph node or other metastatic disease, aggressive surgical resection in conjunction with other treatment modalities has proven to be the most effective treatment for FLC. Consequently, patients will often receive multiple surgical treatments during the course of the disease [37]. Due to the high propensity for metastases, except in exceptional circumstances, liver transplantation is usually not considered a viable option for treatment. In patients with FLC treated by surgical resection, the presence of multiple tumor nodules [hazard ratio (HR) 3.15, 95% confidence interval (CI) 1.2–8.6], elevated serum alpha fetoprotein (AFP) >15 ng/mL (HR 2.81, 95% CI 1.08–7.33), and positive regional lymph nodes (HR 2.83, 95% CI 1.15–6.96) were independently associated with worse survival [38]. Overall, there was no difference in a 5-year survival between patients with FLC and those with HCC who received treatment with curative intent, including surgical resection, local ablation, or liver transplantation [2].

Nonsurgical Treatment of Fibrolamellar Carcinoma

Local Ablation and Locoregional Treatment

In the rare instance when a single FLC tumor is <3 cm at the time of diagnosis, local ablation with microwave or radiofrequency ablation can be used with curative intent. Patients who are not candidates for surgical resection are considered for

loco-regional treatment with transarterial hepatic artery embolization (HAE), chemoembolization (TACE), or radioembolization using Y90 impregnated glass microspheres or resin beads (TARE). These local and locoregional therapies are discussed in more detail in Chapter 1. In patients who respond to locoregional therapy, combined treatment with subsequent surgical resection is encouraged if feasible [39].

Systemic Therapy

Thus far, there have been no approved agents shown to effectively target FLC. Standard antineoplastic systemic chemotherapies are usually used for treatment of FLC, including gemcitabine, cisplatin, oxaliplatin, 5-fluorouracil, cyclophosphamide, and interferon. Anti-angiogenic agents such as thalidomide have also been used [40]. Immune checkpoint inhibitors such as nivolumab have not proven to be effective.

The identification of the fusion protein of DNAJB1 with PRKACA as the driving oncogene in FLC has prompted an active investigative effort to identify effective systemic therapeutic options against FLC. The recent observation of mammalian target of rapamycin 1 (mTORC1) activity in FLC, based on the increased expression of phospho-S6 (pS6) in FLC, has stimulated interest in the potential efficacy of the mTOR inhibitor everolimus in FLC. Indeed, in a case report, a patient with end-stage FLC that was found to stain positive for pS6 by immunohistochemistry showed a substantial response to everolimus lasting about 10 months, before developing resistance and eventually fatal progression [41]. Unfortunately, a Phase II study comparing everolimus versus estrogen deprivation therapy using the combination of letrozole and leuprolide versus everolimus plus combination letrozole and leuprolide (NCT01642186) failed to show a benefit of everolimus.

Although there is no difference in survival outcomes of FLC patients receiving curative treatment compared to patients with HCC, there is a substantial difference in overall outcomes of FLC patients compared to HCC patients, with FLC patients achieving better 5-year survival of 34% overall, compared to 16% 5-year survival of patients with HCC [2].

References

1. El-Serag HB, Davila JA. Is fibrolamellar carcinoma different from hepatocellular carcinoma? A US population-based study. Hepatology. 2004;39(3):798–803.
2. Eggert T, McGlynn KA, Duffy A, Manns MP, Greten TF, Altekruse SF. Fibrolamellar hepatocellular carcinoma in the USA, 2000-2010: a detailed report on frequency, treatment and outcome based on the surveillance, epidemiology, and end results database. United European Gastroenterol J. 2013;1(5):351–7.

3. Honeyman JN, Simon EP, Robine N, Chiaroni-Clarke R, Darcy DG, Lim II, et al. Detection of a recurrent DNAJB1-PRKACA chimeric transcript in fibrolamellar hepatocellular carcinoma. Science. 2014;343(6174):1010–4.
4. Cao B, Lu TW, Martinez Fiesco JA, Tomasini M, Fan L, Simon SM, et al. Structures of the PKA RIalpha holoenzyme with the FLHCC driver J-PKAcalpha or wild-type PKAcalpha. Structure. 2019;27(5):816–28 e4.
5. Torbenson M. Review of the clinicopathologic features of fibrolamellar carcinoma. Adv Anat Pathol. 2007;14(3):217–23.
6. Ross HM, Daniel HD, Vivekanandan P, Kannangai R, Yeh MM, Wu TT, et al. Fibrolamellar carcinomas are positive for CD68. Mod Pathol. 2011;24(3):390–5.
7. Graham RP, Yeh MM, Lam-Himlin D, Roberts LR, Terracciano L, Cruise MW, et al. Molecular testing for the clinical diagnosis of fibrolamellar carcinoma. Mod Pathol. 2018;31(1):141–9.
8. Engelholm LH, Riaz A, Serra D, Dagnaes-Hansen F, Johansen JV, Santoni-Rugiu E, et al. CRISPR/Cas9 engineering of adult mouse liver demonstrates that the Dnajb1-Prkaca gene fusion is sufficient to induce tumors resembling Fibrolamellar hepatocellular carcinoma. Gastroenterology. 2017;153(6):1662–73 e10.
9. Dinh TA, Vitucci EC, Wauthier E, Graham RP, Pitman WA, Oikawa T, et al. Comprehensive analysis of the Cancer genome atlas reveals a unique gene and non-coding RNA signature of fibrolamellar carcinoma. Sci Rep. 2017;7:44653.
10. Carney JA, Gordon H, Carpenter PC, Shenoy BV, Go VL. The complex of myxomas, spotty pigmentation, and endocrine overactivity. Medicine (Baltimore). 1985;64(4):270–83.
11. Graham RP, Lackner C, Terracciano L, Gonzalez-Cantu Y, Maleszewski JJ, Greipp PT, et al. Fibrolamellar carcinoma in the Carney complex: PRKAR1A loss instead of the classic DNAJB1-PRKACA fusion. Hepatology 2018;68(4):1441–47. https://doi.org/10.1002/hep.29719.
12. Kirschner LS, Carney JA, Pack SD, Taymans SE, Giatzakis C, Cho YS, et al. Mutations of the gene encoding the protein kinase a type I-alpha regulatory subunit in patients with the Carney complex. Nat Genet. 2000;26(1):89–92.
13. Casey M, Vaughan CJ, He J, Hatcher CJ, Winter JM, Weremowicz S, et al. Mutations in the protein kinase a R1alpha regulatory subunit cause familial cardiac myxomas and Carney complex. J Clin Invest. 2000;106(5):R31–8.
14. Sethi S, Tageja N, Singh J, Arabi H, Dave M, Badheka A, et al. Hyperammonemic encephalopathy: a rare presentation of fibrolamellar hepatocellular carcinoma. Am J Med Sci. 2009;338(6):522–4.
15. Cho J, Chen JCY, Paludo J, Conboy EE, Lanpher BC, Alberts SR, et al. Hyperammonemic encephalopathy in a patient with fibrolamellar hepatocellular carcinoma: case report and literature review. J Gastrointest Oncol. 2019;10(3):582–8.
16. Surjan RC, Dos Santos ES, Basseres T, Makdissi FF, Machado MA. A proposed Physiopathological pathway to Hyperammonemic encephalopathy in a non-cirrhotic patient with Fibrolamellar hepatocellular carcinoma without ornithine Transcarbamylase (OTC) mutation. Am J Case Rep. 2017;18:234–41.
17. Thakral N, Simonetto DA. Hyperammonemic encephalopathy: an unusual presentation of fibrolamellar hepatocellular carcinoma. Clin Mol Hepatol. 2020;26(1):74–7.
18. Suarez O, Perez M, Garzon M, Daza R, Hernandez G, Salinas C, et al. Fibrolamellar hepatocellular carcinoma and noncirrhotic Hyperammonemic encephalopathy. Case Reports Hepatol. 2018;2018:7521986.
19. Brandt DJ, Johnson CD, Stephens DH, Weiland LH. Imaging of fibrolamellar hepatocellular carcinoma. AJR Am J Roentgenol. 1988;151(2):295–9.
20. Friedman AC, Lichtenstein JE, Goodman Z, Fishman EK, Siegelman SS, Dachman AH. Fibrolamellar hepatocellular carcinoma. Radiology. 1985;157(3):583–7.
21. Ganeshan D, Szklaruk J, Kundra V, Kaseb A, Rashid A, Elsayes KM. Imaging features of fibrolamellar hepatocellular carcinoma. AJR Am J Roentgenol. 2014;202(3):544–52.
22. Soyer P, Roche A, Levesque M, Legmann P. CT of fibrolamellar hepatocellular carcinoma. J Comput Assist Tomogr. 1991;15(4):533–8.

23. Titelbaum DS, Burke DR, Meranze SG, Saul SH. Fibrolamellar hepatocellular carcinoma: pitfalls in nonoperative diagnosis. Radiology. 1988;167(1):25–30.
24. Smith MT, Blatt ER, Jedlicka P, Strain JD, Fenton LZ. Best cases from the AFIP: fibrolamellar hepatocellular carcinoma. Radiographics. 2008;28(2):609–13.
25. Mandry D, Bressenot A, Galloy MA, Chastagner P, Branchereau S, Claudon M. Contrast-enhanced ultrasound in fibro-lamellar hepatocellular carcinoma: a case report. Ultraschall Med. 2007;28(6):547–52.
26. Blachar A, Federle MP, Ferris JV, Lacomis JM, Waltz JS, Armfield DR, et al. Radiologists' performance in the diagnosis of liver tumors with central scars by using specific CT criteria. Radiology. 2002;223(2):532–9.
27. Do RK, McErlean A, Ang CS, DeMatteo RP, Abou-Alfa GK. CT and MRI of primary and metastatic fibrolamellar carcinoma: a case series of 37 patients. Br J Radiol. 2014;87(1040):20140024.
28. Ichikawa T, Federle MP, Grazioli L, Madariaga J, Nalesnik M, Marsh W. Fibrolamellar hepatocellular carcinoma: imaging and pathologic findings in 31 recent cases. Radiology. 1999;213(2):352–61.
29. McLarney JK, Rucker PT, Bender GN, Goodman ZD, Kashitani N, Ros PR. Fibrolamellar carcinoma of the liver: radiologic-pathologic correlation. Radiographics. 1999;19(2):453–71.
30. Palm V, Sheng R, Mayer P, Weiss KH, Springfeld C, Mehrabi A, et al. Imaging features of fibrolamellar hepatocellular carcinoma in gadoxetic acid-enhanced MRI. Cancer Imaging : Official Publication of International Cancer Imaging Society. 2018;18(1):9.
31. Ichikawa T, Federle MP, Grazioli L, Marsh W. Fibrolamellar hepatocellular carcinoma: pre- and posttherapy evaluation with CT and MR imaging. Radiology. 2000;217(1):145–51.
32. Thompson SM, Wang J, Chandan VS, Glaser KJ, Roberts LR, Ehman RL, et al. MR elastography of hepatocellular carcinoma: correlation of tumor stiffness with histopathology features-preliminary findings. Magn Reson Imaging. 2017;37:41–5.
33. Liu S, Wah Chan K, Tong J, Wang Y, Wang B, Qiao L. PET-CT scan is a valuable modality in the diagnosis of fibrolamellar hepatocellular carcinoma: a case report and a summary of recent literature. QJM. 2011;104(6):477–83.
34. Maniaci V, Davidson BR, Rolles K, Dhillon AP, Hackshaw A, Begent RH, et al. Fibrolamellar hepatocellular carcinoma: prolonged survival with multimodality therapy. Eur J Surg Oncol. 2009;35(6):617–21.
35. von Falck C, Rodt T, Shin HO, Knapp WH, Galanski M. F-18 FDG PET imaging of fibrolamellar hepatocellular carcinoma. Clin Nucl Med. 2008;33(9):633–4.
36. Stevens WR, Johnson CD, Stephens DH, Nagorney DM. Fibrolamellar hepatocellular carcinoma: stage at presentation and results of aggressive surgical management. AJR Am J Roentgenol. 1995;164(5):1153–8.
37. Mayo SC, Mavros MN, Nathan H, Cosgrove D, Herman JM, Kamel I, et al. Treatment and prognosis of patients with fibrolamellar hepatocellular carcinoma: a national perspective. J Am Coll Surg. 2014;218(2):196–205.
38. McDonald JD, Gupta S, Shindorf ML, Gamble LA, Ruff SM, Drake J, et al. Elevated Serum alpha-Fetoprotein is Associated with Abbreviated Survival for Patients with Fibrolamellar Hepatocellular Carcinoma Who Undergo a Curative Resection. Ann Surg Oncol. 2020.
39. Mafeld S, French J, Tiniakos D, Haugk B, Manas D, Littler P. Fibrolamellar hepatocellular carcinoma: treatment with Yttrium-90 and subsequent surgical resection. Cardiovasc Intervent Radiol. 2018;41(5):816–20.
40. Okur A, Eser EP, Yilmaz G, Dalgic A, Akdemir UO, Oguz A, et al. Successful multimodal treatment for aggressive metastatic and recurrent fibrolamellar hepatocellular carcinoma in a child. J Pediatr Hematol Oncol. 2014;36(5):e328–32.
41. Bill R, Montani M, Blum B, Dufour JF, Escher R, Buhlmann M. Favorable response to mammalian target of rapamycin inhibition in a young patient with unresectable fibrolamellar carcinoma of the liver. Hepatology. 2018;68(1):384–6.

Chapter 11
Gallbladder Cancer

Amit Mahipal, Anuhya Kommalapati, Sri Harsha Tella, Gaurav Goyal, Tushar C. Patel, Candice A. Bookwalter, Sean P. Cleary, Christopher L. Hallemeier, and Rondell P. Graham

Introduction

Gallbladder cancer (GBC), although considered an uncommon cancer of the gastrointestinal tract, constitutes about two thirds of the malignancies arising from the extrahepatic biliary tract in the United States. Other malignancies associated with the biliary tract including intrahepatic, perihilar and distal cholangiocarcinoma, and ampullary cancers are distinct from gallbladder cancers in their presentation and natural history and are less common. The prognosis of GBC is highly dependent on tumor stage at presentation. Many cases of GBC are identified incidentally during surgery, cholecystectomy, or pathological examination of resected gallbladders.

A. Mahipal (✉) · G. Goyal
Department of Medical Oncology, Mayo Clinic, Rochester, MN, USA
e-mail: mahipal.amit@mayo.edu

A. Kommalapati · S. H. Tella
Department of Internal Medicine, University of South Carolina School of Medicine, Columbia, SC, USA

T. C. Patel
Department of Transplantation, and Division of Gastroenterology and Hepatology, Mayo Clinic, Jacksonville, FL, USA

C. A. Bookwalter
Department of Radiology, Mayo Clinic, Rochester, MN, USA

S. P. Cleary
Department of Surgery, Mayo Clinic, Rochester, MN, USA

C. L. Hallemeier
Department of Radiation Oncology, Mayo Clinic, Rochester, MN, USA

R. P. Graham
Department of Laboratory Medicine and Pathology, Mayo Clinic, Rochester, MN, USA

L. R. Roberts et al. (eds.), *Evaluation and Management of Liver Masses*,
https://doi.org/10.1007/978-3-030-46699-2_11

Given the vague, nonspecific presentation, symptomatic GBC tends to present at an advanced stage, and survival is generally poor, except for the minority of cases that are identified at early stages. Unlike other extrahepatic biliary tract cancers, the presence of jaundice is associated with unresectability, often due to hilar involvement, and the prognosis is poor. Overall, 5-year survival for patients with T1 tumors approaches 50% and is lower for more advanced tumors. In this chapter, we detail the current literature on the pathophysiology, diagnosis, and management of GBC with a special focus on recent advances in the field.

Epidemiology

The incidence of GBC cancer varies widely worldwide depending upon the geographical location and ethnicity. High incidence rates of GBC (>15 per 100,000 women) are seen in Chile, Northern India, and Southern Pakistan followed by Japan and Thailand, while Northern America, parts of western Europe, and Mediterranean Europe have the lowest incidences (<10 per 100,000 women) [1]. Even within the US, the incidence varies depending on ethnic background with a higher incidence in American Indian, Hispanic, and Alaskan native populations, and a lower incidence in African Americans and Caucasians. In addition, the incidence of GBC increases with age, being usually seen in elderly persons (>65 years) with a female predilection [2]. In general, the incidence of GBC varies with the prevalance of two major risk factors, gallstones and typhoid infection, as well as other factors such as environmental exposure to carcinogens, liver fluke infections and patient-related factors such as intrinsic predisposition to tumorigenesis [3].

Etiology

The etiology of GBC is complex, but chronic gallbladder injury and inflammation are the most commonly associated etiological factors for GBC. Proposed risk factors for GBC are summarized in Table 11.1.

Gallstones

Gallstones are present in most (70–90%) patients with gallbladder cancer. The risk is further correlated with the size of the gallstones – the presence of gallstones >3 cm increases the risk of GBC by ten-fold compared to gallstones of size <1 cm [4]. Autopsy data also suggest that gallstones are associated with an almost

Table 11.1 Proposed risk/etiological factors for gallbladder cancer

Gallstones
Chronic inflammation and infection
Congenital anomalies (anomalous pancreatobiliary duct)
Drugs (isoniazid, methyldopa)
Environmental risk factors (exposure to cadmium, nickel, radon)
Porcelain gallbladder
Typhoid carrier
Adenomatous polyp (size of the polyp is strongest predictor of malignant transformation)
Multiparity
Syndromic association (Van-Hippel Lindau syndrome, neurofibromatosis-1)

seven-fold increase in the risk of GBC. Though substantial evidence favors the association between the two diseases, it is not yet clear if the association represents a direct causal link [5, 6]. The presence of gallstones is thought to induce chronic irritation and inflammation of the gallbladder mucosa, thereby leading to dysplasia of mucosal cells. These chronic inflammatory insults may act as inciting agents for oncogenic transformation by causing deoxyribonucleic acid (DNA) damage and DNA methylation defects, as well as by releasing inflammatory cytokines and growth factors leading to angiogenesis [7, 8]. Another possible explanation for the metaplasia-dysplasia transformation of gallbladder epithelium is alteration of the chemical composition of bile leading to the formation of free radical oxidation products and secondary bile acids [9]. However, environmental and genetic factors may also play key roles in the development of GBC, as about 10–25% of patients GBC do not have associated cholelithiasis [5]. The first-line imaging test for evaluation of gallstones is a right upper quadrant abdominal ultrasound (USG). On ultrasound, gallstones are typically mobile, echogenic foci with posterior acoustic shadowing as shown in Fig. 11.1.

Chronic Inflammation

Chronic bacterial infection has been linked to GBC. Bacterial colonization may alter the bile acid milieu. The most common organisms implicated with this association are *Salmonella* (*S. typhi* and *S. paratyphi*) and *Helicobacter* (*H. bilis*) species [10]. Ecologically, there is a geographical correlation between the endemicity of typhoid infection and GBC, especially in Chile and North India [11, 12]. Moreover, a registry-based cohort study concluded that chronic typhoid and paratyphoid carriers showed a large excess risk (observed/expected cases) for GBC (167·0; 95% confidence interval 54·1–389) [13]. Similarly, a 12-fold increase in risk of GBC in patients with a history of typhoid infection (OR = 12.7 [CI, 1.5–598]) was reported

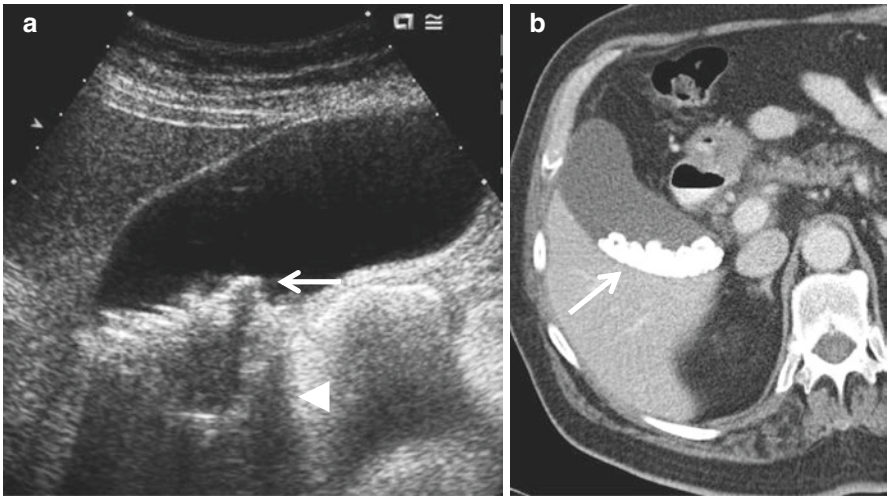

Fig. 11.1 A 79-year-old male patient being evaluated for epigastric pain demonstrates multiple echogenic foci (white arrow) layering within the gallbladder with posterior acoustic shadowing (white arrowhead) within the gallbladder (**a**). The same patient subsequently underwent a CT examination of the abdomen showing radiopaque gallstones (white arrow)

in a case control study [14]. Retrospective case control studies from Japan and Thailand also showed an association of *Helicobacter bilis* with GBC (almost six-fold increase) [10].

About 10–20% of patients with primary sclerosing cholangitis (PSC) will develop hepatobiliary malignancy [15]. PSC is known to cause high frequencies of pyloric metaplasia, intestinal metaplasia/dysplasia, and invasive adenocarcinoma at rates significantly higher than the general population [15]. Retrospective studies found that GB adenocarcinomas arose out of a background of flat mucosal dysplasia, supporting the concept of a metaplasia-dysplasia-carcinoma sequence [16]. Given this strong association, it is recommended that patients with PSC should have annual gallbladder cancer surveillance (abdominal ultrasound screening) to identify gallbladder masses, and cholecystectomy should be performed if any suspicious lesions, polyps, or masses are identified [17].

Calcified/Porcelain Gallbladder

Chronic irritation and inflammation may lead to calcium deposition in the gallbladder wall. The gallbladder calcification can be of distinct types – diffuse intramural calcification (porcelain gallbladder) or isolated mucosal calcification. Calcification within the gallbladder wall is best seen on CT examination, but can also be seen on

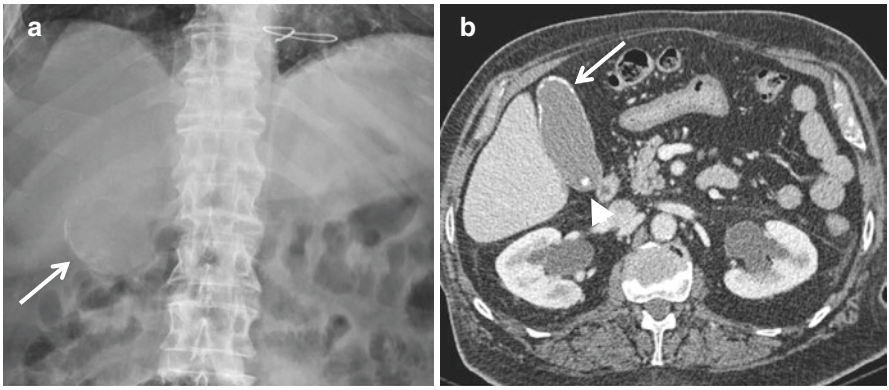

Fig. 11.2 A 72-year-old male with porcelain gallbladder (white arrow) shown on plain frontal supine radiograph of the abdomen (**a**) and CT (**b**). Notice a small radiopaque gallstone in the dependent gallbladder (white arrowhead)

ultrasound or plain X-ray as seen in Fig. 11.2. Based on previous reports, gallbladder calcification is associated with increased risk of GBC (range 2–61%), and the risk is much higher in gallbladders with isolated mucosal calcifications leading to stippled, multiple punctate calcifications (compared to diffuse intramural calcifications) [18, 19]. Hence, gallbladders with partial calcification, stippled, or multiple punctate calcifications warrant extensive evaluation, and prophylactic cholecystectomy may be needed.

Gallbladder Polyps

Gallbladder polyps are present in 5% of the adult population and are usually asymptomatic [16]. Gallbladder polyps can be differentiated from gallstones by their typical sonographic appearance. Polyps are intraluminal, nonmobile, echogenic foci which lack posterior acoustic shadowing (Fig. 11.3). Features of polyps that predict malignancy are: size >1 cm, solitary and/or sessile masses, associated gallstones, a vascular stalk, concomitant PSC or PBC, and most importantly, rapid polyp growth [20]. Cholecystectomy is recommended in polyps with such features. By consensus guidelines, incidentally found gallbladder polyps ≤6 mm in size are considered benign and no further evaluation or follow-up is recommended. Gallbladder polyps measuring 7–9 mm are considered indeterminate and should be followed by serial ultrasonography at 12-month intervals [21]. Whether gallbladder polyps in *BRCA* 1/2 mutation carriers merit cholecystectomy is not conclusively proven, but given the increased risk of biliary cancers, a lower threshold for cholecystectomy is often applied to these patients.

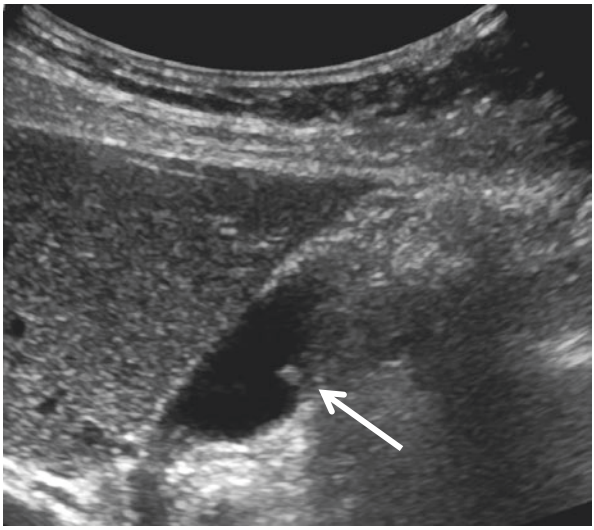

Fig. 11.3 Gallbladder polyp. A 45-year-old female with small 3 mm gallbladder polyp that underwent surveillance and was unchanged compared to the earliest exam, 5 years earlier

Environmental Risk Factors/Exposure to Carcinogens

Various environmental factors such as nickel, cadmium, radon, cigarette smoking, and drugs (methyldopa and isoniazid) have been implicated in the development of GBC. Despite the fact that some studies have hypothesized an etiological role for oral contraceptive pills in GBC, the association remains unclear [16].

Congenital Abnormalities and Association with Hereditary Syndromes

About 10% of GBC patients were have an anomalous junction of the pancreaticobiliary duct leading to regurgitation of pancreatic secretions into the gallbladder. Interestingly, these anomalies are more common in patients of Asian descent, in whom the incidence of GBC is high [16]. It is hypothesized that reflux of pancreatic secretions through the common channel into the biliary tree gives rise to metaplastic and dysplastic changes in the gallbladder mucosa.

Rare cases of GBC are reported in hereditary syndromes such as Gardner Syndrome, NF-1, MEN-1, and Von-Hippel Lindau syndrome (neuroendocrine tumors of gallbladder) [22], as well as in persons with *BRCA2* mutations.

Pathology of GBC

GBC usually leads to asymmetric thickening of the gallbladder wall with infiltration of surrounding structures. Most cancers originate in the gallbladder fundus (60%), followed by the body (30%) and neck (10%) [23]. Macroscopically, GBCs can be divided into papillary, tubular, and nodular forms. Tubular and nodular forms of the disease are aggressive, whereas papillary tumors are less likely to invade the liver directly and have a lower incidence of lymph-node metastasis [5].

Histologically, the majority of carcinomas of the gallbladder are adenocarcinomas (80–95%) and can be papillary, tubular, mucinous (colloid) adenocarcinoma, signet ring adenocarcinoma, cribriform carcinoma, clear cell adenocarcinoma, and hepatoid adenocarcinoma variants. Less common types of GBC include adenosquamous carcinoma, squamous cell carcinoma, and undifferentiated or anaplastic carcinoma (2–7%) [5]. Other rare variants include small-cell carcinoma and neuroendocrine tumors. Involvement of the gallbladder by malignant melanoma, lymphoma, and sarcomas is particularly rare [24].

Two distinct types of precursor lesions are associated with GBC, flat lesions with either low- or high-grade dysplasia and adenomas [25]. Most GBCs arise from flat dysplastic lesions (metaplasia-dysplasia-carcinoma sequence) while mass-forming precursor lesions (adenoma-carcinoma pathway) are identified only in a minority of cases. It is estimated that it takes about 15 years for dysplasia to progress to carcinoma in situ and finally to GBC.

Oncogenes that were shown to be associated with GBC are *KRAS* (10–67%), *HER2 (ERBB2)*, epidermal growth factor receptor (*EGFR*)/HER-1, and cyclins-D1 and E [26]. *KRAS* mutations were seen with high frequency (50–80%) in anomalous pancreatic biliary malformation patients from Japan [27]. *HER2* (transmembrane receptor tyrosine kinase) amplification was reported in 33–70% of GBC cases [28]. *EGFR* (a member of the erbB protein family that also encodes a receptor tyrosine kinase) mutations were identified more often in GBC (70.7%) and dysplastic precancerous lesions (85.7%) than in cases with simple hyperplasia (27%) and normal gallbladder (0%) [29]. Cell cycle progression promoter cyclin D1 overexpression was seen in about 40% of cases of GBC and seemed to be associated with early venous and lymphatic invasion [26]. Tumor suppressor genes that were associated with GBC include *TP53*, *CDKN2A*, p21/CDKN1A (associated with better survival), and Fragile Histidine Triad (FHIT) (frameshift mutations, loss of function). Other studies have identified higher levels of microsatellite instability, angiogenic-inflammatory pathway gene mutations (cyclooxygenase−2 [COX-2], nitric oxide synthase [iNOS], and vascular endothelial growth factor (VEGF)), MUC-1 overexpression (associated with lymphatic spread and poor prognosis), and telomerase (hTERT) re-expression in the pathogenesis of GBC [26].

It is important to understand the mechanism of GBC metastasis for the optimal management approach. As with any other cancer, the common routes of spread of

GBC are direct, lymphatic, vascular, intraperitoneal, intraductal, and neural. Locoregional spread of the disease to adjacent liver segments IV and V or surrounding organs such as the duodenum, colon, peritoneum, or anterior abdominal wall is the most common mode of spread. Peritoneal spread is more common than distant spread. Lymph node metastases typically follow the lymphatic drainage of the gallbladder – gallbladder-retro-pancreatic pathway: involvement of cystic duct and peri-choledochal nodes occurs first, followed by posterior nodes to the head of the pancreas and then to inter-aortocaval lymph nodes; gallbladder-celiac pathway: spreads through the retro-portal and right celiac lymph nodes via gastro-hepatic ligament; gallbladder-mesenteric pathway: spreads to the aortocaval lymph nodes via pancreas [30]. However, involvement of aortocaval nodes can be positive even when cystic nodes are negative [31]. Segment IV of the liver is most commonly involved in cases of vascular metastases due to the direct communicating veins [5]. Distant metastases occur in cases of retroperitoneal vein invasion and are associated with very dismal prognosis and median survival of less than 4 months. Intraductal spread is seen in about 19% of papillary carcinomas. Intraductal growth leads to obstruction of the biliary tree, resulting in early clinical presentation and an overall better prognosis [30].

Clinical Presentation

Most cases of GBC are detected incidentally during surgery for cholecystectomy, or on histologic examination of a resected polyp or may be missed only to present with recurrence during follow-up. Due to the vague or delayed symptomatic presentation of GBC, especially occurring in the background of acute cholecystitis, the disease is usually diagnosed in late stages with dismal prognosis. GBC should be considered in the differential diagnosis if an elderly patient (>65 years) presents with right hypochondrial pain, weight loss, anorexia, and jaundice. Mirizzi syndrome (right upper quadrant pain due to common hepatic duct obstruction caused by extrinsic compression from an impacted stone in the cystic duct or gallbladder), a complication of long-standing cholelithiasis, was shown to be associated with GBC in 5–28% of cases [32, 33]. Patients with advanced GBC may present with a palpable gallbladder mass, hard nodular liver, malignant ascites from carcinomatosis, and jaundice. The presence of jaundice in GBC usually portends a poor prognosis [34]. Only about 20% of the patients have disease confined to the gallbladder at the time of diagnosis. The majority (about 80%) have locoregionally advanced disease with invasion of adjacent structures or distant metastases leading to varied symptoms such as acute abdominal pain due to intestinal perforation, ascites, paraneoplastic syndromes, neuropathy, and venous thromboembolism [5]. GBC should be suspected in patients with a long-standing history of chronic cholecystitis with gallstones who have sudden weight loss and have developed new symptoms of pain.

Diagnostic Evaluation

Imaging Studies

As in any other cancer management, preoperative imaging for tumor recognition and staging play a key role in the appropriate management of GBC. Roentgenographic studies have a relatively high sensitivity for the detection of GBC in advanced stages, but imaging findings of early GBC lesions appear similar to more common benign entities. For example, it is difficult to differentiate between cholecystitis and early carcinoma because thickening of the gallbladder wall is a feature of both diseases [5]. Tumefactive sludge and adenomyomatosis are also benign entities which in some cases can mimic early GBC. Nonetheless, an US can identify findings that are suggestive of GBC such as intramural wall thickening or calcification, polyps, irregular mass, loss of the interface between the liver and gallbladder, or direct liver infiltration. The diagnostic accuracy of polyps or intramural mass in the gallbladder by US is over 80% [20]. A gallbladder mass is shown in Fig. 11.4 with corresponding CT images.

Although US may be a good initial test, it is not very helpful in evaluating extent of locally advanced disease, involved lymph nodes or staging of disease [20]. To better characterize potentially malignant gallbladder lesions, contrast-enhanced magnetic resonance imaging (MRI) is the preferred imaging modality. GBC typically is heterogeneously hyperintense on T2-weighted images and relatively iso- or hypo-intense on T1-weighted images (Fig. 11.5). All GBC show enhancement on contrast-enhanced imaging, but note that imaging appearance can overlap with chronic cholecystitis in early GBC. Focal or diffuse mural thickening of more than 1 cm is highly suggestive of GBC [35]. Early irregular enhancement along the margin and invasion into surrounding structures are also features of GBC. MRI of the

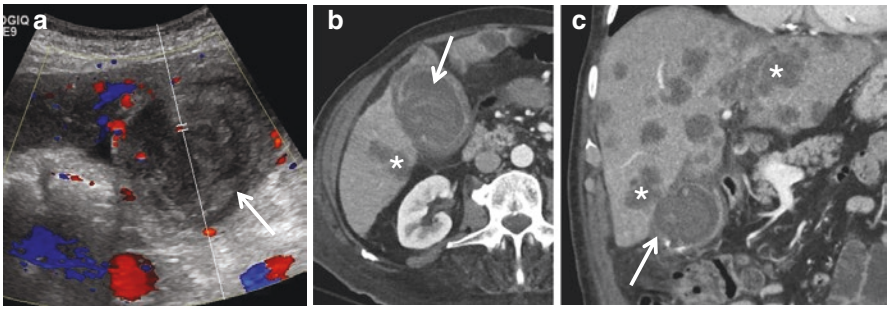

Fig. 11.4 Gallbladder carcinoma with metastatic spread. An 87-year-old male with prior history of cholelithiasis and biliary colic presented with an upper abdominal mass on physical examination and obstructive jaundice. On ultrasound examination, there is a heterogeneous gallbladder mass with internal vascularity (**a**). Subsequent staging CT axial and coronal images (**b** and **c**, respectively) demonstrate an infiltrative gallbladder mass disrupting the enhancing gallbladder wall mucosa and invading the liver (white arrow). Innumerable liver metastases are also seen (white asterisks)

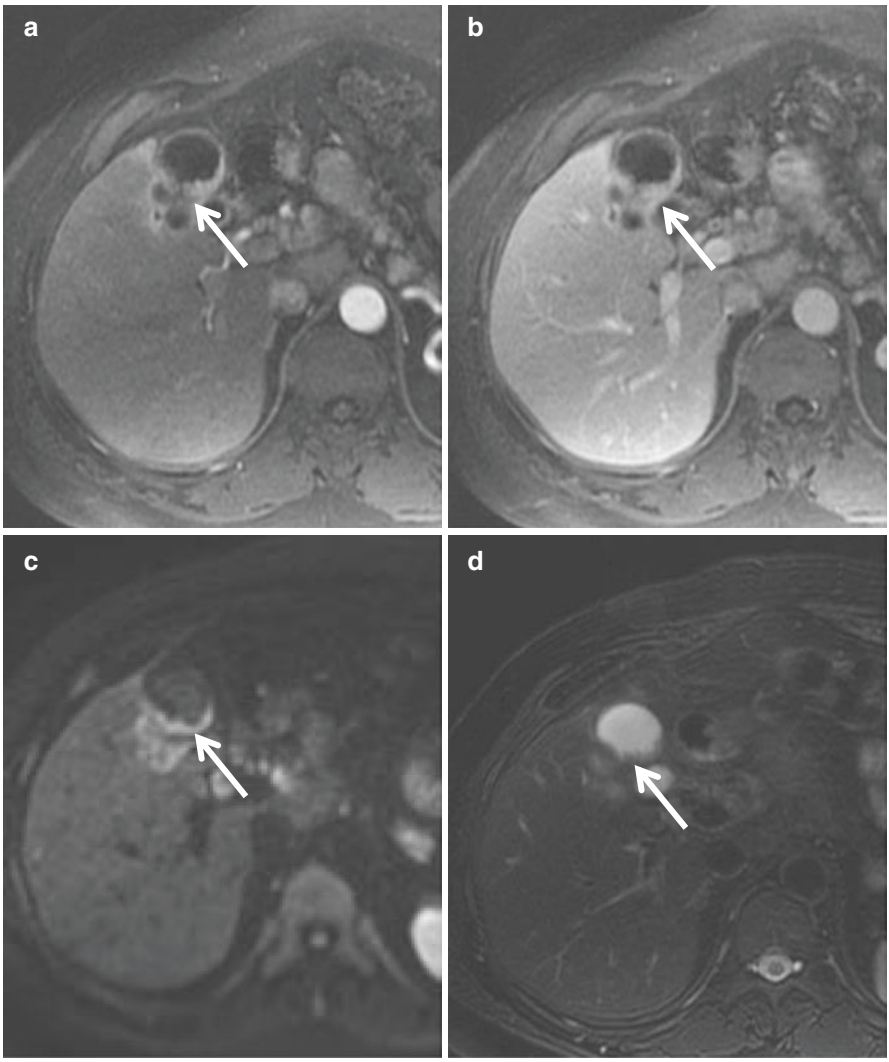

Fig. 11.5 Gallbladder carcinoma with direct invasion into the adjacent liver. A 62-year-old male with gallbladder cancer. Axial arterial phase postcontrast T1-weighted image (**a**), portal venous phase postcontrast T1-weighted image (**b**), high b-value diffusion weighted image (**c**), and T2-weighted image (**d**) all show thickened gallbladder wall infiltrating into the adjacent liver (white arrow)

abdomen is preferred over CT as the former has a better diagnostic accuracy for assessing metastatic spread to the hepatoduodenal ligament, portal vein encasement, regional lymph nodes, and liver [20]. Multiphase MRI with arterial phase images should be obtained to determine the degree of vascular involvement and

anatomic course of the hepatic arteries relative to the tumor mass, which helps the surgeon in determining resectability [20].

For a detailed metastatic survey for the presence of distant metastases, cross-sectional imaging of the chest, abdomen, and pelvis should be obtained using multidetector contrast-enhanced CT [36]. Endoscopic ultrasound is useful for the evaluation and biopsy of regional lymph nodes and should be considered when local expertise is available. Unlike for other cancers, positron emission tomography (PET) scan is not routinely used in GBC management, but it may be selectively utilized when questionable or concerning features for regional or distant metastases are apparent on CT, MRI, or endoscopic retrograde cholangiopancreatography (ERCP).

Laboratory Evaluation

Laboratory studies are neither specific nor sensitive for the diagnosis of GBC. In stage I and II disease, the liver enzymes may not be elevated unless the biliary tract is obstructed. Elevated serum carcinoembryonic antigen (CEA) and serum carbohydrate antigen 19–9 (CA 19–9) in the setting of elevated alkaline phosphatase (ALP) should raise the suspicion of biliary tract or pancreatic malignancy, and GBC should be in the differential. However, it is important to note that serum CA 19–9 can also be raised in the setting of benign biliary obstruction or inflammation, and hence, the serum CA 19–9 should be interpreted cautiously.

Diagnostic Staging Laparoscopy

Metastases of GBC may not always be seen on diagnostic imaging studies. Moreover, the presence of lymph node (LN) disease is often difficult to determine preoperatively as abdominal CT and MRI have a detection rate of only about 24% [37]. Hence, staging laparoscopy is usually performed for better staging of the disease before proceeding to surgery. There is considerable debate about the utility of diagnostic laparoscopy. Based on the analysis of a retrospective study, staging laparoscopy is high yield if T3 disease is suspected on imaging studies or the patient had a poorly differentiated tumor or positive margins on the previously excised mass [38]. To increase sensitivity, laparoscopy can be combined with laparoscopic ultrasound to identify satellite lesions in the liver and other adjacent structures in order to determine the anatomical extension of the tumor and to evaluate for vascular invasion. Inter-aortocaval LN frozen-section evaluation during staging laparoscopy further increases the sensitivity of detection of LN metastases [39].

Table 11.2 AJCC/IUCC 8th edition TNM staging of gallbladder cancer

Primary tumor (T)	
T category	T criteria
TX	Primary tumor cannot be assessed
T0	No evidence of primary tumor
Tis	Carcinoma in situ
T1	Tumor invades the lamina propria or muscular layer
T1a	Tumor invades the lamina propria
T1b	Tumor invades the muscular layer
T2	Tumor invades the perimuscular connective tissue on the peritoneal side, without involvement of the serosa (visceral peritoneum) Or tumor invades the perimuscular connective tissue on the hepatic side, with no extension into the liver
T2a	Tumor invades the perimuscular connective tissue on the peritoneal side, without involvement of the serosa (visceral peritoneum)
T2b	Tumor invades the perimuscular connective tissue on the hepatic side, with no extension into the liver
T3	Tumor perforates the serosa (visceral peritoneum) and/or directly invades the liver and/or one other adjacent organ or structure, such as the stomach, duodenum, colon, pancreas, omentum, or extrahepatic bile ducts
T4	Tumor invades the main portal vein or hepatic artery or invades two or more extrahepatic organs or structures
Regional lymph nodes (N)	
N category	N criteria
NX	Regional lymph nodes cannot be assessed
N0	No regional lymph node metastasis
N1	Metastases to one or three regional lymph nodes
N2	Metastases to four or more regional lymph nodes
Distant metastasis (M)	
M category	M criteria
M0	No distant metastasis
M1	Distant metastasis

Staging of GBC

GBC is staged using the American Joint Committee on Cancer-Tumor Node Metastasis (AJCC TNM) staging system (Table 11.2). According to the eighth edition of the American Joint Committee on Cancer staging manual for gallbladder carcinoma (effective January 1, 2018), primary gallbladder carcinoma can be classified as T1, confined to the lamina propria (T1a) and the muscle layer (T1b) of the gallbladder; T2, extending to the serosa, further classified into T2a (peritoneal side extension) and T2b (hepatic side extension) [40]; T3, perforating the serosa or directly invading one adjacent structure such as liver, stomach, duodenum, colon,

pancreas, omentum, or extrahepatic bile ducts; or T4, invading the main portal vein, the hepatic artery, or multiple extrahepatic organs. GBC disseminates via lymphatic, hematogenous, intraductal (cystic duct) and neural pathways, and intraperitoneal "drop" metastases [41]. Lymphatic spread is present in more than half of the patients at initial diagnosis and common sites of nodal metastases are nodes along the cystic duct, common bile duct, hilar, hepatic artery and/or portal vein, periaortic, portacaval, superior mesenteric and celiac arteries. The disease is classified as N1 if one to three positive nodes are involved, whereas N2 disease is four or more positive nodes. T1 or T2 primary lesions without lymph node metastasis are classified as stage IA or IB disease, respectively. Stage IIA represents T3 lesions without nodal spread. T1, T2, or T3 lesions with N1 lymph node involvement are defined as stage IIB. A T4 lesion without distant metastasis is considered stage III, and distant metastases represents stage IV. The most common sites of metastases are the liver, peritoneum, lung, and brain.

Management of GBC

GBC is an aggressive malignancy often diagnosed at late stages, and surgery is the only potentially curative option. Unfortunately, only one fourth of the patients will undergo curative surgery. Surgical options are dependent on the staging of the disease and may involve the resection of one or more adjacent organs. Given the dismal prognosis of metastatic GBC, attempts of curative surgery are limited to localized resectable disease.

Surgical Management of GBC

Achieving a tumor-free surgical margin (R0 resection) should be the primary goal of the surgery as it forms one of the important prognostic indicators.

Management of Resectable GBC When Identified as an Incidental Mass on Imaging Studies or Incidental Finding at Surgery

GBC patients should always be referred to a cancer center with available expertise in its management. As per National Comprehensive Cancer Care network (NCCN) guidelines version 1. 2017, any suspicious GBC mass need not undergo preoperative biopsy as it may lead to peritoneal spread. If the diagnosis of GBC is not conclusive, it is always prudent to have an intraoperative frozen section evaluation followed by a definitive resection in case the pathology confirms cancer. As discussed above in the section "Diagnostic Staging Laparoscopy", staging laparoscopy is recommended and is often combined with the surgical

procedure. This staging laparoscopy gives a detailed picture to the surgeon, and a stage-based surgical resection can be performed. In the event of incidental discovery of GBC during a laparoscopic surgical procedure, it should be referred promptly for definitive oncologic resection once the pathologic analysis is finalized.

For stage 0-I disease (T1aN0M0) (early GBC), simple cholecystectomy should suffice as the risk of lymph node dissemination and residual cancer is low. Retrospective studies demonstrate a >95% five-year survival in T1aNx disease treated by cholecystectomy alone. No benefit has been demonstrated for re-resection or more aggressive resection in T1a disease. However, utmost care must be taken by the surgeon to avoid any biliary spillage as it may be contaminated with malignant cells and may increase the chances of intraoperative spread of cancer cells [42]. As the primary goal of the surgery is to achieve R0 resection, in T1a disease, if simple cholecystectomy did not achieve R0 resection, the surgical resection should be extended to involve lymphadenectomy, hepatic resection (segments IVB and V), and hepatic/biliary duct resection (performed in case of positive margins in the cystic duct). In contrast, in T1b disease, lymphadenectomy and hepatic segmental resection (IVB and V) along with cholecystectomy have shown reduced recurrence rates compared to simple cholecystectomy alone (2% vs. 12.5%) [43].

Due to the involvement of deeper layers of the gallbladder and the high probability of lymphatic, perineural, and vascular metastases in stage II and III (T1b, T2, and T3; N0–1) disease, surgical resection involving extended cholecystectomy, extended lymphadenectomy (including celiac/superior mesenteric artery lymph nodes), and hepatectomy (segments IVA, V) is indicated in patients deemed to be appropriate surgical candidates [2]. It is important to note that the extent of surgery is determined by the resection required to achieve a R0 margin. Early series advocated increasingly aggressive "standard" resections for GBC with improvements in long-term outcome. However, it is likely that these aggressive resections improved outcomes by improving the R0 resection rates. Routine major hepatectomy involving the caudate lobe of the liver and extensive hepatic resection beyond the IVA and V segments are associated with higher postoperative morbidity and not associated with survival benefit [44, 45]. Hence, the surgeon should aim to achieve the R0 resection with as limited a resection as possible [43]. Having said that, major hepatectomies are indicated in case of nonachievability of R0 resection with limited resection or if the tumor invades the main vasculature of the liver [2]. Similarly, routine resection of the common bile duct does not improve outcomes but is indicated in patients with preoperative jaundice, a positive cystic duct margin, or evidence of bile duct invasion on preoperative imaging [2, 46].

Though surgery is the only potentially curative therapy for GBC, outcomes may be poor even after complete resection, particularly in stage III (T3 and/or node-positive) disease. Adjuvant chemotherapy and radiotherapy are commonly administered in margin positive resections and node positive disease. Postsurgical adjuvant therapy is discussed in detail in the section "Role of Adjuvant Therapy in the Management of GBC".

Management of Resectable GBC When Identified on Postsurgical Pathology Review

In case of T1a disease, if the prior surgery achieved negative margins, close monitoring and periodic surveillance are recommended. In case of disease recurrence, if the patient is a surgical candidate (based on the medical comorbidities and stage of the disease), extended surgical resection to achieve R0 resection can be considered. Based on previous studies, patients who had incidental diagnosis of T1b or greater GBC based on the postsurgical pathology review required a second procedure. Despite the increased surgical risk of a second procedure, reoperation with successful R0 resections has shown significant improvements in overall survival (OS) [47–50]. Laparoscopic port site disease is often seen in patients with T2 and T3 disease and correlates with peritoneal spread. Given the correlation with peritoneal spread and the lack of benefit in OS, port site resection is not recommended during reoperation [43]. A recent multi-institutional retrospective analysis that evaluated the optimal time to reoperation concluded that surgeries performed between 4 and 8 weeks from the initial surgery are associated with better outcomes. One possible explanation for the better results for surgeries performed between 4 and 8 weeks is that the 4 weeks time frame allows the initial surgical inflammation to resolve, leading to a better appreciation of cancer spread. Moreover, waiting >8 weeks may allow disease dissemination yielding poor results.

Criteria for Unresectability of GBC

Contraindications to curative surgery include the presence of stage IV disease with liver metastasis, distant/extrahepatic metastases, peritoneal disease, malignant ascites, evidence of extensive hepatoduodenal ligament involvement, distant nodal disease (para-aortic lymph nodes), and major vessel involvement that is not amenable to vascular resection and reconstruction. It is important to note that T3 disease with direct involvement of the duodenum, colon, or liver may be amenable to surgery if an R0 en bloc resection can be achieved without significant morbidity. Although curative surgery is contraindicated in extensive stage IV disease, palliative cholecystectomy may be performed in select cases with recurrent episodes of cholecystitis, especially when other options like endoscopic stenting have failed.

Role of Surgery in Unresectable or Stage IV GBC

For patients with regional nodal involvement, radical resection yields a 5-year overall survival (OS) of 10–28% [51, 52]. In contrast, surgery may not be beneficial in prolonging survival for patients with distant metastatic nodal disease (involvement beyond the hepatoduodenal ligament, pancreaticoduodenal area, and along the common hepatic artery area) [51]. Simple cholecystectomy may be performed in GBC

with extensive nodal involvement, unresectable disease, or stage IV disease for palliative purposes when other maneuvers like endoscopic stent placement or biliary bypass have failed or if the patient suffers from recurrent episodes of cholecystitis [2].

Only 20–30% of patients with GBC can undergo surgical resection as the disease is most often diagnosed at late stages when surgery may not prolong survival. For patients who are not good surgical candidates, palliative therapy with external beam radiotherapy (EBRT), systemic chemotherapy, and/or enrollment into clinical trials are available options.

Role of Adjuvant Therapy in the Management of GBC

Despite achieving R0 resection of the primary tumor, outcomes in GBC are generally poor, especially when the disease has spread to adjacent organs at the time of presentation. The risk of recurrence and metastatic spread of GBC is directly related to the T stage at the time of diagnosis. Though radical excision of the cancerous lesion followed by adjuvant therapy is the mainstay of treatment, the data supporting the adjuvant approach are conflicting.

Role of Adjuvant Radiotherapy and Chemoradiotherapy

The current literature on the role of adjuvant radiotherapy or chemoradiotherapy in the management of GBC is primarily derived from retrospective institutional and national database analyses. The lack of data from randomized trials makes it hard to determine whether there is an overall survival benefit. Nonetheless, many, but not all, retrospective analyses have shown favorable outcomes in prolonging survival, with the greatest benefits in the high stage tumors, node positive disease, and R1 resections [53, 54].

Analysis of the SEER database (1992-2002) showed that patients who received postsurgical radiotherapy had a significantly longer median survival than their counterparts who did not receive radiotherapy (14 months versus 8 months; $p < 0.0001$). Patients who had lymph node metastases (16 months vs. 5 months; $p < 0.0001$) and higher stage (T3 stage) (14 months vs. 11 months; $p = 0.01$) benefitted the most. In comparison, patients with stage 1 disease did not appear to benefit from radiotherapy. A recent multi-institutional retrospective analysis found survival benefits in GBC patients who received postoperative adjuvant chemotherapy (hazard ratio [HR] 0.38, 95% CI: 0.23–0.65) and chemoradiotherapy (HR 0.26, 95% CI: 0.15–0.43) [55]. The survival benefit of adjuvant therapy was specifically seen in the patients with T3/T4 disease, lymph node metastases at presentation, and who had R1 resection. Benefit for radiotherapy alone, chemotherapy alone, and chemoradiotherapy is further supported by a National Cancer Database (NCDB) analysis that showed improved 3-year overall survival (chemotherapy, HR: 0.77 [95% CI:

0.61–0.97]; radiotherapy, HR: 0.63 [95% CI 0.44–0.92]; and chemoradiotherapy, HR: 0.47 [95% CI: 0.39–0.58]). However, neither of the therapies showed a survival advantage in T1N0 stage disease [56]. Selected radiotherapy and chemoradiotherapy studies in GBC are summarized in Table 11.3. The results of these retrospective analyses are to be interpreted with caution as there might be a component of selection bias as fitter and relatively younger patients received adjuvant therapy. In contrast, an NCDB analysis showed that patients who had larger primary tumors, advanced stage, and lymph node metastases had a higher likelihood of receiving adjuvant therapy.

A recent multicenter phase II trial (Southwest Oncology Group S0809) evaluated the safety and efficacy of postoperative combined modality therapy in patients with resected EHCC or GBC [57]. Therapy consisted of four cycles of gemcitabine and capecitabine, followed by conformal radiotherapy (45 Gy to regional lymphatics and 54–59.4 Gy to the tumor bed) and concurrent capecitabine. Twenty-five patients enrolled had GBC, with most having stage III–IV disease and/or positive surgical margins. Two-year overall survival, disease-free survival, and local recurrence rates were 56%, 48%, and 8%, respectively. These data provide evidence in support of this regimen in patients with resected GBC at high risk for recurrence.

Improving Safety of Radiotherapy: Despite the potential benefits of radiotherapy in the management of GBC, the dose of radiotherapy is limited by the proximity of the disease to vital structures including the bowel, liver, and kidneys. The risk of acute and late treatment-related adverse effects may be minimized by the use of advanced radiotherapy techniques such as three-dimensional conformal radiotherapy (3D-CRT), intensity-modulated radiotherapy (IMRT), and proton beam radiotherapy. Specifically, IMRT may reduce radiation exposure to the liver and right kidney [58]. A preliminary study evaluated the feasibility of IMRT with image guidance for target localization in ten patients with GBC [59]. The median prescription dose was 59 Gy. Treatment was well tolerated with only one patient experiencing grade 3 toxicity. Recently, a retrospective study evaluated the use of neoadjuvant chemoradiotherapy using IMRT for 28 patients with locally advanced GBC [60]. Patients received a median dose of 57 Gy in 25 fractions to the primary tumor and involved lymph nodes and 45 Gy in 25 fractions to the at-risk regional lymph nodes. Three patients (11%) experienced grade 3 acute treatment-related adverse events during chemoradiotherapy. Two patients experienced grade 3 late treatment-related adverse events after RT. An example of an IMRT treatment plan for gallbladder cancer is shown in Fig. 11.6.

Role of Adjuvant Chemotherapy in the Management of GBC

Chemotherapy, given either alone or in combination with radiotherapy is used as adjuvant therapy following surgical resection of the primary tumor. Chemotherapy is also used in GBC patients with locally advanced unresectable disease or in patients with metastatic disease. As discussed in the section "Role of Adjuvant Radiotherapy and

Table 11.3 Selected studies that evaluated adjuvant radiotherapy and chemoradiotherapy in gallbladder cancer

Study	Regimen	Significance/outcome	Comments
Mitin T et al. [56] (n = 5029)	National Cancer Data Base (NCDB) retrospective analysis (2005–2013)	Adjuvant chemoradiotherapy (HR 0.47) and chemotherapy (HR 0.77) were associated with better survival	Apparent benefit of adjuvant therapy was seen in all subgroups except T1N0 patients. The magnitude of benefit was greatest in patients with N+ disease or positive margins
Mojica P et al. [108] (n = 31w87)	SEER retrospective analysis (1992–2002)	Median survival of 14 months with adjuvant radiotherapy vs. 8 months with no adjuvant radiotherapy ($p < 0.0001$)	Adjuvant radiotherapy was used in 17% of cases. Radiotherapy was associated with survival benefit in patients with regional spread ($p = 0.0001$) and tumors infiltrating the liver ($p = 0.011$)
Gold et al. [105] (n = 73)	Adjuvant therapy with 5-fluorouracil chemotherapy concurrently with radiotherapy (median dosage, 50.4 Gy in 28 fractions)	Overall, no significant difference in median OS was noted between the chemoradiation (4.8 years) vs. no therapy (4.2 years) groups. After adjusting for T, N category and histologic features, chemoradiotherapy was associated with improved survival (hazard ratio for death, 0.3; 95% confidence interval, 0.13–0.69; $p = 0.004$)	Retrospective study of 48 patients who received no adjuvant therapy and 25 patients who received adjuvant chemoradiotherapy
Cho SY et al. [109] (n = 100)	Adjuvant chemotherapy with 5-fluorouracil or cisplatin + capecitabine or gemcitabine concurrently with radiotherapy (dosage, 45 Gy in 25 fractions for 25 days)	Disease-free survival in adjuvant therapy group was higher compared to no adjuvant therapy group in lymph node positive disease only ($p = 0.0006$)	Adjuvant chemoradiotherapy was associated with improved survival in lymph node positive disease only
Gonzalez ME et al. [110] (n = 67)	Abdominal irradiation (20 Gy at 100 cGy daily) plus a boost to the tumor bed for a total of 45–59.4 Gy + fluoropyrimidines	Five-year OS was higher in adjuvant chemoradiotherapy cohort as compared to no adjuvant therapy cohort (57% vs. 27%) ($p = 0.005$)	Evaluation of the role of adjuvant chemoradiotherapy in T1b-3 N0–1M0 disease

Table 11.3 (continued)

Study	Regimen	Significance/outcome	Comments
Kim et al. [55] ($n = 291$)	Gemcitabine, gemcitabine + cisplatin in 67% of the patients + radiotherapy (no specific mention on the type of chemotherapy received in about 33% of patients)	Receipt of chemoradiotherapy was associated with better OS as compared to surgery-only group (HR: 0.26, $p < 0.001$)	Only patients with T3/T4 disease, R1 disease, lymph node metastasis had benefit with chemotherapy or chemoradiotherapy
Gu B et al. [111] ($n = 94$)	Adjuvant radiotherapy with concurrent mono chemotherapy (capecitabine or S-1) or 2-drug chemotherapy (oxaliplatin combined with 5-fluorouracil (5-FU) / capecitabine/ gemcitabine)	Propensity score matched analysis of patients with surgery + chemoradiotherapy and surgery only. Median survival was higher in patients who received adjuvant chemoradiotherapy as compared to surgery alone (27 vs. 13 months; $p = 0.004$)	Disease-free survival was also high in adjuvant chemoradiotherapy group as compared to surgery-only group (23 vs. 7 months; $p = 0.004$) in stage II-IVA GBC patients

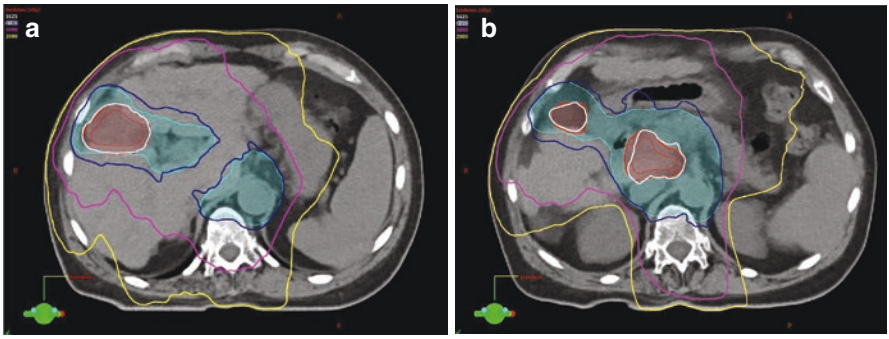

Fig. 11.6 Intensity-modulated radiotherapy (IMRT) plan for a patient with locally advanced, unresectable gallbladder adenocarcinoma. Treatment was delivered in 25 fractions over 5 weeks with concurrent capecitabine. The gallbladder primary tumor and involved portocaval lymph node (red volume) received a dose of 56.25 Gy, and the regional lymph nodes (cyan volume) received 45 Gy. Volumes receiving 56.25 Gy (white), 45 Gy (blue), 30 Gy (magenta), and 20 Gy (yellow) are shown

Chemoradiotherapy", given the rarity of GBC, most of the data are obtained from retrospective analyses, and most studies grouped all patients with biliary tract cancer, including cholangiocarcinoma and GBC. Though the two cancer types are often analyzed in combination, subgroup analyses showed discordant responses to the therapy [61, 62]. Moreover, compared to advanced cholangiocarcinoma (median OS:

Table 11.4 Prospective randomized trials of chemotherapy in the management of gallbladder cancer

Study	Regimen	Significance/outcome	Comments
Takada et al. [112] (n = 112 GBC)	Mitomycin C (6 mg/m^2 IV) at the time of surgery and 5-FU (310 mg/m^2 IV) in 2 courses of treatment for 5 consecutive days during postoperative weeks 1 & 3, followed by 5-FU (100 mg/m^2 orally) daily from postoperative week 5 until disease recurrence	GBC patients who received adjuvant chemotherapy had a better 5-year survival compared to the surgery-only group (26 vs. 14.4%, p = 0.03). A similar trend in DFS was noted (20% vs. 13%, p = 0.02)	Multivariate analysis showed a tendency to lower recurrence rate and lower risk of mortality ($p > 0.05$)
Primrose et al. [65] (n = 79 GBC)	Adjuvant capecitabine (1250 mg/m^2 D1–14 every 21 days, for 8 cycles) vs. no adjuvant therapy	Per protocol analysis, median OS was better in the capecitabine group compared to no adjuvant therapy (53 months vs. 36 months, p = 0.02)	The study included all biliary tract cancers, and survival analysis included all biliary tract cancers
Edeline et al. [113] (n = 196 biliary tract cancers)	Postsurgical adjuvant gemcitabine + oxaliplatin (GEMOX) 85 for 12 cycles vs. no adjuvant therapy	No significant difference in relapse-free survival between the cohorts. Though quality of life did not change with GEMOX, it was associated with high rates of peripheral neuropathy (50 vs. 1%) and neutropenia (22 vs. 0%) compared to no adjuvant therapy	French multicenter study. No GBC specific analysis was performed

24–44 weeks), GBC is a more aggressive disease (median OS: 12 weeks) [63]. Genomic analyses of resection specimens of the two types of cancers show varying rates of driver genomic mutations, including *KRAS*, isocitrate dehydrogenase (*IDH1/2*), and fibroblast growth factor receptor 2 (*FGFR2*) and differences in gene expression [64]. Despite the differences in the aggressiveness and molecular pathogenesis of GBC and biliary tract cancers, randomized controlled trials usually combine the two cancers in the survival analyses, and GBC comprise a relatively small number of the patients analyzed (36% in the Advanced Biliary Cancer [ABC]-02 trial and 18% in the BILCAP trial) [65, 66].

Previous retrospective studies suggested some degree of benefit from adjuvant chemotherapy [67–69]. Few prospective randomized trials have been conducted, and the small number of patients with GBC enrolled in these trials compromises interpretation of the results (Table 11.4).

Encouraging results of improved median survival (53 vs. 36 months, HR 0.75, 95% CI: 0.58–0.97) were seen in the phase III BILCAP trial that evaluated capecitabine as adjuvant therapy (1250 mg/m2 D1–14 every 21 days, for 8 cycles/6 months) in biliary tract cancers including GBC (n = 79, 18% of total biliary tract patients enrolled) [65]. Patients with T1a GBC were excluded from this clinical trial. In the subgroup analysis of GBC patients, survival was numerically

better in the capecitabine arm (HR of 0.84, [95% CI: 0.43–1.63]; $p = 0.097$). In the intention to treat analysis, median relapse-free survival (RFS) of the capecitabine group was 25 months (95% CI: 19–37 months), whereas the observational group had an RFS of 18 months (95% CI: 13–28 months). Common grade 3–4 adverse events included plantar palmar erythema (21%), fatigue (8%), diarrhea (8%), neutropenia (2%), nausea (1%), stomatitis (1%), and hyperbilirubinemia (1%). Interestingly, high rates of R1 resections (38%) were reported in this trial. The benefit of adjuvant chemotherapy was more pronounced in patients with R0 resection compared to those with R1 resection (HR: 0.73 vs. 0.90).

It is important to note that these randomized trials had only limited numbers of cases of GBC. Nonetheless, given the modest survival advantage, tolerable toxicity profile, and extrapolation from clinical trials in the metastatic setting, platinum-based compounds were often combined with gemcitabine [66]. However, the BILCAP study has established capecitabine as a new standard of care option for resected GBC.

Role of Neoadjuvant Therapy in the Management of GBC

Neoadjuvant therapy is currently being employed in locally advanced gastrointestinal malignancies with the primary aim of downstaging the disease and achieving R0 resection. There are limited data in the treatment of GBC in the neoadjuvant setting. An Indian prospective case series that evaluated the role of neoadjuvant chemotherapy with gemcitabine and cisplatin in locally advanced disease concluded that 83.3% (15/18) of patients had a good radiological response and 56.3% (9/16 patients) achieved R0 resection [70]. The study concluded that neoadjuvant chemotherapy may downsize the tumor in approximately half of patients, allowing R0 resection. Similarly, encouraging results were seen in a retrospective analysis that evaluated gemcitabine and cisplatin neoadjuvant chemotherapy in locally advanced GBC. A total of 17/37 patients (46%) could undergo R0 resection, and the patients who underwent surgery had a significantly better progression-free survival and OS [71]. A retrospective case series from India demonstrated the feasibility of administrating neoadjuvant concurrent chemoradiotherapy for locally advanced (stage III) gallbladder cancer [60, 72]. Of the 28 patients treated, 71% experienced partial or complete radiologic response, and 56% underwent R0 resection. Overall survival at 5 years was 24% for all patients and 47% for patients with an R0 resection. A single-arm prospective phase II study in Chile evaluated the feasibility of neoadjuvant chemoradiotherapy for potentially resectable gallbladder cancer [73]. Eighteen patients with stage II–IV disease received preoperative RT (45 Gy in 25 fractions) with concurrent 5-FU. Thirteen patients (72%) underwent potentially curative resection, and of these seven (54%) were alive and free of disease recurrence at a median follow-up of 2 years. To better characterize the benefit of neoadjuvant therapy in GBC, large prospective studies are needed to assess the rates of downsizing and resectability.

Management of Advanced GBC

Palliation of Obstructive Jaundice

Due to infiltration of the common hepatic duct, jaundice is a presenting complaint in 30–60% of patients with advanced GBC. In GBC patients presenting with jaundice, baseline CA 19–9 should be drawn after biliary drainage as it might be falsely elevated in patients with biliary obstruction. The CA-19-9 level can be followed every 3–4 months to determine the progression of the disease. Biliary drainage can be achieved by either percutaneous or endoscopic stenting. A randomized controlled trial evaluated percutaneous transhepatic biliary drainage vs. endoscopic stenting methods of biliary drainage in 54 patients with advanced GBC [74]. Though survival was same in both arms, the percutaneous procedure was associated with better success rates (89% vs. 41%) and lower rates of cholangitis (48 vs. 11%). Despite the lower rates of cholangitis and high success rates with percutaneous procedure, in practical settings, the percutaneous procedure is associated with higher patient discomfort due to open external drainage and comparatively higher rates of bile leak and bleeding [75].

Role of Radiotherapy and/or Chemoradiotherapy in Advanced GBC

Limited data exist on the role of radiotherapy in advanced unresectable GBC, and the available data are mainly obtained from the small number of GBC cases included in studies that evaluated all biliary tact cancers [68, 76]. Given this limited data, patients with unresectable GBC should be encouraged to participate in clinical trials.

Despite uncertainty in survival benefit, chemoradiotherapy is an acceptable choice for locoregional therapy of a locally advanced unresectable GBC in selected cases. Chemotherapy, especially fluoropyrimidine based, is frequently administered in addition to radiotherapy [68]. Systemic chemotherapy should be used as a first choice in advanced disease; and radiotherapy may be considered in patients with localized unresectable disease without metastases after initiation of first-line chemotherapy [77].

Role of Systemic Chemotherapy in Advanced GBC

Gemcitabine and fluorouracil-based therapies are commonly evaluated systemic therapies for treatment of GBC in the palliative setting. The oral fluoropyrimidine derivative, capecitabine, alone or in combination with cisplatin or oxaliplatin showed encouraging results of marginal survival benefit in unresectable GBC [78–80]. Similar encouraging results were reported in another study that evaluated capecitabine in combination with oxaliplatin [79]. The therapy was well tolerated, and the study concluded that of 27 unresectable GBC patients, one had complete response, 7 had partial response, and 9 had a stable disease, with a total disease control rate of 63% and median survival of 11.3 months.

Gemcitabine, either alone or in combination, has been extensively studied in patients with GBC (Table 11.5). Three phase II trials that evaluated gemcitabine alone in unresectable GBC concluded that the drug was well tolerated with response rates ranging from 0 to 30% [81–83]. Gemcitabine was also evaluated in combination with capecitabine in three phase II trials of metastatic, unresectable GBC [84–86]. Results of the three trials showed a response rate of about 30% with a median OS of 13–14 months. This combination regimen was well tolerated, with neutropenia and thrombocytopenia as the most significant toxicities.

In addition, gemcitabine was also evaluated in combination with cisplatin or oxaliplatin in phase II and III trials, and the results (response rates and median OS) were encouraging. In gemcitabine plus cisplatin combination phase II trials, response rates of 21–34.5% and median OS of 9.3–11 months were noted [87–90]. The combination was also evaluated in a phase III randomized trial (ABC-02 trial), which also demonstrated similar encouraging results making it the current standard of care therapy in unresectable GBC [91]. In this clinical trial of 410 patients with biliary tract cancers, 149 subjects had GBC. Compared to gemcitabine monotherapy, the combination therapy resulted in a better progression-free survival (8.4 vs. 6.5 months; HR: 0.72; 95% CI: 0.57–0.90; $p = 0.003$) and OS (11.7 vs. 8.3 months; HR:0.70; 95% CI: 0.54–0.89; $p = 0.002$). The combination therapy was tolerated well without significant added toxicity. In addition, the rate of tumor control was significantly increased among patients in the combination therapy group (81.4% vs. 71.8%, $P = 0.049$). In the GBC subgroup, 37.7% of the patients receiving combination therapy had a partial response compared to 21.4% with single agent gemcitabine. Adverse events were similar in both the cohorts. Though neutropenia was more frequent in the cisplatin–gemcitabine group, the number of neutropenia-associated infections was similar in the two groups.

The gemcitabine–oxaliplatin combination was evaluated in phase II trials [92–94]. The regimen was well tolerated even among patients with higher ECOG scores reflecting poor functional status. A phase III trial of 260 patients compared the combination of gemcitabine–cisplatin with gemcitabine–oxaliplatin in unresectable and metastatic GBC patients [95]. The objective response rates (23% vs. 24%) and median OS (8 vs. 9 months) were similar in both treatment cohorts; however, the combination of gemcitabine and oxaliplatin had more grade 1 or 2 peripheral neuropathy and grade 3 or 4 diarrhea.

Gemcitabine has also been evaluated in combination with fluorouracil-leucovorin and carboplatin. Patients who received the combination with fluorouracil-leucovorin had modest improvements in progression-free survival but it was not superior to gemcitabine alone [96, 97]. In a phase II trial that evaluated the combination of gemcitabine and carboplatin in a group of 20 patients with advanced GBC, 4 patients (21%) achieved a complete response and 3 (15.7%) had a partial response with an overall response rate of 36.7% [98]. Grade III and IV side effects of anemia, neutropenia, and thrombocytopenia were observed in a few patients.

Based on the above data, the combination of gemcitabine and cisplatin is the standard of care for first-line treatment of advanced GBC. The combination of gemcitabine and oxaliplatin is also a reasonable choice. Other alternative regimens include single-agent gemcitabine, gemcitabine and carboplatin, or 5-FU-based

Table 11.5 Gemcitabine-based systemic chemotherapy trials of unresectable gallbladder cancer

Study	Regimen	Significance/outcome	Comments
Kubicka et al.[81] (n = 23 cholangiocellular carcinoma)	Gemcitabine weekly (3 times/month)	Seven/23 patients had clinical benefit (overall response rate of 30%)	Nausea and neutropenia were most commonly noted side effects No GBC specific analysis was performed
Mezger et al. [82] (n = 13 biliary tract cancers)	Gemcitabine 1000 mg/m^2 weekly for 7 weeks, then cycles of 3 weeks with 1 week pause	Only 1 patient had partial remission lasting more than 5 months. No survival advantage demonstrated	No GBC specific analysis was performed
Penz et al. [83] (n = 32 biliary tract cancers)	Gemcitabine 2200 mg/m^2 every 2 weeks for a duration of 6 months	Seven / 32 (22%) patients had a partial response. 14/32 (44%) had stable disease	3/32 patients developed grade 3 hematologic toxicities
Knox et al. [84] (n = 20)	Capecitabine at 650 mg/m^2 + Gemcitabine 1000 mg/m^2	Median OS was 14 months. Median progression-free survival was 7 months (95% CI: 4.6–11.8 months)	Most common side effects observed were transient neutropenia, thrombocytopenia, fatigue, and hand-foot syndrome. No GBC specific analysis was performed
Cho et al. [85] (n = 7)	Capecitabine at 650 mg/m^2 + Gemcitabine 1000 mg/m^2	Median time to disease progression and OS were 6.0 and 14 months, respectively. The 1-year survival rate was 58%	No grade 4 adverse events were seen. No GBC specific analysis was performed
Riechelmann et al. [86] (n = 75 biliary tract cancers)	Capecitabine at 650 mg/m^2 + Gemcitabine 1000 mg/m^2	Overall response rate was 29% (95% CI: 19.4–41%), with a median duration of 9.7 months. 3 patients achieved complete responses, with a median duration of 17 months. The median progression-free survival and OS were 6.2 and 12.7 months, respectively	No GBC specific analysis was performed
Meyerhardt et al. [87] (n = 33 biliary tact cancers)	Gemcitabine at 1000 mg/m^2 and cisplatin at 30 mg/m^2	Seven/33 (21%) experienced a partial response; 12/33 (36%) had stable disease for 3 months. The median progression-free survival and OS were 6.3 and 9.7 months, respectively. After 1 year, 39% of patients were alive	Most common grade 3–4 hematologic toxicities were neutropenia, thrombocytopenia and anemia

Table 11.5 (continued)

Study	Regimen	Significance/outcome	Comments
Thongprasert et al. [88] (n = 40 biliary tract cancers, 1 GBC)	Gemcitabine at 1000 mg/m^2 and cisplatin at 30 mg/m^2	Partial response was seen in 11/40 (27.5%), 13/40 (32.5%) had stable disease and/or minor response. Median survival time was 36 weeks	Anemia and leukopenia were common grade 3 hematologic toxicities
Kim et al. [89] (n = 29 biliary tact cancers)	Gemcitabine at 1000 mg/m^2 days 1 and 8; cisplatin at 60 mg/m^2 every 3 weeks	Ten/29 had partial response. None had complete response. Overall response rate was 34.5%. 4/29 (13.8%) had stable disease. Positive correlation of CA 19–9 increase with disease progression	Grade 3 and 4 hematologic toxicities seen were neutropenia (14%) and anemia (3%)

regimens. Figure 11.7 shows a flow diagram summarizing the overall management of gallbladder carcinoma.

Role of Molecular-Targeted Therapy

The molecular pathology of GBC is discussed in detail in section "Pathology of GBC". The characteristic molecular features include mutation of *KRAS, TP53*, and *p16/CDKN2/INK4A*, as well as human epidermal growth factor receptor *(HER)-2/Neu* amplification. Angiogenic-inflammatory pathway gene mutations in cyclooxygenase-2 [COX-2], nitric oxide synthase [iNOS], and vascular endothelial growth factor [VEGF] are also implicated in the pathogenesis of GBC.

Tyrosine kinase inhibitors, erlotinib and lapatinib, that act by blocking the EGFR pathway (lapatinib also blocks the HER2/EGFR2 pathway) were evaluated in advanced biliary tract cancers (erlotinib) and GBC (lapatinib). These tyrosine kinase inhibitors resulted in modest benefit (~17% progression-free survival) at their best, and all responding patients had mild skin toxicity (grades 1 and 2). A multicenter, randomized phase II trial evaluated the combination of cetuximab (an EGFR inhibitor) with gemcitabine–oxaliplatin in unresectable biliary tract cancers (24% patients had GBC) [99]. The addition of cetuximab resulted in improved 4-month progression-free survival compared to the gemcitabine–oxaliplatin group (61% vs. 44%). Toxicity was comparable in both groups with slightly higher rash/hypersensitivity reactions in the cetuximab group.

Sorafenib, a tyrosine kinase inhibitor that targets VEGFR-2, 3 and platelet-derived growth factor and less potently BRAF kinases was evaluated in a phase II clinical trial involving unresectable or metastatic GBC or cholangiocarcinoma (n = 31) [100]. Twenty-nine % of the patients had stable disease and median progression-free survival was 2 months. Grade 3 or 4 toxicities were significant,

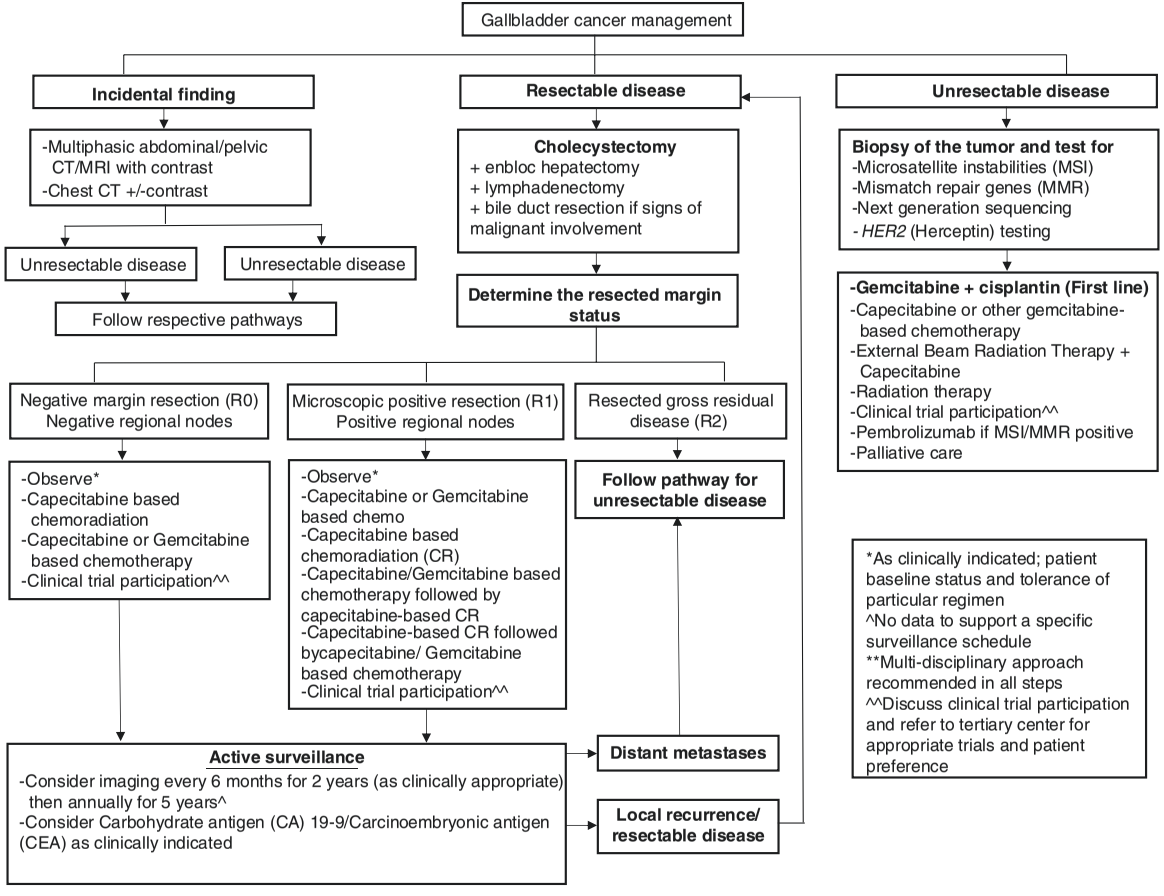

Fig. 11.7 Flow diagram summarizing the overall management of gallbladder carcinoma

affecting about two-thirds of the patients. One patient died of supraventricular tachycardia and thromboembolism.

Bevacizumab, a humanized monoclonal antibody against VEGF, was evaluated in a phase II trial in combination with gemcitabine and oxaliplatin in unresectable biliary tract cancers (28% [n = 10] of enrolled patients had GBC) [101]. In the subset of GBC patients, the median progression-free survival and OS were 6.1 and 8.5 months, respectively. Most common side effects noted were grade 3 or 4 hypertension (n = 5), proteinuria (n = 1), thrombosis (n = 2), and cardiac ischemia (n = 1). Bevacizumab was also evaluated in combination with erlotinib in a phase II trial in biliary tract cancers (n = 53; 10 patients with GBC and 43 with non-GBC) [102]. This biologic combination regimen resulted in stable disease in 51% of patients; the median OS of the entire group was 9.9 months. It is important to note that the results of the study were not stratified based on the tumor location and so cannot be extrapolated to GBC. Another study evaluated the addition of bevacizumab to gemcitabine and oxaliplatin (GEMOX) [103]. The combination was associated with a better progression-free survival compared to GEMOX therapy (6.5 vs. 3.7 months, p = 0.049). No significant difference in adverse events was noted between the groups.

Although these biologic agents are promising, more definitive randomized studies are required to define the role of antiangiogenic agents in advanced GBC, particularly among those harboring *KRAS* and *BRAF* mutations.

Role of Immunotherapy

Given the background of chronic inflammation in the pathogenesis of GBC, immunotherapy may be a potentially attractive targeted therapy [104]. A couple of tumor-related antigens have also been identified in gallbladder carcinoma – Wilms tumor 1 (WT1) and mucin-1 (MUC-1) in 68–80% and 90% of gallbladder cancers, respectively [105]. Trials of both a dendritic-based cell vaccine against WT-1 and MUC-1 antigens, as well as a randomized trial of chemotherapy and a WT1 vaccine in patients with advanced GBC have been described [106]. In addition, in the interim analysis of a phase II trial (KEYNOTE-028, NCT02054806) that evaluated the role of pembrolizumab in advanced biliary tract cancer (including GBC), 34% (n = 8) of patients with positive PD-L1 expression had a partial response or stable disease [107]. Half of the patients (52%, n = 12) had progressive disease.

The role of pembrolizumab alone (NCT03260712) in advanced GBC is being evaluated in a phase II clinical trial. This trial will hopefully provide us with more details about the role of immune-targeted therapy in advanced, inoperable GBC. A phase II clinical trial of nivolumab (NCT02829918) in patients with advanced biliary tract cancers including GBC is also currently underway. These and other clinical trials will help in defining the role of checkpoint inhibitors in patients with GBC.

Conclusion

GBC continues to represent a major challenge in gastrointestinal oncology and often has a dismal prognosis. Surgical resection remains the mainstay of treatment if diagnosed at an early stage. The roles of chemotherapy and chemoradiotherapy in the neoadjuvant and adjuvant settings remain to be defined in randomized, prospective clinical trials. Recent clinical trials have suggested a survival benefit for capecitabine as adjuvant therapy. Molecularly targeted agents that inhibit angiogenesis and *EGFR* and *BRAF* pathways are currently being evaluated in clinical trials, and patients with unresectable GBC should be highly encouraged to enroll in these trials. Despite being a distinct entity compared to other biliary tract cancers, GBCs have been frequently combined with other biliary tract cancers in therapeutic studies. This has prevented a true understanding of the most effective treatment options. Given the relative rarity of GBC, collaboration across academic and community centers with experience in the management of these cancers will be necessary to achieve continued progress in the field and to obtain better outcomes for our patients.

References

1. Randi G, Franceschi S, La Vecchia C. Gallbladder cancer worldwide: geographical distribution and risk factors. Int J Cancer. 2006;118(7):1591–602. https://doi.org/10.1002/ijc.21683.
2. Al-alem F, Mattar RE, Madkhali A, Alsharabi A, Alsaif F, Hassanain M. Incidental gallbladder cancer. In: Abdeldayem HM, editor. Updates in gallbladder diseases. Ch. 06. Rijeka: InTech; 2017.
3. Hundal R, Shaffer EA. Gallbladder cancer: epidemiology and outcome. Clin Epidemiol. 2014;6:99–109. https://doi.org/10.2147/CLEP.S37357.
4. Diehl AK. Gallstone size and the risk of gallbladder cancer. JAMA. 1983;250(17):2323–6.
5. Misra S, Chaturvedi A, Misra NC, Sharma ID. Carcinoma of the gallbladder. Lancet Oncol. 2003;4(3):167–76.
6. Nagorney DM, McPherson GA. Carcinoma of the gallbladder and extrahepatic bile ducts. Semin Oncol. 1988;15(2):106–15.
7. Shukla VK, Tiwari SC, Roy SK. Biliary bile acids in cholelithiasis and carcinoma of the gall bladder. Eur J Cancer Prev. 1993;2(2):155–60.
8. Niu X-J, Wang Z-R, Wu S-L, Geng Z-M, Zhang Y-F, Qing X-L. Relationship between inducible nitric oxide synthase expression and angiogenesis in primary gallbladder carcinoma tissue. World J Gastroenterol. 2004;10(5):725–8. https://doi.org/10.3748/wjg.v10.i5.725.
9. Shukla VK, Tiwari SC, Roy SK. Biliary bile acids in cholelithiasis and carcinoma of the gall bladder. European J Cancer Prevention: Official Journal of the European Cancer Prevention Organisation (ECP). 1993;2(2):155–60.
10. Kumar S, Kumar S, Kumar S. Infection as a risk factor for gallbladder cancer. J Surg Oncol. 2006;93(8):633–9. https://doi.org/10.1002/jso.20530.
11. Nervi F, Duarte I, Gomez G, Rodriguez G, Del Pino G, Ferrerio O, et al. Frequency of gallbladder cancer in Chile, a high-risk area. Int J Cancer. 1988;41(5):657–60.
12. Shukla VK, Khandelwal C, Roy SK, Vaidya MP. Primary carcinoma of the gall bladder: a review of a 16-year period at the university hospital. J Surg Oncol. 1985;28(1):32–5.
13. Caygill CP, Hill MJ, Braddick M, Sharp JC. Cancer mortality in chronic typhoid and paratyphoid carriers. Lancet (London, England). 1994;343(8889):83–4.

14. Strom BL, Soloway RD, Rios-Dalenz JL, Rodriguez-Martinez HA, West SL, Kinman JL, et al. Risk factors for gallbladder cancer. An international collaborative case-control study. Cancer. 1995;76(10):1747–56.
15. Lewis JT, Talwalkar JA, Rosen CB, Smyrk TC, Abraham SC. Prevalence and risk factors for gallbladder neoplasia in patients with primary sclerosing cholangitis: evidence for a metaplasia-dysplasia-carcinoma sequence. Am J Surg Pathol. 2007;31(6):907–13. https://doi.org/10.1097/01.pas.0000213435.99492.8a.
16. Hundal R, Shaffer EA. Gallbladder cancer: epidemiology and outcome. Clin Epidemiol. 2014;6:99–109. https://doi.org/10.2147/clep.s37357.
17. Razumilava N, Gores GJ, Lindor KD. Cancer surveillance in patients with primary sclerosing cholangitis. Hepatology (Baltimore, Md). 2011;54(5):1842–52. https://doi.org/10.1002/hep.24570.
18. Stephen AE, Berger DL. Carcinoma in the porcelain gallbladder: a relationship revisited. Surgery. 2001;129(6):699–703. https://doi.org/10.1067/msy.2001.113888.
19. Khan ZS, Livingston EH, Huerta S. Reassessing the need for prophylactic surgery in patients with porcelain gallbladder: case series and systematic review of the literature. Arch Surg (Chicago, Ill: 1960). 2011;146(10):1143–7. https://doi.org/10.1001/archsurg.2011.257.
20. Wiles R, Thoeni RF, Barbu ST, Vashist YK, Rafaelsen SR, Dewhurst C, et al. Management and follow-up of gallbladder polyps: Joint guidelines between the European Society of Gastrointestinal and Abdominal Radiology (ESGAR), European Association for Endoscopic Surgery and other Interventional Techniques (EAES), International Society of Digestive Surgery - European Federation (EFISDS) and European Society of Gastrointestinal Endoscopy (ESGE). Eur Radiol. 2017;27(9):3856–66. https://doi.org/10.1007/s00330-017-4742-y.
21. Sebastian S, Araujo C, Neitlich JD, Berland LL. Managing incidental findings on abdominal and pelvic CT and MRI, part 4: white paper of the ACR incidental findings committee II on gallbladder and biliary findings. J Am Coll Radiol: JACR. 2013;10(12):953–6. https://doi.org/10.1016/j.jacr.2013.05.022.
22. Mori Y, Sato N, Matayoshi N, Tamura T, Minagawa N, Shibao K, et al. Rare combination of familial adenomatous polyposis and gallbladder polyps. World J Gastroenterol: WJG. 2014;20(46):17661–5. https://doi.org/10.3748/wjg.v20.i46.17661.
23. Shaffer EA. Gallbladder Cancer: the basics. Gastroenterol Hepatol. 2008;4(10):737–41.
24. Buscemi S, Orlando E, Damiano G, Portelli F, Palumbo VD, Valentino A, et al. "Pure" large cell neuroendocrine carcinoma of the gallbladder. Report of a case and review of the literature. Inter J Surg (London, England). 2016;28(Suppl 1):S128–32. https://doi.org/10.1016/j.ijsu.2015.12.045.
25. Dursun N, Escalona OT, Roa JC, Basturk O, Bagci P, Cakir A, et al. Mucinous carcinomas of the gallbladder: Clinicopathologic analysis of 15 cases identified in 606 carcinomas. Arch Pathol Lab Med. 2012;136(11):1347–58. https://doi.org/10.5858/arpa.2011-0447-OA.
26. Bal MM, Ramadwar M, Deodhar K, Shrikhande S. Pathology of gallbladder carcinoma: current understanding and new perspectives. Pathol Oncol Res. 2015;21(3):509–25. https://doi.org/10.1007/s12253-014-9886-3.
27. Saetta AA. K-ras, p53 mutations, and microsatellite instability (MSI) in gallbladder cancer. J Surg Oncol. 2006;93(8):644–9. https://doi.org/10.1002/jso.20532.
28. Chaube A, Tewari M, Garbyal RS, Singh U, Shukla HS. Preliminary study of p53 and c-erbB-2 expression in gallbladder cancer in Indian patients manuscript id: 8962091628764582. BMC Cancer. 2006;6:126. https://doi.org/10.1186/1471-2407-6-126.
29. Zhou YM, Li YM, Cao N, Feng Y, Zeng F. [significance of expression of epidermal growth factor (EGF) and its receptor (EGFR) in chronic cholecystitis and gallbladder carcinoma]. Ai zheng = Aizheng =. Chin J Cancer. 2003;22(3):262–5.
30. Dwivedi AND, Jain S, Dixit R. Gall bladder carcinoma: Aggressive malignancy with protean loco-regional and distant spread. World J Clin Cases: WJCC. 2015;3(3):231–44. https://doi.org/10.12998/wjcc.v3.i3.231.
31. Vega EA, Vinuela E, Yamashita S, Sanhueza M, Cavada G, Diaz C, et al. Extended lymphadenectomy is required for incidental gallbladder Cancer independent of cystic duct lymph node status. J Gastrointest Surg. 2018;22(1):43–51. https://doi.org/10.1007/s11605-017-3507-x.

32. Redaelli CA, Buchler MW, Schilling MK, Krahenbuhl L, Ruchti C, Blumgart LH, et al. High coincidence of Mirizzi syndrome and gallbladder carcinoma. Surgery. 1997;121(1):58–63.
33. Prasad TL, Kumar A, Sikora SS, Saxena R, Kapoor VK. Mirizzi syndrome and gallbladder cancer. J Hepato-Biliary-Pancreat Surg. 2006;13(4):323–6. https://doi.org/10.1007/s00534-005-1072-2.
34. Regimbeau JM, Fuks D, Bachellier P, Le Treut YP, Pruvot FR, Navarro F, et al. Prognostic value of jaundice in patients with gallbladder cancer by the AFC-GBC-2009 study group. European Journal Of Surgical Oncology: The Journal of the European Society of Surgical Oncology and the British Association of Surgical Oncology. 2011;37(6):505–12. https://doi.org/10.1016/j.ejso.2011.03.135.
35. Rooholamini SA, Tehrani NS, Razavi MK, Au AH, Hansen GC, Ostrzega N, et al. Imaging of gallbladder carcinoma. Radiographics: A Review Publication of the Radiological Society of North America, Inc. 1994;14(2):291–306. https://doi.org/10.1148/radiographics.14.2.8190955.
36. Kim JH, Kim TK, Eun HW, Kim BS, Lee MG, Kim PN, et al. Preoperative evaluation of gallbladder carcinoma: efficacy of combined use of MR imaging, MR cholangiography, and contrast-enhanced dual-phase three-dimensional MR angiography. J Magn Reson Imaging: JMRI. 2002;16(6):676–84. https://doi.org/10.1002/jmri.10212.
37. Kokudo N, Makuuchi M, Natori T, Sakamoto Y, Yamamoto J, Seki M, et al. Strategies for surgical treatment of gallbladder carcinoma based on information available before resection. Arch Surg (Chicago, Ill: 1960). 2003;138(7):741–50.; ; discussion 50. https://doi.org/10.1001/archsurg.138.7.741.
38. Butte JM, Gonen M, Allen PJ, D'Angelica MI, Kingham TP, Fong Y, et al. The role of laparoscopic staging in patients with incidental gallbladder cancer. HPB (Oxford). 2011;13(7):463–72. https://doi.org/10.1111/j.1477-2574.2011.00325.x.
39. Agarwal AK, Kalayarasan R, Javed A, Gupta N, Nag HH. The role of staging laparoscopy in primary gall bladder cancer--an analysis of 409 patients: a prospective study to evaluate the role of staging laparoscopy in the management of gallbladder cancer. Ann Surg. 2013;258(2):318–23. https://doi.org/10.1097/SLA.0b013e318271497e.
40. Chun YS, Pawlik TM, Vauthey J-N. 8th edition of the AJCC Cancer staging manual: pancreas and hepatobiliary cancers. Ann Surg Oncol. 2017; https://doi.org/10.1245/s10434-017-6025-x.
41. Reid KM. Ramos-De la Medina a, Donohue JH. Diagnosis and surgical management of gallbladder cancer: a review. J Gastrointest Surg. 2007;11(5):671–81. https://doi.org/10.1007/s11605-006-0075-x.
42. Lee JM, Kim BW, Kim WH, Wang HJ, Kim MW. Clinical implication of bile spillage in patients undergoing laparoscopic cholecystectomy for gallbladder cancer. Am Surg. 2011;77(6):697–701.
43. Aloia TA, Járufe N, Javle M, Maithel SK, Roa JC, Adsay V, et al. Gallbladder Cancer: expert consensus statement. HPB (Oxford). 2015;17(8):681–90. https://doi.org/10.1111/hpb.12444.
44. Shirai Y, Wakai T, Sakata J, Hatakeyama K. Regional lymphadenectomy for gallbladder cancer: rational extent, technical details, and patient outcomes. World J Gastroenterol. 2012;18(22):2775–83. https://doi.org/10.3748/wjg.v18.i22.2775.
45. D'Angelica M, Dalal KM, DeMatteo RP, Fong Y, Blumgart LH, Jarnagin WR. Analysis of the extent of resection for adenocarcinoma of the gallbladder. Ann Surg Oncol. 2009;16(4):806–16. https://doi.org/10.1245/s10434-008-0189-3.
46. Miyazaki M, Yoshitomi H, Miyakawa S, Uesaka K, Unno M, Endo I, et al. Clinical practice guidelines for the management of biliary tract cancers 2015: the 2nd English edition. J Hepatobiliary Pancreat Sci. 2015;22(4):249–73. https://doi.org/10.1002/jhbp.233.
47. Pawlik TM, Gleisner AL, Vigano L, Kooby DA, Bauer TW, Frilling A, et al. Incidence of finding residual disease for incidental gallbladder carcinoma: implications for re-resection. J Gastrointest Surg. 2007;11(11):1478–86.; ; discussion 86-7. https://doi.org/10.1007/s11605-007-0309-6.

48. Fong Y, Jarnagin W, Blumgart LH. Gallbladder cancer: comparison of patients presenting initially for definitive operation with those presenting after prior noncurative intervention. Ann Surg. 2000;232(4):557–69.
49. Ouchi K, Mikuni J, Kakugawa Y. Laparoscopic cholecystectomy for gallbladder carcinoma: results of a Japanese survey of 498 patients. J Hepato-Biliary-Pancreat Surg. 2002;9(2):256–60. https://doi.org/10.1007/s005340200028.
50. Goetze TO, Paolucci V. Benefits of reoperation of T2 and more advanced incidental gallbladder carcinoma: analysis of the German registry. Ann Surg. 2008;247(1):104–8. https://doi.org/10.1097/SLA.0b013e318154bf5d.
51. Chijiiwa K, Noshiro H, Nakano K, Okido M, Sugitani A, Yamaguchi K, et al. Role of surgery for gallbladder carcinoma with special reference to lymph node metastasis and stage using western and Japanese classification systems. World J Surg. 2000;24(10):1271–6; discussion 7.
52. Yamamoto M, Onoyama H, Ajiki T, Yamada I, Fujita T, Saitoh Y. Surgical results of operations for carcinoma of the gallbladder. Hepato-Gastroenterology. 1999;46(27):1552–6.
53. Itoh H, Nishijima K, Kurosaka Y, Takegawa S, Kiriyama M, Dohba S, et al. Magnitude of combination therapy of radical resection and external beam radiotherapy for patients with carcinomas of the extrahepatic bile duct and gallbladder. Dig Dis Sci. 2005;50(12):2231–42. https://doi.org/10.1007/s10620-005-3040-8.
54. Todoroki T, Kawamoto T, Otsuka M, Koike N, Yoshida S, Takada Y, et al. Benefits of combining radiotherapy with aggressive resection for stage IV gallbladder cancer. Hepato-Gastroenterology. 1999;46(27):1585–91.
55. Kim Y, Amini N, Wilson A, Margonis GA, Ethun CG, Poultsides G, et al. Impact of chemotherapy and external-beam radiation therapy on outcomes among patients with resected gallbladder Cancer: a multi-institutional analysis. Ann Surg Oncol. 2016;23(9):2998–3008. https://doi.org/10.1245/s10434-016-5262-8.
56. Mitin T, Enestvedt CK, Jemal A, Sineshaw HM. Limited Use of Adjuvant Therapy in Patients With Resected Gallbladder Cancer Despite a Strong Association With Survival. J Natl Cancer Inst. 2017;109(7) https://doi.org/10.1093/jnci/djw324.
57. Ben-Josef E, Guthrie KA, El-Khoueiry AB, Corless CL, Zalupski MM, Lowy AM, et al. SWOG S0809: a phase II intergroup trial of adjuvant Capecitabine and gemcitabine followed by radiotherapy and concurrent Capecitabine in extrahepatic Cholangiocarcinoma and gallbladder carcinoma. J Clin Oncol: Official Journal of the American Society of Clinical Oncology. 2015;33(24):2617–22. https://doi.org/10.1200/jco.2014.60.2219.
58. Sun XN, Wang Q, Gu BX, Zhu YH, Hu JB, Shi GZ, et al. Adjuvant radiotherapy for gallbladder cancer: a dosimetric comparison of conformal radiotherapy and intensity-modulated radiotherapy. World J Gastroenterol. 2011;17(3):397–402. https://doi.org/10.3748/wjg.v17.i3.397.
59. Fuller CD, Thomas CR Jr, Wong A, Cavanaugh SX, Salter BJ, Herman TS, et al. Image-guided intensity-modulated radiation therapy for gallbladder carcinoma. Radiotherapy and Oncology: Journal of the European Society for Therapeutic Radiology and Oncology. 2006;81(1):65–72. https://doi.org/10.1016/j.radonc.2006.08.013.
60. Engineer R, Goel M, Chopra S, Patil P, Purandare N, Rangarajan V, et al. Neoadjuvant Chemoradiation followed by surgery for locally advanced gallbladder cancers: a new paradigm. Ann Surg Oncol. 2016;23(9):3009–15. https://doi.org/10.1245/s10434-016-5197-0.
61. Eckel F, Schmid RM. Chemotherapy in advanced biliary tract carcinoma: a pooled analysis of clinical trials. Br J Cancer. 2007;96(6):896–902. https://doi.org/10.1038/sj.bjc.6603648.
62. Yonemoto N, Furuse J, Okusaka T, Yamao K, Funakoshi A, Ohkawa S, et al. A multi-center retrospective analysis of survival benefits of chemotherapy for Unresectable biliary tract Cancer. Jpn J Clin Oncol. 2007;37(11):843–51. https://doi.org/10.1093/jjco/hym116.
63. Gallardo J, Rubio B, Villanueva L, Barajas O. Gallbladder Cancer, a different disease that needs individual trials. J Clin Oncol. 2005;23(30):7753–4. https://doi.org/10.1200/JCO.2005.02.7524.

64. Kelley RK, Bardeesy N. Biliary tract cancers: finding better ways to lump and Split. J Clin Oncol. 2015;33(24):2588–90. https://doi.org/10.1200/JCO.2015.61.6953.
65. Primrose JN, Fox R, Palmer DH, Prasad R, Mirza D, Anthoney DA, et al. Adjuvant capecitabine for biliary tract cancer: The BILCAP randomized study. Journal of Clinical Oncology. 2017;35(15_suppl):4006. https://doi.org/10.1200/JCO.2017.35.15_suppl.4006.
66. Valle J, Wasan H, Palmer DH, Cunningham D, Anthoney A, Maraveyas A, et al. Cisplatin plus gemcitabine versus gemcitabine for biliary tract Cancer. N Engl J Med. 2010;362(14):1273–81. https://doi.org/10.1056/NEJMoa0908721.
67. Murakami Y, Uemura K, Sudo T, Hayashidani Y, Hashimoto Y, Nakamura H, et al. Adjuvant gemcitabine plus S-1 chemotherapy improves survival after aggressive surgical resection for advanced biliary carcinoma. Ann Surg. 2009;250(6):950–6.
68. Sirohi B, Singh A, Jagannath P, Shrikhande SV. Chemotherapy and targeted therapy for gall bladder Cancer. Indian J Surg Oncol. 2014;5(2):134–41. https://doi.org/10.1007/s13193-014-0317-4.
69. Oswalt CE, Cruz AB Jr. Effectiveness of chemotherapy in addition to surgery in treating carcinoma of the gallbladder. Rev Surg. 1977;34(6):436–8.
70. Raj D, Singh S, Gupta N, Rathi S. Neoadjuvant chemotherapy for gall bladder cancer: Does it increase resectability? J Clin Oncol. 2016;34(4_suppl):406. https://doi.org/10.1200/jco.2016.34.4_suppl.406.
71. Sirohi B, Mitra A, Jagannath P, Singh A, Ramadvar M, Kulkarni S, et al. Neoadjuvant chemotherapy in patients with locally advanced gallbladder cancer. Future Oncol (London, England). 2015;11(10):1501–9. https://doi.org/10.2217/fon.14.308.
72. Engineer R, Wadasadawala T, Mehta S, Mahantshetty U, Purandare N, Rangarajan V, et al. Chemoradiation for unresectable gall bladder cancer: time to review historic nihilism? J Gastrointest Cancer. 2011;42(4):222–7. https://doi.org/10.1007/s12029-010-9179-3.
73. de Aretxabala X, Roa I, Burgos L, Cartes R, Silva J, Yañez E, et al. Preoperative chemoradiotherapy in the treatment of gallbladder cancer. Am Surg. 1999;65(3):241–6.
74. Saluja SS, Gulati M, Garg PK, Pal H, Pal S, Sahni P, et al. Endoscopic or Percutaneous Biliary Drainage for Gallbladder Cancer: A Randomized Trial and Quality of Life Assessment. Clin Gastroenterol Hepatol. 2008;6(8):944–50.e3. https://doi.org/10.1016/j.cgh.2008.03.028.
75. Pinol V, Castells A, Bordas JM, Real MI, Llach J, Montana X, et al. Percutaneous self-expanding metal stents versus endoscopic polyethylene endoprostheses for treating malignant biliary obstruction: randomized clinical trial. Radiology. 2002;225(1):27–34. https://doi.org/10.1148/radiol.2243011517.
76. Ben-David MA, Griffith KA, Abu-Isa E, Lawrence TS, Knol J, Zalupski M, et al. External-beam radiotherapy for localized extrahepatic cholangiocarcinoma. Int J Radiat Oncol Biol Phys. 2006;66(3):772–9. https://doi.org/10.1016/j.ijrobp.2006.05.061.
77. Valle JW, Borbath I, Khan SA, Huguet F, Gruenberger T, Arnold D. Biliary cancer: ESMO clinical practice guidelines for diagnosis, treatment and follow-up. Annals of Oncology: Official Journal of the European Society for Medical Oncology. 2016;27(suppl 5):v28–37. https://doi.org/10.1093/annonc/mdw324.
78. Patt YZ, Hassan MM, Aguayo A, Nooka AK, Lozano RD, Curley SA, et al. Oral capecitabine for the treatment of hepatocellular carcinoma, cholangiocarcinoma, and gallbladder carcinoma. Cancer. 2004;101(3):578–86. https://doi.org/10.1002/cncr.20368.
79. Nehls O, Oettle H, Hartmann JT, Hofheinz RD, Hass HG, Horger MS, et al. Capecitabine plus oxaliplatin as first-line treatment in patients with advanced biliary system adenocarcinoma: a prospective multicentre phase II trial. Br J Cancer. 2008;98(2):309–15. https://doi.org/10.1038/sj.bjc.6604178.
80. Kim TW, Chang HM, Kang HJ, Lee JR, Ryu MH, Ahn JH, et al. Phase II study of capecitabine plus cisplatin as first-line chemotherapy in advanced biliary cancer. Annals of Ooncology: Official Journal of the European Society for Medical Oncology. 2003;14(7):1115–20.
81. Kubicka S, Rudolph KL, Tietze MK, Lorenz M, Manns M. Phase II study of systemic gemcitabine chemotherapy for advanced unresectable hepatobiliary carcinomas. Hepato-Gastroenterology. 2001;48(39):783–9.

82. Mezger J, Sauerbruch T, Ko Y, Wolter H, Funk C, Glasmacher A. Phase II study with gemcitabine in gallbladder and biliary tract carcinomas. Oncol Res Treat. 1998;21(3):232–4.
83. Penz M, Kornek GV, Raderer M, Ulrich-Pur H, Fiebiger W, Lenauer A, et al. Phase II trial of two-weekly gemcitabine in patients with advanced biliary tract cancer. Ann Oncol. 2001;12(2):183–6.
84. Knox JJ, Hedley D, Oza A, Feld R, Siu LL, Chen E, et al. Combining gemcitabine and capecitabine in patients with advanced biliary cancer: a phase II trial. J Clin Oncol Off J Am Soc Clin Oncol. 2005;23(10):2332–8. https://doi.org/10.1200/jco.2005.51.008.
85. Cho JY, Paik YH, Chang YS, Lee SJ, Lee DK, Song SY, et al. Capecitabine combined with gemcitabine (CapGem) as first-line treatment in patients with advanced/metastatic biliary tract carcinoma. Cancer. 2005;104(12):2753–8. https://doi.org/10.1002/cncr.21591.
86. Riechelmann RP, Townsley CA, Chin SN, Pond GR, Knox JJ. Expanded phase II trial of gemcitabine and capecitabine for advanced biliary cancer. Cancer. 2007;110(6):1307–12. https://doi.org/10.1002/cncr.22902.
87. Meyerhardt JA, Zhu AX, Stuart K, Ryan DP, Blaszkowsky L, Lehman N, et al. Phase-II study of gemcitabine and cisplatin in patients with metastatic biliary and gallbladder cancer. Dig Dis Sci. 2008;53(2):564–70. https://doi.org/10.1007/s10620-007-9885-2.
88. Thongprasert S, Napapan S, Charoentum C, Moonprakan S. Phase II study of gemcitabine and cisplatin as first-line chemotherapy in inoperable biliary tract carcinoma. Ann Oncol. 2005;16(2):279–81. https://doi.org/10.1093/annonc/mdi046.
89. Kim ST, Park JO, Lee J, Lee KT, Lee JK, Choi SH, et al. A phase II study of gemcitabine and cisplatin in advanced biliary tract cancer. Cancer. 2006;106(6):1339–46. https://doi.org/10.1002/cncr.21741.
90. Zhu AX, Hong TS, Hezel AF, Kooby DA. Current management of gallbladder carcinoma. Oncologist. 2010;15(2):168–81. https://doi.org/10.1634/theoncologist.2009-0302.
91. Valle J, Wasan H, Palmer DH, Cunningham D, Anthoney A, Maraveyas A, et al. Cisplatin plus gemcitabine versus gemcitabine for biliary tract cancer. N Engl J Med. 2010;362(14):1273–81. https://doi.org/10.1056/NEJMoa0908721.
92. Andre T, Tournigand C, Rosmorduc O, Provent S, Maindrault-Goebel F, Avenin D, et al. Gemcitabine combined with oxaliplatin (GEMOX) in advanced biliary tract adenocarcinoma: a GERCOR study. Ann Oncol. 2004;15(9):1339–43. https://doi.org/10.1093/annonc/mdh351.
93. Harder J, Riecken B, Kummer O, Lohrmann C, Otto F, Usadel H, et al. Outpatient chemotherapy with gemcitabine and oxaliplatin in patients with biliary tract cancer. Br J Cancer. 2006;95(7):848–52. https://doi.org/10.1038/sj.bjc.6603334.
94. Gebbia N, Verderame F, Di Leo R, Santangelo D, Cicero G, Valerio MR, et al. A phase II study of oxaliplatin (O) and gemcitabine (G) first line chemotherapy in patients with advanced biliary tract cancers. J Clin Oncol. 2005;23(16_suppl):4132. https://doi.org/10.1200/jco.2005.23.16_suppl.4132.
95. Sharma A, Shukla NK, Chaudhary SP, Sahoo R, Mohanti BK, Deo SVS, et al. Final results of a phase III randomized controlled trial comparing modified gemcitabine + oxaliplatin (mGEMOX) to gemcitabine+ cisplatin in management of unresectable gall bladder cancer (GBC). J Clin Oncol. 2016;34(15_suppl):4077. https://doi.org/10.1200/JCO.2016.34.15_suppl.4077.
96. Alberts SR, Al-Khatib H, Mahoney MR, Burgart L, Cera PJ, Flynn PJ, et al. Gemcitabine, 5-fluorouracil, and leucovorin in advanced biliary tract and gallbladder carcinoma: a north central Cancer treatment group phase II trial. Cancer. 2005;103(1):111–8. https://doi.org/10.1002/cncr.20753.
97. Gebbia V, Giuliani F, Maiello E, Colucci G, Verderame F, Borsellino N, et al. Treatment of inoperable and/or metastatic biliary tree carcinomas with single-agent gemcitabine or in combination with levofolinic acid and infusional fluorouracil: results of a multicenter phase II study. J Clin Oncol: Official Journal of the American Society of Clinical Oncology. 2001;19(20):4089–91. https://doi.org/10.1200/jco.2001.19.20.4089.
98. Julka PK, Puri T, Rath GK. A phase II study of gemcitabine and carboplatin combination chemotherapy in gallbladder carcinoma. Hepatobiliary Pancreat Dis Int: HBPD INT. 2006;5(1):110–4.

99. Malka D, Trarbach T, Fartoux L, Mendiboure J, de la Fouchardière C, Viret F, et al. A multicenter, randomized phase II trial of gemcitabine and oxaliplatin (GEMOX) alone or in combination with biweekly cetuximab in the first-line treatment of advanced biliary cancer: Interim analysis of the BINGO trial. J Clin Oncol. 2009;27(15S):4520. https://doi.org/10.1200/jco.2009.27.15s.4520.
100. El-Khoueiry AB, Rankin C, Lenz HJ, Philip P, Rivkin SE, Blanke CD. SWOG 0514: A phase II study of sorafenib (BAY 43–9006) as single agent in patients (pts) with unresectable or metastatic gallbladder cancer or cholangiocarcinomas. J Clin Oncol. 2007;25(18_suppl):4639. https://doi.org/10.1200/jco.2007.25.18_suppl.4639.
101. Zhu AX, Meyerhardt JA, Blaszkowsky LS, Kambadakone AR, Muzikansky A, Zheng H, et al. Efficacy and safety of gemcitabine, oxaliplatin, and bevacizumab in advanced biliary-tract cancers and correlation of changes in 18-fluorodeoxyglucose PET with clinical outcome: a phase 2 study. Lancet Oncol. 2010;11(1):48–54. https://doi.org/10.1016/s1470-2045(09)70333-x.
102. Lubner SJ, Mahoney MR, Kolesar JL, Loconte NK, Kim GP, Pitot HC, et al. Report of a multicenter phase II trial testing a combination of biweekly bevacizumab and daily erlotinib in patients with unresectable biliary cancer: a phase II consortium study. J Clinical Oncology: Official Journal of the American Society of Clinical Oncology. 2010;28(21):3491–7. https://doi.org/10.1200/jco.2010.28.4075.
103. Brechon M, Dior M, Dreanic J, Brieau B, Guillaumot MA, Brezault C, et al. Addition of an antiangiogenic therapy, bevacizumab, to gemcitabine plus oxaliplatin improves survival in advanced biliary tract cancers. Investig New Drugs. 2017; https://doi.org/10.1007/s10637-017-0492-6.
104. Trinchieri G. Cancer and inflammation: an old intuition with rapidly evolving new concepts. Annu Rev Immunol. 2012;30:677–706. https://doi.org/10.1146/annurev-immunol-020711-075008.
105. Goldstein D, Lemech C, Valle J. New molecular and immunotherapeutic approaches in biliary cancer. ESMO Open. 2017;2(Suppl 1) https://doi.org/10.1136/esmoopen-2016-000152.
106. Marks EI, Yee NS. Immunotherapeutic approaches in biliary tract carcinoma: current status and emerging strategies. World J Gastrointest Oncol. 2015;7(11):338–46. https://doi.org/10.4251/wjgo.v7.i11.338.
107. Bang YJ, Doi T, Braud FD, Piha-Paul S, Hollebecque A, Razak ARA, et al. 525 safety and efficacy of pembrolizumab (MK-3475) in patients (pts) with advanced biliary tract cancer: interim results of KEYNOTE-028. Eur J Cancer. 51:S112. https://doi.org/10.1016/S0959-8049(16)30326-4.
108. Mojica P, Smith D, Ellenhorn J. Adjuvant radiation therapy is associated with improved survival for gallbladder carcinoma with regional metastatic disease. Journal of Surgical Oncology 2007;96(1):8–13. https://doi.org/10.1002/jso.20831.
109. Cho SY, Kim SH, Park SJ, Han SS, Kim YK, Lee KW, et al. Adjuvant chemoradiation therapy in gallbladder cancer. Journal of Surgical Oncology 102(1):87–93. https://doi.org/10.1002/jso.21544.
110. González ME, Giannini OH, González P, Saldaña B. Adjuvant radio-chemotherapy after extended or simple cholecystectomy in gallbladder cancer. Clinical and Translational Oncology 2011;13(7):480–4. https://doi.org/10.1007/s12094-011-0685-y.
111. Gu B, Qian L, Yu H, Hu J, Wang Q, Shan J, et al. Concurrent Chemoradiotherapy in Curatively Resected Gallbladder Carcinoma: A Propensity Score–Matched Analysis. International Journal of Radiation Oncology*Biology*Physics 2018;100(1):138–45. https://doi.org/10.1016/j.ijrobp.2017.09.029.
112. Takada T, Amano H, Yasuda H, Nimura Y, Matsushiro T, Kato H, et al. Is postoperative adjuvant chemotherapy useful for gallbladder carcinoma?. Cancer 2002;95(8):1685–95. https://doi.org/10.1002/cncr.10831.
113. Edeline J, Benabdelghani M, Bertaut A, Watelet J, Hammel P, Joly JP, et al. Gemcitabine and Oxaliplatin Chemotherapy or Surveillance in Resected Biliary Tract Cancer (PRODIGE 12-ACCORD 18-UNICANCER GI): A Randomized Phase III Study. Journal of Clinical Oncology 2019;37(8):658–67. https://doi.org/10.1200/JCO.18.00050.

Chapter 12
Cystic Lesions of the Liver

Newton B. Neidert and Sudhakar K. Venkatesh

Introduction

Cystic lesions of the liver are frequently encountered on abdominal imaging studies and represent a spectrum of fluid-filled lesions within the liver parenchyma. Hepatic cystic lesions have an estimated prevalence of up to 15–18% in the United States [1]. While the majority of these lesions are benign simple cysts, some can be premalignant or malignant cystic lesions. There are key imaging features of these cystic lesions that prompt further diagnostic evaluation to differentiate benign simple cysts from premalignant and malignant cystic lesions. Additionally, although many of these cystic lesions are asymptomatic, hepatic cystic lesions can become symptomatic and need intervention for relief of symptoms. The focus of this chapter is to describe the different types of common hepatic cystic lesions, highlight multimodality imaging characteristics, and review the different management strategies. Parasitic cysts and abscesses are discussed in the chapter on infections within this book (Chap. 5).

Simple Cysts

Simple cysts account for the majority of hepatic cystic lesions and have a prevalence of 3–18% [2–4]. Simple cysts are often multiple and less than 10 in number. When more than 10 cysts are present, the possibility of polycystic liver disease should be considered. Simple cysts are characterized by a thin, smooth wall and are lined with cuboidal biliary epithelium that secretes a serous fluid [5]. While believed to be a result of an aberration in biliary development, simple hepatic cysts have no

N. B. Neidert (✉) · S. K. Venkatesh
Department of Radiology, Mayo Clinic, Rochester, MN, USA
e-mail: neidert.newton@mayo.edu; Venkatesh.Sudhakar@mayo.edu

L. R. Roberts et al. (eds.), *Evaluation and Management of Liver Masses*,
https://doi.org/10.1007/978-3-030-46699-2_12

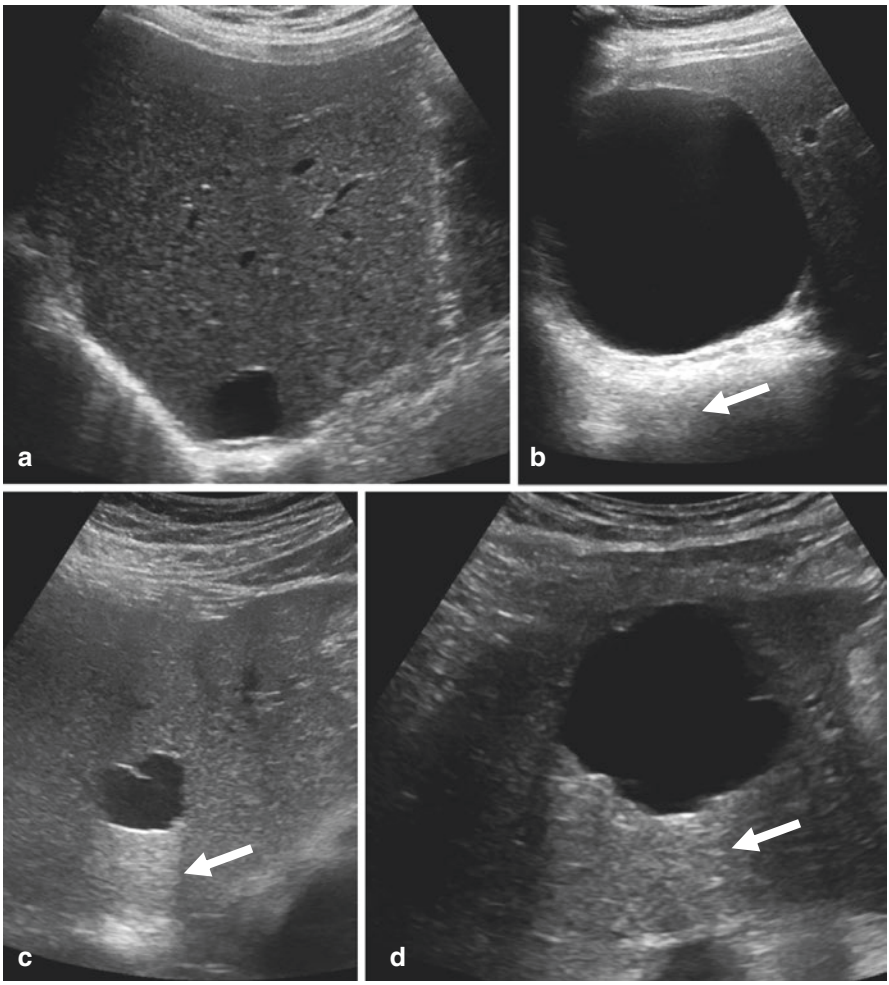

Fig. 12.1 Examples of simple cysts of the liver on ultrasound. Small cyst in the dome of right lobe of the liver (**a**), large cyst in the right lobe (**b**), small septate cyst (**c**), and large lobulated cyst (**d**). All cysts are anechoic. Note posterior acoustic enhancement (arrow)

communication with the biliary tree [6]. Imaging features are typical of cysts found in other organs. On ultrasound (US), simple cysts have distinct margins, an imperceptible wall, an anechoic fluid-filled cavity, and increased posterior through transmission (Fig. 12.1). The presence of wall thickening, multiple internal septations, or calcifications on ultrasound should prompt further evaluation with computed tomography (CT) or magnetic resonance imaging (MRI). Simple cysts are characterized by their water-like properties on CT with low attenuation (Hounsfield units of 0–15), an imperceptible wall, and no wall enhancement (Fig. 12.2). On MRI, simple cysts show high T2 signal intensity and low T1 signal intensity and no wall. The cyst contents do not show any restricted diffusion on diffusion–weighted images (Fig. 12.3).

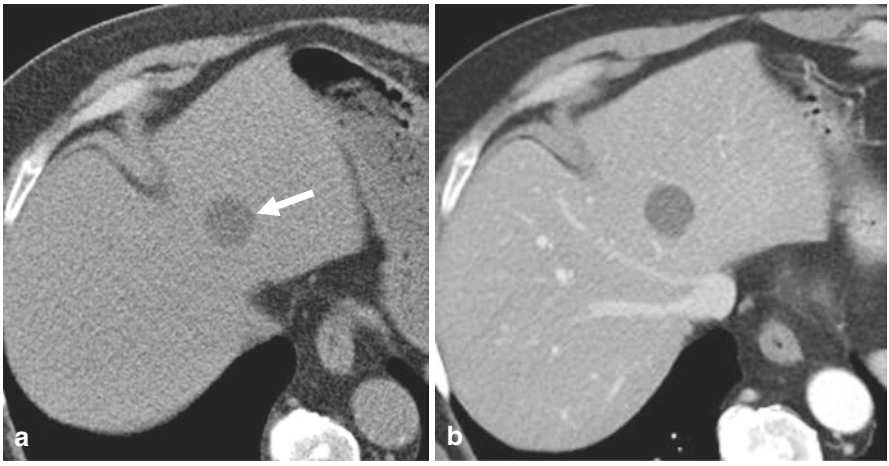

Fig. 12.2 CT appearance of a simple cyst. A small cyst (arrow) in the left lobe appears hypodense compared to normal liver parenchyma on non-contrast-enhanced CT (**a**) and post–contrast-enhanced CT (**b**). Note there is no wall or enhancement of the cyst

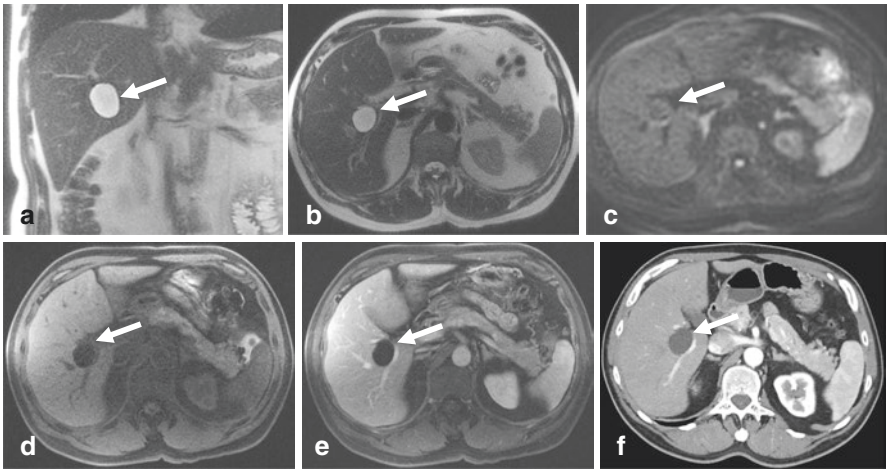

Fig. 12.3 MRI appearance of a simple cyst in the right lobe of the liver (arrow). The cyst appears hyperintense on coronal (**a**) and axial (**b**) T2-weighted images, shows no restricted diffusion (no high signal) on diffusion-weighted image (**c**), and appears hypointense on T1-weighted image (**d**). On post-contrast image (**e**), there is no enhancement of cyst and note there is no presence of wall. A contrast-enhanced CT (**f**) at the same level for comparison

The vast majority of simple hepatic cysts are asymptomatic. However, symptoms can develop with increasing number and size of cysts. Symptoms are often non-specific but relate to mass effect. Such symptoms include abdominal pain, bloating, early satiety, nausea, emesis, and shortness of breath [7]. Rarely, mass

effect from a cyst can cause biliary obstruction with jaundice or inferior vena caval obstruction with leg edema. Infrequently, simple cysts can be complicated by internal hemorrhage or infection [8]. Hemorrhage into a simple cyst can occur as a result of trauma. Hemorrhage or infection of the cyst can change the appearance of the simple cyst with the development of internal debris, septations, a reactive, thickened, and often enhancing wall (Fig. 12.4), and uncommonly calcifications within the wall. The development of an enhancing nodule should raise the possibility of a neoplasm. Treatment of symptomatic hepatic cysts is well described. Cyst aspiration alone will invariably result in recurrence. However, cyst aspiration and sclerotherapy (Fig. 12.5) using sclerosing agents such as polidocanol and dehydrated alcohol has been demonstrated to be safe and effective in reducing the size of hepatic cysts and improving symptoms [9–11]. Surgical treatment is also an effective treatment, albeit with higher morbidity, and includes open or laparoscopic cyst fenestration or deroofing [12–15].

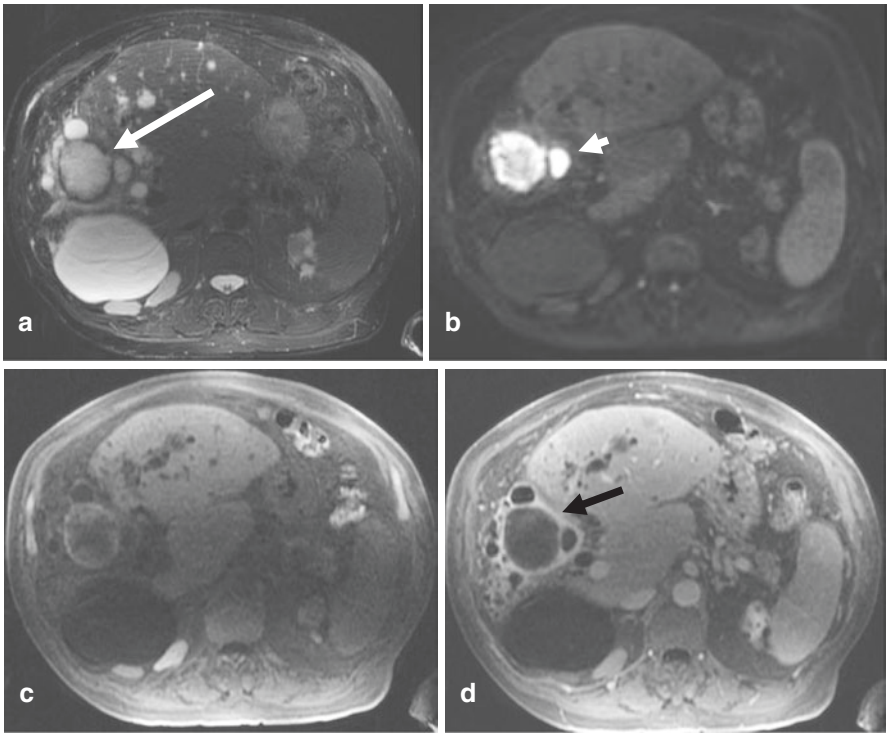

Fig. 12.4 An infected cyst in a patient with polycystic liver disease. Axial T2W image (**a**) shows a septate cyst in the inferior right lobe, demonstrating a thick hypointense (dark) wall (arrow). The cyst contents show restricted diffusion (arrow head) on DWI (**b**), hyperintensity on T1W (**c**) and a thick enhancing rim (black arrow) on post-contrast imaging (**d**)

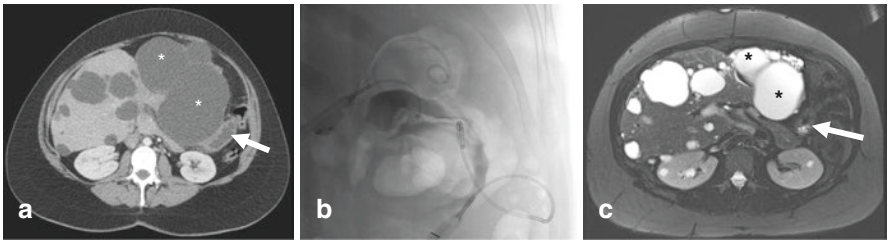

Fig. 12.5 Cyst aspiration and sclerotherapy. Axial CT (**a**) of the abdomen with IV contrast demonstrates polycystic liver disease, including two large cysts (asterisks) in the left hepatic lobe that compress the stomach (arrow). Fluoroscopic image (**b**) during cyst aspiration and sclerotherapy of the two largest cysts in the left hepatic lobe. MRI axial T2W image (**c**) of the abdomen four months after sclerotherapy demonstrates significant volume reduction of the treated left hepatic lobe cysts (asterisks) and decreased compression of the stomach (arrow). The patient's symptoms of abdominal pain, nausea, and vomiting were dramatically improved after sclerotherapy

Polycystic Liver Disease

Polycystic liver disease (PLD) is a rare fibrocystic condition that most commonly occurs in the setting of autosomal dominant polycystic kidney disease (ADPKD). The liver is the most frequent extrarenal site of involvement in ADPKD, occurring in about 40% of patients [16, 17]. Tuberous sclerosis is also associated with polycystic liver disease. The disease typically manifests as numerous cysts that progressively increase in size and number. The imaging features are similar to those of simple cysts except that numerous cysts may be seen throughout the liver and often nearly completely replace the liver parenchyma (Fig. 12.6). PLD can rarely give rise to portal hypertension due to compression of the intrahepatic portal venous system. The large cysts often show evidence of hemorrhage or debris within them. The cysts can grow to large sizes, resulting in hepatomegaly with stretching of the liver capsule or mass impression on adjacent organs. As with symptomatic hepatic cysts, aspiration and sclerotherapy is an effective therapy that can be directed toward large cysts to decrease cyst volume and improve symptoms. In patients with advanced PLD with severely symptomatic and massive hepatomegaly, partial hepatectomy with cyst fenestration can provide long-term reductions in hepatic volume [18]. Liver transplantation is the only curative treatment and is reserved for patients with end-stage PLD [19].

Biliary Hamartoma

Biliary hamartomas have a reported prevalence of 5–6% [20] and represent benign, congenitally dilated small bile ducts enclosed by fibrous stroma [21]. Biliary hamartomas are also referred to as von Meyenberg complex. They are characterized on imaging by multiple small (<15 mm) round or irregular cysts scattered throughout

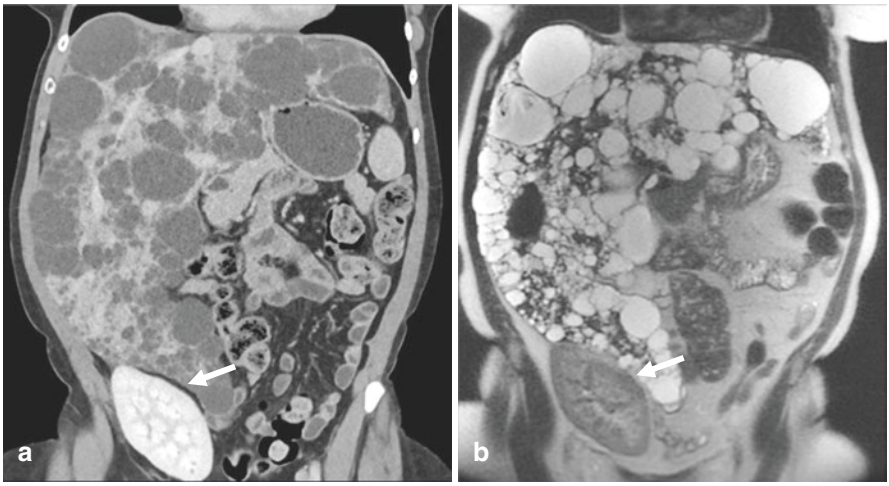

Fig. 12.6 CT and MRI of a patient with polycystic liver disease. Note multiple cysts in both lobes of liver on CT (**a**) and coronal T2-weighted image from MRI (**b**). Patient also had autosomal dominant polycystic kidney disease and underwent bilateral nephrectomies and a transplant. The renal transplant (arrow) is seen in the right lower abdomen

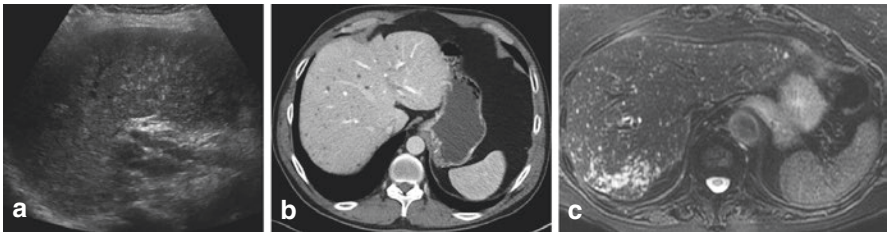

Fig. 12.7 Biliary hamartomas. Ultrasound (**a**), CT (**b**), and T2W MRI image (**c**) of different patients showing multiple hamartomas throughout the liver. On ultrasound, multiple echogenic foci are seen throughout the liver. On CT, tiny non-enhancing hypodensities represent the hamartomas. On T2W images, the hamartomas are seen as tiny hyperintensities with more in the right lobe of liver in this example

the liver and do not communicate with the biliary tree (Fig. 12.7). The small size of biliary hamartomas results in a varied appearance on US that can be anywhere between anechoic to hyperechoic and can also have reverberation artifact from the compressed interfaces [22]. Biliary hamartomas have typical cystic imaging characteristics on CT (i.e., low attention) and MRI (i.e., high T2 signal). The differentiation is from common simple cysts, polycystic liver disease, and Caroli's disease. The presence of fibrous stroma (solid and sometimes enhancing) may render their appearance different from cystic lesions, and rarely, they may be mistaken for necrotic metastases that have solid and cystic areas with variable enhancement. No

treatment is necessary, as biliary hamartomas are usually asymptomatic and discovered incidentally.

Biliary Cystic Neoplasms

Biliary cystic neoplasms include biliary cystadenomas (BCA), biliary cystadenocarcinomas (BCAC), and intraductal papillary mucinous neoplasms of biliary origin (IPMN-B). The recent WHO classification proposed that BCA and BCAC should be classified as mucinous cystic neoplasms (MCN) when ovarian stroma (OS) is present or as IPMN-B when biliary communication is present [23]. Biliary cystic neoplasms represent up to 5% of hepatic cystic lesions and have a female predilection, particularly BCA, which have a 9:1 female–male ratio [24, 25]. While most are asymptomatic, BCA and BCAC can present with symptoms related to mass effect when the lesions are large in size [26]. BCAC are believed to represent malignant transformation of BCA, but predicting this transformation has proven difficult. Biliary cystic tumors are thought to be slow-growing neoplasms of aberrant biliary ductal tissue. Histologically BCAs are composed of three layers – a mucin-secreting epithelial layer composed of columnar cells, a stromal layer (usually ovarian stroma type), and an outer collagenous layer which is thought to be reactive from surrounding liver parenchyma [27]. The stroma consists of bland spindle-shaped cells with round-to-oval nuclei and resembles ovarian stroma (OS), but this also resembles primitive embryonic mesoderm of the gallbladder and bile ducts and therefore has been suggested to be derived from ectopic rests of primitive foregut sequestered in the liver [28]. The exact origin of these neoplasms still remains to be determined.

The imaging characteristics of BCA and BCAC overlap, and imaging studies have yet to reliably distinguish between the two [27, 29, 30]. Both BCA and BCAC are most commonly multilocular with irregular internal septations, cyst wall thickening and enhancement (Fig. 12.8), and occasional calcifications [31, 32]. The internal septations of these lesions are best demonstrated with US or MRI. Cyst contents are typically hyperintense on T2-weighted imaging on MRI but can be heterogenous depending on the amount of mucinous content. The presence of enhancing mural nodules, particularly those greater than 10 mm, is suggestive of BCAC [33]. BCA and BCAC are managed with surgical excision and biopsy and/or aspiration are not advised to avoid malignant dissemination if there is an underlying biliary cystadenocarcinoma [34]. Aspiration, if done, shows bile-tinged mucin and may be useful for differentiating infected cysts. Determination of cystic fluid carbohydrate antigen 19-9 (CA 19-9) and carcinoembryonic antigen (CEA) are not thought to be useful for differentiating BCA from BCAC and remain controversial as there is a risk of seeding the tumor into the peritoneal and/or pleural cavities [32, 34–37].

IPMN-Bs are characterized by intraluminal papillary growth within the bile ducts and produce mucin [38]. They are similar to IPMNs occurring in pancreas

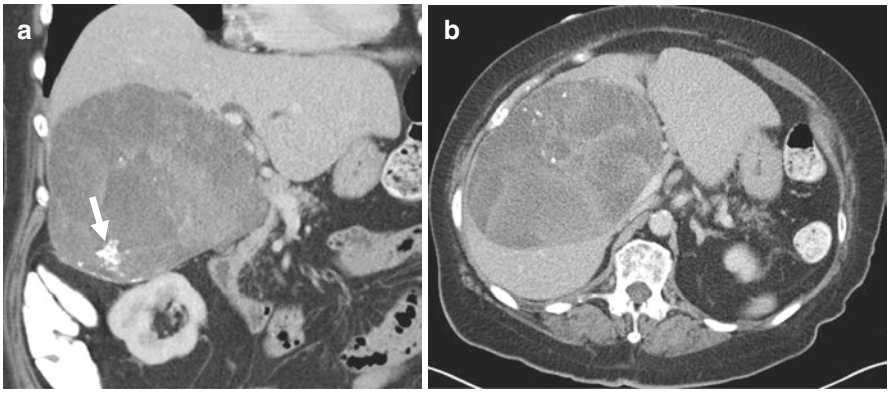

Fig. 12.8 Mucinous cystadenocarcinoma of liver. Coronal (**a**) and axial (**b**) contrast-enhanced CT of the liver showing a heterogeneous attenuation cystic mass in the right lobe of the liver. There is some heterogeneous enhancement of the cystic mass and focal areas of calcification (arrows)

(IPMN-P). IPMN-Bs do not have ovarian stroma and have been previously referred to as papilloma, mucin-producing cholangiocarcinoma, and intraductal variant of cholangiocarcinoma. IPMN-B can produce a lot of mucin and lead to biliary dilatation or a cystic mass that has both solid and cystic components similar to IPMN-P. The cystic type can be mistaken for a BCA [39]. Patients with IPMN-B are mostly asymptomatic, but communication with the biliary tree is characteristic, which may be difficult to show on CT and MRI and may require cholangiography [40]. IPMN-B carries a higher risk of malignant transformation compared to IPMN-P and therefore requires resection. The prognosis of IPMN-B is better than that of cholangiocarcinomas [41, 42].

Choledochal Cyst and Caroli's Disease

Choledochal cyst represents a spectrum of disease characterized by congenital segmental aneurysmal dilatation of the bile ducts and most commonly involves the extrahepatic common bile duct. The most characteristic feature is the communication with bile ducts that can be demonstrated on imaging (Fig. 12.9). Patients are usually asymptomatic, and although congenital, choledochal cysts are usually diagnosed in adult life. Choledochal cysts are classified into five major types (types I through V) with type IV and type V (Caroli's disease) manifesting with intrahepatic cystic dilatation of the biliary ducts [43]. On imaging, the key feature to demonstrate is the communication with the bile ducts on US, CT, or MRI. ERCP may be required if all of the non-invasive methods fail. These segmental dilatations may often contain debris, hemorrhage, and stones. Rarely they may have malignant degeneration into cholangiocarcinoma. Surgical excision of symptomatic cysts offers the best treatment.

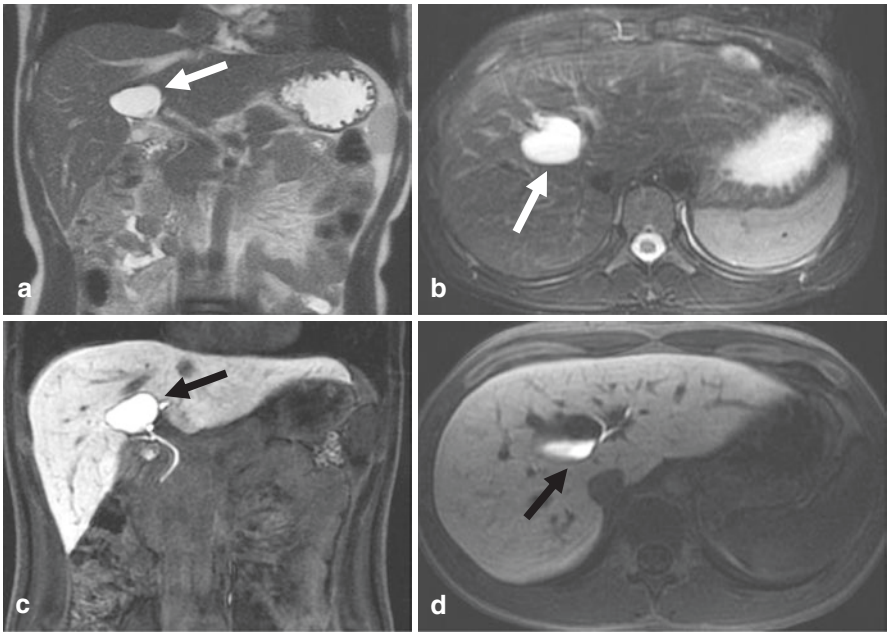

Fig. 12.9 Intrahepatic choledochal cyst. Coronal and axial T2W images (**a**, **b**) showing a central cyst (white arrow). Coronal (**c**) and axial (**d**) T1W images in the delayed hepatobiliary phase (20 minutes) performed with a hepatobiliary contrast agent (gadoxetate sodium) showing contrast in the biliary tree and in the cyst (black arrows) confirming the biliary communication

Caroli's disease is an autosomal recessive disease characterized by multiple small intrahepatic biliary cystic dilatations (Fig. 12.10) and is thought to arise from a ductal plate malformation. The disease represents a fibropolycystic disease similar to ADPKD. A second type – designated the periportal fibrosis type – is autosomal recessive and frequently associated with renal tubular ectasia and polycystic disease. According to the Todani classification, this disease represents type V choledochal cyst. In contrast to other choledochal cysts, Caroli's disease can be symptomatic and often presents with pain and hepatosplenomegaly with elevated liver function tests. When numerous cysts are present, these can be mistaken for biliary hamartomas or peribiliary cysts. A characteristic central dot sign on contrast-enhanced CT has been described which is due to cystic dilatations of the hepatic ducts surround the accompanying portal vein branch which represents the dot. The most common complications are recurrent cholangitis, stone formation, and infected cysts leading to abscess formation. Uncommonly cirrhosis and portal hypertension can result and cholangiocarcinoma can develop. Treatment is by resection of symptomatic cysts and may require liver transplantation if associated with cirrhosis and portal hypertension.

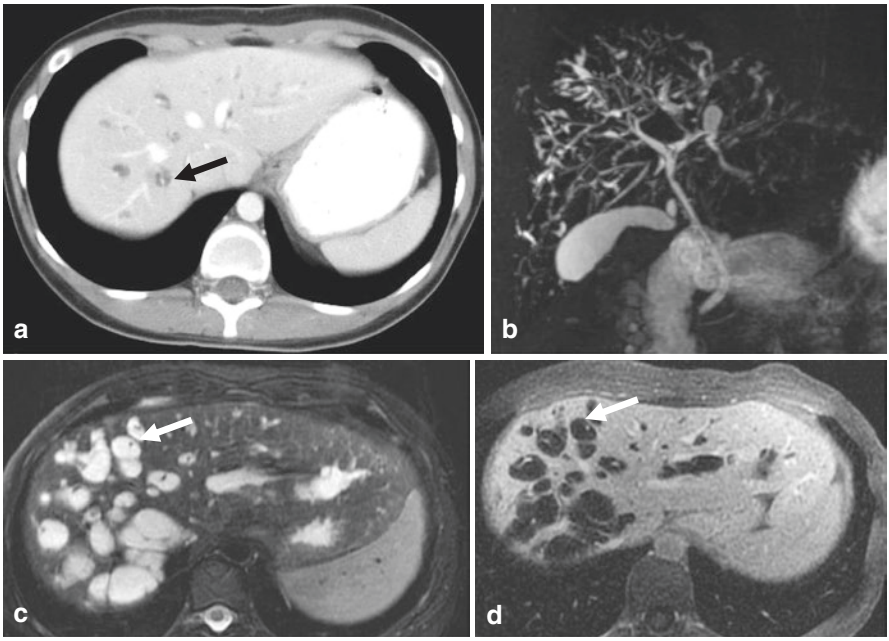

Fig. 12.10 Caroli's disease. Contrast-enhanced CT (**a**) showing central dot sign (black arrow). Magnetic resonance cholangiopancreatography (MRCP) (**b**) showing saccular dilatations of the multiple intrahepatic ducts. MRI in a different patient showing dilated ducts on T2W (**c**) image and central dot sign on post–contrast-enhanced T1W image (**d**) (white arrows)

Peribiliary Cysts

Peribiliary cysts result from cystic dilatation of the obstructed periductal glands in the bile duct wall. These variable-sized cysts are usually found in the liver hilum and can be seen intrahepatically up to about fourth-order biliary ductal branches (Fig. 12.11). When extensive, peribiliary cysts can mimic biliary dilatation and can lead to compression of portal vein branches resulting in portal hypertension. Up to 50% of peribiliary cysts are found in patients with cirrhosis, and they are often symptomatic to the associated disease [44, 45]. Peribiliary cysts are underdiagnosed as they are asymptomatic and demonstrated on imaging in only 9% of patients with cirrhosis. The size and number of cysts increase with the progression of cirrhosis. Obstructive jaundice can occur [46]. Peribiliary cysts are diagnosed on CT or MRI by their characteristic presence along the portal vein branches and the absence of communication with the biliary tree; however, when they cause compression of the biliary tree it may be difficult to rule out a communication. Due to their rarity, peribiliary cysts can be misdiagnosed and this may lead to therapeutic misadventures. A correct diagnosis with MRI/MRCP may avoid such complications.

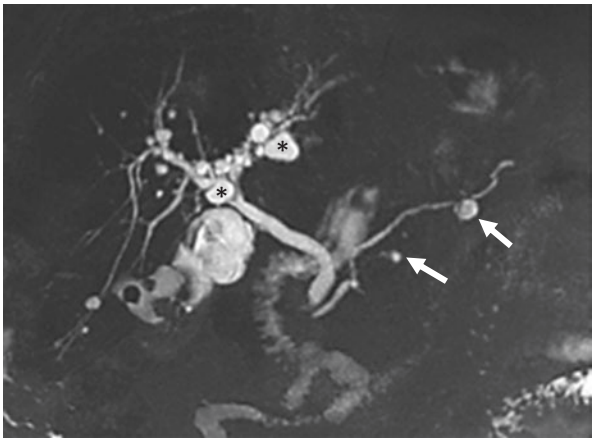

Fig. 12.11 Peribiliary cyst. MRCP image showing multiple cysts along the biliary tree (asterisks). These were not communicating with the biliary system. Note the patient also has cystic lesions in the tail of pancreas (arrows)

Cystic Hepatocellular Carcinoma

Hepatocellular carcinoma (HCC) is typically a solid, hypervascular mass on imaging, but can rarely present as a cystic mass with enhancing septa. The cystic appearance is attributed to areas of necrosis and internal hemorrhage [29, 47, 48]. This cystic appearance is most commonly attributed to percutaneous treatments, such as transarterial embolization or thermal ablation, leading to liquefactive necrosis [8].

Cystic Metastases

The necrosis and internal hemorrhage that can account for the cystic appearance of HCC can also be seen with tumors that have metastasized to the liver. This is especially true of malignancies with rapid growth, such as neuroendocrine tumors, melanoma, sarcoma, and gastrointestinal stromal tumors [8]. In addition, metastases with mucinous secretion, such as mucinous ovarian and colorectal carcinomas, can have a cystic appearance (Figs. 12.12 and 12.13). Lastly, chemotherapy treatment effect can result in cystic degeneration and necrosis of liver metastases.

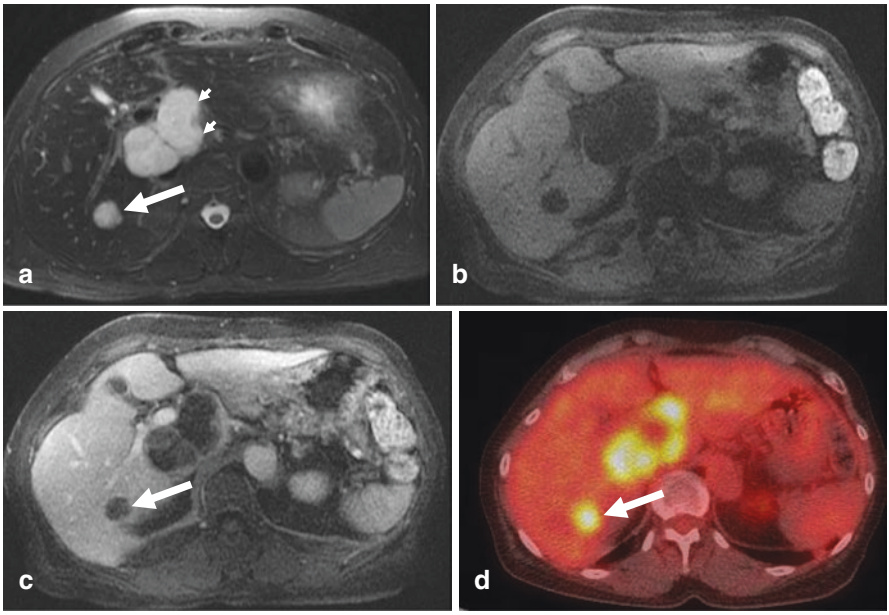

Fig. 12.12 Mucinous carcinoma colon metastases mimicking cystic lesion. Axial T2W (**a**), T1W (**b**), post-contrast T1W (**c**) and positron emission tomography (PET) (**d**) images showing cystic appearing metastatic lesion in the right lobe (white arrow) that shows some peripheral enhancement and uptake on PET similar to the hilar lymph nodes (arrow heads)

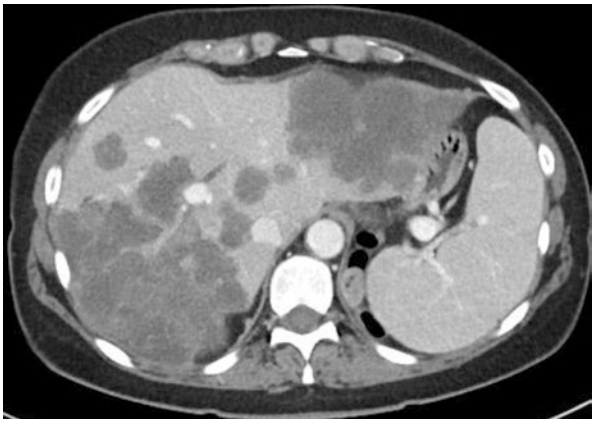

Fig. 12.13 Cystic metastases from ovarian carcinoma. Note similar appearance to polycystic liver disease

Traumatic Lesions

Trauma and iatrogenic injury to the liver can lead to the development of lesions within the liver that appear cystic. Bilomas and seromas typically appear as a simple collection of fluid and can be difficult to distinguish on imaging, unless a biliary

leak can be established which indicates the former [49]. Hematomas have a varied imaging appearance depending on the age of the blood products. On CT, hematomas are typically intermediate attenuation. The most sensitive method for detecting blood products is with a gradient-echo T2-weighted MRI sequence. Arterial pseudoaneurysms can appear cystic on grayscale US and non-contrast imaging studies. Doppler US and post-contrast imaging demonstrating enhancement similar to blood pool can readily establish the diagnosis of a pseudoaneurysm. Hepatic pseudoaneurysms should be treated due to the risk of rupture [50].

Conclusion

Imaging has a valuable role in the diagnosis and management of cystic liver disease. Although the majority of hepatic cystic lesions are benign and do not require any further workup, it is important to recognize imaging characteristics that could indicate a cystic primary malignancy or cystic metastasis. Surgical and non-surgical interventions for cystic hepatic lesions continue to evolve with progress in technology and procedural techniques.

References

1. Marrero JA, Ahn J, Rajender Reddy K. ACG clinical guideline: the diagnosis and management of focal liver lesions. Am J Gastroenterol. 2014;109:1328–47.
2. Gaines PA, Sampson MA. The prevalence and characterization of simple hepatic cysts by ultrasound examination. Br J Radiol. 1989;62:335–7.
3. Carrim ZI, Murchison JT. The prevalence of simple renal and hepatic cysts detected by spiral computed tomography. Clin Radiol. 2003;58:626–9.
4. Larssen TB, Rørvik J, Hoff SR, et al. The occurrence of asymptomatic and symptomatic simple hepatic cysts. A prospective, hospital-based study. Clin Radiol. 2005;60:1026–9.
5. Lantinga MA, Gevers TJ, Drenth JP. Evaluation of hepatic cystic lesions. World J Gastroenterol. 2013;19:3543–54.
6. Benhamou J, Menu Y. Nonparasitic cystic disease of the liver and intrahepatic biliary tree. In: Blumgart LH, editor. Surgery of the liver and biliary tract. Edinburgh: Churchill Livingstone; 1994. p. 1197–210.
7. Bahirwani R, Reddy KR. Review article: the evaluation of solitary liver masses. Aliment Pharmacol Ther. 2008;28:953–65.
8. Borhani AA, Wiant A, Heller MT. Cystic hepatic lesions: a review and an algorithmic approach. AJR Am J Roentgenol. 2014;203:1192–204.
9. Spârchez Z, Radu P, Zaharie F, et al. Percutaneous treatment of symptomatic non-parasitic hepatic cysts. Initial experience with single-session sclerotherapy with polidocanol. Med Ultrason. 2014;16:222–8.
10. van Keimpema L, de Koning DB, Strijk SP, Drenth JP. Aspiration-sclerotherapy results in effective control of liver volume in patients with liver cysts. Dig Dis Sci. 2008;53:2251–7.
11. Yang CF, Liang HL, Pan HB, Lin YH, Mok KT, Lo GH, et al. Single-session prolonged alcohol-retention sclerotherapy for large hepatic cysts. AJR Am J Roentgenol. 2006;187:940–3.

12. Neri V, Ambrosi A, Fersini A, Valentino TP. Laparoscopic treatment of biliary hepatic cysts: short- and medium-term results. HPB (Oxford). 2006;8:306–10.
13. Tocchi A, Mazzoni G, Costa G, et al. Symptomatic nonparasitic hepatic cysts: options for and results of surgical management. Arch Surg. 2002;137:154–8.
14. Garcea G, Rajesh A, Dennison AR. Surgical management of cystic lesions in the liver. ANZ J Surg. 2013;83:516–22.
15. Hansen P, Bhoyrul S, Legha P, Wetter A, Way LW. Laparoscopic treatment of liver cysts. J Gastrointest Surg. 1997;1:53–9.
16. Bae KT, Zhu F, Chapman AB, et al. Magnetic resonance imaging evaluation of hepatic cysts in early autosomaldominant polycystic kidney disease: the consortium for radiologic imaging studies of polycystic kidney disease cohort. Clin J Am Soc Nephrol. 2006;1:64–9.
17. Everson GT, Taylor MR, Doctor RB. Polycystic disease of the liver. Hepatology. 2004;40:774–82.
18. Chebib FT, et al. Outcomes and durability of hepatic reduction after combined partial hepatectomy and cyst fenestration for massive polycystic liver disease. J Am Coll Surg. 2016;223(1):118–126.e1.
19. Arrazola L, Moonka D, Gish RG, Everson GT. Model for end-stage liver disease (MELD) exception for polycystic liver disease. Liver Transpl. 2006;12:S110–1.
20. Redston MS, Wanless IR. The hepatic von Meyenburg complex: prevalence and association with hepatic and renal cysts among 2843 autopsies. Mod Pathol. 1996;9:233–7.
21. Lev-Toaff AS, Bach AM, Wechsler RJ, Hilpert PL, Gatalica Z, Rubin R. The radiologic and pathologic spectrum of biliary hamartomas. AJR. 1995;165:309–13.
22. Zheng RQ, Zhang B, Kudo M, Onda H, Inoue T. Imaging findings of biliary hamartomas. World J Gastroenterol. 2005;11:6354–9.
23. Nakanuma Y, et al. Mucinous cystic neoplasms. In: Bosman FT, et al., editors. World Helath Organization classification of tumours of the digestive system, vol. 3. 4th ed. Geneva: International Agency for Research on Cancer; 2010. p. 217–24.
24. Garcea G, Pattenden CJ, Stephenson J, et al. Nine-year single-center experience with nonparastic liver cysts: diagnosis and management. Dig Dis Sci. 2007;52:185–91.
25. Soares KC, Arnaoutakis DJ, Kamel I, et al. Cystic neoplasms of the liver: biliary cystadenoma and cystadenocarcinoma. J Am Coll Surg. 2014;218:119–28.
26. Ishak KG, Willis GW, Cummins SD, et al. Biliary cystadenoma and cystadenocarcinoma: report of 14 cases and review of the literature. Cancer. 1977;39:322–38.
27. Qian LJ, Zhu J, Zhuang ZG, Xia Q, Liu Q, Xu JR. Spectrum of multilocular cystic hepatic lesions: CT and MR imaging findings with pathologic correlation. Radiographics. 2013;33:1419–33.
28. Wheeler DA, Edmondson HA. Cystadenoma with mesenchymal stroma (CMS) in the liver and bile ducts. A clinicopathologic study of 17 cases, 4 with malignant change. Cancer. 1985;56:1434–45.
29. Bakoyiannis A, Delis S, Triantopoulou C, Dervenis C. Rare cystic liver lesions: a diagnostic and managing challenge. World J Gastroenterol. 2013;19:7603–19.
30. Dong Y, Wang WP, Mao F, Fan M, Ignee A, Serra C, et al. Contrast enhanced ultrasound features of hepatic cystadenoma and hepatic cystadenocarcinoma. Scand J Gastroenterol. 2017;52:365–72.
31. Choi BI, Lim JH, Han MC, et al. Biliary cystadenoma and cystadenocarcinoma: CT and sonographic findings. Radiology. 1989;171:57–61.
32. Kim JY, Kim SH, Eun HW, et al. Differentiation between biliary cystic neoplasms and simple cysts of the liver: accuracy of CT. AJR Am J Roentgenol. 2010;195:1142–8.
33. Mavilia MG, Pakala T, Molina M, Wu GY. Differentiating cystic liver lesions: a review of imaging modalities, diagnosis and management. J Clin Transl Hepatol. 2018;6(2):208–16.
34. Hai S, Hirohashi K, Uenishi T, et al. Surgical management of cystic hepatic neoplasms. J Gastroenterol. 2003;38:759–64.

35. Choi HK, Lee JK, Lee KH, et al. Differential diagnosis for intrahepatic biliary cystadenoma and hepatic simple cyst: significance of cystic fluid analysis and radiologic findings. J Clin Gastroenterol. 2010;44:289–93.
36. Teoh AY, Ng SS, Lee KF, Lai PB. Biliary cystadenoma and other complicated cystic lesions of the liver: diagnostic and therapeutic challenges. World J Surg. 2006;30:1560–6.
37. Pinto MM, Kaye AD. Fine needle aspiration of cystic liver lesions. Cytologic examination and carcinoembryonic antigen assay of cyst contents. Acta Cytol. 1989;33:852–6.
38. Nakanuma Y, et al. Biliary papillary neoplasm of the liver. Histol Histopathol. 2002;27:851–61.
39. Sakamoto E, et al. Clinicopathological studies of mucin producing cholangiocarcinoma. J Hepatobiliary Pancreat Surg. 1997;4:157–62.
40. Zen Y, et al. Biliary cystic tumors with bile duct communication: a cystic variant of intraductal papillary neoplasm of the bile duct. Mod Pathol. 2006;19:1243–54.
41. Zen Y, Fujii T, Itatsu K, et al. Biliary cystic tumors with bile duct communication: a cystic variant of intraductal papillary neoplasm of the bile duct. Mod Pathol. 2006;19:1243–54.
42. Zen Y, Pedica F, Patcha VR, et al. Mucinous cystic neoplasms of the liver: a clinicopathological study and comparison with intraductal papillary neoplasms of the bile duct. Mod Pathol. 2011;24:1079–89.
43. Todani T, Watanabe Y, Narusue M, Tabuchi K, Okajima K. Congenital bile duct cysts: classification, operative procedures, and review of thirty-seven cases including cancer arising from choledochal cyst. Am J Surg. 1977;134(2):263–9.
44. Terada T, Matsushita H, Tashiro J, Sairenji T, Eriguchi M, Osada I. Cholesterol hepatolithiasis with peribiliary cysts. Pathol Int. 2003;53(10):716–20.
45. Hoshiba K, Matsui O, Kadoya M, Yoshikawa J, Gabata T, Terayama N, Takashima T. Peribiliary cysts in cirrhotic liver: observation on computed tomography. Abdom Imaging. 1996;21(3):228–32.
46. Bazerbachi F, Haffar S, Sugihara T, Mounajjed TM, Takahashi N, Murad MH, Abu Dayyeh BK. Peribiliary cysts: a systematic review and proposal of a classification framework. BMJ Open Gastroenterol. 2018;5(1):e000204.
47. Paul SB, Gulati MS. Spectrum of hepatocellular carcinoma on triple phase helical CT: a pictorial essay. Clin Imaging. 2002;26:270–9.
48. Hagiwara S, Ogino T, Takahashi Y, et al. Hepatocellular carcinoma mimicking liver abscesses in a cirrhotic patient with severe septic shock as a result of Salmonella O9 HG infection. Case Rep Gastroenterol. 2009;3:56–60.
49. Yoon W, Jeong YY, Kim JK, et al. CT in blunt liver trauma. Radiographics. 2005;25:87–104.
50. Pachter HL, Knudson MM, Esrig B, et al. Status of nonoperative management of blunt hepatic injuries in 1995: a multicenter experience with 404 patients. J Trauma. 1996;40:31–8.

Index

L. R. Roberts et al. (eds.), *Evaluation and Management of Liver Masses*,
https://doi.org/10.1007/978-3-030-46699-2